

Advanced Techniques and Applications

X-ray and Neutron Diffraction
Techniques and Applications

Resources

X-rays

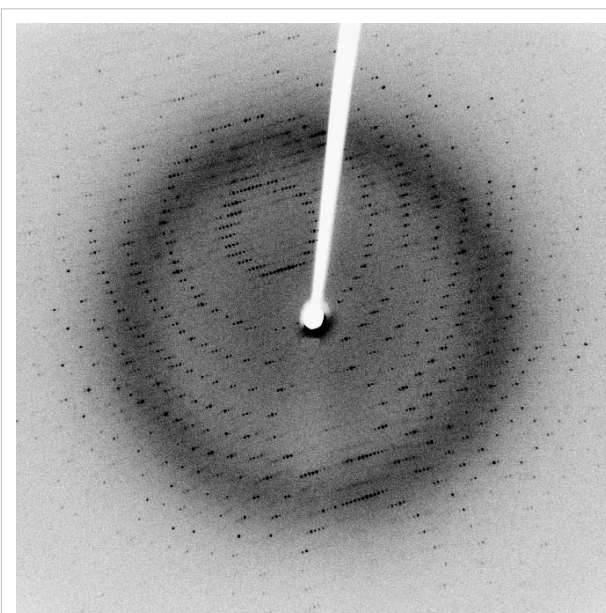
1. REDIRECT X-ray

X-ray scattering techniques

X-ray scattering techniques are a family of non-destructive analytical techniques which reveal information about the crystallographic structure, chemical composition, and physical properties of materials and thin films. These techniques are based on observing the scattered intensity of an X-ray beam hitting a sample as a function of incident and scattered angle, polarization, and wavelength or energy.

X-ray diffraction techniques

X-ray diffraction finds the geometry or shape of a molecule using X-rays. X-ray diffraction techniques are based on the elastic scattering of X-rays from structures that have long range order. The most comprehensive description of scattering from crystals is given by the dynamical theory of diffraction.^[1]



This is an X-ray diffraction pattern formed when X-rays are focused on a crystalline material, in this case a protein. Each dot, called a reflection, forms from the coherent interference of scattered X-rays passing through the crystal.

- Single-crystal X-ray diffraction is a technique used to solve the complete structure of crystalline materials, ranging from simple inorganic solids to complex macromolecules, such as proteins.
- Powder diffraction (XRD) is a technique used to characterize the crystallographic structure, crystallite size (grain size), and preferred orientation in polycrystalline or powdered solid samples. Powder diffraction is commonly used to identify unknown substances, by comparing diffraction data against a database maintained by the International Centre for Diffraction Data. It may also be used to characterize heterogeneous solid mixtures to determine relative abundance of crystalline compounds and, when coupled with lattice refinement techniques, such as Rietveld refinement, can provide structural information on unknown materials. Powder diffraction is also a common method for determining strains in crystalline materials. An effect of the finite

crystallite sizes is seen as a broadening of the peaks in an X-ray diffraction as is explained by the Scherrer Equation.

- Thin film diffraction and grazing incidence X-ray diffraction may be used to characterize the crystallographic structure and preferred orientation of substrate-anchored thin films.
- High-resolution X-ray diffraction is used to characterize thickness, crystallographic structure, and strain in thin epitaxial films. It employs parallel-beam optics.
- X-ray pole figure analysis enables one to analyze and determine the distribution of crystalline orientations within a crystalline thin-film sample.
- X-ray rocking curve analysis is used to quantify grain size and mosaic spread in crystalline materials.

Scattering techniques

Elastic scattering

Materials that do not have long range order may also be studied by scattering methods that rely on elastic scattering of monochromatic X-rays.

- Small angle X-ray scattering (SAXS) probes structure in the nanometer to micrometer range by measuring scattering intensity at scattering angles 2θ close to 0° .^[2]
- X-ray reflectivity is an analytical technique for determining thickness, roughness, and density of single layer and multilayer thin films.
- Wide angle X-ray scattering (WAXS), a technique concentrating on scattering angles 2θ larger than 5° .

Inelastic scattering

When the energy and angle of the inelastically scattered X-rays are monitored scattering techniques can be used to probe the electronic band structure of materials.

- Compton scattering
- Resonant inelastic X-ray scattering (RIXS)
- X-ray Raman scattering
- X-ray diffraction pattern

References

- [1] Azároff, L. V.; R. Kaplow, N. Kato, R. J. Weiss, A. J. C. Wilson, R. A. Young (1974). *X-ray diffraction*. McGraw-Hill.
- [2] Glatter, O.; O. Kratky (1982). <http://physchem.kfunigraz.ac.at/sm/Software.htm>|*Small Angle X-ray Scattering*. Academic Press. <http://physchem.kfunigraz.ac.at/sm/Software.htm>.

See also

- Structure determination
 - Materials Science
 - Metallurgy
 - Mineralogy
 - X-ray crystallography
-

External links

- International Union of Crystallography (<http://www.iucr.ac.uk/>)
 - IUCr Crystallography Online (<http://www.iucr.org/cww-top/crystal.index.html>)
- The International Centre for Diffraction Data (ICDD) (<http://www.icdd.com/>)
- Archives of XRD@JISCMail.AC.UK (<http://www.jiscmail.ac.uk/lists/xrd.html>)
- The British Crystallographic Association (<http://crystallography.org.uk/>)
- Introduction to X-ray Diffraction (<http://www.mrl.ucsb.edu/mrl/centralfacilities/xray/xray-basics/index.html>) at University of California, Santa Barbara

Crystal

A **crystal** or **crystalline solid** is a solid material whose constituent atoms, molecules, or ions are arranged in an orderly repeating pattern extending in all three spatial dimensions. The scientific study of crystals and crystal formation is crystallography. The process of crystal formation via mechanisms of crystal growth is called crystallization or solidification.

The word *crystal* is derived from the ancient Greek word κρύσταλλος (*krustallos*), which had the same meaning, but according to the ancient understanding of crystal. At root it means anything congealed by freezing, such as *ice*.^[1] The word once referred particularly to quartz, or "rock crystal".

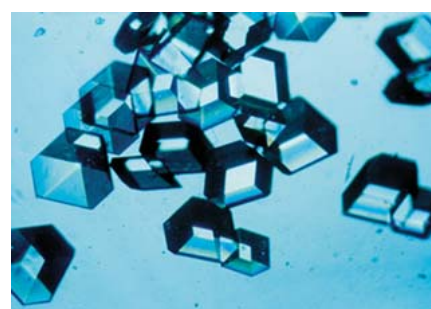
Most metals encountered in everyday life are polycrystals. Crystals are often symmetrically intergrown to form crystal twins.



Quartz crystal. The individual grains of this polycrystalline mineral sample are clearly visible.

Crystal structure

The process of forming a crystalline structure from a fluid or from materials dissolved in the fluid is often referred to as **crystallization**. In the ancient example referenced by the root meaning of the word crystal, water being cooled undergoes a phase change from liquid to solid beginning with small ice crystals that grow until they fuse, forming a polycrystalline structure. The physical properties of the ice depend on the size and arrangement of the individual crystals, or grains, and the same may be said of metals solidifying from a molten state.



Insulin crystals

Which crystal structure the fluid will form depends on the chemistry of the fluid, the conditions under which it is being solidified, and also on the ambient pressure. While the cooling process usually results in the

generation of a crystalline material, under certain conditions, the fluid may be frozen in a noncrystalline state. In most cases, this involves cooling the fluid so rapidly that atoms cannot travel to their lattice sites before they lose mobility. A noncrystalline material, which has no long-range order, is called an amorphous, vitreous, or glassy material. It is also often referred to as an amorphous solid, although there are distinct differences between solids and glasses: most notably, the process of forming a glass does not release the latent heat of fusion.



Halite (sodium chloride) - a single, large crystal

Crystalline structures occur in all classes of materials, with all types of chemical bonds. Almost all metal exists in a polycrystalline state; amorphous or single-crystal metals must be produced synthetically, often with great difficulty. Ionically bonded crystals can form upon solidification of salts, either from a molten fluid or when it condenses from a solution. Covalently bonded crystals are also very common, notable examples being diamond, silica, and graphite. Polymer materials generally will form crystalline regions, but the lengths of the molecules usually prevent complete crystallization. Weak Van der Waals forces can also play a role in a crystal structure; for example, this type of bonding loosely holds together the hexagonal-patterned sheets in graphite.

Most crystalline materials have a variety of crystallographic defects. The types and structures of these defects can have a profound effect on the properties of the materials.

Crystal phases or forms

See: Phase transformations in solids

Polymorphism is the ability of a solid to exist in more than one crystal form. For example, water ice is ordinarily found in the hexagonal form Ice I_h , but can also exist as the cubic Ice I_c , the rhombohedral ice II, and many other forms.

Amorphous phases are also possible with the same molecule, such as amorphous ice. In this case, the phenomenon is known as polyamorphism.

For pure chemical elements, polymorphism is known as allotropy. For example, diamond, graphite, and fullerenes are different allotropes of carbon.

Other meanings and characteristics

Since the initial discovery of crystal-like individual arrays of atoms that are not regularly repeated, made in 1982 by Dan Shechtman, the acceptance of the concept and the word quasicrystal have led the International Union of Crystallography to redefine the term crystal to mean "any solid having an essentially discrete diffraction diagram", thereby shifting the essential attribute of crystallinity from position space to Fourier space. Within the family of crystals one distinguishes between traditional crystals, which are periodic, or repeating, at the atomic scale, and aperiodic (incommensurate) crystals which are not. This broader definition adopted in 1996 reflects the current understanding that microscopic periodicity is a sufficient but not a necessary condition for crystals.



A large monocrystal of potassium dihydrogen phosphate grown from solution by Saint-Gobain for the megajoule laser of CEA.



Gallium, a metal that easily forms large single crystals



Ice crystals

While the term "crystal" has a precise meaning within materials science and solid-state physics, colloquially "crystal" refers to solid objects that exhibit well-defined and often pleasing geometric shapes. In this sense of the word, many types of crystals are found in nature. The shape of these crystals is dependent on the types of molecular bonds between the atoms to determine the structure, as well as on the conditions under which they formed. Snowflakes, diamonds, and table salt are common examples of crystals.

Some crystalline materials may exhibit special electrical properties such as the ferroelectric effect or the piezoelectric effect. Additionally, light passing through a crystal is often refracted or bent in different directions, producing an array of colors; crystal optics is the study of these effects. In periodic dielectric structures a range of unique optical properties can be expected as seen in photonic crystals.

Crystalline rocks

Inorganic matter, if free to take that physical state in which it is most stable, tends to crystallize. There is no practical limit to the size a crystal may attain under the right conditions, and selenite single crystals in excess of 10 m are found in the Cave of the Crystals in Naica, Mexico.^[2]

Crystalline rock masses have consolidated from aqueous solution or from molten magma. The vast majority of igneous rocks belong to this group and the degree of crystallization depends primarily on the conditions under which they solidified. Such rocks as granite, which have cooled very slowly and under great pressures, have completely crystallized, but many lavas were poured out at the surface and cooled very rapidly; in this latter group a small amount of amorphous or glassy matter is frequent. Other crystalline rocks, the evaporites such as rock salt, gypsum and some limestones have been deposited from aqueous solution, mostly owing to evaporation in arid climates. Still another group, the metamorphic rocks which includes the marbles, mica-schists and quartzites; are recrystallized, that is to say, they were at first fragmental rocks, like limestone, shale and sandstone and have never been in a molten condition nor entirely in solution. The high temperature and pressure conditions of metamorphism have acted on them erasing their original structures, and inducing recrystallization in the solid state.^[1]



Fossil shell with calcite crystals

Properties

Crystal	Particles	Attractive forces	Melting point	Other properties
Ionic	Positive and negative ions	Electrostatic attractions	High	Hard, brittle, good electrical conductor in molten state
Molecular	Polar molecules	London force and dipole-dipole attraction	Low	Soft, non-conductor or extremely poor conductor of electricity in liquid state
Molecular	Non-polar molecules	London force	Low	Soft conductor

See also

- Amorphous solid
- Artificial Snow Crystal
- Atomic packing factor
- Biom mineralisation
- Colloidal crystal
- Crystal growth
- Crystal habit
- Crystal system
- Glass
- Physics of glass
- Inorganic Crystal Structure Database
- Laser Heated Pedestal Growth
- Lead crystal
- Liquid crystal
- Metallic crystal
- Micro-Pulling-Down

- Crystallite
- Crystallographic database
- Quasicrystal
- Seed crystal
- Single crystal

References

- [1] <http://www.bartleby.com/61/roots/IE243.html>|"kreus-", *The American Heritage Dictionary of the English Language: Fourth Edition: Appendix I: Indo-European Roots*, 2000.
- [2] National Geographic, 2008. Cavern of Crystal Giants (<http://ngm.nationalgeographic.com/2008/11/crystal-giants/shear-text>)

External links

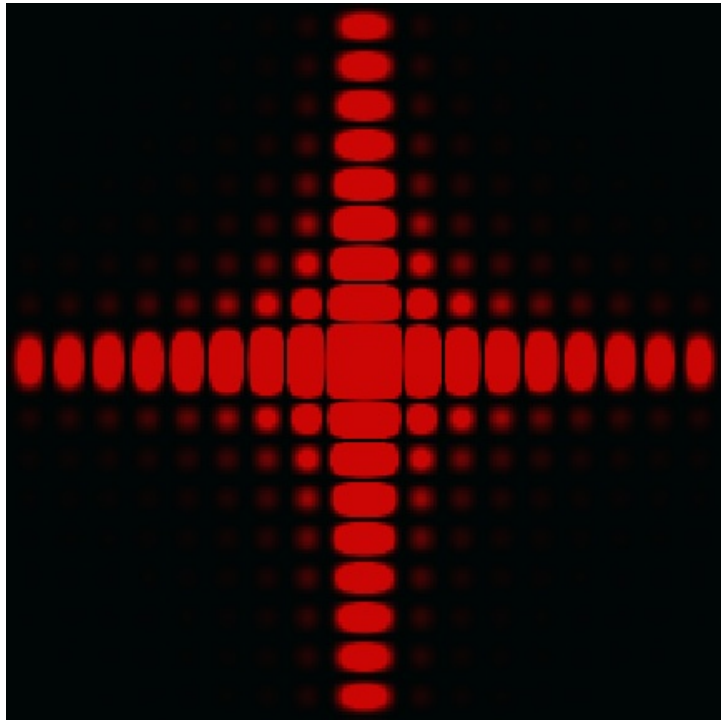
- Howard, J. Michael; Darcy Howard (Illustrator) (1998). <http://www.rockhounds.com/rockshop/xtal/index.html>|"Introduction to Crystallography and Mineral Crystal Systems" (html). Bob's Rock Shop. <http://www.rockhounds.com/rockshop/xtal/index.html>. Retrieved on 2008-04-20.
- Krassmann, Thomas (2005–2008). <http://giantcrystals.strahlen.org/>"The Giant Crystal Project" (html). Krassmann. <http://giantcrystals.strahlen.org>. Retrieved on 2008-04-20.
- Various authors (2007). <http://www.iucr.ac.uk/iucr-top/comm/cteach/pamphlets.html>|"Teaching Pamphlets" (html). Commission on Crystallographic Teaching. <http://www.iucr.ac.uk/iucr-top/comm/cteach/pamphlets.html>. Retrieved on 2008-04-20.
- Various authors (2004). <http://cst-www.nrl.navy.mil/lattice/spcgrp/>"Crystal Lattice Structures:Index by Space Group" (html). U.S. Naval Research Laboratory, Center for Computational Materials Science. <http://cst-www.nrl.navy.mil/lattice/spcgrp/>. Retrieved on 2008-04-20.

Diffraction

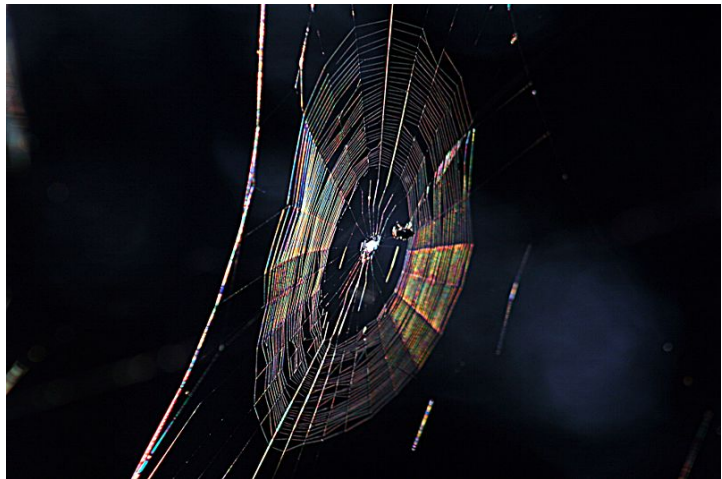
Diffraction is normally taken to refer to various phenomena which occur when a wave encounters an obstacle. It is described as the apparent bending of waves around small obstacles and the spreading out of waves past small openings.^[2] Very similar effects are observed when there is an alteration in the properties of the medium in which the wave is travelling, for example a variation in refractive index for light waves or in acoustic impedance for sound waves and these can also be referred to as diffraction effects. Diffraction occurs with all waves, including sound waves, water waves, and electromagnetic waves such as visible light, x-rays and radio waves. As physical objects have wave-like properties (at the atomic level), diffraction also occurs with matter and can be studied according to the principles of quantum mechanics.

While diffraction occurs whenever propagating waves encounter such changes, its effects are generally most pronounced for waves where the wavelength is on the order of the size of the diffracting objects. If the obstructing object provides multiple, closely-spaced openings, a complex pattern of varying intensity can result. This is due to the superposition, or interference, of different parts of a wave that traveled to the observer by different paths (see diffraction grating).

The formalism of diffraction can also describe the way in which waves of finite extent propagate in free space. For example, the expanding profile of a laser beam, the beam shape of a radar antenna and the field of view of an ultrasonic transducer are all explained by diffraction theory.



The intensity pattern formed on a screen by diffraction from a square aperture



Colors seen in a spider web are partially due to diffraction, according to some analyses.^[1]

Examples of diffraction in everyday life

The effects of diffraction can be regularly seen in everyday life. The most colorful examples of diffraction are those involving light; for example, the closely spaced tracks on a CD or DVD act as a diffraction grating to form the familiar rainbow pattern we see when looking at a disk. This principle can be extended to engineer a grating with a structure such that it will produce any diffraction pattern desired; the hologram on a credit card is an example. Diffraction in the atmosphere by small particles can cause a bright ring to be visible around a bright light source like the sun or the moon. A shadow of a solid object, using light from a compact source, shows small fringes near its edges. The speckle pattern which is observed when laser light falls on an optically rough surface is also a diffraction phenomenon. All these effects are a consequence of the fact that light is a wave.

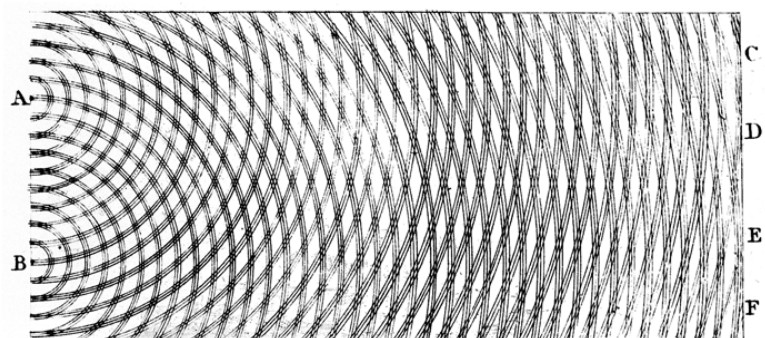


Solar glory at the steam from hot springs. A **glory** is an optical phenomenon produced by light backscattered (a combination of diffraction, reflection and refraction) towards its source by a cloud of uniformly-sized water droplets.

Diffraction can occur with any kind of wave. Ocean waves diffract around jetties and other obstacles. Sound waves can diffract around objects, which is why one can still hear someone calling even when hiding behind a tree.^[3] Diffraction can also be a concern in some technical applications; it sets a fundamental limit to the resolution of a camera, telescope, or microscope.

History

The effects of diffraction of light were first carefully observed and characterized by Francesco Maria Grimaldi, who also coined the term *diffraction*, from the Latin *diffringere*, 'to break into pieces', referring to light breaking up into different directions. The results of Grimaldi's observations were published posthumously in 1665.^[4] ^[5] Isaac Newton

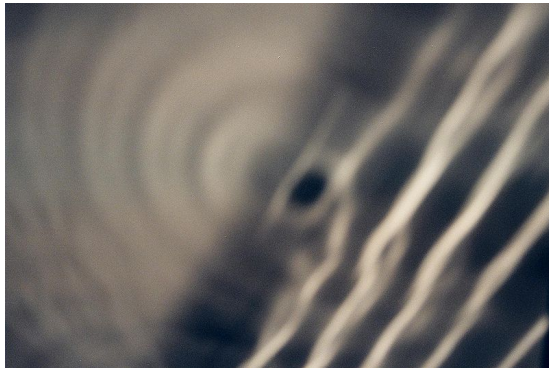


Thomas Young's sketch of two-slit diffraction, which he presented to the Royal Society in 1803

studied these effects and attributed them to *inflexion* of light rays. James Gregory (1638-1675) observed the diffraction patterns caused by a bird feather, which was

effectively the first diffraction grating. In 1803 Thomas Young did his famous experiment observing interference from two closely spaced slits. Explaining his results by interference of the waves emanating from the two different slits, he deduced that light must propagate as waves. Augustin-Jean Fresnel did more definitive studies and calculations of diffraction, published in 1815 and 1818, and thereby gave great support to the wave theory of light that had been advanced by Christiaan Huygens and reinvigorated by Young, against Newton's particle theory. In addition, Young's experiment was one of the experiments used to prove that light acts as both a particle and a wave.

The mechanism of diffraction



Photograph of single-slit diffraction in a circular ripple tank

Diffraction arises because of the way in which waves propagate; this is described by the Huygens-Fresnel principle. The propagation of a wave can be visualized by considering every point on a wavefront as a point source for a secondary radial wave. The subsequent propagation and addition of all these radial waves form the new wavefront. When waves are added together, their sum is determined by the relative phases as well as the amplitudes of the individual waves, an effect which is often known as wave interference. The summed amplitude of the waves can have any value

between zero and the sum of the individual amplitudes. Hence, diffraction patterns usually have a series of maxima and minima.

To determine the form of a diffraction pattern, we must determine the phase and amplitude of each of the Huygens wavelets at each point in space and then find the sum of these waves. There are various analytical models which can be used to do this including the Fraunhofer diffraction equation for the far field and the Fresnel Diffraction equation for the near-field. Most configurations cannot be solved analytically; solutions can be found using various numerical analytical methods including Finite element and boundary element methods

Diffraction systems

It is possible to obtain a qualitative understanding of many diffraction phenomena by considering how the relative phases of the individual secondary wave sources vary, and in particular, the conditions in which the phase difference equals half a cycle in which case waves will cancel one another out.

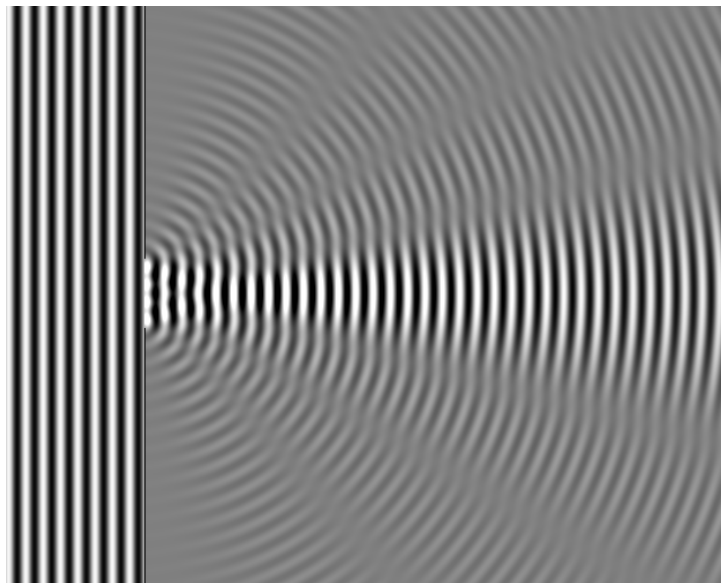
The simplest descriptions of diffraction are those in which the situation can be reduced to a two dimensional problem. For water waves, this is already the case, water waves propagate only on the surface of the water. For light, we can often neglect one direction if the diffracting object extends in that direction over a distance far greater than the wavelength. In the case of light shining through small circular holes we will have to take into account the full three dimensional nature of the problem.

Some of the simpler cases of diffraction are considered below.

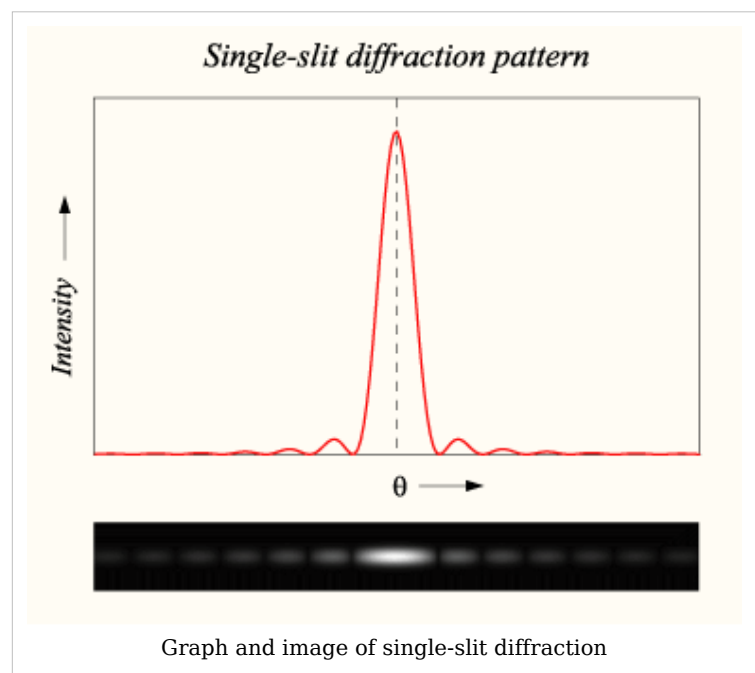
Single-slit diffraction

A long slit of infinitesimal width which is illuminated by light diffracts the light into a series of circular waves and the wavefront which emerges from the slit is a cylindrical wave of uniform intensity.

A slit which is wider than a wavelength has a large number of point sources spaced evenly across the width of the slit. The light at a given angle is made up of contributions from each of these point sources and if the relative phases of these contributions vary by more than 2π , we expect to find minima and maxima in the diffracted light.



Numerical approximation of diffraction pattern from a slit of width four wavelengths with an incident plane wave. The main central beam, nulls, and phase reversals are apparent.



We can find the angle at which a first minimum is obtained in the diffracted light by the following reasoning. The light from a source located at the top edge of the slit interferes destructively with a source located at the middle of the slit, when the path difference between them is equal to $\lambda/2$. Similarly, the source just below the top of the slit will interfere destructively with the source located just below the middle of the slit at the same angle. We can continue this reasoning along the entire height of the slit to conclude that the condition for destructive interference for the entire slit is the same as the condition for destructive interference between two narrow slits a distance apart that is half the width of

the slit. The path difference is given by $\frac{d \sin(\theta)}{2}$ so that the minimum intensity occurs at an angle

$$\theta_{\min} \text{ given by } d \sin \theta_{\min} = \lambda$$

where d is the width of the slit.

A similar argument can be used to show that if we imagine the slit to be divided into four, six eight parts, etc, minima are obtained at angles θ_n given by

$$d \sin \theta_n = n\lambda$$

where n is an integer greater than zero.

There is no such simple argument to enable us to find the maxima of the diffraction pattern. The intensity profile can be calculated using the Fraunhofer diffraction integral as

$$I(\theta) = I_0 \text{sinc}^2(d \sin \theta / \lambda)$$

where the sinc function is given by $\text{sinc}(x) = \sin(\pi x) / (\pi x)$ if $x \neq 0$, and $\text{sinc}(0) = 1$.

It should be noted that this analysis applies only to the far field, that is at a distance much larger than the width of the slit.

Diffraction grating

A diffraction grating is an optical component with a regular pattern. The form of the light diffracted by a grating depends on the structure of the elements and the number of elements present, but all gratings have intensity maxima at angles θ_m which are given by the grating equation

$$d (\sin \theta_m + \sin \theta_i) = m\lambda.$$

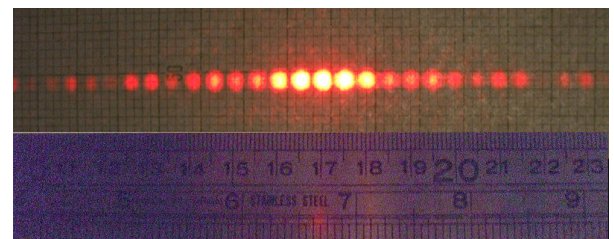
where θ_i is the angle at which the light is incident, d is the separation of grating elements and m is an integer which can be positive or negative.

The light diffracted by a grating is found by summing the light diffracted from each of the elements, and is essentially a convolution of diffraction and interference patterns.

The figure shows the light diffracted by 2-element and 5-element gratings where the grating spacings are the same; it can be seen that the maxima are in the same position, but the detailed structures of the intensities are different.



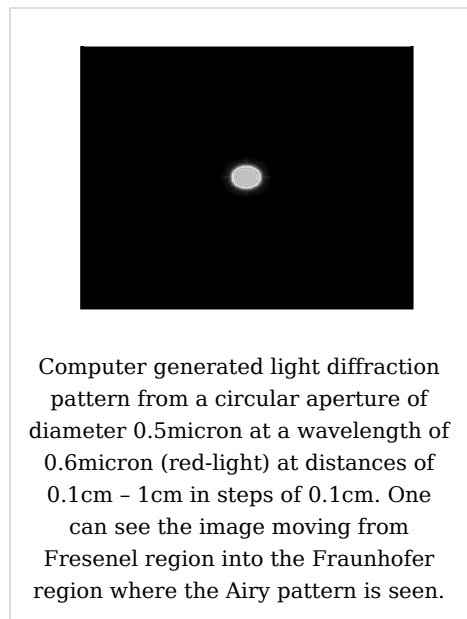
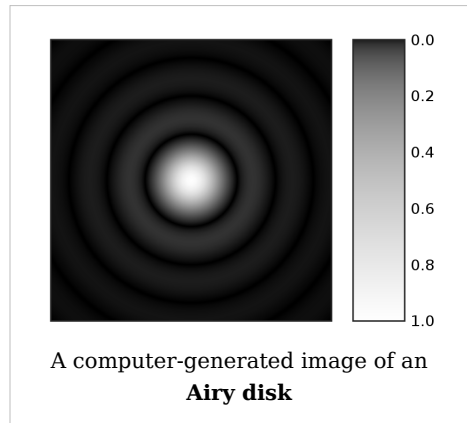
2-slit (top) and 5-slit diffraction of red laser light



A diffraction pattern of a 633 nm laser through a grid of 150 slits

Diffraction by a circular aperture

The far-field diffraction of a plane wave incident on a circular aperture is often referred to as the Airy Disk. The variation in intensity with angle is given by



$$I(\theta) = I_0 \left(\frac{2J_1(ka \sin \theta)}{ka \sin \theta} \right)^2$$

where a is the radius of the circular aperture, k is equal to $2\pi/\lambda$ and J_1 is a Bessel function. The smaller the aperture, the larger the spot size at a given distance, and the greater the divergence of the diffracted beams.

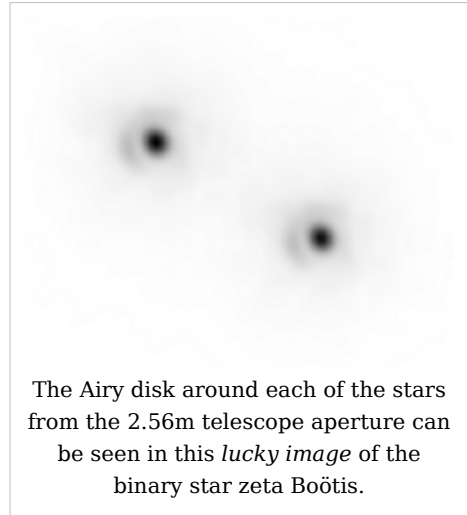
Propagation of a laser beam

The way in which the profile of a laser beam changes as it propagates is determined by diffraction. The output mirror of the laser is an aperture, and the subsequent beam shape is determined by that aperture. Hence, the smaller the output beam, the quicker it diverges. Diode lasers have much greater divergence than He-Ne lasers for this reason.

Paradoxically, it is possible to reduce the divergence of a laser beam by first expanding it with one convex lens, and then collimating it with a second convex lens whose focal point is coincident with that of the first lens. The resulting beam has a larger aperture, and hence a lower divergence.

Diffraction-limited imaging

The ability of an imaging system to resolve detail is ultimately limited by diffraction. This is because a plane wave incident on a circular lens or mirror is diffracted as described above. The light is not focused to a point but forms an Airy disk having a central spot in the focal plane with radius to first null of



$$d = 1.22\lambda N,$$

where λ is the wavelength of the light and N is the f-number (focal length divided by diameter) of the imaging optics. In object space, the corresponding angular resolution is

$$\sin \theta = 1.22 \frac{\lambda}{D},$$

where D is the diameter of the entrance pupil of the imaging lens (e.g., of a telescope's main mirror).

Two point sources will each produce an Airy pattern – see the photo of a binary star. As the point sources move closer together, the patterns will start to overlap, and ultimately they will merge to form a single pattern, in which case the two point sources cannot be resolved in the image. The Rayleigh criterion specifies that two point sources can be considered to be resolvable if the separation of the two images is at least the radius of the Airy disk, i.e. if the first minimum of one coincides with the maximum of the other.

Thus, the larger the aperture of the lens, and the smaller the wavelength, the finer the resolution of an imaging system. This is why telescopes have very large lenses or mirrors, and why optical microscopes are limited in the detail which they can see.

Speckle patterns

The speckle pattern which is seen when using a laser pointer is another diffraction phenomenon. It is a result of the superposition of many waves with different phases, which are produced when a laser beam illuminates a rough surface. They add together to give a resultant wave whose amplitude, and therefore intensity varies randomly.

Common features of diffraction patterns

Several qualitative observations can be made of diffraction in general:

- The angular spacing of the features in the diffraction pattern is inversely proportional to the dimensions of the object causing the diffraction. In other words: The smaller the diffracting object, the 'wider' the resulting diffraction pattern, and vice versa. (More precisely, this is true of the sines of the angles.)

- The diffraction angles are invariant under scaling; that is, they depend only on the ratio of the wavelength to the size of the diffracting object.
- When the diffracting object has a periodic structure, for example in a diffraction grating, the features generally become sharper. The third figure, for example, shows a comparison of a double-slit pattern with a pattern formed by five slits, both sets of slits having the same spacing, between the center of one slit and the next.

Particle diffraction

Quantum theory tells us that every particle exhibits wave properties. In particular, massive particles can interfere and therefore diffract. Diffraction of electrons and neutrons stood as one of the powerful arguments in favor of quantum mechanics. The wavelength associated with a particle is the de Broglie wavelength

$$\lambda = \frac{h}{p}$$

where h is Planck's constant and p is the momentum of the particle (mass \times velocity for slow-moving particles). For most macroscopic objects, this wavelength is so short that it is not meaningful to assign a wavelength to them. A sodium atom traveling at about 3000 m/s would have a De Broglie wavelength of about 5 pico meters.

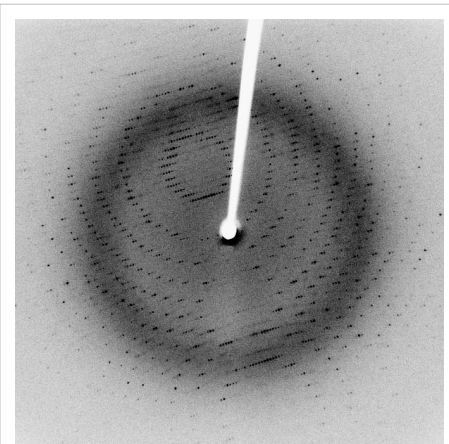
Because the wavelength for even the smallest of macroscopic objects is extremely small, diffraction of matter waves is only visible for small particles, like electrons, neutrons, atoms and small molecules. The short wavelength of these matter waves makes them ideally suited to study the atomic crystal structure of solids and large molecules like proteins.

Relatively recently, larger molecules like buckyballs were also shown to diffract.^[6]

Bragg diffraction

Diffraction from a three dimensional periodic structure such as atoms in a crystal is called Bragg diffraction. It is similar to what occurs when waves are scattered from a diffraction grating. Bragg diffraction is a consequence of interference between waves reflecting from different crystal planes. The condition of constructive interference is given by *Bragg's law*:

$$m\lambda = 2d \sin \theta$$



Following Bragg's law, each dot (or reflection), in this diffraction pattern forms from the constructive interference of X-rays passing through a crystal. The data can be used to determine the crystal's atomic structure.

where

λ is the wavelength,

d is the distance between crystal planes,

θ is the angle of the diffracted wave.

and m is an integer known as the *order* of the diffracted beam.

Bragg diffraction may be carried out using either light of very short wavelength like x-rays or matter waves like neutrons (and electrons) whose wavelength is on the order of (or much smaller than) the atomic spacing^[7]. The pattern produced gives information of the separations of crystallographic planes d , allowing one to deduce the crystal structure. Diffraction contrast, in electron microscopes and x-topography devices in particular, is also a powerful tool for examining individual defects and local strain fields in crystals.

Coherence

The description of diffraction relies on the interference of waves emanating from the same source taking different paths to the same point on a screen. In this description, the difference in phase between waves that took different paths is only dependent on the effective path length. This does not take into account the fact that waves that arrive at the screen at the same time were emitted by the source at different times. The initial phase with which the source emits waves can change over time in an unpredictable way. This means that waves emitted by the source at times that are too far apart can no longer form a constant interference pattern since the relation between their phases is no longer time independent.

The length over which the phase in a beam of light is correlated, is called the Coherence length. In order for interference to occur, the path length difference must be smaller than the coherence length. This is sometimes referred to as spectral coherence, as it is related to the presence of different frequency components in the wave. In the case of light emitted by an atomic transition, the coherence length is related to the lifetime of the excited state from which the atom made its transition.

If waves are emitted from an extended source, this can lead to incoherence in the transversal direction. When looking at a cross section of a beam of light, the length over which the phase is correlated is called the transverse coherence length. In the case of Young's double slit experiment, this would mean that if the transverse coherence length is smaller than the spacing between the two slits, the resulting pattern on a screen would look like two single slit diffraction patterns.

In the case of particles like electrons, neutrons and atoms, the coherence length is related to the spatial extent of the wave function that describes the particle.

See also

- Atmospheric diffraction
- Bragg diffraction
- Cloud iridescence
- Diffraction formalism
- Diffractometer
- Dynamical theory of diffraction
- Diffraction grating
- Electron diffraction
- Fraunhofer diffraction
- Fresnel diffraction
- Fresnel number
- Fresnel zone
- Neutron diffraction
- Prism
- Powder diffraction
- Refraction
- Schaefer-Bergmann diffraction
- Thinned array curse
- X-ray scattering techniques

References

- [1] Dietrich Zawischa. <http://www.itp.uni-hannover.de/~zawischa/ITP/spiderweb.html>|"Optical effects on spider webs". <http://www.itp.uni-hannover.de/%7Ezawischa/ITP/spiderweb.html>. Retrieved on 2007-09-21.
- [2] Diffraction concepts (<http://hyperphysics.phy-astr.gsu.edu/Hbase/phyopt/diffrac.html#c1>)
- [3] Andrew Norton (2000). http://books.google.com/books?id=XRRMxjr24pwC&pg=PA102&dq=sound+wave+diffraction+behind+tree&lr=&as_drrb_is=q&as_minm_is=1&as_miny_is=2009&as_maxm_is=12&as_maxy_is=2009&as_brr=3&as_pt=ALLTYPES&ei=EjjDSbulDJG4kwSBY6yADg *fields and waves*. CRC Press. p. 102. ISBN 9780750307192. http://books.google.com/books?id=XRRMxjr24pwC&pg=PA102&dq=sound+wave+diffraction+behind+tree&lr=&as_drrb_is=q&as_minm_is=1&as_miny_is=2009&as_maxm_is=12&as_maxy_is=2009&as_brr=3&as_pt=ALLTYPES&ei=EjjDSbulDJG4kwSBY6yADg
- [4] Jean Louis Aubert (1760). <http://books.google.com/books?vid=OCLC58901501&id=3OgDAAAAMAAJ&pg=PP151&lpg=PP151&dq=grimaldi+diffraction+pour+l'histoire+des+sciences+et+des+beaux+arts>. Paris: Impr. de S. A. S.; Chez E. Ganeau. pp. 149. http://books.google.com/books?vid=OCLC58901501&id=3OgDAAAAMAAJ&pg=PP151&lpg=PP151&dq=grimaldi+diffraction+date:0-1800&as_brr=1.
- [5] Sir David Brewster (1831). <http://books.google.com/books?vid=OCLC03255091&id=opYAAAAAMAAJ&pg=RA1-PA95&lpg=RA1-PA95&dq=grimaldi+diffraction+treatise+on+optics> *Treatise on Optics*. London: Longman, Rees, Orme, Brown & Green and John Taylor. pp. 95. http://books.google.com/books?vid=OCLC03255091&id=opYAAAAAMAAJ&pg=RA1-PA95&lpg=RA1-PA95&dq=grimaldi+diffraction+date:0-1840&as_brr=1.
- [6] Brezger, B.; Hackermüller, L.; Uttenthaler, S.; Petschinka, J.; Arndt, M.; Zeilinger, A. (February 2002). "http://homepage.univie.ac.at/Lucia.Hackermueller/unsereArtikel/Brezger2002a.pdf|Matter-Wave Interferometer for Large Molecules" (reprint). *Physical Review Letters* **88** (10): 100404. doi: 10.1103/PhysRevLett.88.100404 (<http://dx.doi.org/10.1103/PhysRevLett.88.100404>). <http://homepage.univie.ac.at/Lucia.Hackermueller/unsereArtikel/Brezger2002a.pdf>. Retrieved on 2007-04-30.
- [7] John M. Cowley (1975) *Diffraction physics* (North-Holland, Amsterdam) ISBN 0 444 10791 6

External links

- Do Sensors “Outresolve” Lenses? (<http://luminous-landscape.com/tutorials/resolution.shtml>); on lens and sensor resolution interaction.
 - Diffraction and acoustics. (<http://www.acoustics.salford.ac.uk/feschools/waves/diffract.htm>)
 - Diffraction in photography. (<http://sankey.ws/diffraction.html>)
 - On Diffraction (<http://www.mathpages.com/home/kmath636/kmath636.htm>) at MathPages.
 - Diffraction pattern calculators (<http://demonstrations.wolfram.com/search.html?query=diffraction>) at The Wolfram Demonstrations Project
 - Wave Optics (http://www.lightandmatter.com/html_books/5op/ch05/ch05.html) – A chapter of an online textbook.
 - 2-D wave Java applet (<http://www.falstad.com/wave2d/>) – Displays diffraction patterns of various slit configurations.
 - Diffraction Java applet (<http://www.falstad.com/diffraction/>) – Displays diffraction patterns of various 2-D apertures.
 - Diffraction approximations illustrated (<http://www.mit.edu/~birge/diffraction/>) – MIT site that illustrates the various approximations in diffraction and intuitively explains the Fraunhofer regime from the perspective of linear system theory.
 - Gap (<http://www.phy.hk/wiki/englishhtm/Diffraction.htm>) Obstacle (<http://www.phy.hk/wiki/englishhtm/Diffraction2.htm>) Corner (<http://www.phy.hk/wiki/englishhtm/Diffraction3.htm>) – Java simulation of diffraction of water wave.
 - Google Maps (<http://maps.google.com/maps?q=Panama+canal&hl=en&ie=UTF8&om=1&z=16&ll=9.385048,-79.918799&spn=0.015539,0.027122&t=k&iwloc=addr>) – Satellite image of Panama Canal entry ocean wave diffraction.
-

Uniform theory of diffraction

In numerical analysis, the **uniform geometrical theory of diffraction** (**UTD**) is a high frequency method for solving electromagnetic scattering problems from electrically small discontinuities or discontinuities in more than one dimension at the same point.^[1] UTD is an extension of Joseph Keller's "Geometrical Theory of Diffraction" (GTD).^[2]

The uniform theory of diffraction approximates near field electromagnetic fields as quasi optical and uses ray diffraction to determine diffraction coefficients for each diffracting object-source combination. These coefficients are then used to calculate the field strength and phase for each direction away from the diffracting point.

These fields are then added to the incident fields and reflected fields to obtain a total solution.

See also

- Electromagnetic modeling

References

- [1] R. G. Kouyoumjian and P. H. Pathak, "A uniform geometrical theory of diffraction for an edge in a perfectly conducting surface," *Proc. IEEE*, vol. 62, pp. 1448-1461, November 1974.
- [2] J. B. Keller, "Geometrical theory of diffraction" (<http://www.opticsinfobase.org/abstract.cfm?URI=josa-52-2-116>), *J. Opt. Soc. Am.*, vol. 52, no. 2, pp. 116-130, 1962.

External links

- Overview of Asymptotic Expansion Methods in Electromagnetics (<http://www.cvel.clemson.edu/modeling/tutorials/techniques/gtd-utd/gtd-utd.html>)

Crystallography

Crystallography is the experimental science of determining the arrangement of atoms in solids. In older usage, it is the scientific study of crystals. The word "crystallography" is derived from the Greek words *crystallon* = cold drop / frozen drop, with its meaning extending to all solids with some degree of transparency, and *graphein* = write.

Before the development of X-ray diffraction crystallography (see below), the study of crystals was based on the geometry of the crystals. This involves measuring the angles of crystal faces relative to theoretical reference axes (crystallographic axes), and establishing the symmetry of the crystal in question. The former is carried out using a goniometer. The position in 3D space of each crystal face is plotted on a stereographic net, e.g. Wulff net or Lambert net. In fact, the pole to each face is plotted on the net. Each point is labelled with its Miller index. The final plot allows the symmetry of the crystal to be established.

Crystallographic methods now depend on the analysis of the diffraction patterns that emerge from a sample that is targeted by a beam of some type. The beam is not always electromagnetic radiation, even though X-rays are the most common choice. For some purposes electrons or neutrons are used, which is possible due to the wave properties of the particles. Crystallographers often explicitly state the type of illumination used when referring to a method, as with the terms **X-ray diffraction**, **neutron diffraction** and **electron diffraction**.

These three types of radiation interact with the specimen in different ways. X-rays interact with the spatial distribution of the valence electrons, while electrons are charged particles and therefore feel the total charge distribution of both the atomic nuclei and the surrounding electrons. Neutrons are scattered by the atomic nuclei through the strong nuclear forces, but in addition, the magnetic moment of neutrons is non-zero. They are therefore also scattered by magnetic fields. When neutrons are scattered from hydrogen-containing materials, they produce diffraction patterns with high noise levels. However, the material can sometimes be treated to substitute hydrogen for deuterium. Because of these different forms of interaction, the three types of radiation are suitable for different crystallographic studies.

Theory

An image of a small object is usually generated by using a lens to focus the illuminating radiation, as is done with the rays of the visible spectrum in light microscopy. However, the wavelength of visible light (about 4000 to 7000 Angstroms) is three orders of magnitude longer than the length of typical atomic bonds and atoms themselves (about 1 to 2 Angstroms). Therefore, obtaining information about the spatial arrangement of atoms requires the use of radiation with shorter wavelengths, such as X-rays. Employing shorter wavelengths implied abandoning microscopy and true imaging, however, because there exists no material from which a lens capable of focusing this type of radiation can be created. (That said, scientists have had some success focusing X-rays with microscopic Fresnel zone plates made from gold, and by critical-angle reflection inside long tapered capillaries[1]). Diffracted x-ray beams cannot be focused to produce images, so the sample structure must be reconstructed from the diffraction pattern. Sharp features in the diffraction pattern arise from periodic, repeating structure in the sample, which are often very strong due to coherent reflection of many photons from many regularly spaced

instances of similar structure, while non-periodic components of the structure result in diffuse (and usually weak) diffraction features.

Because of their highly ordered and repetitive structure, crystals give diffraction patterns of sharp Bragg reflection spots, and are ideal for analyzing the structure of solids.

Notation

See Miller index for a full treatment of this topic.

- Coordinates in *square brackets* such as **[100]** denote a direction vector (in real space).
- Coordinates in *angle brackets* or *chevrons* such as **<100>** denote a *family* of directions which are related by symmetry operations. In the cubic crystal system for example, **<100>** would mean [100], [010], [001] or the negative of any of those directions.
- Miller indices in *parentheses* such as **(100)** denote a plane of the crystal structure, and regular repetitions of that plane with a particular spacing. In the cubic system, the normal to the (hkl) plane is the direction [hkl], but in lower-symmetry cases, the normal to (hkl) is not parallel to [hkl].
- Indices in *curly brackets* or *braces* such as **{100}** denote a family of planes and their normals which are equivalent in cubic materials due to symmetry operations, much the way angle brackets denote a family of directions. In non-cubic materials, <hkl> is not necessarily perpendicular to {hkl}.

Technique

Some materials studied using crystallography, proteins for example, do not occur naturally as crystals. Typically, such molecules are placed in solution and allowed to crystallize over days, weeks, or months through vapor diffusion. A drop of solution containing the molecule, buffer, and precipitants is sealed in a container with a reservoir containing a hygroscopic solution. Water in the drop diffuses to the reservoir, slowly increasing the concentration and allowing a crystal to form. If the concentration were to rise more quickly, the molecule would simply precipitate out of solution, resulting in disorderly granules rather than an orderly and hence usable crystal.

Once a crystal is obtained, data can be collected using a beam of radiation. Although many universities that engage in crystallographic research have their own X-ray producing equipment, synchrotrons are often used as X-ray sources, because of the purer and more complete patterns such sources can generate. Synchrotron sources also have a much higher intensity of X-ray beams, so data collection takes a fraction of the time normally necessary at weaker sources.

Producing an image from a diffraction pattern requires sophisticated mathematics and often an iterative process of **modelling and refinement**. In this process, the mathematically predicted diffraction patterns of an hypothesized or "model" structure are compared to the actual pattern generated by the crystalline sample. Ideally, researchers make several initial guesses, which through refinement all converge on the same answer. Models are refined until their predicted patterns match to as great a degree as can be achieved without radical revision of the model. This is a painstaking process, made much easier today by computers.

The mathematical methods for the analysis of diffraction data only apply to *patterns*, which in turn result only when waves diffract from orderly arrays. Hence crystallography applies

for the most part only to crystals, or to molecules which can be coaxed to crystallize for the sake of measurement. In spite of this, a certain amount of molecular information can be deduced from the patterns that are generated by fibers and powders, which while not as perfect as a solid crystal, may exhibit a degree of order. This level of order can be sufficient to deduce the structure of simple molecules, or to determine the coarse features of more complicated molecules (the double-helical structure of DNA, for example, was deduced from an X-ray diffraction pattern that had been generated by a fibrous sample).

Crystallography in materials engineering

Crystallography is a tool that is often employed by materials scientists. In single crystals, the effects of the crystalline arrangement of atoms is often easy to see macroscopically, because the natural shapes of crystals reflect the atomic structure. In addition, physical properties are often controlled by crystalline defects. The understanding of crystal structures is an important prerequisite for understanding crystallographic defects. Mostly, materials do not occur in a single crystalline, but poly-crystalline form, such that the powder diffraction method plays a most important role in structural determination.

A number of other physical properties are linked to crystallography. For example, the minerals in clay form small, flat, platelike structures. Clay can be easily deformed because the platelike particles can slip along each other in the plane of the plates, yet remain strongly connected in the direction perpendicular to the plates. Such mechanisms can be studied by crystallographic texture measurements.

In another example, iron transforms from a body-centered cubic (bcc) structure to a face-centered cubic (fcc) structure called austenite when it is heated. The fcc structure is a close-packed structure, and the bcc structure is not, which explains why the volume of the iron decreases when this transformation occurs.

Crystallography is useful in phase identification. When performing any process on a material, it may be desired to find out what compounds and what phases are present in the material. Each phase has a characteristic arrangement of atoms. Techniques like X-ray diffraction can be used to identify which patterns are present in the material, and thus which compounds are present (note: the determination of the "phases" within a material should not be confused with the more general problem of "phase determination," which refers to the phase of waves as they diffract from planes within a crystal, and which is a necessary step in the interpretation of complicated diffraction patterns).

Crystallography covers the enumeration of the symmetry patterns which can be formed by atoms in a crystal and for this reason has a relation to group theory and geometry. See symmetry group.

Biology

X-ray crystallography is the primary method for determining the molecular conformations of biological macromolecules, particularly protein and nucleic acids such as DNA and RNA. In fact, the double-helical structure of DNA was deduced from crystallographic data. The first crystal structure of a macromolecule was solved in 1958 (Kendrew, J.C. et al. (1958) A three-dimensional model of the myoglobin molecule obtained by X-ray analysis (*Nature* 181, 662–666). The Protein Data Bank (PDB) is a freely accessible repository for the structures of proteins and other biological macromolecules. Computer programs like RasMol or Pymol

can be used to visualize biological molecular structures.

Electron crystallography has been used to determine some protein structures, most notably membrane proteins and viral capsids.

Scientists of note

- William Henry Bragg
- William Lawrence Bragg
- Auguste Bravais
- Francis Crick
- Pierre Curie
- Boris Delone
- Paul Peter Ewald
- Rosalind Franklin
- Georges Friedel
- René Just Haüy
- Carl Hermann
- Dorothy Crowfoot Hodgkin
- Robert Huber
- Max von Laue
- Kathleen Lonsdale
- Ernest-François Mallard
- Charles-Victor Mauguin
- William Hallows Miller
- Max Perutz
- Hugo Rietveld
- Jean-Baptiste L. Romé de l'Isle
- Constance Tipper
- Don Craig Wiley
- Ada Yonath

See also

- Atomic packing factor
 - Condensed Matter Physics
 - Crystal engineering
 - Crystal growth
 - Crystal optics
 - Crystal system
 - Crystal
 - Crystallite
 - Crystallization processes
 - Crystallographic database
 - Crystallographic group
 - Diffraction
 - Dynamical theory of diffraction
 - Electron crystallography
 - Electron diffraction
-

- Euclidean plane isometry
- Fixed points of isometry groups in Euclidean space
- Group action
- Laser-heated pedestal growth
- Materials Science
- Metallurgy
- Mineralogy
- Neutron crystallography
- Neutron diffraction
- Neutron Diffraction at OPAL
- Permutation group
- Point group
- Powder diffraction
- Solid state chemistry
- Space group
- Symmetric group
- Symmetry group
- Symmetry
- X-ray crystallography
- X-ray diffraction

Further reading

- Burns, G.; Glazer, A.M. (1990). *Space Groups for Scientists and Engineers* (2nd ed.). Boston: Academic Press, Inc. ISBN 0-12-145761-3.
 - Clegg, W (1998). *Crystal Structure Determination (Oxford Chemistry Primer)*. Oxford: Oxford University Press. ISBN 0-19-855-901-1.
 - Drenth, J (1999). *Principles of Protein X-Ray Crystallography*. New York: Springer-Verlag. ISBN 0-387-98587-5.
 - Giacovazzo, C; Monaco HL, Viterbo D, Scordari F, Gilli G, Zanotti G, and Catti M (1992). *Fundamentals of Crystallography*. Oxford: Oxford University Press. ISBN 0-19-855578-4.
 - Glusker, JP; Lewis M, Rossi M (1994). *Crystal Structure Analysis for Chemists and Biologists*. New York: VCH Publishers. ISBN 0-471-18543-4.
 - O'Keeffe, M.; Hyde, B.G. (1996). *Crystal Structures; I. Patterns and Symmetry*. Washington, DC: Mineralogical Society of America, *Monograph Series*. ISBN 0-939950-40-5.
-

Applied Computational Powder Diffraction Data Analysis

- Young, R.A., ed (1993). *The Rietveld Method*. Oxford: Oxford University Press & International Union of Crystallography. ISBN 0-19-855577-6.

External links

- Introduction to Crystallography and Mineral Crystal Systems ^[2]
- Crystallographic Teaching Pamphlets ^[3]
- Crystal Lattice Structures ^[4]
- Freely Available Crystallographic Software for Academia ^[5]
- NetSci Software Listing for Crystallography ^[6]
- SINCRIS Information Server for Crystallography ^[7]
- ORTEP a professional grade viewer for use on a PC which is based on the FORTRAN code which came from Oak Ridge ^[8]
- Vega Science Trust Interviews on Crystallography ^[9] Freeview video interviews with Max Pertuz, Rober Huber and Aaron Klug.
- Commission on Crystallographic Teaching, Pamphlets ^[10]
- Crystallography site of Steffen Weber with lots of Java Applets ^[11]
- IUCr Online Dictionary of Crystallography ^[12]
- American Crystallographic Association ^[13]
- Laue Measurement of Single-Crystal Turbine Blades ^[14]
- Ames Laboratory, US DOE Crystallography Research Resources ^[15]

References

- [1] <http://scripts.iucr.org/cgi-bin/paper?kv5037>
 - [2] <http://www.rockhounds.com/rockshop/xtal/index.html>
 - [3] <http://www.mineralogie.uni-wuerzburg.de/links/teach/crysteach.html>
 - [4] <http://cst-www.nrl.navy.mil/lattice/spcgrp/>
 - [5] <http://www.ccp14.ac.uk/>
 - [6] <http://www.netsci.org/Resources/Software/Struct/xray.html>
 - [7] <http://www.iucr.org/sincris-top/>
 - [8] <http://www.chem.gla.ac.uk/~louis/software/ortep3/download.html>
 - [9] <http://www.vega.org.uk>
 - [10] <http://www.iucr.org/iucr-top/comm/cteach/pamphlets.html>
 - [11] <http://www.jcrystal.com/steffenweber/>
 - [12] http://reference.iucr.org/dictionary/Main_Page
 - [13] <http://aca.hwi.buffalo.edu/>
 - [14] <http://www.geocities.com/psistar@sbcglobal.net/Laue.pdf>
 - [15] <http://www.mcbmm.ameslab.gov/index.html>
-

Paracrystalline

Paracrystalline materials are defined as having short and medium range ordering in their lattice (similar to the liquid crystal phases) but lacking long-range ordering at least in one direction.^[1]

Ordering is the regularity in which atoms appear in a predictable lattice, as measured from one point. In a highly ordered, perfectly crystalline material, or single crystal, the location of every atom in the structure can be described exactly measuring out from a single origin. Conversely, in a disordered structure such as a liquid or amorphous solid, the location of the first and perhaps second nearest neighbors can be described from an origin (with some degree of uncertainty) and the ability to predict locations decreases rapidly from there out. The distance at which atom locations can be predicted is referred to as the correlation length ξ . A paracrystalline material exhibits correlation somewhere between the fully amorphous and fully crystalline.

The primary, most accessible source of crystallinity information is X-ray diffraction, although other techniques may be needed to observe the complex structure of paracrystalline materials, such as fluctuation electron microscopy^[2] in combination with Density of states modeling^[3] of electronic and vibrational states.

Paracrystalline Model

The paracrystalline model is a revision of the Continuous Random Network model first proposed by W. H. Zachariasen in 1932^[4]. The paracrystal model is defined as highly strained, microcrystalline grains surrounded by fully amorphous material^[5]. This is a higher energy state than the continuous random network model. The important distinction between this model and the microcrystalline phases is the lack of defined grain boundaries and highly strained lattice parameters, which makes calculations of molecular and lattice dynamics difficult. A general theory of paracrystals has been formulated in a basic textbook^[6], and then further developed/refined by various authors.

Applications

The paracrystal model has been useful, for example, in describing the state of partially amorphous semiconductor materials after deposition. It has also been successfully applied to: synthetic polymers, liquid crystals, biopolymers^[7],^[8] and biomembranes^[9].

See also

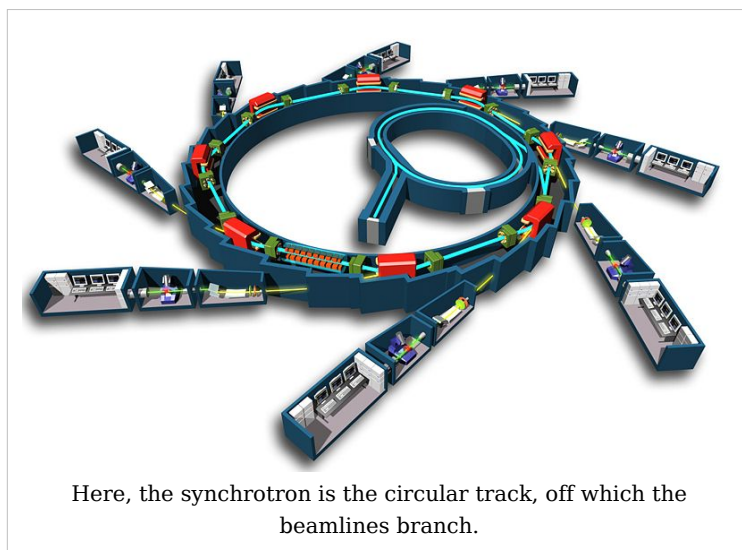
- X-ray scattering
 - Amorphous solid
 - Single Crystal
 - Polycrystalline
 - Crystallography
 - DNA
 - X-ray pattern of a B-DNA Paracrystal^[10]
-

Notes

- [1] Voyles, et al. Structure and physical properties of paracrystalline atomistic models of amorphous silicon. *J. Ap. Phys.*, **90**(2001) 4437, doi: 10.1063/1.1407319
- [2] Biswas, P, et al. *J. Phys.:Condens. Matter*, **19** (2007) 455202, doi:10.1088/0953-8984/19/45/455202
- [3] Nakhmanson, Voyles, Mousseau, Barkema, and Drabold. *Phys. Rev. B* **63**(2001) 235207. doi: 10.1103/PhysRevB.63.235207
- [4] Zachariasen, W.H., *J. Am. Chem. Soc.*, **54**(1932) 3841.
- [5] J.M. Cowley, *Diffraction Studies on Non-Cryst. Substan.* 13 (1981)
- [6] Hosemann R., Bagchi R.N., *Direct analysis of diffraction by matter*, North-Holland Publs., Amsterdam – New York, 1962
- [7] Bessel functions and diffraction by helical structures <http://planetphysics.org/encyclopedia/BesselFunctionsAndTheirApplicationsToDiffractionByHelicalStructures.html>
- [8] X-Ray Diffraction Patterns of Double-Helical Deoxyribonucleic Acid (DNA) Crystals and Paracrystalline Fibers <http://planetphysics.org/encyclopedia/BesselFunctionsApplicationsToDiffractionByHelicalStructures.html>
- [9] Baianu I.C., X-ray scattering by partially disordered membrane systems, *Acta Cryst. A*, **34** (1978), 751–753.
- [10] <http://commons.wikimedia.org/wiki/File:ABDNAXrpgj.jpg>

Synchrotron

A **synchrotron** is a particular type of cyclic particle accelerator in which the magnetic field (to turn the particles so they circulate) and the electric field (to accelerate the particles) are carefully synchronized with the travelling particle beam. The proton synchrotron was originally conceived by Sir Marcus Oliphant^[1]. The honour of the first to publish the idea belongs to Vladimir Veksler, and the first electron synchrotron was constructed by Oliphant's supervisor Edwin McMillan.



Characteristics

While a cyclotron uses a constant magnetic field and a constant-frequency applied electric field (one of these is varied in the synchrocyclotron), both of these fields are varied in the synchrotron. By increasing these parameters appropriately as the particles gain energy, their path can be held constant as they are accelerated. This allows the vacuum chamber for the particles to be a large thin torus. In reality it is easier to use some straight sections between the bending magnets and some bent sections within the magnets giving the torus the shape of a round-cornered polygon. A path of large effective radius may thus be constructed using simple straight and curved pipe segments, unlike the disc-shaped chamber of the cyclotron type devices. The shape also allows and requires the use of multiple magnets to bend the particle beams. Straight sections are required at spacings around a ring for both radiofrequency cavities, and in third generation light sources allow

space for insertion devices such as wigglers and undulators.

The maximum energy that a cyclic accelerator can impart is typically limited by the strength of the magnetic field(s) and the minimum radius (maximum curvature) of the particle path.

In a cyclotron the maximum radius is quite limited as the particles start at the center and spiral outward, thus the entire path must be a self-supporting disc-shaped evacuated chamber. Since the radius is limited, the power of the machine becomes limited by the strength of the magnetic field. In the case of an ordinary electromagnet the

field strength is limited by the saturation of the core (when all magnetic domains are aligned the field may not be further increased to any practical extent). The arrangement of the single pair of magnets the full width of the device also limits the economic size of the device.

Synchrotrons overcome these limitations, using a narrow beam pipe which can be surrounded by much smaller and more tightly focusing magnets. The ability of this device to accelerate particles is limited by the fact that the particles must be charged to be accelerated at all, but charged particles under acceleration emit photons (light), thereby losing energy. The limiting beam energy is reached when the energy lost to the lateral acceleration required to maintain the beam path in a circle equals the energy added each cycle. More powerful accelerators are built by using large radius paths and by using more numerous and more powerful microwave cavities to accelerate the particle beam between corners. Lighter particles (such as electrons) lose a larger fraction of their energy when turning. Practically speaking, the energy of electron/positron accelerators is limited by this radiation loss, while it does not play a significant role in the dynamics of proton or ion accelerators. The energy of those is limited strictly by the strength of magnets and by the cost.



The interior of the Australian Synchrotron facility. Dominating the image is the storage ring, showing the optical diagnostic beamline at front right. In the middle of the storage ring is the booster synchrotron and linac

Design and operation

Particles are injected into the main ring at substantial energies by either a linear accelerator or by an intermediate synchrotron which is in turn fed by a linear accelerator. The "linac" is in turn fed by particles accelerated to intermediate energy by a simple high voltage power supply, typically a Cockcroft-Walton generator.

Starting from an appropriate initial value determined by the injection velocity the magnetic field is then increased. The particles pass through an electrostatic accelerator driven by a high alternating voltage. At particle speeds not close to the speed of light the frequency of the accelerating voltage can be made roughly proportional to the current in the bending magnets. A finer control of the frequency is performed by a servo loop which responds to the detection of the passing of the traveling group of particles. At particle speeds

approaching light speed the frequency becomes more nearly constant, while the current in the bending magnets continues to increase. The maximum energy that can be applied to the particles (for a given ring size and magnet count) is determined by the saturation of the cores of the bending magnets (the point at which increasing current does not produce additional magnetic field). One way to obtain additional power is to make the torus larger and add additional bending magnets. This allows the amount of particle redirection at saturation to be less and so the particles can be more energetic. Another means of obtaining higher power is to use superconducting magnets, these not being limited by core saturation.

Large synchrotrons

One of the early large synchrotrons, now retired, is the Bevatron, constructed in 1950 at the Lawrence Berkeley Laboratory. The name of this proton accelerator comes from its power, in the range of 6.3 GeV (then called BeV for billion electron volts; the name predates the adoption of the SI prefix giga-). A number of heavy elements, unseen in the natural world, were first created with this machine. This site is also the location of one of the first large bubble chambers used to examine the results of the atomic collisions produced here.



Modern industrial-scale synchrotrons can be very large (here, Soleil near Paris)

Another early large synchrotron is the Cosmotron built at Brookhaven National Laboratory which reached 3.3 GeV in 1953.^[2]

Until August 2008, the highest energy synchrotron in the world was the Tevatron, at the Fermi National Accelerator Laboratory, in the United States. It accelerates protons and antiprotons to slightly less than 1 TeV of kinetic energy and collides them together. The Large Hadron Collider (LHC), which has been built at the European Laboratory for High Energy Physics (CERN), has roughly seven times this energy. It is housed in the 27 km tunnel which formerly housed the Large Electron Positron (LEP) collider, so it will maintain the claim as the largest scientific device ever built. The LHC will also accelerate heavy ions (such as lead) up to an energy of 1.15 PeV.

The largest device of this type seriously proposed was the Superconducting Super Collider (SSC), which was to be built in the United States. This design, like others, used superconducting magnets which allow more intense magnetic fields to be created without the limitations of core saturation. While construction was begun, the project was cancelled in 1994, citing excessive budget overruns — this was due to naïve cost estimation and economic management issues rather than any basic engineering flaws. It can also be argued that the end of the Cold War resulted in a change of scientific funding priorities that contributed to its ultimate cancellation.

While there is still potential for yet more powerful proton and heavy particle cyclic accelerators, it appears that the next step up in electron beam energy must avoid losses due to synchrotron radiation. This will require a return to the linear accelerator, but with devices significantly longer than those currently in use. There is at present a major effort to design and build the International Linear Collider (ILC), which will consist of two opposing linear accelerators, one for electrons and one for positrons. These will collide at a total center of mass energy of 0.5 TeV.

However, synchrotron radiation also has a wide range of applications (see synchrotron light) and many 2nd and 3rd generation synchrotrons have been built especially to harness it. The largest of those 3rd generation synchrotron light sources are the European Synchrotron Radiation Facility (ESRF) in Grenoble, France, the Advanced Photon Source (APS) near Chicago, USA, and SPring-8 in Japan, accelerating electrons up to 6, 7 and 8 GeV, respectively.

Synchrotrons which are useful for cutting edge research are large machines, costing tens or hundreds of millions of dollars to construct, and each beamline (there may be 20 to 50 at a large synchrotron) costs another two or three million dollars on average. These installations are mostly built by the science funding agencies of governments of developed countries, or by collaborations between several countries in a region, and operated as infrastructure facilities available to scientists from universities and research organisations throughout the country, region, or world. More compact models, however, have been developed, such as the Compact Light Source.

List of installations

Synchrotron	Location & Country	Energy (GeV)	Circumference (m)	Commissioned	Decommissioned
Advanced Photon Source (APS)	Argonne National Laboratory, USA	7.0	1104	1995	
ISIS	Rutherford Appleton Laboratory, UK	0.8	163	1985	
Australian Synchrotron	Melbourne, Australia	3	216	2006	
LNLS	Campinas, Brazil	1.37	93.2	1997	
SESAME	Allaan, Jordan	2.5	125	Under Design	
Bevatron	Lawrence Berkeley Laboratory, USA	6	114	1954	1993
Advanced Light Source	Lawrence Berkeley Laboratory, USA	1.9	196.8	1993	
Cosmotron	Brookhaven National Laboratory, USA	3	72	1953	1968
Nimrod	Rutherford Appleton Laboratory, UK	7		1957	1978
Alternating Gradient Synchrotron (AGS)	Brookhaven National Laboratory, USA	33	800	1960	

Stanford Synchrotron Radiation Lightsource	SLAC National Accelerator Laboratory, USA	3	234	1973	
Cornell High Energy Synchrotron Source (CHESS)	Cornell University, USA	5.5	768	1979	
Soleil	Paris, France	3	354	2006	
Shanghai Synchrotron Radiation Facility (SSRF)	Shanghai, China	3.5	432	2007	
Proton Synchrotron	CERN, Switzerland	28	628.3	1959	
Tevatron	Fermi National Accelerator Laboratory, USA	1000	6300	1983	
Swiss Light Source	Paul Scherrer Institute, Switzerland	2.8	288	2001	
Large Hadron Collider (LHC)	CERN, Switzerland	7000	26659	2008	
BESSY II	Helmholtz-Zentrum Berlin in Berlin, Germany	1.7	240	1998	
European Synchrotron Radiation Facility (ESRF)	Grenoble, France	6	844	1988	
MAX-I	MAX-lab, Sweden	0.55	30	1986	
MAX-II	MAX-lab, Sweden	1.5	90	1997	
MAX-III	MAX-lab, Sweden	0.7	36	2008	
ELETTRA	Trieste, Italy	2-2.4	260	1993	
Diamond Light Source	Oxfordshire, UK	3	561.6	2002	
DORIS III	DESY, Germany	4.5	289	1980	
PETRA II	DESY, Germany	12	2304	1995	2007
Canadian Light Source	University of Saskatchewan, Canada	2.9	171	2002	
SPring-8	RIKEN, Japan	8	1436	1997	
Taiwanese National Synchrotron Radiation Research Center	Hsinchu Science Park, Taiwan	3.3	518.4	2008	
Synchrotron Light Research Institute (SLRI)	Nakhon Ratchasima, Thailand	1.2	81.4	2004	

Indus 1	Raja Ramanna Centre for Advanced Technology, Indore, India	0.45		1999	
Indus 2	Raja Ramanna Centre for Advanced Technology, Indore, India	2.5	36	2005	
Synchrophasotron	JINR, Dubna, USSR	10	180	1957	2005
U-70	IHEP, Protvino, USSR	70		1967	
CAMD	LSU, Louisiana, US	1.5	-	-	

- Note: in the case of colliders, the quoted power is often double what is shown here. The above table shows the power of one beam but if two opposing beams collide head on, the effective power is doubled.

Applications

- Life sciences: protein and large molecule crystallography
- Drug discovery and research
- "Burning" computer chip designs into metal wafers
- Studying molecule shapes and protein crystals
- Analyzing chemicals to determine their composition
- Observing the reaction of living cells to drugs
- Inorganic material crystallography and microanalysis
- Fluorescence studies
- Semiconductor material analysis and structural studies
- Geological material analysis
- Medical imaging
- Proton therapy to treat some forms of cancer

See also

- List of synchrotron radiation facilities
- Synchrotron X-ray tomographic microscopy
- Energy amplifier
- Superconducting Radio Frequency

References

- [1] Nature 407, 468 (28 September 2000) (<http://www.nature.com/nature/journal/v407/n6803/full/407468a0.html>).
- [2] The Cosmotron (<http://www.bnl.gov/bnlweb/history/cosmotron.asp>)

External links

- Australian Synchrotron (<http://www.synchrotron.org.au>)
- Diamond UK Synchrotron (<http://www.diamond.ac.uk>)
- Lightsources.org (<http://www.lightsources.org/cms/>)
- CERN Large Hadron Collider (<http://lhc-new-homepage.web.cern.ch/lhc-new-homepage>)
- Synchrotron Light Sources of the World (http://www-als.lbl.gov/als/synchrotron_sources.html)
- A Miniature Synchrotron: (<http://www.technologyreview.com/Biotech/20149/>) room-size synchrotron offers scientists a new way to perform high-quality x-ray experiments in their own labs, *Technology Review*, February 04, 2008
- Brazilian Synchrotron Light Laboratory (http://www.lnls.br/lnls/cgi/cgilua.exe/sys/start.htm?UserActiveTemplate=lnls_2007_english&tpl=home)
- Podcast interview (<http://omegataupodcast.net/2009/03/28/11-synchrotron-radiation-science-at-esrf/>) with a scientist at the European Synchrotron Radiation Facility

X-ray microscope

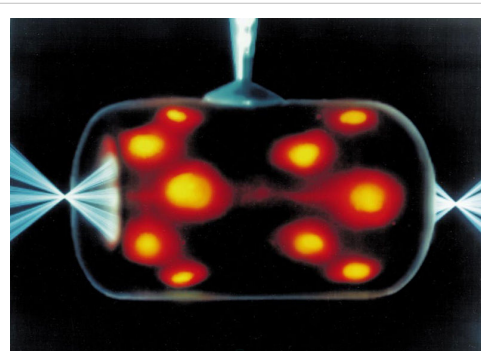
An **X-ray microscope** uses electromagnetic radiation in the soft X-ray band to produce images of very small objects.

Unlike visible light, X-rays do not reflect or refract easily, and they are invisible to the human eye. Therefore the basic process of an X-ray microscope is to expose film or use a charge-coupled device (CCD) detector to detect X-rays that pass through the specimen. It is a contrast imaging technology using the difference in absorption of soft x-ray in the water window region (wavelength region: 2.3 - 4.4 nm, photon energy region: 0.28 - 0.53 keV) by the carbon atom (main element composing the living cell) and the oxygen atom (main element for water).

Early X-ray microscopes by Paul Kirkpatrick and Albert Baez used grazing-incidence reflective optics to focus the X-rays, which grazed X-rays off parabolic curved mirrors at a very high angle of incidence. An alternative method of focusing X-rays is to use a tiny fresnel zone plate of concentric gold or nickel rings on a silicon dioxide substrate. Sir Lawrence Bragg produced some of the first usable X-ray images with his apparatus in the late 1940's.

In the 1950's Newberry produced a shadow X-ray microscope which placed the specimen between the source and a target plate, this became the basis for the first commercial X-ray microscopes from the General Electric Company.

The Advanced Light Source (ALS)[1] in Berkeley CA is home to XM-1 (<http://www.cxro.lbl.gov/BL612/>), a full field soft X-ray microscope operated by the Center for X-ray Optics [2] and dedicated to various applications in modern nanoscience, such as nanomagnetic materials, environmental and materials sciences and biology. XM-1 uses an X-ray lens to focus X-rays on a CCD, in a manner similar to an optical microscope. XM-1 still holds the world record in spatial resolution with Fresnel zone plates down to 15nm and is able to combine high spatial resolution with a sub-100ps time resolution to study e.g. ultrafast spin dynamics.



Indirect drive laser inertial confinement fusion uses a "hohlraum" which is irradiated with laser beam cones from either side on its inner surface to bathe a fusion microcapsule inside with smooth high intensity X-rays. The highest energy X-rays which penetrate the hohlraum can be visualized using an X-ray microscope such as here, where X-radiation is represented in orange/red.

The ALS is also home to the world's first soft x-ray microscope designed for biological and biomedical research. This new instrument, XM-2 was designed and built by scientists from the National Center for X-ray Tomography (<http://ncxt.lbl.gov>). XM-2 is capable of producing 3-Dimensional tomograms of cells.

Sources of soft X-rays suitable for microscopy, such as synchrotron radiation sources, have fairly low brightness of the required wavelengths, so an alternative method of image formation is scanning transmission soft X-ray microscopy. Here the X-rays are focused to a point and the sample is mechanically scanned through the produced focal spot. At each point the transmitted X-rays are recorded with a detector such as a proportional counter or an avalanche photodiode. This type of Scanning Transmission X-ray Microscope (STXM) was first developed by researchers at Stony Brook University and was employed at the National Synchrotron Light Source at Brookhaven National Laboratory.

The resolution of X-ray microscopy lies between that of the optical microscope and the electron microscope. It has an advantage over conventional electron microscopy in that it can view biological samples in their natural state. Electron microscopy is widely used to obtain images with nanometer level resolution but the relatively thick living cell cannot be observed as the sample has to be chemically fixed, dehydrated, embedded in resin, then sliced ultra thin. However, it should be mentioned that cryo-electron microscopy allows the observation of biological specimens in their hydrated natural state. Until now, resolutions of 30 nanometer are possible using the Fresnel zone plate lens which forms the image using the soft x-rays emitted from a synchrotron. Recently, more researchers have begun to use the soft x-rays emitted from laser-produced plasma rather than synchrotron radiation.

Additionally, X-rays cause fluorescence in most materials, and these emissions can be analyzed to determine the chemical elements of an imaged object. Another use is to generate diffraction patterns, a process used in X-ray crystallography. By analyzing the internal reflections of a diffraction pattern (usually with a computer program), the three-dimensional structure of a crystal can be determined down to the placement of individual atoms within its molecules. X-ray microscopes are sometimes used for these

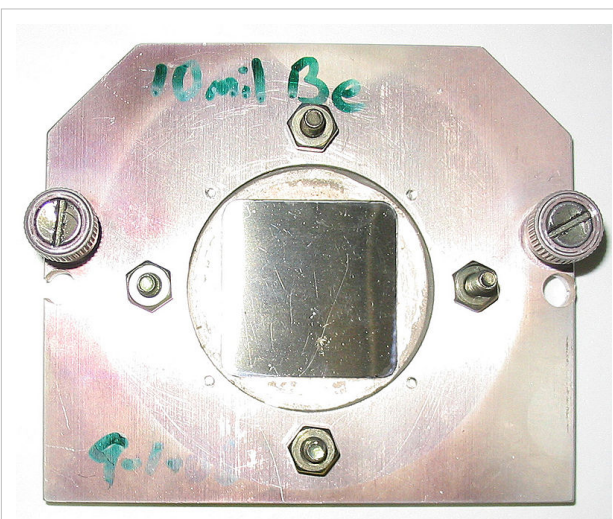
analyses because the samples are too small to be analyzed in any other way.

See also

- Synchrotron X-ray tomographic microscopy

External links

- Application of X-ray microscopy in analysis of living hydrated cells ^[3]
- Hard X-ray microbeam experiments with a sputtered-sliced Fresnel zone plate and its applications ^[4]
- Scientific applications of soft x-ray microscopy ^[5]
- Microarrays products ^[6]



A square beryllium foil mounted in a steel case to be used as a window between a vacuum chamber and an X-ray microscope. Beryllium, due to its low Z number is highly transparent to X-rays.

References

- [1] <http://www-als.lbl.gov>
- [2] <http://www.cxro.lbl.gov>
- [3] http://www.ncbi.nlm.nih.gov/entrez/query.fcgi?cmd=Retrieve&db=pubmed&dopt=Abstract&list_uids=12379938
- [4] http://www.ncbi.nlm.nih.gov/entrez/query.fcgi?cmd=Retrieve&db=pubmed&dopt=Abstract&list_uids=11972376
- [5] <http://www.cxro.lbl.gov/BL612/index.php?content=research.html>
- [6] <http://www.ibio.co.il/Products.aspx?level=2&prodID=17>

Extended X-ray absorption fine structure

X-ray Absorption Spectroscopy (XAS) includes both **Extended X-Ray Absorption Fine Structure** (EXAFS) and **X-ray Absorption Near Edge Structure** (XANES). XAS is the measurement of the x-ray absorption coefficient of a material. X-rays of a narrow energy resolution are shined on the sample and the incident and transmitted x-ray intensity is recorded as the incident x-ray energy is incremented. The number of x-rays that are transmitted through a sample (I_t) is equal to the number of x-rays shined on the sample (I_0) multiplied by a decreasing exponential that depends of the type of atoms in the sample, the absorption coefficient μ , and the thickness of the sample x .

$$I_t = I_0 e^{-\mu x}$$

The absorption coefficient is obtained by taking the log ratio of the incident x-ray intensity to the transmitted x-ray intensity.

$$\mu = \frac{-\ln(I_t/I_0)}{x}$$

When the incident x-ray energy matches the binding energy of an electron of an atom within the sample, the number of x-rays absorbed by the sample increases dramatically, causing a drop in the transmitted x-ray intensity. This results in an absorption edge. Each element on the periodic table has a set of unique absorption edges corresponding to different binding energies of its electrons. This gives XAS element selectivity. XAS spectra are most often collected at synchrotrons. Because X-rays are highly penetrating, XAS samples can be gases, solids or liquids. And because of the brilliance of Synchrotron X-ray sources the concentration of the absorbing element can be as low as a few ppm.

EXAFS spectra are displayed as graphs of the absorption coefficient of a given material versus energy, typically in a 500 – 1000 eV range beginning before an absorption edge of an element in the sample. The x-ray absorption coefficient is usually normalized to unit step height. This is done by regressing a line to the region before and after the absorption edge, subtracting the pre-edge line from the entire data set and dividing by the absorption step height, which is determined by the difference between the pre-edge and post-edge lines at the value of E_0 (on the absorption edge).

The normalized absorption spectra are often called XANES spectra. These spectra can be used to determine the average oxidation state of the element in the sample. The XANES spectra are also sensitive to the coordination environment of the absorbing atom in the sample. Finger printing methods have been used to match the XANES spectra of an unknown sample to those of known "standards". Linear combination fitting of several different standard spectra can give an estimate to the amount of each of the known standard spectra within an unknown sample.

X-ray absorption spectra are produced over the range of 200 – 35,000 eV. The dominant physical process is one where the absorbed photon ejects a core photoelectron from the absorbing atom, leaving behind a core hole. The atom with the core hole is now excited. The ejected photoelectron's energy will be equal to that of the absorbed photon minus the binding energy of the initial core state. The ejected photoelectron interacts with electrons in the surrounding non-excited atoms.

If the ejected photoelectron is taken to have a wave-like nature and the surrounding atoms are described as point scatterers, it is possible to imagine the backscattered electron waves interfering with the forward-propagating waves. The resulting interference pattern shows up as a modulation of the measured absorption coefficient, thereby causing the oscillation in the EXAFS spectra. A simplified plane-wave single-scattering theory has been used for interpretation of EXAFS spectra for many years, although modern methods (like FEFF, GNXAS) have shown that curved-wave corrections and multiple-scattering effects can not be neglected. The photoelectron scattering amplitude in the low energy range (5-200 eV) of the photoelectron kinetic energy become much larger so that multiple scattering events become dominant in the NEXAFS (or XANES) spectra.

The wavelength of the photoelectron is dependent on the energy and phase of the backscattered wave which exists at the central atom. The wavelength changes as a function of the energy of the incoming photon. The phase and amplitude of the backscattered wave are dependent on the type of atom doing the backscattering and the distance of the backscattering atom from the central atom. The dependence of the scattering on atomic species makes it possible to obtain information pertaining to the chemical coordination environment of the original absorbing (centrally excited) atom by analyzing these EXAFS data.

Experimental considerations

Since EXAFS requires a tunable x-ray source, data are always collected at synchrotrons, often at beamlines which are especially optimized for the purpose. The utility of a particular synchrotron to study a particular solid depends on the brightness of the x-ray flux at the absorption edges of the relevant elements.

Applications

XAS is an interdisciplinary technique and its unique properties, as compared to x-ray diffraction, have been exploited for understanding the details of local structure in:

- glass, amorphous and liquid systems
- solid solutions
- Doping and ionic implantation materials for electronics
- local distortions of crystal lattices
- organometallic compounds
- metalloproteins
- metal clusters
- vibrational dynamics
- ions in solutions
- speciation of elements

Example of Significance

EXAFS is, like NEXAFS/XANES, a highly sensitive technique with elemental specificity. As such, EXAFS is an extremely useful way to determine the chemical state of practically important species which occur in very low abundance or concentration. Frequent use of EXAFS occurs in environmental chemistry, where scientists try to understand the propagation of pollutants through an ecosystem. EXAFS can be used along with accelerator

mass spectrometry in forensic examinations, particularly in nuclear non-proliferation applications.

For an example of an EXAFS study of uranium chemistry in glass see [1], and for a general study of trivalent lanthanides and actinides in chloride containing aqueous media can be read at [2]

See also

- XANES
- NEXAFS
- SEXAFS

History

A very detailed, balanced and informative account about the history of EXAFS (originally called Kossel's structures) is given in the paper "A History of the X-ray Absorption Fine Structure} by R. Stumm von Bordwehr", Ann. Phys. Fr. vol. 14, 377-466 (1989) (author's name is C. Brouder).

References

- [1] <http://www.osti.gov/bridge/servlets/purl/459339-8dNh9T/webviewable/459339.pdf>
- [2] http://www-ssrl.slac.stanford.edu/pubs/activity_rep/ar98/2525-edelstein.pdf

Relevant Websites

- International XAFS Society (<http://www.i-x-s.org/>)
- FEFF Project, University of Washington, Seattle (<http://leonardo.phys.washington.edu/feff/>)
- GNXAS project and XAS laboratory, Università di Camerino (<http://gnxas.unicam.it>)
- EXAFS theory Introduction (<http://srs.dl.ac.uk/xrs/Theory/theory.html>)
- Community web site for XAFS (<http://xafs.org/XAFS>)

Books

- B.-K. Teo, *EXAFS: basic principles and data analysis*, Springer 1986
- *X-ray Absorption: principles, applications and techniques of EXAFS, SEXAFS and XANES*, a cura di D.C. Koeningsberger, R. Prins, Wiley 1988

Book Chapters

- Kelly, S.D., Hesterberg, D., and Ravel, B., *Analysis of Soils and Minerals Using X-ray Absorption Spectroscopy* in Methods of Soil Analysis, Part 5 -Mineralogical Methods, (A.L. Ulery and L.R. Drees, Eds.) p. 367. Soil Science Society of America, Madison, WI, USA, 2008.

Papers

- J.J. Rehr and R.C. Albers, "Theoretical approaches to X-ray absorption fine structure", *Reviews of Modern Physics* 72 (2000), 621-654
- A. Filipponi, A. Di Cicco and C.R. Natoli, "X-ray absorption spectroscopy and n-body distribution functions in condensed matter", *Physical Review B* 52/21 (1995) 15122-15148
- F. de Groot, "High-resolution X-ray emission and X-ray absorption spectroscopy", *Chemical Reviews* 101 (2001) 1779-1808
- F.W. Lytle, "The EXAFS family tree: a personal history of the development of extended X-ray absorption fine structure", *Journal of Synchrotron Radiation* 6 (1999), 123-134
- Dale E. Sayers, Edward A. Stern, and Farrel W. Lytle, New Technique for Investigating Noncrystalline Structures: Fourier Analysis of the Extended X-Ray—Absorption Fine Structure, (<http://dx.doi.org/10.1103/PhysRevLett.27.1204>)Phys. Rev. Lett. 27, 1204-1207 (1971).
- A. Kodre, I. Arčon, Proceedings of 36th International Conference on Microelectronics, Devices and Materials, MIDEM, Postojna, Slovenia, October 28-20, (2000), p. 191-196

Surface extended X-ray absorption fine structure

Surface extended X-ray absorption fine structure is the surface sensitive equivalent of the EXAFS technique. This technique involves the illumination of the sample by high intensity X-ray beams from a synchrotron and monitoring their photoabsorption by detecting in the intensity of Auger electrons as a function of the incident photon energy. Surface sensitivity is achieved by the fact that the interpretation of data depends on the intensity of the Auger electrons (which have an escape depth of $\sim 1\text{--}2\text{ nm}$) instead of looking at the relative absorption of the X-rays as in the parent method, EXAFS.

The photon energies are tuned through the characteristic energy for the onset of core level excitation for surface atoms. The core holes thus created can then be filled by nonradiative decay of a higher lying electron and communication of energy to yet another electron, which can then escape from the surface (Auger emission). The photoabsorption can therefore be monitored by direct detection of these Auger electrons to the total photoelectron yield. The absorption coefficient versus incident photon energy contains oscillations which are due to the interference of the backscattered Auger electrons with the outward propagating waves. The period of this oscillations depends on the type of the backscattering atom and its distance from the central atom. Thus, this technique enables the investigation of interatomic distances for adsorbates and their coordination chemistry.

This technique benefits from the fact that long range order is not required which sometimes becomes a limitation in the other conventional techniques like LEED (about 10 nm). This method also largely eliminates the background from the signal. It also benefits from the fact that it can probe different species in the sample by just tuning the X-ray photon energy to the absorption edge of that species. Joachim Stöhr played a major role in the initial development of this technique.

Experimental setup

Synchrotron radiation sources

Normally, the SEXAFS work is done using synchrotron radiation as it has highly collimated, plane polarized and precisely pulsed X-ray sources, with fluxes of 10^{12} to 10^{14} photons/sec/mrad/mA and greatly improves the signal-to-noise ratio over than obtainable from conventional sources. The experimental setup for the conventional EXAFS is shown here in Figure 2. A bright source X-ray source is illuminating the sample and the transmission is being measured as the absorption coefficient as

$$\mu = \frac{\ln(I)}{\ln(I_o)},$$

where I is the transmitted and I_o is the incident intensity of the X-rays. Then it is plotted against the energy of the incoming X-ray photon energy.

Electron detectors

In SEXAFS, an electron detector and a high vacuum chamber is required to calculate the Auger yields instead of the intensity of the transmitted X-ray waves. The detector can be either an energy analyzer, as in the case of Auger measurements, or an electron multiplier, as in the case of total or partial secondary electron yield. The energy analyzer gives rise to better resolution while the electron multiplier has larger solid angle acceptance.

Signal to noise ratio

The equation governing the signal to noise ratio is

$$\frac{S}{N} = \sqrt{\frac{\left(\frac{\Omega}{4\pi}\epsilon_n\mu_A\right)}{\left(1 + \frac{I_b}{I_n}(\mu_T + n)\right)}} \left(\frac{\delta\mu_A}{\mu_A} I_o^{1/2}\right),$$

where

- μ_A is the absorption coefficient;
- I_n is the nonradiative contribution in electron counts/sec;
- I_b is the background contribution in electron counts/sec;
- μ_A is the absorption by the SEXAFS-producing element;
- μ_T is the total absorption by all the elements;
- I_o is the incident intensity;
- n is the attenuation length;
- $\Omega/(4\pi)$ is the solid angle acceptance for the detector;
- ϵ_n is the nonradiative yield which is the probability that the electron will not decay radiatively and will actually get emitted as an Auger electron.

Physics of SEXAFS

Basics

The absorption of a X-ray photon by the atom excites a core level electron thus generating a core hole. This generates a spherical electron wave with the excited atom as the center. This wave propagates outwards and get scattered off from the neighbouring atoms and is turned back towards the central ionized atom. The oscillatory component of the photoabsorption originates from the coupling of this reflected wave to the initial state via the dipole operator M_{fs} as in (1). The Fourier transform of the oscillations gives us the information about the spacing of the neighboring atoms and their chemical environment. This phase information is carried over to the oscillations

in the Auger signal because the transition time in Auger emission is of the same order of magnitude as the average time for a photoelectron in the energy range of interest. Thus, with a proper choice of the absorption edge and characteristic Auger transition, measurement of the variation of the intensity in a particular Auger line as a function of incident photon energy would be a measure of the photoabsorption cross section.

This excitation also triggers various decay mechanisms. These can be of radiative (fluorescence) or nonradiative (Auger and Coster-Kronig) nature. The intensity ratio between the Auger electron and x-ray emissions depends on the atomic number Z . The yield of the Auger electrons decreases with increasing Z .

Theory of EXAFS

The cross section of photoabsorption is given by the Fermi golden rule formula, which, in the dipole approximation, is given as

$$P = \frac{2\pi}{\hbar} \sum_f |M_{fs}|^2 \delta(E_i + \hbar\omega - E_f),$$

$$M_{fs} = \langle f | e\mathbf{e} \cdot \mathbf{r} | i \rangle,$$

where the initial state, i with energy E_i , consists of the atomic core and the Fermi sea, and the incident radiation field, the final state, f with energy E_f (larger than the Fermi level), consists of a core hole and an excited electron. \mathbf{e} is the polarization vector of the electric field, e the electron charge, and $\hbar\omega$ the x-ray photon energy. The photoabsorption signal contains a peak when the core level excitation is neared. It is followed by an oscillatory component which originates from the coupling of that part of the electron wave which upon scattering by the medium is turned back towards the central ionized atom, where it couples to the initial state via the dipole operator, M_i .

Assuming single-scattering and small atom approximation for $kR_j \gg 1$, where R_j is the distance from the central excited atom to the j th shell of neighbors and k is the photoelectrons wave vector,

$$k = \frac{1}{\hbar} \sqrt{2m(\hbar(\omega - \omega_T) + V_o)},$$

where $\hbar\omega_T$ is the absorption edge energy and V_o is the inner potential of the solid associated with exchange and correlation, the following expression for the oscillatory component of the photoabsorption cross section (for K-shell excitation) is obtained:

$$\chi(k) = k^{-1} |f(k, \pi)| \sum_j W_j \sin[2kR_j + \alpha(k)] \exp(-\gamma R_j - 2\sigma_j^2 k^2),$$

where the atomic scattering factor in a partial wave expansion with partial wave phase-shifts δ_l is given by

$$f(k, \theta) = (1/k) \sum_{l=0}^{\infty} (2l+1) [\exp(2i\delta_l(k)) - 1] P_l(\cos \theta).$$

$P_l(x)$ is the l th Legendre polynomial, γ is an attenuation coefficient, $\exp(-2\sigma_j^2 k^2)$ is a Debye-Waller factor and weight W_j is given in terms of the number of atoms in the j th shell and their distance as

$$W_j = \frac{N_j}{R_j^2}.$$

The above equation for the $\chi(k)$ forms the basis of a direct, Fourier transform, method of analysis which has been successfully applied to the analysis of the EXAFS data.

Incorporation of EXAFS-Augur

The number of electrons arriving at the detector with an energy of the characteristic W_{α}^{XY} Auger line (where W_{α} is the absorption edge core-level of element α , to which the incident x-ray line has been tuned) can be written as

$$N_T = N_{W_{\alpha}^{XY}}(\hbar\omega) + N_B(\hbar\omega),$$

where $N_B(\hbar\omega)$ is the background signal and $N_{W_{\alpha}^{XY}}(\hbar\omega)$ is the Auger signal we are interested in, where

$$N_{W_{\alpha}^{XY}}(\hbar\omega) = (4\pi)^{-1} \psi_{W_{\alpha}^{XY}} [1 - \kappa] \int_{\Omega} \int_0^{\infty} \rho_{\alpha}(z) P_{W_{\alpha}}(\hbar\omega; z) \exp \left[\frac{-z}{\lambda(W_{\alpha}^{XY})} \cos \theta \right] dz d\Omega,$$

where $\psi_{W_{\alpha}^{XY}}$ is the probability that an excited atom will decay via W_{α}^{XY} Auger transition, $\rho_{\alpha}(z)$ is the atomic concentration of the element α at depth z , $\lambda(W_{\alpha}^{XY})$ is the mean free path for an W_{α}^{XY} Auger electron, θ is the angle that the escaping Auger electron makes with the surface normal and κ is the photon emission probability which is dictated the atomic number. As the photoabsorption probability, $P_{W_{\alpha}}(\hbar\omega; z)$ is the only term that is dependent on the photon energy, the oscillations in it as a function of energy would give rise to similar oscillations in the $N_{W_{\alpha}^{XY}}(\hbar\omega)$.

References

- First paper of SEXAFS ^[1], U. Landman D.L. Adams, Extended x-ray-absorption fine structure—Auger process for surface structure analysis: Theoretical considerations of a proposed experiment.
- Possibility of adsorbate position determination using final-state interference effects ^[2], Phys. Rev. B 13, 5261 - 5270 (1976)

External links

- Koningsberger, D.C (1988). *X-Ray Absorption: Principles, Applications, Techniques of EXAFS, SEXAFS and XANES*. Wiley InterScience. ISBN 0471875473.
- Details about SEXAFS ^[3]

References

- [1] <http://www.pnas.org/content/73/8/2550.abstract>
 [2] <http://dx.doi.org/10.1103/PhysRevB.13.5261>
 [3] http://www.phys.au.dk/~philip/q1_05/surflec/node24.html

XANES

X-ray Absorption Near Edge Structure (XANES) is a type of absorption spectroscopy.

XANES data indicate the absorption peaks due to the photoabsorption cross section in the X-ray Absorption Spectra (XAS) observed in the energy region, extending over a range of about 100 eV, between the edge region and the EXAFS region. Here the XANES spectroscopy and its applications in these last 26 years is described. XANES is also known as NEXAFS (Near Edge X-ray Absorption Fine Structure) when applied to surface and molecular science and it is described elsewhere.

XANES has to be distinguished from edge and EXAFS spectroscopy. The first difference concerns the energy range above the absorption edge.

Energy Range

Edge energy range

In the absorption edge region of metals, the photoelectron is excited to the first unoccupied level above the Fermi level. Therefore its mean free path in a pure single crystal at zero temperature is as large as infinite, and it remains very large, increasing the energy of the final state up to about 5 eV above the Fermi level. Beyond the role of the unoccupied density of states and matrix elements in single electron excitations, many-body effects appear as an "infrared singularity" at the absorption threshold in metals.

In the absorption edge region of insulators the photoelectron is excited to the first unoccupied level above the chemical potential but the unscreened core hole forms a localized bound state called core exciton.

EXAFS energy range

The fine structure in the x-ray absorption spectra in the high energy range extending from about 150 eV beyond the ionization potential is a powerful tool to determine the atomic pair distribution (i.e. interatomic distances) with a time scale of about 10^{-15} s. In fact the final state of the excited photoelectron in the high kinetic energy range (150-2000 eV) is determined only by single backscattering events due to the low amplitude photoelectron scattering.

XANES energy range

In the XANES region, starting about 5 eV beyond the absorption threshold, because of the low kinetic energy range (5-150 eV) the photoelectron backscattering amplitude by neighbor atoms is very large so that multiple scattering events become dominant in the XANES spectra.

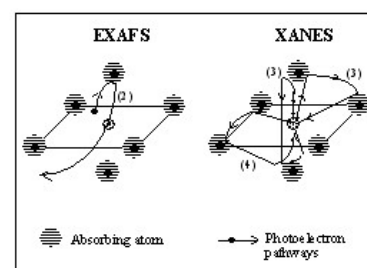
The different energy range between XANES and EXAFS can be also explained in a very simple manner by the comparison between the photoelectron wavelength λ and the interatomic distance of the photoabsorber-backscatterer pair. The photoelectron kinetic energy is connected with the wavelength λ by the following relation:

$$E_{\text{kinetic}} = h\nu - E_{\text{binding}} = \hbar^2 k^2 / (2m) = (2\pi)^2 \hbar^2 / (2m\lambda^2)$$

that means that for high energy the wavelength is shorter than interatomic distances and hence the EXAFS region corresponds to a single scattering regime; while for lower E, λ is larger than interatomic distances and the XANES region is associated with a multiple scattering regime.

Final States

The absorption peaks of XANES spectra are determined by multiple scattering resonances of the photoelectron excited at the atomic absorption site and scattered by neighbor atoms. The local character of the final states is determined by the short photoelectron mean free path, that is strongly reduced (down to about 0.3 nm at 50 eV) in this energy range because of inelastic scattering of the photoelectron by electron-hole excitations (excitons) and collective electronic oscillations of the valence electrons called plasmons.



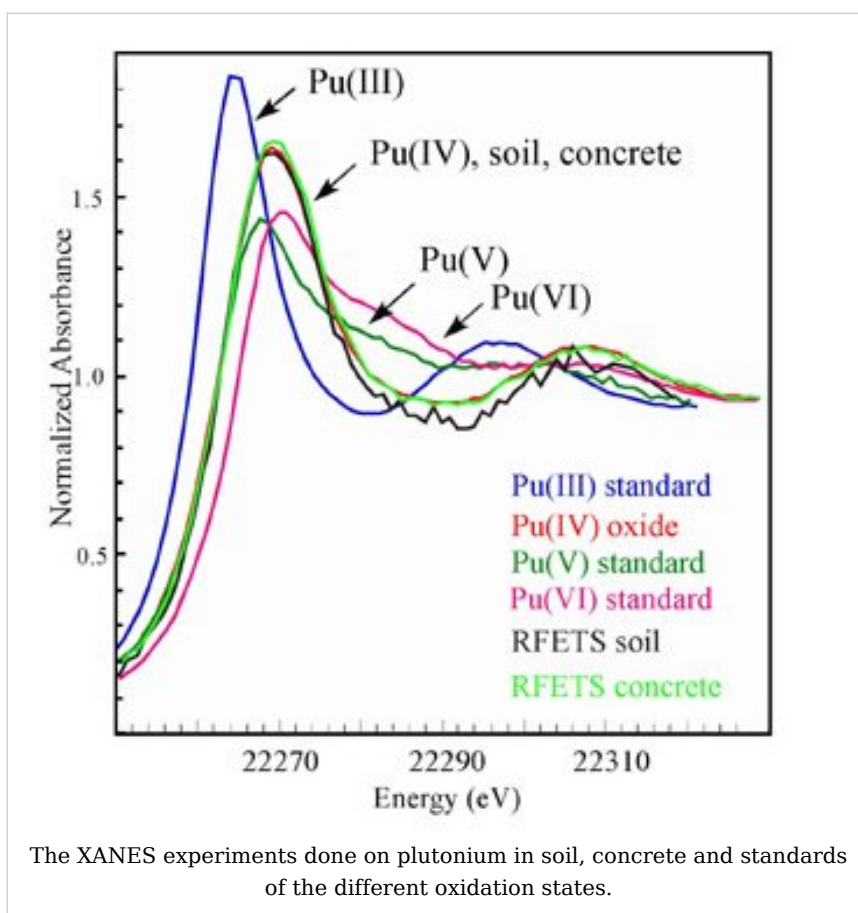
Pictorial view of photoelectron scattering processes in the single-scattering regime, EXAFS, and in the multiple scattering regime, XANES. In EXAFS the photoelectron is scattered only by a single neighbour atom, in XANES all the scattering pathways, classified according to the number of scattering event (3), (4), (5) etc. contribute to the absorption cross section.

Applications

Much chemical information can be extracted from the XANES region: formal valence (very difficult to experimentally determine in a nondestructive way); coordination environment (e.g., octahedral, tetrahedral coordination) and subtle geometrical distortions of it.

Transitions to bound vacant states just above the Fermi level can be seen. Thus XANES spectra can be used as a probe of the unoccupied band structure of a material.

The near-edge structure is characteristic of an environment and valence state hence one of its more common uses is in fingerprinting: if you have a mixture of sites/compounds in a sample you can fit the measured spectra with a linear combinations of XANES spectra of known species and determine the proportion of each site/compound in the sample. One example of such a use is the determination of the oxidation state of the plutonium in the soil at Rocky Flats.



History

The acronym XANES has been first introduced in 1980 to interpret the XANES spectra measured at the Stanford Synchrotron Radiation Laboratory (SSRL) determined by multiple scattering resonances by A. Bianconi. In 1982 the first paper on the application of XANES spectroscopy for determination of the local structural geometrical distortions using multiple scattering theory was published by the collaboration between A. Bianconi, P. J. Durham, J. B. Pendry. In 1983 the first NEXAFS paper appeared for molecules adsorbed on surfaces. The first XAFS paper appeared in 1987 for the interpretation of the intermediate region between EXAFS and XANES.

Software for XANES analysis

FDMNES Calculation of XANES using finite difference method and full multiple scattering theory.

FEFF8 Calculation of XANES using full multiple scattering theory.

FitIt XANES fitting using multidimensional interpolation approximation.

PARATEC XANES calculation using plane-wave pseudopotential approach

WIEN2k XANES calculation on the basis of full-potential (linearized) augmented plane-wave approach.

References

- A. Bianconi "Surface X-ray Absorption Spectroscopy: Surface EXAFS and Surface XANES" Appl. Surf. Sci. Vol. 6 pag. 392-418 (1980)[1]
- A. Bianconi, M. Dell'Araccia, P. J. Durham and J. B. Pendry Multiple-scattering resonances and structural effects in the x-ray-absorption near-edge spectra of Fe II and Fe III hexacyanide complexes" Phys. Rev. B 26, 6502-6508 (1982)[2]

External links

- International XAFS Society ^[3]
- XAFS Spectroscopy at Daresbury ^[4]

Lectures

- M. Newville, *The fundamentals of XAFS* ^[5]
- S. Bare, *XANES measurements and interpretation* ^[6]
- B. Ravel, *A practical introduction to multiple scattering* ^[7]

Bibliography

- Xray Absorption: Principles, Applications, Techniques of EXAFS, SEXAFS, and XANES, in Chemical Analysis 92, D. C. Koningsberger and R. Prins, ed., John Wiley & Sons, 1988.
- Principles and Applications of EXAFS, Chapter 10 in Handbook of Synchrotron Radiation, pp 995-1014. E. A. Stern and S. M. Heald, E. E. Koch, ed., North-Holland, 1983.

References

- [1] http://www.sciencedirect.com/science?_ob=ArticleURL&_udi=B6X3T-46G2PH5-5Y&_coverDate=12%2F31%2F1980&_alid=393547239&_rdoc=1&_fmt=&_orig=search&_qd=1&_cdi=7307&_sort=d&view=c&_acct=C000058858&_version=1&_urlVersion=0&_userid=2814622&md5=4640d16228b2ef420ad2946f50b108ed
- [2] http://prola.aps.org/abstract/PRB/v26/i12/p6502_1?qid=df0eb646d5d96a83&qseq=165&show=10
- [3] <http://ixs.iit.edu/>
- [4] <http://srs.dl.ac.uk/XRS/index.html>
- [5] http://cars9.uchicago.edu/xafs/xas_fun/xas_fundamentals.pdf
- [6] http://cars9.uchicago.edu/xafs/APS_2005/Bare_XANNES.pdf
- [7] <http://cars9.uchicago.edu/~ravel/talks/pimst.pdf>

NEXAFS

1. REDIRECT Near edge X-ray absorption fine structure

Small angle X-ray scattering

1. REDIRECT Small-angle X-ray scattering

Imaging

Imaging is the representation or reproduction of an object's outward form; especially a visual representation (i.e., the formation of an image).

Imaging methodologies and technologies

- Chemical imaging, the simultaneous measurement of spectra and pictures
 - Creation of a disk image, a file which contains the exact content of a non-volatile computer data storage medium. See also disk cloning
 - Digital imaging, creating digital images, generally by scanning, or through digital photography
 - Document imaging, replicating documents commonly used in business
 - Geophysical imaging
 - Medical imaging, creating images of the human body or parts of it, to diagnose or examine disease
 - Magnetic resonance imaging
 - Molecular imaging
 - Optical imaging
 - Personal imaging, real-time sharing of personal experience through images
 - Radar imaging, or imaging radar, for obtaining an image of an object, not just its location and speed
 - Reprography, reproduction of graphics through electrical and mechanical means
 - Cinematography
 - Photography, the process of creating still images
 - Xerography, the method of photocopying
 - Speckle imaging, a method of shift-and-add for astronomical imaging
 - Stereo imaging, an aspect of sound recording and reproduction concerning spatial locations of the performers
 - Thermography, infrared imaging
-

Proper names

- Imaging for Windows, a software product for scanning paper documents

See also

- Image processing
- Imaging technology
- Imaging science, which includes many fields of science
- Remote sensing, imaging the Earth or a planet from space or aircraft

Compton scattering

Compton scattering	
Feynman diagrams	
<p>s-channel</p>	
<p>u-channel</p>	
Light-matter interaction	
Low energy phenomena	Photoelectric effect
Mid-energy phenomena	Compton scattering
High energy phenomena	Pair production

In physics, **Compton scattering** or the **Compton effect** is the decrease in energy (increase in wavelength) of an X-ray or gamma ray photon, when it interacts with matter. Because of the change in photon energy, it is an inelastic scattering process. **Inverse Compton scattering** also exists, where the photon gains energy (decreasing in wavelength) upon interaction with matter. The amount the wavelength changes by is called the **Compton shift**. Although nuclear compton scattering exists^[1] , Compton scattering usually refers to the interaction involving only the electrons of an atom. The Compton effect

was observed by Arthur Holly Compton in 1923 and further verified by his graduate student Y. H. Woo in the years following. Arthur Compton earned the 1927 Nobel Prize in Physics for the discovery.

The effect is important because it demonstrates that light cannot be explained purely as a wave phenomenon. Thomson scattering, the classical theory of an electromagnetic wave scattered by charged particles, cannot explain low intensity shift in wavelength (Classically, light of sufficient intensity for the electric field to accelerate a charged particle to a relativistic speed will cause radiation-pressure recoil and an associated Doppler shift of the scattered light, but the effect would become arbitrarily small at sufficiently low light intensities regardless of wavelength.). Light must behave as if it consists of particles in order to explain the low-intensity Compton scattering. Compton's experiment convinced physicists that light can behave as a stream of particle-like objects (quanta) whose energy is proportional to the frequency.

The interaction between electrons and high energy photons ($\sim \text{keV}$) results in the electron being given part of the energy (making it recoil), and a photon containing the remaining energy being emitted in a different direction from the original, so that the overall momentum of the system is conserved. If the photon still has enough energy left, the process may be repeated. In this scenario, the electron is treated as free or loosely bound. Experimental verification of momentum conservation in individual Compton scattering processes by Bothe and Geiger as well as by Compton and Simon has been important in disproving the BKS theory.

If the photon is of lower energy, but still has sufficient energy (in general a few eV, right around the energy of visible light), it can eject an electron from its host atom entirely (a process known as the photoelectric effect), instead of undergoing Compton scattering. Higher energy photons ($\sim \text{MeV}$) may be able to bombard the nucleus and cause an electron and a positron to be formed, a process called pair production.

The Compton shift formula

Compton used a combination of three fundamental formulas representing the various aspects of classical and modern physics, combining them to describe the quantum behavior of light.

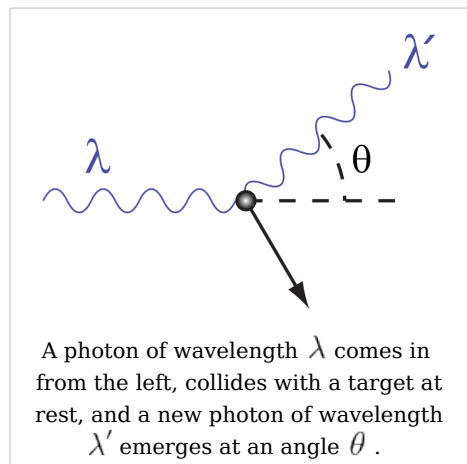
- Light as a particle, as noted previously in the photoelectric effect.
- Relativistic dynamics: special theory of relativity
- Trigonometry: law of cosines

The final result gives us the **Compton scattering equation**:

$$\lambda' - \lambda = \frac{h}{m_e c} (1 - \cos \theta)$$

where

λ is the wavelength of the photon **before** scattering,



λ' is the wavelength of the photon **after** scattering,

m_e is the mass of the electron,

θ is the angle by which the photon's heading changes (between 0° and 180°),

h is Planck's constant, and

c is the speed of light.

$\frac{h}{m_e c} = 2.43 \times 10^{-12}$ m is known as the Compton wavelength. $\lambda' - \lambda$ can be between 0 (for $\theta = 0^\circ$) and two times the Compton wavelength (for $\theta = 180^\circ$).

Derivation

Begin with conservation of energy and conservation of momentum:

$$E_\gamma + E_e = E_{\gamma'} + E_{e'} \quad (1)$$

$$\vec{p}_\gamma = \vec{p}_{\gamma'} + \vec{p}_{e'} \quad (2)$$

where

E_γ and p_γ are the energy and momentum of the photon and

E_e and p_e are the energy and momentum of the electron.

Solving (Part 1)

Now we fill in for the energy part:

$$E_\gamma + E_e = E_{\gamma'} + E_{e'}$$

$$hf + mc^2 = hf' + \sqrt{(p_{e'}c)^2 + (mc^2)^2}$$

The square of the second equation gives an equation for $p_{e'}$:

$$p_{e'}^2 c^2 = (hf + mc^2 - hf')^2 - m^2 c^4 \quad (3)$$

Solving (Part 2)

Rearrange equation (2)

$$\vec{p}_{e'} = \vec{p}_\gamma - \vec{p}_{\gamma'}$$

and square it to see

$$p_{e'}^2 = (\vec{p}_\gamma - \vec{p}_{\gamma'}) \cdot (\vec{p}_\gamma - \vec{p}_{\gamma'})$$

$$p_{e'}^2 = p_\gamma^2 + p_{\gamma'}^2 - 2\vec{p}_\gamma \cdot \vec{p}_{\gamma'}$$

$$p_{e'}^2 = p_\gamma^2 + p_{\gamma'}^2 - 2|p_\gamma||p_{\gamma'}|\cos(\theta)$$

Energy and momentum of photons are connected by the relativistic equation $p_\gamma = \frac{E_\gamma}{c}$, so

$$E_\gamma^2 = p_\gamma^2 c^2 = (hf)^2.$$

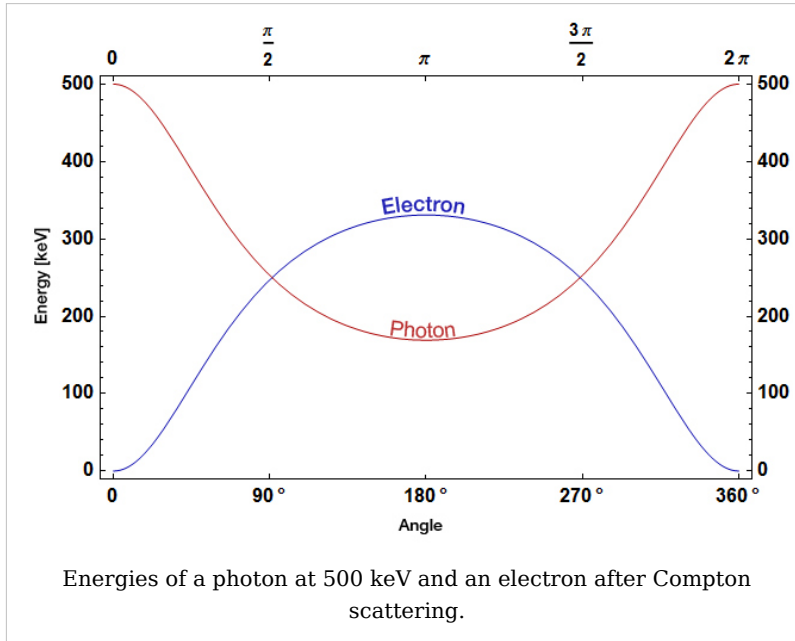
Therefore, multiplying by c^2 , we have also

$$p_{e'}^2 c^2 = (hf)^2 + (hf')^2 - 2(hf)(hf')\cos\theta \quad (4)$$

Putting it together

Now we have the two equations (3 & 4) for $p_e^2 c^2$, which we equate:

$$(hf)^2 + (hf')^2 - 2h^2 f f' \cos \theta = (hf + mc^2 - hf')^2 - m^2 c^4$$



$$-2h^2 f f' \cos \theta = -2h^2 f f' + 2hfmc^2 - 2hf'mc^2.$$

Combining two terms, this becomes:

$$2h^2 f f' (1 - \cos(\theta)) = 2hfmc^2 - 2hf'mc^2.$$

After dividing both sides by $(2hf f' mc^2)$, we get:

$$\frac{h}{mc^2} (1 - \cos \theta) = \frac{1}{f'} - \frac{1}{f}$$

This is equivalent to the **Compton scattering equation**, but it is usually written in terms of wavelength rather than frequency. To make that switch use

$$f = \frac{c}{\lambda}$$

so that finally,

$$\lambda' - \lambda = \frac{h}{mc} (1 - \cos \theta)$$

Applications

Compton scattering

Compton scattering is of prime importance to radiobiology, as it happens to be the most probable interaction of high energy X rays with atomic nuclei in living beings and is applied in radiation therapy.^[2]

In material physics, Compton scattering can be used to probe the wave function of the electrons in matter in the momentum representation.

Compton scattering is an important effect in gamma spectroscopy which gives rise to the Compton edge, as it is possible for the gamma rays to scatter out of the detectors used. Compton suppression is used to detect stray scatter gamma rays to counteract this effect.

Inverse Compton scattering

Inverse Compton scattering is important in astrophysics. In X-ray astronomy, the accretion disk surrounding a black hole is believed to produce a thermal spectrum. The lower energy photons produced from this spectrum are scattered to higher energies by relativistic electrons in the surrounding corona. This is believed to cause the power law component in the X-ray spectra (0.2-10 keV) of accreting black holes.

The effect is also observed when photons from the cosmic microwave background move through the hot gas surrounding a galaxy cluster. The CMB photons are scattered to higher energies by the electrons in this gas, resulting in the Sunyaev-Zel'dovich effect. Observations of the Sunyaev-Zel'dovich effect provide a nearly redshift-independent means of detecting galaxy clusters.

See also

- Thomson scattering
- Klein-Nishina formula
- Photoelectric effect
- Pair production
- Timeline of cosmic microwave background astronomy
- Peter Debye
- Walther Bothe
- List of astronomical topics
- List of physics topics
- Washington University in St. Louis (Site of discovery)

Notes

- [1] P Christillin (1986). "http://www.iop.org/EJ/abstract/0305-4616/12/9/008|Nuclear Compton scattering". *J. Phys. G: Nucl. Phys.* **12**: 837–851. doi: 10.1088/0305-4616/12/9/008 (<http://dx.doi.org/10.1088/0305-4616/12/9/008>). <http://www.iop.org/EJ/abstract/0305-4616/12/9/008>.
- [2] Camphausen KA, Lawrence RC. "Principles of Radiation Therapy" (<http://www.cancernetwork.com/cancer-management-11/chapter02/article/10165/1399960>) in Pazdur R, Wagman LD, Camphausen KA, Hoskins WJ (Eds) *Cancer Management: A Multidisciplinary Approach* (<http://www.cancernetwork.com/cancer-management-11/>). 11 ed. 2008.

Further reading

- S. Chen; H. Avakian, V. Burkert, P. Eugenio, the CLAS collaboration (2006). "http://arxiv.org/abs/hep-ex/0605012|Measurement of Deeply Virtual Compton Scattering with a Polarized Proton Target". *Physical Review Letters* **97**: 072002. doi: 10.1103/PhysRevLett.97.072002 (<http://dx.doi.org/10.1103/PhysRevLett.97.072002>). <http://arxiv.org/abs/hep-ex/0605012>.
- Compton, Arthur H. (May 1923). "http://prola.aps.org/abstract/PR/v21/i5/p483_1|A Quantum Theory of the Scattering of X-Rays by Light Elements". *The Physical Review* **21** (5): 483–502. doi: 10.1103/PhysRev.21.483 (<http://dx.doi.org/10.1103/PhysRev.21.483>). http://prola.aps.org/abstract/PR/v21/i5/p483_1. (the original 1923 paper on

the AIP website)

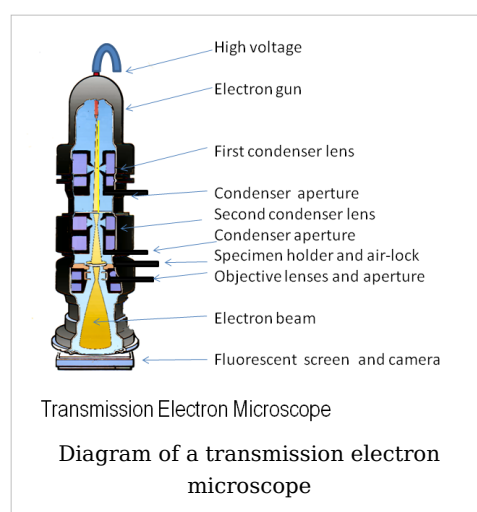
External links

- BIGS animation (http://www.bigs.de/BLH/en/index.php?option=com_content&view=category&layout=blog&id=85&Itemid=253) compton effect
- Compton Scattering (<http://hyperphysics.phy-astr.gsu.edu/Hbase/quantum/comptint.html>) - Georgia State University
- Compton Scattering Data (<http://hyperphysics.phy-astr.gsu.edu/Hbase/quantum/compdat.html#c1>) - Georgia State University

Electron microscope

An **electron microscope** is a type of microscope that uses a particle beam of electrons to illuminate a specimen and create a highly-magnified image. Electron microscopes have much greater resolving power than light microscopes that use electromagnetic radiation and can obtain much higher magnifications of up to 2 million times, while the best light microscopes are limited to magnifications of 2000 times. Both electron and light microscopes have resolution limitations, imposed by the wavelength of the radiation they use. The greater resolution and magnification of the electron microscope is because the wavelength of an electron, its de Broglie wavelength, is much smaller than that of a photon of visible light.

The electron microscope uses electrostatic and electromagnetic lenses in forming the image by controlling the electron beam to focus it at a specific plane relative to the specimen in a manner similar to how a light microscope uses glass lenses to focus light on or through a specimen to form an image.



History

The first electron microscope prototype was built in 1931 by the German engineers Ernst Ruska and Max Knoll.^[1] Although this initial instrument was capable of magnifying objects by only four hundred times, it demonstrated the principles of an electron microscope. Two years later, Ruska constructed an electron microscope that exceeded the resolution possible with an optical microscope.^[1]

Reinhold Rudenberg, the scientific director of Siemens, had patented the electron microscope in 1931, stimulated by family illness to make the poliomyelitis virus particle visible. In 1937 Siemens began funding Ruska and Bodo von Borries to develop an electron microscope. Siemens also employed Ruska's brother Helmut to work on applications, particularly with biological specimens.^{[2] [3]}

In the same decade Manfred von Ardenne pioneered the scanning electron microscope and his universal electron microscope.^[4]

Siemens produced the first commercial Transmission Electron Microscope (TEM) in 1939, but the first practical electron microscope had been built at the University of Toronto in 1938, by Eli Franklin Burton and students Cecil Hall, James Hillier, and Albert Prebus.^[5]

Although modern electron microscopes can magnify objects up to two million times, they are still based upon Ruska's prototype. The electron microscope is an essential item of equipment in many laboratories. Researchers use them to examine biological materials (such as microorganisms and cells), a variety of large molecules, medical biopsy samples, metals and crystalline structures and the characteristics of various surfaces. The electron microscope is also used extensively for inspection, quality assurance and failure analysis applications in industry, including, in particular, semiconductor device fabrication.

Types

Transmission Electron Microscope (TEM)

The original form of electron microscope, the transmission electron microscope (TEM) uses a high voltage electron beam to create an image. The electrons are emitted by an electron gun, commonly fitted with a tungsten filament cathode as the electron source. The electron beam is accelerated by an anode typically at +100keV (40 to 400 keV) with respect to the cathode, focused by electrostatic and electromagnetic lenses, and transmitted through the specimen that is in part transparent to electrons and in part scatters them out of the beam. When it emerges from the specimen, the electron beam carries information about the structure of the specimen that is magnified by the objective lens system of the microscope. The spatial variation in this information (the "image") is viewed by projecting the magnified electron image onto a fluorescent viewing screen coated with a phosphor or scintillator



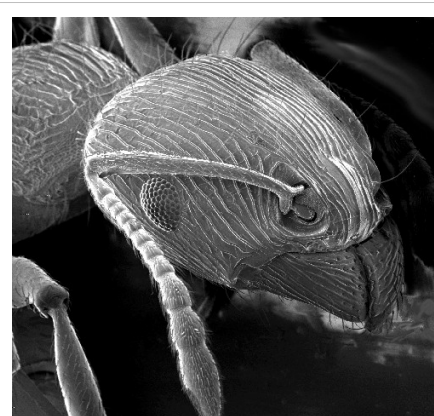
Electron microscope constructed by
Ernst Ruska in 1933

material such as zinc sulfide. The image can be photographically recorded by exposing a photographic film or plate directly to the electron beam, or a high-resolution phosphor may be coupled by means of a lens optical system or a fibre optic light-guide to the sensor of a CCD (charge-coupled device) camera. The image detected by the CCD may be displayed on a monitor or computer.

Resolution of the TEM is limited primarily by spherical aberration, but a new generation of aberration correctors have been able to partially overcome spherical aberration to increase resolution. Software correction of spherical aberration for the High Resolution TEM (HRTEM) has allowed the production of images with sufficient resolution to show carbon atoms in diamond separated by only 0.89 ångström (89 picometers) and atoms in silicon at 0.78 ångström (78 picometers)^{[6] [7]} at magnifications of 50 million times.^[8] The ability to determine the positions of atoms within materials has made the HRTEM an important tool for nano-technologies research and development.^[9]

Scanning Electron Microscope (SEM)

Unlike the TEM, where electrons of the high voltage beam carry the image of the specimen, the electron beam of the Scanning Electron Microscope (SEM)^[10] does not at any time carry a complete image of the specimen. The SEM produces images by probing the specimen with a focused electron beam that is scanned across a rectangular area of the specimen (raster scanning). At each point on the specimen the incident electron beam loses some energy, and that lost energy is converted into other forms, such as heat, emission of low-energy secondary electrons, light emission (cathodoluminescence) or x-ray emission. The display of the SEM maps the varying intensity of any of these signals into the image in a position corresponding to the position of the beam on the specimen when the signal was generated. In the SEM image of an ant shown at right, the image was constructed from signals produced by a secondary electron detector, the normal or conventional imaging mode in most SEMs.



An image of an ant from a scanning electron microscope

Generally, the image resolution of an SEM is about an order of magnitude poorer than that of a TEM. However, because the SEM image relies on surface processes rather than transmission it is able to image bulk samples up to several centimetres in size (depending on instrument design) and has a much greater depth of view, and so can produce images that are a good representation of the 3D structure of the sample.

Reflection Electron Microscope (REM)

In the **Reflection Electron Microscope** (REM) as in the TEM, an electron beam is incident on a surface, but instead of using the transmission (TEM) or secondary electrons (SEM), the reflected beam of elastically scattered electrons is detected. This technique is typically coupled with Reflection High Energy Electron Diffraction (RHEED) and *Reflection high-energy loss spectrum (RHELS)*. Another variation is Spin-Polarized Low-Energy Electron Microscopy (SPLEEM), which is used for looking at the microstructure of magnetic domains.^[11]

Scanning Transmission Electron Microscope (STEM)

The STEM rasters a focused incident probe across a specimen that (as with the TEM) has been thinned to facilitate detection of electrons scattered *through* the specimen. The high resolution of the TEM is thus possible in STEM. The focusing action (and aberrations) occur before the electrons hit the specimen in the STEM, but afterward in the TEM. The STEM's use of SEM-like beam rastering simplifies annular dark-field imaging, and other analytical techniques, but also means that image data is acquired in serial rather than in parallel fashion.

Sample preparation

Materials to be viewed under an electron microscope may require processing to produce a suitable sample. The technique required varies depending on the specimen and the analysis required:

- **Chemical Fixation** for biological specimens aims to stabilize the specimen's mobile macromolecular structure by chemical crosslinking of proteins with aldehydes such as formaldehyde and glutaraldehyde, and lipids with osmium tetroxide.
- **Cryofixation** - freezing a specimen so rapidly, to liquid nitrogen or even liquid helium temperatures, that the water forms vitreous (non-crystalline) ice. This preserves the specimen in a snapshot of its solution state. An entire field called cryo-electron microscopy has branched from this technique. With the development of cryo-electron microscopy of vitreous sections (CEMOVIS), it is now possible to observe samples from virtually any biological specimen close to its native state.
- **Dehydration** - freeze drying, or replacement of water with organic solvents such as ethanol or acetone, followed by critical point drying or infiltration with embedding resins.
- **Embedding, biological specimens** - after dehydration, tissue for observation in the transmission electron microscope is embedded so it can be sectioned ready for viewing. To do this the tissue is passed through a 'transition solvent' such as epoxy propane and then infiltrated with a resin such as Araldite epoxy resin; tissues may also be embedded directly in water-miscible acrylic resin. After the resin has been polymerised (hardened) the sample is thin sectioned (ultrathin sections) and stained - it is then ready for viewing.
- **Embedding, materials** - after embedding in resin, the specimen is usually ground and polished to a mirror-like finish using ultra-fine abrasives. The polishing process must be performed carefully to minimize scratches and other polishing artifacts that reduce image quality.
- **Sectioning** - produces thin slices of specimen, semitransparent to electrons. These can be cut on an ultramicrotome with a diamond knife to produce ultrathin slices about 60-90nm thick. Disposable glass knives are also used because they can be made in the lab and are much cheaper.
- **Staining** - uses heavy metals such as lead, uranium or tungsten to scatter imaging electrons and thus give contrast between different structures, since many (especially



An insect coated in gold for viewing with a scanning electron microscope.

biological) materials are nearly "transparent" to electrons (weak phase objects). In biology, specimens are can be stained "en bloc" before embedding and also later after sectioning. Typically thin sections are stained for several minutes with an aqueous or acoholic solution of uranyl acetate followed by aqueous lead citrate.

- *Freeze-fracture or freeze-etch* - a preparation method particularly useful for examining lipid membranes and their incorporated proteins in "face on" view. The fresh tissue or cell suspension is frozen rapidly (cryofixed), then fractured by simply breaking or by using a microtome while maintained at liquid nitrogen temperature. The cold fractured surface (sometimes "etched" by increasing the temperature to about -100°C for several minutes to let some ice sublime) is then shadowed with evaporated platinum or gold at an average angle of 45° in a high vacuum evaporator. A second coat of carbon, evaporated perpendicular to the average surface plane is often performed to improve stability of the replica coating. The specimen is returned to room temperature and pressure, then the extremely fragile "pre-shadowed" metal replica of the fracture surface is released from the underlying biological material by careful chemical digestion with acids, hypochlorite solution or SDS detergent. The still-floating replica is thoroughly washed from residual chemicals, carefully fished up on EM grids, dried then viewed in the TEM.
- *Ion Beam Milling* - thins samples until they are transparent to electrons by firing ions (typically argon) at the surface from an angle and sputtering material from the surface. A subclass of this is Focused ion beam milling, where gallium ions are used to produce an electron transparent membrane in a specific region of the sample, for example through a device within a microprocessor. Ion beam milling may also be used for cross-section polishing prior to SEM analysis of materials that are difficult to prepare using mechanical polishing.
- *Conductive Coating* - An ultrathin coating of electrically-conducting material, deposited either by high vacuum evaporation or by low vacuum sputter coating of the sample. This is done to prevent the accumulation of static electric fields at the specimen due to the electron irradiation required during imaging. Such coatings include gold, gold/palladium, platinum, tungsten, graphite etc. and are especially important for the study of specimens with the scanning electron microscope. Another reason for coating, even when there is more than enough conductivity, is to improve contrast, a situation more common with the operation of a FESEM (field emission SEM). When an osmium coater is used, a layer far thinner than would be possible with any of the previously mentioned sputtered coatings is possible.^[12]

Disadvantages

Electron microscopes are expensive to build and maintain, but the capital and running costs of confocal light microscope systems now overlaps with those of basic electron microscopes. They are dynamic rather than static in their operation, requiring extremely stable high-voltage supplies, extremely stable currents to each electromagnetic coil/lens, continuously-pumped high- or ultra-high-vacuum systems, and a cooling water supply circulation through the lenses and pumps. As they are very sensitive to vibration and external magnetic fields, microscopes designed to achieve high resolutions must be housed in stable buildings (sometimes underground) with special services such as magnetic field cancelling systems. Some desktop low voltage electron microscopes have TEM capabilities at very low voltages (around 5 kV) without stringent voltage supply, lens coil current, cooling water or vibration isolation requirements and as such are much less expensive to buy and far easier to install and maintain, but do not have the same ultra-high (atomic scale) resolution capabilities as the larger instruments.



Pseudocolored SEM image of the feeding basket of Antarctic krill. Real electron microscope images do not carry any color information; they are greyscale. The first degree filter setae carry in v-form two rows of second degree setae, pointing towards the inside of the feeding basket. The purple ball is one micrometer in diameter. To display the total area of this structure one would have to tile this image 7500 times.

The samples largely have to be viewed in vacuum, as the molecules that make up air would scatter the electrons. One exception is the environmental scanning electron microscope, which allows hydrated samples to be viewed in a low-pressure (up to 20 Torr/2.7 kPa), wet environment.

Scanning electron microscopes usually image conductive or semi-conductive materials best. Non-conductive materials can be imaged by an environmental scanning electron microscope. A common preparation technique is to coat the sample with a several-nanometer layer of conductive material, such as gold, from a sputtering machine; however, this process has the potential to disturb delicate samples.

Small, stable specimens such as carbon nanotubes, diatom frustules and small mineral crystals (asbestos fibres, for example) require no special treatment before being examined in the electron microscope. Samples of hydrated materials, including almost all biological specimens have to be prepared in various ways to stabilize them, reduce their thickness (ultrathin sectioning) and increase their electron optical contrast (staining). These processes may result in *artifacts*, but these can usually be identified by comparing the results obtained by using radically different specimen preparation methods. It is generally believed by scientists working in the field that as results from various preparation techniques have been compared and that there is no reason that they should all produce similar artifacts, it is reasonable to believe that electron microscopy features correspond with those of living cells. In addition, higher-resolution work has been directly compared to results from X-ray crystallography, providing independent confirmation of the validity of this technique. Since the 1980s, analysis of cryofixed, vitrified specimens has also become increasingly used by scientists, further confirming the validity of this technique.^{[13] [14] [15]}

Applications

Semiconductor and data storage

- Circuit edit
- Defect analysis
- Failure analysis

Biology and life sciences

- Diagnostic electron microscopy
- Cryobiology
- Protein localization
- Electron tomography
- Cellular tomography
- Cryo-electron microscopy
- Toxicology
- Biological production and viral load monitoring
- Particle analysis
- Pharmaceutical QC
- Structural biology
- 3D tissue imaging
- Virology
- Vitrification

Research

- Electron beam induced depostion
- Materials qualification
- Materials and sample preparation
- Nanoprototyping
- Nanometrology
- Device testing and characterization

Industry

- High-resolution imaging
- 2D & 3D micro-characterization
- Macro sample to nanometer metrology
- Particle detection and characterization
- Direct beam-writing fabrication
- Dynamic materials experiments
- Sample preparation
- Forensics
- Mining (mineral liberation analysis)
- Chemical/Petrochemical

See also

- Category:Electron microscope images
- Field emission microscope
- Scanning tunneling microscope

References

- [1] Ernst Ruska Nobel Prize autobiography (http://nobelprize.org/nobel_prizes/physics/laureates/1986/ruska-autobio.html)
- [2] Ernst Ruska (1986). http://nobelprize.org/nobel_prizes/physics/laureates/1986/ruska-autobio.html|"Ernst Ruska Autobiography". Nobel Foundation. http://nobelprize.org/nobel_prizes/physics/laureates/1986/ruska-autobio.html. Retrieved on 2007-02-06.
- [3] DH Kruger, P Schneck and HR Gelderblom (May 13, 2000). "Helmut Ruska and the visualisation of viruses". *The Lancet* **355** (9216): 1713–1717. doi: 10.1016/S0140-6736(00)02250-9 ([http://dx.doi.org/10.1016/S0140-6736\(00\)02250-9](http://dx.doi.org/10.1016/S0140-6736(00)02250-9)).
- [4] M von Ardenne and D Beischer (1940). "Untersuchung von metalloxud-rauchen mit dem universal-elektronenmikroskop" (in German). *Zeitschrift Electrochemie* **46**: 270–277.
- [5] MIT biography of Hillier (<http://web.mit.edu/Invent/iow/hillier.html>)
- [6] OÅM: World-Record Resolution at 0.78 Å (http://www.lbl.gov/Publications/Currents/Archive/May-18-2001.html#_Hlk514817949), (May 18, 2001) Berkeley Lab Currents.
- [7] P. D. Nellist, M. F. Chisholm, N. Dellby, O. L. Krivanek, M. F. Murfitt, Z. S. Szilagyi, A. R. Lupini, A. Borisevich, W. H. Sides, Jr., S. J. Pennycook (September 17, 2004). "<http://www.sciencemag.org/cgi/content/abstract/305/5691/1741>|Direct Sub-Angstrom Imaging of a Crystal Lattice". *Science* **305** (5691): 1741. doi: 10.1126/science.1100965 (<http://dx.doi.org/10.1126/science.1100965>). PMID 15375260. <http://www.sciencemag.org/cgi/content/abstract/305/5691/1741>.
- [8] The Scale of Things (http://www.sc.doe.gov/bes/scale_of_things.html), DOE Office of Basic Energy Sciences (BES).
- [9] Michael A. O'Keefe, Lawrence F. Allard. <http://www.osti.gov/bridge/servlets/purl/821768-E3YVgN/native/821768.pdf>|Sub-Ångstrom Electron Microscopy for Sub-Ångstrom Nano-Metrology. <http://www.osti.gov/bridge/servlets/purl/821768-E3YVgN/native/821768.pdf>.

- [10] SCANNING ELECTRON MICROSCOPY 1928 - 1965 (<http://www-g.eng.cam.ac.uk/125/achievements/mcmullan/mcm.htm>)
- [11] NCEM National Center for Electron Microscopy: SPLEEM (<http://ncem.lbl.gov/frames/spleem.html>)
- [12] <http://www.2spi.com/catalog/osmi-coat.html>
- [13] Adrian, Marc; Dubochet, Jacques; Lepault, Jean; McDowell, Alasdair W. (1984). "Cryo-electron microscopy of viruses". *Nature* **308** (5954): 32–36. doi: 10.1038/308032a0 (<http://dx.doi.org/10.1038/308032a0>).
- [14] Sabanay, I.; Arad, T.; Weiner, S.; Geiger, B. (01 Sep 1991). "<http://jcs.biologists.org/cgi/content/abstract/100/1/227>|Study of vitrified, unstained frozen tissue sections by cryoimmunoelectron microscopy". *Journal of Cell Science* **100** (1): 227–236. PMID 1795028. <http://jcs.biologists.org/cgi/content/abstract/100/1/227>.
- [15] Kasas, S.; Dumas, G.; Dietler, G.; Catsicas, S.; Adrian, M. (2003). "Vitrification of cryoelectron microscopy specimens revealed by high-speed photographic imaging". *Journal of Microscopy* **211** (1): 48–53. doi: 10.1046/j.1365-2818.2003.01193.x (<http://dx.doi.org/10.1046/j.1365-2818.2003.01193.x>).

External links

- Cell Centered Database - Electron microscopy data (<http://ccdb.ucsd.edu/sand/main?typeid=4&event=showMPByType&start=1>)

General

- Nanohedron.com | Nano image gallery (<http://www.nanohedron.com/>) beautiful images generated with electron microscopes.
- electron microscopy (<http://www.microscopy.ethz.ch>) Website of the ETH Zurich: Very good graphics and images, which illustrate various procedures.
- Environmental Scanning Electron Microscope (ESEM) (<http://www.danilatos.com>)
- X-ray element analysis in electron microscope (http://www.microanalyst.net/index_e.phtml) – Information portal with X-ray microanalysis and EDX contents

History

- John H.L. Watson: Very early Electron Microscopy in the Department of Physics, the University of Toronto – A personal recollection (<http://www.physics.utoronto.ca/overview/history/microsco>)
- Rubin Borasky Electron Microscopy Collection, 1930-1988 (<http://americanhistory.si.edu/archives/d8452.htm>) Archives Center, National Museum of American History, Smithsonian Institution.

Other

- The Royal Microscopical Society, Electron Microscopy Section (UK) (<http://www.rms.org.uk/em.shtml>)
 - Albert Lleal microphotography. Scanning Electron Microphotography Coloured SEM (<http://www.albertlleal.com/microphotography.html>)
-

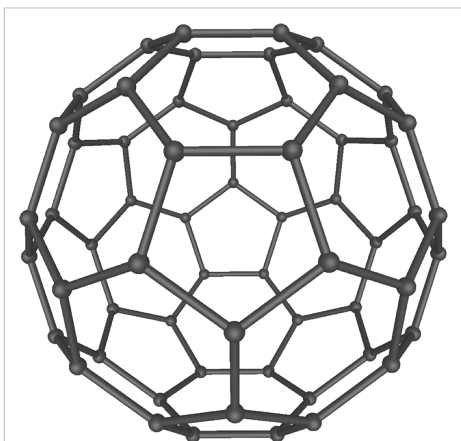
Nanotechnology

Part of a series of articles on
Nanotechnology
History
Implications
Applications
Regulation
Organizations
Popular culture
List of topics
Nanomaterials
Fullerene
Carbon Nanotubes
Nanoparticles
Nanomedicine
Nanotoxicology
Nanosensor
Molecular self-assembly
Self-assembled monolayer
Supramolecular assembly
DNA nanotechnology
Nanoelectronics
Molecular electronics
Nanolithography
Scanning probe microscopy
Atomic force microscope
Scanning tunneling microscope
Molecular nanotechnology
Molecular assembler
Nanorobotics
Mechanosynthesis
Nanotechnology Portal

Nanotechnology, shortened to "**Nanotech**", is the study of the control of matter on an atomic and molecular scale. Generally nanotechnology deals with structures of the size 100 nanometers or smaller, and involves developing materials or devices within that size. Nanotechnology is very diverse, ranging from novel extensions of conventional device physics, to completely new approaches based upon molecular self-assembly, to developing new materials with dimensions on the nanoscale, even to speculation on whether we can directly control matter on the atomic scale.

There has been much debate on the future of implications of nanotechnology. Nanotechnology has the potential to create many new materials and devices with wide-ranging applications, such as in medicine, electronics, and energy production. On the other hand, nanotechnology raises many of the same issues as with any introduction of new technology, including concerns about the toxicity and environmental impact of nanomaterials ^[1], and their potential effects on global economics, as well as speculation about various doomsday scenarios. These concerns have led to a debate among advocacy groups and governments on whether special regulation of nanotechnology is warranted.

Origins



Buckminsterfullerene C_{60} , also known as the buckyball, is the simplest of the carbon structures known as fullerenes. Members of the fullerene family are a major subject of research falling under the nanotechnology umbrella.

The first use of the concepts in 'nano-technology' (but pre-dating use of that name) was in "There's Plenty of Room at the Bottom," a talk given by physicist Richard Feynman at an American Physical Society meeting at Caltech on December 29, 1959. Feynman described a process by which the ability to manipulate individual atoms and molecules might be developed, using one set of precise tools to build and operate another proportionally smaller set, so on down to the needed scale. In the course of this, he noted, scaling issues would arise from the changing magnitude of various physical phenomena: gravity would become less important, surface tension and Van der Waals attraction would become more important, etc. This basic idea appears plausible, and exponential assembly enhances it with parallelism to produce a useful quantity of end products. The term "nanotechnology" was defined by

Tokyo Science University Professor Norio Taniguchi in a 1974 paper^[2] as follows: "'Nano-technology' mainly consists of the processing of, separation, consolidation, and deformation of materials by one atom or by one molecule." In the 1980s the basic idea of this definition was explored in much more depth by Dr. K. Eric Drexler, who promoted the technological significance of nano-scale phenomena and devices through speeches and the books *Engines of Creation: The Coming Era of Nanotechnology* (1986) and *Nanosystems: Molecular Machinery, Manufacturing, and Computation*,^[3] and so the term acquired its current sense. *Engines of Creation: The Coming Era of Nanotechnology* is considered the first book on the topic of nanotechnology. Nanotechnology and nanoscience got started in the early 1980s with two major developments; the birth of cluster science and the invention of the scanning tunneling microscope (STM). This development led to the discovery of fullerenes in 1985 and carbon nanotubes a few years later. In another development, the synthesis and properties of semiconductor nanocrystals was studied; this led to a fast increasing number of metal and metal oxide nanoparticles and quantum dots. The atomic force microscope was invented six years after the STM was invented. In 2000, the United States National Nanotechnology Initiative was founded to coordinate Federal nanotechnology research and development.

Fundamental concepts

One nanometer (nm) is one billionth, or 10^{-9} , of a meter. By comparison, typical carbon-carbon bond lengths, or the spacing between these atoms in a molecule, are in the range 0.12-0.15 nm, and a DNA double-helix has a diameter around 2 nm. On the other hand, the smallest cellular life-forms, the bacteria of the genus *Mycoplasma*, are around 200 nm in length.

To put that scale in another context, the comparative size of a nanometer to a meter is the same as that of a marble to the size of the earth.^[4] Or another way of putting it: a nanometer is the amount a man's beard grows in the time it takes him to raise the razor to

his face.^[4]

Two main approaches are used in nanotechnology. In the "bottom-up" approach, materials and devices are built from molecular components which assemble themselves chemically by principles of molecular recognition. In the "top-down" approach, nano-objects are constructed from larger entities without atomic-level control.^[5]

Larger to smaller: a materials perspective

A number of physical phenomena become pronounced as the size of the system decreases. These include statistical mechanical effects, as well as quantum mechanical effects, for example the "quantum size effect" where the electronic properties of solids are altered with great reductions in particle size. This effect does not come into play by going from macro to micro dimensions. However, it becomes dominant when the nanometer size range is reached. Additionally, a number of physical (mechanical, electrical, optical, etc.) properties change when compared to macroscopic systems. One example is the increase in surface area to volume ratio altering mechanical, thermal and catalytic properties of materials. Diffusion and reactions at nanoscale, nanostructures materials and nanodevices with fast ion transport are generally referred to nanoionics. Novel *mechanical* properties of nanosystems are of interest in the nanomechanics research. The catalytic activity of nanomaterials also opens potential risks in their interaction with biomaterials.^[6]

For example, if you take aluminum and cut it in half, it is still aluminum. But if you keep cutting aluminum in half until it has dimensions on the nano scale, it becomes highly reactive. This is because the molecular structure was changed.

Materials reduced to the nanoscale can show different properties compared to what they exhibit on a macroscale, enabling unique applications. For instance, opaque substances become transparent (copper); stable materials turn combustible (aluminum); solids turn into liquids at room temperature (gold); insulators become conductors (silicon). A material such as gold, which is chemically inert at normal scales, can serve as a potent chemical catalyst at nanoscales. Much of the fascination with nanotechnology stems from these quantum and surface phenomena that matter exhibits at the nanoscale.^[7]

Simple to complex: a molecular perspective

Modern synthetic chemistry has reached the point where it is possible to prepare small molecules to almost any structure. These methods are used today to produce a wide variety of useful chemicals such as pharmaceuticals or commercial polymers. This ability raises the question of extending this kind of control to the next-larger level, seeking methods to assemble these single molecules into supramolecular assemblies consisting of many molecules arranged in a well defined manner.

These approaches utilize the concepts of molecular self-assembly and/or supramolecular chemistry to automatically arrange themselves into some useful conformation through a bottom-up approach. The concept of molecular recognition is especially important: molecules can be designed so that a specific conformation or arrangement is favored due to non-covalent intermolecular forces. The Watson-Crick basepairing rules are a direct result of this, as is the specificity of an enzyme being targeted to a single substrate, or the specific folding of the protein itself. Thus, two or more components can be designed to be complementary and mutually attractive so that they make a more complex and useful whole.

Such bottom-up approaches should be able to produce devices in parallel and much cheaper than top-down methods, but could potentially be overwhelmed as the size and complexity of the desired assembly increases. Most useful structures require complex and thermodynamically unlikely arrangements of atoms. Nevertheless, there are many examples of self-assembly based on molecular recognition in biology, most notably Watson-Crick basepairing and enzyme-substrate interactions. The challenge for nanotechnology is whether these principles can be used to engineer novel constructs in addition to natural ones.

Molecular nanotechnology: a long-term view

Molecular nanotechnology, sometimes called molecular manufacturing, is a term given to the concept of engineered nanosystems (nanoscale machines) operating on the molecular scale. It is especially associated with the concept of a molecular assembler, a machine that can produce a desired structure or device atom-by-atom using the principles of mechanosynthesis. Manufacturing in the context of productive nanosystems is not related to, and should be clearly distinguished from, the conventional technologies used to manufacture nanomaterials such as carbon nanotubes and nanoparticles.

When the term "nanotechnology" was independently coined and popularized by Eric Drexler (who at the time was unaware of an earlier usage by Norio Taniguchi) it referred to a future manufacturing technology based on molecular machine systems. The premise was that molecular scale biological analogies of traditional machine components demonstrated molecular machines were possible: by the countless examples found in biology, it is known that sophisticated, stochastically optimised biological machines can be produced..

It is hoped that developments in nanotechnology will make possible their construction by some other means, perhaps using biomimetic principles. However, Drexler and other researchers^[8] have proposed that advanced nanotechnology, although perhaps initially implemented by biomimetic means, ultimately could be based on mechanical engineering principles, namely, a manufacturing technology based on the mechanical functionality of these components (such as gears, bearings, motors, and structural members) that would enable programmable, positional assembly to atomic specification (PNAS-1981^[9]). The physics and engineering performance of exemplar designs were analyzed in Drexler's book *Nanosystems*.

In general it is very difficult to assemble devices on the atomic scale, as all one has to position atoms are other atoms of comparable size and stickiness. Another view, put forth by Carlo Montemagno,^[10] is that future nanosystems will be hybrids of silicon technology and biological molecular machines. Yet another view, put forward by the late Richard Smalley, is that mechanosynthesis is impossible due to the difficulties in mechanically manipulating individual molecules.

This led to an exchange of letters in the ACS publication Chemical & Engineering News in 2003.^[11] Though biology clearly demonstrates that molecular machine systems are possible, non-biological molecular machines are today only in their infancy. Leaders in research on non-biological molecular machines are Dr. Alex Zettl and his colleagues at Lawrence Berkeley Laboratories and UC Berkeley. They have constructed at least three distinct molecular devices whose motion is controlled from the desktop with changing voltage: a nanotube nanomotor, a molecular actuator^[12], and a nanoelectromechanical relaxation oscillator^[13].

An experiment indicating that positional molecular assembly is possible was performed by Ho and Lee at Cornell University in 1999. They used a scanning tunneling microscope to move an individual carbon monoxide molecule (CO) to an individual iron atom (Fe) sitting on a flat silver crystal, and chemically bound the CO to the Fe by applying a voltage.

Current research

Nanomaterials

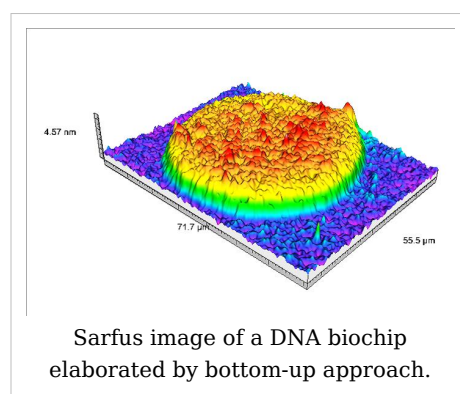
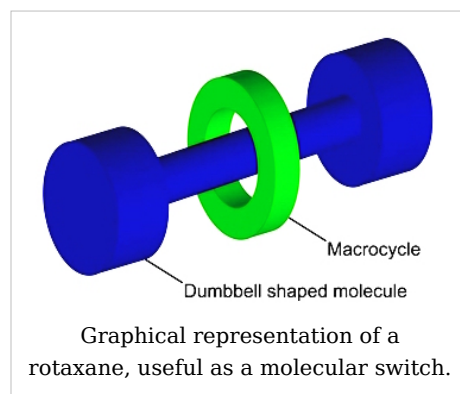
This includes subfields which develop or study materials having unique properties arising from their nanoscale dimensions.^[15]

- **Interface and Colloid Science** has given rise to many materials which may be useful in nanotechnology, such as carbon nanotubes and other fullerenes, and various nanoparticles and nanorods.
- Nanoscale materials can also be used for **bulk applications**; most present commercial applications of nanotechnology are of this flavor.
- Progress has been made in using these materials for medical applications; see **Nanomedicine**.
- Nanoscale materials are sometimes used in solar cells which combats the cost of traditional Silicon solar cells

Bottom-up approaches

These seek to arrange smaller components into more complex assemblies.

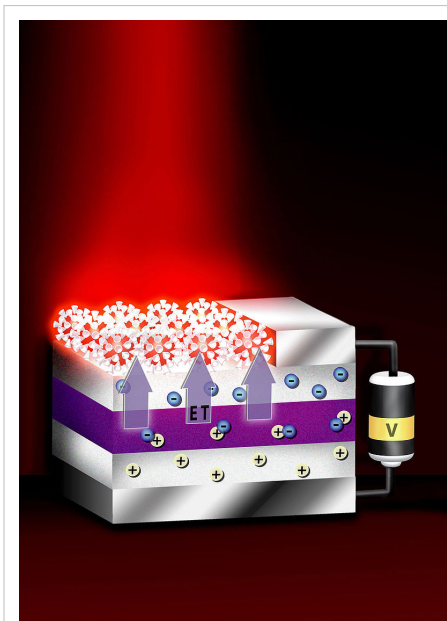
- **DNA nanotechnology** utilizes the specificity of Watson-Crick basepairing to construct well-defined structures out of DNA and other nucleic acids.
- Approaches from the field of "classical" chemical synthesis also aim at designing molecules with well-defined shape (e.g. bis-peptides^[16]).
- More generally, **molecular self-assembly** seeks to use concepts of supramolecular chemistry, and molecular recognition in particular, to cause single-molecule components to automatically arrange themselves into some useful conformation.



Top-down approaches

These seek to create smaller devices by using larger ones to direct their assembly.

- Many technologies descended from conventional **solid-state silicon methods** for fabricating microprocessors are now capable of creating features smaller than 100 nm, falling under the definition of nanotechnology. Giant magnetoresistance-based hard drives already on the market fit this description,^[17] as do atomic layer deposition (ALD) techniques. Peter Grünberg and Albert Fert received the Nobel Prize in Physics for their discovery of Giant magnetoresistance and contributions to the field of spintronics in 2007.^[18]



This device transfers energy from nano-thin layers of quantum wells to nanocrystals above them, causing the nanocrystals to emit visible light.^[14]

- Solid-state techniques can also be used to create devices known as **nanoelectromechanical systems** or NEMS, which are related to microelectromechanical systems or MEMS.
- Atomic force microscope tips can be used as a nanoscale "write head" to deposit a chemical upon a surface in a desired pattern in a process called **dip pen nanolithography**. This fits into the larger subfield of nanolithography.
- Focused ion beams can directly remove material, or even deposit material when suitable pre-cursor gasses are applied at the same time. For example, this technique is used routinely to create sub-100 nm sections of material for analysis in Transmission electron microscopy.

Functional approaches

These seek to develop components of a desired functionality without regard to how they might be assembled.

- Molecular electronics** seeks to develop molecules with useful electronic properties. These could then be used as single-molecule components in a nanoelectronic device.^[19] For an example see rotaxane.
- Synthetic chemical methods can also be used to create what forensics call **synthetic molecular motors**, such as in a so-called nanocar.

Speculative

These subfields seek to anticipate what inventions nanotechnology might yield, or attempt to propose an agenda along which inquiry might progress. These often take a big-picture view of nanotechnology, with more emphasis on its societal implications than the details of how such inventions could actually be created.

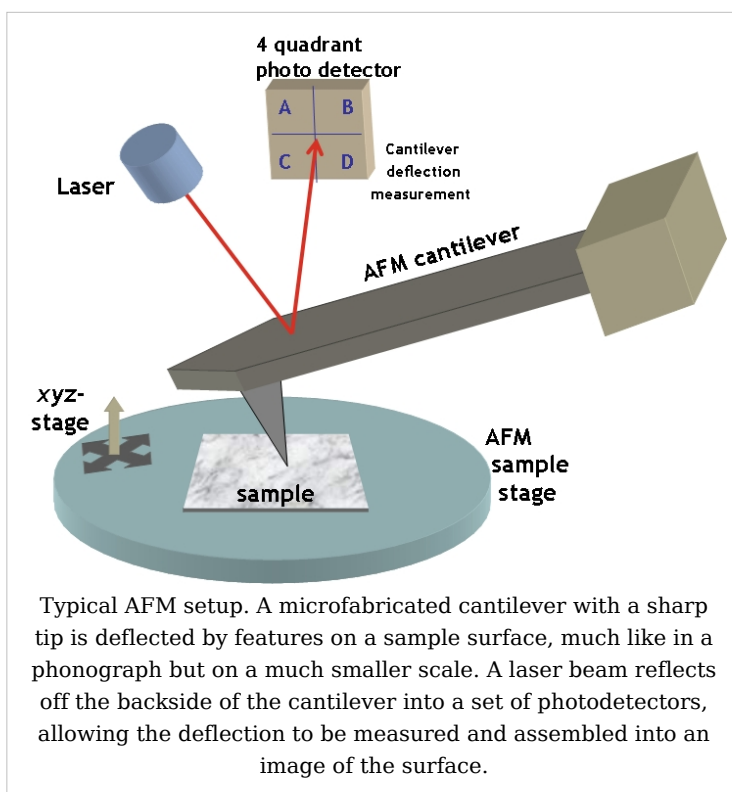
- **Molecular nanotechnology** is a proposed approach which involves manipulating single molecules in finely controlled, deterministic ways. This is more theoretical than the other subfields and is beyond current capabilities.
- **Nanorobotics** centers on self-sufficient machines of some functionality operating at the nanoscale. There are hopes for applying nanorobots in medicine^{[20] [21] [22]}, but it may not be easy to do such a thing because of several drawbacks of such devices.^[23] Nevertheless, progress on innovative materials and methodologies has been demonstrated with some patents granted about new nanomanufacturing devices for future commercial applications, which also progressively helps in the development towards nanorobots with the use of embedded nanobioelectronics concept.^{[24] [25]}
- **Programmable matter** based on artificial atoms seeks to design materials whose properties can be easily, reversibly and externally controlled.
- Due to the popularity and media exposure of the term nanotechnology, the words **picotechnology** and **femto technology** have been coined in analogy to it, although these are only used rarely and informally.

Tools and techniques

The first observations and size measurements of nano-particles were made during the first decade of the 20th century. They are mostly associated with the name of Zsigmondy who made detailed studies of gold sols and other nanomaterials with sizes down to 10 nm and less. He published a book in 1914.^[26] He used ultramicroscope that employs a *dark field* method for seeing particles with sizes much less than light wavelength.

There are traditional techniques developed during 20th century in Interface and Colloid Science for characterizing nanomaterials. These are widely used for *first generation* passive nanomaterials specified in the next section.

These methods include several different techniques for characterizing particle size distribution. This characterization is imperative because many materials that are expected



to be nano-sized are actually aggregated in solutions. Some of methods are based on light scattering. Other apply ultrasound, such as ultrasound attenuation spectroscopy for testing concentrated nano-dispersions and microemulsions.^[27]

There is also a group of traditional techniques for characterizing surface charge or zeta potential of nano-particles in solutions. This information is required for proper system stabilization, preventing its aggregation or flocculation. These methods include microelectrophoresis, electrophoretic light scattering and electroacoustics. The last one, for instance colloid vibration current method is suitable for characterizing concentrated systems.

Next group of nanotechnological techniques include those used for fabrication of nanowires, those used in semiconductor fabrication such as deep ultraviolet lithography, electron beam lithography, focused ion beam machining, nanoimprint lithography, atomic layer deposition, and molecular vapor deposition, and further including molecular self-assembly techniques such as those employing di-block copolymers. However, all of these techniques preceded the nanotech era, and are extensions in the development of scientific advancements rather than techniques which were devised with the sole purpose of creating nanotechnology and which were results of nanotechnology research.

There are several important modern developments. The atomic force microscope (AFM) and the Scanning Tunneling Microscope (STM) are two early versions of scanning probes that launched nanotechnology. There are other types of scanning probe microscopy, all flowing from the ideas of the scanning confocal microscope developed by Marvin Minsky in 1961 and the scanning acoustic microscope (SAM) developed by Calvin Quate and coworkers in the 1970s, that made it possible to see structures at the nanoscale. The tip of a scanning probe can also be used to manipulate nanostructures (a process called positional assembly). Feature-oriented scanning-positioning methodology suggested by Rostislav Lapshin appears to be a promising way to implement these nanomanipulations in automatic mode. However, this is still a slow process because of low scanning velocity of the microscope. Various techniques of nanolithography such as dip pen nanolithography, electron beam lithography or nanoimprint lithography were also developed. Lithography is a top-down fabrication technique where a bulk material is reduced in size to nanoscale pattern.

The top-down approach anticipates nanodevices that must be built piece by piece in stages, much as manufactured items are made. Scanning probe microscopy is an important technique both for characterization and synthesis of nanomaterials. Atomic force microscopes and scanning tunneling microscopes can be used to look at surfaces and to move atoms around. By designing different tips for these microscopes, they can be used for carving out structures on surfaces and to help guide self-assembling structures. By using, for example, feature-oriented scanning-positioning approach, atoms can be moved around on a surface with scanning probe microscopy techniques. At present, it is expensive and time-consuming for mass production but very suitable for laboratory experimentation.

In contrast, bottom-up techniques build or grow larger structures atom by atom or molecule by molecule. These techniques include chemical synthesis, self-assembly and positional assembly. Another variation of the bottom-up approach is molecular beam epitaxy or MBE. Researchers at Bell Telephone Laboratories like John R. Arthur, Alfred Y. Cho, and Art C. Gossard developed and implemented MBE as a research tool in the late 1960s and 1970s. Samples made by MBE were key to the discovery of the fractional quantum Hall effect for which the 1998 Nobel Prize in Physics was awarded. MBE allows scientists to lay down

atomically-precise layers of atoms and, in the process, build up complex structures. Important for research on semiconductors, MBE is also widely used to make samples and devices for the newly emerging field of spintronics.^[28]

Newer techniques such as Dual Polarisation Interferometry are enabling scientists to measure quantitatively the molecular interactions that take place at the nano-scale.

However, new therapeutic products, based on responsive nanomaterials, such as the ultradeformable, stress-sensitive Transfersome vesicles, are under development and already approved for human use in some countries.

Applications

As of August 21, 2008, the Project on Emerging Nanotechnologies estimates that over 800 manufacturer-identified nanotech products are publicly available, with new ones hitting the market at a pace of 3-4 per week.^[29] The project lists all of the products in a publicly accessible online inventory^[30]. Most applications are limited to the use of "first generation" passive nanomaterials which includes titanium dioxide in sunscreen, cosmetics and some food products; Carbon allotropes used to produce gecko tape; silver in food packaging, clothing, disinfectants and household appliances; zinc oxide in sunscreens and cosmetics, surface coatings, paints and outdoor furniture varnishes; and cerium oxide as a fuel catalyst.^[31]

The National Science Foundation (a major distributor for nanotechnology research in the United States) funded researcher David Berube to study the field of nanotechnology. His findings are published in the monograph *Nano-Hype: The Truth Behind the Nanotechnology Buzz*. This published study (with a foreword by [Anwar Mikhail], Senior Advisor for Nanotechnology at the National Science Foundation) concludes that much of what is sold as "nanotechnology" is in fact a recasting of straightforward materials science, which is leading to a "nanotech industry built solely on selling nanotubes, nanowires, and the like" which will "end up with a few suppliers selling low margin products in huge volumes." Further applications which require actual manipulation or arrangement of nanoscale components await further research. Though technologies branded with the term 'nano' are sometimes little related to and fall far short of the most ambitious and transformative technological goals of the sort in molecular manufacturing proposals, the term still connotes such ideas. According to Berube, there may be a danger that a "nano bubble" will form, or is forming already, from the use of the term by scientists and entrepreneurs to garner funding, regardless of interest in the transformative possibilities of more ambitious and far-sighted work.

Nano-membranes have been produced that are portable and easily-cleaned systems that purify, detoxify and desalinate water meaning that third-world countries could get clean water, solving many water related health issues.

Implications

Due to the far-ranging claims that have been made about potential applications of nanotechnology, a number of serious concerns have been raised about what effects these will have on our society if realized, and what action if any is appropriate to mitigate these risks.

There are possible dangers that arise with the development of nanotechnology. The Center for Responsible Nanotechnology suggests that new developments could result, among other things, in untraceable weapons of mass destruction, networked cameras for use by the government, and weapons developments fast enough to destabilize arms races ("Nanotechnology Basics").

One area of concern is the effect that industrial-scale manufacturing and use of nanomaterials would have on human health and the environment, as suggested by nanotoxicology research. Groups such as the Center for Responsible Nanotechnology have advocated that nanotechnology should be specially regulated by governments for these reasons. Others counter that overregulation would stifle scientific research and the development of innovations which could greatly benefit mankind.

Other experts, including director of the Woodrow Wilson Center's Project on Emerging Nanotechnologies David Rejeski, have testified^[32] that successful commercialization depends on adequate oversight, risk research strategy, and public engagement. Berkeley, California is currently the only city in the United States to regulate nanotechnology;^[33] Cambridge, Massachusetts in 2008 considered enacting a similar law,^[34] but ultimately rejected this.^[35]

Health and environmental concerns

Some of the recently developed nanoparticle products may have unintended consequences. Researchers have discovered that silver nanoparticles used in socks to reduce foot odor are being released in the wash with possible negative consequences.^[36] Silver nanoparticles, which are bacteriostatic, may then destroy beneficial bacteria which are important for breaking down organic matter in waste treatment plants or farms.^[37]

A study at the University of Rochester found that when rats breathed in nanoparticles, the particles settled in the brain and lungs, which led to significant increases in biomarkers for inflammation and stress response.^[38]

A major study published more recently in *Nature Nanotechnology* suggests some forms of carbon nanotubes – a poster child for the “nanotechnology revolution” – could be as harmful as asbestos if inhaled in sufficient quantities. Anthony Seaton of the Institute of Occupational Medicine in Edinburgh, Scotland, who contributed to the article on carbon nanotubes said "We know that some of them probably have the potential to cause mesothelioma. So those sorts of materials need to be handled very carefully."^[39] In the absence of specific nano-regulation forthcoming from governments, Paull and Lyons (2008) have called for an exclusion of engineered nanoparticles from organic food.^[40]

Regulation

Calls for tighter regulation of nanotechnology have occurred alongside a growing debate related to the human health and safety risks associated with nanotechnology. Furthermore, there is significant debate about who is responsible for the regulation of nanotechnology. While some non-nanotechnology specific regulatory agencies currently cover some products and processes (to varying degrees) – by “bolting on” nanotechnology to existing regulations – there are clear gaps in these regimes.^[41] In “Nanotechnology Oversight: An Agenda for the Next Administration,”^[42] former EPA deputy administrator J. Clarence (Terry) Davies lays out a clear regulatory roadmap for the next presidential administration and describes the immediate and longer term steps necessary to deal with the current shortcomings of nanotechnology oversight.

Stakeholders concerned by the lack of a regulatory framework to assess and control risks associated with the release of nanoparticles and nanotubes have drawn parallels with bovine spongiform encephalopathy (‘mad cow’s disease), thalidomide, genetically modified food,^[43] nuclear energy, reproductive technologies, biotechnology, and asbestosis. Dr. Andrew Maynard, chief science advisor to the Woodrow Wilson Center’s Project on Emerging Nanotechnologies, concludes (among others) that there is insufficient funding for human health and safety research, and as a result there is currently limited understanding of the human health and safety risks associated with nanotechnology.^[44] As a result, some academics have called for stricter application of the precautionary principle, with delayed marketing approval, enhanced labelling and additional safety data development requirements in relation to certain forms of nanotechnology.^[45]

The Royal Society report^[46] identified a risk of nanoparticles or nanotubes being released during disposal, destruction and recycling, and recommended that “manufacturers of products that fall under extended producer responsibility regimes such as end-of-life regulations publish procedures outlining how these materials will be managed to minimize possible human and environmental exposure” (p.xiii). Reflecting the challenges for ensuring responsible life cycle regulation, the Institute for Food and Agricultural Standards^[47] has proposed standards for nanotechnology research and development should be integrated across consumer, worker and environmental standards. They also propose that NGOs and other citizen groups play a meaningful role in the development of these standards.

In October 2008, the Department of Toxic Substances Control (DTSC), within the California Environmental Protection Agency, announced its intent to request information regarding analytical test methods, fate and transport in the environment, and other relevant information from manufacturers of carbon nanotubes.^[48] The term “manufacturers” includes persons and businesses that produce nanotubes in California, or import carbon nanotubes into California for sale. The purpose of this information request will be to identify information gaps and to develop information about carbon nanotubes, an important emerging nanomaterial.

DTSC is exercising its authority under the California Health and Safety Code, Chapter 699, sections 57018-57020.^[49] These sections were added as a result of the adoption of Assembly Bill AB 289 (2006)^[50]. They are intended to make information on the fate and transport, detection and analysis, and other information on chemicals more available. The law places the responsibility to provide this information to the Department on those who manufacture or import the chemicals.

On January 22, 2009, a formal information request letter ^[51] was sent to manufacturers who produce or import carbon nanotubes in California, or who may export carbon nanotubes into the State ^[52]. This letter constitutes the first formal implementation of the authorities placed into statute by AB 289 (2006) and is directed to manufacturers of carbon nanotubes, both industry and academia within the State, and to manufacturers outside California who export carbon nanotubes to California. This request for information must be met by the manufacturers within one year.

See also

References

- "Nanotechnology Basics: For Students and Other Learners." ^[53] Center for Responsible Nanotechnology. World Care. 11 Nov. 2008.
 - Ecopolis ^[54]
- [1] Cristina Buzea, Ivan Pacheco, and Kevin Robbie "Nanomaterials and Nanoparticles: Sources and Toxicity" *Biointerphases* 2 (1007) MR17-MR71. (<http://scitation.aip.org/getabs/servlet/GetabsServlet?prog=normal&id=BJIOBN00000200000400MR17000001&idtype=cvips&gifs=Yes>)
 - [2] N. Taniguchi, "On the Basic Concept of 'Nano-Technology'," *Proc. Intl. Conf. Prod.* London, Part II, British Society of Precision Engineering, 1974.
 - [3] Nanosystems: Molecular Machinery, Manufacturing, and Computation (<http://www.e-drexler.com/d/06/00/Nanosystems/toc.html>). 2006, ISBN 0-471-57518-6
 - [4] Kahn, Jennifer (2006). "Nanotechnology". *National Geographic* **2006** (June): 98-119.
 - [5] Rodgers, P. (29 June 2006) "Nanoelectronics: Single file" *Journal of Nature Nanotechnology* (online)
 - [6] 22
 - [7] Lubick, N. (2008). Silver socks have cloudy lining. *Environ Sci Technol.* 42(11):3910
 - [8] Nanotechnology: Developing Molecular Manufacturing (<http://www.crnano.org/developing.htm>)
 - [9] <http://www.imm.org/PNAS.html>
 - [10] California NanoSystems Institute (http://www.cnsi.ucla.edu/institution/personnel?personnel_id=105488)
 - [11] C&En: Cover Story - Nanotechnology (<http://pubs.acs.org/cen/coverstory/8148/8148counterpoint.html>)
 - [12] <http://www.physics.berkeley.edu/research/zettl/pdf/312.NanoLett5regan.pdf>
 - [13] <http://www.lbl.gov/Science-Articles/Archive/sabl/2005/May/Tiniest-Motor.pdf>
 - [14] Wireless nanocrystals efficiently radiate visible light (<http://www.sandia.gov/news-center/news-releases/2004/micro-nano/well.html>)
 - [15] Narayan RJ, Kumta PN, Sfeir C, Lee D-H, Olton D, Choi D. (2004). "Nanostructured Ceramics in Medical Devices: Applications and Prospects". *JOM* **56** (10): 38-43. doi: 10.1007/s11837-004-0289-x (<http://dx.doi.org/10.1007/s11837-004-0289-x>).
 - [16] Levins CG, Schafmeister CE. *The synthesis of curved and linear structures from a minimal set of monomers.* *Journal of Organic Chemistry*, **70**, p. 9002, 2005. doi: 10.1002/chin.200605222 (<http://dx.doi.org/10.1002/chin.200605222>)
 - [17] <http://www.nano.gov/html/facts/appsprod.html> "Applications/Products". National Nanotechnology Initiative. <http://www.nano.gov/html/facts/appsprod.html>. Retrieved on 2007-10-19.
 - [18] http://nobelprize.org/nobel_prizes/physics/laureates/2007/index.html "The Nobel Prize in Physics 2007". Nobelprize.org. http://nobelprize.org/nobel_prizes/physics/laureates/2007/index.html. Retrieved on 2007-10-19.
 - [19] Das S, Gates AJ, Abdu HA, Rose GS, Picconatto CA, Ellenbogen JC. (2007). "Designs for Ultra-Tiny, Special-Purpose Nanoelectronic Circuits". *IEEE Transactions on Circuits and Systems I* **54** (11): 2528-2540. doi: 10.1109/TCSI.2007.907864 (<http://dx.doi.org/10.1109/TCSI.2007.907864>).
 - [20] Ghalanbor Z, Marashi SA, Ranjbar B (2005). "Nanotechnology helps medicine: nanoscale swimmers and their future applications". *Med Hypotheses* **65** (1): 198-199. doi: 10.1016/j.mehy.2005.01.023 (<http://dx.doi.org/10.1016/j.mehy.2005.01.023>). PMID 15893147.
 - [21] Kubik T, Bogunia-Kubik K, Sugisaka M. (2005). "Nanotechnology on duty in medical applications". *Curr Pharm Biotechnol.* **6** (1): 17-33. PMID 15727553.
 - [22] Leary SP, Liu CY, Apuzzo MLJ. (2006). "Toward the Emergence of Nanoneurosurgery: Part III-Nanomedicine: Targeted Nanotherapy, Nanosurgery, and Progress Toward the Realization of Nanoneurosurgery". *Neurosurgery* **58** (6): 1009-1026. doi: 10.1227/01.NEU.0000217016.79256.16 (<http://dx.doi.org/10.1227/>

- 01.NEU.0000217016.79256.16).
- [23] Shetty RC (2005). "Potential pitfalls of nanotechnology in its applications to medicine: immune incompatibility of nanodevices". *Med Hypotheses* **65** (5): 998-9. doi: 10.1016/j.mehy.2005.05.022 (<http://dx.doi.org/10.1016/j.mehy.2005.05.022>). PMID 16023299.
- [24] Cavalcanti A, Shirinzadeh B, Freitas RA Jr., Kretly LC. (2007). "Medical Nanorobot Architecture Based on Nanobioelectronics". *Recent Patents on Nanotechnology* (<http://bentham.org/nanotec/>). **1** (1): 1-10. doi: 10.2174/187221007779814745 (<http://dx.doi.org/10.2174/187221007779814745>).
- [25] Boukallel M, Gauthier M, Dauge M, Piat E, Abadie J. (2007). "Smart microrobots for mechanical cell characterization and cell conveying". *IEEE Trans. Biomed. Eng.* **54** (8): 1536-40. doi: 10.1109/TBME.2007.891171 (<http://dx.doi.org/10.1109/TBME.2007.891171>). PMID 17694877.
- [26] Zsigmondy, R. "Colloids and the Ultramicroscope", J.Wiley and Sons, NY, (1914)
- [27] Dukhin, A.S. and Goetz, P.J. "Ultrasound for characterizing colloids", Elsevier, 2002
- [28] 21
- [29] Project on Emerging Nanotechnologies. (2008). Analysis: This is the first publicly available on-line inventory of nanotechnology-based consumer products. (http://www.nanotechproject.org/inventories/consumer/analysis_draft/)
- [30] <http://www.nanotechproject.org/inventories/consumer/>
- [31] Applications for Nanotechnology (<http://www.americanelements.com/nanotech.htm>)
- [32] Testimony of David Rejeski for U.S. Senate Committee on Commerce, Science and Transportation (http://www.nanotechproject.org/news/archive/successful_commercialization_depends_on/) Project on Emerging Nanotechnologies. Retrieved on 2008-3-7.
- [33] Berkeley considering need for nano safety (Rick DeVecchio, Chronicle Staff Writer) Friday, November 24, 2006 (<http://www.sfgate.com/cgi-bin/article.cgi?file=/c/a/2006/11/24/MNGP9MJ4KI1.DTL>)
- [34] Cambridge considers nanotech curbs - City may mimic Berkeley bylaws (By Hiawatha Bray, Boston Globe Staff) January 26, 2007 (http://boston.com/business/technology/articles/2007/01/26/cambridge_considers_nanotech_curbs/)
- [35] [<http://www.nanolawreport.com/Cambridge.pdf> Recommendations for a Municipal Health & Safety Policy for Nanomaterials: A Report to the Cambridge City Manager. July 2008.
- [36] Lubick, N. (2008). Silver socks have cloudy lining. (http://pubs.acs.org/subscribe/journals/esthag-w/2008/apr/science/nl_nanosocks.html)
- [37] Murray R.G.E., Advances in Bacterial Paracrystalline Surface Layers (Eds.: T. J. Beveridge, S. F. Koval). Plenum pp. 3 ± 9. [9]
- [38] Elder, A. (2006). Tiny Inhaled Particles Take Easy Route from Nose to Brain. (<http://www.urmc.rochester.edu/pr/news/story.cfm?id=1191>)
- [39] Weiss, R. (2008). Effects of Nanotubes May Lead to Cancer, Study Says. (<http://www.washingtonpost.com/wp-dyn/content/article/2008/05/20/AR2008052001331.html?hpid=sec-health&sid=ST2008052100104>)
- [40] Paull, J. & Lyons, K. (2008) , Nanotechnology: The Next Challenge for Organics ([http://www.organic-systems.org/journal/Vol 3\(1\)/pdf/03-22 NanoPaullJOS3.pdf](http://www.organic-systems.org/journal/Vol%203(1)/pdf/03-22%20NanoPaullJOS3.pdf)), Journal of Organic Systems, 3(1) 3-22
- [41] Bowman D, and Hodge G (2006). "Nanotechnology: Mapping the Wild Regulatory Frontier". *Futures* **38**: 1060-1073. doi: 10.1016/j.futures.2006.02.017 (<http://dx.doi.org/10.1016/j.futures.2006.02.017>).
- [42] Davies, JC. (2008). Nanotechnology Oversight: An Agenda for the Next Administration (<http://www.nanotechproject.org/publications/archive/pen13/>).
- [43] Rowe G, Horlick-Jones T, Walls J, Pidgeon N, (2005). "Difficulties in evaluating public engagement initiatives: reflections on an evaluation of the UK GM Nation?". *Public Understanding of Science* (<http://pus.sagepub.com/cgi/content/abstract/14/4/331>). **14**: 333.
- [44] Maynard, A. Testimony by Dr. Andrew Maynard for the U.S. House Committee on Science and Technology (<http://www.science.house.gov/publications/Testimony.aspx?TID=12957>). (2008-4-16). Retrieved on 2008-11-24.
- [45] Faunce TA et al. Sunscreen Safety: The Precautionary Principle, The Australian Therapeutic Goods Administration and Nanoparticles in Sunscreens Nanoethics (2008) 2:231-240 DOI 10.1007/s11569-008-0041-z. <http://law.anu.edu.au/StaffUploads/236-Nanoethics%20Sunscreens%202008.pdf> (last accessed 18 June 2009)
- [46] Royal Society and Royal Academy of Engineering (2004). <http://www.nanotec.org.uk/finalReport.html> | Nanoscience and nanotechnologies: opportunities and uncertainties. <http://www.nanotec.org.uk/finalReport.htm>. Retrieved on 2008-05-18.
- [47] <https://www.msu.edu/~ifas/>
- [48] <http://www.dtsc.ca.gov/TechnologyDevelopment/Nanotechnology/index.cfm> | Nanotechnology web page. Department of Toxic Substances Control. 2008. <http://www.dtsc.ca.gov/TechnologyDevelopment/Nanotechnology/index.cfm>.

- [49] http://www.dtsc.ca.gov/PollutionPrevention/Chemical_Call_In.cfm|Chemical Information Call-In web page. Department of Toxic Substances Control. 2008. http://www.dtsc.ca.gov/PollutionPrevention/Chemical_Call_In.cfm.
- [50] http://www.dtsc.ca.gov/pollutionprevention/chemical_call_in.cfm
- [51] http://www.dtsc.ca.gov/TechnologyDevelopment/Nanotechnology/upload/Formal_AB289_Call_In_Letter_CNTs.pdf
- [52] http://www.dtsc.ca.gov/TechnologyDevelopment/Nanotechnology/upload/AB289_CNT_Contact_List.pdf
- [53] <http://www.crnano.org/basics.htm>
- [54] <http://www.discoverychannel.com>

Further reading

- " Basic Concepts of Nanotechnology (<http://www.inanot.com/>)" History of Nano-Technology, News, Materials, Potential Risks and Important People. (<http://www.inanot.com/>)
- " Nanotechnology 101 (<http://www.nanotechproject.org/topics/nano101/>)" from the Project on Emerging Nanotechnologies. (<http://www.nanotechproject.org/topics/nano101/>)
- Maynard, Andrew, The Twinkie Guide to Nanotechnology (http://www.nanotechproject.org/news/archive/the_twinkie_guide_to_nanotechnology/) Woodrow Wilson International Center for Scholars. 2007. - "...a friendly, funny, 25-minute travel guide to the technology" (http://www.nanotechproject.org/news/archive/the_twinkie_guide_to_nanotechnology/)
- "Nanotechnology Basics: For Students and Other Learners." Center for Responsible Nanotechnology. World Care. 11 Nov. 2008 <<http://www.crnano.org/basics.htm>>.
- Fritz Allhoff and Patrick Lin (eds.), *Nanotechnology & Society: Current and Emerging Ethical Issues* (Dordrecht: Springer, 2008). (<http://www.springer.com/philosophy/ethics/book/978-1-4020-6208-7>)
- Fritz Allhoff, Patrick Lin, James Moor, and John Weckert (eds.), *Nanoethics: The Ethical and Societal Implications of Nanotechnology* (Hoboken: John Wiley & Sons, 2007). (<http://www.wiley.com/WileyCDA/WileyTitle/productCd-0470084170.html>) (<http://www.nanoethics.org/wiley.html>)
- J. Clarence Davies, EPA and Nanotechnology: Oversight for the 21st Century (http://www.nanotechproject.org/publications/archive/epa_nanotechnology_oversight_for_21st/), *Project on Emerging Nanotechnologies*, PEN 9, May 2007.
- William Sims Bainbridge: *Nanoconvergence: The Unity of Nanoscience, Biotechnology, Information Technology and Cognitive Science*, June 27 2007, Prentice Hall, ISBN 0-13-244643-X
- Lynn E. Foster: *Nanotechnology: Science, Innovation, and Opportunity*, December 21 2005, Prentice Hall, ISBN 0-13-192756-6
- *Impact of Nanotechnology on Biomedical Sciences: Review of Current Concepts on Convergence of Nanotechnology With Biology* (<http://www.azonano.com/details.asp?ArticleID=1242>) by Herbert Ernest and Rahul Shetty, from AZojono, May 2005.
- Hunt, G & Mehta, M (eds)(2008) *Nanotechnology: Risk, Ethics & Law*, Earthscan, London.
- Hari Singh Nalwa (2004), *Encyclopedia of Nanoscience and Nanotechnology* (10-Volume Set), American Scientific Publishers. ISBN 1-58883-001-2
- Michael Rieth and Wolfram Schommers (2006), *Handbook of Theoretical and Computational Nanotechnology* (10-Volume Set), American Scientific Publishers. ISBN

1-58883-042-X

- Akhlesh Lakhtakia (ed) (2004). *The Handbook of Nanotechnology. Nanometer Structures: Theory, Modeling, and Simulation*. SPIE Press, Bellingham, WA, USA. ISBN 0-8194-5186-X.
- Fei Wang & Akhlesh Lakhtakia (eds) (2006). *Selected Papers on Nanotechnology -- Theory & Modeling (Milestone Volume 182)*. SPIE Press, Bellingham, WA, USA. ISBN 0-8194-6354-X.
- Jumana Boussey, Georges Kamarinos, Laurent Montès (editors) (2003), Towards Nanotechnology (<http://www.lavoisier.fr/notice/fr2746208580.html>), "Nano et Micro Technologies", Hermes Sciences Publ., Paris, ISBN 2-7462-0858-X.
- The Silicon Valley Toxics Coalition (April, 2008), Regulating Emerging Technologies in Silicon Valley and Beyond (http://www.eto toxics.org/site/PageServer?pagename=svtc_nanotech)
- Genetic Engineering & Biotechnology News (<http://www.genengnews.com>) (January, 2008), Getting a Handle on Nanobiotech Products (<http://www.genengnews.com/articles/chitem.aspx?aid=2325>) Regulators and Companies Are Laying the Groundwork for a Predicted Bright Future

External links

- What is Nanotechnology? (<http://www.vega.org.uk/video/programme/3>) (A Vega/BBC/OU Video Discussion).
- Nanotec Expo (<http://www.nanotecexpo.com.br/english>) - Fair and Congress Latin American of Nanotechnology
- Nanotechnology (<http://www.dmoz.org/Science/Technology/Nanotechnology/>) at the Open Directory Project

§

DNA nanotechnology

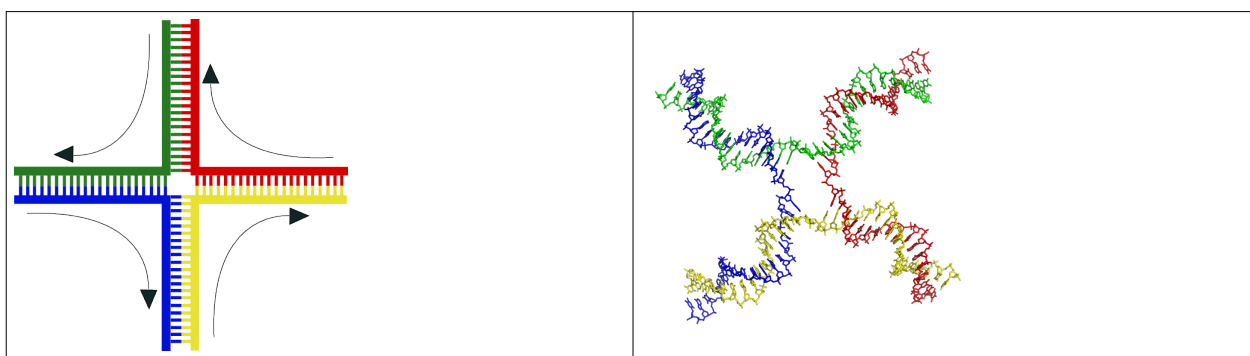
Part of a series of articles on **Molecular self-assembly**

Self-assembled monolayer
Supramolecular assembly
DNA nanotechnology

See also
Nanotechnology

DNA nanotechnology is a subfield of nanotechnology which seeks to use the unique molecular recognition properties of DNA and other nucleic acids to create novel, controllable structures out of DNA. The DNA is thus used as a structural material rather than as a carrier of genetic information, making it an example of bionanotechnology. This has possible applications in molecular self-assembly and in DNA computing.

Introduction: DNA crossover molecules



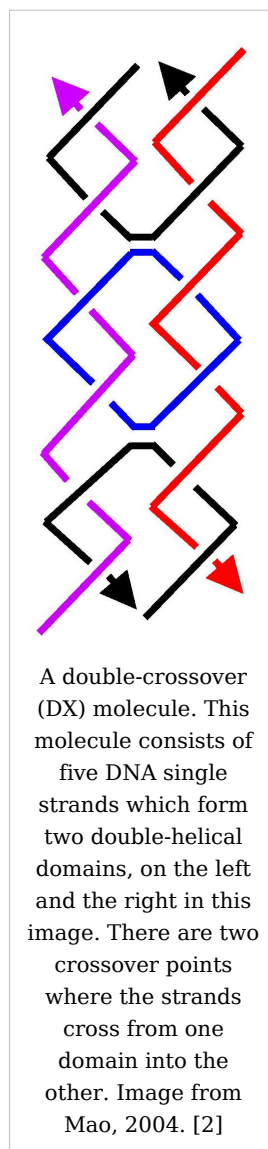
Structure of the 4-arm junction.

Left: A schematic. **Right:** A more realistic model.^[1]

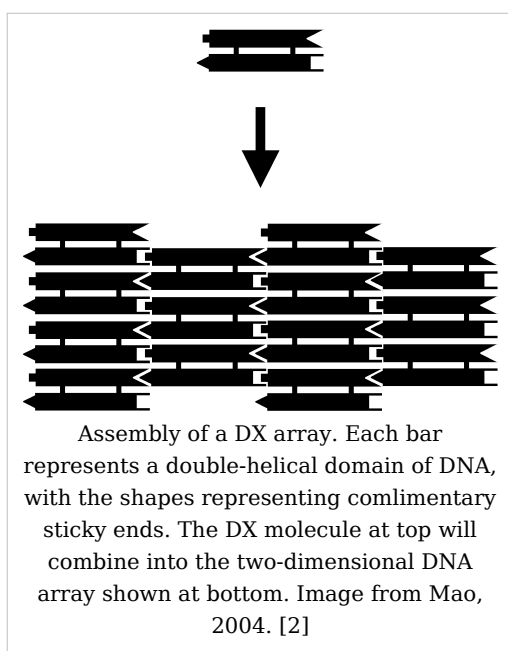
Each of the four separate DNA single strands are shown in different colors.

DNA nanotechnology makes use of branched DNA structures to create DNA complexes with useful properties. DNA is normally a linear molecule, in that its axis is unbranched. However, DNA molecules containing junctions can also be made. For example, a four-arm junction can be made using four individual DNA strands which are complementary to each other in the correct pattern. Due to Watson-Crick base pairing, only portions of the strands which are complementary to each other will attach to each other to form duplex DNA. This four-arm junction is an immobile form of a Holliday junction.

Junctions can be used in more complex molecules. The most important of these is the "double-crossover" or DX motif. Here, two DNA duplexes lie next to each other, and share two junction points where strands cross from one duplex into the other. This molecule has the advantage that the junction points are now constrained to a single orientation as opposed to being flexible as in the four-arm junction. This makes the DX motif suitable as a structural building block for larger DNA complexes.^[3]



Tile-based arrays



DX arrays

DX, Double Crossover, molecules can be equipped with sticky ends in order to combine them into a two-dimensional periodic lattice. Each DX molecule has four termini, one at each end of the two double-helical domains, and these can be equipped with sticky ends that program them to combine into a specific pattern. More than one type of DX can be used which can be made to arrange in rows or any other tessellated pattern. They thus form extended flat sheets which are essentially two-dimensional crystals of DNA.^[4]

DNA nanotubes

In addition to flat sheets, DX arrays have been made to form hollow tubes of 4-20 nm diameter. These

DNA nanotubes are somewhat similar in size and shape to carbon nanotubes, but the carbon nanotubes are stronger and better conductors, whereas the DNA nanotubes are more easily modified and connected to other structures.^[5]

Other tile arrays

Two-dimensional arrays have been made out of other motifs as well, including the Holliday junction rhombus array as well as various DX-based arrays in the shapes of triangles and hexagons.^[6] Another motif, the six-helix bundle, has the ability to form three-dimensional DNA arrays as well.^[7]

DNA origami

As an alternative to the tile-based approach, two-dimensional DNA structures can be made from a single, long DNA strand of arbitrary sequence which is folded into the desired shape by using shorter, "staple" strands. This allows the creation of two-dimensional shapes at the nanoscale using DNA. Demonstrated designs have included the smiley face and a coarse map of North America. DNA origami was the cover story of *Nature* on March 15, 2006.^[8]

DNA polyhedra

A number of three-dimensional DNA molecules have been made which have the connectivity of a polyhedron such as an octahedron or cube. In other words, the DNA duplexes trace the edges of a polyhedron with a DNA junction at each vertex. The earliest demonstrations of DNA polyhedra involved multiple ligations and solid-phase synthesis steps to create catenated polyhedra. More recently, there have been demonstrations of a DNA truncated octahedron made from a long single strand designed to fold into the correct conformation, as well as a tetrahedron which can be produced from four DNA strands in a single step.^[9]

DNA nanomechanical devices

DNA complexes have been made which change their conformation upon some stimulus. These are intended to have applications in nanorobotics. One of the first such devices, called "molecular tweezers," changes from an open to a closed state based upon the presence of control strands.

DNA machines have also been made which show a twisting motion. One of these makes use of the transition between the B-DNA and Z-DNA forms to respond to a change in buffer conditions. Another relies on the presence of control strands to switch from a paranemic-crossover (PX) conformation to a double-junction (JX2) conformation.^[10]

Stem Loop Controllers

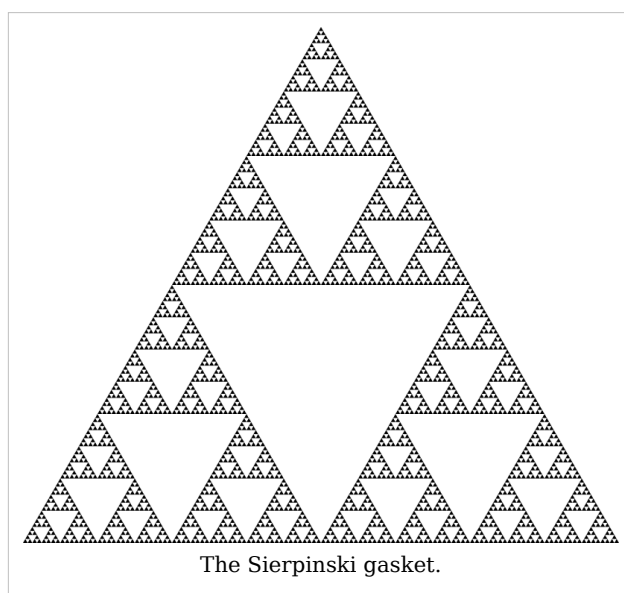
A design called a *stem loop*, consisting of a single strand of DNA which has a loop at an end, are a dynamic structure that opens and closes when a piece of DNA bonds to the loop part. This effect has been exploited to create several logic gates.^{[11] [12]} These logic gates have been used to create the computers MAYA I and MAYA II which can play tick-tac-toe to some extent.^[13]

Applications

Algorithmic self-assembly

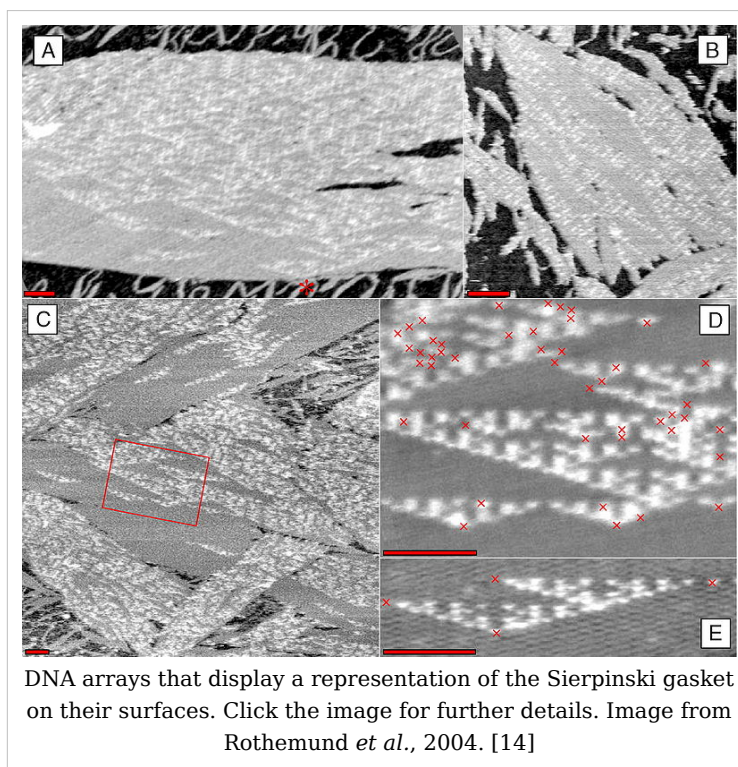
DNA nanotechnology has been applied to the related field of DNA computing. A DX array has been demonstrated whose assembly encodes an XOR operation, which allows the DNA array to implement a cellular automaton which generates a fractal called the Sierpinski gasket. This shows that computation can be incorporated into the assembly of DNA arrays, increasing its scope beyond simple periodic arrays.

Note that DNA computing overlaps with, but is distinct from, DNA nanotechnology. The latter uses the specificity of Watson-Crick basepairing to make novel structures out of DNA. These structures can be used for DNA computing, but they do not have to be. Additionally, DNA computing can be done without using the types of molecules made possible by DNA Nanotechnology.^[15]



Nanoarchitecture

The idea of using DNA arrays to template the assembly of other functional molecules has been around for a while, but only recently has progress been made in reducing these kinds of schemes to practice. In 2006, researchers covalently attached gold nanoparticles to a DX-based tile and showed that self-assembly of the DNA structures also assembled the nanoparticles hosted on them. A non-covalent hosting scheme was shown in 2007, using Dervan polyamides on a DX array to arrange streptavidin proteins on specific kinds of tiles on the DNA array.^[16] Previously in 2006 LaBean demonstrated the letters "D" "N" and "A" created on a 4x4 DX array using streptavidin.^[17]



DNA has also been used to assemble a single walled carbon nanotube Field-effect transistor.^[18]

See also

- Mechanical properties of DNA

External links

- Chengde Mao page at Purdue University [19]
- John Reif lab at Duke University [20]
- Nadrian Seeman lab at NYU [21]
- William M. Shih lab at Harvard Medical School [22]
- Andrew Turberfield lab at Oxford University [23]
- Erik Winfree lab at Caltech [24]
- Hao Yan lab at Arizona State University [25]
- Bernard Yurke formerly at Bell Labs [26] now at Boise State University [27]
- Thom LaBean at Duke University [28]
- Software for 3D DNA design, modeling and/or simulation:
 - Ascalaph Designer^[29]
 - caDNAno^[30]
 - GIDEON^[31]
 - NanoEngineer-1^[32]
- International Society for Nanoscale Science, Computation and Engineering [33]

References

Note: Click on the doi to access the text of the referenced article.

[1] Created from PDB 1M6G (<http://www.rcsb.org/pdb/explore/explore.do?structureId=1M6G>)

[2] <http://dx.doi.org/10.1371/journal.pbio.0020431>

- Seeman, Nadrian C. (1 November 1999). "DNA Engineering and its Application to Nanotechnology". *Trends in Biotechnology* **17** (11): 437–443. doi: 10.1016/S0167-7799(99)01360-8 ([http://dx.doi.org/10.1016/S0167-7799\(99\)01360-8](http://dx.doi.org/10.1016/S0167-7799(99)01360-8)). ISSN 0167-7799 (<http://worldcat.org/issn/0167-7799>).
- Seeman, Nadrian C. (January 2001). "DNA Nicks and Nodes and Nanotechnology". *Nano Letters* **1** (1): 22–26. doi: 10.1021/nl000182v (<http://dx.doi.org/10.1021/nl000182v>). ISSN 1530-6984 (<http://worldcat.org/issn/1530-6984>).
- Mao, Chengde (December 2004). "The Emergence of Complexity: Lessons from DNA". *PLoS Biology* **2** (12): 2036–2038. doi: 10.1371/journal.pbio.0020431 (<http://dx.doi.org/10.1371/journal.pbio.0020431>). ISSN 1544-9173 (<http://worldcat.org/issn/1544-9173>).
- Kumara, Mudalige T. (July 2008). "Assembly pathway analysis of DNA nanostructures and the construction of parallel motifs". *Nano Letters* **8** (7): 1971–1977. doi: 10.1021/nl800907y (<http://dx.doi.org/10.1021/nl800907y>). ISSN .
- Winfree, Erik; Liu, Furong; Wenzler, Lisa A. & Seeman, Nadrian C. (6 August 1998). "Design and self-assembly of two-dimensional DNA crystals". *Nature* **394**: 529–544. doi: 10.1038/28998 (<http://dx.doi.org/10.1038/28998>). ISSN 0028-0836 (<http://worldcat.org/issn/0028-0836>).
- Liu, Furong; Sha, Ruojie & Seeman, Nadrian C. (10 February 1999). "Modifying the Surface Features of Two-Dimensional DNA Crystals". *Journal of the American Chemical Society* **121** (5): 917–922. doi: 10.1021/ja982824a (<http://dx.doi.org/10.1021/ja982824a>). ISSN 0002-7863 (<http://worldcat.org/issn/0002-7863>).
- Rothmund, Paul W. K.; Ekani-Nkodo, Axel; Papadakis, Nick; Kumar, Ashish; Fygenson, Deborah Kuchnir & Winfree, Erik (22 December 2004). "Design and Characterization of Programmable DNA Nanotubes". *Journal of the American Chemical Society* **126** (50): 16344–16352. doi: 10.1021/ja044319l (<http://dx.doi.org/10.1021/ja044319l>). ISSN 0002-7863 (<http://worldcat.org/issn/0002-7863>).
- Mao, Chengde; Sun, Weiqiong & Seeman, Nadrian C. (16 June 1999). "Designed Two-Dimensional DNA Holliday Junction Arrays Visualized by Atomic Force Microscopy". *Journal of the American Chemical Society* **121** (23): 5437–5443. doi: 10.1021/ja9900398 (<http://dx.doi.org/10.1021/ja9900398>). ISSN 0002-7863 (<http://worldcat.org/issn/0002-7863>).
- Constantinou, Pamela E.; Wang, Tong; Kopatsch, Jens; Israel, Lisa B.; Zhang, Xiaoping; Ding, Baoquan; Sherman, William B.; Wang, Xing; Zheng, Jianping; Sha, Ruojie & Seeman, Nadrian C. (2006). "Double cohesion in structural DNA nanotechnology". *Organic and Biomolecular Chemistry* **4**: 3414–3419. doi: 10.1039/b605212f (<http://dx.doi.org/10.1039/b605212f>).
- Mathieu, Frederick; Liao, Shiping; Kopatsch, Jens; Wang, Tong; Mao, Chengde & Seeman, Nadrian C. (April 2005). "Six-Helix Bundles Designed from DNA". *Nano Letters* **5** (4): 661–665. doi: 10.1021/nl050084f (<http://dx.doi.org/10.1021/nl050084f>). ISSN 1530-6984 (<http://worldcat.org/issn/1530-6984>).
- Rothmund, Paul W. K. (2006). "Folding DNA to create nanoscale shapes and patterns". *Nature* **440**: 297–302. doi: 10.1038/nature04586 (<http://dx.doi.org/10.1038/nature04586>). ISSN 0028-0836 (<http://worldcat.org/issn/0028-0836>).
- Zhang, Yuwen; Seeman, Nadrian C. (1994). "Construction of a DNA-truncated octahedron". *Journal of the American Chemical Society* **116** (5): 1661–1669. doi: 10.1021/ja00084a006 (<http://dx.doi.org/10.1021/ja00084a006>). ISSN 0002-7863 (<http://worldcat.org/issn/0002-7863>).
- Shih, William M.; Quispe, Joel D.; Joyce, Gerald F. (12 February 2004). "A 1.7-kilobase single-stranded DNA that folds into a nanoscale octahedron". *Nature* **427**: 618–621. doi: 10.1038/nature02307 (<http://dx.doi.org/10.1038/nature02307>). ISSN 0028-0836 (<http://worldcat.org/issn/0028-0836>).
- Goodman, R.P.; Schaap, I.A.T.; Tardin, C.F.; Erben, C.M.; Berry, R.M.; Schmidt, C.F.; Turberfield, A.J. (9 December 2005). "Rapid chiral assembly of rigid DNA building blocks for molecular nanofabrication". *Science* **310** (5754): 1661–1665. doi: 10.1126/science.1120367 (<http://dx.doi.org/10.1126/science.1120367>). ISSN 0036-8075 (<http://worldcat.org/issn/0036-8075>).
- Yurke, Bernard; Turberfield, Andrew J.; Mills, Allen P., Jr; Simmel, Friedrich C. & Neumann, Jennifer L. (10 August 2000). "A DNA-fuelled molecular machine made of DNA". *Nature* **406**: 605–609. doi: 10.1038/35020524 (<http://dx.doi.org/10.1038/35020524>). ISSN 0028-0836 (<http://worldcat.org/issn/0028-0836>).

- 0028-0836).
- Mao, Chengde; Sun, Weiqiong; Shen, Zhiyong & Seeman, Nadrian C. (14 January 1999). "A DNA Nanomechanical Device Based on the B-Z Transition". *Nature* **397**: 144–146. doi: 10.1038/16437 (<http://dx.doi.org/10.1038/16437>). ISSN .
 - Yan, Hao; Zhang, Xiaoping; Shen, Zhiyong & Seeman, Nadrian C. (3 January 2002). "A robust DNA mechanical device controlled by hybridization topology". *Nature* **415**: 62–65. doi: 10.1038/415062a (<http://dx.doi.org/10.1038/415062a>). ISSN .
- [11] DNA Logic Gates (<https://digamma.cs.unm.edu/wiki/bin/view/McogPublicWeb/MolecularLogicGates>)
- [12] (http://www.duke.edu/~jme17/Joshua_E._Mendoza-Elias/Research_Ideas.html)
- [13] MAYA II (<https://digamma.cs.unm.edu/wiki/bin/view/McogPublicWeb/MolecularAutomataMAYAI>)
- [14] <http://dx.doi.org/10.1371/journal.pbio.0020424>
- Rothmund, Paul W. K.; Papadakis, Nick & Winfree, Erik (December 2004). "Algorithmic Self-Assembly of DNA Sierpinski Triangles". *PLoS Biology* **2** (12): 2041–2053. doi: 10.1371/journal.pbio.0020424 (<http://dx.doi.org/10.1371/journal.pbio.0020424>). ISSN 1544-9173 (<http://worldcat.org/issn/1544-9173>).
 - Robinson, Bruce H.; Seeman, Nadrian C. (August 1987). "The Design of a Biochip: A Self-Assembling Molecular-Scale Memory Device". *Protein Engineering* **1** (4): 295–300. ISSN 0269-2139 (<http://worldcat.org/issn/0269-2139>). Link (<http://peds.oxfordjournals.org/cgi/content/abstract/1/4/295>)
 - Zheng, Jiwen; Constantinou, Pamela E.; Micheel, Christine; Alivisatos, A. Paul; Kiehl, Richard A. & Seeman, Nadrian C. (2006). "2D Nanoparticle Arrays Show the Organizational Power of Robust DNA Motifs". *Nano Letters* **6**: 1502–1504. doi: 10.1021/nl060994c (<http://dx.doi.org/10.1021/nl060994c>). ISSN 1530-6984 (<http://worldcat.org/issn/1530-6984>).
 - Cohen, Justin D.; Sadowski, John P.; Dervan, Peter B. (2007). "Addressing Single Molecules on DNA Nanostructures". *Angewandte Chemie* **46** (42): 7956–7959. doi: 10.1002/anie.200702767 (<http://dx.doi.org/10.1002/anie.200702767>). ISSN 0570-0833 (<http://worldcat.org/issn/0570-0833>).
- [17] Park, Sung Ha; Sung Ha Park, Constantin Pistol, Sang Jung Ahn, John H. Reif, Alvin R. Lebeck, Chris Dwyer, Thomas H. LaBean (October 2006).
["http://www3.interscience.wiley.com/journal/113390879/abstract|Finite-Size, Fully Addressable DNA Tile Lattices Formed by Hierarchical Assembly Procedures"](http://www3.interscience.wiley.com/journal/113390879/abstract|Finite-Size, Fully Addressable DNA Tile Lattices Formed by Hierarchical Assembly Procedures). *Angewandte Chemie* **118** (40): 749–753. doi: 10.1002/ange.200690141 (<http://dx.doi.org/10.1002/ange.200690141>). ISSN 1521-3757 (<http://worldcat.org/issn/1521-3757>). <http://www3.interscience.wiley.com/journal/113390879/abstract>.
- [18] Keren, K.; Kinneret Keren, Rotem S. Berman, Evgeny Buchstab, Uri Sivan, Erez Braun (November 2003).
["http://www.sciencemag.org/cgi/content/abstract/sci;302/5649/1380|DNA-Templated Carbon Nanotube Field-Effect Transistor"](http://www.sciencemag.org/cgi/content/abstract/sci;302/5649/1380|DNA-Templated Carbon Nanotube Field-Effect Transistor). *Science* **302** (6549): 1380–1382. doi: 10.1126/science.1091022 (<http://dx.doi.org/10.1126/science.1091022>). ISSN 1095-9203 (<http://worldcat.org/issn/1095-9203>). <http://www.sciencemag.org/cgi/content/abstract/sci;302/5649/1380>.
- [19] <http://www.chem.purdue.edu/people/faculty/faculty.asp?itemID=46>
- [20] <http://www.cs.duke.edu/~reif/BMC/Reif.BMCproject.html>
- [21] <http://seemanlab4.chem.nyu.edu/>
- [22] http://research2.dfci.harvard.edu/shih/SHIH_LAB/Home.html
- [23] <http://www.physics.ox.ac.uk/cm/people/turberfield.htm>
- [24] <http://dna.caltech.edu/>
- [25] http://chemistry.asu.edu/faculty/hao_yan.asp
- [26] <http://www.bell-labs.com/org/physicalsciences/profiles/yurke.html>
- [27] <http://coen.boisestate.edu/departments/faculty.asp?ID=134>
- [28] <http://www.cs.duke.edu/~thl/>
- [29] http://www.agilemolecule.com/Ascalaph/Ascalaph_Designer.html
- [30] <http://cadnano.org>
- [31] <http://www.subirac.com>
- [32] <http://www.nanoengineer-1.net>
- [33] <http://www.isnsce.org/>

DNA microarray

For terminology, see glossary below.

A **DNA microarray** is a multiplex technology used in molecular biology and in medicine. It consists of an arrayed series of thousands of microscopic spots of DNA oligonucleotides, called features, each containing picomoles of a specific DNA sequence. This can be a short section of a gene or other DNA element that are used as probes to hybridize a cDNA or

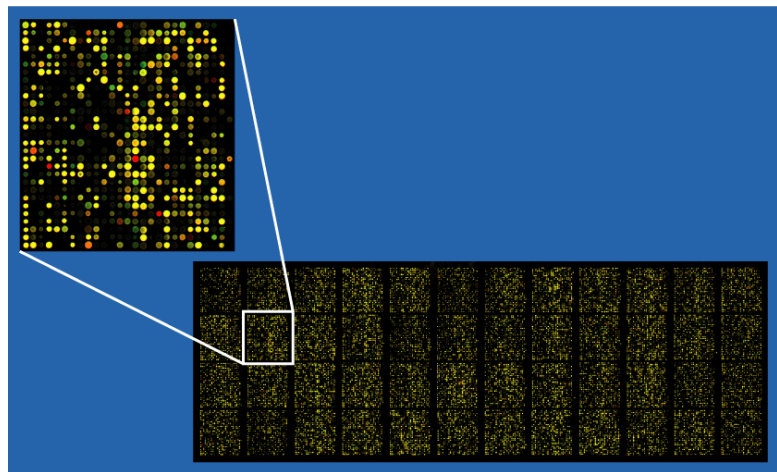
cRNA sample (called target) under high-stringency conditions. Probe-target hybridization is usually detected and quantified by detection of fluorophore-, silver-, or chemiluminescence-labeled targets to determine relative abundance of nucleic acid sequences in the target.

In standard microarrays, the probes are attached to a solid surface by a covalent bond to a chemical matrix (via epoxy-silane, amino-silane, lysine, polyacrylamide or others). The solid surface can be glass or a silicon chip, in which case they are commonly known as *gene chip* or colloquially *Affy chip* when an Affymetrix chip is used. Other microarray platforms, such as Illumina, use microscopic beads, instead of the large solid support. DNA arrays are different from other types of microarray only in that they either measure DNA or use DNA as part of its detection system.

DNA microarrays can be used to measure changes in expression levels, to detect single nucleotide polymorphisms (SNPs) (*see uses and types section*), in genotyping or in resequencing mutant genomes. Microarrays also differ in fabrication, workings, accuracy, efficiency, and cost (*see fabrication section*). Additional factors for microarray experiments are the experimental design and the methods of analyzing the data (*see Bioinformatics section*).

History

Microarray technology evolved from Southern blotting, where fragmented DNA is attached to a substrate and then probed with a known gene or fragment. The use of a collection of distinct DNAs in arrays for expression profiling was first described in 1987, and the arrayed DNAs were used to identify genes whose expression is modulated by interferon.^[1] These early gene arrays were made by spotting cDNAs onto filter paper with a pin-spotting device. The use of miniaturized microarrays for gene expression profiling was first reported in 1995,^[2] and a complete eukaryotic genome (*Saccharomyces cerevisiae*) on a microarray was published in 1997.^[3]



Example of an approximately 40,000 probe spotted oligo microarray with enlarged inset to show detail.

Uses and types

Arrays of DNA can be spatially arranged, as in the commonly known *gene chip* (also called *genome chip*, *DNA chip* or *gene array*), or can be specific DNA sequences labelled such that they can be independently identified in solution. The traditional solid-phase array is a collection of microscopic DNA spots attached to a solid surface, such as glass, plastic or silicon biochip. The affixed DNA segments are known as *probes* (although some sources use different terms such as *reporters*). Thousands of them can be placed in known locations on a single DNA microarray.



DNA microarrays can be used to detect DNA (as in comparative genomic hybridization), or detect RNA (most commonly as cDNA after reverse transcription) that may or may not be translated into proteins. The process of measuring gene expression via cDNA is called expression analysis or expression profiling.

Since an array can contain tens of thousands of probes, a microarray experiment can accomplish that many genetic tests in parallel. Therefore arrays have dramatically accelerated many types of investigation.

Applications include:

Technology or Application	Synopsis
Gene expression profiling	In an mRNA or gene expression profiling experiment the expression levels of thousands of genes are simultaneously monitored to study the effects of certain treatments, diseases, and developmental stages on gene expression. For example, microarray-based gene expression profiling can be used to identify genes whose expression is changed in response to pathogens or other organisms by comparing gene expression in infected to that in uninfected cells or tissues. [4]
Comparative genomic hybridization	Assessing genome content in different cells or closely related organisms. [5] [6]
GeneID	Small microarrays to check IDs of organisms in food and feed (like GMO [7]), mycoplasmas in cell culture, or pathogens for disease detection, mostly combining PCR and microarray technology.
Chromatin immunoprecipitation on Chip	DNA sequences bound to a particular protein can be isolated by immunoprecipitating that protein (ChIP), these fragments can be then hybridized to a microarray (such as a tiling array) allowing the determination of protein binding site occupancy throughout the genome. Example protein to immunoprecipitate are histone modifications (H3K27me3, H3K4me2, H3K9me3, etc), Polycomb-group protein (PRC2:Suz12, PRC1:YY1) and trithorax-group protein (Ash1) to study the epigenetic landscape or RNA Polymerase II to study the transcription landscape.
SNP detection	Identifying single nucleotide polymorphism among alleles within or between populations. [8] Several applications of microarrays make use of SNP detection, including Genotyping, forensic analysis, measuring predisposition to disease, identifying drug-candidates, evaluating germline mutations in individuals or somatic mutations in cancers, assessing loss of heterozygosity, or genetic linkage analysis.

Alternative splicing detection	An ' <i>exon junction array</i> design uses probes specific to the expected or potential splice sites of predicted exons for a gene. It is of intermediate density, or coverage, to a typical gene expression array (with 1-3 probes per gene) and a genomic tiling array (with hundreds or thousands of probes per gene). It is used to assay the expression of alternative splice forms of a gene. Exon arrays have a different design, employing probes designed to detect each individual exon for known or predicted genes, and can be used for detecting different splicing isoforms.
Fusion genes microarray	A Fusion gene microarray can detect fusion transcripts, <i>e.g.</i> from cancer specimens. The principle behind this is building on the alternative splicing micorrays. The oligo design strategy enables combined measurements of chimeric transcript junctions with exon-wise measurements of individual fusion partners.
Tiling array	Genome tiling arrays consist of overlapping probes designed to densely represent a genomic region of interest, sometimes as large as an entire human chromosome. The purpose is to empirically detect expression of transcripts or alternatively splice forms which may not have been previously known or predicted.

Fabrication

Microarrays can be manufactured in different ways, depending on the number of probes under examination, costs, customization requirements, and the type of scientific question being asked. Arrays may have as few as 10 probes or up to 2.1 million (NimbleGen, Roche) micrometre-scale probes from commercial vendors.

Surface engineering

The first step of DNA microarray fabrication involves surface engineering of a substrate in order to obtain desirable surface properties for the application of interest. Optimal surface properties are those which produce high signal to noise ratios for the DNA targets of interest. Generally, this involves maximizing the probe surface density and activity while minimizing the non-specific binding of the targets of interest. Methods of surface engineering vary depending on the platform material, design, and application.

Spotted vs. oligonucleotide arrays

Microarrays can be fabricated using a variety of technologies, including printing with fine-pointed pins onto glass slides, photolithography using pre-made masks, photolithography using dynamic micromirror devices, ink-jet printing,^[9] or electrochemistry on microelectrode arrays.

In *spotted microarrays*, the probes are oligonucleotides, cDNA or small fragments of PCR products that correspond to mRNAs. The probes are synthesized prior to deposition on the array surface and are then "spotted" onto glass. A common approach utilizes an array of fine pins or needles controlled by a robotic arm that is dipped into wells containing DNA probes and then depositing each probe at designated locations on the array surface. The resulting "grid" of probes represents the nucleic acid profiles of the prepared probes and is ready to receive complementary cDNA or cRNA "targets" derived from experimental or clinical samples. This technique is used by research scientists around the world to produce "in-house" printed microarrays from their own labs. These arrays may be easily customized for each experiment, because researchers can choose the probes and printing locations on

the arrays, synthesize the probes in their own lab (or collaborating facility), and spot the arrays. They can then generate their own labeled samples for hybridization, hybridize the samples to the array, and finally scan the arrays with their own equipment. This provides a relatively low-cost microarray that may be customized for each study, and avoids the costs of purchasing often more expensive commercial arrays that may represent vast numbers of genes that are not of interest to the investigator. Publications exist which indicate in-house spotted microarrays may not provide the same level of sensitivity compared to commercial oligonucleotide arrays,^[10] possibly owing to the small batch sizes and reduced printing efficiencies when compared to industrial manufactures of oligo arrays.

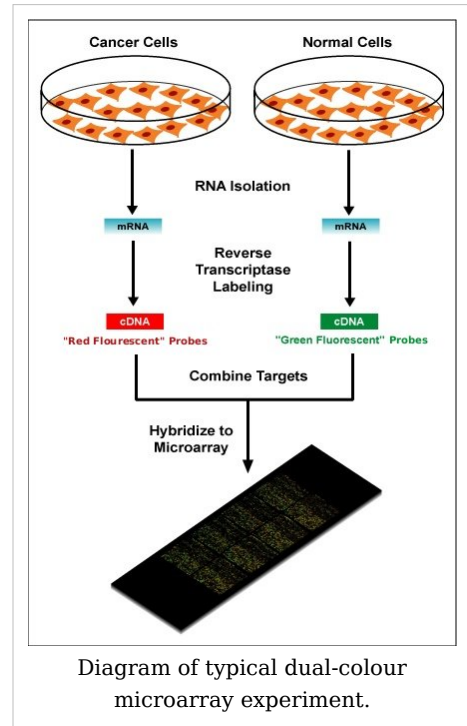
In *oligonucleotide microarrays*, the probes are short sequences designed to match parts of the sequence of known or predicted open reading frames. Although oligonucleotide probes are often used in "spotted" microarrays, the term "oligonucleotide array" most often refers to a specific technique of manufacturing. Oligonucleotide arrays are produced by printing short oligonucleotide sequences designed to represent a single gene or family of gene splice-variants by synthesizing this sequence directly onto the array surface instead of depositing intact sequences. Sequences may be longer (60-mer probes such as the Agilent design) or shorter (25-mer probes produced by Affymetrix) depending on the desired purpose; longer probes are more specific to individual target genes, shorter probes may be spotted in higher density across the array and are cheaper to manufacture. One technique used to produce oligonucleotide arrays include photolithographic synthesis (Agilent and Affymetrix) on a silica substrate where light and light-sensitive masking agents are used to "build" a sequence one nucleotide at a time across the entire array.^[11] Each applicable probe is selectively "unmasked" prior to bathing the array in a solution of a single nucleotide, then a masking reaction takes place and the next set of probes are unmasked in preparation for a different nucleotide exposure. After many repetitions, the sequences of every probe become fully constructed. More recently, Maskless Array Synthesis from NimbleGen Systems has combined flexibility with large numbers of probes.^[12]

Two-channel vs. one-channel detection

Two-color microarrays or *two-channel microarrays* are typically hybridized with cDNA prepared from two samples to be compared (e.g. diseased tissue versus healthy tissue) and that are labeled with two different fluorophores.^[13] Fluorescent dyes commonly used for cDNA labelling include Cy3, which has a fluorescence emission wavelength of 570 nm (corresponding to the green part of the light spectrum), and Cy5 with a fluorescence emission wavelength of 670 nm (corresponding to the red part of the light spectrum). The two Cy-labelled cDNA samples are mixed and hybridized to a single microarray that is then scanned in a microarray scanner to visualize fluorescence of the two fluorophores after excitation with a laser beam of a defined wavelength. Relative intensities of each fluorophore may then be used in ratio-based analysis to identify up-regulated and down-regulated genes.^[14]

Oligonucleotide microarrays often contain control probes designed to hybridize with RNA spike-ins. The degree of hybridization between the spike-ins and the control probes is used to normalize the hybridization measurements for the target probes. Although absolute levels of gene expression may be determined in the two-color array, the relative differences in expression among different spots within a sample and between samples is the preferred method of data analysis for the two-color system. Examples of providers for such microarrays includes Agilent with their Dual-Mode platform, Eppendorf with their DualChip platform for colorimetric Silverquant labeling, and TeleChem International with Arrayit.

In *single-channel microarrays* or *one-color microarrays*, the arrays are designed to give estimations of the absolute levels of gene expression. Therefore the comparison of two conditions requires two separate single-dye hybridizations. As only a single dye is used, the data collected represent absolute values of gene expression. These may be compared to other genes within a sample or to reference "normalizing" probes used to calibrate data across the entire array and across multiple arrays. Three popular single-channel systems are the Affymetrix "Gene Chip", the Applied Microarrays "CodeLink" arrays, and the Eppendorf "DualChip & Silverquant". One strength of the single-dye system lies in the fact that an aberrant sample cannot affect the raw data derived from other samples, because each array chip is exposed to only one sample (as opposed to a two-color system in which a single low-quality sample may drastically impinge on overall data precision even if the other sample was of high quality). Another benefit is that data are more easily compared to arrays from different experiments; the absolute values of gene expression may be compared between studies conducted months or years apart. A drawback to the one-color system is that, when compared to the two-color system, twice as many microarrays are needed to compare samples within an experiment.



Microarrays and bioinformatics

The advent of inexpensive microarray experiments created several specific bioinformatics challenges:

- the multiple levels of replication in experimental design (Experimental design)
- the number of platforms and independent groups and data format (Standardization)
- the treatment of the data (Statistical analysis)
- accuracy and precision (Relation between probe and gene)
- the sheer volume of data and the ability to share it (Data warehousing)

Experimental design

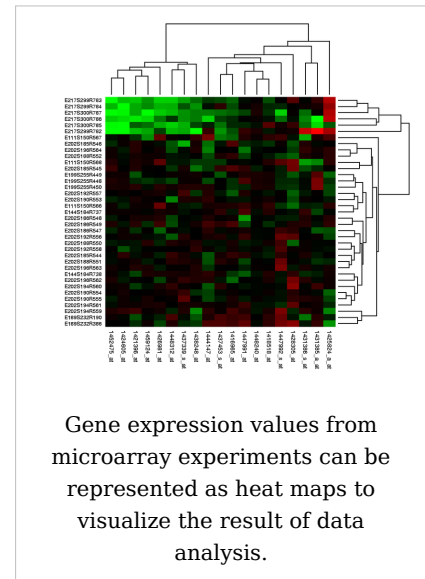
Due to the biological complexity of gene expression, the considerations of experimental design that are discussed in the expression profiling article are of critical importance if statistically and biologically valid conclusions are to be drawn from the data.

There are three main elements to consider when designing a microarray experiment. First, replication of the biological samples is essential for drawing conclusions from the experiment. Second, technical replicates (two RNA samples obtained from each experimental unit) help to ensure precision and allow for testing differences within treatment groups. The technical replicates may be two independent RNA extractions or two aliquots of the same extraction. Third, spots of each cDNA clone or oligonucleotide are present as replicates (at least duplicates) on the microarray slide, to provide a measure of technical precision in each hybridization. It is critical that information about the sample preparation and handling is discussed, in order to help identify the independent units in the experiment and to avoid inflated estimates of statistical significance.^[15]

Standardization

Microarray data is difficult to exchange due to the lack of standardization in platform fabrication, assay protocols, and analysis methods. This presents an interoperability problem in bioinformatics. Various grass-roots open-source projects are trying to ease the exchange and analysis of data produced with non-proprietary chips:

- For example, the "Minimum Information About a Microarray Experiment" (MIAME) checklist helps define the level of detail that should exist and is being adopted by many journals as a requirement for the submission of papers incorporating microarray results. But MIAME does not describe the format for the information, so while many formats can support the MIAME requirements, as of 2007 no format permits verification of complete semantic compliance.
- The "MicroArray Quality Control (MAQC) Project" is being conducted by the US Food and Drug Administration (FDA) to develop standards and quality control metrics which will eventually allow the use of MicroArray data in drug discovery, clinical practice and regulatory decision-making.^[16]



- The MGED Society has developed standards for the representation of gene expression experiment results and relevant annotations.

Statistical analysis

The analysis of DNA microarrays poses a large number of statistical problems, including the normalization of the data. There are several normalization methods in the published literature some of which are platform specific; as in many other cases where authorities disagree, a sound conservative approach is to directly compare different normalization methods to determine the effects of these different methods on the results obtained. This can be done, for example, by investigating the performance of various methods on data from "spike-in" experiments.

Also, experimenters must account for multiple comparisons: even if the statistical P-value assigned to a gene indicates that it is extremely unlikely that differential expression of this gene was due to random rather than treatment effects, the very high number of genes on an array makes it likely that differential expression of some genes represent false positives or false negatives. Statistical methods tailored to microarray analyses have recently become available that assess statistical power based on the variation present in the data and the number of experimental replicates, and can help minimize type I and type II errors in the analyses.^[17]

A basic difference between microarray data analysis and much traditional biomedical research is the dimensionality of the data. A large clinical study might collect 100 data items per patient for thousands of patients. A medium-size microarray study will obtain many thousands of numbers per sample for perhaps a hundred samples. Many analysis techniques treat each sample as a single point in a space with thousands of dimensions, then attempt by various techniques to reduce the dimensionality of the data to something humans can visualize.^[18] An example for such a method is the Local Pooled Error (LPE) test, which pools standard deviations of genes with similar expression levels and thereby overcomes the problem of low replicate numbers.^[19]

Relation between probe and gene

The relation between a probe and the mRNA that it is expected to detect is problematic. On the one hand, some mRNAs may cross-hybridize probes in the array that are supposed to detect another mRNA. On the other hand, probes that are designed to detect the mRNA of a particular gene may be relying on genomic EST information that is incorrectly associated with that gene.

Data warehousing

Microarray data was found to be more useful when compared to other similar datasets. The sheer volume (in bytes), specialized formats (such as MIAME), and curation efforts associated with the datasets require specialized databases to store the data.

See also

- Cyanine dyes, such as Cy3 and Cy5, are commonly used fluorophores with microarrays
- FatiGO
- Full Genome Sequencing
- Microfluidics or lab-on-chip
- Serial analysis of gene expression
- Significance analysis of microarrays
- Systems biology

References

- [1] Kulesh DA, Clive DR, Zarlenga DS, Greene JJ (1987). "Identification of interferon-modulated proliferation-related cDNA sequences". *Proc Natl Acad Sci USA* **84**: 8453–8457. doi: 10.1073/pnas.84.23.8453 (<http://dx.doi.org/10.1073/pnas.84.23.8453>). PMID 2446323.
- [2] Schena M, Shalon D, Davis RW, Brown PO (1995). "Quantitative monitoring of gene expression patterns with a complementary DNA microarray". *Science* **270**: 467–470. doi: 10.1126/science.270.5235.467 (<http://dx.doi.org/10.1126/science.270.5235.467>). PMID 7569999.
- [3] Lashkari DA, DeRisi JL, McCusker JH, Namath AF, Gentile C, Hwang SY, Brown PO, Davis RW (1997). "Yeast microarrays for genome wide parallel genetic and gene expression analysis". *Proc Natl Acad Sci USA* **94**: 13057–13062. doi: 10.1073/pnas.94.24.13057 (<http://dx.doi.org/10.1073/pnas.94.24.13057>). PMID 9371799.
- [4] Adomas A, Heller G, Olson A, Osborne J, Karlsson M, Nahalkova J, Van Zyl L, Sederoff R, Stenlid J, Finlay R, Asiegbu FO (2008). "Comparative analysis of transcript abundance in *Pinus sylvestris* after challenge with a saprotrophic, pathogenic or mutualistic fungus". *Tree Physiol.* **28**: 885–897. PMID 18381269.
- [5] Pollack JR, Perou CM, Alizadeh AA, Eisen MB, Pergamenschikov A, Williams CF, Jeffrey SS, Botstein D, Brown PO (1999). "Genome-wide analysis of DNA copy-number changes using cDNA microarrays". *Nat Genet* **23**: 41–46. doi: 10.1038/14385 (<http://dx.doi.org/10.1038/14385>). PMID 10471496.
- [6] Moran G, Stokes C, Thewes S, Hube B, Coleman DC, Sullivan D (2004). "Comparative genomics using *Candida albicans* DNA microarrays reveals absence and divergence of virulence-associated genes in *Candida dubliniensis*". *Microbiology* **150**: 3363–3382. doi: 10.1099/mic.0.27221-0 (<http://dx.doi.org/10.1099/mic.0.27221-0>). PMID 15470115.
- [7] <http://bgmo.jrc.ec.europa.eu/home/docs.htm>
- [8] Hacia JG, Fan JB, Ryder O, Jin L, Edgemon K, Ghandour G, Mayer RA, Sun B, Hsie L, Robbins CM, Brody LC, Wang D, Lander ES, Lipshutz R, Fodor SP, Collins FS (1999). "Determination of ancestral alleles for human single-nucleotide polymorphisms using high-density oligonucleotide arrays". *Nat Genet* **22**: 164–167. doi: 10.1038/9674 (<http://dx.doi.org/10.1038/9674>). PMID 10369258.
- [9] Lausted C et al. (2004). "http://genomebiology.com/2004/5/8/R58|POSaM: a fast, flexible, open-source, inkjet oligonucleotide synthesizer and microarrayer". *Genome Biology* **5**: R58. doi: 10.1186/gb-2004-5-8-r58 (<http://dx.doi.org/10.1186/gb-2004-5-8-r58>). PMID 15287980. <http://genomebiology.com/2004/5/8/R58>.
- [10] Bammler T, Beyer RP, Bhattacharya S, Boorman GA, Boyles A, Bradford BU, Bumgarner RE, Bushel PR, Chaturvedi K, Choi D, Cunningham ML, Deng S, Dressman HK, Fannin RD, Farin FM, Freedman JH, Fry RC, Harper A, Humble MC, Hurban P, Kavanagh TJ, Kaufmann WK, Kerr KF, Jing L, Lapidus JA, Lasarev MR, Li J, Li YJ, Lobenhofer EK, Lu X, Malek RL, Milton S, Nagalla SR, O'malley JP, Palmer VS, Pattee P, Paules RS, Perou CM, Phillips K, Qin LX, Qiu Y, Quigley SD, Rodland M, Rusyn I, Samson LD, Schwartz DA, Shi Y, Shin JL, Sieber SO, Slifer S, Speer MC, Spencer PS, Sproles DI, Swenberg JA, Suk WA, Sullivan RC, Tian R, Tennant RW, Todd SA, Tucker CJ, Van Houten B, Weis BK, Xuan S, Zarbl H; Members of the Toxicogenomics Research Consortium. (2005). "Standardizing global gene expression analysis between laboratories and across platforms". *Nat Methods* **2**: 351–356. doi: 10.1038/nmeth0605-477a (<http://dx.doi.org/10.1038/nmeth0605-477a>). PMID 15846362.

- [11] Pease AC, Solas D, Sullivan EJ, Cronin MT, Holmes CP, Fodor SP. (1994). "Light-generated oligonucleotide arrays for rapid DNA sequence analysis". *PNAS* **91**: 5022-5026. doi: 10.1073/pnas.91.11.5022 (<http://dx.doi.org/10.1073/pnas.91.11.5022>). PMID 8197176.
- [12] Nuwaysir EF, Huang W, Albert TJ, Singh J, Nuwaysir K, Pitas A, Richmond T, Gorski T, Berg JP, Ballin J, McCormick M, Norton J, Pollock T, Sumwalt T, Butcher L, Porter D, Molla M, Hall C, Blattner F, Sussman MR, Wallace RL, Cerrina F, Green RD. (2002). "Gene expression analysis using oligonucleotide arrays produced by maskless photolithography". *Genome Res* **12**: 1749-1755. doi: 10.1101/gr.362402 (<http://dx.doi.org/10.1101/gr.362402>). PMID 12421762.
- [13] Shalon D, Smith SJ, Brown PO (1996). "A DNA microarray system for analyzing complex DNA samples using two-color fluorescent probe hybridization". *Genome Res* **6**: 639-645. doi: 10.1101/gr.6.7.639 (<http://dx.doi.org/10.1101/gr.6.7.639>). PMID 8796352.
- [14] Tang T, François N, Glatigny A, Agier N, Mucchielli MH, Aggerbeck L, Delacroix H (2007). "Expression ratio evaluation in two-colour microarray experiments is significantly improved by correcting image misalignment". *Bioinformatics* **23**: 2686-2691. doi: 10.1093/bioinformatics/btm399 (<http://dx.doi.org/10.1093/bioinformatics/btm399>). PMID 17698492.
- [15] Churchill GA (2002). "<http://www.vmr.org/research-websites/gcf/Forms/Churchill.pdf>[Fundamentals of experimental design for cDNA microarrays" (- Scholar search (http://scholar.google.co.uk/scholar?hl=en&lr=&q=intitle:Fundamentals+of+experimental+design+for+cDNA+microarrays&as_publication=Nature+genetics+suppliment&as_ylo=2002&as_yhi=2002&btnG=Search)). *Nature genetics suppliment* **32**: 490. doi: 10.1038/ng1031 (<http://dx.doi.org/10.1038/ng1031>). <http://www.vmr.org/research-websites/gcf/Forms/Churchill.pdf>.
- [16] NCTR Center for Toxicoinformatics - MAQC Project (<http://www.fda.gov/nctr/science/centers/toxicoinformatics/maqc/>)
- [17] Wei C, Li J, Bumgarner RE. (2004). "Sample size for detecting differentially expressed genes in microarray experiments". *BMC Genomics* **5**: 87. doi: 10.1186/1471-2164-5-87 (<http://dx.doi.org/10.1186/1471-2164-5-87>). PMID 15533245.
- [18] Wouters L, Göhlmann HW, Bijmens L, Kass SU, Molenberghs G, Lewi PJ (2003). "Graphical exploration of gene expression data: a comparative study of three multivariate methods". *Biometrics* **59**: 1131-1139. doi: 10.1111/j.0006-341X.2003.00130.x (<http://dx.doi.org/10.1111/j.0006-341X.2003.00130.x>).
- [19] Jain N, Thatte J, Braciale T, Ley K, O'Connell M, Lee JK (2003). "Local-pooled-error test for identifying differentially expressed genes with a small number of replicated microarrays". *Bioinformatics* **19**: 1945-1951. doi: 10.1093/bioinformatics/btg264 (<http://dx.doi.org/10.1093/bioinformatics/btg264>).

Glossary

- An **Array** or **slide** is a collection of *features* spatially arranged in a two dimensional grid, arranged in columns and rows.
- **Block** or **subarray**: a group of spots, typically made in one print round; several subarrays/blocks form an array.
- **Case/control**: an experimental design paradigm especially suited to the two-colour array system, in which a condition chosen as control (such as healthy tissue or state) is compared to an altered condition (such as a diseased tissue or state).
- **Channel**: the fluorescence output recorded in the scanner for an individual fluorophore and can even be ultraviolet.
- **Dye flip** or **Dye swap** or **Fluor reversal**: reciprocal labelling of DNA targets with the two dyes to account for dye bias in experiments.
- **Scanner**: an instrument used to detect and quantify the intensity of fluorescence of spots on a microarray slide, by selectively exciting fluorophores with a laser and measuring the fluorescence with a filter (optics) photomultiplier system.
- **Spot** or **feature**: a small area on an array slide that contains picomoles of specific DNA samples.
- For other relevant terms see:

Glossary of gene expression terms

Protocol (natural sciences)

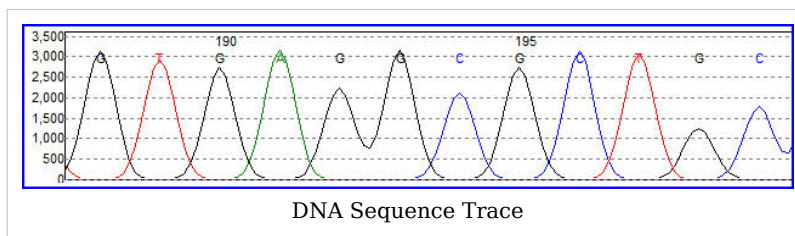
External links

- Many important links can be found at the Open Directory Project
 - Gene Expression (http://www.dmoz.org/Science/Biology/Biochemistry_and_Molecular_Biology/Gene_Expression/) at the Open Directory Project
 - Micro Scale Products and Services for Biochemistry and Molecular Biology (http://www.dmoz.org/Science/Biology/Biochemistry_and_Molecular_Biology/Products_and_Services/Micro_Scale/) at the Open Directory Project
 - Products and Services for Gene Expression (http://www.dmoz.org/Science/Biology/Biochemistry_and_Molecular_Biology/Gene_Expression/Products_and_Services/) at the Open Directory Project
 - PLoS Biology Primer: Microarray Analysis (<http://biology.plosjournals.org/perlserv/?request=get-document&doi=10.1371/journal.pbio.0000015>)
 - Rundown of microarray technology (<http://www.genome.gov/page.cfm?pageID=10000533>)
 - ArrayMining.net (<http://www.arraymining.net>) - a free web-server for online microarray analysis
 - CLASSIFI (<http://pathcuric1.swmed.edu/pathdb/classifi.html>) - Gene Ontology-based gene cluster classification resource
 - Microarray - How does it work? (http://www.unsolvedmysteries.oregonstate.edu/microarray_07)
 - Microarray data processing using Self-Organizing Maps tutorial: Part 1 (<http://blog.peltarion.com/2007/04/10/the-self-organized-gene-part-1>) Part 2 (<http://blog.peltarion.com/2007/06/13/the-self-organized-gene-part-2>)
-

DNA sequencing

The term **DNA sequencing** refers to methods for determining the order of the nucleotide bases, adenine, guanine, cytosine, and thymine, in a molecule of DNA. The first DNA sequences were obtained by academic researchers, using laborious methods based on 2-dimensional chromatography in the early 1970s. Following the development of dye-based sequencing methods with automated analysis, DNA sequencing has become easier and orders of magnitude faster. Knowledge of DNA sequences of genes and other parts of the genome of organisms has become indispensable for basic research studying biological processes, as well as in applied fields such as diagnostic or forensic research. The advent of DNA sequencing has significantly accelerated biological research and discovery. The rapid speed of sequencing attained with modern DNA sequencing technology has been instrumental in the sequencing of the human genome, in the Human Genome Project. Related projects, often by scientific collaboration across continents, have generated the complete DNA sequences of many animal, plant, and microbial genomes.

RNA sequencing, which is technically easier to perform than DNA sequencing, was one of the earliest forms of nucleotide sequencing. The major landmark of RNA sequencing is the sequence of



the first complete gene and the complete genome of Bacteriophage MS2, identified and published by Walter Fiers and his coworkers at the University of Ghent (Ghent, Belgium), between 1972^[1] and 1976.^[2]

Prior to the development of rapid DNA sequencing methods in the early 1970s by Frederick Sanger at the University of Cambridge, in England and Walter Gilbert and Allan Maxam at Harvard,^[3] ^[4] a number of laborious methods were used. For instance, in 1973, Gilbert and Maxam reported the sequence of 24 basepairs using a method known as wandering-spot analysis.^[5]

The chain-termination method developed by Sanger and coworkers in 1975 soon became the method of choice, owing to its relative ease and reliability.^[6] ^[7]

Maxam-Gilbert sequencing

In 1976-1977, Allan Maxam and Walter Gilbert developed a DNA sequencing method based on chemical modification of DNA and subsequent cleavage at specific bases.^[3] Although Maxam and Gilbert published their chemical sequencing method two years after the ground-breaking paper of Sanger and Coulson on plus-minus sequencing,^[6] ^[8] Maxam-Gilbert sequencing rapidly became more popular, since purified DNA could be used directly, while the initial Sanger method required that each read start be cloned for production of single-stranded DNA. However, with the improvement of the chain-termination method (see below), Maxam-Gilbert sequencing has fallen out of favour due to its technical complexity prohibiting its use in standard molecular biology kits, extensive use of hazardous chemicals, and difficulties with scale-up.

The method requires radioactive labelling at one end and purification of the DNA fragment to be sequenced. Chemical treatment generates breaks at a small proportion of one or two of the four nucleotide bases in each of four reactions (G, A+G, C, C+T). Thus a series of labelled fragments is generated, from the radiolabelled end to the first 'cut' site in each molecule. The fragments in the four reactions are arranged side by side in gel electrophoresis for size separation. To visualize the fragments, the gel is exposed to X-ray film for autoradiography, yielding a series of dark bands each corresponding to a radiolabelled DNA fragment, from which the sequence may be inferred.

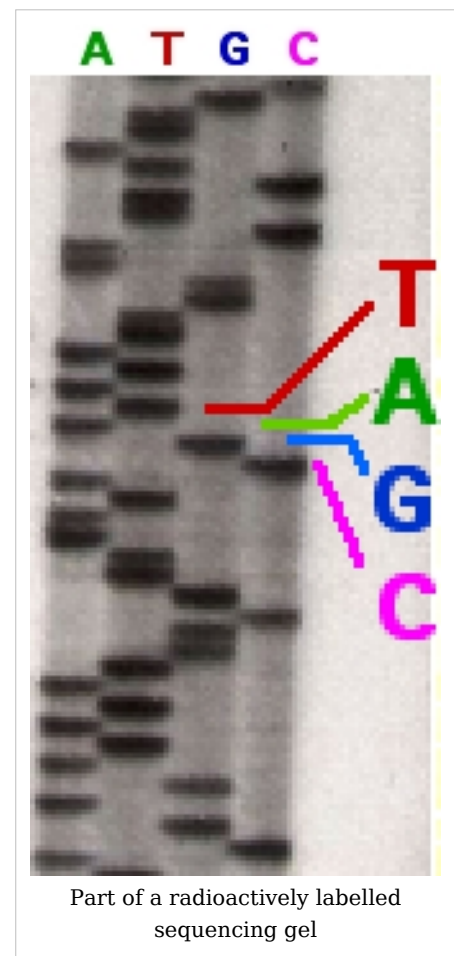
Also sometimes known as 'chemical sequencing', this method originated in the study of DNA-protein interactions (footprinting), nucleic acid structure and epigenetic modifications to DNA, and within these it still has important applications.

Chain-termination methods

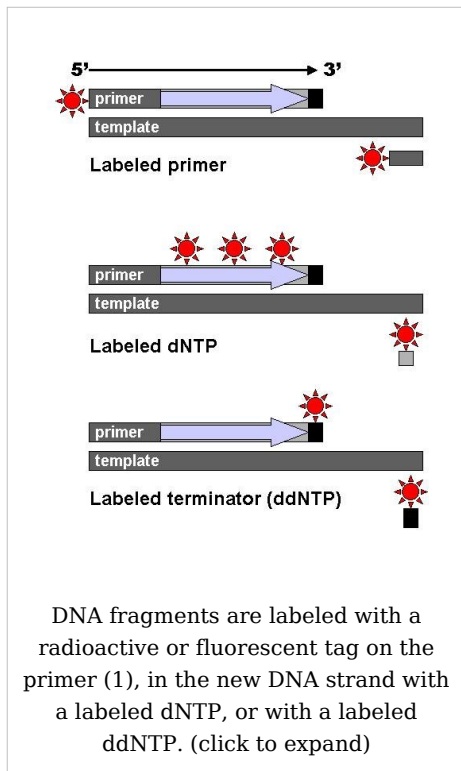
Because the chain-terminator method (or Sanger method after its developer Frederick Sanger) is more efficient and uses fewer toxic chemicals and lower amounts of radioactivity than the method of Maxam and Gilbert, it rapidly became the method of choice. The key principle of the Sanger method was the use of dideoxynucleotide triphosphates (ddNTPs) as DNA chain terminators.

The classical chain-termination method requires a single-stranded DNA template, a DNA primer, a DNA polymerase, radioactively or fluorescently labeled nucleotides, and modified nucleotides that terminate DNA strand elongation. The DNA sample is divided into four separate sequencing reactions, containing all four of the standard deoxynucleotides (dATP, dGTP, dCTP and dTTP) and the DNA polymerase. To each reaction is added only one of the four dideoxynucleotides (ddATP, ddGTP, ddCTP, or ddTTP) which are the chain-terminating nucleotides, lacking a 3'-OH group required for the formation of a phosphodiester bond between two nucleotides, thus terminating DNA strand extension and resulting in various DNA fragments of varying length.

The newly synthesized and labeled DNA fragments are heat denatured, and separated by size (with a resolution of just one nucleotide) by gel electrophoresis on a denaturing polyacrylamide-urea gel with each of the four reactions run in one of four individual lanes (lanes A, T, G, C); the DNA bands are then visualized by autoradiography or UV light, and the DNA sequence can be directly read off the X-ray film or gel image. In the image on the right, X-ray film was exposed to the gel, and the dark bands correspond to DNA fragments of different lengths. A dark band in a lane indicates a DNA fragment that is the result of chain termination after incorporation of a dideoxynucleotide (ddATP, ddGTP, ddCTP, or ddTTP). The relative positions of the different bands among the four lanes are then used to read (from bottom to

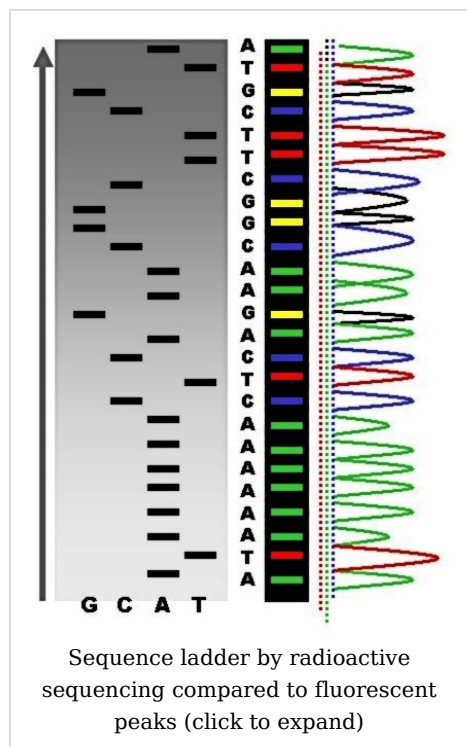


top) the DNA sequence.

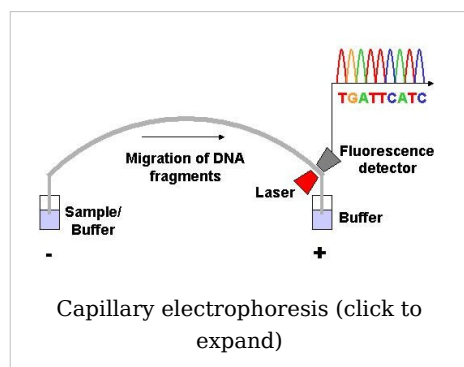


Technical variations of chain-termination sequencing include tagging with nucleotides containing radioactive phosphorus for radiolabelling, or using a primer labeled at the 5' end with a fluorescent dye. Dye-primer sequencing facilitates reading in an optical system for faster and more economical analysis and automation. The later development by Leroy Hood and coworkers^[9]^[10] of fluorescently labeled ddNTPs and primers set the stage for automated, high-throughput DNA sequencing.

Chain-termination methods have greatly simplified DNA sequencing. For example, chain-termination-based kits are commercially available that contain the reagents needed for sequencing, pre-aliquoted and ready to use. Limitations include non-specific binding of the primer to the DNA, affecting accurate read-out of the DNA sequence, and DNA secondary structures affecting the fidelity of the sequence.



Dye-terminator sequencing



Dye-terminator sequencing utilizes labelling of the chain terminator ddNTPs, which permits sequencing in a single reaction, rather than four reactions as in the labelled-primer method. In dye-terminator sequencing, each of the four dideoxynucleotide chain terminators is labelled with fluorescent dyes, each of which with different wavelengths of fluorescence and emission. Owing to its greater expediency and speed, dye-terminator sequencing is now the mainstay in automated sequencing. Its limitations include dye

effects due to differences in the incorporation of the dye-labelled chain terminators into the DNA fragment, resulting in unequal peak heights and shapes in the electronic DNA sequence trace chromatogram after capillary electrophoresis (see figure to the right). This problem has been addressed with the use of modified DNA polymerase enzyme systems and dyes that minimize incorporation variability, as well as methods for eliminating "dye blobs". The dye-terminator sequencing method, along with automated high-throughput DNA sequence analyzers, is now being used for the vast majority of sequencing projects.

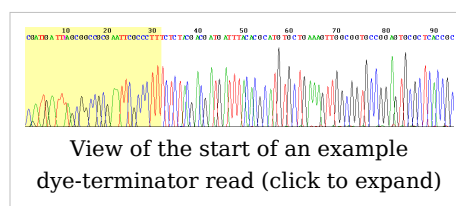
Challenges

Common challenges of DNA sequencing include poor quality in the first 15-40 bases of the sequence and deteriorating quality of sequencing traces after 700-900 bases. Base calling software typically gives an estimate of quality to aid in quality trimming.

In cases where DNA fragments are cloned before sequencing, the resulting sequence may contain parts of the cloning vector. In contrast, PCR-based cloning and emerging sequencing technologies based on pyrosequencing often avoid using cloning vectors.

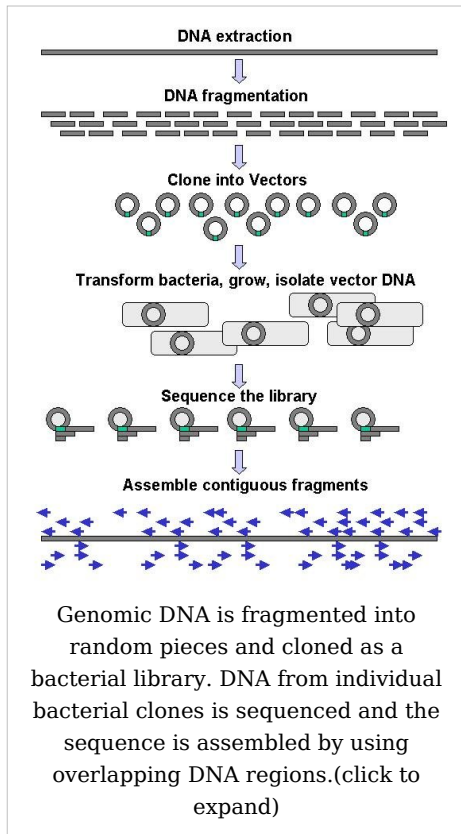
Automation and sample preparation

Automated DNA-sequencing instruments (DNA sequencers) can sequence up to 384 DNA samples in a single batch (run) in up to 24 runs a day. DNA sequencers carry out capillary electrophoresis for size separation, detection and recording of dye fluorescence, and data output as fluorescent peak trace chromatograms. Sequencing reactions by thermocycling, cleanup and re-suspension in a buffer solution before loading onto the sequencer are performed separately. A number of commercial and non-commercial software packages can trim low-quality DNA traces automatically. These programs score the quality of each peak and remove low-quality base peaks (generally located at the ends of the sequence). The accuracy of such algorithms is below visual examination by a human operator, but sufficient for automated processing of large sequence data sets.



Large-scale sequencing strategies

Current methods can directly sequence only relatively short (300-1000 nucleotides long) DNA fragments in a single reaction.^[11] The main obstacle to sequencing DNA fragments above this size limit is insufficient power of separation for resolving large DNA fragments that differ in length by only one nucleotide.



Large-scale sequencing aims at sequencing very long DNA pieces, such as whole chromosomes. Common approaches consist of cutting (with restriction enzymes) or shearing (with mechanical forces) large DNA fragments into shorter DNA fragments. The fragmented DNA is cloned into a DNA vector, and amplified in *Escherichia coli*. Short DNA fragments purified from individual bacterial colonies are individually sequenced and assembled electronically into one long, contiguous sequence. This method does not require any pre-existing information about the sequence of the DNA and is referred to as *de novo* sequencing. Gaps in the assembled sequence may be filled by primer walking. The different strategies have different tradeoffs in speed and accuracy; *shotgun methods* are often used for sequencing large genomes, but its assembly is complex and difficult, particularly with sequence repeats often causing gaps in genome assembly.

New sequencing methods

High-throughput sequencing

The high demand for low-cost sequencing has driven the development of high-throughput sequencing technologies that parallelize the sequencing process, producing thousands or millions of sequences at once.^{[12] [13]} High-throughput sequencing technologies are intended to lower the cost of DNA sequencing beyond what is possible with standard dye-terminator methods.

In vitro clonal amplification

Molecular detection methods are not sensitive enough for single molecule sequencing, so most approaches use an *in vitro* cloning step to amplify individual DNA molecules. Emulsion PCR isolates individual DNA molecules along with primer-coated beads in aqueous droplets within an oil phase. Polymerase chain reaction (PCR) then coats each bead with clonal copies of the DNA molecule followed by immobilization for later sequencing. Emulsion PCR is used in the methods by Margulis et al. (commercialized by 454 Life Sciences), Shendure and Porreca et al. (also known as "polony sequencing") and SOLiD sequencing, (developed by Agencourt, now Applied Biosystems).^{[14] [15] [16]} Another method for *in vitro* clonal amplification is *bridge PCR*, where fragments are amplified upon primers attached to a

solid surface. The single-molecule method developed by Stephen Quake's laboratory (later commercialized by Helicos) skips this amplification step, directly fixing DNA molecules to a surface.^[17]

Parallelized sequencing

DNA molecules are physically bound to a surface, and sequenced in parallel. *Sequencing by synthesis*, like dye-termination electrophoretic sequencing, uses a DNA polymerase to determine the base sequence. Reversible terminator methods (used by Illumina and Helicos) use reversible versions of dye-terminators, adding one nucleotide at a time, detect fluorescence at each position in real time, by repeated removal of the blocking group to allow polymerization of another nucleotide. Pyrosequencing (used by 454) also uses DNA polymerization, adding one nucleotide species at a time and detecting and quantifying the number of nucleotides added to a given location through the light emitted by the release of attached pyrophosphates.^{[14] [18]}

Sequencing by ligation

This enzymatic sequencing method uses a DNA ligase to determine the target sequence.^{[15] [16] [19]} Used in the polony method and in the SOLiD technology, it uses a pool of all possible oligonucleotides of a fixed length, labeled according to the sequenced position. Oligonucleotides are annealed and ligated; the preferential ligation by DNA ligase for matching sequences results in a signal informative of the nucleotide at that position.

Microfluidic Sanger Sequencing

In microfluidic Sanger sequencing the entire thermocycling amplification of DNA fragments as well as their separation by electrophoresis is done on a single chip (approximately 100 μm in diameter) thus reducing the reagent usage as well as cost. In some instances researchers have shown that they can increase the through-put of conventional sequencing through the use of microchips. Research will still need to be done in order to make this use of technology effective.

Other sequencing technologies

Sequencing by hybridization is a non-enzymatic method that uses a DNA microarray. A single pool of DNA whose sequence is to be determined is fluorescently labeled and hybridized to an array containing known sequences. Strong hybridization signals from a given spot on the array identifies its sequence in the DNA being sequenced.^[20] Mass spectrometry may be used to determine mass differences between DNA fragments produced in chain-termination reactions.^[21]

DNA sequencing methods currently under development include labeling the DNA polymerase,^[22] reading the sequence as a DNA strand transits through nanopores,^{[23] [24]} and microscopy-based techniques, such as AFM or electron microscopy that are used to identify the positions of individual nucleotides within long DNA fragments (>5,000 bp) by nucleotide labeling with heavier elements (e.g., halogens) for visual detection and recording.^[25]

In October 2006, the X Prize Foundation established an initiative to promote the development of full genome sequencing technologies, called the Archon X Prize, intending to award \$10 million to "the first Team that can build a device and use it to sequence 100 human genomes within 10 days or less, with an accuracy of no more than one error in every 100,000 bases sequenced, with sequences accurately covering at least 98% of the genome,

and at a recurring cost of no more than \$10,000 (US) per genome."^[26]

Major landmarks in DNA sequencing

- 1953 Discovery of the structure of the DNA double helix.
- 1972 Development of recombinant DNA technology, which permits isolation of defined fragments of DNA; prior to this, the only accessible samples for sequencing were from bacteriophage or virus DNA.
- 1975 The first complete DNA genome to be sequenced is that of bacteriophage ϕ X174
- 1977 Allan Maxam and Walter Gilbert publish "DNA sequencing by chemical degradation".^[3] Frederick Sanger, independently, publishes "DNA sequencing by enzymatic synthesis".
- 1980 Frederick Sanger and Walter Gilbert receive the Nobel Prize in Chemistry
- 1984 Medical Research Council scientists decipher the complete DNA sequence of the Epstein-Barr virus, 170 kb.
- 1986 Leroy E. Hood's laboratory at the California Institute of Technology and Smith announce the first semi-automated DNA sequencing machine.
- 1987 Applied Biosystems markets first automated sequencing machine, the model ABI 370.
- 1990 The U.S. National Institutes of Health (NIH) begins large-scale sequencing trials on *Mycoplasma capricolum*, *Escherichia coli*, *Caenorhabditis elegans*, and *Saccharomyces cerevisiae* (at 75 cents (US)/base).
- 1995 Richard Mathies *et al.* publish dye-based sequencing.^[27]
- 1998 Phil Green and Brent Ewing of the University of Washington publish "phred" for sequencer data analysis^[28].

See also

- Sequencing
 - Full Genome Sequencing
 - Genome project
 - Single Molecule Real Time Sequencing
 - Applied Biosystems
 - 454 Life Sciences
 - Illumina (company)
 - Pacific Biosciences
 - Complete Genomics
 - Joint Genome Institute
 - DNA field-effect transistor
 - DNA sequencing theory
-

References

- [1] Min Jou W, Haegeman G, Ysebaert M, Fiers W (May 1972). "Nucleotide sequence of the gene coding for the bacteriophage MS2 coat protein". *Nature* **237** (5350): 82–8. doi: 10.1038/237082a0 (<http://dx.doi.org/10.1038/237082a0>). PMID 4555447.
- [2] Fiers W, Contreras R, Duerinck F, *et al* (April 1976). "Complete nucleotide sequence of bacteriophage MS2 RNA: primary and secondary structure of the replicase gene". *Nature* **260** (5551): 500–7. doi: 10.1038/260500a0 (<http://dx.doi.org/10.1038/260500a0>). PMID 1264203.
- [3] Maxam AM, Gilbert W (February 1977).
"http://www.pubmedcentral.nih.gov/articlerender.fcgi?tool=pmcentrez&artid=392330|A new method for sequencing DNA". *Proc. Natl. Acad. Sci. U.S.A.* **74** (2): 560–4. doi: 10.1073/pnas.74.2.560 (<http://dx.doi.org/10.1073/pnas.74.2.560>). PMID 265521.
- [4] Gilbert, W. DNA sequencing and gene structure (http://nobelprize.org/nobel_prizes/chemistry/laureates/1980/gilbert-lecture.pdf). Nobel lecture, 8 December 1980.
- [5] Gilbert W, Maxam A (December 1973).
"http://www.pubmedcentral.nih.gov/articlerender.fcgi?tool=pmcentrez&artid=427284|The nucleotide sequence of the lac operator". *Proc. Natl. Acad. Sci. U.S.A.* **70** (12): 3581–4. doi: 10.1073/pnas.70.12.3581 (<http://dx.doi.org/10.1073/pnas.70.12.3581>). PMID 4587255.
- [6] Sanger F, Coulson AR (May 1975). "A rapid method for determining sequences in DNA by primed synthesis with DNA polymerase". *J. Mol. Biol.* **94** (3): 441–8. doi: 10.1016/0022-2836(75)90213-2 ([http://dx.doi.org/10.1016/0022-2836\(75\)90213-2](http://dx.doi.org/10.1016/0022-2836(75)90213-2)). PMID 1100841.
- [7] Sanger F, Nicklen S, Coulson AR (December 1977).
"http://www.pubmedcentral.nih.gov/articlerender.fcgi?tool=pmcentrez&artid=431765|DNA sequencing with chain-terminating inhibitors". *Proc. Natl. Acad. Sci. U.S.A.* **74** (12): 5463–7. doi: 10.1073/pnas.74.12.5463 (<http://dx.doi.org/10.1073/pnas.74.12.5463>). PMID 271968.
- [8] Sanger F. Determination of nucleotide sequences in DNA (http://nobelprize.org/nobel_prizes/chemistry/laureates/1980/sanger-lecture.pdf). Nobel lecture, 8 December 1980.
- [9] Smith LM, Sanders JZ, Kaiser RJ, *et al* (1986). "Fluorescence detection in automated DNA sequence analysis". *Nature* **321** (6071): 674–9. doi: 10.1038/321674a0 (<http://dx.doi.org/10.1038/321674a0>). PMID 3713851.
"We have developed a method for the partial automation of DNA sequence analysis. Fluorescence detection of the DNA fragments is accomplished by means of a fluorophore covalently attached to the oligonucleotide primer used in enzymatic DNA sequence analysis. A different coloured fluorophore is used for each of the reactions specific for the bases A, C, G and T. The reaction mixtures are combined and co-electrophoresed down a single polyacrylamide gel tube, the separated fluorescent bands of DNA are detected near the bottom of the tube, and the sequence information is acquired directly by computer."
- [10] Smith LM, Fung S, Hunkapiller MW, Hunkapiller TJ, Hood LE (April 1985).
"http://nar.oxfordjournals.org/cgi/pmidlookup?view=long&pmid=4000959|The synthesis of oligonucleotides containing an aliphatic amino group at the 5' terminus: synthesis of fluorescent DNA primers for use in DNA sequence analysis". *Nucleic Acids Res.* **13** (7): 2399–412. doi: 10.1093/nar/13.7.2399 (<http://dx.doi.org/10.1093/nar/13.7.2399>). PMID 4000959. PMC: 341163 (<http://www.pubmedcentral.nih.gov/articlerender.fcgi?tool=pmcentrez&artid=341163>). <http://nar.oxfordjournals.org/cgi/pmidlookup?view=long&pmid=4000959>.
- [11] 3730xl DNA Analyzer (<http://www.appliedbiosystems.com/catalog/myab/StoreCatalog/products/CategoryDetails.jsp?hierarchyID=102&category1st=a50&category2nd=a51&category3rd=111907>)
- [12] Hall N (May 2007). "Advanced sequencing technologies and their wider impact in microbiology". *J. Exp. Biol.* **210** (Pt 9): 1518–25. doi: 10.1242/jeb.001370 (<http://dx.doi.org/10.1242/jeb.001370>). PMID 17449817.
- [13] Church GM (January 2006). "Genomes for all". *Sci. Am.* **294** (1): 46–54. PMID 16468433.
- [14] Margulies M, Egholm M, Altman WE, *et al* (September 2005).
"http://www.pubmedcentral.nih.gov/articlerender.fcgi?tool=pmcentrez&artid=1464427|Genome sequencing in microfabricated high-density picolitre reactors". *Nature* **437** (7057): 376–80. doi: 10.1038/nature03959 (<http://dx.doi.org/10.1038/nature03959>). PMID 16056220.
- [15] Shendure J, Porreca GJ, Reppas NB, *et al* (September 2005). "Accurate multiplex polony sequencing of an evolved bacterial genome". *Science* **309** (5741): 1728–32. doi: 10.1126/science.1117389 (<http://dx.doi.org/10.1126/science.1117389>). PMID 16081699.
- [16] Applied Biosystems' SOLiD technology (<http://solid.appliedbiosystems.com/>)
- [17] Braslavsky I, Hebert B, Kartalov E, Quake SR (April 2003).
"http://www.pubmedcentral.nih.gov/articlerender.fcgi?tool=pmcentrez&artid=153030|Sequence information can be obtained from single DNA molecules". *Proc. Natl. Acad. Sci. U.S.A.* **100** (7): 3960–4. doi: 10.1073/pnas.0230489100 (<http://dx.doi.org/10.1073/pnas.0230489100>). PMID 12651960.

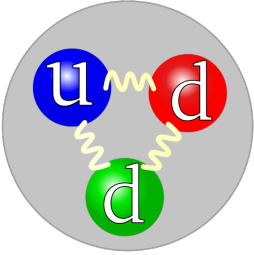
- [18] M. Ronaghi, S. Karamohamed, B. Pettersson, M. Uhlen, and P. Nyren (1996). "Real-time DNA sequencing using detection of pyrophosphate release". *Analytical Biochemistry* **242**: 84–9. doi: 10.1006/abio.1996.0432 (<http://dx.doi.org/10.1006/abio.1996.0432>).
- [19] US5750341 (<http://patft.uspto.gov/netacgi/nph-Parser?patentnumber=5750341>) (1995-04-17) Macevicz SC, *DNA sequencing by parallel oligonucleotide extensions*.
- [20] Hanna GJ, Johnson VA, Kuritzkes DR, *et al* (01 July 2000). "<http://jcm.asm.org/cgi/pmidlookup?view=long&pmid=10878069>|Comparison of sequencing by hybridization and cycle sequencing for genotyping of human immunodeficiency virus type 1 reverse transcriptase". *J. Clin. Microbiol.* **38** (7): 2715–21. PMID 10878069. PMC: 87006 (<http://www.pubmedcentral.nih.gov/articlerender.fcgi?tool=pmcentrez&artid=87006>). <http://jcm.asm.org/cgi/pmidlookup?view=long&pmid=10878069>.
- [21] J.R. Edwards, H. Ruparel, and J. Ju (2005). "Mass-spectrometry DNA sequencing". *Mutation Research* **573** (1-2): 3–12.
- [22] VisiGen Biotechnologies Inc. - Technology Overview (http://visigenbio.com/technology_overview.html)
- [23] The Harvard Nanopore Group (<http://mcb.harvard.edu/branton/index.htm>)
- [24] <http://www.physorg.com/news157378086.html>"Nanopore Sequencing Could Slash DNA Analysis Costs". <http://www.physorg.com/news157378086.html>.
- [25] US20060029957 (<http://patft.uspto.gov/netacgi/nph-Parser?patentnumber=20060029957>) (2005-07-14) ZS Genetics, *Systems and methods of analyzing nucleic acid polymers and related components*.
- [26] "PRIZE Overview: Archon X PRIZE for Genomics" (<http://genomics.xprize.org/genomics/archon-x-prize-for-genomics/prize-overview>)
- [27] Ju J, Ruan C, Fuller CW, Glazer AN, Mathies RA (May 1995). "<http://www.pubmedcentral.nih.gov/articlerender.fcgi?tool=pmcentrez&artid=41941>|Fluorescence energy transfer dye-labeled primers for DNA sequencing and analysis". *Proc. Natl. Acad. Sci. U.S.A.* **92** (10): 4347–51. doi: 10.1073/pnas.92.10.4347 (<http://dx.doi.org/10.1073/pnas.92.10.4347>). PMID 7753809.
- [28] Ewing B, Green P (March 1998). "<http://www.genome.org/cgi/pmidlookup?view=long&pmid=9521922>|Base-calling of automated sequencer traces using phred. II. Error probabilities". *Genome Res.* **8** (3): 186–94. PMID 9521922. <http://www.genome.org/cgi/pmidlookup?view=long&pmid=9521922>.

External links

- Disruptive Gene Sequencing technology (http://en.wikipedia.org/wiki/Single_Molecule_Real_Time_Sequencing) - Single Molecule Real Time (SMRT) sequencing

Neutron resources

Neutron

<i>Neutron</i>	
	
The quark structure of the neutron.	
Classification:	Baryon
Composition:	1 up quark, 2 down quarks
Family:	Fermion
Group:	Hadron
Interaction:	Gravity, Weak, Strong
Antiparticle:	Antineutron
Theorized:	Ernest Rutherford ^[1] (1920)
Discovered:	James Chadwick ^[2] (1932)
Symbol(s):	n, n ⁰ , N ⁰
Mass:	$1.67492729(28) \times 10^{-27} \text{ kg}$ $939.565560(81) \text{ MeV}/c^2$ $1.0086649156(6) \text{ u}$ ^[3]
Mean lifetime:	885.7(8) s (free)
Electric charge:	0 e 0 °C
Electric dipole moment:	$<2.9 \times 10^{-26} \text{ e cm}$
Electric polarizability:	$1.16(15) \times 10^{-3} \text{ fm}^3$
Magnetic moment:	$-1.9130427(5) \mu_N$
Magnetic polarizability:	$3.7(20) \times 10^{-4} \text{ fm}^3$
Spin:	$\frac{1}{2}$
Isospin:	$-\frac{1}{2}$
Parity:	+1

Condensed:	$I(J^P) = 1^{\frac{1}{2}}_2(1^{\frac{1}{2}}_2^+)$
-------------------	---

The **neutron** is a subatomic particle with no net electric charge and a mass slightly larger than that of a proton.

Neutrons are usually found in atomic nuclei. The nuclei of most atoms consist of protons and neutrons, which are therefore collectively referred to as nucleons. The number of protons in a nucleus is the atomic number and defines the type of element the atom forms. The number of neutrons determines the isotope of an element. For example, the carbon-12 isotope has 6 protons and 6 neutrons, while the carbon-14 isotope has 6 protons and 8 neutrons.

While bound neutrons in stable nuclei are stable, free neutrons are unstable; they undergo beta decay with a lifetime of just under 15 minutes (885.7 ± 0.8 s).^[4] Free neutrons are produced in nuclear fission and fusion. Dedicated neutron sources like research reactors and spallation sources produce free neutrons for the use in irradiation and in neutron scattering experiments.

Even though it is not a chemical element, the free neutron is sometimes included in tables of nuclides. It is then considered to have an atomic number of zero and a mass number of one.

Discovery

In 1931 Walther Bothe and Herbert Becker in Germany found that if the very energetic alpha particles emitted from polonium fell on certain light elements, specifically beryllium, boron, or lithium, an unusually penetrating radiation was produced. At first this radiation was thought to be gamma radiation, although it was more penetrating than any gamma rays known, and the details of experimental results were very difficult to interpret on this basis. The next important contribution was reported in 1932 by Irène Joliot-Curie and Frédéric Joliot in Paris. They showed that if this unknown radiation fell on paraffin or any other hydrogen-containing compound it ejected protons of very high energy. This was not in itself inconsistent with the assumed gamma ray nature of the new radiation, but detailed quantitative analysis of the data became increasingly difficult to reconcile with such a hypothesis.

Finally, in 1932 the physicist James Chadwick in the George Holt building at the University of Liverpool performed a series of experiments showing that the gamma ray hypothesis was untenable. He suggested that in fact the new radiation consisted of uncharged particles of approximately the mass of the proton, and he performed a series of experiments verifying his suggestion.^[5] These uncharged particles were called *neutrons*, apparently from the Latin root for *neutral* and the Greek ending *-on* (by imitation of *electron* and *proton*).

The discovery of the neutron immediately explained a known puzzle involving the spin of the nitrogen-14 nucleus, which had been experimentally measured to be 1 basic unit of angular momentum. It was known that atomic nuclei usually had about half as many positive charges as if they were composed completely of protons, and in existing models this was often explained by proposing that nuclei also contained some "nuclear electrons" to neutralize the excess charge. Thus, nitrogen-14 would be composed of 14 protons and 7 electrons to give it a charge of +7 but a mass of 14 atomic mass units. However, it also known that both protons and electrons carried an intrinsic spin of 1/2 unit of angular momentum, and there was no way to arrange 21 particles in one group, or in groups of 7

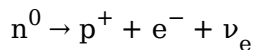
and 14, to give a spin of 1. All possible pairings gave a net spin of 1/2. However, when nitrogen-14 was proposed to consist of 3 pairs of protons and neutrons, with an additional unpaired neutron and proton each contributing a spin of 1/2 in the same direction for a total spin of 1, the model became viable. Soon, nuclear neutrons were used to naturally explain spin differences in many different nuclides in the same way, and the neutron as a basic structural unit of atomic nuclei was accepted.

Intrinsic properties

Stability and beta decay

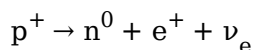
Because the neutron consists of three quarks, the only possible decay mode without a change of baryon number requires the flavour changing of one of the quarks via the weak nuclear force. The neutron consists of two down quarks with charge $-1/3$ and one up quark with charge $+2/3$, and the decay of one of the down quarks into a lighter up quark can be achieved by the emission of a W boson. By this means the neutron decays into a proton (which contains one down and two up quarks), an electron, and an electron antineutrino (antineutrino).

Outside the nucleus, free neutrons are unstable and have a mean lifetime of 885.7 ± 0.8 s (about 15 minutes), decaying by emission of a negative electron and antineutrino to become a proton:^[6]

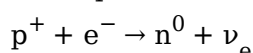


This decay mode, known as beta decay, can also transform the character of neutrons within unstable nuclei.

Bound inside a nucleus, protons can also transform via inverse beta decay into neutrons. In this case, the transformation occurs by emission of a positron (antielectron) and a neutrino (instead of an antineutrino):

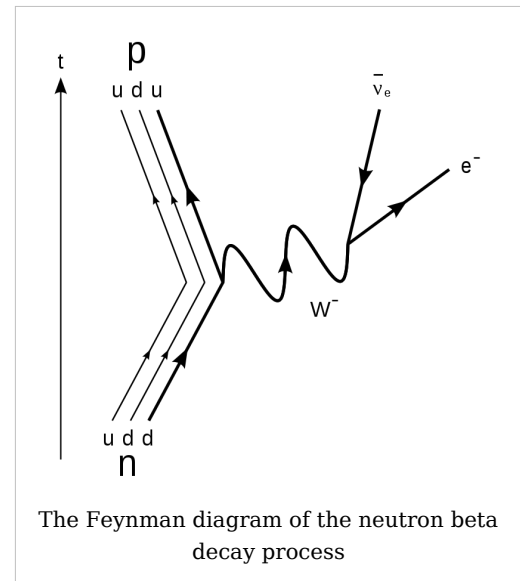


The transformation of a proton to a neutron inside of a nucleus is also possible through electron capture:



Positron capture by neutrons in nuclei that contain an excess of neutrons is also possible, but is hindered because positrons are repelled by the nucleus, and quickly annihilate when they encounter negative electrons.

When bound inside of a nucleus, the instability of a single neutron to beta decay is balanced against the instability that would be acquired by the nucleus as a whole if an additional proton were to participate in repulsive interactions with the other protons that are already present in the nucleus. As such, although free neutrons are unstable, bound neutrons are not necessarily so. The same reasoning explains why protons, which are stable in empty



space, may transform into neutrons when bound inside of a nucleus.

Beta decay and electron capture are types of radioactive decay and are both governed by the weak interaction.

Electric dipole moment

The Standard Model of particle physics predicts a tiny separation of positive and negative charge within the neutron leading to a permanent electric dipole moment. The predicted value is, however, well below the current sensitivity of experiments. From several unsolved puzzles in particle physics, it is clear that the Standard Model is not the final and full description of all particles and their interactions. New theories going beyond the Standard Model generally lead to much larger predictions for the electric dipole moment of the neutron. Currently, there are at least four experiments trying to measure for the first time a finite neutron electric dipole moment.

Anti-neutron

The antineutron is the antiparticle of the neutron. It was discovered by Bruce Cork in the year 1956, a year after the antiproton was discovered. CPT-symmetry puts strong constraints on the relative properties of particles and antiparticles and, therefore, is open to stringent tests. The fractional difference in the masses of the neutron and antineutron is $9 \pm 5 \times 10^{-5}$. Since the difference is only about 2 standard deviations away from zero, this does not give any convincing evidence of CPT-violation.^[3]

Neutron compounds

Dineutrons and tetra-neutrons

The existence of stable clusters of four neutrons, or tetra-neutrons, has been hypothesised by a team led by Francisco-Miguel Marqués at the CNRS Laboratory for Nuclear Physics based on observations of the disintegration of beryllium-14 nuclei. This is particularly interesting because current theory suggests that these clusters should not be stable.

The dineutron is another hypothetical particle.

Neutronium and neutron stars

At extremely high pressures and temperatures, nucleons and electrons are believed to collapse into bulk neutronic matter, called neutronium. Presumably this is what happens in neutron stars.

Detection

The common means of detecting a charged particle by looking for a track of ionization (such as in a cloud chamber) does not work for neutrons directly. Neutrons that elastically scatter off atoms can create an ionization track that is detectable, but the experiments are not as simple to carry out; other means for detecting neutrons, consisting of allowing them to interact with atomic nuclei, are more commonly used.

A common method for detecting neutrons involves converting the energy released from such reactions into electrical signals. The nuclides ^3He , ^6Li , ^{10}B , ^{233}U , ^{235}U , ^{237}Np and ^{239}Pu are useful for this purpose. A good discussion on neutron detection is found in

chapter 14 of the book *Radiation Detection and Measurement* by Glenn F. Knoll (John Wiley & Sons, 1979).

Uses

The neutron plays an important role in many nuclear reactions. For example, neutron capture often results in neutron activation, inducing radioactivity. In particular, knowledge of neutrons and their behavior has been important in the development of nuclear reactors and nuclear weapons. The fissioning of elements like uranium-235 and plutonium-239 is caused by their absorption of neutrons.

Cold, *thermal* and *hot* neutron radiation is commonly employed in neutron scattering facilities, where the radiation is used in a similar way one uses X-rays for the analysis of condensed matter. Neutrons are complementary to the latter in terms of atomic contrasts by different scattering cross sections; sensitivity to magnetism; energy range for inelastic neutron spectroscopy; and deep penetration into matter.

The development of "neutron lenses" based on total internal reflection within hollow glass capillary tubes or by reflection from dimpled aluminum plates has driven ongoing research into neutron microscopy and neutron/gamma ray tomography.^{[7] [8] [9]}

One use of neutron emitters is the detection of light nuclei, particularly the hydrogen found in water molecules. When a fast neutron collides with a light nucleus, it loses a large fraction of its energy. By measuring the rate at which slow neutrons return to the probe after reflecting off of hydrogen nuclei, a neutron probe may determine the water content in soil.

Sources

Because free neutrons are unstable, they can be obtained only from nuclear disintegrations, nuclear reactions, and high-energy reactions (such as in cosmic radiation showers or accelerator collisions). Free neutron beams are obtained from neutron sources by neutron transport. For access to intense neutron sources, researchers must go to specialist facilities, such as the ISIS facility in the UK, which is currently the world's most intense pulsed neutron and muon source.

Neutrons' lack of total electric charge prevents engineers or experimentalists from being able to steer or accelerate them. Charged particles can be accelerated, decelerated, or deflected by electric or magnetic fields. However, these methods have no effect on neutrons except for a small effect of an inhomogeneous magnetic field because of the neutron's magnetic moment.

Protection

Exposure to free neutrons can be hazardous, since the interaction of neutrons with molecules in the body can cause disruption to molecules and atoms, and can also cause reactions which give rise to other forms of radiation (such as protons). The normal precautions of radiation protection apply: avoid exposure, stay as far from the source as possible, and keep exposure time to a minimum. Some particular thought must be given to how to protect from neutron exposure, however. For other types of radiation, e.g. alpha particles, beta particles, or gamma rays, material of a high atomic number and with high density make for good shielding; frequently lead is used. However, this approach will not

work with neutrons, since the absorption of neutrons does not increase straightforwardly with atomic number, as it does with alpha, beta, and gamma radiation. Instead one needs to look at the particular interactions neutrons have with matter (see the section on detection above). For example, hydrogen rich materials are often used to shield against neutrons, since ordinary hydrogen both scatters and slows neutrons. This often means that simple concrete blocks or even paraffin-loaded plastic blocks afford better protection from neutrons than do far more dense materials. After slowing, neutrons may then be absorbed with an isotope which has high affinity for slow neutrons without causing secondary capture-radiation, such as lithium-6.

Hydrogen-rich ordinary water affects neutron absorption in nuclear fission reactors: usually neutrons are so strongly absorbed by normal water that fuel-enrichment with fissionable isotope, is required. The deuterium in heavy water has a very much lower absorption affinity for neutrons than does protium (normal light hydrogen). Deuterium is therefore used in CANDU-type reactors, in order to slow (moderate) neutron velocity, to increase the probability of nuclear fission compared to neutron capture.

Production

Various nuclides become more stable by expelling neutrons as a decay mode; this is known as neutron emission, and happens commonly during spontaneous fission.

Cosmic radiation interacting the Earth's atmosphere continuously generates neutrons that can be detected at the surface. Even stronger neutron radiation is produced at the surface of Mars where the atmosphere is thick enough to generate neutrons from cosmic ray spallation, but not thick enough to provide significant protection from the neutrons produced. These neutrons not only produce a Martian surface neutron radiation hazard from direct downward-going neutron radiation, but also a significant hazard from reflection of neutrons from the Martian surface, which will produces reflected neutron radiation penetrating upward into a Martian craft or habitat from the floor. ^[10]

Nuclear fission reactors naturally produce free neutrons; their role is to sustain the energy-producing chain reaction. The intense neutron radiation can also be used to produce various radioisotopes through the process of neutron activation, which is a type of neutron capture.

Experimental nuclear fusion reactors produce free neutrons as a waste product. However, it is these neutrons that possess most of the energy, and converting that energy to a useful form has proved a difficult engineering challenge. Fusion reactors which generate neutrons are likely to create around twice the amount of radioactive waste of a fission reactor, but the waste is composed of neutron-activated lighter isotopes, which have relatively short (50-100 years) decay periods as compared to typical half lives of 10,000 years for fission waste, which is long primarily due to the long half life of alpha-emitting transuranic actinides. [11] [12]

Neutron temperature

Thermal neutron

A **thermal neutron** is a free neutron that is Boltzmann distributed with $kT = 0.024$ eV (4.0×10^{-21} J) at room temperature. This gives characteristic (not average, or median) speed of 2.2 km/s. The name 'thermal' comes from their energy being that of the room temperature gas or material they are permeating. (see *kinetic theory* for energies and speeds of molecules). After a number of collisions (often in the range of 10–20) with nuclei, neutrons arrive at this energy level, provided that they are not absorbed.

In many substances, thermal neutrons have a much larger effective cross-section than faster neutrons, and can therefore be absorbed more easily by any atomic nuclei that they collide with, creating a heavier — and often unstable — isotope of the chemical element as a result.

Most fission reactors use a neutron moderator to slow down, or *thermalize* the neutrons that are emitted by nuclear fission so that they are more easily captured, causing further fission. Others, called fast breeder reactors, use fission energy neutrons directly.

Cold neutrons

These neutrons are thermal neutrons that have been equilibrated in a very cold substances such as liquid deuterium. These are produced in neutron scattering research facilities.

Ultracold neutrons

Ultracold neutrons are produced by equilibration in substances with a temperature of a few kelvins, such as solid deuterium or superfluid helium. An alternative production method is the mechanical deceleration of cold neutrons.

Fission energy neutron

A **fast neutron** is a free neutron with a kinetic energy level close to 2 MeV (20 TJ/kg), hence a speed of 28,000 km/s. They are named *fission energy* or *fast* neutrons to distinguish them from lower-energy thermal neutrons, and high-energy neutrons produced in cosmic showers or accelerators. Fast neutrons are produced by nuclear processes such as nuclear fission.

Fast neutrons can be made into thermal neutrons via a process called moderation. This is done with a neutron moderator. In reactors, typically heavy water, light water, or graphite are used to moderate neutrons.

Fusion neutron

D-T (deuterium-tritium) fusion is both the easiest fusion reaction to ignite, and produces the most energetic neutrons, with 14.1 MeV of kinetic energy and traveling at 17% of the speed of light. With about 10 times the energy of fission neutrons, they are very effective at fissioning even non-fissile heavy nuclei, and those high-energy fissions tend to produce more neutrons per fission. 14 MeV neutrons can also produce more neutrons by knocking them loose from nuclei. (spallation) On the other hand, they are less likely to simply be captured without causing fission or spallation. For these reasons, nuclear weapon designs extensively utilize 14.1 MeV neutrons to cause more fission.

Other fusion reactions produce much less energetic neutrons; for example, D-D fusion produces a 2.45 MeV neutron and ^3He half of the time. (It produces tritium and a proton but no neutron the other half of the time.)

Intermediate neutrons

A fission energy neutron that is slowing down is often said to have intermediate energy. There are not many non-elastic reactions in this energy region, so most of what happens is just slowing to thermal speeds before eventual capture. Intermediate energy neutrons are a hazard in reactors owing to the existence of a resonance region in the fission cross section of fissile elements. Within this region there exist many local minima and local maxima of probability of causing fission; this means that a reactor operating with a significant population of intermediate neutrons in contact with fuel nuclei could exhibit dangerous transient response. In such reactors, other mechanisms of inherent stability must be provided, such as large hydrogen populations to provide Doppler broadening.

High-energy neutrons

These neutrons have more energy than fission energy neutrons and are generated in accelerators or in the atmosphere from cosmic particles. They can have energies as high as tens of joules per neutron.

See also

- Neutron radiation
- List of particles
- Nuclear reaction
- Thermal reactor
- Fast neutron
- Ionizing radiation
- Isotope
- Neutron flux
- Neutron generator
- Neutron magnetic moment
- Neutron capture nucleosynthesis:
 - R-process
 - S-process
- Neutron radiation and the Sievert radiation scale

Neutron sources

- Neutron sources
- Neutron generator

Processes involving neutrons

- | | |
|-----------------------|---------------------|
| • Neutron bomb | • Neutron flux |
| • Neutron diffraction | • Neutron transport |

References

- [1] 1935 Nobel Prize in Physics (http://nobelprize.org/nobel_prizes/physics/laureates/1935/)
- [2] 1935 Nobel Prize in Physics (http://nobelprize.org/nobel_prizes/physics/laureates/1935/)
- [3] Particle Data Group's Review of Particle Physics 2006 (<http://pdg.lbl.gov/2006/tables/bxxx.pdf>)
- [4] Particle Data Group's Review of Particle Physics 2006 (<http://pdg.lbl.gov/2006/tables/bxxx.pdf>)
- [5] Chadwick, James (1932). "Possible Existence of a Neutron". *Nature* **129**: 312. doi: 10.1038/129312a0 (<http://dx.doi.org/10.1038/129312a0>).
- [6] Particle Data Group Summary Data Table on Baryons (<http://pdg.lbl.gov/2007/tables/bxxx.pdf>)
- [7] Kumakhov, M. A.; Sharov, V. A. (1992). "A neutron lens". *Nature* **357**: 390–391. doi: 10.1038/357390a0 (<http://dx.doi.org/10.1038/357390a0>).
- [8] Physorg.com, "New Way of 'Seeing': A 'Neutron Microscope'" (<http://www.physorg.com/news599.html>)
- [9] NASA.gov: "NASA Develops a Nugget to Search for Life in Space" (<http://www.nasa.gov/vision/earth/technologies/nuggets.html>)
- [10] http://www.physicamedica.com/VOLXVII_S1/20-CLOUDSLEY%20et%20alii.pdf
- [11] <http://news.bbc.co.uk/1/hi/sci/tech/4627237.stm>
- [12] http://en.wikipedia.org/wiki/Nuclear_power#Solid_waste

Further reading

- Krane, K. S. (1998) *Introductory Nuclear Physics*
- G. L. Squires (1997) *Introduction to the Theory of Thermal Neutron Scattering*
- M. S. Dewey, D. M. Gilliam, J. S. Nico, M. S. Snow and F. E. Wietfeldt *NIST Neutron Lifetime Experiment*

Neutron scattering

Neutron scattering encompasses all scientific techniques whereby the deflection of neutron radiation is used as a scientific probe. Neutrons readily interact with atomic nuclei and magnetic fields from unpaired electrons, making a useful probe of both structure and magnetic order. Neutron Scattering falls into two basic categories - elastic and inelastic. Elastic scattering is when a neutron interacts with a nucleus or electronic magnetic field but does not leave it in an excited state, meaning the emitted neutron has the same energy as the injected neutron. Scattering processes that involve an energetic excitation or relaxation by the neutron are inelastic: the injected neutron's energy is used or increased to create an excitation or by absorbing the excess energy from a relaxation, and consequently the emitted neutron's energy is reduced or increased respectively.

For several good reasons, moderated neutrons provide an ideal tool for the study of almost all forms of condensed matter. Firstly, they are readily produced at a nuclear research reactor or a spallation source. Normally in such processes neutrons are however produced with much higher energies than are needed. Therefore moderators are generally used which slow the neutrons down and therefore produce wavelengths that are comparable to the atomic spacing in solids and liquids, and kinetic energies that are comparable to those of dynamic processes in materials. Moderators can be made from Aluminium and filled with liquid hydrogen (for very long wavelength neutrons) or liquid methane (for shorter wavelength neutrons). Fluxes of $10^7/\text{s}$ - $10^8/\text{s}$ are not atypical in most neutron sources from any given moderator.

The neutrons cause pronounced interference and energy transfer effects in scattering experiments. Unlike an x-ray photon with a similar wavelength, which interacts with the electron cloud surrounding the nucleus, neutrons interact with the nucleus itself. Because

the neutron is an electrically neutral particle, it is deeply penetrating, and is therefore more able to probe the bulk material. Consequently, it enables the use of a wide range of sample environments that are difficult to use with synchrotron x-ray sources. It also has the advantage that the cross sections for interaction do not increase with atomic number as they do with radiation from a synchrotron x-ray source. Thus neutrons can be used to analyse materials with low atomic numbers like proteins and surfactants. This can be done at synchrotron sources but very high intensities are needed which may cause the structures to change. Moreover, the nucleus provides a very short range, isotropic potential varying randomly from isotope to isotope, making it possible to tune the nuclear scattering contrast to suit the experiment:

The neutron has an additional advantage over the x-ray photon in the study of condensed matter. It readily interacts with internal magnetic fields in the sample. In fact, the strength of the magnetic scattering signal is often very similar to that of the nuclear scattering signal in many materials, which allows the simultaneous exploration of both nuclear and magnetic structure. Because the neutron scattering amplitude can be measured in absolute units, both the structural and magnetic properties as measured by neutrons can be compared quantitatively with the results of other characterisation techniques.

See also

- Neutron diffraction
- Small angle neutron scattering
- Neutron Reflectometry
- Inelastic neutron scattering
 - neutron triple-axis spectrometry
 - neutron time-of-flight scattering
 - neutron backscattering
 - neutron spin echo
 - neutron resonance spin echo
- Neutron scattering facilities

External links

- Neutron Scattering - A primer ^[1] (LANL-hosted black and white version ^[2]) - An introductory article written by Roger Pynn (Los Alamos National Laboratory)

References

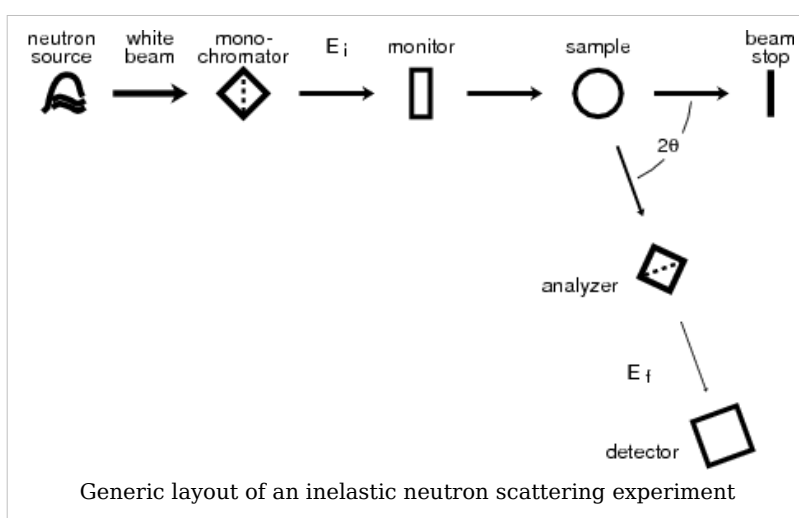
- [1] <http://knocknick.files.wordpress.com/2008/04/neutrons-a-primer-by-roger-pynn.pdf>
[2] <http://library.lanl.gov/cgi-bin/getfile?00326651.pdf>
-

Inelastic neutron scattering

Inelastic neutron scattering is an experimental technique commonly used in condensed matter research to study atomic and molecular motion as well as magnetic and crystal field excitations. It distinguishes itself from other neutron scattering techniques by resolving the change in kinetic energy that occurs when the collision between neutrons and the sample is an inelastic one. Results are generally communicated as the dynamic structure factor (also called inelastic scattering law) $S(q, \omega)$, sometimes also as the dynamic susceptibility $\chi(q, \omega)$ where the scattering vector q is the difference between incoming and outgoing wave vector, and $\hbar\omega$ is the energy change experienced by the sample (negative that of the scattered neutron). When results are plotted as function of ω , they can often be interpreted in the same way as spectra obtained by conventional spectroscopic techniques; insofar as inelastic neutron scattering can be seen as a special spectroscopy.

Inelastic scattering experiments normally require a monochromatization of the incident or outgoing beam and an energy analysis of the scattered neutrons. This can be done either through time-of-flight techniques (neutron time-of-flight scattering) or through Bragg reflection from single crystals (neutron triple-axis spectroscopy, neutron backscattering).

Monochromatization is not needed in echo techniques (neutron spin echo, neutron resonance spin echo), which use the quantum mechanical phase of the neutrons in addition to their amplitudes.



Types of Inelastic Neutron Scattering

- neutron triple-axis scattering
- neutron time-of-flight scattering
- neutron backscattering
- neutron spin echo

Further Information

Literature:

- G L Squires *Introduction to the Theory of Thermal Neutron Scattering* Dover 1997 (reprint?)

External links

- Joachim Wuttke: Introduction to Inelastic Crystal Spectrometers ^[1]

References

- [1] <http://iffwww.iff.kfa-juelich.de/~wuttke/doku/lib/exe/fetch.php?id=spheres%3Aprinciple&cache=cache&media=spheres:np9v05.pdf>

ISIS

1. REDIRECT Isis (disambiguation)

ISIS neutron source

ISIS is a world leading pulsed neutron and muon source. It is situated at the Rutherford Appleton Laboratory in Oxfordshire, United Kingdom and is part of the Science and Technology Facilities Council . It uses the techniques muon spectroscopy and neutron scattering to probe the structure and dynamics of condensed matter on a microscopic scale ranging from the subatomic to the macromolecular.

Hundreds of experiments are performed annually at ISIS by visiting researchers from around the world, in diverse science areas including physics, chemistry, materials engineering, earth sciences, biology and archaeology.

Neutrons and muons

Neutrons are uncharged constituents of atoms and penetrate materials well, deflecting only from the nuclei of atoms. The statistical accumulation of deflected neutrons at different positions beyond the sample can be used to find the structure of a material, and the loss or gain of energy by neutrons can reveal the dynamic behaviour of parts of a sample, for example diffusive processes in solids. At ISIS the neutrons are created by accelerating 'bunches' of protons in a synchrotron, then colliding these with a heavy tantalum metal target, under a constant



ISIS experimental hall for Target Station 1

cooling load to dissipate the heat from the 160 kW proton beam. The tantalum atoms slough off neutrons, and these are channelled through guides, or beamlines, to about 20 instruments, individually optimised for the study of different types of matter. The target station and most of the instruments are set in a large hall. The penetrating neutrons are a dangerous form of radiation so the target and beamlines are heavily shielded with concrete. ISIS produces muons by colliding a fraction of the proton beam with a graphite target, producing pions which decay rapidly into muons, delivered in a spin-polarised beam to sample stations.

Science at ISIS

ISIS is administered and operated by the Science and Technology Facilities Council (previously CCLRC). Experimental time is open to academic users from funding countries and is applied for through a twice-yearly 'call for proposals'. Research allocation, or 'beam-time', is allotted to



Another view of the ISIS experimental hall for Target Station 1

applicants via a peer-review process. Users and their parent institutions do not pay for the running costs of the facility, which are as much as £11,000 per instrument per day. Their transport and living costs are also refunded whilst carrying out the experiment. Most users stay in Ridgeway House, a hotel near the site, or at Cosener's House, an STFC-run conference centre in Abingdon. Over 600 experiments by 1600 users are completed every year.

A large number of support staff operate the facility, aid users, and carry out research, the control room is staffed 24 hours a day, every day of the year. Instrument scientists oversee the running of each instrument and liaise with users, and other divisions provide sample environment, data analysis and computing expertise, maintain the accelerator, and run education programmes.

Among the important and pioneering work carried out was the discovery of the structure of high-temperature superconductors and the solid phase of buckminsterfullerene.

Construction for a second target station started in 2003, and the first neutrons were delivered to the target on December 14 2007^[1]. It will use low-energy neutrons to study soft condensed matter, biological systems, advanced composites and nanomaterials. To supply the extra protons for this, the accelerator is being upgraded.

History and background of ISIS

The source was approved in 1977 for the RAL site on the Harwell campus and recycled components from earlier UK science programmes including the accelerator hall which had previously been occupied by the Nimrod accelerator. The first beam was produced in 1984, and the facility was formally opened by the then Prime Minister Margaret Thatcher in October 1985.^[2]

The name ISIS is not an acronym: it refers to the Ancient Egyptian goddess and the local name for the River Thames. The name was selected for the official opening of the facility in

1985, prior to this it was known as the SNS, or Spallation Neutron Source. The name was considered appropriate as Isis was a goddess who could restore life to the dead, and ISIS made use of equipment previously constructed for the Nimrod and Nina accelerators^[3].

External links

- ISIS facility ^[4]
- ISIS Second Target Station ^[5]
- The Science and Technology Facilities Council ^[6]

References

- [1] ISIS Second Target Station Project (<http://ts-2.isis.rl.ac.uk/>)
- [2] Linacs at the Rutherford Appleton Laboratory (<http://epubs.cclrc.ac.uk/bitstream/692/linacplahistory.pdf>)
- [3] Explanation of the name of ISIS (<http://www.isis.rl.ac.uk/aboutIsis/index.htm>)
- [4] <http://www.isis.rl.ac.uk/>
- [5] <http://ts-2.isis.rl.ac.uk/>
- [6] <http://www.stfc.ac.uk>

Geographical coordinates: 51°34′18″N 1°19′12″W

Sudbury Neutrino Observatory

The **Sudbury Neutrino Observatory (SNO)** is a neutrino observatory located 6800 feet (about 2 km) underground in Vale Inco's Creighton Mine in Sudbury, Ontario, Canada. The detector was designed to detect solar neutrinos through their interactions with a large tank of heavy water. The detector turned on in May 1999, and was turned off on November 28, 2006. While new data is no longer being taken the SNO collaboration will continue to analyze the data taken during that period for the next several years. The equipment is currently being refurbished for use in the SNO+ experiment.

Experimental motivation

The first measurements of the number of solar neutrinos reaching the earth were taken in the 1960s, and all experiments prior to SNO observed a third to a half fewer neutrinos than were predicted by the Standard Solar Model. As several experiments confirmed this deficit the effect became known as the solar neutrino problem. Over several decades many ideas were put forward to try to explain the effect, one of which was the hypothesis of neutrino flavour change. All of the solar neutrino detectors prior to SNO had been sensitive primarily or exclusively to electron neutrinos and not to muon or tau type neutrinos.



Artist's concept of SNO's detector.
(Courtesy of SNO)

In 1984 Herb Chen of the University of California at Irvine first pointed out the advantages of using heavy water as a detector for solar neutrinos. Unlike previous detectors, using heavy water would make the detector sensitive to two reactions, one sensitive to all neutrino flavours, which would allow a detector to measure neutrino oscillations directly. The Creighton mine in Sudbury, among the deepest in the world and blessed with low background radiation, was quickly identified as an ideal place for Chen's proposed experiment to be built.

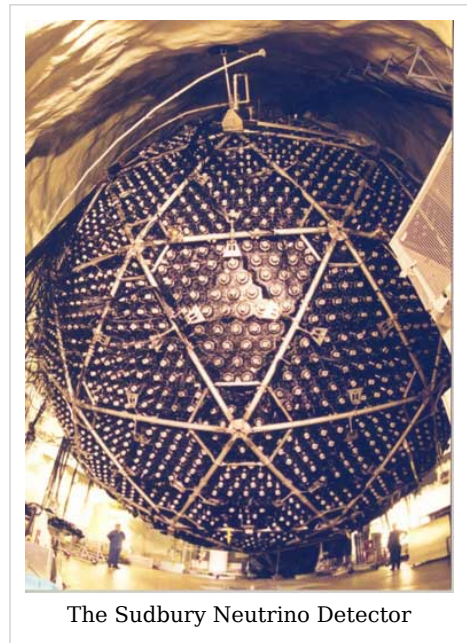
The SNO collaboration held its first meeting in 1984. At the time it competed with TRIUMF's "KAON Factory" proposal for federal funding, and the wide variety of universities backing SNO quickly led to it being selected for development. The official go-ahead was given in 1990.

The experiment did not directly detect neutrinos, but rather observed the light produced by relativistic electrons in the water. As relativistic electrons lose energy they produce a cone of blue light through the Cerenkov effect, and it is this light that is directly detected.

Detector description

The SNO detector target consisted of 1000 tonnes (1102 short tons) of heavy water contained in a 6-metre (20 ft) radius acrylic vessel. The detector cavity outside the vessel was filled with normal water to provide both buoyancy for the vessel and radioactive shielding. The heavy water was viewed by approximately 9600 photomultiplier tubes (PMTs) mounted on a geodesic sphere at a radius of about 850 centimetres (335 in). The cavity housing the detector is the largest manmade underground cavity in the world, requiring a variety of high-performance rock bolting techniques to prevent rock bursts.

The observatory is located at the end of a 1.5-kilometre (0.9 mi) long drift, whimsically named the "SNO drift", isolating it from other mining operations. Along the drift are a number of operations and equipment rooms, all held in a clean room setting. Most of the facility is Class 3000 (fewer than 3000 particles of 1 μm or larger per 1 m^3 of air) but the final cavity containing the detector is Class 1000.^[1]



The Sudbury Neutrino Detector

Charged current interaction

In the charged current interaction a neutrino converts the neutron in a deuteron to a proton. The neutrino is absorbed in the reaction and an electron is produced. Solar neutrinos have energies smaller than the mass of muon and tau particles, so only electron neutrinos can participate in this reaction. The emitted electron carries off most of the neutrino's energy, on the order of 5-15 MeV, and is detectable. The proton which is produced does not have enough energy to be detected easily. The electrons produced in this reaction come off in all directions, but there is a slight tendency for them to point back in the direction the neutrino came from.

Neutral current interaction

In the neutral current interaction a neutrino dissociates the deuteron, breaking it into its constituent neutron and proton. The neutrino continues on with slightly less energy, and all three neutrino flavours are equally likely to participate in this interaction. Heavy water has a small cross section for neutrons, and when neutrons capture on a deuterium nucleus a gamma ray with roughly 6 MeV of energy is produced. The direction of the gamma ray is completely uncorrelated with the direction of the neutrino. Some of the neutrons wander past the acrylic vessel into the light water, and since light water has a very large cross section for neutron capture these neutrons are captured very quickly. A gamma ray with roughly 2 MeV of energy is produced in this reaction, but because this is below the detector's energy threshold they are not observable.

Electron elastic scattering

In the elastic scattering interaction a neutrino collides with an atomic electron and imparts some of its energy to the electron. All three neutrinos can participate in this interaction through the exchange of the neutral Z boson, and electron neutrinos can also participate with the exchange of a charged W boson. For this reason this interaction is dominated by electron type neutrinos, and this is the channel through which the Super-Kamiokande detector can observe solar neutrinos. This interaction is the relativistic equivalent of billiards, and for this reason the electrons produced usually point in the direction that the neutrino was travelling (away from the sun). Because this interaction takes place on atomic electrons it occurs with the same rate in both the heavy and light water.

Experimental results and impact

On June 18, 2001, the first scientific results of the Observatory were published,^[2] ^[3] bringing the first clear evidence that neutrinos change flavour, or oscillate, as they travel from the sun. This oscillation in turn implies that neutrinos have non-zero masses. The total flux of all neutrino flavours measured by SNO agrees well with the theoretical prediction. Further measurements carried out by the Observatory have since confirmed and improved the precision of the original result.

Although Super-Kamiokande had beaten SNO to the punch, having published evidence for neutrino oscillation as early as 1998, the SuperK results were not conclusive and did not specifically deal with solar neutrinos. SNO's results were the first to directly demonstrate oscillations in solar neutrinos. The results of the experiment had a major impact on the field, as evidenced by the fact that two of the SNO papers have been cited over 1300 times, and two others have been cited over 500 times.^[4] In 2007, the Franklin Institute awarded the director of SNO Art McDonald with the Benjamin Franklin Medal in Physics.^[5]

Other possible analyses

The SNO detector would have been capable of detecting a supernova within our galaxy if one had occurred while the detector was online. As neutrinos emitted by a supernova are released earlier than the photons, it is possible to alert the astronomical community before the supernova is visible. SNO was a founding member of the Supernova Early Warning System with Super-Kamiokande and LVD. No such supernovas have yet been detected.

The SNO experiment was also able to observe atmospheric neutrinos produced by cosmic ray interactions in the atmosphere. Due to the limited size of the SNO detector in comparison with Super-K the low cosmic ray neutrino signal is not statistically significant at neutrino energies below 1 GeV.

Participating institutions

Large particle physics experiments require large collaborations. With approximately 100 collaborators, SNO was a rather small group compared to collider experiments. The participating institutions have included:

Canada

- Carleton University
- Laurentian University
- Queen's University - designed and built many calibration sources and the device for deploying sources
- TRIUMF
- University of British Columbia
- University of Guelph

Although no longer a collaborating institution, Chalk River Laboratories led the construction of the acrylic vessel that holds the heavy water, and Atomic Energy of Canada Limited was the source of the heavy water.

United Kingdom

- University of Oxford - developed much of the experiment's Monte Carlo analysis program (SNOMAN), and maintained the program

United States of America

- LBNL - Led the construction of the geodesic structure that holds the PMTs
 - LANL
 - University of Pennsylvania - designed and built the front end electronics and trigger
 - University of Washington - designed and built proportional counter tubes for detection of neutrons in the third phase of the experiment
 - Brookhaven National Laboratory
 - University of Texas at Austin
 - Massachusetts Institute of Technology
-

Trivia

- The day after the experiment was officially turned off, an unusually large earthquake occurred at the mine in which SNO is located.^[6] This damaged the detector to the point of temporary inoperability.
- Asteroid 14724 SNO is named in honour of the Observatory.
- The Sudbury Neutrino Observatory is a major setting in the *Neanderthal Parallax* trilogy by Canadian science fiction author Robert J. Sawyer.
- Although the observatory itself is not open to the public for tours, a video tour of the facility can be seen at Sudbury's interactive science centre, Science North.
- In November 2006 the entire SNO team was awarded the inaugural John C. Polanyi Award for “a recent outstanding advance in any field of the natural sciences or engineering” conducted in Canada.^[7]
- Renowned physicist Stephen Hawking and Nobel prize winners Bertram Brockhouse and Richard Taylor were present at the official opening of the SNO in 1998.

See also

- SNOLAB - A permanent underground physics laboratory being built around SNO

Other neutrino observatories

- Kamioka Observatory
- Baksan Neutrino Observatory
- Laboratori Nazionali del Gran Sasso, Italy
- Partial list of general observatories

Related Articles

- Particle Physics - General Article on Particle Physics
- Raymond Davis Jr. - Former Director of the Homestake Experiment
- Masatoshi Koshiba - Former Director of Kamioka Observatory

References

- [1] <http://cerncourier.com/cws/article/cern/28553>|"The Sudbury Neutrino Observatory - Canada's eye on the universe". *CERN Courier*. CERN / IOP Publishing Ltd. 2001-12-04. <http://cerncourier.com/cws/article/cern/28553>. Retrieved on 2008-06-04.
- [2] Ahmad, QR; et al. (2001-07-25). "<http://link.aps.org/abstract/PRL/v87/e071301>|Measurement of the Rate of $\nu_{e+d \rightarrow p+p+e}$ Interactions Produced by ^8B Solar Neutrinos at the Sudbury Neutrino Observatory". *Physical Review Letters* (American Physical Society) **87** (7): 071301. doi: 10.1103/PhysRevLett.87.071301 (<http://dx.doi.org/10.1103/PhysRevLett.87.071301>). PACS 26.65.+t, 14.60.Pq, 95.85.Ry. <http://link.aps.org/abstract/PRL/v87/e071301>. Retrieved on 2008-06-04.
- [3] http://www.sno.phy.queensu.ca/sno/first_results/|"Sudbury Neutrino Observatory First Scientific Results". 2001-07-03. http://www.sno.phy.queensu.ca/sno/first_results/. Retrieved on 2008-06-04.
- [4] SPIRES HEP Results (<http://www-library.desy.de/cgi-bin/spiface/find/blu/hep/wwwcite?rawcmd=FOUND+COLLABORATION+SNO+and+topcite+500+>)
- [5] http://www.fi.edu/winners/2007/mcdonald_arthur.faw?winner_id=4411|"Arthur B. McDonald, Ph.D.". *Franklin Laureate Database*. Franklin Institute. http://www.fi.edu/winners/2007/mcdonald_arthur.faw?winner_id=4411. Retrieved on 2008-06-04.
- [6] "<http://www.cbc.ca/canada/story/2006/11/29/earthquake-sudbury.html>|Earthquake rattles Sudbury region overnight". *CBC News* (Canadian Broadcasting Corporation). 2006-11-29. <http://www.cbc.ca/canada/story/2006/11/29/earthquake-sudbury.html>. Retrieved on 2008-06-04.
- [7] http://www.nserc.gc.ca/award_e.asp?nav=polanyi&lbi=past|"Past Winners - The Sudbury Neutrino Observatory". Natural Sciences and Engineering Research Council. 2008-03-03. http://www.nserc.gc.ca/award_e.asp?nav=polanyi&lbi=past. Retrieved on 2008-06-04.

External links

- SNO's official site (<http://www.sno.phy.queensu.ca/>)
- Joshua Klein's *Introduction to SNO, Solar Neutrinos, and Penn at SNO* (<http://www.hep.upenn.edu/SNO/intro.html>)
- "http://www.pbs.org/kcet/wiredscience/story/49-experiment_cave.html|Experiment Cave". *WIRED Science* (PBS). 2007-10-24. http://www.pbs.org/kcet/wiredscience/story/49-experiment_cave.html.
- "<http://www.pbs.org/wgbh/nova/neutrino/>|The Ghost Particle". Written and Directed by David Singleton. *Nova* (PBS). 2006-02-21. <http://www.pbs.org/wgbh/nova/neutrino/>. No. 3306 (607), season 34.

Geographical coordinates: 46°28′00″N 81°10′22″W

ATLAS experiment

LHC experiments	
ATLAS	A Toroidal LHC Apparatus
CMS	Compact Muon Solenoid
LHCb	LHC-beauty
ALICE	A Large Ion Collider Experiment
TOTEM	Total Cross Section, Elastic Scattering and Diffraction Dissociation
LHCf	LHC-forward
LHC preaccelerators	
p and Pb	Linear accelerators for protons (Linac 2) and Lead (Linac 3)
(not marked)	Proton Synchrotron Booster
PS	Proton Synchrotron
SPS	Super Proton Synchrotron

Geographical coordinates: 46°14′8″N 6°3′19″E



ATLAS logo.

ATLAS (A Toroidal LHC ApparatuS) is one of the six particle detector experiments (ALICE, ATLAS, CMS, TOTEM, LHCb, and LHCf) constructed at the Large Hadron Collider (LHC), a new particle accelerator at the European Organization for Nuclear Research (CERN) in Switzerland. ATLAS is 44 metres long and 25 metres in diameter, weighing about 7,000 tonnes. The project involves roughly 2,000 scientists and engineers at 165 institutions in 35 countries.^[1] The construction was originally scheduled to be completed in June 2007, but was ready and detected its first beam events on 10 September 2008.^[2] The experiment is designed to observe phenomena that involve highly massive particles which were not observable using earlier lower-energy accelerators and might shed light on new theories of particle physics beyond the Standard Model.

The *ATLAS collaboration*, the group of physicists building the detector, was formed in 1992 when the proposed EAGLE (**E**xperiment for **A**ccurate **G**amma, **L**epton and **E**nergy

Measurements) and ASCOT (**A**pparatus with **S**uper **C**onducting **T**oroids) collaborations merged their efforts into building a single, general-purpose particle detector for the Large Hadron Collider.^[3] The design was a combination of those two previous designs, as well as the detector research and development that had been done for the Superconducting Supercollider. The ATLAS experiment was proposed in its current form in 1994, and officially funded by the CERN member countries beginning in 1995. Additional countries, universities, and laboratories joined in subsequent years, and further institutions and physicists continue to join the collaboration even today. The work of construction began at individual institutions, with detector components shipped to CERN and assembled in the ATLAS experimental pit beginning in 2003.

ATLAS is designed as a general-purpose detector. When the proton beams produced by the Large Hadron Collider interact in the center of the detector, a variety of different particles with a broad range of energies may be produced. Rather than focusing on a particular physical process, ATLAS is designed to measure the broadest possible range of signals. This is intended to ensure that, whatever form any new physical processes or particles might take, ATLAS will be able to detect them and measure their properties. Experiments at earlier colliders, such as the Tevatron and Large Electron-Positron Collider, were designed based on a similar philosophy. However, the unique challenges of the Large Hadron Collider—its unprecedented energy and extremely high rate of collisions—require ATLAS to be larger and more complex than any detector ever built.

Background

The first cyclotron, an early type of particle accelerator, was built by Ernest O. Lawrence in 1931, with a radius of just a few centimetres and a particle energy of 1 MeV. Since then, accelerators have grown enormously in the quest to produce new particles of greater and greater mass. As accelerators have grown, so too has the list of known particles that they might be used to investigate. The most comprehensive model of particle interactions available today is known as the Standard Model of Particle Physics. With the important exception of the Higgs boson, all of the particles predicted by the model have been observed. While the standard model predicts that quarks, electrons, and neutrinos should exist, it does not explain why the masses of the particles are so very different. Due to this violation of

"naturalness" most particle physicists believe it is possible that the Standard Model will break down at energies beyond the current energy frontier of about one TeV (set at the Tevatron). If such beyond-the-Standard-Model physics is observed it is hoped that a new model, which is identical to the Standard Model at energies thus far probed, can be developed to describe particle physics at higher energies. Most of the currently proposed theories predict new higher-mass particles, some of which are hoped to be light enough to be observed by ATLAS. At 27 kilometres in circumference, the Large Hadron Collider (LHC)

will collide two beams of protons together, each proton carrying about 7 TeV of energy — enough energy to produce particles with masses up to roughly ten times more massive than



ATLAS experiment detector under construction in October 2004 in its experimental pit; the current status of construction can be seen here ^[4]. Note the people in the background, for comparison.

any particles currently known — assuming of course that such particles exist. With an energy seven million times that of the first accelerator the LHC represents a "new generation" of particle accelerators.

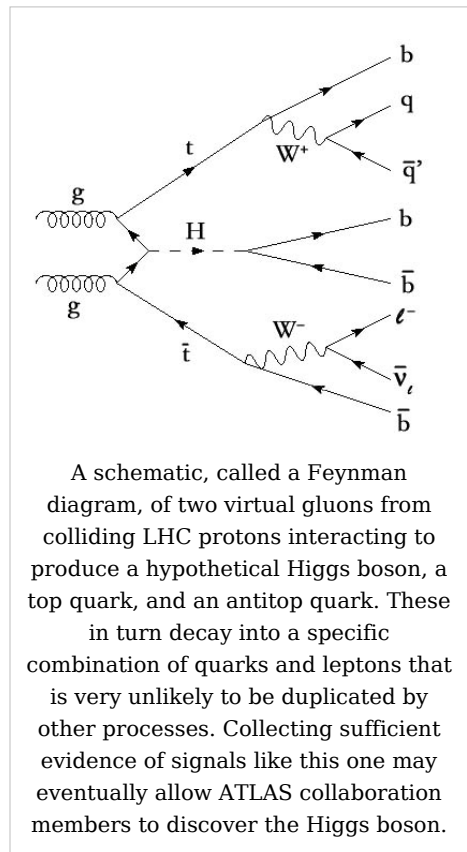
Particles that are produced in accelerators must also be observed, and this is the task of particle detectors. While interesting phenomena may occur when protons collide it is not enough to produce them. Particle detectors must be built to detect particles, their masses, momentum, energies, charges, and nuclear spins. In order to identify all particles produced at the interaction point where the particle beams collide, particle detectors are usually designed with a similarity to an onion. The layers are made up of detectors of different types, each of which is adept at observing specific types of particles. The different features that particles leave in each layer of the detector allow for effective particle identification and accurate measurements of energy and momentum. (The role of each layer in the detector is discussed below.) As the energy of the particles produced by the accelerator increases, the detectors attached to it must grow to effectively measure and stop higher-energy particles. ATLAS is the largest detector ever built at a particle collider as of 2008[5].^[1]

Physics Program

ATLAS is intended to investigate many different types of physics that might become detectable in the energetic collisions of the LHC. Some of these are confirmations or improved measurements of the Standard Model, while many others are searches for new physical theories.

One of the most important goals of ATLAS is to investigate a missing piece of the Standard Model, the Higgs boson.^[6] The Higgs mechanism, which includes the Higgs boson, is invoked to give masses to elementary particles, giving rise to the differences between the weak force and electromagnetism by giving the W and Z bosons masses while leaving the photon massless. If the Higgs boson is not discovered by ATLAS, it is expected that another mechanism of electroweak symmetry breaking that explains the same phenomena, such as technicolour, will be discovered. The Standard Model is simply not mathematically consistent at the energies of the LHC without such a mechanism. The Higgs boson would be detected by the particles it decays into; the easiest to observe are two photons, two bottom quarks, or four leptons. Sometimes these decays can only be definitively identified as originating with the Higgs boson when they are associated with additional particles; for an example of this, see the diagram at right.

The asymmetry between the behavior of matter and antimatter, known as CP violation, will also be investigated.^[6] Current CP-violation experiments, such as BaBar and Belle, have not



yet detected sufficient CP violation in the Standard Model to explain the lack of detectable antimatter in the universe. It is possible that new models of physics will introduce additional CP violation, shedding light on this problem; these models might either be detected directly by the production of new particles, or indirectly by measurements made of the properties of B-mesons. (LHCb, an LHC experiment dedicated to B-mesons, is likely to be better suited to the latter.)^[7]

The top quark, discovered at Fermilab in 1995, has thus far had its properties measured only approximately. With much greater energy and greater collision rates, LHC will produce a tremendous number of top quarks, allowing ATLAS to make much more precise measurements of its mass and interactions with other particles.^[8] These measurements will provide indirect information on the details of the Standard Model, perhaps revealing inconsistencies that point to new physics. Similar precision measurements will be made of other known particles; for example, ATLAS may eventually measure the mass of the W boson twice as accurately as has previously been achieved.

Perhaps the most exciting lines of investigation are those searching directly for new models of physics. One theory that is the subject of much current research is broken supersymmetry. The theory is popular because it could potentially solve a number of problems in theoretical physics and is present in almost all models of string theory. Models of supersymmetry involve new, highly massive particles; in many cases these decay into high-energy quarks and stable heavy particles that are very unlikely to interact with ordinary matter. The stable particles would escape the detector, leaving as a signal one or more high-energy quark jets and a large amount of "missing" momentum. Other hypothetical massive particles, like those in Kaluza-Klein theory, might leave a similar signature, but its discovery would certainly indicate that there was some kind of physics beyond the Standard Model.

One remote possibility (if the universe contains large extra dimensions) is that microscopic black holes might be produced by the LHC.^[9] These would decay immediately by means of Hawking radiation, producing all particles in the Standard Model in equal numbers and leaving an unequivocal signature in the ATLAS detector.^[10] In fact, if this occurs, the primary studies of Higgs bosons and top quarks would be conducted on those produced by the black holes.

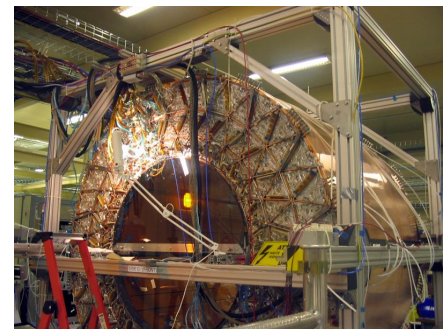
Components

The ATLAS detector consists of a series of ever-larger concentric cylinders around the interaction point where the proton beams from the LHC collide. It can be divided into four major parts: the Inner Detector, the calorimeters, the muon spectrometer and the magnet systems.^[11] Each of these is in turn made of multiple layers. The detectors are complementary: the Inner Detector tracks particles precisely, the calorimeters measure the energy of easily stopped particles, and the muon system makes additional measurements of highly penetrating muons. The two magnet systems bend charged particles in the Inner Detector and the muon spectrometer, allowing their momenta to be measured.

The only established stable particles that cannot be detected directly are neutrinos; their presence is inferred by noticing a momentum imbalance among detected particles. For this to work, the detector must be "hermetic", and detect all non-neutrinos produced, with no blind spots. Maintaining detector performance in the high radiation areas immediately surrounding the proton beams is a significant engineering challenge.

Inner detector

The Inner Detector begins a few centimetres from the proton beam axis, extends to a radius of 1.2 metres, and is seven metres in length along the beam pipe. Its basic function is to track charged particles by detecting their interaction with material at discrete points, revealing detailed information about the type of particle and its momentum.^[12] The magnetic field surrounding the entire inner detector causes charged particles to curve; the direction of the curve reveals a particle's charge and the degree of curvature reveals its momentum. The starting points of the tracks yield useful information for identifying particles; for example, if a group of tracks seem to originate from a point other than the original proton-proton collision, this may be a sign that the particles came from the decay of a bottom quark (see B-tagging). The Inner Detector has three parts, which are explained below.



The **ATLAS TRT** central section, the outermost part of the Inner Detector, as of September 2005, assembled on the surface and taking data from cosmic rays.

The Pixel Detector, the innermost part of the detector, contains three layers and three disks on each end-cap, with a total of 1744 *modules*, each measuring two centimetres by six centimetres. The detecting material is 250 μm thick silicon. Each module contains 16 readout chips and other electronic components. The smallest unit that can be read out is a pixel (each 50 by 400 micrometres); there are roughly 47,000 pixels per module. The minute pixel size is designed for extremely precise tracking very close to the interaction point. In total, the Pixel Detector will have over 80 million readout channels, which is about 50% of the total readout channels; such a large count created a design and engineering challenge. Another challenge was the radiation the Pixel Detector will be exposed to because of its proximity to the interaction point, requiring that all components be radiation hardened in order to continue operating after significant exposures.

The Semi-Conductor Tracker (SCT) is the middle component of the inner detector. It is similar in concept and function to the Pixel Detector but with long, narrow strips rather than small pixels, making coverage of a larger area practical. Each strip measures 80 micrometres by 12.6 centimetres. The SCT is the most critical part of the inner detector for basic tracking in the plane perpendicular to the beam, since it measures particles over a much larger area than the Pixel Detector, with more sampled points and roughly equal (albeit one dimensional) accuracy. It is composed of four double layers of silicon strips, and has 6.2 million readout channels and a total area of 61 square meters.

The Transition radiation tracker (TRT), the outermost component of the inner detector, is a combination of a straw tracker and a transition radiation detector. It was built by groups from CERN, Denmark, Poland, Russia, Sweden, Turkey, and the US. The central, or barrel, section was built in the US by groups at Duke University, Hampton University, and Indiana University. The electronics for the entire TRT was built by the University of Pennsylvania and Yale University. The detecting elements are drift tubes (straws), each four millimetres in diameter and up to 144 centimetres long. The uncertainty of track position measurements (position resolution) is about 200 micrometres, not as precise as those for the other two detectors, a necessary sacrifice for reducing the cost of covering a larger volume and having transition radiation detection capability. Each straw is filled with gas

that becomes ionized when a charged particle passes through. The straws are held at about -1500V, driving the negative ions to a fine wire down the centre of each straw, producing a current pulse (signal) in the wire. The wires with signals create a pattern of 'hit' straws that allow the path of the particle to be determined. Between the straws, materials with widely varying indices of refraction cause ultra-relativistic charged particles to produce transition radiation and leave much stronger signals in some straws. Xenon gas is used to increase the number of straws with strong signals. Since the amount of transition radiation is greatest for highly relativistic particles (those with a speed very near the speed of light), and particles of a particular energy have a higher speed the lighter they are, particle paths with many very strong signals can be identified as the lightest charged particles, electrons. The TRT has about 351,000 straws in total.

Calorimeters

The calorimeters are situated outside the solenoidal magnet that surrounds the inner detector. Their purpose is to measure the energy from particles by absorbing it. There are two basic calorimeter systems: an inner electromagnetic calorimeter and an outer hadronic calorimeter.^[13] Both are *sampling calorimeters*; that is, they absorb energy in high-density metal and periodically sample the shape of the resulting particle shower, inferring the energy of the original particle from this measurement.

The electromagnetic (EM) calorimeter absorbs energy from particles that interact electromagnetically, which include charged particles and photons. It has high precision, both in the amount of energy absorbed and in the precise location of the energy deposited. The angle between the particle's trajectory and the detector's beam axis (or more precisely the pseudorapidity) and its angle within the perpendicular plane are both measured to within roughly 0.025 radians. The energy-absorbing materials are lead and stainless steel, with liquid argon as the sampling material, and a cryostat is required around the EM calorimeter to keep it sufficiently cool.

The hadron calorimeter absorbs energy from particles that pass through the EM calorimeter, but do interact via the strong force; these particles are primarily hadrons. It is less precise, both in energy magnitude and in the localization (within about 0.1 radians only).^[7] The energy-absorbing material is steel, with scintillating tiles that sample the energy deposited. Many of the features of the calorimeter are chosen for their cost-effectiveness; the instrument is large and comprises a huge amount of construction material: the main part of the calorimeter—the tile calorimeter—is eight metres in diameter and covers 12 metres along the beam axis. The far-forward sections of the hadronic calorimeter are contained within the EM calorimeter's cryostat, and use liquid argon as it does.



September 2005: the main barrel section of the ATLAS hadronic calorimeter, waiting to be moved inside the toroid magnets.



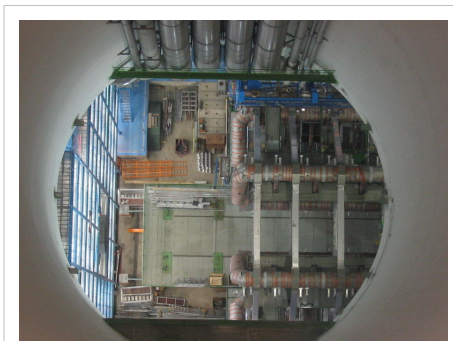
One of the sections of the extensions of the hadronic calorimeter, waiting to be inserted in late February 2006

Muon spectrometer

The muon spectrometer is an extremely large tracking system, extending from a radius of 4.25 m around the calorimeters out to the full radius of the detector (11 m).^[11] Its tremendous size is required to accurately measure the momentum of muons, which penetrate other elements of the detector; the effort is vital because one or more muons are a key element of a number of interesting physical processes, and because the total energy of particles in an event could not be measured accurately if they were ignored. It functions similarly to the inner detector, with muons curving so that their momentum can be measured, albeit with a different magnetic field configuration, lower spatial precision, and a much larger volume. It also serves the function of simply identifying muons—very few particles of other types are expected to pass through the calorimeters and subsequently leave signals in the muon spectrometer. It has roughly one million readout channels, and its layers of detectors have a total area of 12,000 square meters.

Magnet system

The ATLAS detector uses two large superconducting magnet systems to bend charged particles so that their momenta can be measured. This bending is due to the Lorentz force, which is proportional to velocity. Since all particles produced in the LHC's proton collisions will be traveling at very close to the speed of light, the force on particles of different momenta is equal. (In the theory of relativity, momentum is *not* proportional to velocity at such speeds.) Thus high-momentum particles will curve very little, while low-momentum particles will curve significantly; the amount of curvature can be quantified and the particle momentum can be determined from this value.

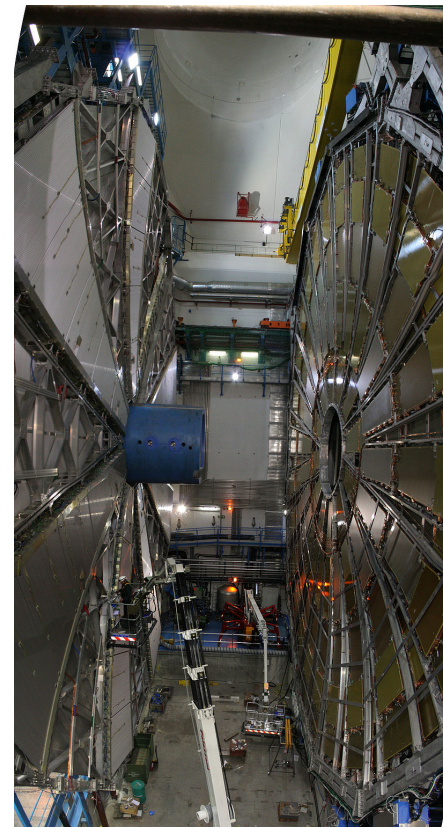


The ends of four of eight ATLAS toroid magnets, seen from the surface, about 90 metres above, in September 2005.

The inner solenoid produces a two tesla magnetic field surrounding the Inner Detector.^[14] This high magnetic field allows even very energetic particles to curve enough for their momentum to be determined, and its nearly uniform direction and strength allow measurements to be made very precisely. Particles with momenta below roughly 400 MeV will be curved so strongly that they will loop repeatedly in the field and most likely not be measured; however, this energy is very small compared to the several TeV of energy released in each proton collision.

The outer toroidal magnetic field is produced by eight very large air-core superconducting barrel loops and two end-caps, all situated outside the calorimeters and within the muon system.^[14] This magnetic field is

26 metres long and 20 metres in diameter, and it stores 1.6 gigajoules of energy. Its magnetic field is not uniform, because a solenoid magnet of sufficient size would be prohibitively expensive to build. Fortunately, measurements need to be much less precise to measure momentum accurately in the large volume of the muon system.



Part of the ATLAS, as it looked
February 2007.

Forward detectors

The ATLAS detector will be complemented with a set of detectors in the very forward region. These detectors will be located in the LHC tunnel far away from the interaction point. The basic idea is to measure elastic scattering at very small angles in order to get a handle on the absolute luminosity at the interaction point of ATLAS.

Data systems and analysis

The detector generates unmanageably large amounts of raw data, about 25 megabytes per event (raw; zero suppression reduces this to 1.6 MB) times 40 million beam crossings per second in the center of the detector, for a total of 1 petabyte/second of raw data.^[15] The trigger system uses simple information to identify, in real time, the most interesting events to retain for detailed analysis. There are three trigger levels, the first based in electronics on the detector and the other two primarily run on a large computer cluster near the detector. After the first-level trigger, about 100,000 events per second have been selected. After the third-level trigger, a few hundred events remain to be stored for further analysis. This amount of data will require over 100 megabytes of disk space per second — at least a petabyte each year.^[16]

Offline event reconstruction will be performed on all permanently stored events, turning the pattern of signals from the detector into physics objects, such as jets, photons, and leptons. Grid computing will be extensively used for event reconstruction, allowing the parallel use of university and laboratory computer networks throughout the world for the

CPU-intensive task of reducing large quantities of raw data into a form suitable for physics analysis. The software for these tasks has been under development for many years, and will continue to be refined once the experiment is running.

Individuals and groups within the collaboration will write their own code to perform further analysis of these objects, searching in the pattern of detected particles for particular physical models or hypothetical particles. These studies are already being developed and tested on detailed simulations of particles and their interactions with the detector. Such simulations give physicists a good sense of which new particles can be detected and how long it will take to confirm them with sufficient statistical certainty.

Notes

- [1] CERN (2006-11-20). <http://press.web.cern.ch/Press/PressReleases/Releases2006/PR17.06E.html>|World's largest superconducting magnet switches on. Press release. <http://press.web.cern.ch/Press/PressReleases/Releases2006/PR17.06E.html>. Retrieved on 2007-03-03.
- [2] CERN. <http://www.atlas.ch/news/2008/first-beam-and-event.html>|"First beam and first events in ATLAS". <http://www.atlas.ch/news/2008/first-beam-and-event.html>. Retrieved on 2008-09-13.
- [3] <http://library.cern.ch/archives/isad/isaatlas.html>|"ATLAS Collaboration records". CERN Archive. <http://library.cern.ch/archives/isad/isaatlas.html>. Retrieved on 2007-02-25.
- [4] http://atlaswebpub.web.cern.ch/atlaswebpub/web-sites/pages/UX15_webcams.htm
- [5] http://en.wikipedia.org/wiki/Atlas_experiment
- [6] <http://atlas.web.cern.ch/Atlas/TP/NEW/HTML/tp9new/node4.html#SECTION00400000000000000000>|"Introduction and Overview". *ATLAS Technical Proposal*. CERN. 1994.
- [7] *N. V. Krasnikov, V. A. Matveev (September 1997). "<http://arxiv.org/abs/hep-ph/9703204>|Physics at LHC". *Physics of Particles and Nuclei* **28** (5): 441–470. doi: 10.1134/1.953049 (<http://dx.doi.org/10.1134/1.953049>). <http://arxiv.org/abs/hep-ph/9703204>.
- [8] <http://atlas.web.cern.ch/Atlas/TP/NEW/HTML/tp9new/node416.html#SECTION00241000000000000000>|"Top-Quark Physics". *ATLAS Technical Proposal*. CERN. 1994.
- [9] C.M. Harris, M.J. Palmer, M.A. Parker, P. Richardson, A. Sabetfakhri and B.R. Webber (2005). "Exploring higher dimensional black holes at the Large Hadron Collider". *Journal of High Energy Physics* **5**: 053. doi: 10.1088/1126-6708/2005/05/053 (<http://dx.doi.org/10.1088/1126-6708/2005/05/053>).
- [10] J. Tanaka, T. Yamamura, S. Asai, J. Kanzaki (2005). "<http://www.springerlink.com/content/x067g845688470r4/>|Study of Black Holes with the ATLAS detector at the LHC". *The European Physical Journal C* **41** (s2): 19–33. doi: 10.1140/epjcd/s2005-02-008-x (<http://dx.doi.org/10.1140/epjcd/s2005-02-008-x>). <http://www.springerlink.com/content/x067g845688470r4/>.
- [11] <http://atlas.web.cern.ch/Atlas/TP/NEW/HTML/tp9new/node6.html#SECTION00420000000000000000>|"Overall detector concept". *ATLAS Technical Proposal*. CERN. 1994.
- [12] <http://atlas.web.cern.ch/Atlas/TP/NEW/HTML/tp9new/node10.html#SECTION00433000000000000000>|"Inner detector". *ATLAS Technical Proposal*. CERN. 1994.
- [13] <http://atlas.web.cern.ch/Atlas/TP/NEW/HTML/tp9new/node9.html#SECTION00432000000000000000>|"Calorimetry". *ATLAS Technical Proposal*. CERN. 1994.
- [14] <http://atlas.web.cern.ch/Atlas/TP/NEW/HTML/tp9new/node8.html#SECTION00431000000000000000>|"Magnet system". *ATLAS Technical Proposal*. CERN. 1994.
- [15] Marjorie Shapiro.. <http://www.youtube.com/watch?v=-cdbnwaW34g>|*Supersymmetry, Extra Dimensions and the Origin of Mass: Exploring the Nature of the Universe Using PetaScale Data Analysis*. Event occurs at 35:00. <http://www.youtube.com/watch?v=-cdbnwaW34g>. Retrieved on 2007-12-08. See also 32:30 for information on the various trigger levels.
- [16] "<http://www.eurekalert.org/features/doe/2004-03/dnal-tsg032604.php>|The sensitive giant". *United States Department of Energy Research News*. March 2004. <http://www.eurekalert.org/features/doe/2004-03/dnal-tsg032604.php>.

References

- ATLAS Technical Proposal. (<http://atlas.web.cern.ch/Atlas/TP/tp.html>) CERN: The Atlas Experiment. Retrieved on 2007-04-10
- ATLAS Detector and Physics Performance Technical Design Report. (<http://atlas.web.cern.ch/Atlas/GROUPS/PHYSICS/TDR/access.html>) CERN: The Atlas Experiment. Retrieved on 2007-04-10
- N. V. Krasnikov, V. A. Matveev (September 1997). "http://arxiv.org/abs/hep-ph/9703204|Physics at LHC". *Physics of Particles and Nuclei* **28** (5): 441–470. doi: 10.1134/1.953049 (<http://dx.doi.org/10.1134/1.953049>). <http://arxiv.org/abs/hep-ph/9703204>.

External links

- Official ATLAS Public Webpage (<http://atlas.ch>) at CERN (*The "award winning ATLAS movie" is a very good general introduction!*)
- Official ATLAS Collaboration Webpage (<http://atlas.web.cern.ch/Atlas/internal/Welcome.html>) at CERN (*Lots of technical and logistical information*)
- ATLAS Cavern Webcams (http://atlaseye-webpub.web.cern.ch/atlaseye-webpub/web-sites/pages/UX15_webcams.htm)
- ATLAS section from US/LHC Website (http://www.uslhq.us/What_is_the_LHC/Experiments/ATLAS)
- PhysicsWorld article on LHC and experiments (<http://physicsweb.org/articles/world/13/5/9/1>)
- New York Times article on LHC and experiments (<http://www.nytimes.com/2000/11/21/science/21HIGG.html?ex=1130040000&en=5282f51cf019f1b7&ei=5070&ex=1082001600&en=39ccf65ca6047eb2&ei=5070>)
- United States Department of Energy article on ATLAS (<http://www.eurekalert.org/features/doe/2004-03/dnal-tsg032604.php>)
- The Large Hadron Collider ATLAS Experiment Virtual Reality (VR) photography panoramas (<http://www.pettermccready.com/portfolio/05091901.html>)
- Large Hadron Collider Project Director Dr Lyn Evans CBE on the engineering behind the ATLAS experiment, *Ingenia* magazine, June 2008 (<http://www.ingenia.org.uk/ingenia/articles.aspx?Index=489>)
- Atlas Experiment News and social networking (<http://www.AtlasExperiment.net>)
- The ATLAS Collaboration, G Aad *et al.* (2008-08-14). "http://www.iop.org/EJ/journal/-page=extra.lhc/jinst|The ATLAS Experiment at the CERN Large Hadron Collider". *Journal of Instrumentation* **3** (S08003): S08003. doi: 10.1088/1748-0221/3/08/S08003 (<http://dx.doi.org/10.1088/1748-0221/3/08/S08003>). <http://www.iop.org/EJ/journal/-page=extra.lhc/jinst>. Retrieved on 2008-08-26. (Full design documentation)

Neutron spin echo

Neutron spin echo spectroscopy is an inelastic neutron scattering technique invented by Ferenc Mezei in the 1970's, and developed in collaboration with John Hayter. In recognition of this work and in other areas, Mezei was awarded the first Walter Haelg Prize ^[1] in 1999.

The spin-echo spectrometer possesses an extremely high energy resolution (roughly one part in 100,000). Additionally, it measures the density-density correlation (or intermediate scattering function) $F(Q,t)$ as a function of momentum transfer Q and time. Other neutron scattering techniques measure the dynamic structure factor, which then must be converted to $F(Q,t)$ by a Fourier transform, which is difficult in practice. Because of these advantages over other neutron scattering techniques, NSE is an ideal method to observe ^[2] internal dynamic modes in materials such as a polymer blend, alkane chain, or microemulsion. The extraordinary power of NSE spectrometry was further demonstrated recently ^[3] by the direct observation of coupled internal protein domain dynamics in the protein Taq polymerase, allowing the visualization of protein nanomachinery in motion.

Technical details

The technique of neutron spin echo exploits the neutron's intrinsic angular momentum, or spin, to access extremely high-resolution inelastic scattering windows.

The core of a neutron spin echo instrument is a *symmetric* field integral around the sample position, and a spin flipper (or the sample itself) to reverse the spin direction, so that any loss in polarisation at the detector position can be directly attributed to inelastic scattering processes in the sample.

Because of the interference of the wavevectors associated with the spin up and spin down quantum states of the neutron, the measured neutron polarisation is proportional to the sample's correlation function *in real time*. This makes it a very useful and intuitive technique for the high-resolution study of low-energy excitations in materials.

In soft matter research the structure of macromolecular objects is often investigated by small angle neutron scattering, SANS. The exchange of hydrogen with deuterium in some of the molecules creates scattering contrast between even equal chemical species. The SANS diffraction pattern --if interpreted in real space-- corresponds to a snapshot picture of the molecular arrangement. Neutron spin echo instruments can analyze the inelastic broadening of the SANS intensity and thereby analyze the motion of the macromolecular objects. A coarse analogy would be a photo with a certain opening time instead of the SANS like snapshot. The opening time corresponds to the Fourier time which depends on the setting of the NSE spectrometer, it is proportional to the magnetic field (integral) and to the third power of the neutron wavelength. Values up to several hundreds of nanoseconds are available. Note that the spatial resolution of the scattering experiment is in the nanometer range, which means that a time range of e.g. 100ns corresponds to effective molecular motion velocities of $1 \text{ nm}/100\text{ns} = 1\text{cm/s}$. This may be compared to the typical neutron velocity of 200..1000 m/s used in these type of experiments.

References

- [1] http://neutron.neutron-eu.net/n_ensa/Prize
- [2] B. Farago (2006). "Neutron spin echo study of well organized soft matter systems". *Physica B: Condensed matter* **385-386**: 688-691. doi: 10.1016/j.physb.2006.05.292 (<http://dx.doi.org/10.1016/j.physb.2006.05.292>).
- [3] Bu Z, Biehl R, Monkenbusch M, Richter D, Callaway DJE (2005). "Coupled protein domain motion in Taq polymerase revealed by neutron spin-echo spectroscopy.". *Proc Natl Acad Sci U S A* **102** (49): 17646-17651. doi: 10.1073/pnas.0503388102 (<http://dx.doi.org/10.1073/pnas.0503388102>). PMID 16306270.

Existing Spectrometers

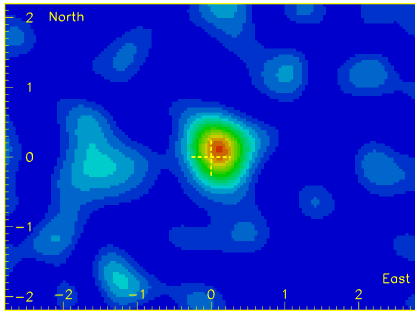
- IN11 (<http://www.ill.eu/in11/>) (Institut Laue-Langevin, ILL (<http://www.ill.fr>), Grenoble, France)
- IN15 (<http://www.ill.eu/in15/>) (Institut Laue-Langevin, ILL (<http://www.ill.fr>), Grenoble, France)
- J-NSE (Juelich Centre for Neutron Science JCNS (<http://www.jcns.info>), Juelich, Germany, hosted by FRMII (<http://wwwnew.frm2.tum.de>), Munich (Garching), Germany)
- NG5-NSE (NIST CNRF (<http://www.ncnr.nist.gov>), Gaithersburg, USA)
- V5/SPAN (Hahn-Meitner Institut (<http://www.hmi.de>), Berlin, Germany)
- C2-2 (ISSP (<http://www.issp.u-tokyo.ac.jp>), Tokai, Japan)

See also

- neutron scattering
 - neutron resonance spin echo
 - Biological small-angle scattering
 - Soft matter
 - NMR
 - Protein domain
 - Larmor precession
 - SAXS
-

Muons and other

Muon

<i>Muon</i>	
	
The Moon's cosmic ray shadow, as seen in secondary muons detected 700m below ground, at the Soudan II detector.	
Composition:	Elementary particle
Family:	Fermion
Group:	Lepton
Generation:	Second
Interaction:	Gravity, Electromagnetic, Weak
Antiparticle:	μ^+ (Antimuon)
Theorized:	—
Discovered:	Carl D. Anderson (1936)
Symbol(s):	μ^-
Mass:	105.658369(9) MeV/c ²
Mean lifetime:	2.19703(4)×10 ^{−6} s ^[1]
Electric charge:	−1 e
Color charge:	None
Spin:	$\frac{1}{2}$

The **muon** (from the Greek letter mu (μ) used to represent it) is an elementary particle similar to the electron, with negative electric charge and a spin of $\frac{1}{2}$. Together with the electron, the tauon, and the three neutrinos, it is classified as a lepton. It is the unstable subatomic particle with the second longest mean lifetime (2.2 μ s), behind the neutron (~15 min). Like all elementary particles, the muon has corresponding antiparticle of opposite charge but equal mass and spin: the **antimuon** (also called a *positive muon*). Muons are denoted by μ^- and antimuons by μ^+ . Muons were sometimes referred to as **mu mesons** in the past, even though they are not classified as mesons by modern particle physicists (*see History*).

Muons have a mass of $105.7\text{ MeV}/c^2$, which is about 200 times the mass of the electrons. Since their interactions are very similar to those of the electron, a muon can be thought of as a much heavier version of the electron. Due to their greater mass, muons do not emit as much bremsstrahlung radiation; consequently, they are highly penetrating, much more so than electrons.

As with the case of the other charged leptons, the muon has an associated muon neutrino. Muon neutrinos are denoted by ν_μ .

History

Muons were discovered by Carl D. Anderson in 1936 while he studied cosmic radiation. He had noticed particles that curved in a manner distinct from that of electrons and other known particles, when passed through a magnetic field. In particular, these new particles were negatively charged but curved to a smaller degree than electrons, but more sharply than protons, for particles of the same velocity. It was assumed that the magnitude of their negative electric charge was equal to that of the electron, and so to account for the difference in curvature, it was supposed that these particles were of intermediate mass (lying somewhere between that of an electron and that of a proton). The discovery of the muon seemed so incongruous and surprising at the time that Nobel laureate I. I. Rabi famously quipped, "Who ordered that?"

For this reason, Anderson initially called the new particle a *mesotron*, adopting the prefix *meso-* from the Greek word for "mid-". Shortly thereafter, additional particles of intermediate mass were discovered, and the more general term *meson* was adopted to refer to any such particle. Faced with the need to differentiate between different types of mesons, the mesotron was in 1947 renamed the *mu meson* (with the Greek letter μ (*mu*) used to approximate the sound of the Latin letter *m*).

However, it was soon found that the mu meson significantly differed from other mesons; for example, its decay products included a neutrino and an antineutrino, rather than just one or the other, as was observed in other mesons. Other mesons were eventually understood to be hadrons—that is, particles made of quarks—and thus subject to the residual strong force. In the quark model, a *meson* is composed of exactly two quarks (a quark and antiquark), unlike baryons which are composed of three quarks. Mu mesons, however, were found to be fundamental particles (leptons) like electrons, with no quark structure. Thus, mu mesons were not mesons at all (in the new sense and use of the term *meson*), and so the term *mu meson* was abandoned, and replaced with the modern term *muon*.

Muon sources

Antimatter
Overview
Annihilation
Devices <ul style="list-style-type: none">Particle acceleratorPenning trap

Antiparticles <ul style="list-style-type: none">• Positron• Antiproton• Antineutron
Uses <ul style="list-style-type: none">• Positron emission tomography• Fuel• Weaponry
Bodies <ul style="list-style-type: none">• ALPHA Collaboration• ATHENA• ATRAP• CERN
People <ul style="list-style-type: none">• Paul Dirac• Carl David Anderson• Andrei Sakharov <div>edit ^[2]</div>

Since the production of muons requires an available center of momentum frame energy of over 105 MeV, neither ordinary radioactive decay events nor nuclear fission and fusion events (such as those occurring in nuclear reactors and nuclear weapons) are energetic enough to produce muons. Only nuclear fission produces single-nuclear-event energies in this range, but due to conservation constraints, muons are not produced.

On Earth, all naturally occurring muons are apparently created by cosmic rays, which consist mostly of protons, many arriving from deep space at very high energy.

About 10,000 muons reach every square meter of the earth's surface a minute; these charged particles form as by-products of cosmic rays colliding with molecules in the upper atmosphere. Traveling at relativistic speeds, muons can penetrate tens of meters into rocks and other matter before attenuating as a result of absorption or deflection by other atoms.

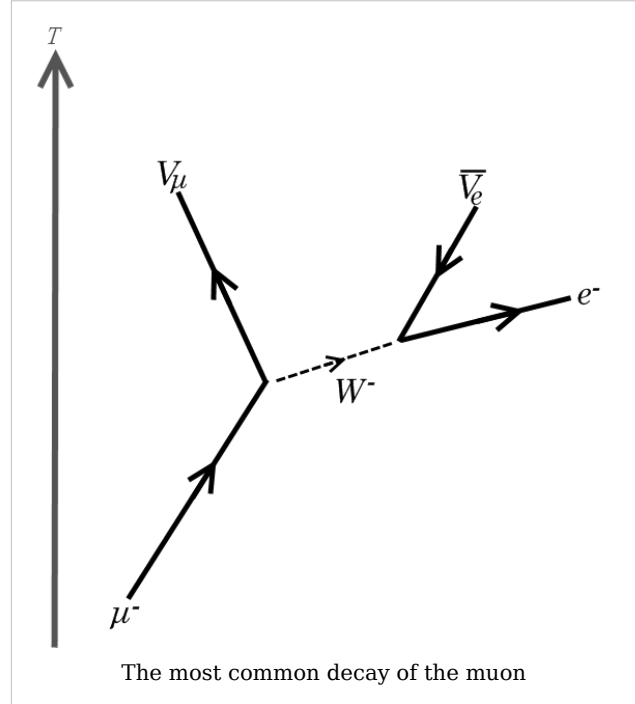
—Mark Wolverton, science writer, *Scientific American* magazine, September 2007, page 26 "Muons for Peace"^[3]

When a cosmic ray proton impacts atomic nuclei of air atoms in the upper atmosphere, pions are created. These decay within a relatively short distance (meters) into muons (the pion's preferred decay product), and neutrinos. The muons from these high energy cosmic rays, generally continuing essentially in the same direction as the original proton, do so at very high velocities. Although their lifetime *without* relativistic effects would allow a half-survival distance of only about 0.66 km at most, the time dilation effect of special relativity allows cosmic ray secondary muons to survive the flight to the earth's surface. Indeed, since muons are unusually penetrative of ordinary matter, like neutrinos, they are also detectable deep underground and underwater, where they form a major part of the natural background ionizing radiation. Like cosmic rays, as noted, this secondary muon radiation is also directional. See the illustration above of the moon's cosmic ray shadow, detected when 700 m of soil and rock filters secondary radiation, but allows enough muons to form a crude image of the moon, in a directional detector.

The same nuclear reaction described above (i.e., hadron-hadron impacts to produce pion beams, which then quickly decay to muon beams over short distances) is used by particle physicists to produce muon beams, such as the beam used for the muon g-2 ^[4] gyromagnetic ratio experiment (see link below). In naturally-produced muons, the very high-energy protons to begin the process are thought to originate from acceleration by electromagnetic fields over long distances between stars or galaxies, in a manner somewhat analogous to the mechanism of proton acceleration used in laboratory particle accelerators.

Muon decay

Muons are unstable elementary particles and are heavier than electrons and neutrinos but lighter than all other matter particles. They decay via the weak interaction to an electron, two neutrinos and possibly other particles with a net charge of zero. Nearly all of the time, they decay into an electron, an electron-antineutrino, and a muon-neutrino. Antimuons decay to a positron, an electron-neutrino, and a muon-antineutrino:



$$\mu^- \rightarrow e^- + \bar{\nu}_e + \nu_\mu, \quad \mu^+ \rightarrow e^+ + \nu_e + \bar{\nu}_\mu.$$

The mean lifetime of the (positive) muon is $2.197\,019 \pm 0.000\,021 \mu\text{s}$ ^[5]. The equality of the muon and anti-muon lifetimes has been established to better than one part in 10^4 .

The tree-level muon decay width is

$$\Gamma = \frac{G_F^2 m_\mu^5}{192\pi^3} I\left(\frac{m_e^2}{m_\mu^2}\right), \text{ where } I(x) = 1 - 8x + 12x^2 \ln\left(\frac{1}{x}\right) + 8x^3 - x^4.$$

A photon or electron-positron pair is also present in the decay products about 1.4% of the time.

The decay distributions of the electron in muon decays have been parametrized using the so-called Michel parameters. The values of these four parameters are predicted unambiguously in the Standard Model of particle physics, thus muon decays represent an excellent laboratory to test the space-time structure of the weak interaction. No deviation from the Standard Model predictions has yet been found.

Certain neutrino-less decay modes are kinematically allowed but forbidden in the Standard Model. Examples, forbidden by lepton flavour conservation, are

$$\mu^- \rightarrow e^- + \gamma \text{ and } \mu^- \rightarrow e^- + e^+ + e^-.$$

Observation of such decay modes would constitute clear evidence for physics beyond the Standard Model (BSM). Upper limits for the branching fractions of such decay modes are in the range 10^{-11} to 10^{-12} .

Muonic atoms

The muon was the first elementary particle discovered that does not appear in ordinary atoms. Negative muons can, however, form muonic atoms by replacing an electron in ordinary atoms. Muonic atoms are much smaller than typical atoms because the larger mass of the muon gives it a smaller ground-state wavefunction than the electron.

A positive muon, when stopped in ordinary matter, can also bind an electron and form an exotic atom known as muonium (Mu) atom, in which the muon acts as the nucleus. The positive muon, in this context, can be considered a pseudo-isotope of hydrogen with one ninth of the mass of the proton. Because the reduced mass of muonium, and hence its Bohr radius, is very close to that of hydrogen, this short-lived "atom" behaves chemically — to a first approximation — like hydrogen, deuterium and tritium.

Anomalous magnetic dipole moment

The anomalous magnetic dipole moment is the difference between the experimentally observed value of the magnetic dipole moment and the theoretical value predicted by the Dirac equation. The measurement and prediction of this value is very important in the precision tests of QED (quantum electrodynamics). The E821 experiment ^[6] at Brookhaven National Laboratory (BNL) studied the precession of muon and anti-muon in a constant external magnetic field as they circulated in a confining storage ring. The E821 Experiment reported the following average value (from the July 2007 review by Particle Data Group) ^[7]

$$a = \frac{g - 2}{2} = 0.00116592080(54)(33)$$

where the first errors are statistical and the second systematic.

The difference between the g-factors of the muon and the electron is due to their difference in mass. Because of the muon's larger mass, contributions to the theoretical calculation of its anomalous magnetic dipole moment from Standard Model weak interactions and from contributions involving hadrons are important at the current level of precision, whereas these effects are not important for the electron. The muon's anomalous magnetic dipole moment is also sensitive to contributions from new physics beyond the Standard Model, such as supersymmetry. For this reason, the muon's anomalous magnetic moment is normally used as a probe for new physics beyond the Standard Model rather than as a test of QED (Phys.Lett. B649, 173 (2007) ^[8]).

See also

- Muonium
- Muon spin spectroscopy
- Muon-catalyzed fusion
- List of particles

References

- [1] W.-M. Yao et al. (Particle Data Group), J. Phys. G 33, 1 (2006)
- [2] <http://en.wikipedia.org/w/index.php?title=Template:Antimatter&action=edit>
- [3] Wolverton, Mark (September 2007), "<http://www.sciam.com/article.cfm?id=muons-for-peace>|Muons for Peace: New way to spot hidden nukes gets ready to debut", *Scientific American* (Scientific American, Inc.) **297** (3): 26–28, <http://www.sciam.com/article.cfm?id=muons-for-peace>, retrieved on 2008-08-01 *Note: only first two paragraphs available on-line*
- [4] <http://www.bnl.gov/bnlweb/pubaf/pr/2002/bnlpr073002.htm>
- [5] (<http://arxiv.org/abs/0704.1981v1>)
- [6] <http://www.g-2.bnl.gov/>
- [7] http://pdg.lbl.gov/2007/reviews/g-2_s004219.pdf
- [8] <http://arxiv.org/abs/hep-ph/0611102>
- S.H. Neddermeyer and C.D. Anderson, "Note on the Nature of Cosmic-Ray Particles", Phys. Rev. 51, 884–886 (1937). Full text available in (http://prola.aps.org/pdf/PR/v51/i10/p884_1"PDF").
- J.C. Street and E.C. Stevenson, "New Evidence for the Existence of a Particle of Mass Intermediate Between the Proton and Electron", Phys. Rev. 52, 1003-1004 (1937). Full text available in (http://prola.aps.org/pdf/PR/v52/i9/p1003_1"PDF").
- Serway & Faughn, *College Physics, Fourth Edition* (Fort Worth TX: Saunders, 1995) page 841
- Emanuel Derman, *My Life As A Quant* (Hoboken, NJ: Wiley, 2004) pp. 58-62.
- Marc Knecht ; *The Anomalous Magnetic Moments of the Electron and the Muon*, Poincaré Seminar (Paris, Oct. 12, 2002), published in : Duplantier, Bertrand; Rivasseau, Vincent (Eds.) ; *Poincaré Seminar 2002*, Progress in Mathematical Physics 30, Birkhäuser (2003) [ISBN 3-7643-0579-7]. Full text available in *PostScript* (<http://parthe.lpthe.jussieu.fr/poincare/textes/octobre2002/Knecht.ps>).

External links

- Muon anomalous magnetic moment and supersymmetry (<http://antwpr.gsfc.nasa.gov/apod/ap050828.html>)
 - g-2 (muon anomalous magnetic moment) experiment (<http://www.g-2.bnl.gov/>)
 - muLan (Measurement of the Positive Muon Lifetime) experiment (<http://www.npl.uiuc.edu/exp/mulan/>)
 - The Review of Particle Physics (<http://pdg.lbl.gov/>)
 - The TRIUMF Weak Interaction Symmetry Test (<http://twist.triumf.ca/>)
-

Ionization cooling

Physical Principle

Ionization cooling is a process by which the beam emittance of a beam of particles may be reduced ^[1]. In ionization cooling, particles are passed through some material. The momentum of the particles is reduced as they ionize atomic electrons in the material. Thus the normalised beam emittance is reduced. By re-accelerating the beam, for example in an RF cavity, the longitudinal momentum may be restored without replacing transverse momentum. Thus overall the angular spread and hence the geometric emittance in the beam will be reduced.

Ionization cooling can be spoiled by stochastic physical processes. Multiple Coulomb scattering in muons as well as nuclear scattering in protons and ions can reduce the cooling or even lead to net heating transverse to the direction of beam motion. In addition, energy straggling can cause heating parallel to the direction of beam motion.

Muon Cooling

The primary use of ionization cooling is envisaged to be for cooling of muon beams. This is because ionization cooling is the only technique that works on the timescale of the muon lifetime. Ionization cooling channels have been designed for use in a Neutrino Factory and a Muon Collider. Muon ionization cooling is expected to be demonstrated for the first time by the Proof of Principle International Muon Ionization Cooling Experiment. Other PoP muon ionization cooling experiments have been devised.

Other Particles

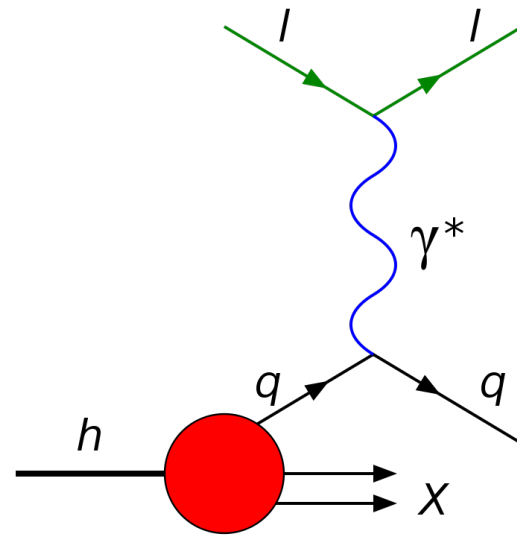
Ionization cooling has also been proposed for use in low energy ion beams and proton beams.

References

- [1] G.I. Budker, in: Proceedings of 15th International Conference on High Energy Physics, Kiev, 1970 A.N. Skrinsky, Intersecting storage rings at Novosibirsk, in: Proceedings of Morges Seminar, 1971 Report CERN/D.PH II/YGC/mng

Deep inelastic scattering

Deep inelastic scattering is the name given to a process used to probe the insides of hadrons (particularly the baryons, such as protons and neutrons), using electrons, muons and neutrinos. It provided the first convincing evidence of the reality of quarks, which up until that point had been considered by many to be a purely mathematical phenomenon. It is a relatively new process, first attempted in the 1960s and 1970s. It is conceptually similar to Rutherford Scattering, but with important differences. The reason why this type of scattering is described as "deep" and "inelastic" is discussed at the Oxford University page.^[1]



Deep Inelastic Scattering of a lepton on a hadron, at leading order in perturbative expansion.

Quarks

The Standard Model of physics, particularly given the work of Murray Gell-Mann in the 1960s, had been successful in uniting much of the previously disparate concepts in particle physics into one, relatively straightforward, scheme. In essence, there were three types of particles.

- The leptons, which were light (as in not particularly massive) particles such as electrons, neutrinos and their antiparticles. They have integer charge
- The bosons, which were particles that exchange forces. These ranged from the massless, easy-to-detect photon (the carrier of the electro-magnetic force) to the exotic (though still massless) gluons that carry the strong nuclear force
- The quarks, which were massive particles that carried fractional charges. They are the "building blocks" of the hadrons. They are also the only particles to be affected by the strong interaction

The leptons had been detected since 1897, when J. J. Thomson had shown that electric current is a flow of electrons. Some bosons were being routinely detected, although the W^+ , W^- and Z^0 particles of the electroweak force were only categorically seen in the early 1980s, and gluons were only firmly pinned down at DESY in Hamburg at about the same time. Quarks, however, were still elusive.

The Experiments

Drawing on Rutherford's groundbreaking experiments in the early years of the Twentieth century, ideas for detecting quarks were formulated. Rutherford had proven that atoms had a small, massive, charged nucleus at their centre by firing alpha particles at atoms in gold. Most had gone through with little or no deviation, but a few were deflected through large angles or came right back. This suggested that atoms had internal structure, and a lot of

empty space.

In order to enter baryons (where quarks were theoretically to be found), a small, penetrating (ie easily accelerated; in reality this meant charged) and easily produced particle needed to be found. Electrons were considered ideal for the role, and in a series of remarkable technological and engineering leaps, electrons were fired as tiny bullets at protons and neutrons in nuclei. As an added bonus, the electrostatic attraction of the positively charged nucleus and the negatively charged electron increased the speed. Later experiments were conducted with muons, but the same principles apply.

The collision absorbs some kinetic energy, and as such it is inelastic (this compares to Rutherford scattering which is elastic, with no loss of kinetic energy, taking into account recoils of the nuclei). The electron emerges from the nucleus, and its trajectory and velocity can be detected.

Analysis of the results led to the following conclusions:

- The hadrons do have internal structure
- In baryons, there are three points of deflection (i.e. baryons consist of three quarks)
- In mesons, there are two points of deflection (i.e. mesons consist of a quark and an anti-quark. The reason they do not consist of two quarks is to do with their colour; see the quark article for more explanation)
- Quarks appear to be point charges, as electrons appear to be, with the fractional charges suggested by the Standard Model

The experiments were important because, not only did they confirm the physical reality of quarks but also proved again that the Standard Model was the correct avenue of research for particle physicists to pursue.

References

- [1] Deep inelastic scattering (<http://www.physics.ox.ac.uk/documents/PUS/dis/DIS.htm>). *Oxford University Physics Department*, 2003.

Timeline of microphysics

Timeline of quantum mechanics, molecular physics, atomic physics, nuclear physics, and particle physics

- 585 BC Buddha states that there were indivisible particles of mind and matter which vibrated 3 trillion times in the blink of an eye which he calls "kalapas"
- 440 BC Democritus speculates about fundamental indivisible particles—calls them "atoms"

The beginning of chemistry

- 1766 Henry Cavendish discovers and studies hydrogen
 - 1778 Carl Scheele and Antoine Lavoisier discover that air is composed mostly of nitrogen and oxygen
 - 1781 Joseph Priestley creates water by igniting hydrogen and oxygen
 - 1800 William Nicholson and Anthony Carlisle use electrolysis to separate water into hydrogen and oxygen
 - 1803 John Dalton introduces atomic ideas into chemistry and states that matter is composed of atoms of different weights
 - 1805 Thomas Young conducts Double-slit experiment (approximate time)
 - 1811 Amedeo Avogadro claims that equal volumes of gases should contain equal numbers of molecules
 - 1832 Michael Faraday states his laws of electrolysis
 - 1871 Dmitri Ivanovich Mendeleev systematically examines the periodic table and predicts the existence of gallium, scandium, and germanium
 - 1873 Johannes van der Waals introduces the idea of weak attractive forces between molecules
 - 1885 Johann Balmer finds a mathematical expression for observed hydrogen line wavelengths
 - 1887 Heinrich Hertz discovers the photoelectric effect
 - 1894 Lord Rayleigh and William Ramsay discover argon by spectroscopically analyzing the gas left over after nitrogen and oxygen are removed from air
 - 1895 William Ramsay discovers terrestrial helium by spectroscopically analyzing gas produced by decaying uranium
 - 1896 Antoine Becquerel discovers the radioactivity of uranium
 - 1896 Pieter Zeeman studies the splitting of sodium D lines when sodium is held in a flame between strong magnetic poles
 - 1897 J.J. Thomson discovers the electron
 - 1898 William Ramsay and Morris Travers discover neon, and negatively charged beta particles
-

The age of quantum mechanics

- 1900 Paul Villard discovers gamma-rays while studying uranium decay
 - 1900 Johannes Rydberg refines the expression for observed hydrogen line wavelengths
 - 1900 Max Planck states his quantum hypothesis and blackbody radiation law
 - 1902 Philipp Lenard observes that maximum photoelectron energies are independent of illuminating intensity but depend on frequency
 - 1902 Theodor Svedberg suggests that fluctuations in molecular bombardment cause the Brownian motion
 - 1905 Albert Einstein explains the photoelectric effect
 - 1906 Charles Barkla discovers that each element has a characteristic X-ray and that the degree of penetration of these X-rays is related to the atomic weight of the element
 - 1909 Hans Geiger and Ernest Marsden discover large angle deflections of alpha particles by thin metal foils
 - 1909 Ernest Rutherford and Thomas Royds demonstrate that alpha particles are doubly ionized helium atoms
 - 1911 Ernest Rutherford explains the Geiger-Marsden experiment by invoking a nuclear atom model and derives the Rutherford cross section
 - 1911 Jean Perrin proves the existence of atoms and molecules
 - 1912 Max von Laue suggests using crystal lattices to diffract X-rays
 - 1912 Walter Friedrich and Paul Knipping diffract X-rays in zinc blende
 - 1913 William Henry Bragg and William Lawrence Bragg work out the Bragg condition for strong X-ray reflection
 - 1913 Henry Moseley shows that nuclear charge is the real basis for numbering the elements
 - 1913 Niels Bohr presents his quantum model of the atom
 - 1913 Robert Millikan measures the fundamental unit of electric charge
 - 1913 Johannes Stark demonstrates that strong electric fields will split the Balmer spectral line series of hydrogen
 - 1914 James Franck and Gustav Hertz observe atomic excitation
 - 1914 Ernest Rutherford suggests that the positively charged atomic nucleus contains protons
 - 1915 Arnold Sommerfeld develops a modified Bohr atomic model with elliptic orbits to explain relativistic fine structure
 - 1916 Gilbert N. Lewis and Irving Langmuir formulate an electron shell model of chemical bonding
 - 1917 Albert Einstein introduces the idea of stimulated radiation emission
 - 1921 Alfred Landé introduces the Landé g-factor
 - 1922 Arthur Compton studies X-ray photon scattering by electrons
 - 1922 Otto Stern and Walther Gerlach show "space quantization"
 - 1923 Louis de Broglie suggests that electrons may have wavelike properties
 - 1923 Lise Meitner discovers the Auger process
 - 1924 John Lennard-Jones proposes a semiempirical interatomic force law
 - 1924 Satyendra Bose and Albert Einstein introduce Bose-Einstein statistics
 - 1925 Wolfgang Pauli states the quantum exclusion principle
 - 1925 George Uhlenbeck and Samuel Goudsmit postulate electron spin
 - 1925 Pierre Auger discovers the Auger process (2 years after Lise Meitner)
-

- 1925 Werner Heisenberg, Max Born, and Pascual Jordan formulate quantum matrix mechanics
 - 1926 Erwin Schrödinger states his nonrelativistic quantum wave equation and formulates quantum wave mechanics
 - 1926 Erwin Schrödinger proves that the wave and matrix formulations of quantum theory are mathematically equivalent
 - 1926 Oskar Klein and Walter Gordon state their relativistic quantum wave equation, now the Klein-Gordon equation
 - 1926 Enrico Fermi discovers the spin-statistics connection
 - 1926 Paul Dirac introduces Fermi-Dirac statistics
 - 1927 Clinton Davisson, Lester Germer, and George Paget Thomson confirm the wavelike nature of electrons
 - 1927 Werner Heisenberg states the quantum uncertainty principle
 - 1927 Max Born interprets the probabilistic nature of wavefunctions
 - 1927 Walter Heitler and Fritz London introduce the concepts of valence bond theory and apply it to the hydrogen molecule.
 - 1927 Thomas and Fermi develop the Thomas-Fermi model
 - 1927 Max Born and Robert Oppenheimer introduce the Born-Oppenheimer approximation
 - 1928 Chandrasekhara Raman studies optical photon scattering by electrons
 - 1928 Paul Dirac states his relativistic electron quantum wave equation
 - 1928 Charles G. Darwin and Walter Gordon solve the Dirac equation for a Coulomb potential
 - 1928 Friedrich Hund and Robert S. Mulliken introduce the concept of molecular orbital
 - 1929 Oskar Klein discovers the Klein paradox
 - 1929 Oskar Klein and Yoshio Nishina derive the Klein-Nishina cross section for high energy photon scattering by electrons
 - 1929 Nevill Mott derives the Mott cross section for the Coulomb scattering of relativistic electrons
 - 1930 Paul Dirac introduces electron hole theory
 - 1930 Erwin Schrödinger predicts the zitterbewegung motion
 - 1930 Fritz London explains van der Waals forces as due to the interacting fluctuating dipole moments between molecules
 - 1931 John Lennard-Jones proposes the Lennard-Jones interatomic potential
 - 1931 Irene Joliot-Curie and Frédéric Joliot observe but misinterpret neutron scattering in paraffin
 - 1931 Wolfgang Pauli puts forth the neutrino hypothesis to explain the apparent violation of energy conservation in beta decay
 - 1931 Linus Pauling discovers resonance bonding and uses it to explain the high stability of symmetric planar molecules
 - 1931 Paul Dirac shows that charge quantization can be explained if magnetic monopoles exist
 - 1931 Harold Urey discovers deuterium using evaporation concentration techniques and spectroscopy
 - 1932 John Cockcroft and Ernest Walton split lithium and boron nuclei using proton bombardment
 - 1932 James Chadwick discovers the neutron
-

- 1932 Werner Heisenberg presents the proton-neutron model of the nucleus and uses it to explain isotopes
 - 1932 Carl D. Anderson discovers the positron
 - 1933 Ernst Stueckelberg (1932), Lev Davidovich Landau (1932), and Clarence Zener discover the Landau-Zener transition
 - 1933 Max Delbruck suggests that quantum effects will cause photons to be scattered by an external electric field
 - 1934 Irene Joliot-Curie and Frédéric Joliot bombard aluminum atoms with alpha particles to create artificially radioactive phosphorus-30
 - 1934 Leó Szilárd realizes that nuclear chain reactions may be possible
 - 1934 Enrico Fermi formulates his theory of beta decay
 - 1934 Lev Davidovich Landau tells Edward Teller that nonlinear molecules may have vibrational modes which remove the degeneracy of an orbitally degenerate state (Jahn-Teller effect)
 - 1934 Enrico Fermi suggests bombarding uranium atoms with neutrons to make a 93 proton element
 - 1934 Pavel Alekseyevich Cherenkov reports that light is emitted by relativistic particles traveling in a nonscintillating liquid
 - 1935 Hideki Yukawa presents a theory of strong interactions and predicts mesons
 - 1935 Albert Einstein, Boris Podolsky, and Nathan Rosen put forth the EPR paradox
 - 1935 Henry Eyring develop the transition state theory
 - 1935 Niels Bohr presents his analysis of the EPR paradox
 - 1936 Eugene Wigner develops the theory of neutron absorption by atomic nuclei
 - 1936 Hermann Arthur Jahn and Edward Teller present their systematic study of the symmetry types for which the Jahn-Teller effect is expected
 - 1937 Hans Hellmann finds the Hellmann-Feynman theorem
 - 1937 Seth Neddermeyer, Carl Anderson, J.C. Street, and E.C. Stevenson discover muons using cloud chamber measurements of cosmic rays
 - 1939 Richard Feynman finds the Hellmann-Feynman theorem
 - 1939 Otto Hahn and Fritz Strassmann bombard uranium salts with thermal neutrons and discover barium among the reaction products
 - 1939 Lise Meitner and Otto Robert Frisch determine that nuclear fission is taking place in the Hahn-Strassmann experiments
 - 1942 Enrico Fermi makes the first controlled nuclear chain reaction
 - 1942 Ernst Stueckelberg introduces the propagator to positron theory and interprets positrons as negative energy electrons moving backwards through spacetime
 - 1943 Sin-Itiro Tomonaga publishes his paper on the basic physical principles of quantum electrodynamics
 - 1947 Willis Lamb and Robert Rethford measure the Lamb-Rethford shift
 - 1947 Cecil Powell, César Lattes, and Giuseppe Occhialini discover the pi-meson by studying cosmic ray tracks
 - 1947 Richard Feynman presents his propagator approach to quantum electrodynamics
 - 1948 Hendrik Casimir predicts a rudimentary attractive Casimir force on a parallel plate capacitor
 - 1951 Martin Deutsch discovers positronium
 - 1952 David Bohm propose his interpretation of quantum mechanics
-

- 1953 Robert Wilson observes Delbruck scattering of 1.33 MeV gamma-rays by the electric fields of lead nuclei
- 1954 Chen Ning Yang and Robert Mills investigate a theory of hadronic isospin by demanding local gauge invariance under isotopic spin space rotations---first non-Abelian gauge theory
- 1955 Owen Chamberlain, Emilio Segrè, Clyde Wiegand, and Thomas Ypsilantis discover the antiproton
- 1956 Frederick Reines and Clyde Cowan detect antineutrino
- 1956 Chen Ning Yang and Tsung Lee propose parity violation by the weak nuclear force
- 1956 Chien Shiung Wu discovers parity violation by the weak force in decaying cobalt
- 1957 Gerhart Luders proves the CPT theorem
- 1957 Richard Feynman, Murray Gell-Mann, Robert Marshak, and E.C.G. Sudarshan propose a vector/axial vector (VA) Lagrangian for weak interactions
- 1958 Marcus Sparnaay experimentally confirms the Casimir effect
- 1959 Yakir Aharonov and David Bohm predict the Aharonov-Bohm effect
- 1960 R.G. Chambers experimentally confirms the Aharonov-Bohm effect
- 1961 Murray Gell-Mann and Yuval Ne'eman discover the Eightfold Way patterns---SU(3) group
- 1961 Jeffrey Goldstone considers the breaking of global phase symmetry
- 1962 Leon Lederman shows that the electron neutrino is distinct from the muon neutrino

The formation and successes of the Standard Model

- 1963 Murray Gell-Mann and George Zweig propose the quark/aces model
- 1964 Peter Higgs considers the breaking of local phase symmetry
- 1964 John Stewart Bell shows that all local hidden variable theories must satisfy Bell's inequality
- 1964 Val Fitch and James Cronin observe CP violation by the weak force in the decay of K mesons
- 1967 Steven Weinberg puts forth his electroweak model of leptons
- 1969 John Clauser, Michael Horne, Abner Shimony and Richard Holt propose a polarization correlation test of Bell's inequality
- 1970 Sheldon Glashow, John Iliopoulos, and Luciano Maiani propose the charm quark
- 1971 Gerard 't Hooft shows that the Glashow-Salam-Weinberg electroweak model can be renormalized
- 1972 Stuart Freedman and John Clauser perform the first polarization correlation test of Bell's inequality
- 1973 David Politzer proposes the asymptotic freedom of quarks
- 1974 Burton Richter and Samuel Ting discover the psi meson implying the existence of the charm quark
- 1974 Robert J. Buenker and Sigrid D. Peyerimhoff introduce the multireference configuration interaction method.
- 1975 Martin Perl discovers the tau lepton
- 1977 Steve Herb finds the upsilon resonance implying the existence of the beauty/bottom quark
- 1982 Alain Aspect, J. Dalibard, and G. Roger perform a polarization correlation test of Bell's inequality that rules out conspiratorial polarizer communication

- 1983 Carlo Rubbia, Simon van der Meer, and the CERN UA-1 collaboration find the W and Z intermediate vector bosons
- 1989 The Z intermediate vector boson resonance width indicates three quark-lepton generations
- 1994 The CERN LEAR Crystal Barrel Experiment justifies the existence of glueballs (exotic meson).
- 1995 after 18 years searching at Fermilab was discovered the top quark, it had very big mass
- 1998 Super-Kamiokande (Japan) observes evidence for neutrino oscillations, implying that at least one neutrino has mass.
- 2001 The Sudbury Neutrino Observatory (Canada) confirms the existence of neutrino oscillations.
- 2005 At the RHIC accelerator of Brookhaven National Laboratory they have created a quark-gluon liquid of very low viscosity, perhaps the quark-gluon plasma
- 2008 The Large Hadron Collider at CERN is scheduled to begin operation in this year and has a big chance to find the Higgs boson later

Automatic calculation of particle interaction or decay

The **automatic calculation of particle interaction or decay** is part of the computational particle physics branch. It refers to computing tools that help calculating the complex particle interactions as studied in high-energy physics, astroparticle physics and cosmology. The goal of the automation is to handle the full sequence of calculations in an automatic (programmed) way: from the Lagrangian expression describing the physics model up to the cross-sections values and to the event generator software.

Particle accelerator or colliders produce collisions (interactions) of particle (like the electron or the proton). The colliding particles form the *Initial State*. In the collision, particles can be annihilated or/and exchanged producing possibly different sets of particles, the *Final States*. The Initial and Final States of the interaction relate through the so-called scattering matrix (S-matrix).

For example at LEP, $e^+ e^- \rightarrow e^+ e^-$ or $e^+ e^- \rightarrow \mu^+ \mu^-$ are processes where the *initial state* is an electron and a positron colliding to produce an electron and a positron or two muons of opposite charge: the *final states*. In these simple cases, no automatic packages are needed and cross-section analytical expression can be easily derived at least for the lowest approximation: the Born approximation also called the leading order or the tree level (as Feynman diagrams have only trunk and branches, no loops)

But particle physics is now requiring much more complex calculations like at LHC $pp \rightarrow n \text{ jets}$ where p are protons and $n \text{ jets}$ means n (2,3,4,...) jets of particles initiated by proton constituents (quarks and gluons). The number of subprocesses describing a given process is so large that automatic tools have been developed to mitigate the burden of hand calculations.

Interactions at higher energies open a large spectrum of possible final states and consequently increase the number of processes to compute.

High precision experiments impose the calculation of higher order calculation, namely the inclusion of subprocesses where more than one virtual particles can be created and annihilated during the interaction lapse creating so-called *loops* which induce much more involved calculations.

Finally new theoretical models like the supersymmetry model (MSSM in its minimal version) predict a flurry of new processes.

The automatic packages, once seen as mere teaching support, have become, this last 10 years an essential component of the data simulation and analysis suite for all experiments. They help constructing event generators and are sometime viewed as *generators of event generators* or *Meta-generators*. A particle physics model is essentially described by its Lagrangian. To simulate the production of events through event generators, 3 steps have to be taken. The Automatic Calculation project is to create the tools to make those steps as automatic (or programmed) as possible:

I Feynman rules, coupling and mass generation

LanHEP is an example of Feynman rules generation. Some model needs an additional step to compute, based on some parameters, the mass and coupling of new predicted particles.

II Matrix element code generation: Various methods are used to automatically produce the Matrix element expression in a computer language (Fortran, C/C++). They use values (i.e. for the masses) or expressions (i.e. for the couplings) produced by step **I** or model specific libraries constructed *by hands* (usually heavily relying on Computer algebra languages). When this expression is integrated (usually numerically) over the internal degrees of freedom it will provide the total and differential cross-sections for a given set of initial parameters like the *initial state* particle energies and polarization.

III Event generator code generation: This code must then be interfaced to other packages to fully provide the actual *final state*. The various effects or phenomenon that need to be implemented are:

Initial state radiation and beamstrahlung for $e^+ e^-$ initial states. Parton Distribution Functions describing the actual content in terms of gluons and quarks of the p or p -bar initial state particles Parton showering describing the way final state quarks or gluons due to the QCD confinement generate additional quark/gluon pairs generating a so-called shower of partons before transforming into hadrons. Hadronization describing how the final quark pairs/triplets form the visible and detectable hadrons. Underlying event takes care of the way the rest, in term of constituent, of the initial protons also contribute to any given event.

The interplay or *matching* of the precise matrix element calculation and the approximations resulting from the simulation of the *parton shower* gives rise to further complications, either within a given level of precision like at leading order (LO) for the production of n jets or between two levels of precision when tempting to connect matrix element computed at next-to-leading (NLO) (1-loop) or next-to-next-leading order (NNLO) (2-loops) with LO partons shower package.

Several methods have been developed for this matching:

- Subtraction methods
- ...

But the only correct way is to match packages at the same level theoretical accuracy like the NLO matrix element calculation with NLO parton shower packages. This is currently in development.

History

in construction

The idea of automation of the calculations in high-energy physics is not new. It dates back to the 1960's when packages such as SCHOONSCHIP and then REDUCE had been developed.

These are symbolic manipulation codes that automatize the algebraic parts of a matrix element evaluation, like traces on Dirac matrices and contraction of Lorentz indices. Such codes have evolved quite a lot with applications not only optimized for high-energy physics like FORM but also more general purpose programs like Mathematica and Maple.

Generation of QED Feynman graphs at any order in the coupling constant was automatized in the late 70's[15]. One of the first major application of these early developments in this field was the calculation of the anomalous magnetic moments of the electron and the muon[16]. The first automatic system incorporating all the steps for the calculation of a cross section, from Feynman graph generation, amplitude generation through a REDUCE source code that produces a FORTRAN code, phase space integration and event generation with BASES/SPRING[17] is GRAND[18]. It was limited to tree-level processes in QED. In the early nineties, a few groups started to develop packages aiming at the automation in the SM[19]. [1] [2] [3] [4] [5] [6] [7] [8] [9] [10]

Matrix element calculation methods

see Feynman diagram

Helicity amplitude

Feynman amplitudes are written in terms of spinor products of wave functions for massless fermions, and then evaluated numerically before the amplitudes are squared. Taking into account fermion masses implies that Feynman amplitudes are decomposed into vertex amplitudes by splitting the internal lines into wave function of fermions and polarization vectors of gauge bosons. All helicity configuration can be computed independently.

Helicity amplitude squared

The method is similar to the previous one, but the numerical calculation is performed after squaring the Feynman Amplitude. The final expression is shorter and therefore faster to compute, but independent helicity information are not anymore available.

Dyson-Schwinger recursive equations

The scattering amplitude is evaluated recursively through a set of Schwinger-Dyson[Dyson-Schwinger equations. The computational cost of this algorithm grows asymptotically as 3^n , where n is the number of particles involved in the process, compared to $n!$ in the traditional Feynman graphs approach. Unitary gauge is used and mass effects are available as well. Additionally, the color and helicity structures are appropriately transformed so the usual summation is replaced by the Monte Carlo

techniques. ^[11].

Higher order calculations

in construction ^[12]

Additional package for Event generation

The integration of the "matrix element" over the multidimensional internal parameters phase space provides the total and differential cross-sections. Each point of this phase space is associated to an event probability. this is used to randomly generate events closely mimicking experimental data. This is called event generation, the first step in the complete chain of event simulation. The initial and final state particles can be elementary particles like electron, muon or photons but also partons, the constituent of the proton (quarks and gluons).

More effects must them be implemented to reproduce real life events as those detected at the colliders.

The initial electron or positron may undergo radiation before they actually interact:Initial state radiation and beamstrahlung

The bare partons that do not exist in nature (there are confined insite the hadrons) must be so to say dressed so that they form the known hadrons or mesons. they is made in two steps: Parton shower and Hadronization.

When the initial state are protons, at high energy it is only their constituent which interact. Therefore the specific parton that will experience the "hard interaction" has to be selected. Structure functions must therefore be implemented. The other parton may interact "softly" must be also be simulated as they contribute to the complexity of the event: Underlying event

Initial state radiation and beamstrahlung

(to be written)

Parton shower and Hadronization

(to be written)

At leading Order (LO)

(to be written)

At Next-to-Leading order (NLO)

(to be written)

Structure and Fragmentation Functions

(to be written)

Underlying event*(to be written)***Model specific packages***(to be written)***MSSM****Related computational issues***(to be written)***Multi-dimensional integrators***(to be written)***Ultra-High Precision Numerical computation***(to be written)***Existing Packages****Feynman rules generators**

- LanHEP
- ...

Tree Level Packages

Name	Model	Max FS	Tested FS	Short description	Publication	Method	Status
Grace	SM/MSSM	2->n	2->6	complete,massive,helicity,color	Manual v2.0 [13]	HA	PD [14]
CompHEP	Model	Max FS	Tested FS	Short description	Publication	method	Status
CalcHEP	Model	Max FS	Tested FS	Short description	Publication	Method	Status
Sherpa	SM/MSSM	2->n	2->8	massive	publication [15]	HA/DS	PD [16]
GenEva	Model	Max FS	Tested FS	Short description	Publication	Method	Status
HELAC	Model	Max FS	Tested FS	Short description	Publication	Method	Status
Name	Model	Max FS	Tested FS	Short description	Publication	Method	Status

PD: Public Domain, SM: Standard Model, MSSM: Minimal Supersymmetric Standard Model
 HA: Helicity Amplitude DS: Dyson Schwinger

Higher-order Packages

Name	Model	Order tested	Max FS	Tested FS	Short description	Publication	Method	Status
Grace L-1	SM/MSSM	1-loop	2->n	2->4	complete,massive,helicity,color	NA	Method	NA
Name	Order	Model	Max FS	Tested FS	Short description	Publication	Method	Status

Additional package for Event generation

References

- [1] Automatic calculation of Feynman amplitudes. (<http://www.slac.stanford.edu/spires/find/hep?key=5471150>) By T. Kaneko. In *Lyon 1990, New computing techniques in physics research* 555-56.
- [2] Automatic calculation in high-energy physics by Grace/Chanel and CompHEP. (<http://www.slac.stanford.edu/spires/find/hep?key=2574861>) By E.E. Boos, et al., Int.J.Mod.Phys.C5:615-628,1994.
- [3] Automatic calculation of Feynman loop diagram. 1. Generation of simplified form of amplitude. (<http://www.slac.stanford.edu/spires/find/hep?key=2719657>) By Jian-Xiong Wang. Comput.Phys.Commun.77:263-285,1993.

Automatic calculation of two loop weak corrections to muon anomalous magnetic moment. (<http://www.slac.stanford.edu/spires/find/hep?key=3147525>) By Toshiaki Kaneko, Nobuya Nakazawa.

In *Pisa 1995, New computing techniques in physics research* 173-17. [hep-ph/9505278]

Automatic calculation of SUSY particle production. (<http://www.slac.stanford.edu/spires/find/hep?key=3360695>) By Minami-Tateya Collaboration

In *Zvenigorod 1995, High energy physics and quantum field theory* 155-16. [hep-ph/9605414]

Automatic calculation of massive two loop self-energies with XLOOPS. (<http://www.slac.stanford.edu/spires/find/hep?key=3461025>) By Johannes Franzkowski.

Nucl.Instrum.Meth.A389:333-338,1997. [hep-ph/9611378]

- [7] Automatic Feynman diagram calculation with xloops: A Short overview. (<http://www.slac.stanford.edu/spires/find/hep?key=4306120>) By Lars Brucher. [hep-ph/0002028] MZ-TH-98-18 (Mar 1998) 5p.

- [8] Automatic amplitude calculation and event generation for collider physics: GRACE and CompHEP. (<http://www.slac.stanford.edu/spires/find/hep?key=4515617>) By D. Perret-Gallix. In *Moscow 1999, High energy physics and quantum field theory* 270-28.

- [9] Automatic calculations in high energy physics and Grace at one-loop. (<http://www.slac.stanford.edu/spires/find/hep?key=5631408>) By G. Belanger, et al., Phys.Rept.430:117-209,2006. [hep-ph/0308080]

Automatic one loop calculation of MSSM processes with GRACE. (<http://www.slac.stanford.edu/spires/find/hep?key=5795915>) By J. Fujimoto, T. Ishikawa, M. Jimbo, T. Kon, M.

Kuroda. Nucl.Instrum.Meth.A534:246-249,2004. [hep-ph/0402145]

- [11] HELAC: A Package to compute electroweak helicity amplitudes. Aggeliki Kanaki, Costas G. Papadopoulos (Democritus Nucl. Res. Ctr.) . DEMO-HEP-2000-01, Feb 2000. 14pp. Published in Comput.Phys.Comm.132:306-315,2000. e-Print: hep-ph/0002082

- [12] Automatic calculations in high energy physics and Grace at one-loop. G. Belanger, F. Boudjema (Annecy, LAPP) , J. Fujimoto, T. Ishikawa, T. Kaneko (KEK, Tsukuba) , K. Kato (Kogakuin U.) , Y. Shimizu (KEK, Tsukuba), LAPTH-982-03, KEK-CP-138, Aug 2003. 83pp. Published in Phys.Rept.430:117-209,2006. e-Print: hep-ph/0308080 URL for hep-ph <http://arxiv.org/abs/hep-ph/0308080>

- [13] <http://minami-home.kek.jp/grace/gracedoc.ps>

- [14] <http://minami-home.kek.jp>

- [15] <http://www.slac.stanford.edu/spires/find/hep/www?rawcmd=HHEP+HEP-PH%2F0311263>

- [16] <http://www.sherpa-mc.de>

Neutrino

Neutrino	
Composition:	Elementary particle
Family:	Fermion
Group:	Lepton
Interaction:	weak interaction and gravitation
Antiparticle:	Antineutrino (possibly identical to the neutrino)
Theorized:	1930 by Wolfgang Pauli
Discovered:	1956 by Clyde Cowan, Frederick Reines, F. B. Harrison, H. W. Kruse, and A. D. McGuire.
Symbol(s):	ν_e, ν_μ, ν_τ
Types:	3 - electron, muon and tau
Mass:	Nonzero, see Mass below
Electric charge:	0
Color charge:	0
Spin:	$\frac{1}{2}$

Neutrinos (*meaning*: "Small neutral ones") are elementary particles that often travel close to the speed of light, lack an electric charge, are able to pass through ordinary matter almost undisturbed and are thus extremely difficult to detect. Neutrinos have a minuscule, but nonzero mass. They are usually denoted by the Greek letter ν (nu).

Neutrinos are created as a result of certain types of radioactive decay or nuclear reactions such as those that take place in the Sun, in nuclear reactors, or when cosmic rays hit atoms. There are three types, or "flavors", of neutrinos: *electron neutrinos*, *muon neutrinos* and *tau neutrinos*; each type also has an antimatter partner, called an antineutrino. Electron neutrinos or antineutrinos are generated whenever neutrons change into protons or vice versa, the two forms of beta decay. Interactions involving neutrinos are generally mediated by the weak force.

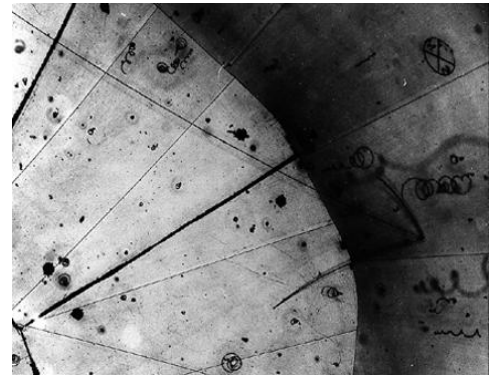
Most neutrinos passing through the Earth emanate from the Sun, and more than 50 trillion solar electron neutrinos pass through the human body every second.^[1]

History

Proposal of neutrino existence, from conservation arguments

The neutrino was first postulated in 1930 by Wolfgang Pauli to preserve conservation of energy, conservation of momentum, and conservation of angular momentum in beta decay – the decay of a neutron into a proton, an electron and an antineutrino.^[2] Pauli theorized that an undetected particle was carrying away the observed difference between the energy, momentum, and angular momentum of the initial and final particles.

The current name *neutrino* was coined by Enrico Fermi, who developed the first theory describing neutrino interactions, as a pun on *neutrone*, the Italian name of the neutron: *neutrone* seems to use the *-one* suffix (even though it is a complete word, not a compound), which in Italian indicates a large object, whereas *-ino* indicates a small one.



Observation of a neutrino hitting a proton in a bubble chamber. The collision occurred at the point where three tracks emanate on the right of the photograph.

Direct detection from induced beta decay

In 1942 Kan-Chang Wang first proposed to use beta-capture to experimentally detect neutrinos.^[3] In 1956 Clyde Cowan, Frederick Reines, F. B. Harrison, H. W. Kruse, and A. D. McGuire published the article "Detection of the Free Neutrino: a Confirmation" in *Science*, a result that was rewarded with the 1995 Nobel Prize. In this experiment, now known as the neutrino experiment, neutrinos created in a nuclear reactor by beta decay were shot into protons producing neutrons and positrons both of which could be detected. It is now known that both the proposed and the observed particles were antineutrinos.

Experimental demonstration of neutrino flavors

In 1962 Leon M. Lederman, Melvin Schwartz and Jack Steinberger showed that more than one type of neutrino exists by first detecting interactions of the muon neutrino (already hypothesised with the name *neutretto*^[4]), which earned them the 1988 Nobel Prize. When a third type of lepton, the tau, was discovered in 1975 at the Stanford Linear Accelerator, it too was expected to have an associated neutrino. First evidence for this third neutrino type came from the observation of missing energy and momentum in tau decays analogous to the beta decay leading to the discovery of the neutrino. The first detection of tau neutrino interactions was announced in summer of 2000 by the DONUT collaboration at Fermilab, making it the latest particle of the Standard Model to have been directly observed; its existence had already been inferred by both theoretical consistency and experimental data from LEP.

The solar neutrino number discrepancy problem

Starting in the late 1960s, several experiments found that the number of electron neutrinos arriving from the sun was between one third and one half the number predicted by the Standard Solar Model, a discrepancy which became known as the solar neutrino problem and remained unresolved for some thirty years.

The Standard Model of particle physics formerly assumed that neutrinos were massless and couldn't change flavor. However, nonzero neutrino mass and accompanying flavor oscillation remained a possibility.

A practical method for investigating neutrino masses (that is, flavor oscillation) was first suggested by Bruno Pontecorvo in 1957 using an analogy with the neutral kaon system; over the subsequent 10 years he developed the mathematical formalism and the modern formulation of vacuum oscillations. In 1985 Stanislav Mikheyev and Alexei Smirnov (expanding on 1978 work by Lincoln Wolfenstein) noted that flavor oscillations can be modified when neutrinos propagate through matter. This so-called MSW effect is important to understand neutrinos emitted by the Sun, which pass through its dense atmosphere on their way to detectors on Earth.

Direct detection of flavor oscillation in solar neutrinos

Starting in 1998, experiments began to show that solar and atmospheric neutrinos change flavors (see Super-Kamiokande, Sudbury Neutrino Observatory). This resolved the solar neutrino problem: the electron neutrinos produced in the sun had partly changed into other flavors which the experiments could not detect.

Although individual experiments, such as the set of solar neutrino experiments, are consistent with non-oscillatory mechanisms of neutrino flavor conversion, taken altogether, neutrino experiments imply the existence of neutrino oscillations. Especially relevant in this context are the reactor experiment KamLAND and the accelerator experiments such as MINOS. The KamLAND experiment has indeed identified oscillations as the neutrino flavor conversion mechanism involved in the solar electron neutrinos. Similarly MINOS confirms the oscillation of atmospheric neutrinos and gives a better determination of the mass squared splitting.^[5]

Detection of supernova neutrinos

Raymond Davis Jr. and Masatoshi Koshihara were jointly awarded the 2002 Nobel Prize in Physics. Ray Davis for his pioneer work on cosmic neutrinos and Koshihara for the first real time observation of supernova neutrinos. The detection of solar neutrinos, and of neutrinos of SN 1987A supernova in 1987 marked the beginning of neutrino astronomy.

Properties and reactions

The neutrino has half-integer spin ($\frac{1}{2}\hbar$) and is therefore a fermion. Neutrinos interact primarily through the weak force. The discovery of neutrino flavor oscillations implies that neutrinos have mass. The existence of a neutrino mass strongly suggests the existence of a tiny neutrino magnetic moment^[6] of the order of 10^{-19} Bohr magneton allowing the possibility that neutrinos may interact electromagnetically as well. An experiment done by C. S. Wu at Columbia University showed that neutrinos always have left-handed chirality.

It is very hard to uniquely identify neutrino interactions among the natural background of radioactivity. For this reason, in early experiments a special reaction channel was chosen to facilitate the identification: the interaction of an antineutrino with one of the hydrogen nuclei in the water molecules. A hydrogen nucleus is a single proton, so simultaneous nuclear interactions, which would occur within a heavier nucleus, don't need to be considered for the detection experiment. Within a cubic metre of water placed right outside a nuclear reactor, only relatively few such interactions can be recorded, but the setup is now used for measuring the reactor's plutonium production rate.

Analogies to the index of refraction and the MSW effect. Neutrinos traveling through matter, in general, undergo a process analogous to light traveling through a transparent material. This process is not directly observable because it doesn't produce ionizing radiation, but gives rise to the MSW effect. Only a small fraction of the neutrino's energy is transferred to the material.

Neutrinos can interact with a more heavy nucleus changing it to another nucleus. This process is used in radiochemical neutrino detectors. In this case, the energy levels and spin states within the target nucleus have to be taken into account to estimate the probability for an interaction. In general the interaction probability increases with the number of neutrons and protons within a nucleus.

Theoretical reactions not yet observed: neutrino induced fission. Very much like neutrons do in nuclear reactors, neutrinos can induce fission reactions within heavy nuclei^[7]. So far, this reaction has not been measured in a laboratory, but is predicted to happen within stars and supernovae. The process affects the abundance of isotopes seen in the universe^[8].

Types of neutrinos

Neutrinos in the Standard Model
of elementary particles

Fermion	Symbol	Mass ^[9]
Generation 1 (electron)		
Electron neutrino	ν_e	< 2.2 eV
Electron antineutrino	$\bar{\nu}_e$	< 2.2 eV
Generation 2 (muon)		
Muon neutrino	ν_μ	< 170 keV
Muon antineutrino	$\bar{\nu}_\mu$	< 170 keV
Generation 3 (tau)		
Tau neutrino	ν_τ	< 15.5 MeV
Tau antineutrino	$\bar{\nu}_\tau$	< 15.5 MeV

There are three known types (*flavors*) of neutrinos: electron neutrino ν_e , muon neutrino ν_μ and tau neutrino ν_τ , named after their partner leptons in the Standard Model (see table at right). The current best measurement of the number of neutrino types comes from observing the decay of the Z boson. This particle can decay into any light neutrino and its antineutrino, and the more types of light neutrinos available, the shorter the lifetime of the Z boson. Measurements of the Z lifetime have shown that the number of light neutrino

types (with "light" meaning of less than half the Z mass) is 3.^[6] The correspondence between the six quarks in the Standard Model and the six leptons, among them the three neutrinos, suggests to physicists' intuition that there should be exactly three types of neutrino. However, actual proof that there are only three kinds of neutrinos remains an elusive goal of particle physics.

The possibility of *sterile* neutrinos — relatively light neutrinos which do not participate in the weak interaction but which could be created through flavor oscillation (see below) — is unaffected by these Z-boson-based measurements, and the existence of such particles is in fact hinted by experimental data from the LSND experiment. However, the currently running MiniBooNE experiment suggested, until recently, that sterile neutrinos are not required to explain the experimental data,^[10] although the latest research into this area is on-going and anomalies in the MiniBooNE data may allow for exotic neutrino types, including sterile neutrinos.^[11]

Flavor oscillations

Neutrinos are most often created or detected with a well defined flavor (electron, muon, tau). However, in a phenomenon known as neutrino flavor oscillation, neutrinos are able to oscillate between the three available flavors while they propagate through space. Specifically, this occurs because the neutrino flavor eigenstates are not the same as the neutrino mass eigenstates (simply called 1, 2, 3). This allows for a neutrino that was produced as an electron neutrino at a given location to have a calculable probability to be detected as either a muon or tau neutrino after it has traveled to another location. This quantum mechanical effect was first hinted by the discrepancy between the number of electron neutrinos detected from the Sun's core failing to match the expected numbers, dubbed as the "solar neutrino problem." In the Standard Model the existence of flavor oscillations implies a nonzero neutrino mass, because the amount of mixing between neutrino flavors at a given time depends on the differences in their squared-masses.

It is possible that the neutrino and antineutrino are in fact the same particle, a hypothesis first proposed by the Italian physicist Ettore Majorana. The neutrino could transform into an antineutrino (and vice versa) by flipping the orientation of its spin state. This is called the Neutrigga Theory.

This change in spin would require the neutrino and antineutrino to have nonzero mass, and therefore travel slower than light, because such a spin flip caused only by a change in point of view, can take place only if inertial frames of reference exist that move faster than the particle: such a particle has a spin of one orientation when seen from a frame which moves slower than the particle, but the opposite spin when observed from a frame that moves faster than the particle.

Speed

Before the idea of neutrino oscillations came up, it was generally assumed that neutrinos travel at the speed of light. The question of neutrino velocity is closely related to their mass. According to relativity, if neutrinos are massless, they must travel at the speed of light. However, if they carry a mass, they cannot reach the speed of light.

In the early 1980s, first measurements of neutrino speed were done using pulsed pion beams (produced by pulsed proton beams hitting a target). The pions decayed producing neutrinos, and the neutrino interactions observed within a time window in a detector at a distance were consistent with the speed of light. This measurement has been repeated using the MINOS detectors, which found the speed of 3 GeV neutrinos to be $1.000051(29)c$. While the central value is higher than the speed of light, the uncertainty is great enough that it is very likely that the true velocity is not greater than the speed of light. This measurement set an upper bound on the mass of the muon neutrino of 50 MeV at 99% confidence.^[12]

The same observation was made, on a somewhat larger scale, with supernova 1987a. The neutrinos from the supernova were detected within a time window that was consistent with a speed of light for the neutrinos. So far, the question of neutrino masses cannot be decided based on measurements of the neutrino speed.

Mass

The Standard Model of particle physics assumed that neutrinos are massless, although adding massive neutrinos to the basic framework is not difficult. Indeed, the experimentally established phenomenon of neutrino oscillation requires neutrinos to have nonzero masses.^[10]

The strongest upper limit on the masses of neutrinos comes from cosmology: the Big Bang model predicts that there is a fixed ratio between the number of neutrinos and the number of photons in the cosmic microwave background. If the total energy of all three types of neutrinos exceeded an average of 50 electronvolts per neutrino, there would be so much mass in the universe that it would collapse. This limit can be circumvented by assuming that the neutrino is unstable; however, there are limits within the Standard Model that make this difficult. A much more stringent constraint comes from a careful analysis of cosmological data, such as the cosmic microwave background radiation, galaxy surveys and the Lyman-alpha forest. These indicate that the sum of the neutrino masses must be less than 0.3 electronvolt.^[13]

In 1998, research results at the Super-Kamiokande neutrino detector determined that neutrinos do indeed flavor oscillate, and therefore have mass. While this shows that neutrinos have mass, the absolute neutrino mass scale is still not known. This is due to the fact that neutrino oscillations are sensitive only to the difference in the squares of the masses.^[14]

The best estimate of the difference in the squares of the masses of mass eigenstates 1 and 2 was published by KamLAND in 2005: $\Delta m_{21}^2 = 0.000079 \text{ eV}^2$.^[15] In 2006, the MINOS experiment measured oscillations from an intense muon neutrino beam, determining the difference in the squares of the masses between neutrino mass eigenstates 2 and 3. The initial results indicate $|\Delta m_{32}^2| = 0.0027 \text{ eV}^2$, consistent with previous results from Super-K.^[16] Since $|\Delta m_{32}^2|$ is the difference of two squared masses, at least one of them has to have a value which is at least the square root of this value. Thus, there exists at least one

neutrino mass eigenstate with a mass of at least 0.04 eV.^[17]

Currently a number of efforts are under way to directly determine the absolute neutrino mass scale in laboratory experiments. The methods applied involve nuclear beta decay (KATRIN and MARE) or neutrinoless double beta decay (e.g. GERDA, CUORE/Cuoricino, NEMO 3 and others).

In 2006, the US-based Main Injector Neutrino Oscillation Search (MINOS) experiment detected flavour oscillations which theoretically suggests that neutrinos have mass, a characteristic not accounted for by the Standard Model.^[18]

Handedness

Experimental results show that (nearly) all produced and observed neutrinos have left-handed helicities (spins antiparallel to momenta), and all antineutrinos have right-handed helicities, within the margin of error. In the massless limit, it means that only one of two possible chiralities is observed for either particle. These are the only chiralities included in the Standard Model of particle interactions.

It is possible that their counterparts (right-handed neutrinos and left-handed antineutrinos) simply do not exist. If they do, their properties are substantially different from observable neutrinos and antineutrinos. It is theorized that they are either very heavy (on the order of GUT scale—see Seesaw mechanism), do not participate in weak interaction (so-called *sterile* neutrinos), or both.

The existence of nonzero neutrino masses somewhat complicates the situation. Neutrinos are produced in weak interactions as chirality eigenstates. However, chirality of a massive particle is not a constant of motion; helicity is, but the chirality operator does not share eigenstates with the helicity operator. Free neutrinos propagate as mixtures of left- and right-handed helicity states, with mixing amplitudes on the order of m_ν/E . This does not significantly affect the experiments, because neutrinos involved are nearly always ultrarelativistic, and thus mixing amplitudes are vanishingly small (for example, most solar neutrinos have energies on the order of 100 keV–1 MeV, so the fraction of neutrinos with "wrong" helicity among them cannot exceed 10^{-10}).^{[19] [20]}

Neutrino sources

Artificially produced neutrinos

Nuclear reactors are the major source of human-generated neutrinos. Anti-neutrinos are made in the beta-decay of neutron-rich daughter fragments in the fission process. Generally, the four main isotopes contributing to the anti-neutrino flux are: uranium-235, uranium-238, plutonium-239, plutonium-241 (e.g. the anti-neutrinos emitted during beta-minus decay of their respective fission fragments). The average nuclear fission releases about 200 MeV of energy, of which roughly 6% (or 9 MeV, depending on quoted reference) are radiated away as anti-neutrinos. For a typical nuclear reactor with a thermal power of 4,000 MW (megawatts) and an electrical power generation of 1,300 MW, this corresponds to a total power production of 4,250 MW, of which 250 MW is radiated away as anti-neutrino radiation. This is to say, 250 MW of fission energy is *lost* from this reactor and does not appear as heat, since the anti-neutrinos penetrate all normal building materials essentially tracelessly. The energy spectrum depends, for example, on the degree to which the fuel is burned.

There is no established experimental method to measure the flux of low energy anti-neutrinos. Only anti-neutrinos with an energy above threshold of 1.8 MeV can be uniquely identified (see *neutrino detection* below). An estimated 3% of all anti-neutrinos from a nuclear reactor carry an energy above this threshold. An average nuclear power plant may generate over 10^{20} anti-neutrinos per second above this threshold, and a much larger number which cannot be seen with present detector technology.

Some particle accelerators have been used to make neutrino beams. The technique is to smash protons into a fixed target, producing charged pions or kaons. These unstable particles are then magnetically focused into a long tunnel where they decay while in flight. Because of the relativistic boost of the decaying particle the neutrinos are produced as a beam rather than isotropically. Efforts to construct an accelerator facility where neutrinos are produced through muon decays are ongoing.^[21] Such a setup is generally known as a *neutrino factory*.

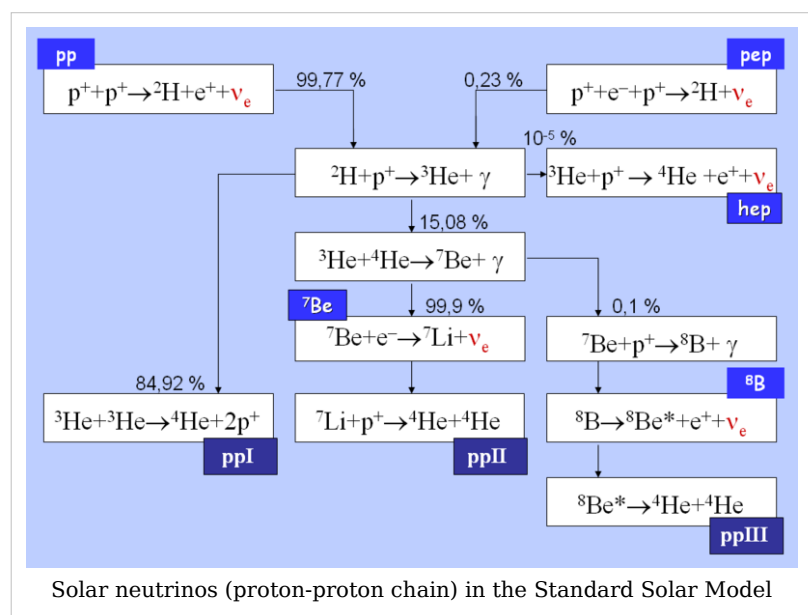
Nuclear bombs also produce very large quantities of neutrinos. Fred Reines and Clyde Cowan considered the detection of neutrinos from a bomb prior to their search for reactor neutrinos.

Geologically produced neutrinos

Neutrinos are produced as a result of natural background radiation. In particular, the decay chains of uranium-238 and thorium-232 isotopes, as well as potassium-40, include beta decays which emit anti-neutrinos. These so-called geoneutrinos can provide valuable information on the Earth's interior. A first indication for geoneutrinos was found by the KamLAND experiment in 2005. KamLAND's main background in the geoneutrino measurement are the anti-neutrinos coming from reactors. Several future experiments aim at improving the geoneutrino measurement and these will necessarily have to be far away from reactors.

Atmospheric neutrinos

Atmospheric neutrinos result from the interaction of cosmic rays with atomic nuclei in the Earth's atmosphere, creating showers of particles, many of which are unstable and produce neutrinos when they decay. A collaboration of particle physicists from Tata Institute of Fundamental Research (TIFR), India, Osaka City University, Japan and Durham University, UK recorded the first cosmic ray neutrino interaction in an underground laboratory in KGF gold mines in India in 1965.



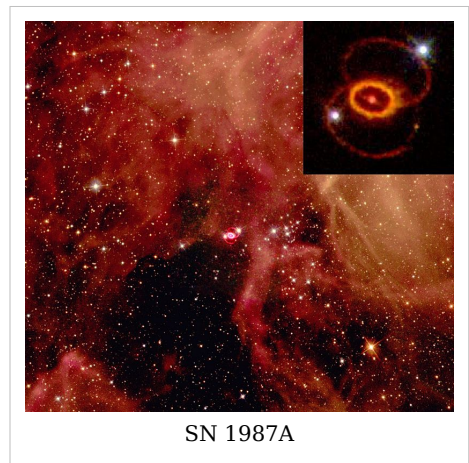
Solar neutrinos

Solar neutrinos originate from the nuclear fusion powering the sun and other stars. The details of the operation of the sun are explained by the Standard Solar Model. In short: when four protons fuse to become one helium nucleus, two of them have to convert into neutrons, and each such conversion releases one electron neutrino.

The sun sends enormous numbers of neutrinos in all directions. Every second, about 65 billion (6.5×10^{10}) solar neutrinos pass through every square centimeter on Earth that faces the sun.^[22] Since neutrinos are insignificantly absorbed by the mass of the Earth, the surface area on the side of the Earth opposite the Sun receives about the same number of neutrinos as the side facing the Sun.

Supernova neutrinos

Neutrinos are an important product of Types Ib, Ic and II (core-collapse) supernovae. In such events, the density at the core becomes so high (10^{17} kg/m^3) that the degeneracy of electrons is not enough to prevent protons and electrons from combining to form a neutron and an electron neutrino. A second and more important neutrino source is the thermal energy (100 billion kelvins) of the newly formed neutron core, which is dissipated via the formation of neutrino-antineutrino pairs of all flavors.^[23] Most of the energy produced in supernovas is thus radiated away in the form of an immense burst of neutrinos. The first experimental evidence of this phenomenon came in 1987, when



SN 1987A

neutrinos from supernova 1987A were detected. The water-based detectors Kamiokande II and IMB detected 11 and 8 antineutrinos of thermal origin,^[23] respectively, while the gallium-71-based Baksan detector found 5 neutrinos (lepton number = 1) of either thermal or electron-capture origin, in a burst lasting less than 13 seconds. It is thought that neutrinos would also be produced from other events such as the collision of neutron stars. What was particularly interesting about this event was that the neutrino signature of the supernova arrived at earth approximately 18 hours *before* the arrival of the first photon signature (Warning: compare with SNEWS where the delay is stated as being 3 hours!). The exceptionally weak interaction with normal matter allowed the neutrinos to pass through the churning mass of the exploding star, while the electromagnetic photons were retarded, with the photon signature of the supernova not being released until the outermost layers of the star were superheated and released a much brighter visible light signature, observed telescopically on earth some 18 hours after the neutrinos had already arrived. This shows how weakly interacting neutrinos truly are.

Because neutrinos interact so little with matter, it is thought that a supernova's neutrino emissions carry information about the innermost regions of the explosion. Much of the *visible* light comes from the decay of radioactive elements produced by the supernova shock wave, and even light from the explosion itself is scattered by dense and turbulent gases. Neutrinos, on the other hand, pass through these gases, providing information about the supernova core (where the densities *were* large enough to influence the neutrino

signal). Furthermore, the neutrino burst is expected to reach Earth before any electromagnetic waves, including visible light, gamma rays or radio waves. The exact time delay is unknown, but for a Type II supernova, astronomers expect the neutrino flood to be released seconds after the stellar core collapse, while the first electromagnetic signal may be hours or days later. The SNEWS project uses a network of neutrino detectors to monitor the sky for candidate supernova events; it is hoped that the neutrino signal will provide a useful advance warning of an exploding star.

The energy of supernova neutrinos ranges from a few to several tens of MeV. However, the sites where cosmic rays are accelerated are expected to produce neutrinos that are one million times more energetic or more, produced from turbulent gaseous environments left over by supernova explosions: the supernova remnants. The connection between cosmic rays and supernova remnants was suggested by Walter Baade and Fritz Zwicky, shown to be consistent with the cosmic ray losses of the Milky Way if the efficiency of acceleration is about 10 percent by Ginzburg and Syrovatsky, and it is supported by a specific mechanism called "shock wave acceleration" based on Fermi ideas (which is still under development). The very high energy neutrinos are still to be seen, but this branch of neutrino astronomy is just in its infancy. The main existing or forthcoming experiments that aim at observing very high energy neutrinos from our galaxy are Baikal, AMANDA, IceCube, Antares, NEMO and Nestor. Related information is provided by very high energy gamma ray observatories, such as HESS and MAGIC. Indeed, the collisions of cosmic rays are supposed to produce charged pions, whose decay give the neutrinos, and also neutral pions, whose decay give gamma rays: the environment of a supernova remnant is transparent to both types of radiation.

Still higher energy neutrinos, resulting from the interactions of extragalactic cosmic rays, could be observed with the Pierre Auger Observatory or with the dedicated experiment named ANITA.

Cosmic background radiation neutrinos

It is thought that, just like the cosmic microwave background radiation left over from the Big Bang, there is a background of low energy neutrinos in our Universe. In the 1980s it was proposed that these may be the explanation for the dark matter thought to exist in the universe. Neutrinos have one important advantage over most other dark matter candidates: we know they exist. However, they also have serious problems.

From particle experiments, it is known that neutrinos are very light. This means that they move at speeds close to the speed of light. Thus, dark matter made from neutrinos is termed "hot dark matter". The problem is that being fast moving, the neutrinos would tend to have spread out evenly in the universe before cosmological expansion made them cold enough to congregate in clumps. This would cause the part of dark matter made of neutrinos to be smeared out and unable to cause the large galactic structures that we see.

Further, these same galaxies and groups of galaxies appear to be surrounded by dark matter which is not fast enough to escape from those galaxies. Presumably this matter provided the gravitational nucleus for formation. This implies that neutrinos make up only a small part of the total amount of dark matter.

From cosmological arguments, relic background neutrinos are estimated to have density of 56 of each type per cubic centimeter and temperature 1.9 K (1.7×10^{-4} eV) if they are massless, much colder if their mass exceeds 0.001 eV. Although their density is quite high,

due to extremely low neutrino cross-sections at sub-eV energies, the relic neutrino background has not yet been observed in the laboratory. In contrast, boron-8 solar neutrinos — which are emitted with a higher energy — have been detected definitively despite having a space density that is lower than that of relic neutrinos by some 6 orders of magnitude.

Neutrino detection

Because neutrinos are very weakly interacting, neutrino detectors must be very large in order to detect a significant number of neutrinos. Neutrino detectors are often built underground in order to isolate the detector from cosmic rays and other background radiation.

Antineutrinos were first detected in the 1950s near a nuclear reactor. Reines and Cowan used two targets containing a solution of cadmium chloride in water. Two scintillation detectors were placed next to the cadmium targets. Antineutrinos with an energy above the threshold of 1.8 MeV caused charged current interactions with the protons in the water, producing positrons and neutrons. The resulting positron annihilations with electrons created photons with an energy of about 0.5 MeV. Pairs of photons in coincidence could be detected by the two scintillation detectors above and below the target. The neutrons were captured by cadmium nuclei resulting in gamma rays of about 8 MeV that were detected a few microseconds after the photons from a positron annihilation event.

Since then, various detection methods have been used. Super Kamiokande is a large volume of water surrounded by photomultiplier tubes that watch for the Cherenkov radiation emitted when an incoming neutrino creates an electron or muon in the water. The Sudbury Neutrino Observatory is similar, but uses heavy water as the detecting medium, which uses the same effects, but also allows the additional reaction any-flavor neutrino photo-dissociation of deuterium, resulting in a free neutron which is then detected from gamma radiation after chlorine-capture. Other detectors have consisted of large volumes of chlorine or gallium which are periodically checked for excesses of argon or germanium, respectively, which are created by electron-neutrinos interacting with the original substance. MINOS uses a solid plastic scintillator coupled to photomultiplier tubes, while Borexino uses a liquid pseudocumene scintillator also watched by photomultiplier tubes and the proposed NOvA detector will use liquid scintillator watched by avalanche photodiodes.

Motivation for scientific interest in the neutrino

The neutrino is of scientific interest because it can make an exceptional probe for environments that are typically concealed from the standpoint of other observation techniques, such as optical and radio observation.

The first such use of neutrinos was proposed in the early 20th century for observation of the core of the Sun. Direct optical observation of the solar core is impossible due to the diffusion of electromagnetic radiation by the huge amount of matter surrounding the core. On the other hand, neutrinos generated in stellar fusion reactions interact very weakly with matter, and pass through the sun with few interactions. While photons emitted by the solar core may require some 40,000 years to diffuse to the outer layers of the Sun, neutrinos are virtually unimpeded and cross this distance at nearly the speed of light.^{[24] [25]}

Neutrinos are also useful for probing astrophysical sources beyond our solar system. Neutrinos are the only known particles that are not significantly attenuated by their travel through the interstellar medium. Optical photons can be obscured or diffused by dust, gas and background radiation. High-energy cosmic rays, in the form of fast-moving protons and atomic nuclei, are not able to travel more than about 100 megaparsecs due to the GZK cutoff. Neutrinos can travel this and greater distances with very little attenuation.

The galactic core of the Milky Way is completely obscured by dense gas and numerous bright objects. Neutrinos produced in the galactic core will be measurable by Earth-based neutrino telescopes in the next decade.

Another important use of the neutrino is in the observation of supernovae, the explosions that end the lives of highly massive stars. The core collapse phase of a supernova is an almost unimaginably dense and energetic event. It is so dense that no known particles are able to escape the advancing core front except for neutrinos. Consequently, supernovae are known to release approximately 99% of their energy in a rapid (10 second) burst of neutrinos. As a result, neutrinos are a very useful probe for these important events.

Determining the mass of the neutrino (see above) is also an important test of cosmology (see *Dark matter*). Many other important uses of the neutrino may be imagined in the future. It is clear that the astrophysical significance of the neutrino as an observational technique is comparable with all other known techniques, and is therefore a major focus of study in astrophysical communities.

In particle physics the main virtue of studying neutrinos is that they are typically the lowest mass, and hence lowest energy examples of particles theorized in extensions of the Standard Model of particle physics. For example, one would expect that if there is a fourth class of fermions beyond the electron, muon, and tau generations of particles, that a fourth generation neutrino would be the easiest to generate in a particle accelerator.

Neutrinos could also be used for studying quantum gravity effects. Because they are not affected by either the strong interaction or electromagnetism (unless they have a magnetic moment), and because they are not normally found in composite particles (unlike quarks) or prone to near instantaneous decay (like many other standard model particles) it might be possible to isolate and measure gravitational effects on neutrinos at a quantum level.

See also

- List of neutrino experiments
- Neutrino factory

Notes

- [1] MIT News Office, "Experiment confirms famous physics model" April 18, 2007 (<http://web.mit.edu/newsoffice/2007/neutrino.html>)
- [2] K. Riesselmann (2007). "<http://www.symmetrymagazine.org/cms/?pid=1000450>|Logbook: Neutrino Invention". *Symmetry* **4** (2). <http://www.symmetrymagazine.org/cms/?pid=1000450>.
- [3] Wang, Kan Chang (January 1942). "http://prola.aps.org/abstract/PR/v61/i1-2/p97_1|A Suggestion on the Detection of the Neutrino". *Physical Review* **61** (1-2): 97. doi: 10.1103/PhysRev.61.97 (<http://dx.doi.org/10.1103/PhysRev.61.97>). http://prola.aps.org/abstract/PR/v61/i1-2/p97_1.
- [4] Ivan V. Anicin (2005). "The Neutrino - Its Past, Present and Future". *arXiv: physics/0503172v1* (<http://www.arxiv.org/abs/physics/0503172v1>) [physics].
- [5] M. Maltoni *et al.* (2004). "Status of global fits to neutrino oscillations". *NJP* **06**: 122. doi: 10.1088/1367-2630/6/1/122 (<http://dx.doi.org/10.1088/1367-2630/6/1/122>). *arXiv:hep-ph/0405172*

- [6] Particle Data Group (S. Eidelman *et al.*) (2004). "<http://pdg.lbl.gov/2005/listings/lxxx.html>|Leptons in the 2005 Review of Particle Physics". *Phys. Lett. B* **592** (1): 1–5. <http://pdg.lbl.gov/2005/listings/lxxx.html>. Retrieved on 2007-11-25.
- [7] G.M. Fuller, E. Kolbe (March 2004). "<http://link.aps.org/doi/10.1103/PhysRevLett.92.111101>|Neutrino-Induced Fission of Neutron-Rich Nuclei". *Phys. Rev. Lett.* **92** (11): 1101. doi: 10.1103/PhysRevLett.92.111101 (<http://dx.doi.org/10.1103/PhysRevLett.92.111101>). <http://link.aps.org/doi/10.1103/PhysRevLett.92.111101>.
- [8] K.-H. Schmidt, A. Kelic (June 2005). "Cross sections and fragment distributions from neutrino-induced fission on r-process nuclei". *Physics Letters B* **616** (1-2): 48–48. doi: 10.1016/j.physletb.2005.04.074 (<http://dx.doi.org/10.1016/j.physletb.2005.04.074>).
- [9] Since neutrino flavor eigenstates are not the same as neutrino mass eigenstates (see neutrino oscillation), the given masses are actually mass expectation values. If the mass of a neutrino could be measured directly, the value would always be that of one of the three mass eigenstates: ν_1 , ν_2 , and ν_3 . In practice, the mass cannot be measured directly. Instead it is measured by looking at the shape of the endpoint of the energy spectrum in particle decays. This sort of measurement directly measures the expectation value of the mass; it is not sensitive to any of the mass eigenstates separately.
- [10] Karagiorgi, G.; A. Aguilar-Arevalo, J. M. Conrad, and M. H. Shaevitz (2007). "<http://scitation.aip.org/getabs/servlet/GetabsServlet?prog=normal&id=PRVDAQ000075000001013011000001&idtype=cvips&gifs=yes> CP violation studies at MiniBooNE in the (3+2) sterile neutrino oscillation hypothesis". *Phys Rev D* **75** (013011): 1–8. doi: 10.1103/PhysRevD.75.013011 (<http://dx.doi.org/10.1103/PhysRevD.75.013011>). <http://scitation.aip.org/getabs/servlet/GetabsServlet?prog=normal&id=PRVDAQ000075000001013011000001&idtype=cvips&gifs=yes>.
- [11] Alpert, M. (August 2007). "<http://www.sciam.com/article.cfm?chanID=sa006&colID=5&articleID=B5CB9C67-E7F2-99DF-3BF7368614D46C5D>|Dimension Shortcuts". *Scientific American*. <http://www.sciam.com/article.cfm?chanID=sa006&colID=5&articleID=B5CB9C67-E7F2-99DF-3BF7368614D46C5D>.
- [12] Measurement of neutrino velocity with the MINOS detectors and NuMI neutrino beam, Adamson *et al.*, arXiv:0706.0437
- [13] Goobar, Ariel; Hannestad, Steen; Mortsell, Edvard; Tu, Huitzu (2006). "The neutrino mass bound from WMAP 3 year data, the baryon acoustic peak, the SNLS supernovae and the Lyman- α forest". *Journal of Cosmology and Astroparticle Physics* **606**: 19. doi: 10.1088/1475-7516/2006/06/019 (<http://dx.doi.org/10.1088/1475-7516/2006/06/019>). arXiv:astro-ph/0602155.
- [14] R. N. Mohapatra *et al.* (APS neutrino theory working group) (2005). "Theory of neutrinos: a white paper". arXiv: [hep-ph/0510213](http://www.arxiv.org/abs/hep-ph/0510213) (<http://www.arxiv.org/abs/hep-ph/0510213>) [hep-ph].
- [15] KamLAND Collaboration (2005). *Physical Review Letters* **94**: 081801.
- [16] http://www.fnal.gov/pub/presspass/press_releases/minos_3-30-06.html|"MINOS experiment sheds light on mystery of neutrino disappearance". Fermilab. 30 March 2006. http://www.fnal.gov/pub/presspass/press_releases/minos_3-30-06.html. Retrieved on 2007-11-25.
- [17] C. Amsler *et al.* (PDG) (2008). "<http://pdg.lbl.gov/2008/reviews/rpp2008-rev-neutrino-mixing.pdf>|The Review of Particle Physics : Neutrino Mass, Mixing, and Flavor Change". *Physics Letters B* **667**: 1. <http://pdg.lbl.gov/2008/reviews/rpp2008-rev-neutrino-mixing.pdf>.
- [18] Morelle, Rebecca (2006-03-31). <http://news.bbc.co.uk/2/hi/science/nature/4862112.stm>|"Light shed on mysterious particle". BBC News. <http://news.bbc.co.uk/2/hi/science/nature/4862112.stm>. Retrieved on 2009-05-29.
- [19] B. Kayser (2005). <http://pdg.lbl.gov/2006/reviews/numixrpp.pdf>|"Neutrino mass, mixing, and flavor change" (PDF). Particle Data Group. <http://pdg.lbl.gov/2006/reviews/numixrpp.pdf>. Retrieved on 2007-11-25.
- [20] Bilenky, S.M.; Giunti, C. (2001). "<http://www.nu.to.infn.it/pap/0102320/>|Lepton Numbers in the framework of Neutrino Mixing". *Int. J. Mod. Phys. A* **16** (3931): 3931. doi: 10.1142/S0217751X01004967 (<http://dx.doi.org/10.1142/S0217751X01004967>). <http://www.nu.to.infn.it/pap/0102320/>. Retrieved on 2007-11-25.
- [21] Bandyopadhyay, A. *et al.* (ISS Physics Working Group) (2007). "Physics at a future Neutrino Factory and super-beam facility". *Preprint*. arXiv:0710.4947
- [22] Bellerive, A (March 2004). "<http://www.worldscinet.com/cgi-bin/details.cgi?id=pii:S0217751X04019093&type=html>|Review of Solar Neutrino Experiments". *International Journal of Modern Physics A* **19** (8): 1167–1179. doi: 10.1142/S0217751X04019093 (<http://dx.doi.org/10.1142/S0217751X04019093>). <http://www.worldscinet.com/cgi-bin/details.cgi?id=pii:S0217751X04019093&type=html>.
- [23] Mann, Alfred K. (<http://www.physics.upenn.edu/facultyinfo/mann.html>) (1997). http://www.whfreeman.com/GeneralReaders/book.asp?disc=TRAD&id_product=1058001008&@id_course=1058000240|Shadow of a star: The neutrino story of Supernova 1987A. New York: W. H. Freeman. pp. 122. ISBN 0716730979. http://www.whfreeman.com/GeneralReaders/book.asp?disc=TRAD&id_product=1058001008&

@id_course=1058000240.

[24] J.N. Bahcall, *Neutrino Astrophysics*, Cambridge, 1989.

[25] Davis, Raymond, Jr. (July 2003). "http://prola.aps.org/abstract/RMP/v75/i3/p985_1|Nobel Lecture: A half-century with solar neutrinos". *Reviews of Modern Physics* **75** (3): 10. doi: 10.1103/RevModPhys.75.985 (<http://dx.doi.org/10.1103/RevModPhys.75.985>). http://prola.aps.org/abstract/RMP/v75/i3/p985_1.

References

- G. A. Tammann, F. K. Thielemann, D. Trautmann (2003). <http://www.europhysicsnews.com/full/20/article8/article8.html>|"Opening new windows in observing the Universe". Europhysics News. <http://www.europhysicsnews.com/full/20/article8/article8.html>. Retrieved on 2006-06-08.
- Bahcall, John N. (1989). *Neutrino Astrophysics*. Cambridge University Press. ISBN 0-521-35113-8.
- Griffiths, David J. (1987). *Introduction to Elementary Particles*. Wiley, John & Sons, Inc. ISBN 0-471-60386-4.
- Perkins, Donald H. (1999). *Introduction to High Energy Physics*. Cambridge University Press. ISBN 0-521-62196-8.
- Povh, Bogdan (1995). *Particles and Nuclei: An Introduction to the Physical Concepts*. Springer-Verlag. ISBN 0-387-59439-6.
- Tipler, Paul; Llewellyn, Ralph (2002). *Modern Physics (4th ed.)*. W. H. Freeman. ISBN 0-7167-4345-0.
- Neutrino Oscillations, Masses And Mixing: W.M.Alberico, Torino University&S.M. Bilenky, Dubna NRI; 2003;<http://arxiv.org/abs/hep-ph/0306239v1>
- Bumfiel, Geoff. "The Milky Way's Hidden Black Hole." Scientific American 01 Oct 2001 1-2. 26 Jan 2009 <<http://www.sciam.com/article.cfm?id=the-milky-ways-hidden-bla>>.

External links

- NEUTRINO UNBOUND (<http://www.nu.to.infn.it>): On-line review and e-archive on Neutrino Physics and Astrophysics
- Nova: The Ghost Particle (<http://www.pbs.org/wgbh/nova/neutrino/>): Documentary on US public television from WGBH
- SNEWS (<http://snews.bnl.gov>): Using neutrino detectors to receive early warning of supernovae
- Measuring the density of the earth's core with neutrinos (<http://www.newscientist.com/channel/fundamentals/mg18524885.900>)
- John Bahcall Website (<http://www.sns.ias.edu/~jnb/>)
- Universe submerged in a sea of chilled neutrinos (http://space.newscientist.com/article/dn13414-universe-submerged-in-a-sea-of-chilled-neutrinos.html?feedId=online-news_rss20), *New Scientist*, 5 March 2008

List of neutrino experiments

This is a list of neutrino experiments, neutrino detectors, and neutrino telescopes.

Abbreviation	Full name	Sensitivity	Type of reaction ^[a]	Type of reaction ^[b]	Detector	Type of detector	Threshold energy	Location	Operation	Home page	
ANTARES	Astronomy with a Neutrino Telescope and Abyss Environmental REsearch							Mediterranean Sea, France	2006–	[1]	
BOREXINO	Neon Experiment	LS	ν_e	$\nu_x + e^- \rightarrow \nu_x + e^-$	ES	LOS shielded by water	Scintillation	250–685 keV	Gran Sasso, Italy	May 2007–	[2] [3]
CLEAN	Cryogenic Low-Energy Astrophysics with Neon	LS, SN, WIMP	ν_e	$\nu_x + e^- \rightarrow \nu_x + e^-$ $\nu_e + {}^{20}\text{Ne} \rightarrow \nu_e + {}^{20}\text{Ne}$	ES ES	Liquid Ne (10 t)	Scintillation		<i>future</i>	[4]	
Daya Bay	Daya Bay Reactor Neutrino Experiment	R	ν_e	$\nu_e + p \rightarrow e^+ + n$	CC	Gd-doped LOS	Scintillation	1.8 MeV	Daya Bay, China	2009–	[5]
Double CHOOZ	Double Chooz Reactor Neutrino Experiment	R	ν_e	$\nu_e + p \rightarrow e^+ + n$	CC	Gd-doped LOS	Scintillation	1.8 MeV	Chooz, France	2008–	[6]
EXO-200	Enriched Xenon Observatory							WIPP, New Mexico	2009–	[7]	

GALLIUM EXperiment	LS	ν_e	$\nu_e + {}^{71}\text{Ga} \rightarrow {}^{71}\text{Ge} + e^-$	CC	GaCl_3 (30 t)	Radiochemical	233.2 keV	Gran Sasso, Italy	1991-1997	[8]
GNO Gallium Neutrino Observatory	LS	ν_e	$\nu_e + {}^{71}\text{Ga} \rightarrow {}^{71}\text{Ge} + e^-$	CC	GaCl_3 (30 t)	Radiochemical	233.2 keV	Gran Sasso, Italy	May 1998-Jan 2002	[9]
HERON Helium Roton Observation of Neutrinos	LS	ν_e (mainly)	$\nu_e + e^- \rightarrow \nu_e + e^-$	NC	Superfluid He	Rotational excitation	1 MeV		future	[10]
HOMESTAKE-CHLORINE Homestake chlorine experiment	S	ν_e	${}^{37}\text{Cl} + \nu_e \rightarrow {}^{37}\text{Ar}^* + e^-$ ${}^{37}\text{Ar}^* \rightarrow {}^{37}\text{Cl} + e^+$ $+ \nu_e$	CC	C_2Cl_4 (615 t)	Radiochemical	814 keV	Homestake Mine, South Dakota	1967-1998	[11]
HOMESTAKE-IODINE Homestake iodine experiment	S	ν_e	$\nu_e + e^- \rightarrow \nu_e + e^-$ $\nu_e + {}^{127}\text{I} \rightarrow {}^{127}\text{Xe} + e^-$	ES CC	NaI in water	Radiochemical	789 keV	Homestake Mine, South Dakota	future	[11]
ICARUS Imaging Cosmic and Rare Underground Signal	S, ATM, GSN	$\nu_e, \nu_{\mu}, \nu_{\tau}$	$\nu_e + e^- \rightarrow \nu_e + e^-$	ES	Liquid Ar	Cherenkov	5.9 MeV	Gran Sasso, Italy		[12]

IceCube	IceCube Neutrino Detector	S, ATM, CR, ?	ν_e, ν_μ, ν_τ	$\nu + e^- \rightarrow \nu + e^-$	ES	Water ice (1 km ³)	Cherenkov	~10 MeV	South Pole, Antarctica	2006-	[13]
Kamioka	Kamioka Nucleon Decay Experiment	S, ATM	ν_e	$\nu + e^- \rightarrow \nu + e^-$	ES	Water (H ₂ O)	Cherenkov	7.5 MeV	Kamioka, Japan	1986-1995	[14]
Kamioka	Kamioka Liquid Scintillator Antineutrino Detector								Kamioka, Japan	2002-	[15]
KM3Net	KM3 Neutrino Telescope								Mediterranean Sea, ?	2009-	[16]
LENs	Low Energy Neutrino Spectroscopy	LS	ν_e	$\nu_e + {}^{115}\text{In} \rightarrow {}^{115}\text{Sn} + \nu_e + 2\gamma$	CC	In-doped LOS	Scintillation	120 keV			[17] [18]
Majorana	Neutrinoless Double Beta Decay in ⁷⁶ Ge to measure neutrino mass								Homestake Mine, South Dakota	future (~2010)	[19]
MOON	Molybdenum Observatory Of Neutrinos	LS, LSN	ν_e	$\nu_e + {}^{100}\text{Mo} \rightarrow {}^{100}\text{Tc} + e^-$	CC	¹⁰⁰ Mo (1 kt) + MoF6 (gas)	Scintillation	168 keV	Washington, USA		[20]
MiniBooNE	Mini Booster Neutrino Experiment	AC	ν_e, ν_μ	$\nu_e + {}^{12}\text{C} \rightarrow e^- + X$	CC	Mineral oil (1 kton)	Cherenkov	~100 keV	Illinois, USA	2002-	[21]
NEMO	Neutrino Telescope Observing								Mediterranean Sea, Italy	2007-	[22]
NOvA	NuMI Off-Axis ν_e Appearance								Illinois and Minnesota, United States	2011-	[23]

OPERA	Oscillation Project with Emulsion-tRacking Apparatus		ν_τ						LNGS (Italy) and CERN	2008-	[24]
SAGE	Soviet-American Gallium Experiment	LS	ν_e	$\nu_e + {}^{71}\text{Ga} \rightarrow {}^{71}\text{Ge} + e^-$	CC	GaCl_3	Radiochemical	233 keV	Baksan Valley, Russia	1990-2006	[25]
SNO	Sudbury Neutrino Observatory	S, ATM, GSN	$\nu_{e'}, \nu_{\mu'}, \nu_\tau$	$\nu_e + {}^2\text{D} \rightarrow 2p + e^-$ $\nu_x + {}^2\text{D} \rightarrow \nu_x + n + p$ $\nu_e + e^- \rightarrow \nu_e + e^-$	CC NC ES	Heavy water (1 kt D_2O)	Cherenkov	3.5 MeV	Creighton Mine, Ontario	1999-2006	[26]
SNO+	SNO with liquid scintillator								Creighton Mine, Ontario	2009-	[26]
SK	Super-Kamiokande	S, ATM, GSN	$\nu_{e'}, \nu_{\mu'}, \nu_\tau$	$\nu_e + e^- \rightarrow \nu_e + e^-$ $\nu_e + n \rightarrow e^- + p$ $\nu_e + p \rightarrow e^+ + n$	ES CC CC	Water (H_2O)	Cherenkov		Kamioka, Japan	1996-	[27] [28]

UNO	Underground Nucleon decay and neutrino Observatory	S, ATM, GSN, RSN	$\nu_e,$ $\nu_{\mu'},$ ν_{τ}	$\nu_e + e^- \rightarrow \nu_e + e^-$	ES	Water (440 kt H ₂ O)	Cherenkov		Henderson Mine, Colorado	<i>future</i>	[29]
-----	---	---------------------------	---	---------------------------------------	----	------------------------------------	-----------	--	--------------------------------	---------------	------

^**[a]** Solar neutrino (S), Low-energy solar neutrino (LS), Reactor neutrino (R), Terrestrial neutrino (T), Atmospheric neutrino (ATM), Accelerator neutrino (AC), Cosmic ray neutrino (CR), Supernova neutrino (SN), Low-energy supernova neutrino (LSN), Active galactic nuclei neutrino (AGN), Pulsar neutrino (PUL)

^**[b]** Elastic scattering (ES), Neutral current (NC), Charged current (CC)

See also

References

- [1] <http://antares.in2p3.fr/index.html>
- [2] <http://www.ge.infn.it/borexino/>
- [3] <http://borex.lngs.infn.it/>
- [4] <http://mckinseygroup.physics.yale.edu/publications/CLEAN.pdf>
- [5] <http://dayawane.ihep.ac.cn/>
- [6] <http://doublechooz.in2p3.fr/>
- [7] <http://www-project.slac.stanford.edu/exo/>
- [8] <http://www.mpi-hd.mpg.de/nuastro/galex.html>
- [9] http://www.lngs.infn.it/lngs_infn/contents/lngs_en/research/experiments_scientific_info/experiments_past/gno/
- [10] http://www.physics.brown.edu/physics/researchpages/cme/heron/LTD_home.html
- [11] <http://www-spires.dur.ac.uk/cgi-bin/spiface/find/experiments/www2?rawcmd=fin+expt+homestake>
- [12] <http://www.aquila.infn.it/icarus/>
- [13] <http://icecube.wisc.edu/>
- [14] <http://www-sk.icrr.u-tokyo.ac.jp/doc/kam/index.html>
- [15] <http://www.awa.tohoku.ac.jp/KamLAND/>
- [16] <http://www.km3net.org/>
- [17] <http://www.phys.vt.edu/~lens/>
- [18] <http://lens.in2p3.fr/>
- [19] <http://majorana.npl.washington.edu/>
- [20] <http://ewi.npl.washington.edu/moon/>
- [21] <http://www-boone.fnal.gov>
- [22] <http://nemoweb.lns.infn.it>
- [23] <http://www-nova.fnal.gov>
- [24] <http://operaweb.web.cern.ch/operaweb/index.shtml>
- [25] <http://ewi.npl.washington.edu/SAGE/sage.html>
- [26] <http://www.sno.phy.queensu.ca/>
- [27] <http://neutrino.phys.washington.edu/~superk/>
- [28] http://www-sk.icrr.u-tokyo.ac.jp/sk/index_e.html
- [29] <http://ale.physics.sunysb.edu/uno/>

List of materials analysis methods

List of materials analysis methods:

Contents Top • 0-9 • A B C D E F G H I J K L M N O P Q R S T U V W X Y Z

- **μSR** - see Muon spin spectroscopy
- **χ** - see Magnetic susceptibility

A

- **Analytical ultracentrifugation** - Analytical ultracentrifugation
- **AAS** - Atomic absorption spectroscopy
- **AED** - Auger electron diffraction
- **AES** - Auger electron spectroscopy
- **AFM** - Atomic force microscopy
- **AFS** - Atomic fluorescence spectroscopy
- **ARPES** - Angle resolved photoemission spectroscopy
- **ARUPS** - Angle resolved ultraviolet photoemission spectroscopy
- **APFIM** - Atom probe field ion microscopy
- **APS** - Appearance potential spectroscopy
- **ATR** - Attenuated total reflectance
- **AXRS** - Anomalous X-ray scattering

B

- **BET** - BET surface area measurement (BET from Brunauer, Emmett, Teller)
- **BKD** - Backscatter Kikuchi diffraction, see **EBSD**
- **BiFC** - Bimolecular fluorescence complementation
- **BRET** - Bioluminescence resonance energy transfer
- **BSED** - Back scattered electron diffraction, see **EBSD**

C

- **CAICISS** - Coaxial impact collision ion scattering spectroscopy
 - **CARS** - Coherent anti-Stokes Raman spectroscopy
 - **CBED** - Convergent beam electron diffraction
 - **CET** - Cryo-electron tomography
 - **CCM** - Charge collection microscopy
 - **CL** - Cathodoluminescence
 - **CLSM** - Confocal laser scanning microscopy
 - **CDI** - Coherent diffraction imaging
 - **COSY** - Correlation spectroscopy
 - **Cryo-EM** - Cryo-electron microscopy
 - **CV** - Cyclic voltammetry
-

D

- **DE(T)A** - Dielectric thermal analysis
- **dHvA** - De Haas-van Alphen effect
- **Dielectric spectroscopy** - Dielectric spectroscopy
- **DIC** - Differential interference contrast microscopy
- **DLS** - Dynamic light scattering
- **DLTS** - Deep-level transient spectroscopy
- **DMA** - Dynamic mechanical analysis
- **DSC** - Differential scanning calorimetry
- **DTA** - Differential thermal analysis
- **DVS** - Dynamic vapour sorption
- **DRS** - Differential reflectance spectroscopy

E

- **EBIC** - Electron beam induced current (and see IBIC: ion beam induced charge)
- **EBS** - Elastic (non-Rutherford) backscattering spectrometry (see RBS)
- **EBSD** - Electron backscatter diffraction
- **ECOSY** - Exclusive correlation spectroscopy
- **ECT** - Electrical capacitance tomography
- **EDAX** - Energy-dispersive analysis of x-rays
- **EDMR** - Electrically detected magnetic resonance, see ESR or EPR
- **EDS** - Energy dispersive spectroscopy
- **EDX** - Energy dispersive X-ray spectroscopy
- **EELS** - Electron energy loss spectroscopy
- **EFTEM** - Energy filtered transmission electron microscopy
- **EID** - Electron induced desorption
- **EIT** and **ERT** - Electrical impedance tomography and Electrical resistivity tomography
- **EL** - Electroluminescence
- **Electron crystallography** - Electron crystallography
- **ELS** - Electrophoretic light scattering
- **ENDOR** - Electron nuclear double resonance, see ESR or EPR
- **EPMA** - Electron probe microanalysis
- **ERD** or **ERDA** - Elastic recoil detection or Elastic recoil detection analysis
- **ESEM** - Environmental scanning electron microscopy
- **ESCA** - Electron spectroscopy for chemical analysis* **see XPS**
- **ESI-MS** or **ES-MS** - Electrospray ionization mass spectrometry or Electrospray mass spectrometry
- **ESTM** - Electrochemical scanning tunneling microscopy
- **EPR** - Electron paramagnetic resonance spectroscopy
- **ESD** - Electron stimulated desorption
- **ESR** - Electron spin resonance spectroscopy
- **EXAFS** - Extended X-ray absorption fine structure
- **EXSY** - Exchange spectroscopy

F

- **FCS** - Fluorescence correlation spectroscopy
- **FCCS** - Fluorescence cross-correlation spectroscopy
- **FEM** - Field emission microscopy
- **FIB** - Focused ion beam microscopy
- **FIM-AP** - Field ion microscopy-atom probe
- **Flow birefringence** - Flow birefringence
- **Fluorescence anisotropy** - Fluorescence anisotropy
- **FLIM** - Fluorescence lifetime imaging
- **Fluorescence microscopy** - Fluorescence microscopy
- **FRET** - Fluorescence resonance energy transfer
- **FRS** - Forward Recoil Spectrometry, a synonym of ERD
- **FTICR** or **FT-MS** - Fourier transform ion cyclotron resonance or Fourier transform mass spectrometry
- **FTIR** - Fourier transform infrared spectroscopy

G

- **GC-MS** - Gas chromatography-mass spectrometry
- **GDMS** - Glow discharge mass spectrometry
- **GDOS** - Glow discharge optical spectroscopy
- **GISAXS** - Grazing incidence small angle X-ray scattering
- **GIXD** - Grazing incidence X-ray diffraction
- **GIXR** - Grazing incidence X-ray reflectivity
- **GLC** - Gas-liquid chromatography

H

- **HAADF** - high angle annular dark-field imaging
- **HAS** - Helium atom scattering
- **HPLC** - High performance liquid chromatography
- **HREELS** - High resolution electron energy loss spectroscopy
- **HREM** - High-resolution electron microscopy
- **HRTEM** - High-resolution transmission electron microscopy

I

- **IAES** - Ion induced Auger electron spectroscopy
 - **IBA** - Ion beam analysis
 - **IBIC** - Ion beam induced charge microscopy
 - **ICP-MS** - Inductively coupled plasma mass spectrometry
 - **Immunofluorescence** - Immunofluorescence
 - **ICR** - Ion cyclotron resonance
 - **IETS** - Inelastic electron tunneling spectroscopy
 - **IGA** - Intelligent gravimetric analysis
 - **IIX** - Ion induced X-ray analysis: See Particle induced X-ray emission
 - **INS** - Ion neutralization spectroscopy
Inelastic neutron scattering
-

- **IRS** - Infrared spectroscopy
- **ISS** - Ion scattering spectroscopy
- **ITC** - Isothermal titration calorimetry
- **IVEM** - Intermediate voltage electron microscopy

L

- List of materials analysis methods (deliberate self-link)
- **LALLS** - Low-angle laser light scattering
- **LC-MS** - Liquid chromatography-mass spectrometry
- **LEED** - Low-energy electron diffraction
- **LEEM** - Low-energy electron microscopy

M

- **MALDI** - Matrix-assisted laser desorption/ionization
- **MBE** - Molecular beam epitaxy
- **MFM** - Magnetic force microscopy
- **MIT** - Magnetic induction tomography
- **MRFM** - Magnetic resonance force microscopy
- **MRI** - Magnetic resonance imaging
- **MS** - Mass spectrometry
- **MS/MS** - Tandem mass spectrometry
- **MEIS** - Medium energy ion scattering
- **Mössbauer spectroscopy** - Mössbauer spectroscopy
- **MTA** - Microthermal analysis

N

- **Nanovid microscopy** - Nanovid microscopy
 - **ND** - Neutron diffraction
 - **NDP** - Neutron depth profiling
 - **NAA** - Neutron activation analysis
 - **NEXAFS** - Near edge X-ray absorption fine structure
 - **NMR** - Nuclear magnetic resonance spectroscopy
 - **NOESY** - Nuclear Overhauser effect spectroscopy
 - **NSOM** - Near-field optical microscopy
 - **NIS** - Nuclear inelastic scattering/absorption
 - **NRA** - Nuclear reaction analysis
-

O

- **OBIC** - Optical beam induced current
- **ODNMR** - Optically detected magnetic resonance, see ESR or EPR
- **OES** - Optical emission spectroscopy
- **Osmometry** - Osmometry

P

- **PAS** - Positron annihilation spectroscopy
- **PAT** or **PACT** - Photoacoustic tomography or photoacoustic computed tomography
- **Photoacoustic spectroscopy** - Photoacoustic spectroscopy
- **PAX** - Photoemission of adsorbed xenon
- **PC** or **PCS** - Photocurrent spectroscopy
- **PD** - Photodesorption
- **PDEIS** - Potentiodynamic electrochemical impedance spectroscopy
- **PDS** - Photothermal deflection spectroscopy
- **PED** - Photoelectron diffraction
- **PEELS** - parallel electron energy-loss spectroscopy
- **PES** - Photoelectron spectroscopy
- **PL** - Photoluminescence
- **Porosimetry** - Porosimetry
- **Phase contrast microscopy** - Phase contrast microscopy
- **PIXE** - Particle (or proton) induced X-ray spectroscopy
- **Powder diffraction** - Powder diffraction
- **PTMS** - Photothermal microspectroscopy
- **PTS** - Photothermal spectroscopy

Q

- **QENS** - Quasi-elastic neutron scattering

R

- **Raman** - Raman spectroscopy
 - **RAXRS** - Resonant anomalous X-ray scattering
 - **RBS** - Rutherford backscattering spectroscopy
 - **REM** - Reflection electron microscopy
 - **RHEED** - Reflection high energy electron diffraction
 - **RIXS** - Resonant inelastic X-ray scattering
 - **RR spectroscopy** - Resonance Raman spectroscopy
-

S

- **SAED** - Selected area electron diffraction
- **SAD** - Selected area diffraction
- **SAM** - Scanning Auger microscopy
- **SANS** - Small angle neutron scattering
- **SAXS** - Small angle X-ray scattering
- **SCANIIR** - Surface composition by analysis of neutral species and ion-impact radiation
- **SCEM** - Scanning confocal electron microscopy
- **SE** - Spectroscopic ellipsometry
- **SEC** - Size exclusion chromatography
- **SEIRA** - Surface enhanced infrared absorption spectroscopy
- **SEM** - Scanning electron microscopy
- **SERS** - Surface enhanced Raman spectroscopy
- **SEXAFS** - Surface extended X-ray absorption fine structure
- **SICM** - Scanning ion-conductance microscopy
- **SIMS** - Secondary ion mass spectrometry
- **SNMS** - Sputtered neutral species mass spectroscopy
- **SNOM** - Scanning near-field optical microscopy
- **SPECT** - Single photon emission computed tomography
- **SPM** - Scanning probe microscopy
- **SRM-CE/MS** - Selected-reaction-monitoring capillary-electrophoresis mass-spectrometry
- **SSNMR** - Solid-state nuclear magnetic resonance
- **Stark spectroscopy** - Stark spectroscopy
- **STEM** - Scanning transmission electron microscopy
- **STM** - Scanning tunneling microscopy
- **STS** - Scanning tunneling spectroscopy
- **SXRD** - Surface X-ray Diffraction (SXRD)

T

- **TEM** - Transmission electron microscopy
 - **TAT** or **TACT** - Thermoacoustic tomography or thermoacoustic computed tomography (see also photoacoustic tomography - PAT)
 - **TEM** - transmission electron microscope/microscopy
 - **TGA** - Thermogravimetric analysis
 - **TIRFM** - Total internal reflection fluorescence microscopy
 - **TMA** - Thermomechanical analysis
 - **TLS** - Photothermal lens spectroscopy, a type of Photothermal spectroscopy
 - **TOF-MS** - Time-of-flight mass spectrometry
 - **TXRF** - Total reflection X-ray fluorescence analysis
 - **Two-photon excitation microscopy** - Two-photon excitation microscopy
-

U

- **Ultrasound attenuation spectroscopy** - Ultrasound attenuation spectroscopy
- **Ultrasonic testing** - Ultrasonic testing
- **UPS** - UV-photoelectron spectroscopy

V

- **VEDIC** - Video-enhanced differential interference contrast microscopy
- **Voltammetry** - Voltammetry

W

- **WAXS** - Wide angle X-ray scattering
- **WDX or WDS** - Wavelength dispersive X-ray spectroscopy

X

- **XAES** - X-ray induced Auger electron spectroscopy
- **XANES** - XANES, synonymous with NEXAFS (Near edge X-ray absorption fine structure)
- **XAS** - X-ray absorption spectroscopy
- **X-CTR** - X-ray crystal truncation rod scattering
- **X-ray crystallography** - X-ray crystallography
- **XDS** - X-ray diffuse scattering
- **XPEEM** - X-ray photoelectron emission microscopy
- **XPS** - X-ray photoelectron spectroscopy
- **XRR** - X-ray reflectivity
- **XRD** - X-ray diffraction
- **XRS** - X-ray Raman scattering
- **XRf** - X-ray fluorescence analysis
- **XSW** - X-ray standing wave technique

References

- Callister, WD (2000). *Materials Science and Engineering - An Introduction*. John Wiley and Sons : London. ISBN 0-471-32013-7.
 - Yao, N, ed (2007). *Focused Ion Beam Systems: Basics and Applications*. Cambridge University Press : Cambridge, UK. ISBN 978-052183-1994.
-

Fourier Transform Spectroscopy and 2D

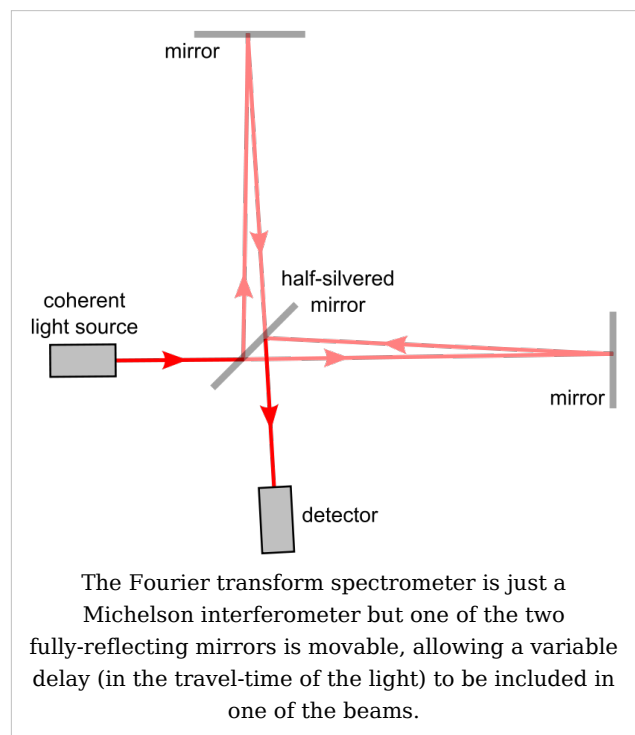
Fourier transform spectroscopy

Fourier transform spectroscopy is a measurement technique whereby spectra are collected based on measurements of the temporal coherence of a radiative source, using time-domain measurements of the electromagnetic radiation or other type of radiation. It can be applied to a variety of types of spectroscopy including optical spectroscopy, infrared spectroscopy (FT IR, FT-NIRS), Fourier transform (FT) nuclear magnetic resonance^[1], mass spectrometry and electron spin resonance spectroscopy. There are several methods for measuring the temporal coherence of the light, including the continuous wave *Michelson* or *Fourier transform* spectrometer and the pulsed Fourier transform spectrograph (which is more sensitive and has a much shorter sampling time than conventional spectroscopic techniques, but is only applicable in a laboratory environment).

Continuous wave *Michelson* or *Fourier transform* spectrograph

The Michelson spectrograph is similar to the instrument used in the Michelson-Morley experiment. Light from the source is split into two beams by a half-silvered mirror, one is reflected off a fixed mirror and one off a moving mirror which introduces a time delay -- the Fourier transform spectrometer is just a Michelson interferometer with a movable mirror. The beams interfere, allowing the temporal coherence of the light to be measured at each different time delay setting, effectively converting the time domain into a spatial coordinate. By making measurements of the signal at many discrete positions of the moving mirror, the spectrum can be reconstructed using a Fourier transform of the temporal coherence of the light. Michelson

spectrographs are capable of very high spectral resolution observations of very bright sources. The Michelson or Fourier transform spectrograph was popular for infra-red applications at a time when infra-red astronomy only had single pixel detectors. Imaging Michelson spectrometers are a possibility, but in general have been supplanted by imaging Fabry-Perot instruments which are easier to construct.



Pulsed *Fourier transform* spectrometer

A pulsed *Fourier transform* spectrometer does not employ transmittance techniques. In the most general description of pulsed FT spectrometry, a sample is exposed to an energizing event which causes a periodic response. The frequency of the periodic response, as governed by the field conditions in the spectrometer, is indicative of the measured properties of the analyte.

Examples of Pulsed *Fourier transform* spectrometry

In magnetic spectroscopy (EPR, NMR), an RF pulse in a strong ambient magnetic field is used as the energizing event. This turns the magnetic particles at an angle to the ambient field, resulting in gyration. The gyrating spins then induce a periodic current in a detector coil. Each spin exhibits a characteristic frequency of gyration (relative to the field strength) which reveals information about the analyte.

In FT-mass spectrometry, the energizing event is the injection of the charged sample into the strong electromagnetic field of a cyclotron. These particles travel in circles, inducing a current in a fixed coil on one point in their circle. Each traveling particle exhibits a characteristic cyclotron frequency-field ratio revealing the masses in the sample.

The Free Induction Decay

Pulsed FT spectrometry gives the advantage of requiring a single, time-dependent measurement which can easily deconvolute a set of similar but distinct signals. The resulting composite signal, is called a *free induction decay*, because typically the signal will decay due to inhomogeneities in sample frequency, or simply unrecoverable loss of signal due to entropic loss of the property being measured.

Fellgett Advantage

One of the most important advantages of Fourier transform spectroscopy was shown by P.B. Fellgett, an early advocate of the method. The Fellgett advantage, also known as the multiplex principle, states that a multiplex spectrometer such as the Fourier transform spectroscopy will produce a gain of the order of the square root of m in the signal-to-noise ratio of the resulting spectrum, when compared with an equivalent scanning monochromator, where m is the number of elements comprising the resulting spectrum when the measurement noise is dominated by detector noise.

Converting spectra from time domain to frequency domain

$$S(t) = \int_{-\infty}^{\infty} I(\nu) e^{-i\nu 2\pi t} d\nu$$

The sum is performed over all contributing frequencies to give a signal $S(t)$ in the time domain.

$$I(\nu) = 2\text{Re} \int_{-\infty}^{\infty} S(t) e^{2i\pi\nu t} dt$$

gives non-zero value when $S(t)$ contains a component that matches the oscillating function. Remember that

$$e^{ix} = \cos x + i \sin x$$

See also

- Applied spectroscopy
- 2D-FT NMRI and Spectroscopy
- Forensic chemistry
- Forensic polymer engineering
- nuclear magnetic resonance
- Infra-red spectroscopy

References and notes

- [1] Antoine Abragam. 1968. *Principles of Nuclear Magnetic Resonance.*, 895 pp., Cambridge University Press: Cambridge, UK.

Further reading

- Ellis, D.I. and Goodacre, R. (2006). "Metabolic fingerprinting in disease diagnosis: biomedical applications of infrared and Raman spectroscopy". *The Analyst* **131**: 875–885. doi: 10.1039/b602376m (<http://dx.doi.org/10.1039/b602376m>).

External links

- Description of how a Fourier transform spectrometer works (<http://scienceworld.wolfram.com/physics/FourierTransformSpectrometer.html>)
 - The Michelson or Fourier transform spectrograph (<http://www.astro.livjm.ac.uk/courses/phys362/notes/>)
 - Internet Journal of Vibrational Spectroscopy - How FTIR works (<http://www.ijvs.com/volume5/edition5/section1.html#Feature>)
 - Fourier Transform Spectroscopy Topical Meeting and Tabletop Exhibit (<http://www.osa.org/meetings/topicalmeetings/fts/default.aspx>)
-

Chemical imaging

Chemical imaging is the simultaneous measurement of spectra (chemical information) and images or pictures (spatial information)^{[1] [2]}. The technique is most often applied to either solid or gel samples, and has applications in chemistry, biology^{[3] [4] [5] [6] [7] [8]}, medicine^{[9] [10]}, pharmacy^[11] (see also for example: Chemical Imaging Without Dyeing^[12]), food science, biotechnology^{[13] [14]}, agriculture and industry (see for example: NIR Chemical Imaging in Pharmaceutical Industry^[15] and Pharmaceutical Process Analytical Technology: ^[16]). NIR, IR and Raman chemical imaging is also referred to as hyperspectral, spectroscopic, spectral or multispectral imaging (also see microspectroscopy). However, other ultra-sensitive and selective, chemical imaging techniques are also in use that involve either UV-visible or fluorescence microspectroscopy. Chemical imaging techniques can be used to analyze samples of all sizes, from the single molecule^{[17] [18]} to the cellular level in biology and medicine^{[19] [20] [21]}, and to images of planetary systems in astronomy, but different instrumentation is employed for making observations on such widely different systems.

Chemical imaging instrumentation is composed of three components: a radiation source to illuminate the sample, a spectrally selective element, and usually a detector array (the camera) to collect the images. When many stacked spectral channels (wavelengths) are collected for different locations of the microspectrometer focus on a line or planar array in the focal plane, the data is called hyperspectral; fewer wavelength data sets are called multispectral. The data format is called a hypercube. The data set may be visualized as a three-dimensional block of data spanning two spatial dimensions (x and y), with a series of wavelengths (λ) making up the third (spectral) axis. The hypercube can be visually and mathematically treated as a series of spectrally resolved images (each image plane corresponding to the image at one wavelength) or a series of spatially resolved spectra. The analyst may choose to view the spectrum measured at a particular spatial location; this is useful for chemical identification. Alternatively, selecting an image plane at a particular wavelength can highlight the spatial distribution of sample components, provided that their spectral signatures are different at the selected wavelength.

Many materials, both manufactured and naturally occurring, derive their functionality from the spatial distribution of sample components. For example, extended release pharmaceutical formulations can be achieved by using a coating that acts as a barrier layer. The release of active ingredient is controlled by the presence of this barrier, and imperfections in the coating, such as discontinuities, may result in altered performance. In the semi-conductor industry, irregularities or contaminants in silicon wafers or printed micro-circuits can lead to failure of these components. The functionality of biological systems is also dependent upon chemical gradients – a single cell, tissue, and even whole organs function because of the very specific arrangement of components. It has been shown that even small changes in chemical composition and distribution may be an early indicator of disease.

Any material that depends on chemical gradients for functionality may be amenable to study by an analytical technique that couples spatial and chemical characterization. To efficiently and effectively design and manufacture such materials, the ‘what’ and the ‘where’ must both be measured. The demand for this type of analysis is increasing as manufactured materials become more complex. Chemical imaging techniques not only

permit visualization of the spatially resolved chemical information that is critical to understanding modern manufactured products, but it is also a non-destructive technique so that samples are preserved for further testing.

History

Commercially available laboratory-based chemical imaging systems emerged in the early 1990s (ref. 1-5). In addition to economic factors, such as the need for sophisticated electronics and extremely high-end computers, a significant barrier to commercialization of infrared imaging was that the focal plane array (FPA) needed to read IR images were not readily available as commercial items. As high-speed electronics and sophisticated computers became more commonplace, and infrared cameras became readily commercially available, laboratory chemical imaging systems were introduced.

Initially used for novel research in specialized laboratories, chemical imaging became a more commonplace analytical technique used for general R&D, quality assurance (QA) and quality control (QC) in less than a decade. The rapid acceptance of the technology in a variety of industries (pharmaceutical, polymers, semiconductors, security, forensics and agriculture) rests in the wealth of information characterizing both chemical composition and morphology. The parallel nature of chemical imaging data makes it possible to analyze multiple samples simultaneously for applications that require high throughput analysis in addition to characterizing a single sample.

Principles

Chemical imaging shares the fundamentals of vibrational spectroscopic techniques, but provides additional information by way of the simultaneous acquisition of spatially resolved spectra. It combines the advantages of digital imaging with the attributes of spectroscopic measurements. Briefly, vibrational spectroscopy measures the interaction of light with matter. Photons that interact with a sample are either absorbed or scattered; photons of specific energy are absorbed, and the pattern of absorption provides information, or a fingerprint, on the molecules that are present in the sample.

On the other hand, in terms of the observation setup, chemical imaging can be carried out in one of the following modes: (optical) absorption, emission (fluorescence), (optical) transmission or scattering (Raman). A consensus currently exists that the fluorescence (emission) and Raman scattering modes are the most sensitive and powerful, but also the most expensive.

In a transmission measurement, the radiation goes through a sample and is measured by a detector placed on the far side of the sample. The energy transferred from the incoming radiation to the molecule(s) can be calculated as the difference between the quantity of photons that were emitted by the source and the quantity that is measured by the detector. In a diffuse reflectance measurement, the same energy difference measurement is made, but the source and detector are located on the same side of the sample, and the photons that are measured have re-emerged from the illuminated side of the sample rather than passed through it. The energy may be measured at one or multiple wavelengths; when a series of measurements are made, the response curve is called a spectrum.

A key element in acquiring spectra is that the radiation must somehow be energy selected – either before or after interacting with the sample. Wavelength selection can be

accomplished with a fixed filter, tunable filter, spectrograph, an interferometer, or other devices. For a fixed filter approach, it is not efficient to collect a significant number of wavelengths, and multispectral data are usually collected. Interferometer-based chemical imaging requires that entire spectral ranges be collected, and therefore results in hyperspectral data. Tunable filters have the flexibility to provide either multi- or hyperspectral data, depending on analytical requirements.

Spectra may be measured one point at a time using a single element detector (single-point mapping), as a line-image using a linear array detector (typically 16 to 28 pixels) (linear array mapping), or as a two-dimensional image using a Focal Plane Array (FPA)(typically 256 to 16,384 pixels) (FPA imaging). For single-point the sample is moved in the x and y directions point-by-point using a computer-controlled stage. With linear array mapping, the sample is moved line-by-line with a computer-controlled stage. FPA imaging data are collected with a two-dimensional FPA detector, hence capturing the full desired field-of-view at one time for each individual wavelength, without having to move the sample. FPA imaging, with its ability to collect tens of thousands of spectra simultaneously is orders of magnitude faster than linear arrays which can typically collect 16 to 28 spectra simultaneously, which are in turn much faster than single-point mapping.

Terminology

Some words common in spectroscopy, optical microscopy and photography have been adapted or their scope modified for their use in chemical imaging. They include: resolution, field of view and magnification. There are two types of resolution in chemical imaging. The spectral resolution refers to the ability to resolve small energy differences; it applies to the spectral axis. The spatial resolution is the minimum distance between two objects that is required for them to be detected as distinct objects. The spatial resolution is influenced by the field of view, a physical measure of the size of the area probed by the analysis. In imaging, the field of view is a product of the magnification and the number of pixels in the detector array. The magnification is a ratio of the physical area of the detector array divided by the area of the sample field of view. Higher magnifications for the same detector image a smaller area of the sample.

Types of vibrational chemical imaging instruments

Chemical imaging has been implemented for mid-infrared, near-infrared spectroscopy and Raman spectroscopy. As with their bulk spectroscopy counterparts, each imaging technique has particular strengths and weaknesses, and are best suited to fulfill different needs.

Mid-infrared chemical imaging

Mid-infrared (MIR) spectroscopy probes fundamental molecular vibrations, which arise in the spectral range 2,500-25,000 nm. Commercial imaging implementations in the MIR region typically employ Fourier Transform Infrared (FT-IR) interferometers and the range is more commonly presented in wavenumber, 4,000 – 400 cm^{-1} . The MIR absorption bands tend to be relatively narrow and well-resolved; direct spectral interpretation is often possible by an experienced spectroscopist. MIR spectroscopy can distinguish subtle changes in chemistry and structure, and is often used for the identification of unknown materials. The absorptions in this spectral range are relatively strong; for this reason, sample presentation is important to limit the amount of material interacting with the

incoming radiation in the MIR region. Most data collected in this range is collected in transmission mode through thin sections (~10 micrometres) of material. Water is a very strong absorber of MIR radiation and wet samples often require advanced sampling procedures (such as attenuated total reflectance). Commercial instruments include point and line mapping, and imaging. All employ an FT-IR interferometer as wavelength selective element and light source.

For types of MIR microscope, see [Microscopy#infrared microscopy](#).

Atmospheric windows in the infrared spectrum are also employed to perform chemical imaging remotely. In these spectral regions the atmospheric gases (mainly water and CO₂) present low absorption and allow infrared viewing over kilometer



Remote chemical imaging of a simultaneous release of SF₆ and NH₃ at 1.5km using the FIRST imaging spectrometer^[22]

distances. Target molecules can then be viewed using the selective absorption/emission processes described above. An example of the chemical imaging of a simultaneous release of SF₆ and NH₃ is shown in the image.

Near-infrared chemical imaging

The analytical near infrared (NIR) region spans the range from approximately 700-2,500 nm. The absorption bands seen in this spectral range arise from overtones and combination bands of O-H, N-H, C-H and S-H stretching and bending vibrations. Absorption is one to two orders of magnitude smaller in the NIR compared to the MIR; this phenomenon eliminates the need for extensive sample preparation. Thick and thin samples can be analyzed without any sample preparation, it is possible to acquire NIR chemical images through some packaging materials, and the technique can be used to examine hydrated samples, within limits. Intact samples can be imaged in transmittance or diffuse reflectance.

The lineshapes for overtone and combination bands tend to be much broader and more overlapped than for the fundamental bands seen in the MIR. Often, multivariate methods are used to separate spectral signatures of sample components. NIR chemical imaging is particularly useful for performing rapid, reproducible and non-destructive analyses of known materials^{[23] [24]}. NIR imaging instruments are typically based on one of two platforms: imaging using a tunable filter and broad band illumination, and line mapping employing an FT-IR interferometer as the wavelength filter and light source.

Raman chemical imaging

The Raman shift chemical imaging spectral range spans from approximately 50 to 4,000 cm⁻¹; the actual spectral range over which a particular Raman measurement is made is a function of the laser excitation frequency. The basic principle behind Raman spectroscopy differs from the MIR and NIR in that the x-axis of the Raman spectrum is measured as a function of energy shift (in cm⁻¹) relative to the frequency of the laser used as the source of radiation. Briefly, the Raman spectrum arises from inelastic scattering of incident photons, which requires a change in polarizability with vibration, as opposed to infrared absorption, which requires a change in dipole moment with vibration. The end result is spectral

information that is similar and in many cases complementary to the MIR. The Raman effect is weak - only about one in 10^7 photons incident to the sample undergoes Raman scattering. Both organic and inorganic materials possess a Raman spectrum; they generally produce sharp bands that are chemically specific. Fluorescence is a competing phenomenon and, depending on the sample, can overwhelm the Raman signal, for both bulk spectroscopy and imaging implementations.

Raman chemical imaging requires little or no sample preparation. However, physical sample sectioning may be used to expose the surface of interest, with care taken to obtain a surface that is as flat as possible. The conditions required for a particular measurement dictate the level of invasiveness of the technique, and samples that are sensitive to high power laser radiation may be damaged during analysis. It is relatively insensitive to the presence of water in the sample and is therefore useful for imaging samples that contain water such as biological material.

Fluorescence imaging (visible and NIR)

This emission microspectroscopy mode is the most sensitive in both visible and FT-NIR microspectroscopy, and has therefore numerous biomedical, biotechnological and agricultural applications. There are several powerful, highly specific and sensitive fluorescence techniques that are currently in use, or still being developed; among the former are FLIM, FRAP, FRET and FLIM-FRET; among the latter are NIR fluorescence and probe-sensitivity enhanced NIR fluorescence microspectroscopy and nanospectroscopy techniques (see "Further reading" section).

Sampling and samples

The value of imaging lies in the ability to resolve spatial heterogeneities in solid-state or gel/gel-like samples. Imaging a liquid or even a suspension has limited use as constant sample motion serves to average spatial information, unless ultra-fast recording techniques are employed as in fluorescence correlation microspectroscopy or FLIM observations where a single molecule may be monitored at extremely high (photon) detection speed. High-throughput experiments (such as imaging multi-well plates) of liquid samples can however provide valuable information. In this case, the parallel acquisition of thousands of spectra can be used to compare differences between samples, rather than the more common implementation of exploring spatial heterogeneity within a single sample.

Similarly, there is no benefit in imaging a truly homogeneous sample, as a single point spectrometer will generate the same spectral information. Of course the definition of homogeneity is dependent on the spatial resolution of the imaging system employed. For MIR imaging, where wavelengths span from 3-10 micrometres, objects on the order of 5 micrometres may theoretically be resolved. The sampled areas are limited by current experimental implementations because illumination is provided by the interferometer. Raman imaging may be able to resolve particles less than 1 micrometre in size, but the sample area that can be illuminated is severely limited. With Raman imaging, it is considered impractical to image large areas and, consequently, large samples. FT-NIR chemical/hyperspectral imaging usually resolves only larger objects (>10 micrometres), and is better suited for large samples because illumination sources are readily available. However, FT-NIR microspectroscopy was recently reported to be capable of about 1.2 micron (micrometer) resolution in biological samples^[25] Furthermore, two-photon

excitation FCS experiments were reported to have attained 15 nanometer resolution on biomembrane thin films with a special coincidence photon-counting setup.

Detection limit

The concept of the detection limit for chemical imaging is quite different than for bulk spectroscopy, as it depends on the sample itself. Because a bulk spectrum represents an average of the materials present, the spectral signatures of trace components are simply overwhelmed by dilution. In imaging however, each pixel has a corresponding spectrum. If the physical size of the trace contaminant is on the order of the pixel size imaged on the sample, its spectral signature will likely be detectable. If however, the trace component is dispersed homogeneously (relative to pixel image size) throughout a sample, it will not be detectable. Therefore, detection limits of chemical imaging techniques are strongly influenced by particle size, the chemical and spatial heterogeneity of the sample, and the spatial resolution of the image.

Data analysis

Data analysis methods for chemical imaging data sets typically employ mathematical algorithms common to single point spectroscopy or to image analysis. The reasoning is that the spectrum acquired by each detector is equivalent to a single point spectrum; therefore pre-processing, chemometrics and pattern recognition techniques are utilized with the similar goal to separate chemical and physical effects and perform a qualitative or quantitative characterization of individual sample components. In the spatial dimension, each chemical image is equivalent to a digital image and standard image analysis and robust statistical analysis can be used for feature extraction.

See also

- Multispectral image
- Microspectroscopy
- Imaging spectroscopy

References

- [1] [http://www.imaging.net/chemical-imaging/Chemical imaging](http://www.imaging.net/chemical-imaging/Chemical%20imaging)
- [2] http://www.malvern.com/LabEng/products/sdi/bibliography/sdi_bibliography.htm E. N. Lewis, E. Lee and L. H. Kidder, Combining Imaging and Spectroscopy: Solving Problems with Near-Infrared Chemical Imaging. *Microscopy Today*, Volume 12, No. 6, 11/2004.
- [3] C.L. Evans and X.S. Xie.2008. Coherent Anti-Stokes Raman Scattering Microscopy: Chemical Imaging for Biology and Medicine., doi:10.1146/annurev.anchem.1.031207.112754 *Annual Review of Analytical Chemistry*, **1**: 883-909.
- [4] Diaspro, A., and Robello, M. (1999). Multi-photon Excitation Microscopy to Study Biosystems. *European Microscopy and Analysis.*, 5:5-7.
- [5] D.S. Mantus and G. H. Morrison. 1991. Chemical imaging in biology and medicine using ion microscopy., *Microchimica Acta*, **104**, (1-6) January 1991, doi: 10.1007/BF01245536
- [6] Bagatolli, L.A., and Gratton, E. (2000). Two-photon fluorescence microscopy of coexisting lipid domains in giant unilamellar vesicles of binary phospholipid mixtures. *Biophys J.*, 78:290-305.
- [7] Schwille, P., Haupts, U., Maiti, S., and Webb. W.(1999). Molecular dynamics in living cells observed by fluorescence correlation spectroscopy with one- and two-photon excitation. *Biophysical Journal*, 77(10):2251-2265.
- [8] 1.Lee, S. C. et al., (2001). One Micrometer Resolution NMR Microscopy. *J. Magn. Res.*, 150: 207-213.

- [9] Near Infrared Microspectroscopy, Fluorescence Microspectroscopy, Infrared Chemical Imaging and High Resolution Nuclear Magnetic Resonance Analysis of Soybean Seeds, Somatic Embryos and Single Cells., Baianu, I.C. et al. 2004., In *Oil Extraction and Analysis.*, D. Luthria, Editor pp.241-273, AOCS Press., Champaign, IL.
- [10] Single Cancer Cell Detection by Near Infrared Microspectroscopy, Infrared Chemical Imaging and Fluorescence Microspectroscopy. 2004. I. C. Baianu, D. Costescu, N. E. Hofmann and S. S. Korban, q-bio/0407006 (July 2004) (<http://arxiv.org/abs/q-bio/0407006>)
- [11] J. Dubois, G. Sando, E. N. Lewis, Near-Infrared Chemical Imaging, A Valuable Tool for the Pharmaceutical Industry, G.I.T. Laboratory Journal Europe, No. 1-2, 2007.
- [12] <http://witec.de/en/download/Raman/ImagingMicroscopy04.pdf>
- [13] Raghavachari, R., Editor. 2001. *Near-Infrared Applications in Biotechnology*, Marcel-Dekker, New York, NY.
- [14] Applications of Novel Techniques to Health Foods, Medical and Agricultural Biotechnology. (June 2004) I. C. Baianu, P. R. Lozano, V. I. Prisecaru and H. C. Lin q-bio/0406047 (<http://arxiv.org/abs/q-bio/0406047>)
- [15] http://www.spectroscopyeurope.com/NIR_14_3.pdf
- [16] <http://www.fda.gov/cder/OPS/PAT.htm>
- [17] Eigen, M., and Rigler, R. (1994). Sorting single molecules: Applications to diagnostics and evolutionary biotechnology, *Proc. Natl. Acad. Sci. USA* 91:5740.
- [18] Rigler R. and Widengren J. (1990). Ultrasensitive detection of single molecules by fluorescence correlation spectroscopy, *BioScience* (Ed. Klinge & Owman) p.180.
- [19] Single Cancer Cell Detection by Near Infrared Microspectroscopy, Infrared Chemical Imaging and Fluorescence Microspectroscopy. 2004. I. C. Baianu, D. Costescu, N. E. Hofmann, S. S. Korban and et al., q-bio/0407006 (July 2004) (<http://arxiv.org/abs/q-bio/0407006>)
- [20] Oehlschläger F., Schwille P. and Eigen M. (1996). Detection of HIV-1 RNA by nucleic acid sequence-based amplification combined with fluorescence correlation spectroscopy, *Proc. Natl. Acad. Sci. USA* 93:1281.
- [21] Near Infrared Microspectroscopy, Fluorescence Microspectroscopy, Infrared Chemical Imaging and High Resolution Nuclear Magnetic Resonance Analysis of Soybean Seeds, Somatic Embryos and Single Cells., Baianu, I.C. et al. 2004., In *Oil Extraction and Analysis.*, D. Luthria, Editor pp.241-273, AOCS Press., Champaign, IL.
- [22] M. Chamberland, V. Farley, A. Vallières, L. Belhumeur, A. Villemaire, J. Giroux et J. Legault, High-Performance Field-Portable Imaging Radiometric Spectrometer Technology For Hyperspectral imaging Applications, *Proc. SPIE* 5994, 59940N, September 2005.
- [23] Novel Techniques for Microspectroscopy and Chemical Imaging Analysis of Soybean Seeds and Embryos. (2002). Baianu, I.C., Costescu, D.M., and You, T. *Soy2002 Conference*, Urbana, Illinois.
- [24] Near Infrared Microspectroscopy, Chemical Imaging and NMR Analysis of Oil in Developing and Mutagenized Soybean Embryos in Culture. (2003). Baianu, I.C., Costescu, D.M., Hofmann, N., and Korban, S.S. *AOCS Meeting, Analytical Division*.
- [25] Near Infrared Microspectroscopy, Fluorescence Microspectroscopy, Infrared Chemical Imaging and High Resolution Nuclear Magnetic Resonance Analysis of Soybean Seeds, Somatic Embryos and Single Cells., Baianu, I.C. et al. 2004., In *Oil Extraction and Analysis.*, D. Luthria, Editor pp.241-273, AOCS Press., Champaign, IL.

Further reading

1. E. N. Lewis, P. J. Treado, I. W. Levin, Near-Infrared and Raman Spectroscopic Imaging, *American Laboratory*, 06/1994:16 (1994)
2. E. N. Lewis, P. J. Treado, R. C. Reeder, G. M. Story, A. E. Dowrey, C. Marcott, I. W. Levin, FTIR spectroscopic imaging using an infrared focal-plane array detector, *Analytical Chemistry*, 67:3377 (1995)
3. P. Colarusso, L. H. Kidder, I. W. Levin, J. C. Fraser, E. N. Lewis Infrared Spectroscopic Imaging: from Planetary to Cellular Systems, *Applied Spectroscopy*, 52 (3):106A (1998)
4. P. J. Treado I. W. Levin, E. N. Lewis, Near-Infrared Spectroscopic Imaging Microscopy of Biological Materials Using an Infrared Focal-Plane Array and an Acousto-Optic Tunable Filter (AOTF), *Applied Spectroscopy*, 48:5 (1994)
5. Hammond, S.V., Clarke, F. C., Near-infrared microspectroscopy. In: *Handbook of Vibrational Spectroscopy*, Vol. 2, J.M. Chalmers and P.R. Griffiths Eds. John Wiley and Sons, West Sussex, UK, 2002, p.1405-1418

6. L.H. Kidder, A.S. Haka, E.N. Lewis, Instrumentation for FT-IR Imaging. In: Handbook of Vibrational Spectroscopy, Vol. 2, J.M. Chalmers and P.R. Griffiths Eds. John Wiley and Sons, West Sussex, UK, 2002, pp.1386-1404
 7. J. Zhang; A. O'Connor; J. F. Turner II, Cosine Histogram Analysis for Spectral Image Data Classification, Applied Spectroscopy, Volume 58, Number 11, November 2004, pp. 1318-1324(7)
 8. J. F. Turner II; J. Zhang; A. O'Connor, A Spectral Identity Mapper for Chemical Image Analysis, Applied Spectroscopy, Volume 58, Number 11, November 2004, pp. 1308-1317(10)
 9. H. R. MORRIS, J. F. TURNER II, B. MUNRO, R. A. RYNTZ, P. J. TREADO, Chemical imaging of thermoplastic olefin (TPO) surface architecture, Langmuir, 1999, vol. 15, no8, pp. 2961-2972
 10. J. F. Turner II, Chemical imaging and spectroscopy using tunable filters: Instrumentation, methodology, and multivariate analysis, Thesis (PhD). UNIVERSITY OF PITTSBURGH, Source DAI-B 59/09, p. 4782, Mar 1999, 286 pages.
 11. P. Schwille.(2001). in *Fluorescence Correlation Spectroscopy. Theory and applications*. R. Rigler & E.S. Elson, eds., p. 360. Springer Verlag: Berlin.
 12. Schwille P., Oehlenschläger F. and Walter N. (1996). Analysis of RNA-DNA hybridization kinetics by fluorescence correlation spectroscopy, *Biochemistry* **35**:10182.
 13. FLIM | Fluorescence Lifetime Imaging Microscopy: Fluorescence, fluorophore chemical imaging, confocal emission microspectroscopy, FRET, cross-correlation fluorescence microspectroscopy (<http://www.nikoninstruments.com/infocenter.php?n=FLIM>).
 14. FLIM Applications: (<http://www.nikoninstruments.com/infocenter.php?n=FLIM>)
"FLIM is able to discriminate between fluorescence emanating from different fluorophores and autofluorescing molecules in a specimen, even if their emission spectra are similar. It is, therefore, ideal for identifying fluorophores in multi-label studies. FLIM can also be used to measure intracellular ion concentrations without extensive calibration procedures (for example, Calcium Green) and to obtain information about the local environment of a fluorophore based on changes in its lifetime." FLIM is also often used in microspectroscopic/chemical imaging, or microscopic, studies to monitor spatial and temporal protein-protein interactions, properties of membranes and interactions with nucleic acids in living cells.
 15. Gadella TW Jr., *FRET and FLIM techniques*, 33. Imprint: Elsevier, ISBN 978-0-08-054958-3. (2008) 560 pages
 16. Langel FD, et al., Multiple protein domains mediate interaction between Bcl10 and Malt1, *J. Biol. Chem.*, (2008) 283(47):32419-31
 17. Clayton AH. , The polarized AB plot for the frequency-domain analysis and representation of fluorophore rotation and resonance energy homotransfer. *J Microscopy*. (2008) 232(2):306-12
 18. Clayton AH, et al., Predominance of activated EGFR higher-order oligomers on the cell surface. *Growth Factors* (2008) 20:1
 19. Plowman et al., Electrostatic Interactions Positively Regulate K-Ras Nanocluster Formation and Function. *Molecular and Cellular Biology* (2008) 4377-4385
 20. Belanis L, et al., Galectin-1 Is a Novel Structural Component and a Major Regulator of H-Ras Nanoclusters. *Molecular Biology of the Cell* (2008) 19:1404-1414
 21. Van Manen HJ, Refractive index sensing of green fluorescent proteins in living cells using fluorescence lifetime imaging microscopy. *Biophys J*. (2008) 94(8):L67-9
-

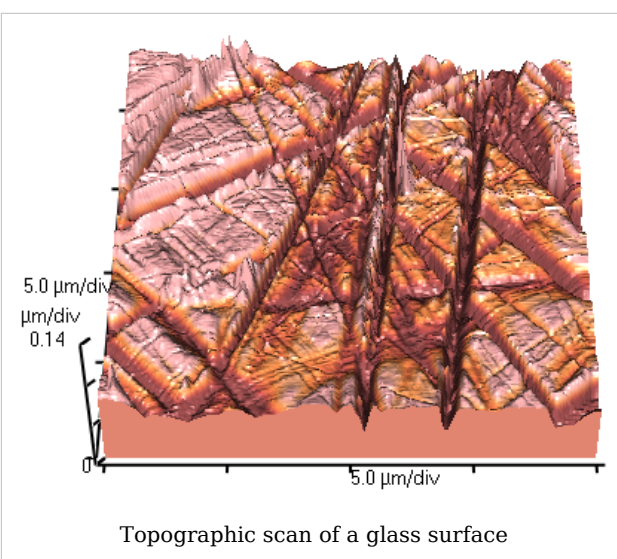
22. Van der Krogt GNM, et al., A Comparison of Donor-Acceptor Pairs for Genetically Encoded FRET Sensors: Application to the Epac cAMP Sensor as an Example, PLoS ONE, (2008) 3(4):e1916
23. Dai X, et al., Fluorescence intensity and lifetime imaging of free and micellar-encapsulated doxorubicin in living cells. *Nanomedicine*. (2008) 4(1):49-56.

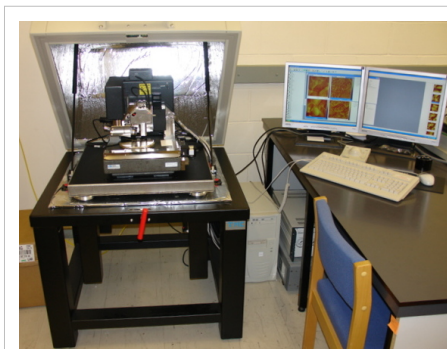
External links

- NIR Chemical Imaging in Pharmaceutical Industry (http://www.spectroscopyeurope.com/NIR_14_3.pdf)
- Pharmaceutical Process Analytical Technology: (<http://www.fda.gov/cder/OPS/PAT.htm>)
- NIR Chemical Imaging for Counterfeit Pharmaceutical Product Analysis (<http://www.spectroscopymag.com/spectroscopy/Near-IR+Spectroscopy/NIR-Chemical-Imaging-for-Counterfeit-Pharmaceutica/ArticleStandard/Article/detail/406629>)
- Chemical Imaging: Potential New Crime Busting Tool (<http://www.sciencedaily.com/releases/2007/08/070802103435.htm>)
- Chemical Imaging Without Dyeing (<http://witec.de/en/download/Raman/ImagingMicroscopy04.pdf>) - Chemical Imaging Without Dyeing

Atomic force microscope

The **atomic force microscope** (AFM) or scanning force microscope (SFM) is a very high-resolution type of scanning probe microscopy, with demonstrated resolution of fractions of a nanometer, more than 1000 times better than the optical diffraction limit. The precursor to the AFM, the scanning tunneling microscope, was developed by Gerd Binnig and Heinrich Rohrer in the early 1980s, a development that earned them the Nobel Prize for Physics in 1986. Binnig, Quate and Gerber invented the first AFM in 1986. The AFM is one of the foremost tools for imaging, measuring and manipulating matter at the nanoscale. The information is gathered by "feeling" the surface with a mechanical probe. Piezoelectric elements that facilitate tiny but accurate and precise movements on (electronic) command enable the very precise scanning.





Microscope AFM

Basic principle

Part of a series of articles on

Nanotechnology

History

Implications

Applications

Regulation

Organizations

Popular culture

List of topics

Nanomaterials

Fullerene

Carbon Nanotubes

Nanoparticles

Nanomedicine

Nanotoxicology

Nanosensor

Molecular self-assembly

Self-assembled monolayer

Supramolecular assembly

DNA nanotechnology

Nanoelectronics

Molecular electronics

Nanolithography

Scanning probe microscopy

Atomic force microscope

Scanning tunneling microscope

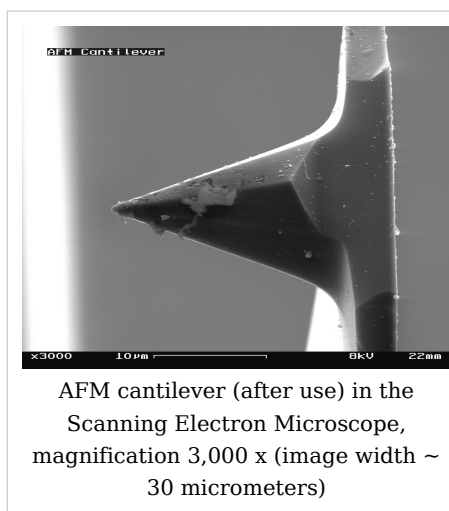
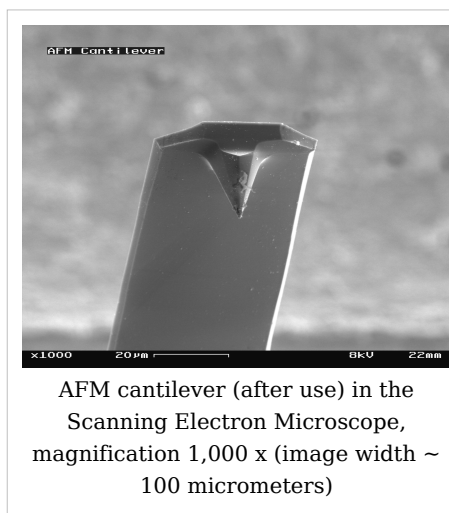
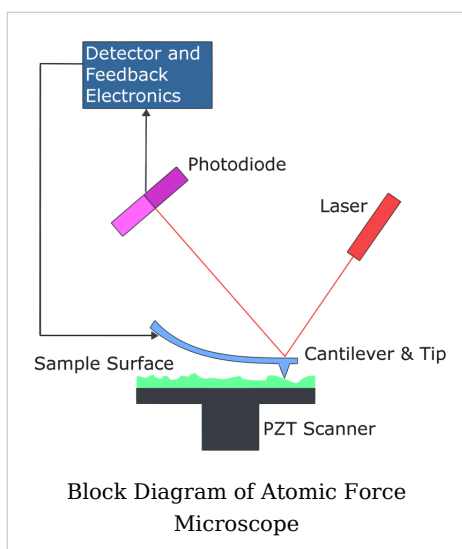
Molecular nanotechnology

Molecular assembler

Nanorobotics

Mechanosynthesis

Nanotechnology Portal



The AFM consists of a microscale cantilever with a sharp tip (probe) at its end that is used to scan the specimen surface. The cantilever is typically silicon or silicon nitride with a tip radius of curvature on the order of nanometers. When the tip is brought into proximity of a sample surface, forces between the tip and the sample lead to a deflection of the cantilever according to Hooke's law. Depending on the situation, forces that are measured in AFM include mechanical contact force, Van der Waals forces, capillary forces, chemical bonding, electrostatic forces, magnetic forces (see Magnetic force microscope (MFM)), Casimir forces, solvation forces etc. As well as force, additional quantities may simultaneously be measured through the use of specialised types of probe (see Scanning thermal microscopy, photothermal microspectroscopy, etc.). Typically, the deflection is measured using a laser spot reflected from the top surface of the cantilever into an array of photodiodes. Other methods that are used include optical interferometry, capacitive sensing or piezoresistive AFM cantilevers. These cantilevers are fabricated with piezoresistive elements that act as a strain gauge. Using a Wheatstone bridge, strain in the AFM cantilever due to deflection can be measured, but this method is not as sensitive as laser deflection or interferometry.

If the tip was scanned at a constant height, a risk would exist that the tip collides with the surface, causing damage. Hence, in most cases a feedback mechanism is employed to adjust the tip-to-sample distance to maintain a constant force between the tip and the sample. Traditionally, the sample is mounted on a piezoelectric tube, that can move the sample in the z direction for maintaining a constant force, and the x and y directions for scanning the sample. Alternatively a 'tripod' configuration of three piezo crystals may be employed, with each responsible for scanning in the x, y and z directions. This eliminates some of the distortion effects seen with a tube scanner. In newer designs, the tip is mounted on a vertical piezo scanner while the sample is being scanned in X and Y using another piezo block. The resulting map of the area $s = f(x, y)$

represents the topography of the sample.

The AFM can be operated in a number of modes, depending on the application. In general, possible imaging modes are divided into static (also called Contact) modes and a variety of dynamic (or non-contact) modes where the cantilever is vibrated.

Imaging modes

The primary modes of operation are static (contact) mode and dynamic mode. In the static mode operation, the static tip deflection is used as a feedback signal. Because the measurement of a static signal is prone to noise and drift, low stiffness cantilevers are used to boost the deflection signal. However, close to the surface of the sample, attractive forces can be quite strong, causing the tip to 'snap-in' to the surface. Thus static mode AFM is almost always done in contact where the overall force is repulsive. Consequently, this technique is typically called 'contact mode'. In contact mode, the force between the tip and the surface is kept constant during scanning by maintaining a constant deflection.

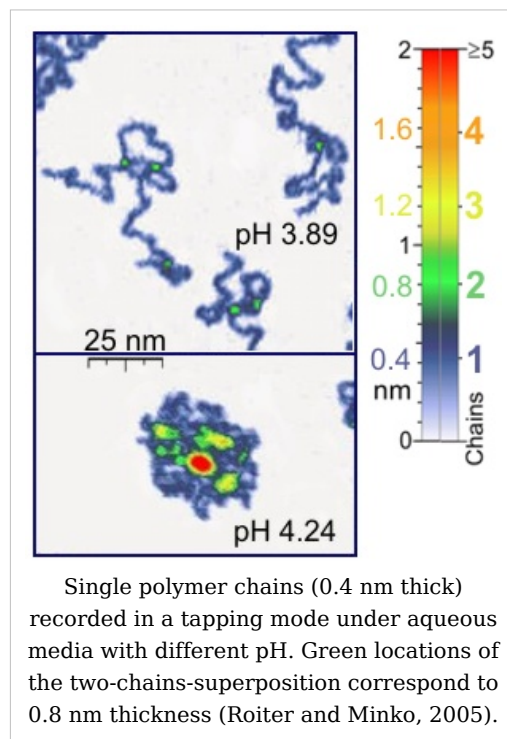
In the dynamic mode, the cantilever is externally oscillated at or close to its fundamental resonance frequency or a harmonic. The oscillation amplitude, phase and resonance frequency are modified by tip-sample interaction forces; these changes in oscillation with respect to the external reference oscillation provide information about the sample's characteristics. Schemes for dynamic mode operation include frequency modulation and the more common amplitude modulation. In frequency modulation, changes in the oscillation frequency provide information about tip-sample interactions. Frequency can be measured with very high sensitivity and thus the frequency modulation mode allows for the use of very stiff cantilevers. Stiff cantilevers provide stability very close to the surface and, as a result, this technique was the first AFM technique to provide true atomic resolution in ultra-high vacuum conditions (Giessibl).

In amplitude modulation, changes in the oscillation amplitude or phase provide the feedback signal for imaging. In amplitude modulation, changes in the phase of oscillation can be used to discriminate between different types of materials on the surface. Amplitude modulation can be operated either in the non-contact or in the intermittent contact regime. In ambient conditions, most samples develop a liquid meniscus layer. Because of this, keeping the probe tip close enough to the sample for short-range forces to become detectable while preventing the tip from sticking to the surface presents a major hurdle for the non-contact dynamic mode in ambient conditions. Dynamic contact mode (also called intermittent contact or tapping mode) was developed to bypass this problem (Zhong et al.). In dynamic contact mode, the cantilever is oscillated such that the separation distance between the cantilever tip and the sample surface is modulated.

Amplitude modulation has also been used in the non-contact regime to image with atomic resolution by using very stiff cantilevers and small amplitudes in an ultra-high vacuum environment.

Tapping Mode

In *tapping mode* the cantilever is driven to oscillate up and down at near its resonance frequency by a small piezoelectric element mounted in the AFM tip holder. The amplitude of this oscillation is greater than 10 nm, typically 100 to 200 nm. Due to the interaction of forces acting on the cantilever when the tip comes close to the surface, Van der Waals force or dipole-dipole interaction, electrostatic forces, etc cause the amplitude of this oscillation to decrease as the tip gets closer to the sample. An electronic servo uses the piezoelectric actuator to control the height of the cantilever above the sample. The servo adjusts the height to maintain a set cantilever oscillation amplitude as the cantilever is scanned over the sample. A *Tapping AFM* image is therefore produced by imaging the force of the oscillating contacts of the tip with the sample surface. This is an improvement on conventional contact AFM, in which the cantilever just drags across the surface at constant force and can result in surface damage. Tapping mode is gentle enough even for the visualization of supported lipid bilayers or adsorbed single polymer molecules (for instance, 0.4 nm thick chains of synthetic polyelectrolytes) under liquid medium. At the application of proper scanning parameters, the conformation of single molecules remains unchanged for hours (Roiter and Minko, 2005).



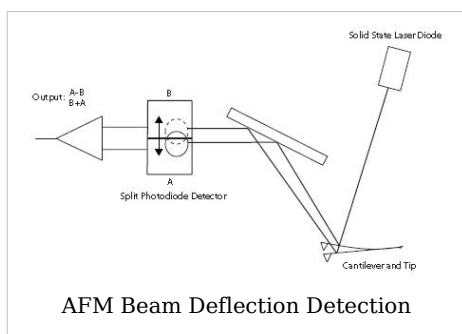
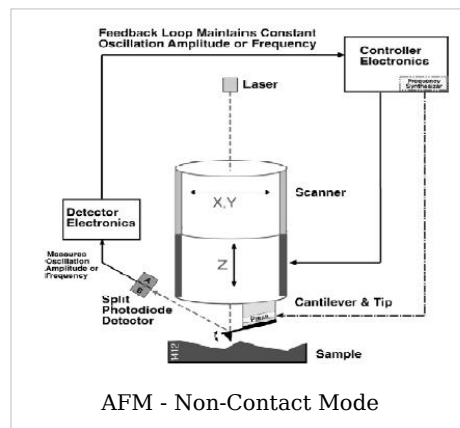
Non-Contact Mode

Here the tip of the cantilever does not contact the sample surface. The cantilever is instead oscillated at a frequency slightly above its resonance frequency where the amplitude of oscillation is typically a few nanometers (<10nm). The van der Waals forces, which are strongest from 1nm to 10nm above the surface, or any other long range force which extends above the surface acts to decrease the resonance frequency of the cantilever. This decrease in resonance frequency combined with the feedback loop system maintains a constant oscillation amplitude or frequency by adjusting the average tip-to-sample distance. Measuring the tip-to-sample distance at each (x,y) data point allows the scanning software to construct a topographic image of the sample surface.

Non-contact mode AFM does not suffer from tip or sample degradation effects that are sometimes observed after taking numerous scans with contact AFM. This makes non-contact AFM preferable to contact AFM for measuring soft samples. In the case of rigid samples, contact and non-contact images may look the same. However, if a few monolayers of adsorbed fluid are lying on the surface of a rigid sample, the images may look quite different. An AFM operating in contact mode will penetrate the liquid layer to image the underlying surface, whereas in non-contact mode an AFM will oscillates above the adsorbed fluid layer to image both the liquid and surface.

AFM -Beam Deflection Detection

Laser light from a solid state diode is reflected off the back of the cantilever and collected by a position sensitive detector (PSD) consisting of two closely spaced photodiodes whose output signal is collected by a differential amplifier. Angular displacement of cantilever results in one photodiode collecting more light than the other photodiode, producing an output signal (the difference between the photodiode signals normalized by their sum) which is proportional to the deflection of the cantilever. It detects cantilever deflections $<1\text{\AA}$ (thermal noise limited). A long beam path (several cm) amplifies changes in beam angle.



Force spectroscopy

Another major application of AFM (besides imaging) is force spectroscopy, the measurement of force-distance curves. For this method, the AFM tip is extended towards and retracted from the surface as the static deflection of the cantilever is monitored as a function of piezoelectric displacement. These measurements have been used to measure nanoscale contacts, atomic bonding, Van der Waals forces, and Casimir forces, dissolution forces in liquids and single molecule stretching and rupture forces (Hinterdorfer & Dufrêne). Forces of the order of a few pico-Newton can now be routinely measured with a vertical distance resolution of better than 0.1 nanometer.

Problems with the technique include no direct measurement of the tip-sample separation and the common need for low stiffness cantilevers which tend to 'snap' to the surface. The snap-in can be reduced by measuring in liquids or by using stiffer cantilevers, but in the latter case a more sensitive deflection sensor is needed. By applying a small dither to the tip, the stiffness (force gradient) of the bond can be measured as well (Hoffmann et al.).

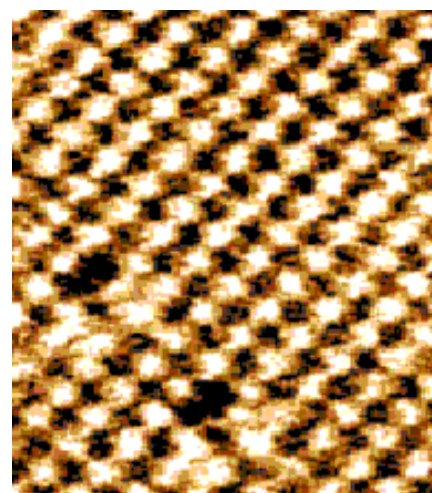
Identification of individual surface atoms

The AFM can be used to image and manipulate atoms and structures on a variety of surfaces. The atom at the apex of the tip "senses" individual atoms on the underlying surface when it forms incipient chemical bonds with each atom. Because these chemical interactions subtly alter the tip's vibration frequency, they can be detected and mapped.

Physicist Oscar Custance (Osaka University, Graduate School of Engineering, Osaka, Japan) and his team used this principle to distinguish between atoms of silicon, tin and lead on an alloy surface (*Nature* 2007, 446, 64).

The trick is to first measure these forces precisely for each type of atom expected in the sample. The team found that the tip interacted most strongly with silicon atoms, and interacted 23% and 41% less strongly with tin and lead atoms, respectively. Thus, each different type of atom can be identified in the matrix as the tip is moved across the surface.

Such a technique has been used now in biology and extended recently to cell biology. Forces corresponding to (i) the unbinding of receptor ligand couples (ii) unfolding of proteins (iii) cell adhesion at single cell scale have been gathered.

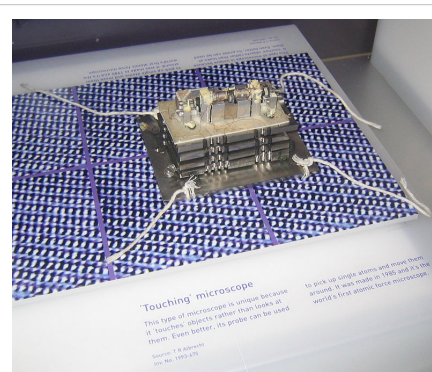


The atoms of a Sodium Chloride crystal viewed with an Atomic Force Microscope

Advantages and disadvantages

The AFM has several advantages over the scanning electron microscope (SEM). Unlike the electron microscope which provides a two-dimensional projection or a two-dimensional image of a sample, the AFM provides a true three-dimensional surface profile. Additionally, samples viewed by AFM do not require any special treatments (such as metal/carbon coatings) that would irreversibly change or damage the sample. While an electron microscope needs an expensive vacuum environment for proper operation, most AFM modes can work perfectly well in ambient air or even a liquid environment. This makes it possible to study biological macromolecules and even living organisms. In principle, AFM can provide higher resolution than SEM. It has been shown to give true atomic resolution in ultra-high vacuum (UHV) and, more recently, in liquid environments. High resolution AFM is comparable in resolution to Scanning Tunneling Microscopy and Transmission Electron Microscopy.

A disadvantage of AFM compared with the scanning electron microscope (SEM) is the image size. The SEM can image an area on the order of millimetres by millimetres with a depth of field on the order of millimetres. The AFM can only image a maximum height on the order of micrometres and a maximum scanning area of around 150 by 150 micrometres.



The first Atomic Force Microscope

Another inconvenience is that an incorrect choice of tip for the required resolution can lead to image artifacts. Traditionally the AFM could not scan images as fast as an SEM, requiring several minutes for a typical scan, while a SEM is capable of scanning at near real-time (although at relatively low quality) after the chamber is evacuated. The relatively slow rate of scanning during AFM imaging often leads to thermal drift in the image (Lapshin, 2004, 2007), making the AFM microscope less suited for measuring accurate distances between artifacts on the image. However, several fast-acting designs were suggested to increase microscope scanning productivity (Lapshin and Obyedkov, 1993) including what is being termed videoAFM (reasonable quality images are being obtained with videoAFM at video rate - faster than the average SEM). To eliminate image distortions induced by thermodrift, several methods were also proposed (Lapshin, 2004, 2007).

AFM images can also be affected by hysteresis of the piezoelectric material (Lapshin, 1995) and cross-talk between the (x,y,z) axes that may require software enhancement and filtering. Such filtering could "flatten" out real topographical features. However, newer AFM use real-time correction software (for example, feature-oriented scanning, Lapshin, 2004, 2007) or closed-loop scanners which practically eliminate these problems. Some AFM also use separated orthogonal scanners (as opposed to a single tube) which also serve to eliminate cross-talk problems.

Due to the nature of AFM probes, they cannot normally measure steep walls or overhangs. Specially made cantilevers can be modulated sideways as well as up and down (as with dynamic contact and non-contact modes) to measure sidewalls, at the cost of more expensive cantilevers and additional artifacts.

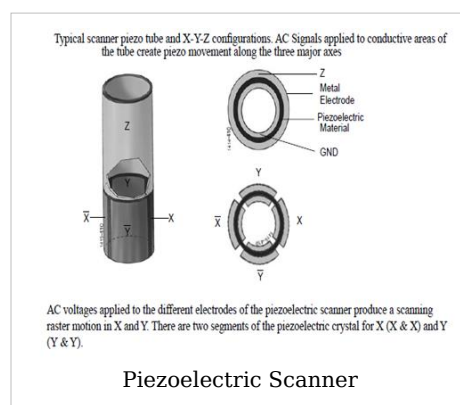
Piezoelectric Scanners

AFM scanners are made from piezoelectric material, which expands and contracts proportionally to an applied voltage. Whether they elongate or contract depends upon the polarity of the voltage applied. The scanner is constructed by combining independently operated piezo electrodes for X, Y, & Z into a single tube, forming a scanner which can manipulate samples and probes with extreme precision in 3 dimensions.

Scanners are characterized by their sensitivity which is the ratio of piezo movement to piezo voltage, i.e. by how much the piezo material extends or contracts per applied volt. Because of differences in material or size, the sensitivity varies from scanner to scanner.

Sensitivity varies non-linearly with respect to scan size. Piezo scanners exhibit more sensitivity at the end than at the beginning of a scan. This causes the forward and reverse scans to behave differently and display hysteresis between the two scan directions. This can be corrected by applying a non-linear voltage to the piezo electrodes to cause linear scanner movement and calibrating the scanner accordingly.

The sensitivity of piezoelectric materials decreases exponentially with time. This causes most of the change in sensitivity to occur in the initial stages of the scanner's life. Piezoelectric scanners are run for approximately 48 hours before they are shipped from the factory so that they are past the point where we can expect large changes in sensitivity. As the scanner ages, the sensitivity will change less with time and the scanner would seldom



require recalibration.

See also

- Interfacial force microscope
- Friction force microscope
- Scanning tunneling microscope
- Scanning probe microscopy
- Scanning voltage microscopy

References

- A. D L. Humphris, M. J. Miles, J. K. Hobbs, A mechanical microscope: High-speed atomic force microscopy ^[1], *Applied Physics Letters* 86, 034106 (2005).
- D. Sarid, *Scanning Force Microscopy*, Oxford Series in Optical and Imaging Sciences, Oxford University Press, New York (1991)
- R. Dagani, Individual Surface Atoms Identified, *Chemical & Engineering News*, 5 March 2007, page 13. Published by American Chemical Society
- Q. Zhong, D. Inniss, K. Kjoller, V. B. Elings, *Surf. Sci. Lett.* 290, L688 (1993).
- V. J. Morris, A. R. Kirby, A. P. Gunning, *Atomic Force Microscopy for Biologists*. (Book) (December 1999) Imperial College Press.
- J. W. Cross *SPM - Scanning Probe Microscopy Website* ^[2]
- P. Hinterdorfer, Y. F. Dufrêne, *Nature Methods*, 3, 5 (2006)
- F. Giessibl, *Advances in Atomic Force Microscopy*, *Reviews of Modern Physics* 75 (3), 949-983 (2003).
- R. H. Eibl, V.T. Moy, Atomic force microscopy measurements of protein-ligand interactions on living cells. *Methods Mol Biol.* 305:439-50 (2005)
- P. M. Hoffmann, A. Oral, R. A. Grimbale, H. Ö. Özer, S. Jeffery, J. B. Pethica, *Proc. Royal Soc. A* 457, 1161 (2001).
- R. V. Lapshin, O. V. Obyedkov, Fast-acting piezoactuator and digital feedback loop for scanning tunneling microscopes ^[3], *Review of Scientific Instruments*, vol. 64, no. 10, pp. 2883-2887, 1993.
- R. V. Lapshin, Analytical model for the approximation of hysteresis loop and its application to the scanning tunneling microscope ^[4], *Review of Scientific Instruments*, vol. 66, no. 9, pp. 4718-4730, 1995.
- R. V. Lapshin, Feature-oriented scanning methodology for probe microscopy and nanotechnology ^[5], *Nanotechnology*, vol. 15, iss. 9, pp. 1135-1151, 2004.
- R. V. Lapshin, Automatic drift elimination in probe microscope images based on techniques of counter-scanning and topography feature recognition ^[6], *Measurement Science and Technology*, vol. 18, iss. 3, pp. 907-927, 2007.
- P. West, *Introduction to Atomic Force Microscopy: Theory, Practice and Applications* --- www.AFMUniversity.org
- R. W. Carpick and M. Salmeron, Scratching the surface: Fundamental investigations of tribology with atomic force microscopy ^[7], *Chemical Reviews*, vol. 97, iss. 4, pp. 1163-1194 (2007).
- Y. Roiter and S. Minko, AFM Single Molecule Experiments at the Solid-Liquid Interface: In Situ Conformation of Adsorbed Flexible Polyelectrolyte Chains ^[8], *Journal of the American Chemical Society*, vol. 127, iss. 45, pp. 15688-15689 (2005).

References

- [1] http://www.infinitema.com/downloads/APL_paper.pdf
- [2] <http://www.mobot.org/jwcross/spm/>
- [3] <http://www.nanoworld.org/homepages/lapshin/publications.htm#fast1993>
- [4] <http://www.nanoworld.org/homepages/lapshin/publications.htm#analytical1995>
- [5] <http://www.nanoworld.org/homepages/lapshin/publications.htm#feature2004>
- [6] <http://www.nanoworld.org/homepages/lapshin/publications.htm#automatic2007>
- [7] <http://dx.doi.org/10.1021/cr960068q>
- [8] <http://dx.doi.org/10.1021/ja0558239>

Nuclear magnetic resonance

Nuclear magnetic resonance (NMR) is a property that magnetic nuclei have in a magnetic field and applied electromagnetic (EM) pulse, which cause the nuclei to absorb energy from the EM pulse and radiate this energy back out. The energy radiated back out is at a specific resonance frequency which depends on the strength of the magnetic field and other factors. This allows the observation of specific quantum mechanical magnetic properties of an atomic nucleus. Many scientific techniques exploit NMR phenomena to study molecular physics, crystals and non-crystalline materials through NMR spectroscopy. NMR is also routinely used in advanced medical imaging techniques, such as in magnetic resonance imaging (MRI).

All nuclei that contain odd numbers of nucleons have an intrinsic magnetic moment and angular momentum, in other words a spin > 0 . The most commonly studied nuclei are ^1H (the most NMR-sensitive isotope after the radioactive ^3H) and ^{13}C ,



World's First 1 GHz NMR Spectrometer currently being final-tested in Kalrsuhe, Germany (1000 MHz, 23.5 T) - which will be installed to the new 'Centre de RMN à Très Hauts Champs' in Lyon, France in July 2009

although nuclei from isotopes of many other elements (e.g. ^2H , ^{10}B , ^{11}B , ^{14}N , ^{15}N , ^{17}O , ^{19}F , ^{23}Na , ^{29}Si , ^{31}P , ^{35}Cl , ^{113}Cd , ^{195}Pt) are studied by high-field NMR spectroscopy as well.

A key feature of NMR is that the resonance frequency of a particular substance is directly proportional to the strength of the applied magnetic field. It is this feature that is exploited in imaging techniques; if a sample is placed in a non-uniform magnetic field then the resonance frequencies of the sample's nuclei depend on where in the field they are located. Since the resolution of the imaging techniques depends on how big the gradient of the field is, many efforts are made to develop more powerful magnets, often using superconductors. The effectiveness of NMR can also be improved using hyperpolarization, and/or using two-dimensional, three-dimensional and higher dimension multi-frequency techniques.

The principle of NMR usually involves two sequential steps:

- The alignment (polarization) of the magnetic nuclear spins in an applied, constant magnetic field \mathbf{H}_0 .
- The perturbation of this alignment of the nuclear spins by employing an electro-magnetic, usually radio frequency (RF) pulse. The required perturbing frequency is dependent upon the static magnetic field (\mathbf{H}_0) and the nuclei of observation.

The two fields are usually chosen to be perpendicular to each other as this maximises the NMR signal strength. The resulting response by the total magnetization (\mathbf{M}) of the nuclear spins is the phenomenon that is exploited in NMR spectroscopy and magnetic resonance imaging. Both use intense applied magnetic fields (\mathbf{H}_0) in order to achieve dispersion and very high stability to deliver spectral resolution, the details of which are described by chemical shifts, the Zeeman effect, and Knight shifts (in metals).

NMR phenomena are also utilized in low-field NMR, NMR spectroscopy and MRI in the Earth's magnetic field (referred to as Earth's field NMR), and in several types of magnetometers.



Pacific Northwest National Laboratory's high magnetic field (800 MHz, 18.8 T) NMR spectrometer being loaded with a sample.

History

Discovery

Nuclear magnetic resonance was first described and measured in molecular beams by Isidor Rabi in 1938.^[1] Eight years later, in 1946, Felix Bloch and Edward Mills Purcell refined the technique for use on liquids and solids, for which they shared the Nobel Prize in physics in 1952.

Purcell had worked on the development and radar applications during World War II at Massachusetts Institute of Technology's Radiation Laboratory. His work during that project on the production and detection of RF energy, and on the absorption of such RF energy by matter, preceded his discovery of NMR.

They noticed that magnetic nuclei, like ^1H and ^{31}P , could absorb RF energy when placed in a magnetic field of a strength specific to the identity of the nuclei. When this absorption occurs, the nucleus is described as being *in resonance*. Different atomic nuclei within a molecule resonate at different (radio) frequencies for the same magnetic field strength. The observation of such magnetic resonance frequencies of the nuclei present in a molecule allows any trained user to discover essential, chemical and structural information about the molecule.

The development of nuclear magnetic resonance as a technique of analytical chemistry and biochemistry parallels the development of electromagnetic technology and its introduction into civilian use.

Theory of nuclear magnetic resonance

Nuclear spin and magnets

All nucleons, that is neutrons and protons, composing any atomic nucleus, have the intrinsic quantum property of spin. The overall spin of the nucleus is determined by the spin quantum number S . If the number of both the protons and neutrons in a given isotope are even then $S = 0$, i.e. there is no overall spin; just as electrons pair up in atomic orbitals, so do even numbers of protons or even numbers of neutrons (which are also spin- $\frac{1}{2}$ particles and hence fermions) pair up giving zero overall spin.

However, a proton and neutron will have lower energy when their spins are parallel, **not anti-parallel**, as this parallel spin alignment does not infringe upon the Pauli principle, but instead has to do with the quark fine structure of these two nucleons. Therefore, the spin ground state for the deuteron (the deuterium nucleus, or the ^2H isotope of hydrogen) --that has only a proton and a neutron--corresponds to a spin value of **1**, *not of zero*; the single, isolated deuteron is therefore exhibiting an NMR absorption spectrum characteristic of a quadrupolar nucleus of spin **1**, which in the 'rigid' state at very low temperatures is a characteristic ('Pake') *doublet*, (not a singlet as for a single, isolated ^1H , or any other isolated fermion or dipolar nucleus of spin $1/2$). On the other hand, because of the Pauli principle, the (radioactive) tritium isotope has to have a pair of anti-parallel spin neutrons (of total spin zero for the neutron spin couple), plus a proton of spin $1/2$; therefore, the character of the tritium nucleus ('triton') is again magnetic dipolar, *not quadrupolar*-- like its non-radioactive deuteron neighbor, and the tritium nucleus total spin value is again $1/2$, just like for the simpler, abundant hydrogen isotope, ^1H nucleus (the *proton*). The NMR absorption (radio) frequency for tritium is however slightly higher for tritium than that of

^1H because the tritium nucleus has a slightly higher gyromagnetic ratio than ^1H . In many other cases of *non-radioactive* nuclei, the overall spin is also non-zero. For example, the ^{27}Al nucleus has an overall spin value $S = \frac{5}{2}$.

A non-zero spin is thus always associated with a non-zero magnetic moment (μ) via the relation $\mu = gS$, where g is the gyromagnetic ratio. It is this magnetic moment that allows the observation of NMR absorption spectra caused by transitions between nuclear spin levels. Most radioactive nuclei (with some rare exceptions) that have both even numbers of protons and even numbers of neutrons, also have zero nuclear magnetic moments-and also have zero magnetic dipole and quadrupole moments; therefore, such radioactive isotopes do not exhibit any NMR absorption spectra. Thus, ^{14}C , ^{32}P , and ^{36}Cl are examples of radioactive nuclear isotopes that have no NMR absorption, whereas ^{13}C , ^{31}P , ^{35}Cl and ^{37}Cl are stable nuclear isotopes that do exhibit NMR absorption spectra; the last two nuclei are quadrupolar nuclei whereas the preceding two nuclei (^{13}C and ^{31}P) are dipolar ones.

Electron spin resonance (ESR) is a related technique which detects transitions between electron spin levels instead of nuclear ones. The basic principles are similar; however, the instrumentation, data analysis and detailed theory are significantly different. Moreover, there is a much smaller number of molecules and materials with unpaired electron spins that exhibit ESR (or electron paramagnetic resonance (EPR)) absorption than those that have NMR absorption spectra. Significantly also, is the much greater sensitivity of ESR and EPR in comparison with NMR. Furthermore, ferromagnetic materials and thin films may exhibit 'very unusual', highly resolved ferromagnetic resonance (FMR) spectra, or ferromagnetic spin wave resonance (FSWR) excitations in non-crystalline solids such as ferromagnetic metallic glasses, well beyond the common single-transitions of most routine NMR, FMR and EPR studies.^{[2] [3]}

Values of spin angular momentum

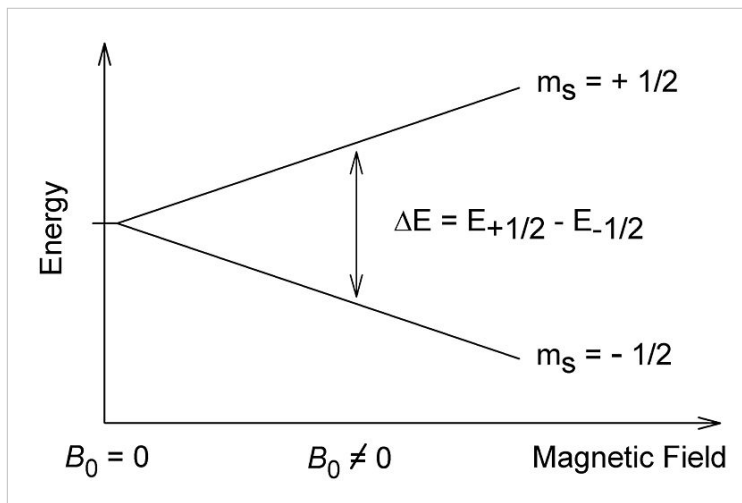
The angular momentum associated with nuclear spin is quantized. This means both that the magnitude of angular momentum is quantized (i.e. S can only take on a restricted range of values), and also that the orientation of the associated angular momentum is quantized. The associated quantum number is known as the magnetic quantum number, m , and can take values from $+S$ to $-S$, in integer steps. Hence for any given nucleus, there is a total of $2S + 1$ angular momentum states.

The z-component of the angular momentum vector (\mathbf{S}) is therefore $S_z = m\hbar$, where \hbar is the reduced Planck constant. The z-component of the magnetic moment is simply:

$$\mu_z = gS_z = gm\hbar$$

Spin behavior in a magnetic field

Consider nuclei which have a spin of one-half, like ^1H , ^{13}C or ^{19}F . The nucleus has two possible spin states: $m = +\frac{1}{2}$ or $m = -\frac{1}{2}$ (also referred to as spin-up and spin-down, or sometimes α and β spin states, respectively). These states are degenerate, i.e. they have the same energy. Hence the number of atoms in these two states will be approximately equal at thermal equilibrium.



If a nucleus is placed in a magnetic field, however, the interaction between the nuclear magnetic moment and the external magnetic field mean the two states no longer have the same energy. The energy of a magnetic moment μ when in a magnetic field \mathbf{B}_0 is given by:

$$E = -\mu \cdot \mathbf{B}_0 = -\mu_z B_0 \cos \theta .$$

Usually \mathbf{B}_0 is chosen to be aligned along the z axis, therefore $\cos\theta=1$:

$$E = -\mu_z B_0 ,$$

or alternatively:

$$E = -gm\hbar B_0 .$$

As a result the different nuclear spin states have different energies in a non-zero magnetic field. In hand-waving terms, we can talk about the two spin states of a spin $\frac{1}{2}$ as being *aligned* either with or against the magnetic field. If g is positive (true for most isotopes) then $m = +\frac{1}{2}$ is the lower energy state.

The energy difference between the two states is:

$$\Delta E = g\hbar B_0 ,$$

and this difference results in a small population bias toward the lower energy state.

Magnetic resonance by nuclei

Resonant absorption by nuclear spins will occur only when electromagnetic radiation of the correct frequency (e.g., equaling the Larmor precession rate) is being applied to match the energy difference between the nuclear spin levels in a constant magnetic field of the appropriate strength. The energy of an absorbed photon is then $E = h\nu_0$, where ν_0 is the resonance radiofrequency that has to match (that is, it has to be equal to) the Larmor precession frequency ν_L of the nuclear magnetization in the constant magnetic field \mathbf{H}_0 . Hence, a magnetic resonance absorption will only occur when $\Delta E = h\nu_0$, which is when $\nu_0 = gB_0/(2\pi)$. Such magnetic resonance frequencies typically correspond to the radio frequency (or RF) range of the electromagnetic spectrum for magnetic fields up to ~ 20 T. It is this magnetic resonant absorption which is detected in NMR.

Nuclear shielding

It might appear from the above that all nuclei of the same nuclide (and hence the same g) would resonate at the same frequency. This is not the case. The most important perturbation of the NMR frequency for applications of NMR is the 'shielding' effect of the surrounding electrons. In general, this electronic shielding reduces the magnetic field *at the nucleus* (which is what determines the NMR frequency).

As a result the energy gap is reduced, and the frequency required to achieve resonance is also reduced. This shift in the NMR frequency due to the electrons' molecular orbital coupling to the external magnetic field is called chemical shift, and it explains why NMR is able to probe the chemical structure of molecules which depends on the electron density distribution in the corresponding molecular orbitals. If a nucleus in a specific chemical group is shielded to a higher degree by a higher electron density of its surrounding molecular orbital, then its NMR frequency will be shifted "upfield" (that is, a lower chemical shift), whereas if it is less shielded by such surrounding electron density, then its NMR frequency will be shifted "downfield" (that is, a higher chemical shift).

Unless the local symmetry of such molecular orbitals is very high (leading to "isotropic" shift), the shielding effect will depend on the orientation of the molecule with respect to the external field (\mathbf{H}_0). In solid-state NMR spectroscopy, magic angle spinning is required to average out this orientation dependence in order to obtain values close to the average chemical shifts. This is unnecessary in conventional NMR investigations of molecules, since rapid molecular tumbling averages out the chemical shift anisotropy (CSA). In this case, the term "average" chemical shift (ACS) is used.

Relaxation

The process called population relaxation refers to nuclei that return to the thermodynamic state in the magnet. This process is also called T_1 , "spin-lattice" or "longitudinal magnetic" relaxation, where T_1 refers to the mean time for an individual nucleus to return to its thermal equilibrium state of the spins. Once the nuclear spin population is relaxed, it can be probed again, since it is in the initial, equilibrium (mixed) state.

The precessing nuclei can also fall out of alignment with each other (returning the net magnetization vector to a non-precessing field) and stop producing a signal. This is called T_2 or *transverse relaxation*. Because of the difference in the actual relaxation mechanisms involved (for example, inter-molecular vs. intra-molecular magnetic dipole-dipole interactions), T_1 is always longer than T_2 (that is, slower spin-lattice relaxation, for example because of smaller dipole-dipole interaction effects). In practice, the value of T_2^* which is the actually observed decay time of the observed NMR signal, or free induction decay, (to 1/e of the initial amplitude immediately after the resonant RF pulse)-- also depends on the static magnetic field inhomogeneity, which is quite significant. (There is also a smaller but significant contribution to the observed FID shortening from the RF inhomogeneity of the resonant pulse). In the corresponding FT-NMR spectrum—meaning the Fourier transform of the free induction decay--the T_2^* time is inversely related to the width of the NMR signal in frequency units. Thus, a nucleus with a long T_2 relaxation time gives rise to a very sharp NMR peak in the FT-NMR spectrum for a very homogeneous ("well-shimmed") static magnetic field, whereas nuclei with shorter T_2 values give rise to broad FT-NMR peaks even when the magnet is shimmed well. Both T_1 and T_2 depend on the rate of molecular motions as well as the gyromagnetic ratios of both the resonating and

their strongly interacting, next-neighbor nuclei that are not at resonance.

NMR spectroscopy

NMR spectroscopy is one of the principal techniques used to obtain physical, chemical, electronic and structural information about molecules due to either the chemical shift Zeeman effect, or the Knight shift effect, or a combination of both, on the resonant frequencies of the nuclei present in the sample. It is a powerful technique that can provide detailed information on the topology, dynamics and three-dimensional structure of molecules in solution and the solid state. Thus, structural and dynamic information is obtainable (with or without "magic angle" spinning (MAS)) from NMR studies of quadrupolar nuclei (that is, those nuclei with spin $S > \frac{1}{2}$) even in the presence of magnetic dipole-dipole interaction broadening (or simply, dipolar broadening) which is always much smaller than the quadrupolar interaction strength because it is a magnetic vs. an electric interaction effect.



900MHz, 21.2 T NMR Magnet at HWB-NMR, Birmingham, UK being loaded with a sample

Additional structural and chemical information may be obtained by performing double-quantum NMR experiments for quadrupolar nuclei such as ^2H . Also, nuclear magnetic resonance is one of the techniques that has been used to design quantum automata, and also build elementary quantum computers.^{[4] [5]}

Continuous wave (CW) spectroscopy

In its first few decades, nuclear magnetic resonance spectrometers used a technique known as continuous-wave spectroscopy (CW spectroscopy). Although NMR spectra could be, and have been, obtained using a fixed magnetic field and sweeping the frequency of the electromagnetic radiation, this more typically involved using a fixed frequency source and varying the current (and hence magnetic field) in an electromagnet to observe the resonant absorption signals. This is the origin of the anachronistic, but still common, "high" and "low" field terminology for low frequency and high frequency regions respectively of the NMR spectrum.

CW spectroscopy is inefficient in comparison to Fourier techniques (see below) as it probes the NMR response at individual frequencies in succession. As the NMR signal is intrinsically weak, the observed spectra suffer from a poor signal-to-noise ratio. This can be mitigated by signal averaging i.e. adding the spectra from repeated measurements. While

the NMR signal is constant between scans and so adds linearly, the random noise adds more slowly—as the square-root of the number of spectra (see Random walk). Hence the overall ratio of the signal to the noise increases as the square-root of the number of spectra measured.

Fourier transform spectroscopy

Most applications of NMR involve full NMR spectra, that is, the intensity of the NMR signal as a function of frequency. Early attempts to acquire the NMR spectrum more efficiently than simple CW methods involved irradiating simultaneously with more than one frequency. It was soon realized, however, that a simpler solution was to use short pulses of radio-frequency (centered at the middle of the NMR spectrum). In simple terms, a short square pulse of a given "carrier" frequency "contains" a range of frequencies centered about the carrier frequency, with the range of excitation (bandwidth) being inversely proportional to the pulse duration (the Fourier transform (FT) of an approximate square wave contains contributions from all the frequencies in the neighborhood of the principal frequency). The restricted range of the NMR frequencies made it relatively easy to use short (millisecond to microsecond) radiofrequency (RF) pulses to excite the entire NMR spectrum.

Applying such a pulse to a set of nuclear spins simultaneously excites all the single-quantum NMR transitions. In terms of the net magnetization vector, this corresponds to tilting the magnetization vector away from its equilibrium position (aligned along the external magnetic field). The out-of-equilibrium magnetization vector precesses about the external magnetic field vector at the NMR frequency of the spins. This oscillating magnetization vector induces a current in a nearby pickup coil, creating an electrical signal oscillating at the NMR frequency. This signal is known as the free induction decay (FID) and contains the vector-sum of the NMR responses from all the excited spins. In order to obtain the frequency-domain NMR spectrum (NMR absorption intensity vs. NMR frequency) this time-domain signal (intensity vs. time) must be FTed. Fortunately the development of FT NMR coincided with the development of digital computers and Fast Fourier Transform algorithms.

Richard R. Ernst was one of the pioneers of pulse (FT) NMR and won a Nobel Prize in chemistry in 1991 for his work on FT NMR and his development of multi-dimensional NMR (see below).

Multi-dimensional NMR Spectroscopy

The use of pulses of different shapes, frequencies and durations in specifically-designed patterns or *pulse sequences* allows the spectroscopist to extract many different types of information about the molecule. Multi-dimensional nuclear magnetic resonance spectroscopy is a kind of FT NMR in which there are at least two pulses and, as the experiment is repeated, the pulse sequence is varied. In *multidimensional nuclear magnetic resonance* there will be a sequence of pulses and, at least, one variable time period. In three dimensions, two time sequences will be varied. In four dimensions, three will be varied.

There are many such experiments. In one, these time intervals allow (amongst other things) magnetization transfer between nuclei and, therefore, the detection of the kinds of nuclear-nuclear interactions that allowed for the magnetization transfer. Interactions that

can be detected are usually classified into two kinds. There are *through-bond* interactions and *through-space* interactions, the latter usually being a consequence of the nuclear Overhauser effect. Experiments of the nuclear Overhauser variety may be employed to establish distances between atoms, as for example by 2D-FT NMR of molecules in solution.

Although the fundamental concept of 2D-FT NMR was proposed by Professor Jean Jeener from the Free University of Brussels at an International Conference, this idea was largely developed by Richard Ernst who won the 1991 Nobel prize in Chemistry for his work in FT NMR, including multi-dimensional FT NMR, and especially 2D-FT NMR of small molecules.^[6] Multi-dimensional FT NMR experiments were then further developed into powerful methodologies for studying biomolecules in solution, in particular for the determination of the structure of biopolymers such as proteins or even small nucleic acids.^[7]

Kurt Wüthrich shared (with John B. Fenn) in 2002 the Nobel Prize in Chemistry for his work in protein FT NMR in solution.

Solid-state NMR spectroscopy

This technique complements biopolymer X-ray crystallography in that it is frequently applicable to biomolecules in a liquid or liquid crystal phase, whereas crystallography, as the name implies, is performed on molecules in a solid phase. Though nuclear magnetic resonance is used to study solids, extensive atomic-level biomolecular structural detail is especially challenging to obtain in the solid state. There is little signal averaging by thermal motion in the solid state, where most molecules can only undergo restricted vibrations and rotations at room temperature, each in a slightly different electronic environment, therefore exhibiting a different NMR absorption peak. Such a variation in the electronic environment of the resonating nuclei results in a blurring of the observed spectra—which is often only a broad Gaussian band for non-quadrupolar spins in a solid—thus making the interpretation of such "dipolar" and "chemical shift anisotropy" (CSA) broadened spectra either very difficult or impossible.

Professor Raymond Andrew at Nottingham University in UK pioneered the development of high-resolution solid-state nuclear magnetic resonance. He was the first to report the introduction of the MAS (magic angle sample spinning; MASS) technique that allowed him to achieve spectral resolution in solids sufficient to distinguish between chemical groups with either different chemical shifts or distinct Knight shifts. In MASS, the sample is spun at several kilohertz around an axis that makes the so-called magic angle θ_m (which is $\sim 54.74^\circ$, where $\cos^2\theta_m = 1/3$, or $3\cos^2\theta_m - 1 = 0$) with respect to the direction of the static magnetic field \mathbf{H}_0 ; as a result of such magic angle sample spinning, the chemical shift anisotropy bands are averaged to their corresponding average (isotropic) chemical shift values. The above expression involving $\cos^2\theta_m$ has its origin in a calculation that predicts the magnetic dipolar interaction effects to cancel out for the specific value of θ_m called the magic angle. One notes that correct alignment of the sample rotation axis as close as possible to θ_m is essential for cancelling out the dipolar interactions whose strength for angles sufficiently far from θ_m is usually greater than ~ 10 kHz for C-H bonds in solids, for example, and it is thus greater than their CSA values.

A concept developed by Sven Hartmann and Erwin Hahn was utilized in transferring magnetization from protons to less sensitive nuclei (popularly known as cross-polarization) by M.G. Gibby, Alex Pines and John S. Waugh. Then, Jake Schaefer and Ed Stejskal

demonstrated also the powerful use of cross-polarization under MASS conditions which is now routinely employed to detect low-abundance and low-sensitivity nuclei.

Sensitivity

Because the intensity of nuclear magnetic resonance signals and, hence, the sensitivity of the technique depends on the strength of the magnetic field the technique has also advanced over the decades with the development of more powerful magnets. Advances made in audio-visual technology have also improved the signal-generation and processing capabilities of newer machines.

As noted above, the sensitivity of nuclear magnetic resonance signals is also dependent on the presence of a magnetically-susceptible nuclide and, therefore, either on the natural abundance of such nuclides or on the ability of the experimentalist to artificially enrich the molecules, under study, with such nuclides. The most abundant naturally-occurring isotopes of hydrogen and phosphorus (for example) are both magnetically susceptible and readily useful for nuclear magnetic resonance spectroscopy. In contrast, carbon and nitrogen have useful isotopes but which occur only in very low natural abundance.

Other limitations on sensitivity arise from the quantum-mechanical nature of the phenomenon. For quantum states separated by energy equivalent to radio frequencies, thermal energy from the environment causes the populations of the states to be close to equal. Since incoming radiation is equally likely to cause stimulated emission (a transition from the upper to the lower state) as absorption, the NMR effect depends on an excess of nuclei in the lower states. Several factors can reduce sensitivity, including

- Increasing temperature, which evens out the population of states. Conversely, low temperature NMR can sometimes yield better results than room-temperature NMR, providing the sample remains liquid.
- Saturation of the sample with energy applied at the resonant radiofrequency. This manifests in both CW and pulsed NMR; in the first, CW, case this happens by using too much continuous power that keeps the upper spin levels completely populated; in the second case, saturation occurs by pulsing too frequently—without allowing time for the nuclei to return to thermal equilibrium through spin-lattice relaxation. For nuclei such as ^{29}Si this is a serious practical problem as the relaxation time is measured in seconds; for protons in "pure" ice, or ^{19}F in high-purity (undoped) LiF crystals the spin-lattice relaxation time can be on the order of an hour or longer. The use of shorter RF pulses that tip the magnetization by less than 90° can partially solve the problem by allowing spectral acquisition without the complete loss of NMR signal.
- Non-magnetic effects, such as electric-quadrupole coupling of spin-1 and spin- $\frac{3}{2}$ nuclei with their local environment, which broaden and weaken absorption peaks. ^{14}N , an abundant spin-1 nucleus, is difficult to study for this reason. High resolution NMR instead probes molecules using the rarer ^{15}N isotope, which has spin- $\frac{1}{2}$.

Isotopes

Many chemical elements can be used for NMR analysis.^[8]

Commonly used nuclei:

- ^1H , the most commonly used, very useful. Highly abundant, the most sensitive nucleus apart from tritium (^3H) which is not commonly used as it is unstable and radioactive. Narrow chemical shift with sharp signals. In particular, the ^1H signal is used in magnetic resonance imaging.
- ^2H , commonly used in the form of deuterated solvents to avoid interference of solvents in measurement of ^1H . Also used in determining the behavior of lipids in lipid membranes and other solids or liquid crystals as it is a relatively non-perturbing label which can selectively replace ^1H .
- ^3He , very sensitive. Low percentage in natural helium, has to be enriched. Used mainly in studies of endohedral fullerenes.
- ^{10}B , lower sensitivity than ^{11}B . Quartz tubes must be used as borosilicate glass interferes with measurement.
- ^{11}B , more sensitive than ^{10}B , yields sharper signals. Quartz tubes must be used as borosilicate glass interferes with measurement.
- ^{13}C , commonly used. There is a low percentage in natural carbon, therefore spectrum acquisition on unlabelled takes a long time. Frequently used for labeling of compounds in synthetic and metabolic studies. Has low sensitivity and wide chemical shift, yields sharp signals. Low percentage makes it useful by preventing spin-spin couplings and makes the spectrum appear less crowded. Slow relaxation means that spectra are not integrable unless long acquisition times are used.
- ^{14}N , medium sensitivity nucleus with wide chemical shift. Its large quadrupole moment interferes in acquisition of high resolution spectra, limiting usefulness to smaller molecules and functional groups with a high degree of symmetry such as the headgroups of lipids.
- ^{15}N , relatively commonly used. Can be used for labeling compounds. Nucleus very insensitive but yields sharp signals. Low percentage in natural nitrogen together with low sensitivity requires high concentrations or expensive isotope enrichment.
- ^{17}O , low sensitivity and very low natural abundance. Used in metabolic and biochemical studies.
- ^{19}F , relatively commonly measured. Sensitive, yields sharp signals, has wide chemical shift.
- ^{31}P , 100% of natural phosphorus. Medium sensitivity, wide chemical shift range, yields sharp lines. Used in biochemical studies.
- ^{35}Cl and ^{37}Cl , broad signal. ^{35}Cl significantly more sensitive, preferred over ^{37}Cl despite its slightly broader signal. Organic chlorides yield very broad signals, its use is limited to inorganic and ionic chlorides and very small organic molecules.
- ^{43}Ca , used in biochemistry to study calcium binding to DNA, proteins, etc. Moderately sensitive, very low natural abundance.
- ^{195}Pt , used in studies of catalysts and complexes.

Other nuclei (usually used in the studies of their complexes and chemical binding, or to detect presence of the element):

- ^6Li , ^7Li
- ^9Be

- ^{19}F
- ^{21}Ne
- ^{23}Na
- ^{25}Mg
- ^{27}Al
- ^{29}Si
- ^{31}P
- ^{33}S
- ^{39}K , ^{40}K , ^{41}K
- ^{45}Sc
- ^{47}Ti , ^{49}Ti
- ^{50}V , ^{51}V
- ^{53}Cr
- ^{53}Mn
- ^{57}Fe
- ^{59}Co
- ^{61}Ni
- ^{63}Cu , ^{65}Cu
- ^{67}Zn
- ^{69}Ga , ^{71}Ga
- ^{73}Ge
- ^{77}Se
- ^{81}Br
- ^{87}Rb
- ^{87}Sr
- ^{95}Mo
- ^{109}Ag
- ^{113}Cd
- ^{125}Te
- ^{127}I
- ^{133}Cs
- ^{135}Ba , ^{137}Ba
- ^{139}La
- ^{183}W
- ^{199}Hg

Applications

Medicine

The use of nuclear magnetic resonance best known to the general public is magnetic resonance imaging for medical diagnosis and MR Microscopy in research settings, however, it is also widely used in chemical studies, notably in NMR spectroscopy such as proton NMR, carbon-13 NMR, deuterium NMR and phosphorus-31 NMR. Biochemical information can also be obtained from living tissue (e.g. human brain tumours) with the technique known as in vivo magnetic resonance spectroscopy or chemical shift NMR Microscopy.

These studies are possible because nuclei are surrounded by orbiting electrons, which are also spinning charged particles such as magnets and, so, will partially shield the nuclei. The

amount of shielding depends on the exact local environment. For example, a hydrogen bonded to an oxygen will be shielded differently than a hydrogen bonded to a carbon atom. In addition, two hydrogen nuclei can interact via a process known as spin-spin coupling, if they are on the same molecule, which will split the lines of the spectra in a recognizable way.

Chemistry

By studying the peaks of nuclear magnetic resonance spectra, chemists can determine the structure of many compounds. It can be a very selective technique, distinguishing among many atoms within a molecule or collection of molecules of the same type but which differ only in terms of their local chemical environment. See the articles on carbon-13 NMR and proton NMR for detailed discussions.

By studying T_2^* information, a chemist can determine the identity of a compound by comparing the observed nuclear precession frequencies to known frequencies. Further structural data can be elucidated by observing *spin-spin coupling*, a process by which the precession frequency of a nucleus can be influenced by the magnetization transfer from nearby nuclei. Spin-spin coupling is most commonly observed in NMR involving common isotopes, such as Hydrogen-1 (^1H NMR).

Because the nuclear magnetic resonance *timescale* is rather slow, compared to other spectroscopic methods, changing the temperature of a T_2^* experiment can also give information about fast reactions, such as the Cope rearrangement or about structural dynamics, such as ring-flipping in cyclohexane. At low enough temperatures, a distinction can be made between the axial and equatorial hydrogens in cyclohexane.

An example of nuclear magnetic resonance being used in the determination of a structure is that of buckminsterfullerene (often called "buckyballs", composition C_{60}). This now famous form of carbon has 60 carbon atoms forming a sphere. The carbon atoms are all in identical environments and so should see the same internal H field. Unfortunately, buckminsterfullerene contains no hydrogen and so ^{13}C nuclear magnetic resonance has to be used. ^{13}C spectra require longer acquisition times since carbon-13 is not the common isotope of carbon (unlike hydrogen, where ^1H is the common isotope). However, in 1990 the spectrum was obtained by R. Taylor and co-workers at the University of Sussex and was found to contain a single peak, confirming the unusual structure of buckminsterfullerene.^[9]

Non-destructive testing

Nuclear magnetic resonance is extremely useful for analyzing samples non-destructively. Radio waves and static magnetic fields easily penetrate many types of matter and anything that is not inherently ferromagnetic. For example, various expensive biological samples, such as nucleic acids, including RNA and DNA, or proteins, can be studied using nuclear magnetic resonance for weeks or months before using destructive biochemical experiments. This also makes nuclear magnetic resonance a good choice for analyzing dangerous samples.

Data acquisition in the petroleum industry

Another use for nuclear magnetic resonance is data acquisition in the petroleum industry for petroleum and natural gas exploration and recovery. A borehole is drilled into rock and sedimentary strata into which nuclear magnetic resonance logging equipment is lowered. Nuclear magnetic resonance analysis of these boreholes is used to measure rock porosity, estimate permeability from pore size distribution and identify pore fluids (water, oil and gas). These instruments are typically low field NMR spectrometers.

Process control

NMR has now entered the arena of real-time process control and process optimization in oil refineries and petrochemical plants. Two different types of NMR analysis are utilized to provide real time analysis of feeds and products in order to control and optimize unit operations. Time-domain NMR (TD-NMR) spectrometers operating at low field (2–20 MHz for ^1H) yield free induction decay data that can be used to determine absolute hydrogen content values, rheological information, and component composition. These spectrometers are used in mining, polymer production, cosmetics and food manufacturing as well as coal analysis. High resolution FT-NMR spectrometers operating in the 60 MHz range with shielded permanent magnet systems yield high resolution ^1H NMR spectra of refinery and petrochemical streams. The variation observed in these spectra with changing physical and chemical properties is modelled utilizing chemometrics to yield predictions on unknown samples. The prediction results are provided to control systems via analogue or digital outputs from the spectrometer.

Earth's field NMR

In the Earth's magnetic field, NMR frequencies are in the audio frequency range. EFNMR is typically stimulated by applying a relatively strong dc magnetic field pulse to the sample and, following the pulse, analysing the resulting low frequency alternating magnetic field that occurs in the Earth's magnetic field due to free induction decay (FID). These effects are exploited in some types of magnetometers, EFNMR spectrometers, and MRI imagers. Their inexpensive portable nature makes these instruments valuable for field use and for teaching the principles of NMR and MRI.

Quantum computing

NMR quantum computing uses the spin states of molecules as qubits. NMR differs from other implementations of quantum computers in that it uses an ensemble of systems, in this case molecules. The ensemble is initialized to be the thermal equilibrium state (see quantum statistical mechanics).

Magnetometers

Various magnetometers use NMR effects to measure magnetic fields, including proton precession magnetometers (PPM) (also known as proton magnetometers), and Overhauser magnetometers. See also Earth's field NMR.

Makers of NMR equipment

Major NMR instrument makers include Oxford Instruments, Bruker, SpinLock SRL, General Electric, JEOL, Kimble Chase, Philips, Siemens AG, Varian, Inc. and SpinCore Technologies, Inc.

See also

- Carbon-13 NMR
 - Chemical shift
 - 2D-FT NMRI and Spectroscopy
 - Dynamic Nuclear Polarisation (DNP)
 - Earth's field NMR (EFNMR)
 - Electromagnetism
 - Electron spin/paramagnetic resonance
 - Ferromagnetic resonance
 - Free induction decay (FID)
 - Gyromagnetic ratio
 - Hyperpolarization
 - In vivo magnetic resonance spectroscopy (MRS)
 - J-coupling
 - Larmor equation (Not to be confused with Larmor formula).
 - Larmor precession
 - Low field NMR
 - Magic angle spinning
 - Magnetic resonance imaging (MRI)
 - Magnetometer
 - NMR spectra database
 - NMR spectroscopy
 - NMR Microscopy
 - Nuclear quadrupole resonance (NQR)
 - Overhauser magnetometer
 - Protein dynamics
 - Protein NMR
 - Proton NMR
 - Proton precession magnetometer (PPM)
 - Proton magnetometer
 - Rabi cycle
 - Relaxometry
 - Relaxation (NMR)
 - Solid-state NMR
 - Stark effect
 - Zeeman effect
-

Notes

- [1] I.I. Rabi, J.R. Zacharias, S. Millman, P. Kusch (1938). "A New Method of Measuring Nuclear Magnetic Moment". *Physical Review* **53**: 318. doi: 10.1103/PhysRev.53.318 (<http://dx.doi.org/10.1103/PhysRev.53.318>).
- [2] I.C. Baianu, K.A. Robinson, J. Patterson (1979). "Ferromagnetic Resonance and Spin Wave Excitations in Metallic Glasses". *J. Phys. Chem. Solids* **40** (12): 941–950. doi: 10.1016/0022-3697(79)90122-7 ([http://dx.doi.org/10.1016/0022-3697\(79\)90122-7](http://dx.doi.org/10.1016/0022-3697(79)90122-7)).
- [3] I.C. Baianu (1979). "Ferromagnetic resonance and spin wave excitations in metallic glasses: The effects of thermal ageing and long-range magnetic ordering". *Solid State Communications* **29**: i–xvi. doi: 10.1016/0038-1098(79)91190-6 ([http://dx.doi.org/10.1016/0038-1098\(79\)91190-6](http://dx.doi.org/10.1016/0038-1098(79)91190-6)).
- [4] (see also references cited therein) (<http://planetphysics.org/encyclopedia/QuantumComputers.html>)
- [5] David P. DiVincenzo (2000). "The Physical Implementation of Quantum Computation": *Experimental Proposals for Quantum Computation*. **arXiv:quant-ph/0002077**. p. 1 through 10. doi: 10.1103/PhysRev.53.318 (<http://dx.doi.org/10.1103/PhysRev.53.318>).
- [6] "Nuclear Magnetic Resonance Fourier Transform Spectroscopy" (http://nobelprize.org/nobel_prizes/chemistry/laureates/1991/ernst-lecture.html)
- [7] I.C. Baianu. <http://planetmath.org/encyclopedia/TwoDimensionalFourierTransforms.html>|"Two-dimensional Fourier transforms". *2D-FT NMR and MRI*. PlanetMath. <http://planetmath.org/encyclopedia/TwoDimensionalFourierTransforms.html>. Retrieved on 2009-02-22.
- [8] (<http://chem.ch.huji.ac.il/nmr/techniques/1d/multi.html>)
- [9] R. Taylor, J.P. Hare, A.K. Abdul-Sada, H.W. Kroto (1990). "Isolation, separation and characterization of the fullerenes C₆₀ and C₇₀: the third form of carbon". *Journal of the Chemical Society, Chemical Communications* **20**: 1423–1425. doi: 10.1039/c39900001423 (<http://dx.doi.org/10.1039/c39900001423>).

References

- G.E Martin, A.S. Zekter (1988). *Two-Dimensional NMR Methods for Establishing Molecular Connectivity*. New York: VCH Publishers. p. 59.
- J.W. Akitt, B.E. Mann (2000). *NMR and Chemistry*. Cheltenham, UK: Stanley Thornes. pp. 273, 287.
- J.P. Hornak. <http://www.cis.rit.edu/htbooks/nmr/>|"The Basics of NMR". <http://www.cis.rit.edu/htbooks/nmr/>. Retrieved on 2009-02-23.
- J. Keeler (2005). *Understanding NMR Spectroscopy*. John Wiley & Sons. ISBN 0470017864.
- K. Wuthrich (1986). *NMR of Proteins and Nucleic Acids*. New York (NY), USA: Wiley-Interscience.
- J.M Tyszka, S.E Fraser, R.E Jacobs (2005). "Magnetic resonance microscopy: recent advances and applications". *Current Opinion in Biotechnology* **16** (1): 93–99. doi: 10.1016/j.copbio.2004.11.004 (<http://dx.doi.org/10.1016/j.copbio.2004.11.004>).
- J.C. Edwards. [http://www.process-nmr.com/pdfs/NMR Overview.pdf](http://www.process-nmr.com/pdfs/NMR%20Overview.pdf)|"Principles of NMR". Process NMR Associates. <http://www.process-nmr.com/pdfs/NMR%20Overview.pdf>. Retrieved on 2009-02-23.

External links

Tutorial

- NMR/MRI tutorial (<http://www.cis.rit.edu/htbooks/nmr/inside.htm>)

Animations and Simulations

- Animations (http://www.bigs.de/BLH/en/index.php?option=com_content&view=category&layout=blog&id=51&Itemid=222)
- Animation of NMR spin ^1H / ^2H precession (<http://www.chem.queensu.ca/FACILITIES/NMR/nmr/webcourse/precess.htm>)
- A free interactive simulation of NMR principles (<http://vam.anest.ufl.edu/forensic/nmr.html>)

Software

- CARA (<http://www.nmr.ch/>) - Computer Aided Resonance Assignment, freeware, developed at the group of Prof. Kurt Wüthrich
- Janocchio (<http://janocchio.sourceforge.net>) Conformation-dependent coupling and NOE prediction for small molecules.
- NMR processing software from ACD/Labs (<http://www.acdlabs.com/>) for 1D (http://www.acdlabs.com/products/spec_lab/exp_spectra/nmr/) and 2D (http://www.acdlabs.com/products/spec_lab/exp_spectra/2d_nmr/) NMR spectra. DB interface available.
- NMR Prediction software ACD/NMR Predictors (http://www.acdlabs.com/products/spec_lab/predict_nmr/)
- NMR simulation software QSim (<http://www.bpc.lu.se/QSim>)
- Free software for simulation of spin coupled multiplets and DNMR spectra WINDNMR-Pro (<http://www.chem.wisc.edu/areas/reich/plt/windnmr.htm>)
- NMR processing software NMRPipe (<http://spin.niddk.nih.gov/bax/software/NMRPipe>)
- RMN (<http://www.grandinetti.org/Software/RMN>) - An NMR data processing program for the Macintosh.

Video

- introduction to NMR and MRI (<http://www.youtube.com/watch?v=7aRKAXD4dAg>)
- Richard Ernst, NL - Developer of Multidimensional NMR techniques (<http://www.vega.org.uk/video/programme/21>) Freeview video provided by the Vega Science Trust.
- 'An Interview with Kurt Wuthrich' (<http://www.vega.org.uk/video/programme/115>) Freeview video by the Vega Science Trust (Wüthrich was awarded a Nobel Prize in Chemistry in 2002 "for his development of nuclear magnetic resonance spectroscopy for determining the three-dimensional structure of biological macromolecules in solution").

Wiki

- NMR Wiki (<http://www.nmrwiki.org>) Open NMR,EPR,MRI web project

2D-FT NMRI and Spectroscopy

2D-FT Nuclear magnetic resonance imaging (2D-FT NMRI), or **Two-dimensional Fourier transform** nuclear magnetic resonance imaging (**NMRI**), is primarily a non—invasive imaging technique most commonly used in biomedical research and medical radiology/nuclear medicine/MRI to visualize structures and functions of the living systems and single cells. For example it can provides fairly detailed images of a human body in any selected cross-sectional plane, such as longitudinal, transversal, sagittal, etc. The basic NMR phenomenon or physical principle^[1] is essentially the same in N(MRI), nuclear magnetic resonance/FT (NMR) spectroscopy, topical NMR, or even in Electron Spin Resonance /EPR; however, the details are significantly different at present for EPR, as only in the early days of NMR the static magnetic field was scanned for obtaining spectra, as it is still the case in many EPR or ESR spectrometers. NMRI, on the other hand, often utilizes a linear magnetic field gradient to obtain an image that combines the visualization of molecular structure and dynamics. It is this dynamic aspect of NMRI, as well as its highest sensitivity for the ^1H nucleus that distinguishes it very dramatically from X-ray CAT scanning that 'misses' hydrogens because of their very low X-ray scattering factor.

Thus, NMRI provides much greater contrast especially for the different soft tissues of the body than computed tomography (CT) as its most sensitive option observes the nuclear spin distribution and dynamics of highly mobile molecules that contain the naturally abundant, stable hydrogen isotope ^1H as in plasma water molecules, blood, dissolved metabolites and fats. This approach makes it most useful in cardiovascular, oncological (cancer), neurological (brain), musculoskeletal, and cartilage imaging. Unlike CT, it uses no ionizing radiation, and also unlike nuclear imaging it does not employ any radioactive isotopes. Some of the first MRI images reported were published in 1973^[2] and the first study performed on a human took place on July 3, 1977.^[3] Earlier papers were also published by Sir Peter Mansfield^[4] in UK (Nobel Laureate in 2003), and R. Damadian in the USA^[5], (together with an approved patent for 'fonar', or magnetic imaging). The detailed physical theory of NMRI was published by Peter Mansfield in 1973^[6]. Unpublished 'high-resolution' (50 micron resolution) images of other living systems, such as hydrated wheat grains, were also obtained and communicated in UK in 1977-1979, and were subsequently confirmed by articles published in *Nature* by Peter Callaghan.

NMR Principle

Certain nuclei such as ^1H nuclei, or 'fermions' have spin-1/2, because there are two spin states, referred to as "up" and "down" states. The nuclear magnetic resonance absorption phenomenon occurs when samples containing such nuclear spins are placed in a static magnetic field and a very short radiofrequency pulse is applied with a center, or carrier, frequency matching that of the transition between the up and down states of the spin-1/2 ^1H nuclei that were polarized by the static magnetic field.^[7] Very low field schemes have also been recently reported.^[8]



Advanced 4.7 T clinical diagnostics and biomedical research NMR Imaging instrument.

Chemical Shifts

NMR is a very useful family of techniques for chemical and biochemical research because of the chemical shift; this effect consists in a frequency shift of the nuclear magnetic resonance for specific chemical groups or atoms as a result of the partial shielding of the corresponding nuclei from the applied, static external magnetic field by the electron orbitals (or molecular orbitals) surrounding such nuclei present in the chemical groups. Thus, the higher the electron density surrounding a specific nucleus the larger the chemical shift will be. The resulting magnetic field at the nucleus is thus lower than the applied external magnetic field and the resonance frequencies observed as a result of such shielding are lower than the value that would be observed in the absence of any electronic orbital shielding. Furthermore, in order to obtain a chemical shift value independent of the strength of the applied magnetic field and allow for the direct comparison of spectra obtained at different magnetic field values, the chemical shift is defined by the ratio of the strength of the local magnetic field value at the observed (electron orbital-shielded) nucleus by the external magnetic field strength, H_{loc}/H_0 . The first NMR observations of the chemical shift, with the correct physical chemistry interpretation, were reported for ^{19}F containing compounds in the early 1950s by Herbert S. Gutowsky and Charles P. Slichter from the University of Illinois at Urbana (USA).

A related effect in metals is called the Knight shift, which is due only to the conduction electrons. Such conduction electrons present in metals induce an "additional" local field at the nuclear site, due to the spin re-orientation of the conduction electrons in the presence of the applied (constant), external magnetic field. This is only broadly 'similar' to the chemical shift in either solutions or diamagnetic solids.

NMR Imaging Principles

A number of methods have been devised for combining magnetic field gradients and radiofrequency pulsed excitation to obtain an image. Two major methods involve either 2D-FT or 3D-FT^[9] reconstruction from projections, somewhat similar to Computed Tomography, with the exception of the image interpretation that in the former case must include dynamic and relaxation/contrast enhancement information as well. Other schemes involve building the NMR image either point-by-point or line-by-line. Some schemes use instead gradients in the rf field rather than in the static magnetic field. The majority of NMR images routinely obtained are either by the Two-Dimensional Fourier Transform (2D-FT) technique^[10] (with slice selection), or by the Three-Dimensional Fourier Transform (3D-FT) techniques that are however much more time consuming at present. 2D-FT NMRI is sometime called in common parlance a "spin-warp". An NMR image corresponds to a spectrum consisting of a number of 'spatial frequencies' at different locations in the sample investigated, or in a patient.^[11] A two-dimensional Fourier transformation of such a "real" image may be considered as a representation of such "real waves" by a matrix of spatial frequencies known as the k-space. We shall see next in some mathematical detail how the 2D-FT computation works to obtain 2D-FT NMR images.

Two-dimensional Fourier transform imaging and spectroscopy

A two-dimensional Fourier transform (2D-FT) is computed numerically or carried out in two stages, both involving 'standard', one-dimensional Fourier transforms. However, the second stage Fourier transform is not the inverse Fourier transform (which would result in the original function that was transformed at the first stage), but a Fourier transform in a second variable—which is 'shifted' in value—relative to that involved in the result of the first Fourier transform. Such 2D-FT analysis is a very powerful method for both NMRI and two-dimensional nuclear magnetic resonance spectroscopy (2D-FT NMRS)^[12] that allows the three-dimensional reconstruction of polymer and biopolymer structures at atomic resolution.^[13] for molecular weights (Mw) of dissolved biopolymers in aqueous solutions (for example) up to about 50,000 Mw. For larger biopolymers or polymers, more complex methods have been developed to obtain limited structural resolution needed for partial 3D-reconstructions of higher molecular structures, e.g. for up 900,000 Mw or even oriented microcrystals in aqueous suspensions or single crystals; such methods have also been reported for *in vivo* 2D-FT NMR spectroscopic studies of algae, bacteria, yeast and certain mammalian cells, including human ones. The 2D-FT method is also widely utilized in optical spectroscopy, such as *2D-FT NIR hyperspectral imaging* (2D-FT NIR-HS), or in MRI imaging for research and clinical, diagnostic applications in Medicine. In the latter case, 2D-FT NIR-HS has recently allowed the identification of single, malignant cancer cells surrounded by healthy human breast tissue at about 1 micron resolution, well-beyond the resolution obtainable by 2D-FT NMRI for such systems in the limited time available for such diagnostic investigations (and also in magnetic fields up to the FDA approved magnetic field strength H_0 of 4.7 T, as shown in the top image of the state-of-the-art NMRI instrument). A more precise mathematical definition of the 'double' (2D) Fourier transform involved in both 2D NMRI and 2D-FT NMRS is specified next, and a precise example follows this generally accepted definition.

2D-FT Definition

A 2D-FT, or two-dimensional Fourier transform, is a standard Fourier transformation of a function of two variables, $f(x_1, x_2)$, carried first in the first variable x_1 , followed by the Fourier transform in the second variable x_2 of the resulting function $F(s_1, x_2)$. Note that in the case of both 2D-FT NMRI and 2D-FT NMRS the two independent variables in this definition are in the time domain, whereas the results of the two successive Fourier transforms have, of course, frequencies as the independent variable in the NMRS, and ultimately spatial coordinates for both 2D NMRI and 2D-FT NMRS following computer structural reconstructions based on special algorithms that are different from FT or 2D-FT. Moreover, such structural algorithms are different for 2D NMRI and 2D-FT NMRS: in the former case they involve macroscopic, or anatomical structure determination, whereas in the latter case of 2D-FT NMRS the atomic structure reconstruction algorithms are based on the quantum theory of a microphysical (quantum) process such as nuclear Overhauser enhancement NOE, or specific magnetic dipole-dipole interactions^[14] between neighbor nuclei.

Example 1

A 2D Fourier transformation and phase correction is applied to a set of 2D NMR (FID) signals: $s(t_1, t_2)$ yielding a real 2D-FT NMR 'spectrum' (collection of 1D FT-NMR spectra) represented by a matrix \mathbf{S} whose elements are

$$S(\nu_1, \nu_2) = \text{Re} \int \int \cos(\nu_1 t_1) \exp(-i\nu_2 t_2) s(t_1, t_2) dt_1 dt_2$$

where ν_1 and ν_2 denote the discrete indirect double-quantum and single-quantum(detection) axes, respectively, in the 2D NMR experiments. Next, the covariance matrix is calculated in the frequency domain according to the following equation

$$C(\nu'_2, \nu_2) = S^T S = \sum_{\nu_1} [S(\nu_1, \nu'_2) S(\nu_1, \nu_2)], \text{ with } \nu_2, \nu'_2 \text{ taking all possible}$$

single-quantum frequency values and with the summation carried out over all discrete, double quantum frequencies ν_1 .

Example 2

Atomic Structure from 2D-FT STEM Images^[15] of electron distributions in a high-temperature cuprate superconductor 'paracrystal' reveal both the domains (or 'location') and the local symmetry of the 'pseudo-gap' in the electron-pair correlation band responsible for the high-temperature superconductivity effect (obtained at Cornell University). So far there have been three Nobel prizes awarded for 2D-FT NMR/MRI during 1992-2003, and an additional, earlier Nobel prize for 2D-FT of X-ray data ('CAT scans'); recently the advanced possibilities of 2D-FT techniques in Chemistry, Physiology and Medicine^[16] received very significant recognition.^[17]

Brief explanation of NMRI diagnostic uses in Pathology

As an example, a diseased tissue such as a malign tumor, can be detected by 2D-FT NMRI because the hydrogen nuclei of molecules in different tissues return to their equilibrium spin state at different relaxation rates, and also because of the manner in which a malign tumor spreads and grows rapidly along the blood vessels adjacent to the tumor, also inducing further vascularization to occur. By changing the pulse delays in the RF pulse

sequence employed, and/or the RF pulse sequence itself, one may obtain a 'relaxation—based contrast', or contrast enhancement between different types of body tissue, such as normal vs. diseased tissue cells for example. Excluded from such diagnostic observations by NMRI are all patients with ferromagnetic metal implants, (e.g., cochlear implants), and all cardiac pacemaker patients who cannot undergo any NMRI scan because of the very intense magnetic and RF fields employed in NMRI which would strongly interfere with the correct functioning of such pacemakers. It is, however, conceivable that future developments may also include along with the NMRI diagnostic treatments with special techniques involving applied magnetic fields and very high frequency RF. Already, surgery with special tools is being experimented on in the presence of NMR imaging of subjects. Thus, NMRI is used to image almost every part of the body, and is especially useful for diagnosis in neurological conditions, disorders of the muscles and joints, for evaluating tumors, such as in lung or skin cancers, abnormalities in the heart (especially in children with hereditary disorders), blood vessels, CAD, atherosclerosis and cardiac infarcts ^[18] (courtesy of Dr. Robert R. Edelman)

See also

- Nuclear magnetic resonance (NMR)
- Edward Mills Purcell
- Felix Bloch
- Medical imaging
- Paul C. Lauterbur
- Magnetic resonance microscopy
- Peter Mansfield
- Computed tomography (CT)
- Solid-state NMR
- Knight shift
- John Hasbrouck Van Vleck
- Chemical shift
- Herbert S. Gutowsky
- John S. Waugh
- Charles Pence Slichter
- Protein nuclear magnetic resonance spectroscopy
- Kurt Wüthrich
- Nuclear Overhauser effect
- Fourier transform spectroscopy(FTS)
- Jean Jeneer
- Richard R. Ernst
- Relaxation
- Earth's field NMR (EFNMR)
- Robinson oscillator
- FT-NIRS (NIR)
- Magnetic resonance elastography

Footnotes

- [1] Antoine Abragam. 1968. *Principles of Nuclear Magnetic Resonance.*, 895 pp., Cambridge University Press: Cambridge, UK.
- [2] Lauterbur, P.C., Nobel Laureate in 2003 (1973). "Image Formation by Induced Local Interactions: Examples of Employing Nuclear Magnetic Resonance". *Nature* **242**: 190-1. doi: 10.1038/242190a0 (<http://dx.doi.org/10.1038/242190a0>).
- [3] Howstuffworks "How MRI Works" (<http://www.howstuffworks.com/mri.htm/printable>)
- [4] Peter Mansfield. 2003. Nobel Laureate in Physiology and Medicine for (2D and 3D) MRI (<http://www.parteqinnovations.com/pdf-doc/fandr-Gaz1006.pdf>)
- [5] Damadian, R. V. "Tumor Detection by Nuclear Magnetic Resonance," *Science*, 171 (March 19, 1971): 1151-1153 (<http://www.sciencemag.org/cgi/content/abstract/171/3976/1151>)
- [6] NMR 'diffraction' in solids? P. Mansfield et al. 1973 *J. Phys. C: Solid State Phys.* 6 L422-L426 doi: 10.1088/0022-3719 (<http://www.iop.org/EJ/article/0022-3719/6/22/007/jcv6i22pL422.pdf>)
- [7] Antoine Abragam. 1968. *Principles of Nuclear Magnetic Resonance.*, 895 pp., Cambridge University Press: Cambridge, UK.
- [8] Raftery D (August 2006).
"http://www.pubmedcentral.nih.gov/articlerender.fcgi?tool=pmcentrez&artid=1568902|MRI without the magnet". *Proc Natl Acad Sci USA*. **103** (34): 12657-8. doi: 10.1073/pnas.0605625103 (<http://dx.doi.org/10.1073/pnas.0605625103>). PMID 16912110.
- [9] Wu Y, Chesler DA, Glimcher MJ, et al. (February 1999).
"http://www.pnas.org/cgi/pmidlookup?view=long&pmid=9990066|Multinuclear solid-state three-dimensional MRI of bone and synthetic calcium phosphates". *Proc. Natl. Acad. Sci. U.S.A.* **96** (4): 1574-8. doi: 10.1073/pnas.96.4.1574 (<http://dx.doi.org/10.1073/pnas.96.4.1574>). PMID 9990066. PMC: 15521 (<http://www.pubmedcentral.nih.gov/articlerender.fcgi?tool=pmcentrez&artid=15521>). <http://www.pnas.org/cgi/pmidlookup?view=long&pmid=9990066>.
- [10] http://www.math.cuhk.edu.hk/course/mat2071a/lec1_08.ppt
- [11] *Haacke, E Mark; Brown, Robert F; Thompson, Michael; Venkatesan, Ramesh (1999). *Magnetic resonance imaging: physical principles and sequence design*. New York: J. Wiley & Sons. ISBN 0-471-35128-8.
- [12] Richard R. Ernst. 1992. Nuclear Magnetic Resonance Fourier Transform (2D-FT) Spectroscopy. Nobel Lecture (http://nobelprize.org/nobel_prizes/chemistry/laureates/1991/ernst-lecture.pdf), on December 9, 1992.
- [13] http://en.wikipedia.org/wiki/Nuclear_magnetic_resonance#Nuclear_spin_and_magnets Kurt Wüthrich in 1982-1986 : 2D-FT NMR of solutions
- [14] Charles P. Slichter.1996. *Principles of Magnetic Resonance*. Springer: Berlin and New York, Third Edition., 651pp. ISBN 0-387-50157-6.
- [15] <http://www.physorg.com/news129395045.html>
- [16] http://nobelprize.org/nobel_prizes/chemistry/laureates/1991/ernst-lecture.pdf
- [17] Protein structure determination in solution by NMR spectroscopy (http://www.ncbi.nlm.nih.gov/entrez/query.fcgi?cmd=Retrieve&db=pubmed&dopt=Abstract&list_uids=2266107&query_hl=33&itool=pubmed_docsum) Kurt Wüthrich. *J Biol Chem*. 1990 December 25;265(36):22059-62.
- [18] <http://www.mr-tip.com/serv1.php?type=img&img=Cardiac%20Infarct%20Short%20Axis%20Cine%204>

References

- Antoine Abragam. 1968. *Principles of Nuclear Magnetic Resonance.*, 895 pp., Cambridge University Press: Cambridge, UK.
- Charles P. Slichter.1996. *Principles of Magnetic Resonance*. Springer: Berlin and New York, Third Edition., 651pp. ISBN 0-387-50157-6.
- Kurt Wüthrich. 1986, *NMR of Proteins and Nucleic Acids.*, J. Wiley and Sons: New York, Chichester, Brisbane, Toronto, Singapore. (Nobel Laureate in 2002 for 2D-FT NMR Studies of Structure and Function of Biological Macromolecules (http://nobelprize.org/nobel_prizes/chemistry/laureates/2002/wutrich-lecture.pdf)
- Protein structure determination in solution by NMR spectroscopy (http://www.ncbi.nlm.nih.gov/entrez/query.fcgi?cmd=Retrieve&db=pubmed&dopt=Abstract&list_uids=2266107&query_hl=33&itool=pubmed_docsum) Kurt Wüthrich. *J Biol Chem*.

1990 December 25;265(36):22059-62

- 2D-FT NMRI Instrument image: A JPG color image of a 2D-FT NMRI 'monster' Instrument (<http://upload.wikimedia.org/wikipedia/en/b/bf/HWB-NMRv900.jpg>).
- Richard R. Ernst. 1992. Nuclear Magnetic Resonance Fourier Transform (2D-FT) Spectroscopy. Nobel Lecture (http://nobelprize.org/nobel_prizes/chemistry/laureates/1991/ernst-lecture.pdf), on December 9, 1992.
- Peter Mansfield. 2003. Nobel Laureate in Physiology and Medicine for (2D and 3D) MRI (<http://www.parteqinnovations.com/pdf-doc/fandr-Gaz1006.pdf>)
- D. Benett. 2007. PhD Thesis. Worcester Polytechnic Institute. PDF of 2D-FT Imaging Applications to NMRI in Medical Research. (<http://www.wpi.edu/Pubs/ETD/Available/etd-081707-080430/unrestricted/dbennett.pdf>) Worcester Polytechnic Institute. (Includes many 2D-FT NMR images of human brains.)
- Paul Lauterbur. 2003. Nobel Laureate in Physiology and Medicine for (2D and 3D) MRI. (http://nobelprize.org/nobel_prizes/medicine/laureates/2003/)
- Jean Jeener. 1971. Two-dimensional Fourier Transform NMR, presented at an Ampere International Summer School, Basko Polje, unpublished. A verbatim quote follows from Richard R. Ernst's Nobel Laureate Lecture delivered on December 2, 1992, "A new approach to measure two-dimensional (2D) spectra." has been proposed by Jean Jeener at an Ampere Summer School in Basko Polje, Yugoslavia, 1971 (Jean Jeener, 1971)). He suggested a 2D Fourier transform experiment consisting of two $\pi/2$ pulses with a variable time t_1 between the pulses and the time variable t_2 measuring the time elapsed after the second pulse as shown in Fig. 6 that expands the principles of Fig. 1. Measuring the response $S(t_1, t_2)$ of the two-pulse sequence and Fourier-transformation with respect to both time variables produces a two-dimensional spectrum $S(O_1, O_2)$ of the desired form. This two-pulse experiment by Jean Jeener is the forefather of a whole class of 2D experiments that can also easily be expanded to multidimensional spectroscopy.
- Dudley, Robert, L (1993). "High-Field NMR Instrumentation". *Ch. 10 in Physical Chemistry of Food Processes* (New York: Van Nostrand-Reinhold) **2**: 421-30. ISBN 0-442-00582-2.
- Baianu, I.C.; Kumosinski, Thomas (August 1993). "NMR Principles and Applications to Structure and Hydration,". *Ch.9 in Physical Chemistry of Food Processes* (New York: Van Nostrand-Reinhold) **2**: 338-420. ISBN 0-442-00582-2.
- Haacke, E Mark; Brown, Robert F; Thompson, Michael; Venkatesan, Ramesh (1999). *Magnetic resonance imaging: physical principles and sequence design*. New York: J. Wiley & Sons. ISBN 0-471-35128-8.
- Raftery D (August 2006). "http://www.pubmedcentral.nih.gov/articlerender.fcgi?tool=pmcentrez&artid=1568902|MRI without the magnet". *Proc Natl Acad Sci USA*. **103** (34): 12657-8. doi: 10.1073/pnas.0605625103 (<http://dx.doi.org/10.1073/pnas.0605625103>). PMID 16912110.
- Wu Y, Chesler DA, Glimcher MJ, *et al.* (February 1999). "http://www.pnas.org/cgi/pmidlookup?view=long&pmid=9990066|Multinuclear solid-state three-dimensional MRI of bone and synthetic calcium phosphates". *Proc. Natl. Acad. Sci. U.S.A.* **96** (4): 1574-8. doi: 10.1073/pnas.96.4.1574 (<http://dx.doi.org/10.1073/pnas.96.4.1574>)

1073/pnas.96.4.1574). PMID 9990066. PMC: 15521 (<http://www.pubmedcentral.nih.gov/articlerender.fcgi?tool=pmcentrez&artid=15521>). <http://www.pnas.org/cgi/pmidlookup?view=long&pmid=9990066>.

External links

- Cardiac Infarct or "heart attack" Imaged in Real Time by 2D-FT NMRI (http://www.mr-tip.com/exam_gifs/cardiac_infarct_short_axis_cine_6.gif)
- Interactive Flash Animation on MRI (<http://www.e-mri.org>) - *Online Magnetic Resonance Imaging physics and technique course*
- Herbert S. Gutowsky
- Jiri Jonas and Charles P. Slichter: NMR Memoires at NAS about Herbert Sander Gutowsky; NAS = National Academy of Sciences, USA, (<http://books.nap.edu/html/biomems/hgutowsky.pdf>)
- 3D Animation Movie about MRI Exam (<http://www.patiencys.com/MRI/>)
- International Society for Magnetic Resonance in Medicine (<http://www.ismrm.org>)
- Danger of objects flying into the scanner (http://www.simplyphysics.com/flying_objects.html)

Related Wikipedia websites

- Medical imaging
- Computed tomography
- Magnetic resonance microscopy
- Fourier transform spectroscopy
- FT-NIRS
- Chemical imaging
- Magnetic resonance elastography
- Nuclear magnetic resonance (NMR)
- Chemical shift
- Relaxation
- Robinson oscillator
- Earth's field NMR (EFNMR)
- Rabi cycle

This article incorporates material by the original author from 2D-FT MR- Imaging and related Nobel awards (<http://planetphysics.org/encyclopedia/2DFTImaging.html>) on PlanetPhysics (<http://planetphysics.org/>), which is licensed under the GFDL.

Infrared spectroscopy







Infrared spectroscopy (IR spectroscopy) is the subset of spectroscopy that deals with the infrared region of the electromagnetic spectrum. It covers a range of techniques, the most common being a form of absorption spectroscopy. As with all spectroscopic techniques, it can be used to identify compounds or investigate sample composition. Infrared spectroscopy correlation tables are tabulated in the literature.

Background and Theory

The infrared portion of the electromagnetic spectrum is divided into three regions; the near-, mid- and far- infrared, named for their relation to the visible spectrum. The far-infrared, approximately $400\text{--}10\text{ cm}^{-1}$ ($1000\text{--}30\text{ }\mu\text{m}$), lying adjacent to the microwave region, has low energy and may be used for rotational spectroscopy. The mid-infrared, approximately $4000\text{--}400\text{ cm}^{-1}$ ($30\text{--}2.5\text{ }\mu\text{m}$) may be used to study the fundamental vibrations and associated rotational-vibrational structure. The higher energy near-IR, approximately $14000\text{--}4000\text{ cm}^{-1}$ ($2.5\text{--}0.8\text{ }\mu\text{m}$) can excite overtone or harmonic vibrations. The names and classifications of these subregions are merely conventions. They are neither strict divisions nor based on exact molecular or electromagnetic properties.

Infrared spectroscopy exploits the fact that molecules have specific frequencies at which they rotate or vibrate corresponding to discrete energy levels (vibrational modes). These resonant frequencies are determined by the shape of the molecular potential energy surfaces, the masses of the atoms and, by the associated vibronic coupling. In order for a vibrational mode in a molecule to be IR active, it must be associated with changes in the permanent dipole. In particular, in the Born-Oppenheimer and harmonic approximations, i.e. when the molecular Hamiltonian corresponding to the electronic ground state can be approximated by a harmonic oscillator in the neighborhood of the equilibrium molecular geometry, the resonant frequencies are determined by the normal modes corresponding to the molecular electronic ground state potential energy surface. Nevertheless, the resonant frequencies can be in a first approach related to the strength of the bond, and the mass of the atoms at either end of it. Thus, the frequency of the vibrations can be associated with a particular bond type.

Simple diatomic molecules have only one bond, which may stretch. More complex molecules have many bonds, and vibrations can be conjugated, leading to infrared absorptions at characteristic frequencies that may be related to chemical groups. For example, the atoms in a CH_2 group, commonly found in organic compounds can vibrate in six different ways: **symmetrical and antisymmetrical stretching, scissoring, rocking, wagging and twisting**:

Symmetrical stretching	Antisymmetrical stretching	Scissoring	Rocking	Wagging	Twisting
					

The infrared spectrum of a sample is collected by passing a beam of infrared light through the sample. Examination of the transmitted light reveals how much energy was absorbed at each wavelength. This can be done with a monochromatic beam, which changes in

wavelength over time, or by using a Fourier transform instrument to measure all wavelengths at once. From this, a transmittance or absorbance spectrum can be produced, showing at which IR wavelengths the sample absorbs. Analysis of these absorption characteristics reveals details about the molecular structure of the sample.

This technique works almost exclusively on samples with covalent bonds. Simple spectra are obtained from samples with few IR active bonds and high levels of purity. More complex molecular structures lead to more absorption bands and more complex spectra. The technique has been used for the characterization of very complex mixtures.

Sample preparation

Gaseous samples require little preparation beyond purification, but a sample cell with a long pathlength (typically 5-10 cm) is normally needed, as gases show relatively weak absorbances.

Liquid samples can be sandwiched between two plates of a high purity salt (commonly sodium chloride, or common salt, although a number of other salts such as potassium bromide or calcium fluoride are also used). The plates are transparent to the infrared light and will not introduce any lines onto the spectra. Some salt plates are highly soluble in water, so the sample and washing reagents must be anhydrous (without water).

Solid samples can be prepared in four major ways. The first is to crush the sample with a mulling agent (usually nujol) in a marble or agate mortar, with a pestle. A thin film of the mull is applied onto salt plates and measured.

The second method is to grind a quantity of the sample with a specially purified salt (usually potassium bromide) finely (to remove scattering effects from large crystals). This powder mixture is then crushed in a mechanical die press to form a translucent pellet through which the beam of the spectrometer can pass.

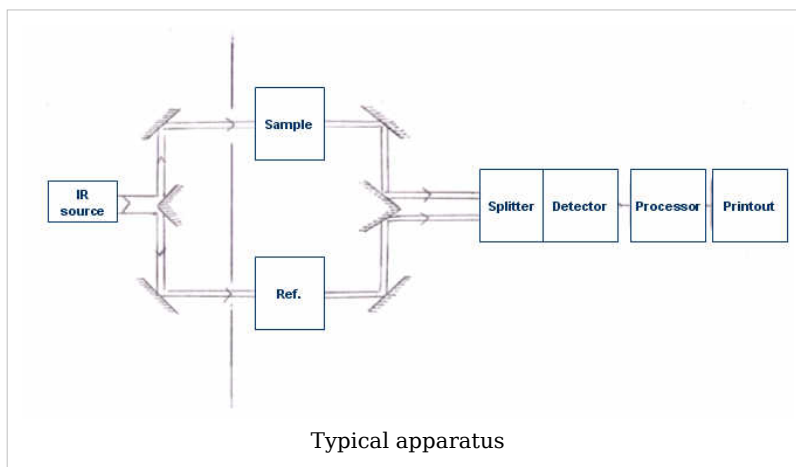
The third technique is the Cast Film technique, which is used mainly for polymeric materials. The sample is first dissolved in a suitable, non hygroscopic solvent. A drop of this solution is deposited on surface of KBr or NaCl cell. The solution is then evaporated to dryness and the film formed on the cell is analysed directly. Care is important to ensure that the film is not too thick otherwise light cannot pass through. This technique is suitable for qualitative analysis.

The final method is to use microtomy to cut a thin (20-100 micrometre) film from a solid sample. This is one of the most important ways of analysing failed plastic products for example because the integrity of the solid is preserved.

It is important to note that spectra obtained from different sample preparation methods will look slightly different from each other due to differences in the samples' physical states.

Typical method

A beam of infrared light is produced and split into two separate beams. One is passed through the sample, the other passed through a reference which is often the substance the sample is dissolved in. The beams are both reflected back towards a detector, however first they pass through a splitter which quickly alternates which of the two beams enters the detector.

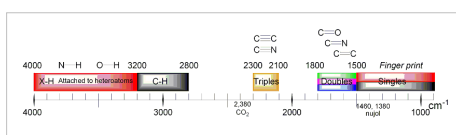


The two signals are then compared and a printout is obtained.

A reference is used for two reasons:

- This prevents fluctuations in the output of the source affecting the data
- This allows the effects of the solvent to be cancelled out (the reference is usually a pure form of the solvent the sample is in)

Summary of absorptions of bonds in organic molecules



Uses and applications

Infrared spectroscopy is widely used in both research and industry as a simple and reliable technique for measurement, quality control and dynamic measurement. It is of especial use in forensic analysis in both criminal and civil cases, enabling identification of polymer degradation for example. It is perhaps the most widely used method of applied spectroscopy.

The instruments are now small, and can be transported, even for use in field trials. With increasing technology in computer filtering and manipulation of the results, samples in solution can now be measured accurately (water produces a broad absorbance across the range of interest, and thus renders the spectra unreadable without this computer treatment). Some instruments will also automatically tell you what substance is being measured from a store of thousands of reference spectra held in storage.

By measuring at a specific frequency over time, changes in the character or quantity of a particular bond can be measured. This is especially useful in measuring the degree of polymerization in polymer manufacture. Modern research instruments can take infrared measurements across the whole range of interest as frequently as 32 times a second. This can be done whilst simultaneous measurements are made using other techniques. This makes the observations of chemical reactions and processes quicker and more accurate.

Techniques have been developed to assess the quality of tea-leaves using infrared spectroscopy. This will mean that highly trained experts (also called 'noses') can be used more sparingly, at a significant cost saving.^[1]

Infrared spectroscopy has been highly successful for applications in both organic and inorganic chemistry. Infrared spectroscopy has also been successfully utilized in the field of semiconductor microelectronics^[2]: for example, infrared spectroscopy can be applied to semiconductors like silicon, gallium arsenide, gallium nitride, zinc selenide, amorphous silicon, silicon nitride, etc.

Isotope effects

The different isotopes in a particular species may give fine detail in infrared spectroscopy. For example, the O-O stretching frequency of oxyhemocyanin is experimentally determined to be 832 and 788 cm⁻¹ for $\nu(^{16}\text{O}-^{16}\text{O})$ and $\nu(^{18}\text{O}-^{18}\text{O})$ respectively.

By considering the O-O as a spring, the wavelength of absorbance, ν can be calculated:

$$\nu = \frac{1}{2\pi} \sqrt{\frac{k}{\mu}}$$

where k is the spring constant for the bond, and μ is the reduced mass of the A-B system:

$$\mu = \frac{m_A m_B}{m_A + m_B}$$

(m_i is the mass of atom i).

The reduced masses for $^{16}\text{O}-^{16}\text{O}$ and $^{18}\text{O}-^{18}\text{O}$ can be approximated as 8 and 9 respectively. Thus

$$\frac{\nu_{^{16}\text{O}}}{\nu_{^{18}\text{O}}} = \sqrt{\frac{9}{8}} \approx \frac{832}{788}.$$

Fourier transform infrared spectroscopy

Fourier transform infrared (FTIR) spectroscopy is a measurement technique for collecting infrared spectra. Instead of recording the amount of energy absorbed when the frequency of the infra-red light is varied (monochromator), the IR light is guided through an interferometer. After passing through the sample, the measured signal is the interferogram. Performing a mathematical Fourier transform on this signal results in a spectrum identical to that from conventional (dispersive) infrared spectroscopy.

FTIR spectrometers are cheaper than conventional spectrometers because building of interferometers is easier than the fabrication of a monochromator. In addition, measurement of a single spectrum is faster for the FTIR technique because the information at all frequencies is collected simultaneously. This allows multiple samples to be collected and averaged together resulting in an improvement in sensitivity. Because of its various advantages, virtually all modern infrared spectrometers are FTIR instruments.

Two-dimensional infrared spectroscopy

Two-dimensional infrared correlation spectroscopy analysis is the application of 2D correlation analysis on infrared spectra. By extending the spectral information of a perturbed sample, spectral analysis is simplified and resolution is enhanced. The 2D synchronous and 2D asynchronous spectra represent a graphical overview of the spectral changes due to a perturbation (such as a changing concentration or changing temperature) as well as the relationship between the spectral changes at two different wavenumbers.

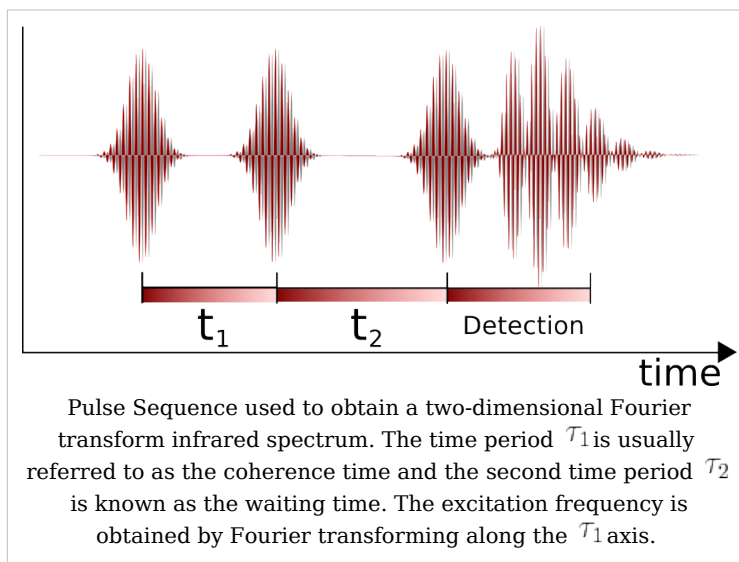
Nonlinear two-dimensional infrared spectroscopy^{[3] [4]}

is the infrared version of correlation spectroscopy.

Nonlinear two-dimensional infrared spectroscopy is a technique that has become available with the development of femtosecond infrared laser pulses. In this experiment first a set of pump pulses are applied to the sample. This is followed by a waiting time, where the system is allowed to relax. The waiting time typically lasts from zero to several

picooseconds and the duration can be controlled with a resolution of tens of femtoseconds. A probe pulse is then applied resulting in the emission of a signal from the sample. The nonlinear two-dimensional infrared spectrum is a two-dimensional correlation plot of the frequency ω_1 that was excited by the initial pump pulses and the frequency ω_3 excited by the probe pulse after the waiting time. This allows the observation of coupling between different vibrational modes. Because of its extremely high time resolution it can be used to monitor molecular dynamics on a picosecond timescale. It is still a largely unexplored technique and is becoming increasingly popular for fundamental research.

Like in two-dimensional nuclear magnetic resonance (2DNMR) spectroscopy this technique spreads the spectrum in two dimensions and allow for the observation of cross peaks that contain information on the coupling between different modes. In contrast to 2DNMR nonlinear two-dimensional infrared spectroscopy also involve the excitation to overtones. These excitations result in excited state absorption peaks located below the diagonal and cross peaks. In 2DNMR two distinct techniques, COSY and NOESY, are frequently used. The cross peaks in the first are related to the scalar coupling, while in the later they are related to the spin transfer between different nuclei. In nonlinear two-dimensional infrared spectroscopy analogs have been drawn to these 2DNMR techniques. Nonlinear two-dimensional infrared spectroscopy with zero waiting time corresponds to COSY and nonlinear two-dimensional infrared spectroscopy with finite waiting time allowing vibrational population transfer corresponds to NOESY. The COSY variant of nonlinear two-dimensional infrared spectroscopy has been used for determination of the secondary structure content proteins.^[5]



See also

- Infrared spectroscopy correlation table
- Fourier transform spectroscopy
- Near infrared spectroscopy
- Vibrational spectroscopy
- Rotational spectroscopy
- Time-resolved spectroscopy
- Spectroscopy
- Quantum vibration
- Raman spectroscopy
- Infrared microscopy
- Photothermal microspectroscopy
- Polymer degradation
- Infrared astronomy
- Far infrared astronomy
- Forensic chemistry
- Forensic engineering
- Forensic polymer engineering
- Forensic science
- Applied spectroscopy

References

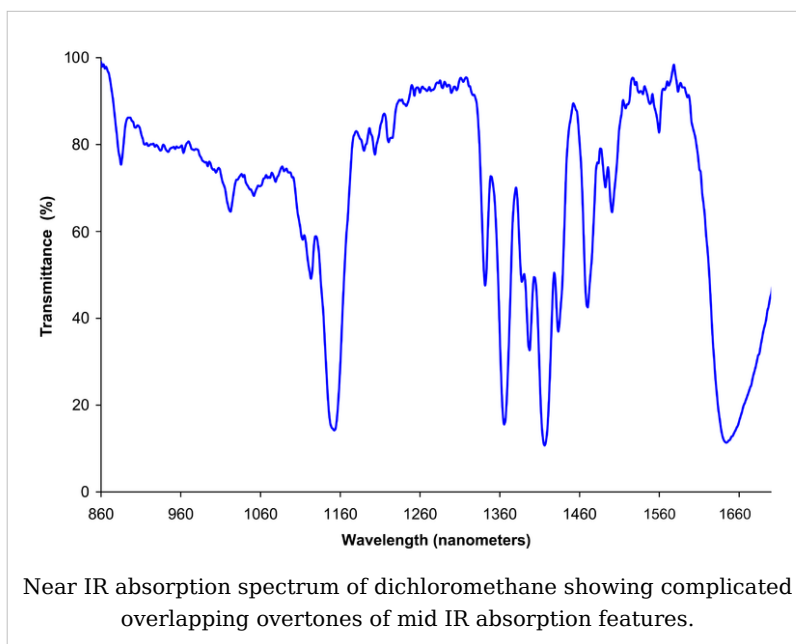
- [1] Luypaert, J.; Zhang, M.H.; Massart, D.L. (2003), "Feasibility study for the use of near infrared spectroscopy in the qualitative and quantitative analysis of green tea, *Camellia sinensis* (L.)", *Analytica Chimica Acta*, **478**(2), Elsevier, pp. 303–312
- [2] Lau, W.S. (1999). *Infrared characterization for microelectronics*. World Scientific.
- [3] P. Hamm, M. H. Lim, R. M. Hochstrasser (1998). "Structure of the amide I band of peptides measured by femtosecond nonlinear-infrared spectroscopy". *J. Phys. Chem. B* **102**: 6123. doi: 10.1021/jp9813286 (<http://dx.doi.org/10.1021/jp9813286>).
- [4] S. Mukamel (2000). "Multidimensional Femtosecond Correlation Spectroscopies of Electronic and Vibrational Excitations". *Annual Review of Physics and Chemistry* **51**: 691. doi: 10.1146/annurev.physchem.51.1.691 (<http://dx.doi.org/10.1146/annurev.physchem.51.1.691>).
- [5] N. Demirdöven, C. M. Cheatum, H. S. Chung, M. Khalil, J. Knoester, A. Tokmakoff (2004). "Two-dimensional infrared spectroscopy of antiparallel beta-sheet secondary structure". *Journal of the American Chemical Society* **126**: 7981. doi: 10.1021/ja049811j (<http://dx.doi.org/10.1021/ja049811j>).

External links

- A useful gif animation of different vibrational modes: here (<http://www.shu.ac.uk/schools/sci/chem/tutorials/molspec/irspec1.htm>)
- Infrared spectroscopy for organic chemists (<http://www.organicworldwide.net/infrared>)
- Organic compounds spectrum database (http://riodb01.ibase.aist.go.jp/sdbs/cgi-bin/cre_index.cgi?lang=eng)

Near infrared spectroscopy

Near infrared spectroscopy (NIRS) is a spectroscopic method which uses the near infrared region of the electromagnetic spectrum (from about 800 nm to 2500 nm). Typical applications include pharmaceutical, medical diagnostics (including blood sugar and oximetry), food and agrochemical quality control, as well as combustion research.



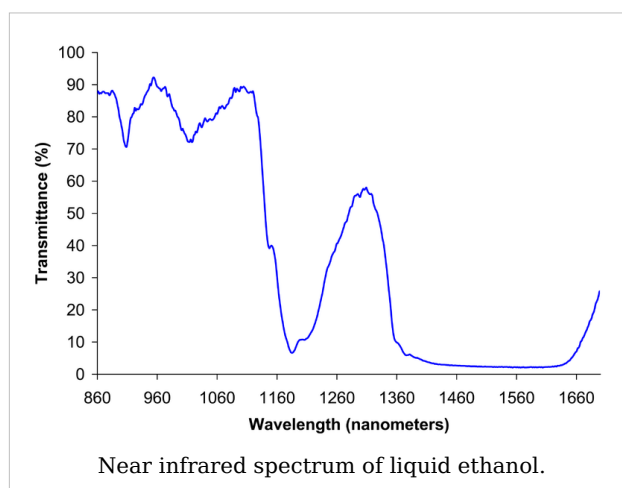
Theory

Near infrared spectroscopy is based on molecular overtone and combination vibrations. Such transitions are forbidden by the selection rules of quantum mechanics. As a result, the molar absorptivity in the near IR region is typically quite small. One advantage is that NIR can typically penetrate much farther into a sample than mid infrared radiation. Near infrared spectroscopy is therefore not a particularly sensitive technique, but it can be very useful in probing bulk material with little or no sample preparation.

The molecular overtone and combination bands seen in the near IR are typically very broad, leading to complex spectra; it can be difficult to assign specific features to specific chemical components. Multivariate (multiple wavelength) calibration techniques (e.g., principal components analysis or partial least squares) are often employed to extract the desired chemical information. Careful development of a set of calibration samples and application of multivariate calibration techniques is essential for near infrared analytical methods.

History

The discovery of near-infrared energy is ascribed to Herschel in the 19th century, but the first industrial application began in the 1950s. In the first applications, NIRS was used only as an add-on unit to other optical devices that used other wavelengths such as ultraviolet (UV), visible (Vis), or mid-infrared (MIR) spectrometers. In the 1980s, a single unit, stand-alone NIRS system was made available, but the application of NIRS was focused more on chemical analysis. With the introduction of light-fiber optics in the mid 80s and the monochromator-detector developments in early nineties, NIRS became a more powerful tool for scientific research.



This optical method can be used in a number of fields of science including physics, physiology, or medicine. It was only in the last few decades that NIRS began to be used as a medical tool for monitoring patients.

Medical uses

Medical applications of NIRS center on the non-invasive measurement of the amount and oxygen content of hemoglobin.

NIRS can be used for non-invasive assessment of brain function through the intact skull in human subjects by detecting changes in blood hemoglobin concentrations associated with neural activity, e.g. in branches of Cognitive psychology as a partial replacement for fMRI techniques. NIRS can be used on infants, where fMRI cannot (at least in the United States), and NIRS is much more portable than fMRI machines, even wireless instrumentation is available, which enables investigations in freely moving subjects^[1]). However, NIRS cannot fully replace fMRI because it can only be used to scan cortical tissue, where fMRI can be used to measure activation throughout the brain.

The application in functional mapping of the human cortex is called optical topography (OT), near infrared imaging (NIRI) or functional NIRS (fNIRS). The term optical tomography is used for three-dimensional NIRS. The terms NIRS, NIRI and OT are often used interchangeably, but they have some distinctions. The most important difference between NIRS and OT/NIRI is that OT/NIRI is mainly used to detect changes in optical properties of tissue simultaneously from multiple measurement points and display the results in the form of a map or image over a specific area, whereas NIRS provides quantitative data in absolute terms on up to a few specific points. The latter is also used to investigate other tissues such as e.g. muscle, breast, and tumors.

By employing several wavelengths and time resolved (frequency or time domain) and/or spatially resolved methods blood flow, volume and oxygenation can be quantified^[2]. These measurements are a form of oximetry. Applications of oximetry by NIRS methods include the detection of illnesses which affect the blood circulation (e.g. peripheral vascular disease), the detection and assessment of breast tumors, and the optimization of training in

sports medicine.

NIRS is starting to be used in pediatric critical care, to help deal with cardiac surgery post-op. Indeed, NIRS is able to measure venous oxygen saturation (SVO₂), which is determined by the cardiac output, as well as other parameters (FiO₂, hemoglobin, oxygen uptake). Therefore, following the NIRS gives critical care physicians a notion of the cardiac output. NIRS is liked by patients, because it is non-invasive, painless and uses non-ionizing radiation.

The instrumental development of NIRS/NIRI/OT has proceeded tremendously during the last years and in particular in terms of quantification, imaging and miniaturisation^[3].

Industrial Uses

As opposed to NIRS used in optical topography, general NIRS used in chemical assays does not provide imaging by mapping. For example, a clinical CO₂ analyzer requires reference techniques and calibration routines to be able to get accurate CO₂ content change. In this case, calibration is performed by adjusting the zero control of the sample being tested after purposefully supplying 0% CO₂ or another known amount of CO₂ in the sample. Normal compressed gas from distributors contains about 95% O₂ and 5% CO₂ which can also be used to adjust %CO₂ meter reading to be exactly 5% at initial calibration.

Instrumentation

Instrumentation for near-IR (NIR) spectroscopy is partially similar to instruments for the visible and mid-IR ranges. There is a source, a detector, and a dispersive element (such as a prism, or more commonly a diffraction grating) to allow the intensity at different wavelengths to be recorded. Fourier transform NIR instruments using an interferometer are also common, especially for wavelengths above ~1000 nm. Depending on the sample, the spectrum can be measured in either in reflection or transmission.

Common incandescent or quartz halogen light bulbs are most often used as broadband sources of near infrared radiation for analytical applications. Light-emitting diodes (LEDs) are also used; they offer greater lifetime and spectral stability and reduced power requirements.^[4]

The type of detector used depends primarily on the range of wavelengths to be measured. Silicon-based CCDs are suitable for the shorter end of the NIR range, but are not sufficiently sensitive over most of the range. InGaAs and PbS devices are more suitable. In certain diode array (DA) NIRS instruments, both silicon-based and InGaAs detectors are employed in the same instrument. Such instruments can record both visible and NIR spectra 'simultaneously'.

Instruments intended for chemical imaging in the NIR may use a 2D array detector with a acousto-optic tunable filter. Multiple images may be recorded sequentially at different narrow wavelength bands.^[5]

Many commercial instruments for UV/vis spectroscopy are capable of recording spectra in the NIR range (to perhaps ~900 nm). In the same way, the range of some mid-IR instruments may extend into the NIR. In these instruments the detector used for the NIR wavelengths is often the same detector used for the instrument's "main" range of interest.

Applications

The primary application of NIRS to the human body uses the fact that the transmission and absorption of NIR light in human body tissues contains information about hemoglobin concentration changes. When a specific area of the brain is activated, the localized blood volume in that area changes quickly. Optical imaging can measure the location and activity of specific regions of the brain by continuously monitoring blood hemoglobin levels through the determination of optical absorption coefficients.

Typical applications of NIR spectroscopy include the analysis of foodstuffs, pharmaceuticals, combustion products and a major branch of astronomical spectroscopy.

Astronomical spectroscopy

Near-infrared spectroscopy is used in astronomy for studying the atmospheres of cool stars where molecules can form. The vibrational and rotational signatures of molecules such as titanium oxide, cyanide and carbon monoxide can be seen in this wavelength range and can give a clue towards the star's spectral type. It is additionally used for studying molecules in other astronomical contexts, such as in molecular clouds where new stars are formed. The astronomical phenomenon known as reddening means that near-infrared wavelengths are less affected by dust in the interstellar medium, such that regions inaccessible by optical spectroscopy can be studied in the near-infrared. Since dust and gas are strongly associated, these dusty regions are exactly those where infrared spectroscopy is most useful. The near-infrared spectra of very young stars provide important information about their ages and masses, which is important for understanding star formation in general.

Remote monitoring

Techniques have been developed for NIR spectroscopic imaging. These have been used for a wide range of uses, including the remote investigation of plants and soils. Data can be collected from instruments on airplanes or satellites to assess ground cover and soil chemistry.

Medical uses

See above

Particle measurement

NIR is often used in particle sizing in a range of different fields, including studying pharmaceutical and agricultural powders.

See also

- fNIR
 - Fourier transform spectroscopy
 - FT-NIRS
 - Infrared spectroscopy
 - Vibrational spectroscopy
 - Rotational spectroscopy
 - Spectroscopy
 - Chemical Imaging
-

- Optical imaging

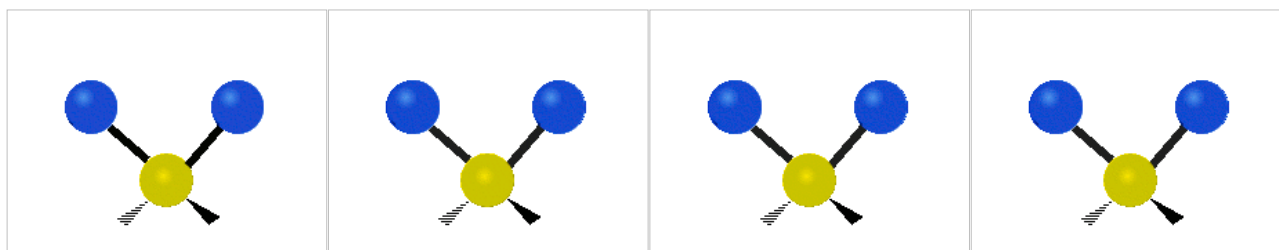
References

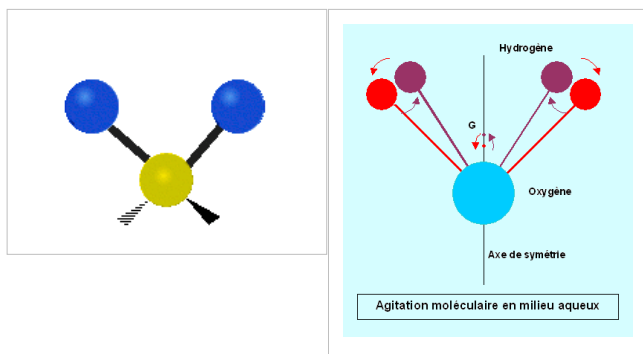
- Kouli, M.: "Experimental investigations of non invasive measuring of cerebral blood flow in adult human using the near infrared spectroscopy." Dissertation, Technical University of Munich, December 2001.
- [1] Muehleemann T, et al. Wireless miniaturized in-vivo near infrared imaging. *Opt. Express* 2008; 16, 10323-10330
- [2] Wolf M, et al. Progress of near infrared spectroscopy and imaging instrumentation for brain and muscle clinical applications. *J. Biomed. Opt.* 2007; 12, 062104. Review
- [3] Wolf M, et al. Progress of near infrared spectroscopy and imaging instrumentation for brain and muscle clinical applications. *J. Biomed. Opt.* 2007; 12, 062104. Review
- [4] Alper Bozkurt et al., *Biomedical Engineering Online* 2005, **4**:29 (doi: 10.1186/1475-925X-4-29 (<http://dx.doi.org/10.1186/1475-925X-4-29>))
- [5] Treado, P. J.; Levin, I. W.; Lewis, E. N. (1992). "Near-Infrared Acousto-Optic Filtered Spectroscopic Microscopy: A Solid-State Approach to Chemical Imaging". *Applied Spectroscopy* **46**: 553-559. doi: 10.1366/0003702924125032 (<http://dx.doi.org/10.1366/0003702924125032>).

Vibrational circular dichroism

Vibrational circular dichroism (VCD) spectroscopy is basically circular dichroism spectroscopy in the infrared and near infrared ranges^[1]. Because VCD is sensitive to the mutual orientation of distinct groups in a molecule, it provides three-dimensional structural information. Thus, it is a powerful technique as VCD spectra of enantiomers can be simulated using *ab initio* calculations, thereby allowing the identification of absolute configurations of small molecules in solution from VCD spectra. Among such quantum computations of VCD spectra resulting from the chiral properties of small organic molecules are those based on density functional theory (DFT) and gauge-invariant atomic orbitals (GIAO). As a simple example of the experimental results that were obtained by VCD are the spectral data obtained within the carbon-hydrogen (C-H) stretching region of 21 amino acids in heavy water solutions. Measurements of vibrational optical activity (VOA) have thus numerous applications, not only for small molecules, but also for large and complex biopolymers such as muscle proteins (myosin, for example) and DNA.

Vibrational modes

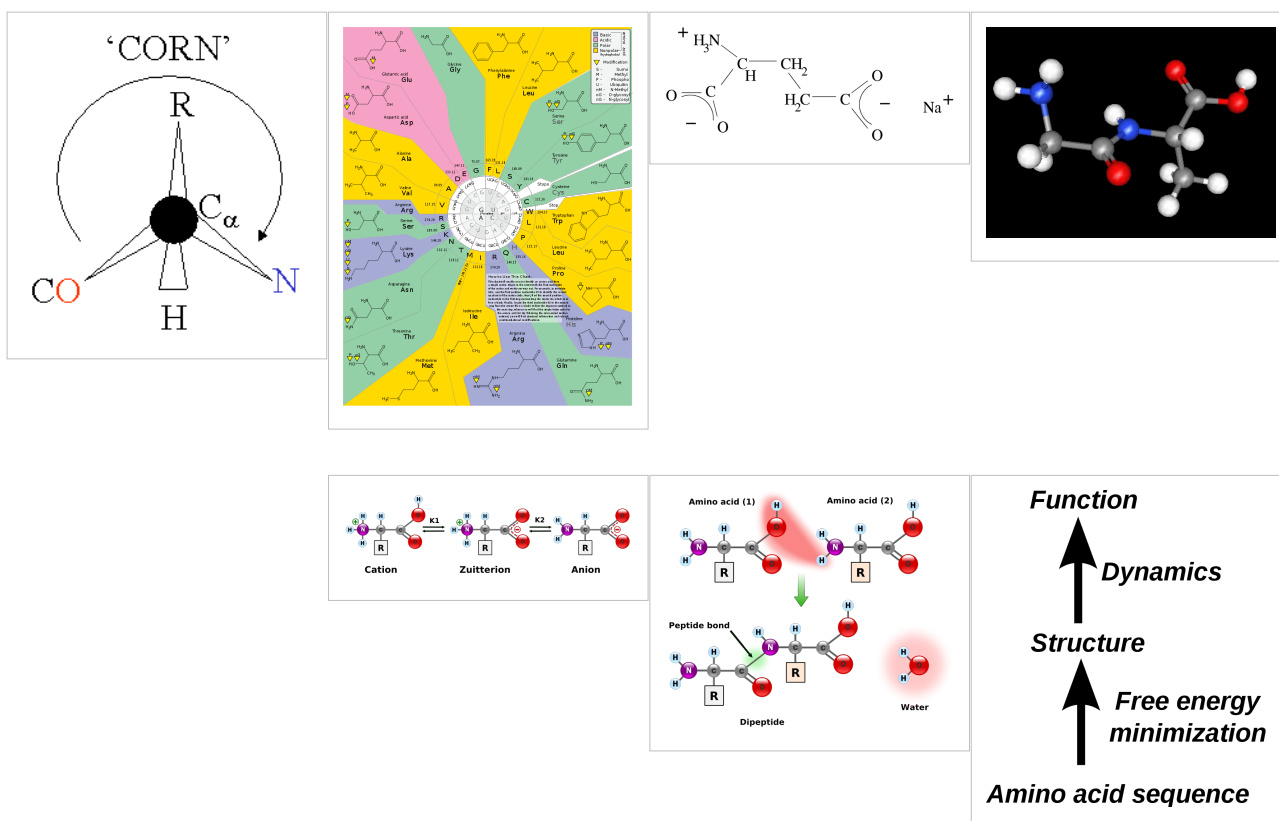


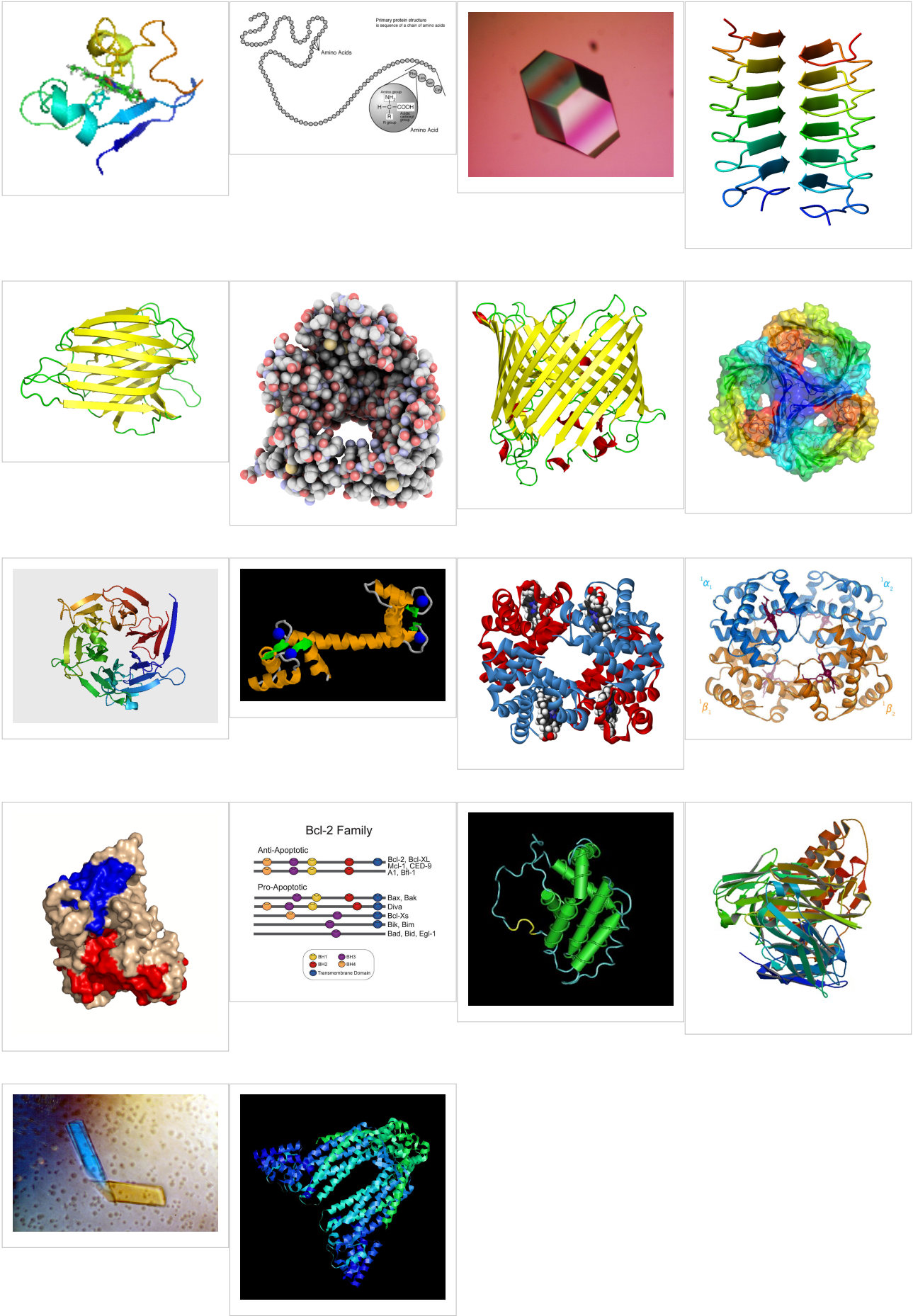


VCD of peptides and proteins

Extensive VCD studies have been reported for both polypeptides and several proteins in solution^{[2] [3] [4]}; several recent reviews were also compiled^{[5] [6] [7] [8]}. An extensive but not comprehensive VCD publications list is also provided in the "References" section. The published reports over the last 22 years have established VCD as a powerful technique with improved results over those previously obtained by visible/UV circular dichroism (CD) or optical rotatory dispersion (ORD) for proteins and nucleic acids.

Amino acid and polypeptide structures



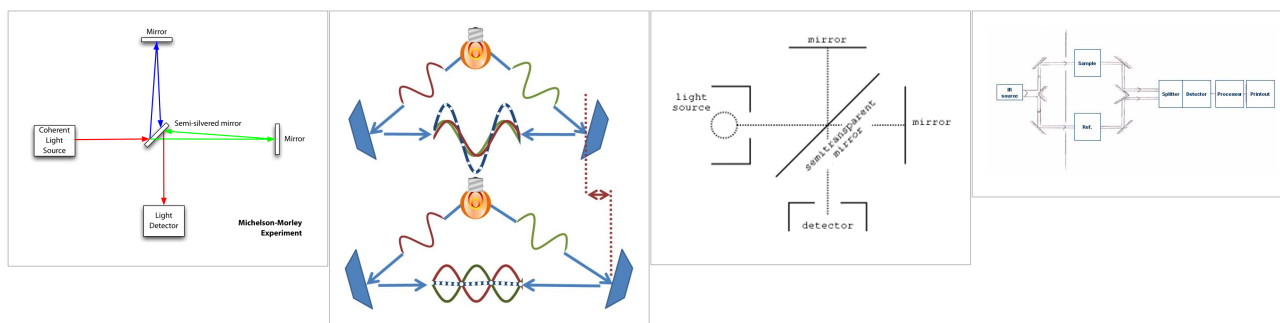


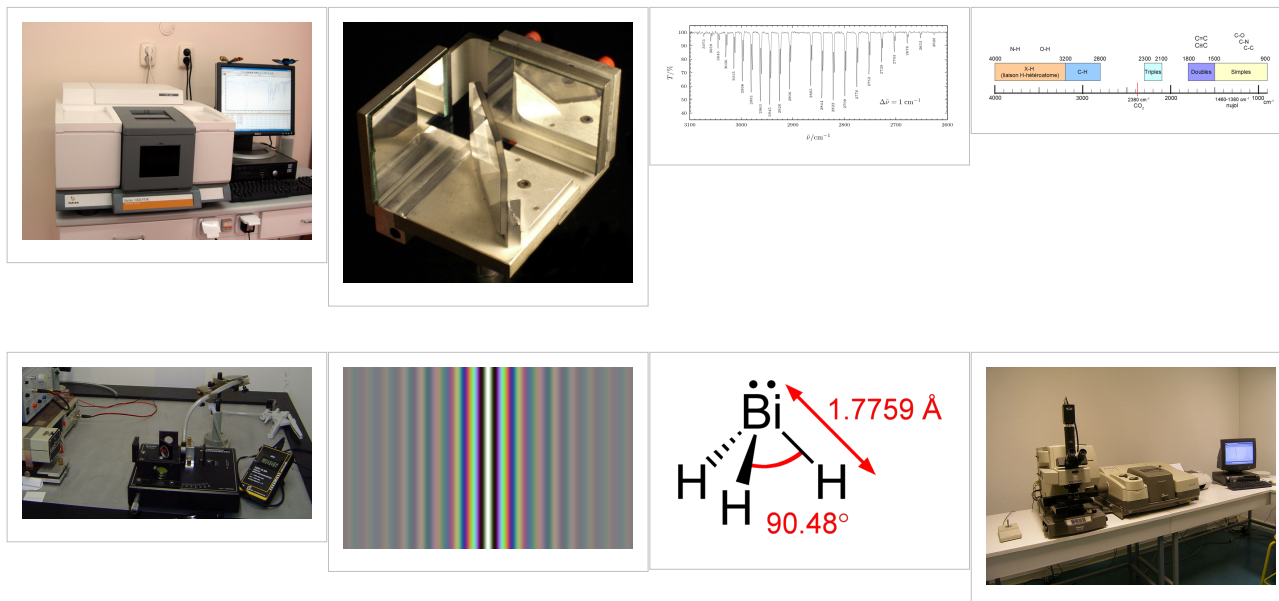
VCD of nucleic acids

VCD spectra of nucleotides, synthetic polynucleotides and several nucleic acids, including DNA, have been reported and assigned in terms of the type and number of helices present in A-, B-, and Z- DNA.

VCD Instrumentation

For biopolymers such as proteins and nucleic acids, the difference in absorbance between the levo- and dextro- configurations is five orders of magnitude smaller than the corresponding (unpolarized) absorbance. Therefore, VCD of biopolymers requires the use of very sensitive, specially built instrumentation as well as time-averaging over relatively long intervals of time even with such sensitive VCD spectrometers. Most CD instruments produce left- and right- circularly polarized light which is then either sine-wave or square-wave modulated, with subsequent phase-sensitive detection and lock-in amplification of the detected signal. In the case of FT-VCD, a photo-elastic modulator (PEM) is employed in conjunction with an FT-IR interferometer set-up. An example is that of a Bomem model MB-100 FT-IR interferometer equipped with additional polarizing optics/accessories needed for recording VCD spectra. A parallel beam emerges through a side port of the interferometer which passes first through a wire grid linear polarizer and then through an octagonal-shaped ZnSe crystal PEM which modulates the polarized beam at a fixed, lower frequency such as 37.5 kHz. A mechanically stressed crystal such as ZnSe exhibits birefringence when stressed by an adjacent piezoelectric transducer. The linear polarizer is positioned close to, and at 45 degrees, with respect to the ZnSe crystal axis. The polarized radiation focused onto the detector is doubly modulated, both by the PEM and by the interferometer setup. A very low noise detector, such as MCT (HgCdTe), is also selected for the VCD signal phase-sensitive detection. Quasi-complete commercial FT-VCD instruments are also available from a few manufacturers but these are quite expensive and also have to be still considered as being at the prototype stage. To prevent detector saturation an appropriate, long wave pass filter is placed before the very low noise MCT detector, which allows only radiation below 1750 cm^{-1} to reach the MCT detector; the latter however measures radiation only down to 750 cm^{-1} . FT-VCD spectra accumulation of the selected sample solution is then carried out, digitized and stored by an in-line computer. Published reviews that compare various VCD methods are also available.^{[9] [10]}





Magnetic VCD

VCD spectra have also been reported in the presence of an applied external magnetic field^[11]. This method can enhance the VCD spectral resolution for small molecules^[12] [13] [14] [15] [16].

Raman optical activity (ROA)

ROA is a technique complementary to VCD especially useful in the 50–1600 cm⁻¹ spectral region; it is considered as the technique of choice for determining optical activity for photon energies less than 600 cm⁻¹.

Notes

- [1] <http://planetphysics.org/?op=getobj;from=objects;id=410> Principles of IR and NIR Spectroscopy
- [2] "Vibrational Circular Dichroism of Polypeptides XII. Re-evaluation of the Fourier Transform Vibrational Circular Dichroism of Poly-gamma-Benzyl-L-Glutamate," P. Malon, R. Kobrinskaya, T. A. Keiderling, *Biopolymers* 27, 733-746 (1988).
- [3] "Vibrational Circular Dichroism of Biopolymers," T. A. Keiderling, S. C. Yasui, U. Narayanan, A. Annamalai, P. Malon, R. Kobrinskaya, L. Yang, in *Spectroscopy of Biological Molecules New Advances* ed. E. D. Schmid, F. W. Schneider, F. Siebert, p. 73-76 (1988).
- [4] "Vibrational Circular Dichroism of Polypeptides and Proteins," S. C. Yasui, T. A. Keiderling, *Mikrochimica Acta*, II, 325-327, (1988).
- [5] "Vibrational Circular Dichroism of Proteins Polysaccharides and Nucleic Acids" T. A. Keiderling, Chapter 8 in *Physical Chemistry of Food Processes, Vol. 2 Advanced Techniques, Structures and Applications.*, eds. I.C. Baianu, H. Pessen, T. Kumosinski, Van Norstrand-Reinhold, New York (1993), pp 307-337.
- [6] "Spectroscopic characterization of Unfolded peptides and proteins studied with infrared absorption and vibrational circular dichroism spectra" T. A. Keiderling and Qi Xu, *Advances in Protein Chemistry Volume 62*, [Unfolded Proteins, Dedicated to John Edsall, Ed.: George Rose, Academic Press:New York] (2002), pp. 111-161.
- [7] "Protein and Peptide Secondary Structure and Conformational Determination with Vibrational Circular Dichroism " Timothy A. Keiderling, *Current Opinions in Chemical Biology* (Ed. Julie Leary and Mark Arnold) 6, 682-688 (2002).
- [8] *Review: Conformational Studies of Peptides with Infrared Techniques. Timothy A. Keiderling and R. A. G. D. Silva, in *Synthesis of Peptides and Peptidomimetics*, Ed. M. Goodman and G. Herrman, Houben-Weyl, Vol 22Eb, Georg Thiem Verlag, New York (2002) pp. 715-738, (written and accepted in 2000).

- [9] "Polarization Modulation Fourier Transform Infrared Spectroscopy with Digital Signal Processing: Comparison of Vibrational Circular Dichroism Methods." Jovencio Hilario, David Drapcho, Raul Curbelo, Timothy A. Keiderling, *Applied Spectroscopy* 55, 1435-1447 (2001)--
- [10] "Vibrational circular dichroism of biopolymers. Summary of methods and applications.", Timothy A. Keiderling, Jan Kubelka, Jovencio Hilario, in *Vibrational spectroscopy of polymers and biological systems*, Ed. Mark Braiman, Vasilis Gregoriou, Taylor & Francis, Atlanta (CRC Press, Boca Raton, FL) (2006) pp. 253-324 (originally written in 2000, updated in 2003)
- [11] "Observation of Magnetic Vibrational Circular Dichroism," T. A. Keiderling, *Journal of Chemical Physics*, 75, 3639-41 (1981).
- [12] "Vibrational Spectral Assignment and Enhanced Resolution Using Magnetic Vibrational Circular Dichroism," T. R. Devine and T. A. Keiderling, *Spectrochimica Acta*, 43A, 627-629 (1987).
- [13] "Magnetic Vibrational Circular Dichroism with an FTIR" P. V. Croatto, R. K. Yoo, T. A. Keiderling, SPIE Proceedings 1145 (7th International Conference on FTS, ed. D. G. Cameron) 152-153 (1989).
- [14] "Direct Measurement of the Rotational g-Value in the Ground State of Acetylene by Magnetic Vibrational Circular Dichroism." C. N. Tam and T. A. Keiderling, *Chemical Physics Letters*, 243, 55-58 (1995).
- [15] "Ab initio calculation of the vibrational magnetic dipole moment" P. Bour, C. N. Tam, T. A. Keiderling, *Journal of Physical Chemistry* 99, 17810-17813 (1995)
- [16] "Rotationally Resolved Magnetic Vibrational Circular Dichroism. Experimental Spectra and Theoretical Simulation for Diamagnetic Molecules." P. Bour, C. N. Tam, B. Wang, T. A. Keiderling, *Molecular Physics* 87, 299-318, (1996).

References

Peptides and proteins

- Huang R, Wu L, McElheny D, Bour P, Roy A, Keiderling TA. Cross-Strand Coupling and Site-Specific Unfolding Thermodynamics of a Trpzip beta-Hairpin Peptide Using (13)C Isotopic Labeling and IR Spectroscopy. *The journal of physical chemistry. B*. 2009 Apr;113(16):5661-74.
- "Vibrational Circular Dichroism of Poly alpha-Benzyl-L-Glutamate," R. D. Singh, and T. A. Keiderling, *Biopolymers*, 20, 237-40 (1981).
- "Vibrational Circular Dichroism of Polypeptides II. Solution Amide II and Deuteration Results," A. C. Sen and T. A. Keiderling, *Biopolymers*, 23, 1519-32 (1984).
- "Vibrational Circular Dichroism of Polypeptides III. Film Studies of Several alpha-Helical and β -Sheet Polypeptides," A. C. Sen and T. A. Keiderling, *Biopolymers*, 23, 1533-46 (1984).
- "Vibrational Circular Dichroism of Polypeptides IV. Film Studies of L-Alanine Homologous Oligopeptides," U. Narayanan, T. A. Keiderling, G. M. Bonora, and C. Toniolo, *Biopolymers* 24, 1257-63 (1985).
- "Vibrational Circular Dichroism of Polypeptides, T. A. Keiderling, S. C. Yasui, A. C. Sen, C. Toniolo, G. M. Bonora, in *Peptides Structure and Function*, Proceedings of the 9th American Peptide Symposium," ed. C. M. Deber, K. Kopple, V. Hruby; Pierce Chemical: Rockford, IL; 167-172 (1985).
- "Vibrational Circular Dichroism of Polypeptides V. A Study of 310 Helical-Octapeptides" S. C. Yasui, T. A. Keiderling, G. M. Bonora, C. Toniolo, *Biopolymers* 25, 79-89 (1986).
- "Vibrational Circular Dichroism of Polypeptides VI. Polytyrosine alpha-helical and Random Coil Results," S. C. Yasui and T. A. Keiderling, *Biopolymers* 25, 5-15 (1986).
- "Vibrational Circular Dichroism of Polypeptides VII. Film and Solution Studies of alpha-forming Homologous Oligopeptides," U. Narayanan, T. A. Keiderling, G. M. Bonora, C. Toniolo, *Journal of the American Chemical Society*, 108, 2431-2437 (1986).
- "Vibrational Circular Dichroism of Polypeptides VIII. Poly Lysine Conformations as a Function of pH in Aqueous Solution," S. C. Yasui, T. A. Keiderling, *Journal of the*

- American Chemical Society, 108, 5576-5581 (1986).
- "Vibrational Circular Dichroism of Polypeptides IX. A Study of Chain Length Dependence for 310-Helix Formation in Solution." S. C. Yasui, T. A. Keiderling, F. Formaggio, G. M. Bonora, C. Toniolo, *Journal of the American Chemical Society* 108, 4988-4993 (1986).
 - "Vibrational Circular Dichroism of Biopolymers." T. A. Keiderling, *Nature*, 322, 851-852 (1986).
 - "Vibrational Circular Dichroism of Polypeptides X. A Study of alpha-Helical Oligopeptides in Solution." S. C. Yasui, T. A. Keiderling, R. Katachai, *Biopolymers* 26, 1407-1412 (1987).
 - "Vibrational Circular Dichroism of Polypeptides XI. Conformation of Poly(L-Lysine(Z)-L-Lysine(Z)-L-1-Pyrenylalanine) and Poly(L-Lysine(Z)-L-Lysine(Z)-L-1-Naphthylalanine) in Solution" S. C. Yasui, T. A. Keiderling, and M. Sisido, *Macromolecules* 20, 2403-2406 (1987).
 - "Vibrational Circular Dichroism of Biopolymers" T. A. Keiderling, S. C. Yasui, A. C. Sen, U. Narayanan, A. Annamalai, P. Malon, R. Kobrinskaya, L. Yang, in "F.E.C.S. Second International Conference on Circular Dichroism, Conference Proceedings," ed. M. Kajtar, L. Eötvös Univ., Budapest, 1987, p. 155-161.
 - "Vibrational Circular Dichroism of Poly-L-Proline and Other Helical Poly-peptides," R. Kobrinskaya, S. C. Yasui, T. A. Keiderling, in "Peptides: Chemistry and Biology, Proceedings of the 10th American Peptide Symposium," ed. G. R. Marshall, ESCOM, Leiden, 1988, p. 65-67.
 - "Vibrational Circular Dichroism of Polypeptides with Aromatic Side Chains," S. C. Yasui, T. A. Keiderling, in "Peptides: Chemistry and Biology, Proceedings of the 10th American Peptide Symposium," ed. G. R. Marshall, ESCOM, Leiden, 1988, p. 90-92.
 - "Vibrational Circular Dichroism of Polypeptides XII. Re-evaluation of the Fourier Transform Vibrational Circular Dichroism of Poly-gamma-Benzyl-L-Glutamate," P. Malon, R. Kobrinskaya, T. A. Keiderling, *Biopolymers* 27, 733-746 (1988).
 - "Vibrational Circular Dichroism of Biopolymers," T. A. Keiderling, S. C. Yasui, U. Narayanan, A. Annamalai, P. Malon, R. Kobrinskaya, L. Yang, in *Spectroscopy of Biological Molecules New Advances* ed. E. D. Schmid, F. W. Schneider, F. Siebert, p. 73-76 (1988).
 - "Vibrational Circular Dichroism of Polypeptides and Proteins," S. C. Yasui, T. A. Keiderling, *Mikrochimica Acta*, II, 325-327, (1988).
 - "(1R,7R)-7-Methyl-6,9,-Diazatricyclo[6,3,0,01,6]Tridecane-5,10-Dione, A Tricyclic Spirodilactam Containing Non-planar Amide Groups: Synthesis, NMR, Crystal Structure, Absolute Configuration, Electronic and Vibrational Circular Dichroism" P. Malon, C. L. Barness, M. Budesinsky, R. K. Dukor, D. van der Helm, T. A. Keiderling, Z. Koblicova, F. Pavlikova, M. Tichy, K. Blaha, *Collections of Czechoslovak Chemical Communications* 53, 2447-2472 (1988).
 - "Vibrational Circular Dichroism of Poly Glutamic Acid" R. K. Dukor, T. A. Keiderling, in *Peptides 1988* (ed. G. Jung, E. Bayer) Walter de Gruyter, Berlin (1989) pp 519-521.
 - "Biopolymer Conformational Studies with Vibrational Circular Dichroism" T. A. Keiderling, S. C. Yasui, P. Pancoska, R. K. Dukor, L. Yang, *SPIE Proceeding* 1057, ("Biomolecular Spectroscopy," ed. H. H. Mantsch, R. R. Birge) 7-14 (1989).
 - "Vibrational Circular Dichroism. Comparison of Techniques and Practical Considerations" T. A. Keiderling, in "Practical Fourier Transform Infrared Spectroscopy. Industrial and Laboratory Chemical Analysis," ed. J. R. Ferraro, K. Krishnan (Academic Press, San Diego, 1990) p. 203-284.
-

- "Vibrational Circular Dichroism Study of Unblocked Proline Oligomers," R. K. Dukor, T. A. Keiderling, V. Gut, *International Journal of Peptide and Protein Research*, 38, 198-203 (1991).
- "Reassessment of the Random Coil Conformation. Vibrational CD Study of Proline Oligopeptides and Related Polypeptides" R. K. Dukor and T. A. Keiderling, *Biopolymers* 31 1747-1761 (1991).
- "Vibrational CD of the Amide II band in Some Model Polypeptides and Proteins" V. P. Gupta, T. A. Keiderling, *Biopolymers* 32 239-248 (1992).
- "Vibrational Circular Dichroism of Proteins Polysaccharides and Nucleic Acids" T. A. Keiderling, Chapter 8 in *Physical Chemistry of Food Processes, Vol. 2 Advanced Techniques, Structures and Applications.*, eds. I.C. Baianu, H. Pessen, T. Kumosinski, Van Norstrand—Reinhold, New York (1993), pp 307-337.
- "Structural Studies of Biological Macromolecules using Vibrational Circular Dichroism" T. A. Keiderling, P. Pancoska, Chapter 6 in *Advances in Spectroscopy Vol. 21, Biomolecular Spectroscopy Part B* eds. R. E. Hester, R. J. H. Clarke, John Wiley Chichester (1993) pp 267-315.
- "Ab Initio Simulations of the Vibrational Circular Dichroism of Coupled Peptides" P. Bour and T. A. Keiderling, *Journal of the American Chemical Society* 115 9602-9607 (1993).
- "Ab initio Simulations of Coupled Peptide Vibrational Circular Dichroism" P. Bour, T. A. Keiderling in "Fifth International Conference on The Spectroscopy of Biological Molecules" Th. Theophanides, J. Anastassopoulou, N. Fotopoulos (Eds), Kluwen Academic Publ., Dortrecht, 1993, p. 29-30.
- "Vibrational Circular Dichroism Spectroscopy of Peptides and Proteins" T. A. Keiderling, in "Circular Dichroism Interpretations and Applications," K. Nakanishi, N. Berova, R. Woody, Eds., VCH Publishers, New York, (1994) pp 497-521.
- "Conformational Study of Sequential Lys-Leu Based Polymers and Oligomers using Vibrational and Electronic Circular Dichroism Spectra" V. Baumruk, D. Huo, R. K. Dukor, T. A. Keiderling, D. LeLeivre and A. Brack *Biopolymers* 34, 1115-1121 (1994).
- "Vibrational Optical Activity of Oligopeptides" T. B. Freedman, L. A. Nafie, T. A. Keiderling *Biopolymers* (Peptide Science) 37 (ed. C. Toniolo) 265-279 (1995).
- "Characterization of β -bend ribbon spiral forming peptides using electronic and vibrational circular dichroism" G. Yoder, T. A. Keiderling, F. Formaggio, M. Crisma, C. Toniolo *Biopolymers* 35, 103-111 (1995).
- "Vibrational Circular Dichroism as a Tool for Determination of Peptide Secondary Structure" P. Bour, T. A. Keiderling, P. Malon, in "Peptides 1994 (Proceedings of the 23rd European Peptide Symposium, 1994," (H.L.S. Maia, ed.), Escom, Leiden 1995, p.517-518.
- "Helical Screw Sense of homo-oligopeptides of C-alpha-methylated alpha-amino acids as Determined with Vibrational Circular Dichroism." G. Yoder, T. A. Keiderling, M. Crisma, F. Formaggio, C. Toniolo, J. Kamphuis, *Tetrahedron Asymmetry* 6, 687 -690 (1995).
- "Conformational Study of Linear Alternating and Mixed D- and L-Proline Oligomers Using Electronic and Vibrational CD and Fourier Transform IR." W. Mästle, R. K. Dukor, G. Yoder, T. A. Keiderling *Biopolymers* 36, 623-631 (1995).
- Review: "Vibrational Circular Dichroism Applications to Conformational Analysis of Biomolecules" T. A. Keiderling in *Circular Dichroism and the Conformational Analysis of Biomolecules* ed. G. D. Fasman, Plenum, New York (1996) p. 555-585.
- "Mutarotation studies of Poly L-Proline using FT-IR, Electronic and Vibrational Circular Dichroism" R. K. Dukor, T. A. Keiderling, *Biospectroscopy* 2, 83-100 (1996).

- "Vibrational Circular Dichroism Applications in Proteins and Peptides" T. A. Keiderling, Proceedings of the NATO ASI in Biomolecular Structure and Dynamics, Loutrakii Greece, May 1996, Ed. G. Vergoten (delayed second volume to 1998).
- "Transfer of Molecular Property Tensors in Cartesian Coordinates: A new algorithm for simulation of vibrational spectra" Petr Bour, Jana Sopkova, Lucie Bednarova, Petr Malon, T. A. Keiderling, *Journal of Computational Chemistry* 18, 6 46-659 (1997).
- "Vibrational Circular Dichroism Characterization of Alanine-Rich Peptides." Gorm Yoder and Timothy A. Keiderling, "Spectroscopy of Biological Molecules: Modern Trends," Ed. P. Carmona, R. Navarro, A. Hernanz, Kluwer Acad. Pub., Netherlands (1997) p p. 27-28.
- "Ionic strength effect on the thermal unfolding of alpha-spectrin peptides." D. Lusitani, N. Menhart, T.A. Keiderling and L. W. M. Fung. *Biochemistry* 37(1998)16546-16554.
- "In search of the earliest events of hCgb folding: structural studies of the 60-87 peptide fragment" S. Sherman, L. Kirnarsky, O. Prakash, H. M. Rogers, R.A.G.D. Silva, T.A. Keiderling, D. Smith, A.M. Hanly, F. Perini, and R.W. Ruddon, American Peptide Symposium Proceedings, 1997.
- "Cold Denaturation Studies of (LKELPKEL)_n Peptide Using Vibrational Circular Dichroism and FT-IR". R. A. G. D. Silva, Vladimir Baumruk, Petr Pancoska, T. A. Keiderling, Eric Lacassie, and Yves Trudelle, American Peptide Symposium Proceedings, 1997.
- "Simulations of oligopeptide vibrational CD. Effects of isotopic labeling." Petr Bour, Jan Kubelka, T. A. Keiderling *Biopolymers* 53, 380-395 (2000).
- "Site specific conformational determination in thermal unfolding studies of helical peptides using vibrational circular dichroism with isotopic substitution" R. A. G. D. Silva, Jan Kubelka, Petr Bour, Sean M. Decatur, Timothy A. Keiderling, *Proceedings of the National Academy of Sciences* (PNAS:USA) 97, 8318-8323 (2000).
- "Folding studies on the human chorionic gonadotropin b -subunit using optical spectroscopy of peptide fragments" R. A. G. D. Silva, S. A. Sherman, F. Perini, E. Bedows, T. A. Keiderling, *Journal of the American Chemical Society*, 122, 8623-8630 (2000).
- "Peptide and Protein Conformational Studies with Vibrational Circular Dichroism and Related Spectroscopies", Timothy A. Keiderling, (Revised and Expanded Chapter) In *Circular Dichroism: Principles and Applications*, 2nd Edition. (Eds. K. Nakanishi, N. Berova and R. A. Woody, John Wiley & Sons, New York (2000) p. 621-666.
- "Conformation studies with Optical Spectroscopy of peptides taken from hairpin sequences in the Human Chorionic Gonadotropin " R. A. G. D. Silva, S. A. Sherman, E. Bedows, T. A. Keiderling, *Peptides for the New Millenium*, Proceedings of the 16th American Peptide Symposium, (June, 1999 Minneapolis, MN) Ed.G. B. Fields, J. P. Tam, G. Barany, Kluwer Acad. Pub., Dordrecht,(2000) p. 325-326.
- "Analysis of Local Conformation within Helical Peptides via Isotope-Edited Vibrational Spectroscopy." S. M. Decatur, T. A. Keiderling, R. A. G. D.Silva, and P. Bour, *Peptides for the New Millenium*, Proceedings of the 16th American Peptide Symposium, (June, 1999 Minneapolis, MN) Ed. Ed.G. B. Fields, J. P. Tam, G. Barany, Kluwer Acad. Pub., Dordrecht, (2000) p. 414-416.
- "The anomalous infrared amide I intensity distribution in C-13 isotopically labeled peptide beta-sheets comes from extended, multiple stranded structures. An *Ab Initio* study." Jan Kubelka and T. A. Keiderling , *Journal of the American Chemical Society*. 123, 6142-6150 (2001).

- "Vibrational Circular Dichroism of Peptides and Proteins: Survey of Techniques, Qualitative and Quantitative Analyses, and Applications" Timothy A. Keiderling, Chapter in *Infrared and Raman Spectroscopy of Biological Materials*, Ed. Bing Yan and H.-U. Gremlich, Marcel Dekker, New York (2001) p.55-100.
- "Chirality in peptide vibrations. Ab initio computational studies of length, solvation, hydrogen bond, dipole coupling and isotope effects on vibrational CD. " Jan Kubelka, Petr Bour, R. A. Gangani D. Silva, Sean M. Decatur, Timothy A. Keiderling, ACS Symposium Series 810, ["Chirality: Physical Chemistry," (Ed. Janice Hicks) American Chemical Society, Washington, DC] (2002), pp. 50-64.
- "Spectroscopic Characterization of Selected β -Sheet Hairpin Models", J. Hilario, J. Kubelka, F. A. Syud, S. H. Gellman, and T. A. Keiderling. *Biopolymers (Biospectroscopy)* 67: 233-236 (2002)
- " Discrimination between peptide 3_{10} - and α -helices. Theoretical analysis of the impact of α -methyl substitution on experimental spectra " Jan Kubelka, R. A. Gangani D. Silva, and T. A. Keiderling, *Journal of the American Chemical Society*, 124, 5325-5332 (2002).
- "Ab Initio Quantum Mechanical Models of Peptide Helices and their Vibrational Spectra" Petr Bour, Jan Kubelka and T. A. Keiderling, *Biopolymers* 65, 45-59 (2002).
- "Discriminating 3_{10} - from α -helices. Vibrational and electronic CD and IR Absorption study of related Aib-containing oligopeptides" R. A. Gangani D. Silva, Sritana Yasui, Jan Kubelka, Fernando Formaggio, Marco Crisma, Claudio Toniolo, and Timothy A. Keiderling, *Biopolymers* 65, 229-243 (2002).
- "Spectroscopic characterization of Unfolded peptides and proteins studied with infrared absorption and vibrational circular dichroism spectra" T. A. Keiderling and Qi Xu, *Advances in Protein Chemistry Volume 62*, [Unfolded Proteins, Dedicated to John Edsall, Ed.: George Rose, Academic Press:New York] (2002), pp. 111-161.
- "Protein and Peptide Secondary Structure and Conformational Determination with Vibrational Circular Dichroism " Timothy A. Keiderling, *Current Opinions in Chemical Biology* (Ed. Julie Leary and Mark Arnold) 6, 682-688 (2002).
- Review: Conformational Studies of Peptides with Infrared Techniques. Timothy A. Keiderling and R. A. G. D. Silva, in *Synthesis of Peptides and Peptidomimetics*, Ed. M. Goodman and G. Herrman, Houben-Weyl, Vol 22Eb, Georg Thieme Verlag, New York (2002) pp. 715-738, (written and accepted in 2000).
- "Spectroscopic Studies of Structural Changes in Two β -Sheet Forming Peptides Show an Ensemble of Structures That Unfold Non-Cooperatively" Serguei V. Kuznetsov, Jovencio Hilario, T. A. Keiderling, Anjum Ansari, *Biochemistry*, 42 :4321-4332, (2003).
- "Optical spectroscopic investigations of model β -sheet hairpins in aqueous solution" Jovencio Hilario, Jan Kubelka, T. A. Keiderling, *Journal of the American Chemical Society* 125, 7562-7574 (2003).
- "Synthesis and conformational study of homopeptides based on (S)-Bin, a C₂-symmetric binaphthyl-derived Caa-disubstituted glycine with only axial chirality" J.-P. Mazaleyrat, K. Wright, A. Gaucher, M. Wakselman, S. Oancea, F. Formaggio, C. Toniolo, V. Setnicka, J. Kapitan, T. A. Keiderling, *Tetrahedron Asymmetry*, 14, 1879-1893 (2003).
- "Empirical modeling of the peptide amide I band IR intensity in water solution," Petr Bour, Timothy A. Keiderling, *Journal of Chemical Physics*, 119, 11253-11262 (2003)
- "The Nature of Vibrational Coupling in Helical Peptides: An Isotope Labeling Study" by R. Huang, J. Kubelka, W. Barber-Armstrong, R. A. G. D Silva, S. M. Decatur, and T. A.

- Keiderling, *Journal of the American Chemical Society*, 126, 2346-2354 (2004).
- "The Complete Chiro-spectroscopic Signature of the Peptide 3_{10} Helix in Aqueous Solution" Claudio Toniolo, Fernando Formaggio, Sabrina Tognon, Quirinus B. Broxterman, Bernard Kaptein, Rong Huang, Vladimir Setnicka, Timothy A. Keiderling, Iain H. McColl, Lutz Hecht, Laurence D. Barron, *Biopolymers* 75, 32-45 (2004).
 - "Induced axial chirality in the biphenyl core for the Ca-tetrasubstituted α -amino acid residue Bip and subsequent propagation of chirality in (Bip) $_n$ /Val oligopeptides" J.-P. Mazaleyrat, K. Wright, A. Gaucher, N. Toulemonde, M. Wakselman, S. Oancea, C. Peggion, F. Formaggio, V. Setnicka, T. A. Keiderling, C. Toniolo, *Journal of the American Chemical Society* 126; 12874-12879 (2004).
 - *Ab initio* modeling of amide I coupling in anti-parallel β -sheets and the effect of the ^{13}C isotopic labeling on vibrational spectra" Petr Bour, Timothy A. Keiderling, *Journal of Physical Chemistry B*, 109, 5348-5357 (2005)
 - Solvent Effects on IR And VCD Spectra of Helical Peptides: Insights from *Ab Initio* Spectral Simulations with Explicit Water" Jan Kubelka and Timothy A. Keiderling, *Journal of Physical Chemistry B* 109, 8231-8243 (2005)
 - IR Study of Cross-Strand Coupling in a β -Hairpin Peptide Using Isotopic Labels., Vladimir Setnicka, Rong Huang, Catherine L. Thomas, Marcus A. Etienne, Jan Kubelka, Robert P. Hammer, Timothy A. Keiderling *Journal of the American Chemical Society* 127, 4992-4993 (2005).
 - Vibrational spectral simulation for peptides of mixed secondary structure: Method comparisons with the trpzip model hairpin. Petr Bour and Timothy A. Keiderling, *Journal of Physical Chemistry B* 109, 232687-23697 (2005).
 - Isotopically labeled peptides provide site-resolved structural data with infrared spectra. Probing the structural limit of optical spectroscopy, Timothy A. Keiderling, Rong Huang, Jan Kubelka, Petr Bour, Vladimir Setnicka, Robert P. Hammer, Marcus *A. Etienne, R. A. Gangani D. Silva, Sean M. Decatur Collections Symposium Series, 8, 42-49 (2005)—["Biologically Active Peptides" IXth Conference, Prague Czech Republic, April 20-22, 2005.

Nucleic acids and polynucleotides

- "Application of Vibrational Circular Dichroism to Synthetic Polypeptides and Polynucleic Acids" T. A. Keiderling, S. C. Yasui, R. K. Dukor, L. Yang, *Polymer Preprints* 30, 423-424 (1989).
- "Vibrational Circular Dichroism of Polyribonucleic Acids. A Comparative Study in Aqueous Solution." A. Annamalai and T. A. Keiderling, *Journal of the American Chemical Society*, 109, 3125-3132 (1987).
- "Conformational phase transitions (A-B and B-Z) of DNA and models using vibrational circular dichroism" L. Wang, L. Yang, T. A. Keiderling in *Spectroscopy of Biological Molecules.*, eds. R. E. Hester, R. B. Girling, Special Publication 94 Royal Society of Chemistry, Cambridge (1991) p. 137-38.
- "Vibrational Circular Dichroism of Proteins Polysaccharides and Nucleic Acids" T. A. Keiderling, Chapter 8 in *Physical Chemistry of Food Processes, Vol. 2 Advanced Techniques, Structures and Applications* eds. I. C. Baianu, H. Pessen, T. Kumosinski, Van Norstrand—Reinhold, New York (1993) pp. 307-337.
- "Structural Studies of Biological Macromolecules using Vibrational Circular Dichroism" T. A. Keiderling, P. Pancoska, Chapter 6 in *Advances in Spectroscopy* Vol. 21,

- "Biomolecular Spectroscopy Part B" ed. R. E. Hester, R. J. H. Clarke, John Wiley Chichester (1993) pp 267–315.
- "Detection of Triple Helical Nucleic Acids with Vibrational Circular Dichroism," L. Wang, P. Pancoska, T. A. Keiderling in "Fifth International Conference on The Spectroscopy of Biological Molecules" Th. Theophanides, J. Anastassopoulou, N. Fotopoulos (Eds), Kluwer Academic Publ., Dordrecht, 1993, p. 81-82.
 - "Helical Nature of Poly (dI-dC) ♦ Poly (dI-dC). Vibrational Circular Dichroism Results" L. Wang and T. A. Keiderling *Nucleic Acids Research* 21 4127-4132 (1993).
 - "Detection and Characterization of Triple Helical Pyrimidine-Purine-Pyrimidine Nucleic Acids with Vibrational Circular Dichroism" L. Wang, P. Pancoska, T. A. Keiderling, *Biochemistry* 33 8428-8435 (1994).
 - "Vibrational Circular Dichroism of A-, B- and Z- form Nucleic Acids in the PO₂- Stretching Region" L. Wang, L. Yang, T. A. Keiderling, *Biophysical Journal* 67, 2460-2467 (1994).
 - "Studies of multiple stranded RNA and DNA with FTIR, vibrational and electronic circular dichroism," Zhihua Huang, Lijiang Wang and Timothy A. Keiderling, in *Spectroscopy of Biological Molecules*, Ed. J. C. Merlin, Kluwer Acad. Pub., Dordrecht, 1995, pp . 321-322.
 - "Vibrational Circular Dichroism Applications to Conformational Analysis of Biomolecules" T. A. Keiderling in "Circular Dichroism and the Conformational Analysis of Biomolecules" ed G. D. Fasman, Plenum, New York (1996) pp. 555–598.
 - "Vibrational Circular Dichroism Techniques and Application to Nucleic Acids" T. A. Keiderling, In "Biomolecular Structure and Dynamics", NATO ASI series, Series E: Applied Sciences- Vol.342, Eds: G. Vergoten and T. Theophanides, Kluwer Academic Publishers, Dordrecht, The Netherlands, pp. 299–317 (1997).

See also

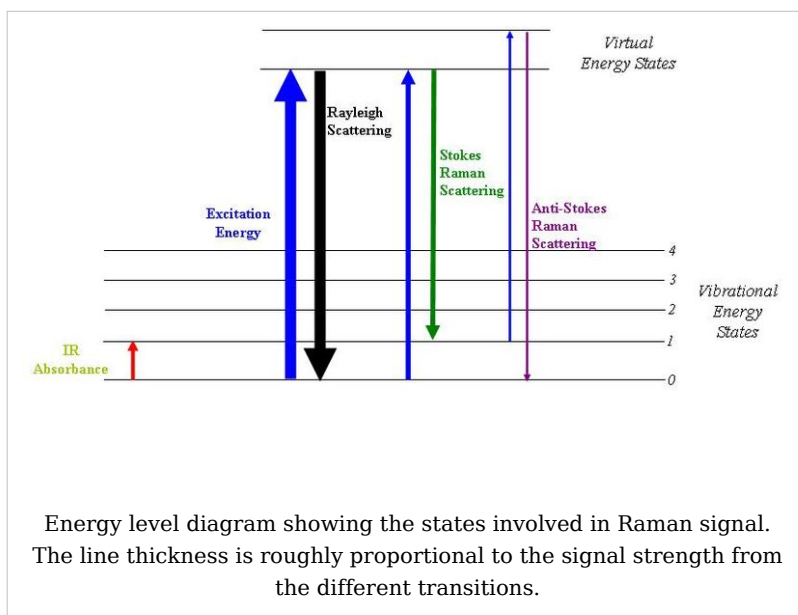
- Circular dichroism
 - Birefringence
 - Optical rotatory dispersion
 - IR spectroscopy
 - Polarization
 - Proteins
 - Nucleic Acids
 - DNA
 - Molecular models of DNA
 - DNA structure
 - Protein structure
 - Amino acids
 - Density functional theory
 - Quantum chemistry
 - Raman optical activity (ROA)
-

Raman spectroscopy

Raman spectroscopy

(pronounced: [rə.mən] S—, named after C. V. Raman) is a spectroscopic technique used in condensed matter physics and chemistry to study vibrational, rotational, and other low-frequency modes in a system.^[1] It relies on inelastic scattering, or Raman scattering, of monochromatic light, usually from a laser in the visible, near infrared, or near ultraviolet range. The laser light interacts with phonons or other excitations

in the system, resulting in the energy of the laser photons being shifted up or down. The shift in energy gives information about the phonon modes in the system. Infrared spectroscopy yields similar, but complementary, information.



Typically, a sample is illuminated with a laser beam. Light from the illuminated spot is collected with a lens and sent through a monochromator. Wavelengths close to the laser line, due to elastic Rayleigh scattering, are filtered out while the rest of the collected light is dispersed onto a detector.

Spontaneous Raman scattering is typically very weak, and as a result the main difficulty of Raman spectroscopy is separating the weak inelastically scattered light from the intense Rayleigh scattered laser light. Historically, Raman spectrometers used holographic gratings and multiple dispersion stages to achieve a high degree of laser rejection. In the past, photomultipliers were the detectors of choice for dispersive Raman setups, which resulted in long acquisition times. However, modern instrumentation almost universally employs notch or edge filters for laser rejection and spectrographs (either axial transmissive (AT), Czerny-Turner (CT) monochromator) or FT (Fourier transform spectroscopy based), and CCD detectors.

There are a number of advanced types of Raman spectroscopy, including surface-enhanced Raman, tip-enhanced Raman, polarised Raman, stimulated Raman (analogous to stimulated emission), transmission Raman, spatially-offset Raman, and hyper Raman.

Basic theory

The Raman effect occurs when light impinges upon a molecule and interacts with the electron cloud and the bonds of that molecule. The incident photon excites the molecule into a virtual state. For the spontaneous Raman effect, the molecule will be excited from the ground state to a virtual energy state, and relax into a vibrational excited state. Two series of lines exist around this central vibrational transition. They correspond to the complimentary rotational transition. Anti-Stokes lines correspond to rotational relaxation

whereas Stokes lines correspond to rotational excitation.

A change in the molecular polarization potential — or amount of deformation of the electron cloud — with respect to the vibrational coordinate is required for the molecule to exhibit the Raman effect. The amount of the polarizability change will determine the Raman scattering intensity, whereas the Raman shift is equal to the vibrational level that is involved.

History

Although the inelastic scattering of light was predicted by Adolf Smekal in 1923, it was not until 1928 that it was observed in practice. The Raman effect was named after one of its discoverers, the Indian scientist Sir C. V. Raman who observed the effect by means of sunlight (1928, together with K. S. Krishnan and independently by Grigory Landsberg and Leonid Mandelstam).^[1] Raman won the Nobel Prize in Physics in 1930 for this discovery accomplished using sunlight, a narrow band photographic filter to create monochromatic light and a "crossed" filter to block this monochromatic light. He found that light of changed frequency passed through the "crossed" filter.

Systematic pioneering theory of the Raman effect was developed by Czechoslovak physicist George Placzek between 1930 and 1934.^[2] The mercury arc became the principal light source, first with photographic detection and then with spectrophotometric detection. Currently lasers are used as light sources.

Applications

Raman spectroscopy is commonly used in chemistry, since vibrational information is specific for the chemical bonds in molecules. It therefore provides a fingerprint by which the molecule can be identified. For instance, the vibrational frequencies of SiO, Si₂O₂, and Si₃O₃ were identified and assigned on the basis of normal coordinate analyses using infrared and Raman spectra.^[3] The fingerprint region of organic molecules is in the (wavenumber) range 500-2000 cm⁻¹. Another way that the technique is used is to study changes in chemical bonding, e.g., when a substrate is added to an enzyme.

Raman gas analyzers have many practical applications. For instance, they are used in medicine for real-time monitoring of anaesthetic and respiratory gas mixtures during surgery.

In solid state physics, spontaneous Raman spectroscopy is used to, among other things, characterize materials, measure temperature, and find the crystallographic orientation of a sample. As with single molecules, a given solid material has characteristic phonon modes that can help an experimenter identify it. In addition, Raman spectroscopy can be used to observe other low frequency excitations of the solid, such as plasmons, magnons, and superconducting gap excitations. The spontaneous Raman signal gives information on the population of a given phonon mode in the ratio between the Stokes (downshifted) intensity and anti-Stokes (upshifted) intensity.

Raman scattering by an anisotropic crystal gives information on the crystal orientation. The polarization of the Raman scattered light with respect to the crystal and the polarization of the laser light can be used to find the orientation of the crystal, if the crystal structure (specifically, its point group) is known.

Raman active fibers, such as aramid and carbon, have vibrational modes that show a shift in Raman frequency with applied stress. Polypropylene fibers also exhibit similar shifts. The radial breathing mode is a commonly used technique to evaluate the diameter of carbon nanotubes. In nanotechnology, a Raman microscope can be used to analyze nanowires to better understand the composition of the structures.

Spatially Offset Raman Spectroscopy (SORS), which is less sensitive to surface layers than conventional Raman, can be used to discover counterfeit drugs without opening their internal packaging, and for non-invasive monitoring of biological tissue.^[4] Raman spectroscopy can be used to investigate the chemical composition of historical documents such as the Book of Kells and contribute to knowledge of the social and economic conditions at the time the documents were produced.^[5] This is especially helpful because Raman spectroscopy offers a non-invasive way to determine the best course of preservation or conservation treatment for such materials.

Raman spectroscopy is being investigated as a means to detect explosives for airport security.^[6]

Microspectroscopy

Raman spectroscopy offers several advantages for microscopic analysis. Since it is a scattering technique, specimens do not need to be fixed or sectioned. Raman spectra can be collected from a very small volume ($< 1 \mu\text{m}$ in diameter); these spectra allow the identification of species present in that volume. Water does not generally interfere with Raman spectral analysis. Thus, Raman spectroscopy is suitable for the microscopic examination of minerals, materials such as polymers and ceramics, cells and proteins. A Raman microscope begins with a standard optical microscope, and adds an excitation laser, a monochromator, and a sensitive detector (such as a charge-coupled device (CCD), or photomultiplier tube (PMT)). FT-Raman has also been used with microscopes.

In *direct imaging*, the whole field of view is examined for scattering over a small range of wavenumbers (Raman shifts). For instance, a wavenumber characteristic for cholesterol could be used to record the distribution of cholesterol within a cell culture.

The other approach is *hyperspectral imaging* or *chemical imaging*, in which thousands of Raman spectra are acquired from all over the field of view. The data can then be used to generate images showing the location and amount of different components. Taking the cell culture example, a hyperspectral image could show the distribution of cholesterol, as well as proteins, nucleic acids, and fatty acids. Sophisticated signal- and image-processing techniques can be used to ignore the presence of water, culture media, buffers, and other interferents.

Raman microscopy, and in particular confocal microscopy, has very high spatial resolution. For example, the lateral and depth resolutions were 250 nm and 1.7 μm , respectively, using a confocal Raman microspectrometer with the 632.8 nm line from a He-Ne laser with a pinhole of 100 μm diameter. Since the objective lenses of microscopes focus the laser beam to several micrometres in diameter, the resulting photon flux is much higher than achieved in conventional Raman setups. This has the added benefit of enhanced fluorescence quenching. However, the high photon flux can also cause sample degradation, and for this reason some setups require a thermally conducting substrate (which acts as a heat sink) in order to mitigate this process.

By using Raman microspectroscopy, *in vivo* time- and space-resolved Raman spectra of microscopic regions of samples can be measured. As a result, the fluorescence of water, media, and buffers can be removed. Consequently *in vivo* time- and space-resolved Raman spectroscopy is suitable to examine proteins, cells and organs.

Raman microscopy for biological and medical specimens generally uses near-infrared (NIR) lasers (785 nm diodes and 1064 nm Nd:YAG are especially common). This reduces the risk of damaging the specimen by applying higher energy wavelengths. However, the intensity of NIR Raman is low (owing to the ω^{-4} dependence of Raman scattering intensity), and most detectors required very long collection times. Recently, more sensitive detectors have become available, making the technique better suited to general use. Raman microscopy of inorganic specimens, such as rocks and ceramics and polymers, can use a broader range of excitation wavelengths.^[7]

Polarized analysis

The polarization of the Raman scattered light also contains useful information. This property can be measured using (plane) polarized laser excitation and a polarization analyzer. Spectra acquired with the analyzer set at both perpendicular and parallel to the excitation plane can be used to calculate the depolarization ratio. Study of the technique is pedagogically useful in teaching the connections between group theory, symmetry, Raman activity and peaks in the corresponding Raman spectra.

The spectral information arising from this analysis gives insight into molecular orientation and vibrational symmetry. In essence, it allows the user to obtain valuable information relating to the molecular shape, for example in synthetic chemistry or polymorph analysis. It is often used to understand macromolecular orientation in crystal lattices, liquid crystals or polymer samples.^[8]

Variations

Several variations of Raman spectroscopy have been developed. The usual purpose is to enhance the sensitivity (e.g., surface-enhanced Raman), to improve the spatial resolution (Raman microscopy), or to acquire very specific information (resonance Raman).

- **Surface Enhanced Raman Spectroscopy (SERS)** - Normally done in a silver or gold colloid or a substrate containing silver or gold. Surface plasmons of silver and gold are excited by the laser, resulting in an increase in the electric fields surrounding the metal. Given that Raman intensities are proportional to the electric field, there is large increase in the measured signal (by up to 10^{11}). This effect was originally observed by Martin Fleischmann but the prevailing explanation was proposed by Van Duyne in 1977.^[9]
- **Resonance Raman spectroscopy** - The excitation wavelength is matched to an electronic transition of the molecule or crystal, so that vibrational modes associated with the excited electronic state are greatly enhanced. This is useful for studying large molecules such as polypeptides, which might show hundreds of bands in "conventional" Raman spectra. It is also useful for associating normal modes with their observed frequency shifts.^[10]
- **Surface Enhanced Resonance Raman Spectroscopy (SERRS)** - A combination of SERS and resonance Raman spectroscopy which uses proximity to a surface to increase Raman intensity, and excitation wavelength matched to the maximum absorbance of the molecule being analysed.

- **Hyper Raman** - A non-linear effect in which the vibrational modes interact with the second harmonic of the excitation beam. This requires very high power, but allows the observation of vibrational modes which are normally "silent". It frequently relies on SERS-type enhancement to boost the sensitivity.^[11]
- **Spontaneous Raman Spectroscopy** - Used to study the temperature dependence of the Raman spectra of molecules.
- **Optical Tweezers Raman Spectroscopy (OTRS)** - Used to study individual particles, and even biochemical processes in single cells trapped by optical tweezers.
- **Stimulated Raman Spectroscopy** - A two color pulse transfers the population from ground to a rovibrationally excited state, if the difference in energy corresponds to an allowed Raman transition. Two photon UV ionization, applied after the population transfer but before relaxation, allows the intra-molecular or inter-molecular Raman spectrum of a gas or molecular cluster (indeed, a given conformation of molecular cluster) to be collected. This is a useful molecular dynamics technique.
- **Spatially Offset Raman Spectroscopy (SORS)** - The Raman scatter is collected from regions laterally offset away from the excitation laser spot, leading to significantly lower contributions from the surface layer than with traditional Raman spectroscopy.^[12]
- **Coherent anti-Stokes Raman spectroscopy (CARS)** - Two laser beams are used to generate a coherent anti-Stokes frequency beam, which can be enhanced by resonance.
- **Raman optical activity (ROA)** - Measures vibrational optical activity by means of a small difference in the intensity of Raman scattering from chiral molecules in right- and left-circularly polarized incident light or, equivalently, a small circularly polarized component in the scattered light.^[13]
- **Transmission Raman** - Allows probing of a significant bulk of a turbid material, such as powders, capsules, living tissue, etc. It was largely ignored following investigations in the late 1960s^[14] but was rediscovered in 2006 as a means of rapid assay of pharmaceutical dosage forms.^[15] There are also medical diagnostic applications.^[16]
- **Inverse Raman spectroscopy.**
- **Tip-Enhanced Raman Spectroscopy (TERS)** - Uses a silver or gold tip to enhance the Raman signals of molecules situated in its vicinity. The spatial resolution is approximately the size of the tip apex (20-30 nm). TERS has been shown to have sensitivity down to the single molecule level.

References

- [1] Gardiner, D.J. (1989). *Practical Raman spectroscopy*. Springer-Verlag. ISBN 978-0387502540.
- [2] Placzek G.: "Rayleigh Streueung und Raman Effekt", In: Hdb. der Radiologie, Vol. VI., 2, 1934, p. 209
- [3] Khanna, R.K. (1981). "Raman-spectroscopy of oligomeric SiO species isolated in solid methane". *Journal of Chemical Physics*. doi: 10.1063/1.441393 (<http://dx.doi.org/10.1063/1.441393>).
- [4] . BBC News. 2007-01-31. <http://news.bbc.co.uk/2/hi/health/6314287.stm>. Retrieved on 2008-12-08.
- [5] Irish Classic Is Still a Hit (in Calfskin, Not Paperback) - New York Times (<http://www.nytimes.com/2007/05/28/world/europe/28kells.html>)
- [6] Ben Vogel (29 August 2008). http://www.janes.com/news/transport/business/jar/jar080829_1_n.shtml|"Raman spectroscopy portends well for standoff explosives detection". Jane's. http://www.janes.com/news/transport/business/jar/jar080829_1_n.shtml. Retrieved on 2008-08-29.
- [7] Ellis DI, Goodacre R (August 2006). "Metabolic fingerprinting in disease diagnosis: biomedical applications of infrared and Raman spectroscopy". *Analyst* **131** (8): 875-85. doi: 10.1039/b602376m (<http://dx.doi.org/10.1039/b602376m>). PMID 17028718.
- [8] Khanna, R.K. (1957). *Evidence of ion-pairing in the polarized Raman spectra of a Ba2+CrO doped KI single crystal*. John Wiley & Sons, Ltd. doi: 10.1002/jrs.1250040104 (<http://dx.doi.org/10.1002/jrs.1250040104>).

- [9] Jeanmaire DL, van Duyne RP (1977). "Surface Raman Electrochemistry Part I. Heterocyclic, Aromatic and Aliphatic Amines Adsorbed on the Anodized Silver Electrode". *Journal of Electroanalytical Chemistry* (Elsevier Sequoia S.A.) **84**: 1-20. doi: 10.1016/S0022-0728(77)80224-6 ([http://dx.doi.org/10.1016/S0022-0728\(77\)80224-6](http://dx.doi.org/10.1016/S0022-0728(77)80224-6)).
- [10] Chao RS, Khanna RK, Lippincott ER (1974). "Theoretical and experimental resonance Raman intensities for the manganate ion". *J Raman Spectroscopy* **3**: 121. doi: 10.1002/jrs.1250030203 (<http://dx.doi.org/10.1002/jrs.1250030203>).
- [11] Kneipp K, *et al.* (1999). "Surface-Enhanced Non-Linear Raman Scattering at the Single Molecule Level". *Chem. Phys.* **247**: 155-162. doi: 10.1016/S0301-0104(99)00165-2 ([http://dx.doi.org/10.1016/S0301-0104\(99\)00165-2](http://dx.doi.org/10.1016/S0301-0104(99)00165-2)).
- [12] Matousek P, Clark IP, Draper ERC, *et al.* (2005). "Subsurface Probing in Diffusely Scattering Media using Spatially Offset Raman Spectroscopy". *Applied Spectroscopy* **59**: 393. doi: 10.1366/000370205775142548 (<http://dx.doi.org/10.1366/000370205775142548>).
- [13] Barron LD, Hecht L, McColl IH, Blanch EW (2004). "Raman optical activity comes of age". *Molec. Phys.* **102** (8): 731-744. doi: 10.1080/00268970410001704399 (<http://dx.doi.org/10.1080/00268970410001704399>).
- [14] B. Schrader, G. Bergmann, Fresenius. Z. (1967). *Anal. Chem.*: 225-230.
- [15] P. Matousek, A. W. Parker (2006). "Bulk Raman Analysis of Pharmaceutical Tablets". *Applied Spectroscopy* **60**: 1353-1357. doi: 10.1366/000370206779321463 (<http://dx.doi.org/10.1366/000370206779321463>).
- [16] P. Matousek, N. Stone (2007). "Prospects for the diagnosis of breast cancer by noninvasive probing of calcifications using transmission Raman spectroscopy". *Journal of Biomedical Optics* **12**: 024008. doi: 10.1117/1.2718934 (<http://dx.doi.org/10.1117/1.2718934>).

External links

- Chemical Imaging Without Dyeing (<http://witec.de/en/download/Raman/ImagingMicroscopy04.pdf>) - Chemical Imaging Without Dyeing
- An introduction to Raman spectroscopy (<http://www.jobinyvon.com/Raman/Tutorial-Intro>)
- Raman Fundamentals 'What is Raman Spectroscopy?' (<http://www.andor.com/chemistry/?app=64>)
- DoITPoMS Teaching and Learning Package - Raman Spectroscopy (<http://www.doitpoms.ac.uk/tlplib/raman/index.php>) - an introduction, aimed at undergraduate level
- Raman Spectroscopy Tutorial (http://161.58.205.25/Raman_Spectroscopy/rtr-ramantutorial.php?ss=800) - A detailed explanation of Raman Spectroscopy including Resonance-Enhanced Raman Scattering and Surface-Enhanced Raman Scattering.
- The Science Show, ABC Radio National (<http://www.abc.net.au/rn/science/ss/stories/s1581469.htm>) - Interview with Scientist on NASA funded project to build Raman Spectrometer for the 2009 Mars mission: a cellular phone size device to detect almost any substance known, with commercial <USD\$5000 commercial spin-off, prototyped by June 2006.
- Raman spectroscopy for medical diagnosis (http://pubs.acs.org/subscribe/journals/ancham/79/i11/pdf/0607feature_griffiths.pdf) from the June 1, 2007 issue of *Analytical Chemistry* (<http://pubs3.acs.org/acs/journals/toc.page?incoden=ancham&indecade=0&involume=79&inissue=11>)

CARS

CARS is a four-letter acronym that can stand for:

- Cyprus Amateur Radio Society
- Cable television relay service station
- Canadian Aviation Regulations
- Childhood Autism Rating Scale
- Charlottesville-Albemarle Rescue Squad, the busiest volunteer rescue squad in the US
- Customer Access and Retrieval System
- Citizens Against Road Slaughter
- Coherent anti-Stokes Raman spectroscopy
- Consortium for Advanced Radiation Sources, a cooperative effort of the University of Chicago and Argonne National Laboratories
- The Combat Arms Regimental System of the United States Army
- Compensatory Anti-Inflammatory Syndrome
- Computer Assisted Radiology and Surgery^[1], an annual international academic conference.
- Community Aerodrome Radio Station^[2]
- Cumulative average adjusted returns

References

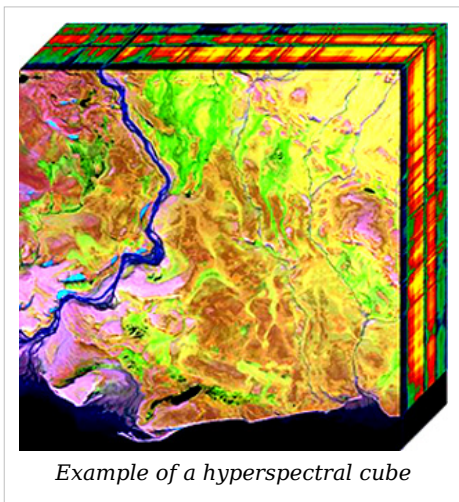
- [1] Computer Assisted Radiology and Surgery (<http://www.cars-int.org>)
- [2] Transport Canada (<http://www.navcanada.ca/NavCanada.asp?Language=en&Content=ContentDefinitionFiles\AboutUs\WhatWeDo\Facilities\default.xml#cars>)
-

Hyperspectral imaging

Hyperspectral imaging collects and processes information from across the electromagnetic spectrum. Unlike the human eye, which just sees visible light, hyperspectral imaging is more like the eyes of the mantis shrimp, which can see visible light as well as from the ultraviolet to infrared. Hyperspectral capabilities enable the mantis shrimp to recognize different types of coral, prey, or predators, all which may appear as the same color to the human eye.

Humans build sensors and processing systems to provide the same type of capability for application in agriculture, mineralogy, physics, and surveillance. Hyperspectral sensors look at objects using a vast portion of the electromagnetic spectrum. Certain objects leave unique 'fingerprints' across the electromagnetic spectrum. These 'fingerprints' are known as spectral signatures and enable identification of the materials that make up a scanned object. For example, having the spectral signature for oil helps mineralogists find new oil fields.

Acquisition and Analysis



Hyperspectral sensors collect information as a set of 'images'. Each image represents a range of the electromagnetic spectrum and is also known as a spectral band. These 'images' are then combined and form a three dimensional hyperspectral cube for processing and analysis.

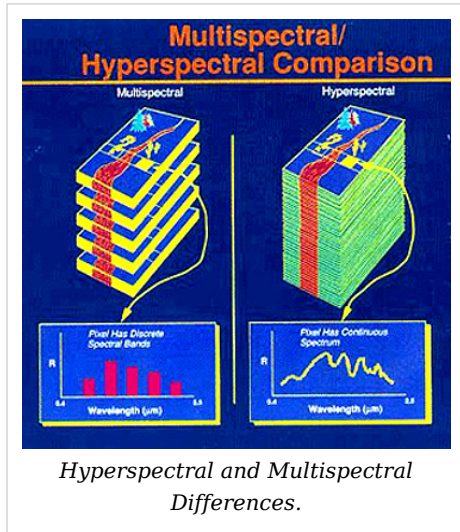
Hyperspectral cubes are generated from airborne sensors like the NASA's *Airborne Visible/Infrared Imaging Spectrometer* (AVIRIS), or from satellites like NASA's Hyperion.^[1] However, for many development and validation studies handheld sensors are used.^[2]

The precision of these sensors is typically measured in spectral resolution, which is the width of each band of the spectrum that is captured. If the scanner picks up on a large number of fairly narrow frequency bands, it is possible to identify objects even if said objects are only captured in a handful of pixels. However, spatial resolution is a factor in addition to spectral resolution. If the pixels are too large, then multiple objects are captured in the same pixel and become difficult to identify. If the pixels are too small, then the energy captured by each sensor-cell is low, and the decreased signal-to-noise ratio reduces the reliability of measured features.

MicroMSI, Opticks and Envi are three remote sensing applications that support the processing and analysis of hyperspectral data. The acquisition and processing of hyperspectral images is also referred to as imaging spectroscopy.

Differences between Hyperspectral and Multispectral

Hyperspectral Imaging is part of a class of techniques commonly referred to as spectral imaging or spectral analysis. Hyperspectral Imaging is related to multispectral imaging. The distinction between hyperspectral and multispectral is usually defined as the number of spectral bands. Multispectral data contains from tens to hundreds of bands. Hyperspectral data contains hundreds to thousands of bands. However, hyperspectral imaging may be best defined by the manner in which the data is collected. Hyperspectral data is a set of contiguous bands (usually by one sensor). Multispectral is a set of optimally chosen spectral bands that are typically not contiguous and can be collected from multiple sensors.



Applications

Hyperspectral remote sensing is used in a wide array of real-life applications. Although originally developed for mining and geology (The ability of hyperspectral imaging to identify various minerals makes it ideal for the mining and oil industries, where it can be used to look for ore and oil^{[2] [3]} it has now spread into fields as wide-spread as ecology and surveillance, as well as historical manuscript research such as the imaging of the Archimedes Palimpsest. This technology is continually becoming more available to the public, and has been used in a wide variety of ways. Organizations such as NASA and the USGS have catalogues of various minerals and their spectral signatures, and have posted them online to make them readily available for researchers.

Agriculture

Although the costs of acquiring hyperspectral images is typically high, for specific crops and in specific climates hyperspectral remote sensing is used more and more for monitoring the development and health of crops. In Australia work is underway to use imaging spectrometers to detect grape variety, and develop an early warning system for disease outbreaks.^[4] Furthermore work is underway to use hyperspectral data to detect the chemical composition of plants^[5] which can be used to detect the nutrient and water status of wheat in irrigated systems^[6]

Mineralogy

The original field of development for hyperspectral remote sensing, hyperspectral sensing of minerals is now well developed. Many minerals can be identified from images, and their relation to the presence of valuable minerals such as gold and diamonds is well understood. Currently the move is towards understanding the relation between oil and gas leakages from pipelines and natural wells; their effect on the vegetation and the spectral signatures. Recent work includes the PhD dissertations of Werff^[7] and Noomen^[8].

Physics

Physicists use an electron microscopy technique that involves microanalysis using either Energy dispersive X-ray spectroscopy (EDS), Electron energy loss spectroscopy (EELS), Infrared Spectroscopy (IR), Raman Spectroscopy, or cathodoluminescence (CL) spectroscopy, in which the entire spectrum measured at each point is recorded. EELS hyperspectral imaging is performed in a scanning transmission electron microscope (STEM); EDS and CL mapping can be performed in STEM as well, or in a scanning electron microscope or electron probe microanalyzer (EPMA). Often, multiple techniques (EDS, EELS, CL) are used simultaneously.

In a "normal" mapping experiment, an image of the sample will be made that is simply the intensity of a particular emission mapped in an XY raster. For example, an EDS map could be made of a steel sample, in which iron x-ray intensity is used for the intensity grayscale of the image. Dark areas in the image would indicate not-iron-bearing impurities. This could potentially give misleading results; if the steel contained tungsten inclusions, for example, the high atomic number of tungsten could result in bremsstrahlung radiation that made the iron-free areas *appear* to be rich in iron.

By hyperspectral mapping, instead, the entire spectrum at each mapping point is acquired, and a quantitative analysis can be performed by computer post-processing of the data, and a quantitative map of iron content produced. This would show which areas contained no iron, despite the anomalous x-ray counts caused by bremsstrahlung. Because EELS core-loss edges are small signals on top of a large background, hyperspectral imaging allows large improvements to the quality of EELS chemical maps.

Similarly, in CL mapping, small shifts in the peak emission energy could be mapped, which would give information regarding slight chemical composition changes or changes in the stress state of a sample.

Surveillance

Hyperspectral surveillance is the implementation of hyperspectral scanning technology for surveillance purposes. Hyperspectral imaging is particularly useful in military surveillance because of measures that military entities now take to avoid airborne surveillance. Airborne surveillance has been in effect since soldiers used tethered balloons to spy on troops during the American Civil War, and since that time we have learned not only to hide from the naked eye, but to mask our heat signature to blend in to the surroundings and avoid infrared scanning, as well. The idea that drives hyperspectral surveillance is that hyperspectral scanning draws information from such a large portion of the light spectrum that any given object should have unique spectral signature in at least a few of the many bands that get scanned.^[1]

Advantages and Disadvantages

The primary advantages to hyperspectral imaging is that, because an entire spectrum is acquired at each point, the operator needs no a priori knowledge of the sample, and post-processing allows all available information from the dataset to be mined.

The primary disadvantages are cost and complexity. Fast computers, sensitive detectors, and large data storage capacities are needed for analyzing hyperspectral data. Significant data storage capacity is necessary since hyperspectral cubes are large multi-dimensional datasets, potentially exceeding hundreds of megabytes. All of these factors greatly increase the cost of acquiring and processing hyperspectral data. Also, one of the hurdles that researchers have had to face is finding ways to program hyperspectral satellites to sort through data on their own and transmit only the most important images, as both transmission and storage of that much data could prove difficult and costly.^[1] As a relatively new analytical technique, the full potential of hyperspectral imaging has not yet been realized.

See also

- Airborne Real-time Cueing Hyperspectral Enhanced Reconnaissance
- Full Spectral Imaging
- Multi-spectral image
- Chemical imaging
- Remote Sensing
- Sensor fusion

External Links

ITT Visual Information Solutions - ENVI Hyperspectral Image Processing Software ^[9]

References

- [1] Schurmer, J.H., (Dec 2003) *Hyperspectral imaging from space* (<http://www.afrlhorizons.com/Briefs/Dec03/VS0302.html>), Air Force Research Laboratories Technology Horizons
- [2] Ellis, J., (Jan 2001) *Searching for oil seeps and oil-impacted soil with hyperspectral imagery* (<http://www.eonline.com/Common/currentissues/Jan01/ellis.htm>), Earth Observation Magazine.
- [3] Smith, R.B. (July 14, 2006), *Introduction to hyperspectral imaging with TMIPS* (<http://www.microimages.com/getstart/pdf/hyprspec.pdf>), MicroImages Tutorial Web site
- [4] Lacar, F.M., et al., *Use of hyperspectral imagery for mapping grape varieties in the Barossa Valley, South Australia* (<http://hdl.handle.net/2440/39292>), Geoscience and remote sensing symposium (IGARSS'01) - IEEE 2001 International, vol.6 2875-2877p. doi: 10.1109/IGARSS.2001.978191 (<http://dx.doi.org/10.1109/IGARSS.2001.978191>)
- [5] Ferwerda, J.G. (2005), *Charting the quality of forage: measuring and mapping the variation of chemical components in foliage with hyperspectral remote sensing* (http://www.itc.nl/library/Papers_2005/phd/ferwerda.pdf), Wageningen University , ITC Dissertation 126, 166p. ISBN 90-8504-209-7
- [6] Tilling, A.K., et al., (2006) *Remote sensing to detect nitrogen and water stress in wheat* (http://www.regional.org.au/au/asa/2006/plenary/technology/4584_tillingak.htm), The Australian Society of Agronomy
- [7] Werff H. (2006), *Knowledge based remote sensing of complex objects: recognition of spectral and spatial patterns resulting from natural hydrocarbon seepages* (http://www.itc.nl/library/papers_2006/phd/vdwerff.pdf), Utrecht University, ITC Dissertation 131, 138p. ISBN 90-6164-238-8
- [8] Noomen, M.F. (2007), *Hyperspectral reflectance of vegetation affected by underground hydrocarbon gas seepage* (http://www.itc.nl/library/papers_2007/phd/noomen.pdf), Enschede, ITC 151p. ISBN 978-90-8504-671-4.
- [9] <http://www.ittvis.com/ProductServices/ENVI.aspx>

Multispectral imaging

1. Redirect Multi-spectral image

Confocal microscope

1. REDIRECT Confocal microscopy

Fluorescence microscope

■ A **fluorescence microscope** (colloquially synonymous with *epifluorescent microscope*) is a light microscope used to study properties of organic or inorganic substances using the phenomena of fluorescence and phosphorescence instead of, or in addition to, reflection and absorption.^{[1] [2]}



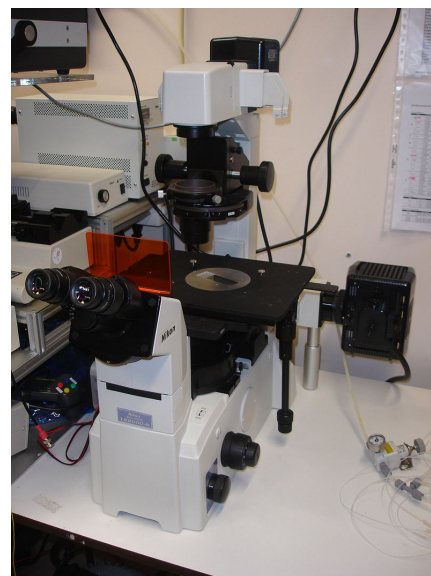
A fluorescent microscope (Olympus BX61), coupled with a digital camera.

Technique

In most cases, a component of interest in the specimen is specifically labeled with a fluorescent molecule called a fluorophore (such as green fluorescent protein (GFP), fluorescein or DyLight 488).^[1] The specimen is illuminated with light of a specific wavelength (or wavelengths) which is absorbed by the fluorophores, causing them to emit longer wavelengths of light (of a different color than the absorbed light). The illumination light is separated from the much weaker emitted fluorescence through the use of an emission filter. Typical components of a fluorescence microscope are the light source (xenon arc lamp or mercury-vapor lamp), the excitation filter, the dichroic mirror (or dichromatic beamsplitter), and the emission filter (see figure below). The filters and the dichroic are chosen to match the spectral excitation and emission characteristics of the fluorophore used to label the specimen.^[1] In this manner, a single fluorophore (color) is imaged at a time. Multi-color images of several fluorophores must be composed by combining several single-color images.^[1]

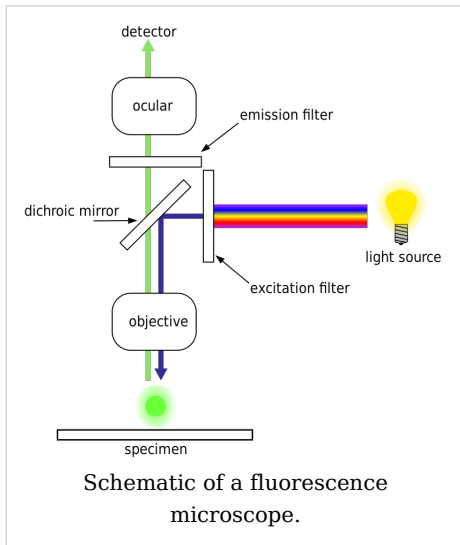
Most fluorescence microscopes in use are epifluorescence microscopes (i.e. excitation and observation of the fluorescence are from above (*epi*-) the specimen). These microscopes have become an important part in the field of biology, opening the doors for more advanced microscope designs, such as the confocal laser scanning microscope and the total internal reflection fluorescence microscope (TIRF). The Vertico SMI combining localisation microscopy with spatially modulated illumination uses standard fluorescence dyes and reaches an optical resolution below 10 nanometers (1 nanometer = 1 nm = 1×10^{-9} m).

Fluorophores lose their ability to fluoresce as they are illuminated in a process called photobleaching. Special care must be taken to prevent photobleaching through the use of more robust fluorophores, by minimizing illumination, or by introducing a scavenger system to reduce the rate of photobleaching.



An inverted fluorescent microscope (Nikon TE2000). Note the orange plate that allows the user to look at the sample while protecting his eyes from the excitation UV light.

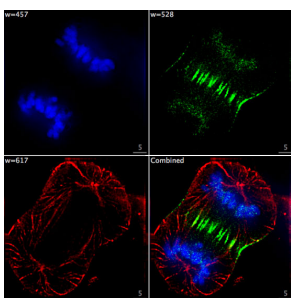
Epifluorescence microscopy



Epifluorescence microscopy is a method of fluorescence microscopy that is widely used in life sciences. The excitatory light is passed from above (or, for inverted microscopes, from below), through the objective and then onto the specimen instead of passing it first through the specimen. (In the latter case the transmitted excitatory light reaches the objective together with light emitted from the specimen). The fluorescence in the specimen gives rise to emitted light which is focused to the detector by the same objective that is used for the excitation. A filter between the objective and the detector filters out the excitation light from fluorescent light. Since most of the excitatory light is transmitted through the specimen, only reflected excitatory light reaches the objective together with the

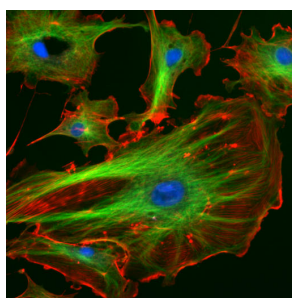
emitted light and this method therefore gives an improved signal to noise ratio. A common use in biology is to apply fluorescent or fluorochrome stains to the specimen in order to image a protein or other molecule of interest.

Gallery

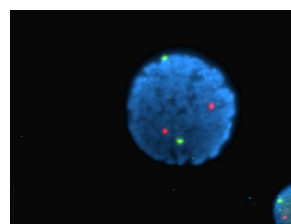


Epifluorescent imaging of the three components in a dividing human cancer cell. DNA is stained blue, a protein called INCENP is green, and the microtubules are red.

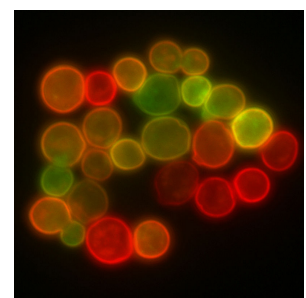
Each fluorophore is imaged separately using a different combination of excitation and emission filters, and the images are captured sequentially using a digital CCD camera, then overlaid to give a complete image.



Endothelial cells under the microscope. Nuclei are stained blue with DAPI, microtubules are marked green by an antibody bound to FITC and actin filaments are labelled red with phalloidin bound to TRITC. Bovine pulmonary artery endothelial (BPAE) cells



human lymphocyte nucleus stained with DAPI with chromosome 13 (green) and 21 (red) centromere probes hybridized (Fluorescent in situ hybridization (FISH))



Yeast cell membrane visualized by some membrane proteins fused with RFP and GFP fluorescent markers. Imposition of light from both of markers results in yellow colour.

See also

- Microscope
- Mercury-vapor lamp
- Xenon arc lamp
- Stokes shift

References

- [1] Spring KR, Davidson MW.
<http://www.microscopyu.com/articles/fluorescence/fluorescenceintro.html>|"Introduction to Fluorescence Microscopy". *Nikon MicroscopyU*. <http://www.microscopyu.com/articles/fluorescence/fluorescenceintro.html>. Retrieved on 2008-09-28.
- [2] http://nobelprize.org/educational_games/physics/microscopes/fluorescence/|"The Fluorescence Microscope". *Microscopes—Help Scientists Explore Hidden Worlds*. The Nobel Foundation. http://nobelprize.org/educational_games/physics/microscopes/fluorescence/. Retrieved on 2008-09-28.

Further reading

- Bradbury, S. and Evennett, P., Fluorescence microscopy., Contrast Techniques in Light Microscopy., BIOS Scientific Publishers, Ltd., Oxford, United Kingdom (1996).
- Rost, F., Quantitative fluorescence microscopy. Cambridge University Press, Cambridge, United Kingdom (1991).
- Rost, F., Fluorescence microscopy. Vol. I. Cambridge University Press, Cambridge, United Kingdom (1992). Reprinted with update, 1996.
- Rost, F., Fluorescence microscopy. Vol. II. Cambridge University Press, Cambridge, United Kingdom (1995).
- Rost, F. and Oldfield, R., Fluorescence microscopy., Photography with a Microscope, Cambridge University Press, Cambridge, United Kingdom (2000).

External links

- WikiScope (<http://wikiscope.org>)
 - Fluorophores.org (<http://www.fluorophores.org>) - Database of fluorescent dyes.
-

Fluorescence correlation spectroscopy

Fluorescence correlation spectroscopy (FCS) is a common technique used by physicists, chemists, and biologists to experimentally characterize the dynamics of fluorescent species (e.g. single fluorescent dye molecules in nanostructured materials, autofluorescent proteins in living cells, etc.). Although the name indicates a specific link to fluorescence, the method is used today also for exploring other forms of luminescence (like reflections, luminescence from gold-beads or quantum dots or phosphorescent species). The "spectroscopy" in the name is not readily found as in common usage a spectrum is generally understood to be a frequency spectrum. The autocorrelation is a genuine form of spectrum, however: It is the time-spectrum generated from the power spectrum (via inverse fourier transform).

Commonly, FCS is employed in the context of optical microscopy, in particular confocal or two photon microscopy. In these techniques light is focused on a sample and the measured fluorescence intensity fluctuations (due to diffusion, physical or chemical reactions, aggregation, etc.) are analyzed using the temporal autocorrelation. Because the measured property is essentially related to the magnitude and/or the amount of fluctuations, there is an optimum measurement regime at the level when individual species enter or exit the observation volume (or turn on and off in the volume). When too many entities are measured at the same time the overall fluctuations are small in comparison to the total signal and may not be resolvable - in the other direction, if the individual fluctuation-events are too sparse in time, one measurement may take prohibitively too long. FCS is in a way the fluorescent counterpart to dynamic light scattering, which uses coherent light scattering, instead of (incoherent) fluorescence.

When an appropriate model is known, FCS can be used to obtain quantitative information such as

- diffusion coefficients
- hydrodynamic radii
- average concentrations
- kinetic chemical reaction rates
- singlet-triplet dynamics

Because fluorescent markers come in a variety of colors and can be specifically bound to a particular molecule (e.g. proteins, polymers, metal-complexes, etc.), it is possible to study the behavior of individual molecules (in rapid succession in composite solutions). With the development of sensitive detectors such as avalanche photodiodes the detection of the fluorescence signal coming from individual molecules in highly dilute samples has become practical. With this emerged the possibility to conduct FCS experiments in a wide variety of specimens, ranging from materials science to biology. The advent of engineered cells with genetically tagged proteins (like green fluorescent protein) has made FCS a common tool for studying molecular dynamics in living cells.

History

Signal-correlation techniques have first been experimentally applied to fluorescence in 1972 by Magde, Elson, and Webb^[1], who are therefore commonly credited as the "inventors" of FCS. The technique was further developed in a group of papers by these and other authors soon after, establishing the theoretical foundations and types of applications.^{[2] [3] [4]} See Thompson (1991)^[5] for a review of that period.

Beginning in 1993^[6], a number of improvements in the measurement techniques--notably using confocal microscopy, and then two photon microscopy--to better define the measurement volume and reject background greatly improved the signal-to-noise and allowed single molecule sensitivity.^{[7] [8]} Since then, there has been a renewed interest in FCS, and as of August 2007 there has been over 3,000 papers using FCS found in Web of Science. See Krichevsky and Bonnet^[9] for a recent review. In addition, there has been a flurry of activity extending FCS in various ways, for instance to laser scanning and spinning disk confocal microscopy (from a stationary, single point measurement), in using cross-correlation (FCCS) between two fluorescent channels instead of autocorrelation, and in using Förster Resonance Energy Transfer (FRET) instead of fluorescence.

Typical FCS setup

The typical FCS setup consists of a laser line (wavelengths ranging typically from 405 - 633 nm (cw), and from 690 - 1100 nm (pulsed)), which is reflected into a microscope objective by a dichroic mirror. The laser beam is focused in the sample, which contains fluorescent particles (molecules) in such high dilution, that only few are within the focal spot (usually 1 - 100 molecules in one fL). When the particles cross the focal volume, they fluoresce. This light is collected by the same objective and, because it is red-shifted with respect to the excitation light it passes the dichroic reaching a detector, typically a photomultiplier tube or avalanche photodiode detector. The resulting electronic signal can be stored either directly as an intensity versus time trace to be analyzed at a later point, or, computed to generate the autocorrelation directly (which requires special acquisition cards). The FCS curve by itself only represents a time-spectrum. Conclusions on physical phenomena have to be extracted from there with appropriate models. The parameters of interest are found after fitting the autocorrelation curve to modeled functional forms.^[10] The setup is shown in Figure 1.

The Measurement Volume

The measurement volume is a convolution of illumination (excitation) and detection geometries, which result from the optical elements involved. The resulting volume is described mathematically by the point spread function (or PSF), it is essentially the image of a point source. The PSF is often described as an ellipsoid (with unsharp boundaries) of few hundred nanometers in focus diameter, and almost one micrometre along the optical axis. The shape varies significantly (and has a large impact on the resulting FCS curves) depending on the quality of the optical elements (it is crucial to avoid astigmatism and to check the real shape of the PSF on the instrument). In the case of confocal microscopy, and for small pinholes (around one Airy unit), the PSF is well approximated by Gaussians:

$$PSF(r, z) = I_0 e^{-2r^2/\omega_{xy}^2} e^{-2z^2/\omega_z^2}$$

where I_0 is the peak intensity, r and z are radial and axial position, and ω_{xy} and ω_z are the radial and axial radii, and $\omega_z > \omega_{xy}$. This Gaussian form is assumed in deriving the functional form of the autocorrelation.

Typically ω_{xy} is 200-300 nm, and ω_z is **2-6** times larger.^[11] One common way of calibrating the measurement volume parameters is to perform FCS on a species with known diffusion coefficient and concentration (see below). Diffusion coefficients for common fluorophores in water are given in a later section.

The Gaussian approximation works to varying degrees depending on the optical details, and corrections can sometimes be applied to offset the errors in approximation.^[12]

Autocorrelation Function

The (temporal) autocorrelation function is the correlation of a time series with itself shifted by time τ , as a function of τ :

$$G(\tau) = \frac{\langle \delta I(t) \delta I(t + \tau) \rangle}{\langle I(t) \rangle^2} = \frac{\langle I(t) I(t + \tau) \rangle}{\langle I(t) \rangle^2} - 1$$

where $\delta I(t) = I(t) - \langle I(t) \rangle$ is the deviation from the mean intensity. The normalization (denominator) here is the most commonly used for FCS, because then the correlation at $\tau = 0$, $G(0)$, is related to the average number of particles in the measurement volume.

Interpreting the Autocorrelation Function

To extract quantities of interest, the autocorrelation data can be fitted, typically using a nonlinear least squares algorithm. The fit's functional form depends on the type of dynamics (and the optical geometry in question).

Normal Diffusion

The fluorescent particles used in FCS are small and thus experience thermal motions in solution. The simplest FCS experiment is thus normal 3D diffusion, for which the autocorrelation is:

$$G(\tau) = G(0) \frac{1}{(1 + (\tau/\tau_D)) (1 + a^{-2}(\tau/\tau_D))^{1/2}} + G(\infty)$$

where $a = \omega_z/\omega_{xy}$ is the ratio of axial to radial e^{-2} radii of the measurement volume, and τ_D is the characteristic residence time. This form was derived assuming a Gaussian measurement volume. Typically, the fit would have three free parameters-- $G(0)$, $G(\infty)$, and τ_D --from which the diffusion coefficient and fluorophore concentration can be obtained. With the normalization used in the previous section, $G(0)$ gives the mean number of diffusers in the volume $\langle N \rangle$, or equivalently--with knowledge of the observation volume size--the mean concentration:

$$G(0) = \frac{1}{\langle N \rangle} = \frac{1}{V_{eff} \langle C \rangle},$$

where the effective volume is found from integrating the Gaussian form of the measurement volume and is given by:

$$V_{eff} = \pi^{3/2} \omega_{xy}^2 \omega_z.$$

τ_D gives the diffusion coefficient: $D = \omega_{xy}^2 / 4\tau_D$.

Anomalous diffusion

If the diffusing particles are hindered by obstacles or pushed by a force (molecular motors, flow, etc.) the dynamics is often not sufficiently well-described by the normal diffusion model, where the mean squared displacement (MSD) grows linearly with time. Instead the diffusion may be better described as anomalous diffusion, where the temporal dependence of the MSD is non-linear as in the power-law:

$$MSD = 6D_a t^\alpha$$

where D_a is an anomalous diffusion coefficient. "Anomalous diffusion" commonly refers only to this very generic model, and not the many other possibilities that might be described as anomalous. Also, a power law is, in a strict sense, the expected form only for a narrow range of rigorously defined systems, for instance when the distribution of obstacles is fractal. Nonetheless a power law can be a useful approximation for a wider range of systems.

The FCS autocorrelation function for anomalous diffusion is:

$$G(\tau) = G(0) \frac{1}{(1 + (\tau/\tau_D)^\alpha)(1 + a^{-2}(\tau/\tau_D)^\alpha)^{1/2}} + G(\infty),$$

where the anomalous exponent α is the same as above, and becomes a free parameter in the fitting.

Using FCS, the anomalous exponent has been shown to be an indication of the degree of molecular crowding (it is less than one and smaller for greater degrees of crowding)^[13].

Polydisperse diffusion

If there are diffusing particles with different sizes (diffusion coefficients), it is common to fit to a function that is the sum of single component forms:

$$G(\tau) = G(0) \sum_i \frac{\alpha_i}{(1 + (\tau/\tau_{D,i})) (1 + a^{-2}(\tau/\tau_{D,i}))^{1/2}} + G(\infty)$$

where the sum is over the number different sizes of particle, indexed by i , and α_i gives the weighting, which is related to the quantum yield and concentration of each type. This introduces new parameters, which makes the fitting more difficult as a higher dimensional space must be searched. Nonlinear least square fitting typically becomes unstable with even a small number of $\tau_{D,i}$ s. A more robust fitting scheme, especially useful for polydisperse samples, is the Maximum Entropy Method^[14].

Diffusion with flow

With diffusion together with a uniform flow with velocity v in the lateral direction, the autocorrelation is^[15]:

$$G(\tau) = G(0) \frac{1}{(1 + (\tau/\tau_D)) (1 + a^{-2}(\tau/\tau_D))^{1/2}} \times \exp[-(\tau/\tau_v)^2 \times \frac{1}{1 + \tau/\tau_D}] + G(\infty)$$

where $\tau_v = \omega_{xy}/v$ is the average residence time if there is only a flow (no diffusion).

Chemical relaxation

A wide range of possible FCS experiments involve chemical reactions that continually fluctuate from equilibrium because of thermal motions (and then "relax"). In contrast to diffusion, which is also a relaxation process, the fluctuations cause changes between states of different energies. One very simple system showing chemical relaxation would be a stationary binding site in the measurement volume, where particles only produce signal when bound (e.g. by FRET, or if the diffusion time is much faster than the sampling interval). In this case the autocorrelation is:

$$G(\tau) = G(0) \exp(-\tau/\tau_B) + G(\infty)$$

where

$$\tau_B = (k_{on} + k_{off})^{-1}$$

is the relaxation time and depends on the reaction kinetics (on and off rates), and:

$$G(0) = \frac{1}{\langle N \rangle} \frac{k_{on}}{k_{off}} = \frac{1}{\langle N \rangle} K$$

is related to the equilibrium constant K .

Most systems with chemical relaxation also show measureable diffusion as well, and the autocorrelation function will depend on the details of the system. If the diffusion and chemical reaction are decoupled, the combined autocorrelation is the product of the chemical and diffusive autocorrelations.

Triplet State Correction

The autocorrelations above assume that the fluctuations are not due to changes in the fluorescent properties of the particles. However, for the majority of (bio)organic fluorophores--e.g. green fluorescent protein, rhodamine, Cy3 and Alexa Fluor dyes--some fraction of illuminated particles are excited to a triplet state (or other non-radiative decaying states) and then do not emit photons for a characteristic relaxation time τ_F . Typically τ_F is on the order of microseconds, which is usually smaller than the dynamics of interest (e.g. τ_D) but large enough to be measured. A multiplicative term is added to the autocorrelation account for the triplet state. For normal diffusion:

$$G(\tau) = G(0) \frac{1 - F + F e^{-\tau/\tau_F}}{1 - F} \frac{1}{(1 + (\tau/\tau_{D,i})) (1 + a^{-2}(\tau/\tau_{D,i}))^{1/2}} + G(\infty)$$

where F is the fraction of particles that have entered the triplet state and τ_F is the corresponding triplet state relaxation time. If the dynamics of interest are much slower than the triplet state relaxation, the short time component of the autocorrelation can simply be truncated and the triplet term is unnecessary.

Common fluorescent probes

The fluorescent species used in FCS is typically a biomolecule of interest that has been tagged with a fluorophore (using immunohistochemistry for instance), or is a naked fluorophore that is used to probe some environment of interest (e.g. the cytoskeleton of a cell). The following table gives diffusion coefficients of some common fluorophores in water at room temperature, and their excitation wavelengths.

Fluorescent dye	D ($\times 10^{-10} \text{ m}^2 \text{ s}^{-1}$)	Excitation wavelength (nm)	Reference

Rhodamine 6G	2.8, 3.0, 4.14 ± 0.05 @ 25.00 °C	514	[16] , [17] , [18]
Rhodamine 110	2.7	488	[19]
Tetramethyl rhodamine	2.6	543	
Cy3	2.8	543	
Cy5	2.5, 3.7 ± 0.15 @ 25.00 °C	633	[20] , [21]
carboxyfluorescein	3.2	488	
Alexa-488	1.96	488	[22]
Atto655-maleimide	4.07 ± 0.1 @ 25.00 °C	663	[23]
Atto655-carboxylicacid	4.26 ± 0.08 @ 25.00 °C	663	[24]
2', 7'-difluorofluorescein (Oregon Green488)	4.11 ± 0.06 @ 25.00 °C	498	[25]

Variations of FCS

FCS almost always refers to the single point, single channel, temporal autocorrelation measurement, although the term "fluorescence correlation spectroscopy" out of its historical scientific context implies no such restriction. FCS has been extended in a number of variations by different researchers, with each extension generating another name (usually an acronym).

Fluorescence Cross-Correlation Spectroscopy (FCCS)

FCS is sometimes used to study molecular interactions using differences in diffusion times (e.g. the product of an association reaction will be larger and thus have larger diffusion times than the reactants individually); however, FCS is relatively insensitive to molecular mass as can be seen from the following equation relating molecular mass to the diffusion time of globular particles (e.g. proteins):

$$\tau_D = \frac{3\pi\omega_{xy}^2\eta}{2kT}(M)^{1/3}$$

where η is the viscosity of the sample and M is the molecular mass of the fluorescent species. In practice, the diffusion times need to be sufficiently different--a factor of at least **1.6**--which means the molecular masses must differ by a factor of **4**.^[26] Dual color fluorescence cross-correlation spectroscopy (FCCS) measures interactions by cross-correlating two or more fluorescent channels (one channel for each reactant), which distinguishes interactions more sensitively than FCS, particularly when the mass change in the reaction is small.

Two- and three- photon FCS excitation

Several advantages in both spatial resolution and minimizing photodamage/photobleaching in organic and/or biological samples are obtained by two-photon or three-photon excitation FCS^{[27] [28] [29] [30] [31]}.

FRET-FCS

Another FCS based approach to studying molecular interactions uses fluorescence resonance energy transfer (FRET) instead of fluorescence, and is called FRET-FCS.^[32] With FRET, there are two types of probes, as with FCCS; however, there is only one channel and light is only detected when the two probes are very close--close enough to ensure an interaction. The FRET signal is weaker than with fluorescence, but has the advantage that there is only signal during a reaction (aside from autofluorescence).

Image Correlation Spectroscopy (ICS)

When the motion is slow (in biology, for example, diffusion in a membrane), getting adequate statistics from a single-point FCS experiment may take a prohibitively long time. More data can be obtained by performing the experiment in multiple spatial points in parallel, using a laser scanning confocal microscope. This approach has been called Image Correlation Spectroscopy (ICS)^[33]. The measurements can then be averaged together.

Another variation of ICS performs a spatial autocorrelation on images, which gives information about the concentration of particles^[34]. The correlation is then averaged in time.

A natural extension of the temporal and spatial correlation versions is spatio-temporal ICS (STICS)^[35]. In STICS there is no explicit averaging in space or time (only the averaging inherent in correlation). In systems with non-isotropic motion (e.g. directed flow, asymmetric diffusion), STICS can extract the directional information. A variation that is closely related to STICS (by the Fourier transform) is k-space Image Correlation Spectroscopy (kICS).^[36]

There are cross-correlation versions of ICS as well.^[33]

Scanning FCS variations

Some variations of FCS are only applicable to serial scanning laser microscopes. Image Correlation Spectroscopy and its variations all were implemented on a scanning confocal or scanning two photon microscope, but transfer to other microscopes, like a spinning disk confocal microscope. Raster ICS (RICS)^[37], and position sensitive FCS (PSFCS)^[38] incorporate the time delay between parts of the image scan into the analysis. Also, low dimensional scans (e.g. a circular ring)^[39]--only possible on a scanning system--can access time scales between single point and full image measurements. Scanning path has also been made to adaptively follow particles.^[40]

Spinning disk FCS, and spatial mapping

Any of the image correlation spectroscopy methods can also be performed on a spinning disk confocal microscope, which in practice can obtain faster imaging speeds compared to a laser scanning confocal microscope. This approach has recently been applied to diffusion in a spatially varying complex environment, producing a pixel resolution map of diffusion coefficient.^[41] The spatial mapping of diffusion with FCS has subsequently been extended to TIRF system.^[42] Spatial mapping of dynamics using correlation techniques had been applied before, but only at sparse points^[43] or at coarse resolution^[35].

Total internal reflection FCS

Total internal reflection fluorescence (TIRF) is a microscopy approach that is only sensitive to a thin layer near the surface of a coverslip, which greatly minimizes background fluorescence. FCS has been extended to that type of microscope, and is called TIR-FCS^[44]. Because the fluorescence intensity in TIRF falls off exponentially with distance from the coverslip (instead of as a Gaussian with a confocal), the autocorrelation function is different.

Other fluorescent dynamical approaches

There are two main non-correlation alternatives to FCS that are widely used to study the dynamics of fluorescent species.

Fluorescence recovery after photobleaching (FRAP)

In FRAP, a region is briefly exposed to intense light, irrecoverably photobleaching fluorophores, and the fluorescence recovery due to diffusion of nearby (non-bleached) fluorophores is imaged. A primary advantage of FRAP over FCS is the ease of interpreting qualitative experiments common in cell biology. Differences between cell lines, or regions of a cell, or before and after application of drug, can often be characterized by simple inspection of movies. FCS experiments require a level of processing and are more sensitive to potentially confounding influences like: rotational diffusion, vibrations, photobleaching, dependence on illumination and fluorescence color, inadequate statistics, etc. It is much easier to change the measurement volume in FRAP, which allows greater control. In practice, the volumes are typically larger than in FCS. While FRAP experiments are typically more qualitative, some researchers are studying FRAP quantitatively and including binding dynamics.^[45] A disadvantage of FRAP in cell biology is the free radical perturbation of the cell caused by the photobleaching. It is also less versatile, as it cannot measure concentration or rotational diffusion, or co-localization. FRAP requires a significantly higher concentration of fluorophores than FCS.

Particle tracking

In particle tracking, the trajectories of a set of particles are measured, typically by applying particle tracking algorithms to movies.^[46] Particle tracking has the advantage that all the dynamical information is maintained in the measurement, unlike FCS where correlation averages the dynamics to a single smooth curve. The advantage is apparent in systems showing complex diffusion, where directly computing the mean squared displacement allows straightforward comparison to normal or power law diffusion. To apply particle tracking, the particles have to be distinguishable and thus at lower concentration than

required of FCS. Also, particle tracking is more sensitive to noise, which can sometimes affect the results unpredictably.

References

- [1] Magde, D., Elson, E. L., Webb, W. W. Thermodynamic fluctuations in a reacting system: Measurement by fluorescence correlation spectroscopy, (1972) *Phys Rev Lett*, **29**, 705-708.
- [2] Ehrenberg, M., Rigler, R. Rotational brownian motion and fluorescence intensity fluctuations, (1974) *Chem Phys*, **4**, 390-401.
- [3] Elson, E. L., Magde, D. Fluorescence correlation spectroscopy I. Conceptual basis and theory, (1974) *Biopolymers*, **13**, 1-27.
- [4] Magde, D., Elson, E. L., Webb, W. W. Fluorescence correlation spectroscopy II. An experimental realization, (1974) *Biopolymers*, **13**, 29-61.
- [5] Thompson N L 1991 Topics in Fluorescence Spectroscopy Techniques vol 1, ed J R Lakowicz (New York: Plenum) pp 337-78
- [6] Rigler, R., Mets, J., Widengren, P., Kask, K. Fluorescence correlation spectroscopy with high count rate and low background: analysis of translational diffusion. *European Biophysics Journal* (1993) **22**(3), 159.
- [7] Eigen, M., Rigler, M. Sorting single molecules: application to diagnostics and evolutionary biotechnology, (1994) *Proc. Natl. Acad. Sci. USA*, **91**, 5740-5747.
- [8] Rigler, M. Fluorescence correlations, single molecule detection and large number screening. Applications in biotechnology, (1995) *J. Biotechnol.*, **41**, 177-186.
- [9] O. Krichinsky, G. Bonnet, "Fluorescence correlation spectroscopy: the technique and its applications," *Rep. Prog. Phys.* **65**, 251-297 (2002).
- [10] Medina, M. A., Schwille, P. Fluorescence correlation spectroscopy for the detection and study of single molecules in biology, (2002) *BioEssays*, **24**, 758-764.
- [11] Mayboroda, O. A., van Remoortere, A., Tanke H. J., Hokke, C. H., Deelder, A. M., A new approach for fluorescence correlation spectroscopy (FCS) based immunoassays, (2003), *J. Biotechnol.*, **107**, 185-192.
- [12] Hess, S.T., and W.W. Webb. 2002. Focal volume optics and experimental artifacts in confocal fluorescence correlation spectroscopy. *Biophys. J.* **83**:2300-2317.
- [13] Banks, D. S., and C. Fradin. 2005. Anomalous diffusion of proteins due to molecular crowding. *Biophys. J.* **89**:2960-2971.
- [14] Sengupta, P., K. Garai, J. Balaji, N. Periasamy, and S. Maiti. 2003. Measuring Size Distribution in Highly Heterogeneous Systems with Fluorescence Correlation Spectroscopy. *Biophys. J.* **84**(3):1977-1984.
- [15] Kohler, R.H., P. Schwille, W.W. Webb, and M.R. Hanson. 2000. Active protein transport through plastid tubules: velocity quantified by fluorescence correlation spectroscopy. *J Cell Sci* **113**(22):3921-3930
- [16] Magde, D., Elson, E. L., Webb, W. W. Fluorescence correlation spectroscopy II. An experimental realization, (1974) *Biopolymers*, **13**, 29-61.
- [17] Berland, K. M. Detection of specific DNA sequences using dual-color two-photon fluorescence correlation spectroscopy. (2004) *J. Biotechnol*, **108**(2), 127-136.
- [18] Müller, C.B., Loman, A., Pacheco, V., Koberling, F., Willbold, D., Richtering, W., Enderlein, J. Precise measurement of diffusion by multi-color dual-focus fluorescence correlation spectroscopy (2008), *EPL*, **83**, 46001.
- [19] Pristinski, D., Kozlovskaya, V., Sukhishvili, S. A. Fluorescence correlation spectroscopy studies of diffusion of a weak polyelectrolyte in aqueous solutions. (2005), *J. Chem. Phys.*, **122**, 014907.
- [20] Widengren, J., Schwille, P., Characterization of photoinduced isomerization and back-isomerization of the cyanine dye Cy5 by fluorescence correlation spectroscopy. (2000), *J. Phys. Chem. A*, **104**, 6416-6428.
- [21] Loman, A., Dertinger, T., Koberling, F., Enderlein, J. Comparison of optical saturation effects in conventional and dual-focus fluorescence correlation spectroscopy (2008), *Chem. Phys. Lett.*, **459**, 18-21.
- [22] Pristinski, D., Kozlovskaya, V., Sukhishvili, S. A. Fluorescence correlation spectroscopy studies of diffusion of a weak polyelectrolyte in aqueous solutions. (2005), *J. Chem. Phys.*, **122**, 014907.
- [23] Müller, C.B., Loman, A., Pacheco, V., Koberling, F., Willbold, D., Richtering, W., Enderlein, J. Precise measurement of diffusion by multi-color dual-focus fluorescence correlation spectroscopy (2008), *EPL*, **83**, 46001.
- [24] Müller, C.B., Loman, A., Pacheco, V., Koberling, F., Willbold, D., Richtering, W., Enderlein, J. Precise measurement of diffusion by multi-color dual-focus fluorescence correlation spectroscopy (2008), *EPL*, **83**, 46001.
- [25] Müller, C.B., Loman, A., Pacheco, V., Koberling, F., Willbold, D., Richtering, W., Enderlein, J. Precise measurement of diffusion by multi-color dual-focus fluorescence correlation spectroscopy (2008), *EPL*, **83**, 46001.

- [26] Meseth, U., Wohland, T., Rigler, R., Vogel, H. Resolution of fluorescence correlation measurements. (1999) *Biophys. J.*, **76**, 1619-1631.
- [27] Diaspro, A., and Robello, M. (1999). Multi-photon Excitation Microscopy to Study Biosystems. *European Microscopy and Analysis.*, 5:5-7.
- [28] Bagatolli, L.A., and Gratton, E. (2000). Two-photon fluorescence microscopy of coexisting lipid domains in giant unilamellar vesicles of binary phospholipid mixtures. *Biophys J.*, 78:290-305.
- [29] Schwille, P., Haupts, U., Maiti, S., and Webb, W. (1999). Molecular dynamics in living cells observed by fluorescence correlation spectroscopy with one- and two- photon excitation. *Biophysical Journal*, **77**(10):2251-2265.
- [30] Near Infrared Microspectroscopy, Fluorescence Microspectroscopy, Infrared Chemical Imaging and High Resolution Nuclear Magnetic Resonance Analysis of Soybean Seeds, Somatic Embryos and Single Cells., Baianu, I.C. et al. 2004., In *Oil Extraction and Analysis.*, D. Luthria, Editor pp.241-273, AOCS Press., Champaign, IL.
- [31] Single Cancer Cell Detection by Near Infrared Microspectroscopy, Infrared Chemical Imaging and Fluorescence Microspectroscopy. 2004. I. C. Baianu, D. Costescu, N. E. Hofmann and S. S. Korban, q-bio/0407006 (July 2004) (<http://arxiv.org/abs/q-bio/0407006>)
- [32] K. Remaut, B. Lucas, K. Braeckmans, N.N. Sanders, S.C. De Smedt and J. Demeester, FRET-FCS as a tool to evaluate the stability of oligonucleotide drugs after intracellular delivery, *J Control Rel* 103 (2005) (1), pp. 259-271.
- [33] Wiseman, P. W., J. A. Squier, M. H. Ellisman, and K. R. Wilson. 2000. Two-photon video rate image correlation spectroscopy (ICS) and image cross-correlation spectroscopy (ICCS). *J. Microsc.* 200:14-25.
- [34] Petersen, N. O., P. L. Höddelius, P. W. Wiseman, O. Seger, and K. E. Magnusson. 1993. Quantitation of membrane receptor distributions by image correlation spectroscopy: concept and application. *Biophys. J.* 65:1135-1146.
- [35] Hebert, B., S. Constantino, and P. W. Wiseman. 2005. Spatio-temporal image correlation spectroscopy (STICS): theory, verification and application to protein velocity mapping in living CHO cells. *Biophys. J.* 88:3601-3614.
- [36] Kolin, D.L., D. Ronis, and P.W. Wiseman. 2006. k-Space Image Correlation Spectroscopy: A Method for Accurate Transport Measurements Independent of Fluorophore Photophysics. *Biophys. J.* 91(8):3061-3075.
- [37] Digman, M.A., P. Sengupta, P.W. Wiseman, C.M. Brown, A.R. Horwitz, and E. Gratton. 2005. Fluctuation Correlation Spectroscopy with a Laser-Scanning Microscope: Exploiting the Hidden Time Structure. *Biophys. J.* 88(5):L33-36.
- [38] Skinner, J.P., Y. Chen, and J.D. Mueller. 2005. Position-Sensitive Scanning Fluorescence Correlation Spectroscopy. *Biophys. J.*:biophysj.105.060749.
- [39] Ruan, Q., M.A. Cheng, M. Levi, E. Gratton, and W.W. Mantulin. 2004. Spatial-temporal studies of membrane dynamics: scanning fluorescence correlation spectroscopy (SFCS). *Biophys. J.* 87:1260-1267.
- [40] A. Berglund and H. Mabuchi, "Tracking-FCS: Fluorescence correlation spectroscopy of individual particles," *Opt. Express* 13, 8069-8082 (2005).
- [41] Sisan, D.R., R. Arevalo, C. Graves, R. McAllister, and J.S. Urbach. 2006. Spatially resolved fluorescence correlation spectroscopy using a spinning disk confocal microscope. *Biophysical Journal* 91(11):4241-4252.
- [42] Kannan, B., L. Guo, T. Sudhakaran, S. Ahmed, I. Maruyama, and T. Wohland. 2007. Spatially resolved total internal reflection fluorescence correlation microscopy using an electron multiplying charge-coupled device camera. *Analytical Chemistry* 79(12):4463-4470
- [43] Wachsmuth, M., W. Waldeck, and J. Langowski. 2000. Anomalous diffusion of fluorescent probes inside living cell nuclei investigated by spatially-resolved fluorescence correlation spectroscopy. *J. Mol. Biol.* 298(4):677-689.
- [44] Lieto, A.M., and N.L. Thompson. 2004. Total Internal Reflection with Fluorescence Correlation Spectroscopy: Nonfluorescent Competitors. *Biophys. J.* 87(2):1268-1278.
- [45] Sprague, B.L., and J.G. McNally. 2005. FRAP analysis of binding: proper and fitting. *Trends in Cell Biology* 15(2):84-91.
- [46] <http://www.physics.emory.edu/~weeks/idl/>

See also

- Confocal microscopy
- Fluorescence cross-correlation spectroscopy
- FRET
- Dynamic light scattering
- Diffusion coefficient

External links

- Single-molecule spectroscopic methods (<http://dx.doi.org/10.1016/j.sbi.2004.09.004>)
- FCS Classroom (<http://www.fcsxpert.com/classroom>)

Fluorescence cross-correlation spectroscopy

Fluorescence cross-correlation spectroscopy (FCCS) was introduced by Eigen and Rigler in 1994 and experimentally realized by Schwille in 1997. It extends the fluorescence correlation spectroscopy (FCS) procedure by introducing high sensitivity for distinguishing fluorescent particles which have a similar diffusion coefficient. FCCS uses two species which are independently labelled with two spectrally separated fluorescent probes. These fluorescent probes are excited and detected by two different laser light sources and detectors commonly known as green and red respectively. Both laser light beams are focused into the sample and tuned so that they overlap to form a superimposed confocal observation volume.

The normalized cross-correlation function is defined for two fluorescent species G and R which are independent green, G and red, R channels as follows:

$$G_{GR}(\tau) = 1 + \frac{\langle \delta I_G(t) \delta I_R(t + \tau) \rangle}{\langle I_G(t) \rangle \langle I_R(t) \rangle} = \frac{\langle I_G(t) I_R(t + \tau) \rangle}{\langle I_G(t) \rangle \langle I_R(t) \rangle}$$

where differential fluorescent signals δI_G at a specific time, t and δI_R at a delay time, τ later is correlated with each other.

Modeling

Cross-correlation curves are modeled according to a slightly more complicated mathematical function than applied in FCS. First of all, the effective superimposed observation volume in which the G and R channels form a single observation volume, $V_{eff, RG}$ in the solution:

$$V_{eff, RG} = \pi^{3/2} (\omega_{xy, G}^2 + \omega_{xy, R}^2) (\omega_{z, G}^2 + \omega_{z, R}^2)^{1/2} / 2^{3/2}$$

where $\omega_{xy, G}^2$ and $\omega_{xy, R}^2$ are radial parameters and $\omega_{z, G}$ and $\omega_{z, R}$ are the axial parameters for the G and R channels respectively.

The diffusion time, $\tau_{D, GR}$ for a doubly (G and R) fluorescent species is therefore described as follows:

$$\tau_{D,GR} = \frac{\omega_{xy,G}^2 + \omega_{xy,R}^2}{8D_{GR}}$$

where D_{GR} is the diffusion coefficient of the doubly fluorescent particle.

The cross-correlation curve generated from diffusing doubly labelled fluorescent particles can be modelled in separate channels as follows:

$$G_G(\tau) = 1 + \frac{(\langle C_G \rangle Diff_k(\tau) + \langle C_{GR} \rangle Diff_k(\tau))}{V_{eff,GR}(\langle C_G \rangle + \langle C_{GR} \rangle)^2}$$

$$G_R(\tau) = 1 + \frac{(\langle C_R \rangle Diff_k(\tau) + \langle C_{GR} \rangle Diff_k(\tau))}{V_{eff,GR}(\langle C_R \rangle + \langle C_{GR} \rangle)^2}$$

In the ideal case, the cross-correlation function is proportional to the concentration of the doubly labeled fluorescent complex:

$$G_{GR}(\tau) = 1 + \frac{\langle C_{GR} \rangle Diff_{GR}(\tau)}{V_{eff}(\langle C_G \rangle + \langle C_{GR} \rangle)(\langle C_R \rangle + \langle C_{GR} \rangle)}$$

$$\text{with } Diff_k(\tau) = \frac{1}{(1 + \frac{\tau}{\tau_{D,i}})(1 + a^{-2}(\frac{\tau}{\tau_{D,i}})^{1/2})}$$

Contrary to FCS, the intercept of the cross-correlation curve does not yield information about the doubly labelled fluorescent particles in solution.

See also

- Fluorescence correlation spectroscopy
- Dynamic light scattering
- Fluorescence spectroscopy
- Diffusion coefficient

External links

- FCS Classroom ^[1]

References

- [1] <http://www.fcsxpert.com/classroom>

Forster resonance energy transfer

1. REDIRECT Förster resonance energy transfer

Molecular graphics

Molecular graphics (MG) is the discipline and philosophy of studying molecules and their properties through graphical representation.^[1] IUPAC limits the definition to representations on a "graphical display device".^[2] Ever since Dalton's atoms and Kekule's benzene, there has been a rich history of hand-drawn atoms and molecules, and these representations have had an important influence on modern molecular graphics. This article concentrates on the use of computers to create molecular graphics. Note, however, that many molecular graphics programs and systems have close coupling between the graphics and editing commands or calculations such as in molecular modelling.

Relation to molecular models

There has been a long tradition of creating molecular models from physical materials. Perhaps the best known is Crick and Watson's model of DNA built from rods and planar sheets, but the most widely used approach is to represent all atoms and bonds explicitly using the "ball and stick" approach. This can demonstrate a wide range of properties, such as shape, relative size, and flexibility. Many chemistry courses expect that students will have access to ball and stick models. One goal of mainstream molecular graphics has been to represent the "ball and stick" model as realistically as possible and to couple this with calculations of molecular properties.

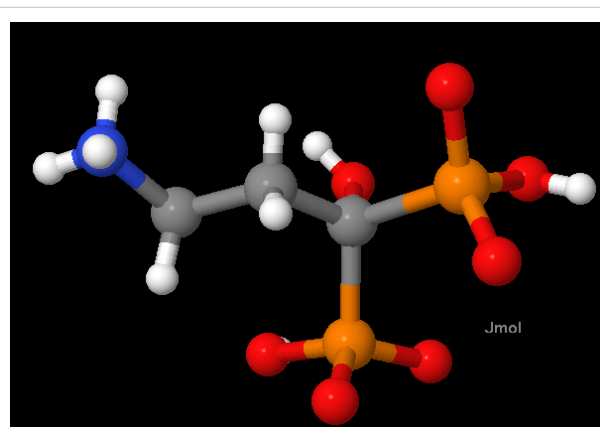


Fig. 1. Key: Hydrogen = white, carbon = grey, nitrogen = blue, oxygen = red, and phosphorus = orange.

Figure 1 shows a small molecule ($\text{NH}_3\text{CH}_2\text{CH}_2\text{C}(\text{OH})(\text{PO}_3\text{H})(\text{PO}_3\text{H})^-$), as drawn by the Jmol program. It is important to realise that the colours are purely a convention. Molecules can never be visible under any light microscope and atoms are not coloured, do not have hard surfaces and do not reflect light. Bonds are not rod-shaped. If physical molecular models had not existed, it is unlikely that molecular graphics would currently use this metaphor.

Comparison of physical models with molecular graphics

Physical models and computer models have partially complementary strengths and weaknesses. Physical models can be used by those without access to a computer and now can be made cheaply out of plastic materials. Their tactile and visual aspects cannot be easily reproduced by computers (although haptic devices have occasionally been built). On a computer screen, the flexibility of molecules is also difficult to appreciate; illustrating the

pseudorotation of cyclohexane is a good example of the value of mechanical models.

However, it is difficult to build large physical molecules, and all-atom physical models of even simple proteins could take weeks or months to build. Moreover, physical models are not robust and they decay over time. Molecular graphics is particularly valuable for representing global and local properties of molecules, such as electrostatic potential. Graphics can also be animated to represent molecular processes and chemical reactions, a feat that is not easy to reproduce physically.

History

Initially the rendering was on early CRT screens or through plotters drawing on paper. Molecular structures have always been an attractive choice for developing new computer graphics tools, since the input data are easy to create and the results are usually highly appealing. The first example of MG was a display of a protein molecule (Project MAC, 1966) by Cyrus Levinthal and Robert Langridge. Among the milestones in high-performance MG was the work of Nelson Max in "realistic" rendering of macromolecules using reflecting spheres.

By about 1980 many laboratories both in academia and industry had recognized the power of the computer to analyse and predict the properties of molecules, especially in materials science and the pharmaceutical industry. The discipline was often called "molecular graphics" and in 1982 a group of academics and industrialists in the UK set up the Molecular Graphics Society (MGS). Initially much of the technology concentrated either on high-performance 3D graphics, including interactive rotation or 3D rendering of atoms as spheres (sometimes with radiosity). During the 1980s a number of programs for calculating molecular properties (such as molecular dynamics and quantum mechanics) became available and the term "molecular graphics" often included these. As a result the MGS has now changed its name to the Molecular Graphics and Modelling Society (MGMS).

The requirements of macromolecular crystallography also drove MG because the traditional techniques of physical model-building could not scale. Alwyn Jones' FRODO program (and later "O") were developed to overlay the molecular electron density determined from X-ray crystallography and the hypothetical molecular structure.

Art, science and technology in molecular graphics

Both computer technology and graphic arts have contributed to molecular graphics. The development of structural biology in the 1950s led to a requirement to display molecules with thousands of atoms. The existing computer technology was limited in power, and in any case a naive depiction of all atoms left viewers overwhelmed. Most systems therefore used conventions where information was implicit or stylistic. Two vectors meeting at a point implied an atom or (in macromolecules) a complete residue (10-20 atoms).

The macromolecular approach was popularized by Dickerson and Geis' presentation of proteins and the graphic work of Jane Richardson through high-quality hand-drawn diagrams such as the "ribbon" representation. In this they strove to capture the intrinsic 'meaning' of the molecule. This search for the "messages in the molecule" has always accompanied the increasing power of computer graphics processing. Typically the depiction would concentrate on specific areas of the molecule (such as the active site) and this might have different colours or more detail in the number of explicit atoms or the type of depiction (e.g., spheres for atoms).

In some cases the limitations of technology have led to serendipitous methods for rendering. Most early graphics devices used vector graphics, which meant that rendering spheres and surfaces was impossible. Michael Connolly's program "MS" calculated points on the surface-accessible surface of a molecule, and the points were rendered as dots with good visibility using the new vector graphics technology, such as the Evans and Sutherland PS300 series. Thin sections ("slabs") through the structural display showed very clearly the complementarity of the surfaces for molecules binding to active sites, and the "Connolly surface" became a universal metaphor.

The relationship between the art and science of molecular graphics is shown in the exhibitions^[3] sponsored by the Molecular Graphics Society. Some exhibits are created with molecular graphics programs alone, while others are collages, or involve physical materials. An example from Mike Hann (1994), inspired by Magritte's painting *Ceci n'est pas une pipe*, uses an image of a salmeterol molecule.

"*Ceci n'est pas une molecule*," writes Mike Hann, "serves to remind us that all of the graphics images presented here are not molecules, not even pictures of molecules, but pictures of icons which we believe represent some aspects of the molecule's properties."

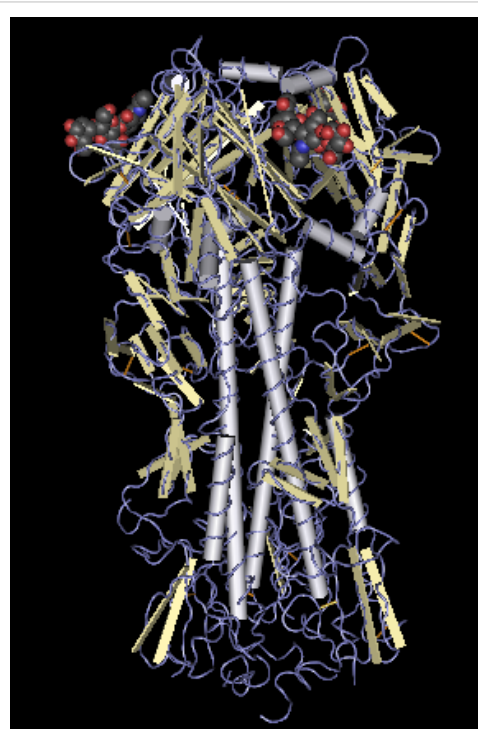
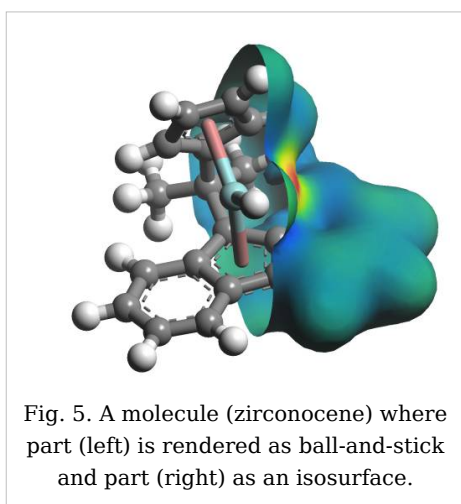
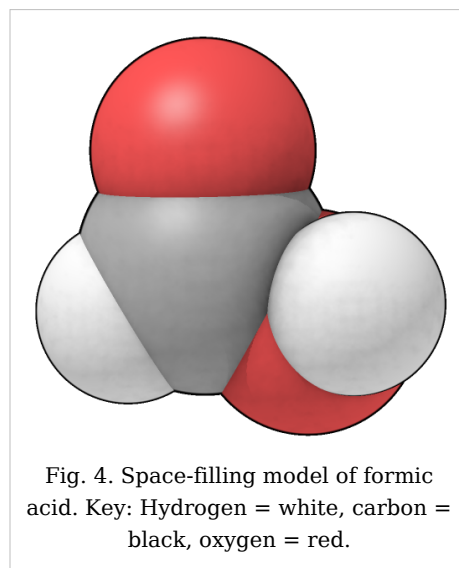


Fig. 2. Image of hemagglutinin with alpha helices depicted as cylinders and the rest of the chain as silver coils. The individual protein atoms (several thousand) have been hidden. All of the non-hydrogen atoms in the two ligands (presumably sialic acid) have been shown near the top of the diagram. Key: Carbon = grey, oxygen = red, nitrogen = blue.

Space-filling models

Fig. 4 is a "space-filling" representation of formic acid, where atoms are drawn to suggest the amount of space they occupy. This is necessarily an icon: in the quantum mechanical representation of molecules, there are only (positively charged) nuclei and a "cloud" of negative electrons. The electron cloud defines an approximate size for the molecule, though there can be no single precise definition of size. For many years the size of atoms has been approximated by mechanical models (CPK), where the atoms have been represented by plastic spheres whose radius (van der Waals radius) describes a sphere within which "most" of the electron density can be found. These spheres could be clicked together to show the steric aspects of the molecule rather than the positions of the nuclei. Fig. 4 shows the intricacy required to make sure that all spheres intersect correctly, and also demonstrates a reflective model.



Since the atomic radii (e.g. in Fig. 4) are only slightly less than the distance between bonded atoms, the iconic spheres intersect, and in the CPK models, this was achieved by planar truncations along the bonding directions, the section being circular. When raster graphics became affordable, one of the common approaches was to replicate CPK models *in silico*. It is relatively straightforward to calculate the circles of intersection, but more complex to represent a model with hidden surface removal. A useful side product is that a conventional value for the molecular volume can be calculated.

The use of spheres is often for convenience, being limited both by graphics libraries and the additional effort required to compute complete electronic density or other space-filling quantities. It is now relatively common to see images of isosurfaces that have been coloured to show quantities such as electrostatic potential. The commonest isosurfaces are the Connolly surface, or the volume within which a given proportion of the electron density lies. The isosurface in Fig. 5 appears to show the electrostatic potential, with blue colours being negative and red/yellow (near the metal) positive. (There is no absolute convention of colouring, and red/positive, blue/negative are often confusingly reversed!) Opaque isosurfaces do not allow the atoms to be seen and identified and it is not easy to deduce them. Because of this, isosurfaces are often drawn with a degree of transparency.

Technology

Molecular graphics has always pushed the limits of display technology, and has seen a number of cycles of integration and separation of compute-host and display. Early systems like Project MAC were bespoke and unique, but in the 1970s the MMS-X and similar systems used (relatively) low-cost terminals, such as the Tektronix 4014 series, often over dial-up lines to multi-user hosts. The devices could only display static pictures but, were able to evangelize MG. In the late 1970s, it was possible for departments (such as crystallography) to afford their own hosts (e.g., PDP-11) and to attach a display (such as Evans & Sutherland's MPS) directly to the bus. The display list was kept on the host, and interactivity was good since updates were rapidly reflected in the display—at the cost of reducing most machines to a single-user system.

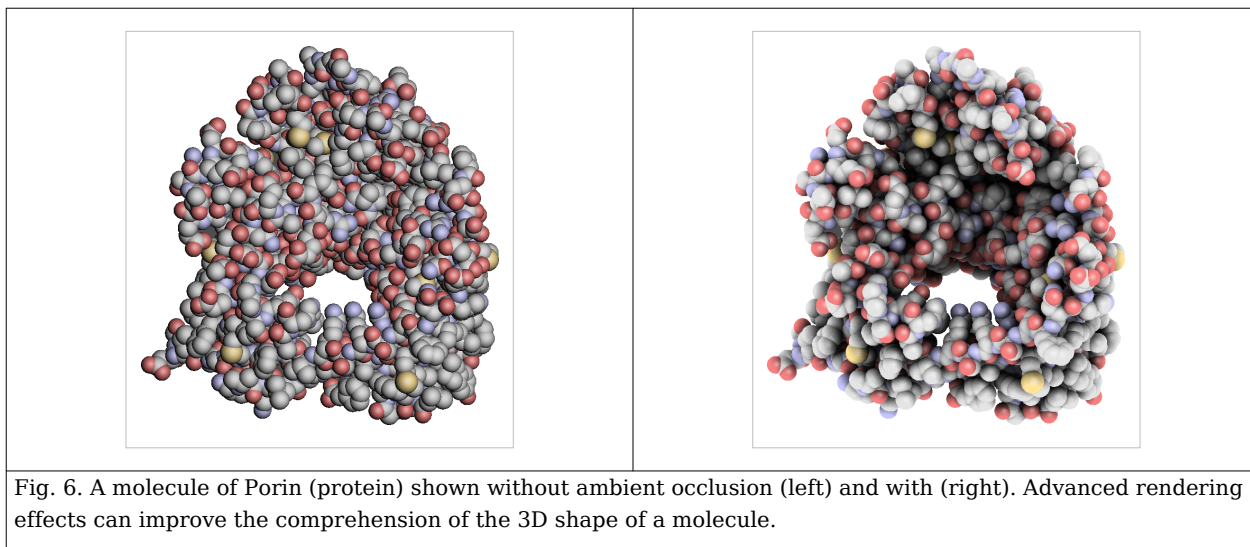
In the early 1980s, Evans & Sutherland (E&S) decoupled their PS300 display, which contained its own display information transformable through a dataflow architecture. Complex graphical objects could be downloaded over a serial line (e.g. 9600 baud) and then manipulated without impact on the host. The architecture was excellent for high performance display but very inconvenient for domain-specific calculations, such as electron-density fitting and energy calculations. Many crystallographers and modellers spent arduous months trying to fit such activities into this architecture.

The benefits for MG were considerable, but by the later 1980s, UNIX workstations such as Sun-3 with raster graphics (initially at a resolution of 256 by 256) had started to appear. Computer-assisted drug design in particular required raster graphics for the display of computed properties such as atomic charge and electrostatic potential. Although E&S had a high-end range of raster graphics (primarily aimed at the aerospace industry) they failed to respond to the low-end market challenge where single users, rather than engineering departments, bought workstations. As a result the market for MG displays passed to Silicon Graphics, coupled with the development of minisupercomputers (e.g., CONVEX and Alliant) which were affordable for well-supported MG laboratories. Silicon Graphics provided a graphics language, IrisGL, which was easier to use and more productive than the PS300 architecture. Commercial companies (e.g., Biosym, Polygen/MSI) ported their code to Silicon Graphics, and by the early 1990s, this was the "industry standard".

Stereoscopic displays were developed based on liquid crystal polarized spectacles, and while this had been very expensive on the PS300, it now became a commodity item. A common alternative was to add a polarizable screen to the front of the display and to provide viewers with extremely cheap spectacles with orthogonal polarization for separate eyes. With projectors such as Barco, it was possible to project stereoscopic display onto special silvered screens and supply an audience of hundreds with spectacles. In this way molecular graphics became universally known within large sectors of chemical and biochemical science, especially in the pharmaceutical industry. Because the backgrounds of many displays were black by default, it was common for modelling sessions and lectures to be held with almost all lighting turned off.

In the last decade almost all of this technology has become commoditized. IrisGL evolved to OpenGL so that molecular graphics can be run on any machine. In 1992, Roger Sayle released his RasMol program into the public domain. RasMol contained a very high-performance molecular renderer that ran on Unix/X Window, and Sayle later ported this to the Windows and Macintosh platforms. The Richardsons developed kinemages and the Mage software, which was also multi-platform. By specifying the chemical MIME type,

molecular models could be served over the Internet, so that for the first time MG could be distributed at zero cost regardless of platform. In 1995, Birkbeck College's crystallography department used this to run "Principles of Protein Structure", the first multimedia course on the Internet, which reached 100 to 200 scientists.



MG continues to see innovation that balances technology and art, and currently zero-cost or open source programs such as PyMOL and Jmol have very wide use and acceptance.

Recently the wide spread diffusion of advanced graphics hardware, has improved the rendering capabilities of the visualization tools. The capabilities of current shading languages allow the inclusion of advanced graphic effects (like ambient occlusion, cast shadows and non-photorealistic rendering techniques) in the interactive visualization of molecules. These graphic effects, beside being eye candy, can improve the comprehension of the three dimensional shapes of the molecules. An example of the effects that can be achieved exploiting recent graphics hardware can be seen in the simple open source visualization system QuteMol.

Algorithms

Reference frames

Drawing molecules requires a transformation between molecular coordinates (usually, but not always, in Angstrom units) and the screen. Because many molecules are chiral it is essential that the handedness of the system (almost always right-handed) is preserved. In molecular graphics the origin (0, 0) is usually at the lower left, while in many computer systems the origin is at top left. If the z-coordinate is out of the screen (towards the viewer) the molecule will be referred to right-handed axes, while the screen display will be left-handed.

Molecular transformations normally require:

- scaling of the display (but not the molecule).
- translations of the molecule and objects on the screen.
- rotations about points and lines.

Conformational changes (e.g. rotations about bonds) require rotation of one part of the molecule relative to another. The programmer must decide whether a transformation on the

screen reflects a change of view or a change in the molecule or its reference frame.

Simple

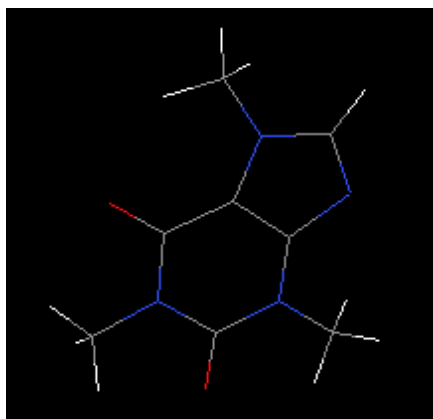


Fig. 7. Stick model of caffeine drawn in Jmol.

In early displays only vectors could be drawn e.g. (Fig. 7) which are easy to draw because no rendering or hidden surface removal is required.

On vector machines the lines would be smooth but on raster devices Bresenham's algorithm is used (note the "jaggies" on some of the bonds, which can be largely removed with antialiasing software.)

Atoms can be drawn as circles, but these should be sorted so that those with the largest z-coordinates (nearest the screen) are drawn last. Although imperfect, this often gives a reasonably attractive display. Other simple tricks which do not include hidden surface algorithms are:

- colouring each end of a bond with the same colour as the atom to which it is attached (Fig. 7).
- drawing less than the whole length of the bond (e.g. 10%-90%) to simulate the bond sticking out of a circle.
- adding a small offset white circle within the circle for an atom to simulate reflection.

Typical pseudocode for creating Fig. 7 (to fit the molecule exactly to the screen):

```
// assume:
// atoms with x, y, z coordinates (Angstrom) and elementSymbol
// bonds with pointers/references to atoms at ends
// table of colours for elementTypes
// find limits of molecule in molecule coordinates as xMin, yMin, xMax,
yMax
scale = min(xScreenMax/(xMax-xMin), yScreenMax/(yMax-yMin))
xOffset = -xMin * scale; yOffset = -yMin * scale
for (bond in $bonds) {
    atom0 = bond.getAtom(0)
    atom1 = bond.getAtom(1)
    x0 = xOffset+atom0.getX()*scale; y0 = yOffset+atom0.getY()*scale //
(1)
    x1 = xOffset+atom1.getX()*scale; y1 = yOffset+atom1.getY()*scale //
(2)
    x1 = atom1.getX(); y1 = atom1.getY()
    xMid = (x0 + x1) / 2; yMid = (y0 + y1) / 2;
    colour0 = ColourTable.getColour(atom0.getSymbol())
    drawLine (colour0, x0, y0, xMid, yMid)
    colour1 = ColourTable.getColour(atom1.getSymbol())
    drawLine (colour1, x1, y1, xMid, yMid)
}
```

Note that this assumes the origin is in the bottom left corner of the screen, with Y up the screen. Many graphics systems have the origin at the top left, with Y down the screen. In this case the lines (1) and (2) should have the y coordinate generation as:

```
y0 = yScreenMax - (yOffset+atom0.getY()*scale) // (1)
y1 = yScreenMax - (yOffset+atom1.getY()*scale) // (2)
```

Changes of this sort change the handedness of the axes so it is easy to reverse the chirality of the displayed molecule unless care is taken.

Advanced

For greater realism and better comprehension of the 3D structure of a molecule many computer graphics algorithms can be used. For many years molecular graphics has stressed the capabilities of graphics hardware and has required hardware-specific approaches. With the increasing power of machines on the desktop, portability is more important and programs such as Jmol have advanced algorithms that do not rely on hardware. On the other hand recent graphics hardware is able to interactively render very complex molecule shapes with a quality that would not be possible with standard software techniques.

Chronology

This table provides an incomplete chronology of molecular graphics advances.

Developer(s)	Approximate date	Technology	Comments
Crystallographers	< 1960	Hand-drawn	Crystal structures, with hidden atom and bond removal. Often clinographic projections.
Cyrus Levinthal, Bob Langridge	1960s	CRT	First protein display on screen (Project MAC).
Johnson, Motherwell	ca 1970	Pen plotter	ORTEP, PLUTO. Very widely deployed for publishing crystal structures.
Langridge, White, Marshall	Late 1970s	Departmental systems (PDP-11, Tektronix displays or DEC-VT11, e.g. MMS-X)	Mixture of commodity computing with early displays.
T. Alwyn Jones	1978	FRODO	Crystallographic structure solution.
Davies, Hubbard	Mid-1980s	CHEM-X, HYDRA	Laboratory systems with multicolor, raster and vector devices (Sigmex, PS300).
Biosym, Tripos, Polygen	Mid-1980s	PS300 and lower cost dumb terminals (VT200, SIGMEX)	Commercial integrated modelling and display packages.
Silicon Graphics, Sun	Late 1980s	IRIS GL (UNIX) workstations	Commodity-priced single-user workstations with stereoscopic display.
EMBL - WHAT IF ^[4]	1989, 2000	Machine independent	Nearly free, multifunctional, still fully supported, many free servers ^[5] based on it

Sayle, Richardson	1992, 1993	RasMol, Kinemage	Platform-independent MG.
MDL (van Vliet, Maffett, Adler, Holt)	1995-1998	Chime	proprietary C++ ; free browser plugin for Mac (OS9) and PCs
ChemAxon	1998-	MarvinSketch ^[6] & MarvinView ^[7] MarvinSpace ^[8] (2005)	proprietary Java applet or stand-alone application.
Community efforts	2000-	Jmol, PyMol, Protein Workshop (www.pdb.org)	Open-source Java applet or stand-alone application.
NOCH	2002-	NOC ^[9]	Powerful and open source code molecular structure explorer
LION Bioscience / EMBL	2004-	SRS 3D ^[10]	Free, open-source system based on Java3D. Integrates 3D structures with sequence and feature data (domains, SNPs, etc.).
San Diego Supercomputer Center	2006-	Sirius	Free for academic/non-profit institutions
Weizmann Institute of Science - Community efforts	2008-	Proteopedia	Collaborative, 3D wiki encyclopedia of proteins & other molecules

References

- [1] Dickerson, R.E.; Geis, I. (1969). *The structure and action of proteins*. Menlo Park, CA: W.A. Benjamin.
- [2] International Union of Pure and Applied Chemistry (1997). "molecular graphics (<http://goldbook.iupac.org/MT06970.html>)". *Compendium of Chemical Terminology* Internet edition.
- [3] http://www.scripps.edu/mb/goodsell/mgs_art/
- [4] <http://swift.cmbi.ru.nl/whatif/>
- [5] <http://swift.cmbi.ru.nl/>
- [6] <http://www.chemaxon.com/product/msketch.html>
- [7] <http://www.chemaxon.com/product/mview.html>
- [8] <http://www.chemaxon.com/product/mspace.html>
- [9] <http://noch.sourceforge.net>
- [10] <http://srs3d.org>

See also

- List of Molecular Graphics Systems
- Molecular Design software
- Molecular model
- Molecular modelling
- Molecular geometry
- Software for molecular mechanics modeling

External links

- The PyMOL Molecular Graphics System (<http://pymol.sf.net>) -- open source
 - PyMOLWiki (<http://pymolwiki.org>) -- community supported wiki for PyMOL
- History of Visualization of Biological Macromolecules (<http://www.umass.edu/microbio/rasmol/history.htm>) by Eric Martz and Eric Francoeur.
- Brief History of Molecular Mechanics/Graphics (<http://stanley.chem.lsu.edu/webpub/7770-Lecture-1-intro.pdf>) in LSU CHEM7770 lecture notes.
- Historical slides (<http://luminary.stanford.edu/langridge/slides.htm>) from Robert (Bob) Langridge. These show the influence of Crick and Watson on molecular graphics (including Levinthal's) and the development of early display technology, finishing with displays which were common in the mid-1980s on machines such as Evans and Sutherland's PS300 series.
- Interview with Langridge. (<http://luminary.stanford.edu/langridge/langridge.html>) The display looking down the axis of B-DNA has been likened to a rose window.
- Nelson Max's home page (<http://accad.osu.edu/~waynec/history/tree/max.html>) with links to 1982 classics.
- Jmol home page (<http://jmol.sourceforge.net/>) contains an applet with an automatic display of many features of molecular graphics including metaphors, scripting, annotation and animation.
- Richardson Lab (<http://kinemage.biochem.duke.edu/>) includes Kinemage and molecular graphics images.
- History of RasMol. (<http://www.openrasmol.org/history.html>)
- Molecule of the Month (http://www.rcsb.org/pdb/static.do?p=education_discussion/molecule_of_the_month/index.html) at RCSB/PDB.
- xeo (<http://sourceforge.net/projects/xeo>) xeo is a free (GPL) open project management for nanostructures using Java
- Exhibitions of Molecular Graphics Art (http://www.scripps.edu/mb/goodsell/mgs_art/), 1994, 1998.
- NOCH home page (<http://noch.sourceforge.net>) A powerful, efficient and open source molecular graphics tool.
- eMovie (<http://www.weizmann.ac.il/ISPC/eMovie.html>): a tool for creation of molecular animations with PyMOL.
- Proteopedia (<http://www.proteopedia.org>): The collaborative, 3D encyclopedia of proteins and other molecules.
- Ascalaph Graphics (http://www.agilemolecule.com/Ascalaph/Ascalaph_Graphics.html): a molecular viewer with some geometry editing capabilities.
- Molecular Graphics and Modelling Society. (<http://www.mgms.org/>)
- *Journal of Molecular Graphics and Modelling* (http://www.sciencedirect.com/science?_ob=JournalURL&_cdi=5260&_auth=y&_acct=C000053194&_version=1&_urlVersion=0&_userid=1495569&md5=1e86bcce088e98890cea52f6eda84b64) (formally *Journal of Molecular Graphics*). This journal is not open access.

Molecular dynamics

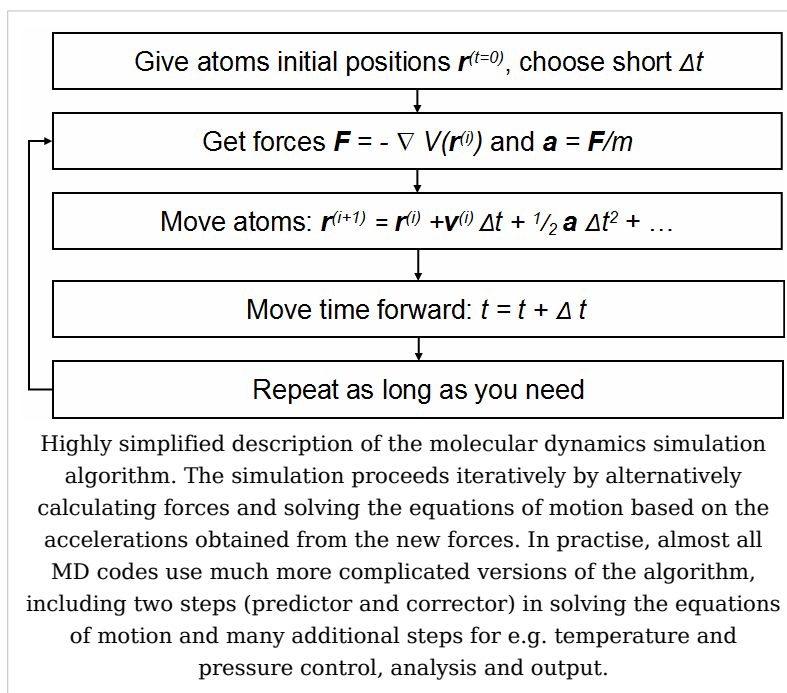
Molecular dynamics (MD) is a form of computer simulation in which atoms and molecules are allowed to interact for a period of time by approximations of known physics, giving a view of the motion of the atoms. Because molecular systems generally consist of a vast number of particles, it is impossible to find the properties of such complex systems analytically. When the number of bodies are more than two no analytical solutions can be found and result in chaotic motion (see n-body problem). MD simulation circumvents this problem by using numerical methods. It represents an interface between laboratory experiments and theory, and can be understood as a "virtual experiment". MD probes the relationship between molecular structure, movement and function. Molecular dynamics is a multidisciplinary method. Its laws and theories stem from mathematics, physics, and chemistry, and it employs algorithms from computer science and information theory. It was originally conceived within theoretical physics in the late 1950s^[1] and early 1960s^[2], but is applied today mostly in materials science and modeling of biomolecules.

Before it became possible to simulate molecular dynamics with computers, some undertook the hard work of trying it with physical models such as macroscopic spheres. The idea was to arrange them to replicate the properties of a liquid. J.D. Bernal said, in 1962: "... I took a number of rubber balls and stuck them together with rods of a selection of different lengths ranging from 2.75 to 4 inches. I tried to do this in the first place as casually as possible, working in my own office, being interrupted every five minutes or so and not remembering what I had done before the interruption."^[3] Fortunately, now computers keep track of bonds during a simulation.

Molecular dynamics is a specialized discipline of molecular modeling and computer simulation based on statistical mechanics; the main justification of the MD method is that statistical ensemble averages are equal to time averages of the system, known as the ergodic hypothesis. MD has also been termed "statistical mechanics by numbers" and "Laplace's vision of Newtonian mechanics" of predicting the future by animating nature's forces^[4] ^[5] and allowing insight into molecular motion on an atomic scale. However, long MD simulations are mathematically ill-conditioned, generating cumulative errors in numerical integration that can be minimized with proper selection of algorithms and parameters, but not eliminated entirely. Furthermore, current potential functions are, in many cases, not sufficiently accurate to reproduce the dynamics of molecular systems, so the much more computationally demanding Ab Initio Molecular Dynamics method must be used. Nevertheless, molecular dynamics techniques allow detailed time and space resolution into representative behavior in phase space.

Areas of Application

There is a significant difference between the focus and methods used by chemists and physicists, and this is reflected in differences in the jargon used by the different fields. In chemistry and biophysics, the interaction between the particles is either described by a "force field" (**classical MD**), a quantum chemical model, or a mix between the two. These terms are not used in physics, where the interactions are usually described by the name of the theory or approximation being used and called the potential energy, or just "potential".



Beginning in theoretical physics, the method of MD gained popularity in materials science and since the 1970s also in biochemistry and biophysics. In chemistry, MD serves as an important tool in protein structure determination and refinement using experimental tools such as X-ray crystallography and NMR. It has also been applied with limited success as a method of refining protein structure predictions. In physics, MD is used to examine the dynamics of atomic-level phenomena that cannot be observed directly, such as thin film growth and ion-subplantation. It is also used to examine the physical properties of nanotechnological devices that have not or cannot yet be created.

In applied mathematics and theoretical physics, molecular dynamics is a part of the research realm of dynamical systems, ergodic theory and statistical mechanics in general. The concepts of energy conservation and molecular entropy come from thermodynamics. Some techniques to calculate conformational entropy such as principal components analysis come from information theory. Mathematical techniques such as the transfer operator become applicable when MD is seen as a Markov chain. Also, there is a large community of mathematicians working on volume preserving, symplectic integrators for more computationally efficient MD simulations.

MD can also be seen as a special case of the discrete element method (DEM) in which the particles have spherical shape (e.g. with the size of their van der Waals radii.) Some authors in the DEM community employ the term MD rather loosely, even when their simulations do not model actual molecules.

Design Constraints

Design of a molecular dynamics simulation should account for the available computational power. Simulation size (n =number of particles), timestep and total time duration must be selected so that the calculation can finish within a reasonable time period. However, the simulations should be long enough to be relevant to the time scales of the natural processes being studied. To make statistically valid conclusions from the simulations, the time span simulated should match the kinetics of the natural process. Otherwise, it is analogous to making conclusions about how a human walks from less than one footstep. Most scientific publications about the dynamics of proteins and DNA use data from simulations spanning nanoseconds ($1\text{E-}9$ s) to microseconds ($1\text{E-}6$ s). To obtain these simulations, several CPU-days to CPU-years are needed. Parallel algorithms allow the load to be distributed among CPUs; an example is the spatial decomposition in LAMMPS.

During a classical MD simulation, the most CPU intensive task is the evaluation of the potential (force field) as a function of the particles' internal coordinates. Within that energy evaluation, the most expensive one is the non-bonded or non-covalent part. In Big O notation, common molecular dynamics simulations scale by $O(n^2)$ if all pair-wise electrostatic and van der Waals interactions must be accounted for explicitly. This computational cost can be reduced by employing electrostatics methods such as Particle Mesh Ewald ($O(n \log(n))$) or good spherical cutoff techniques ($O(n)$).

Another factor that impacts total CPU time required by a simulation is the size of the integration timestep. This is the time length between evaluations of the potential. The timestep must be chosen small enough to avoid discretization errors (i.e. smaller than the fastest vibrational frequency in the system). Typical timesteps for classical MD are in the order of 1 femtosecond ($1\text{E-}15$ s). This value may be extended by using algorithms such as SHAKE, which fix the vibrations of the fastest atoms (e.g. hydrogens) into place. Multiple time scale methods have also been developed, which allow for extended times between updates of slower long-range forces.^{[6] [7] [8]}

For simulating molecules in a solvent, a choice should be made between explicit solvent and implicit solvent. Explicit solvent particles (such as the TIP3P and SPC/E water models) must be calculated expensively by the force field, while implicit solvents use a mean-field approach. Using an explicit solvent is computationally expensive, requiring inclusion of about ten times more particles in the simulation. But the granularity and viscosity of explicit solvent is essential to reproduce certain properties of the solute molecules. This is especially important to reproduce kinetics.

In all kinds of molecular dynamics simulations, the simulation box size must be large enough to avoid boundary condition artifacts. Boundary conditions are often treated by choosing fixed values at the edges, or by employing periodic boundary conditions in which one side of the simulation loops back to the opposite side, mimicking a bulk phase.

Microcanonical ensemble (NVE)

In the **microcanonical**, or **NVE** ensemble, the system is isolated from changes in moles (N), volume (V) and energy (E). It corresponds to an adiabatic process with no heat exchange. A microcanonical molecular dynamics trajectory may be seen as an exchange of potential and kinetic energy, with total energy being conserved. For a system of N particles with coordinates X and velocities V , the following pair of first order differential equations may be written in Newton's notation as

$$F(X) = -\nabla U(X) = M\dot{V}(t)$$

$$V(t) = \dot{X}(t).$$

The potential energy function $U(X)$ of the system is a function of the particle coordinates X . It is referred to simply as the "potential" in Physics, or the "force field" in Chemistry. The first equation comes from Newton's laws; the force F acting on each particle in the system can be calculated as the negative gradient of $U(X)$.

For every timestep, each particle's position X and velocity V may be integrated with a symplectic method such as Verlet. The time evolution of X and V is called a trajectory. Given the initial positions (e.g. from theoretical knowledge) and velocities (e.g. randomized Gaussian), we can calculate all future (or past) positions and velocities.

One frequent source of confusion is the meaning of temperature in MD. Commonly we have experience with macroscopic temperatures, which involve a huge number of particles. But temperature is a statistical quantity. If there is a large enough number of atoms, statistical temperature can be estimated from the *instantaneous temperature*, which is found by equating the kinetic energy of the system to $nk_B T/2$ where n is the number of degrees of freedom of the system.

A temperature-related phenomenon arises due to the small number of atoms that are used in MD simulations. For example, consider simulating the growth of a copper film starting with a substrate containing 500 atoms and a deposition energy of 100 eV. In the real world, the 100 eV from the deposited atom would rapidly be transported through and shared among a large number of atoms (10^{10} or more) with no big change in temperature. When there are only 500 atoms, however, the substrate is almost immediately vaporized by the deposition. Something similar happens in biophysical simulations. The temperature of the system in NVE is naturally raised when macromolecules such as proteins undergo exothermic conformational changes and binding.

Canonical ensemble (NVT)

In the canonical ensemble, moles (N), volume (V) and temperature (T) are conserved. It is also sometimes called constant temperature molecular dynamics (CTMD). In NVT, the energy of endothermic and exothermic processes is exchanged with a thermostat.

A variety of thermostat methods are available to add and remove energy from the boundaries of an MD system in a realistic way, approximating the canonical ensemble. Popular techniques to control temperature include the Nosé-Hoover thermostat, the Berendsen thermostat, and Langevin dynamics. Note that the Berendsen thermostat might introduce the flying ice cube effect, which leads to unphysical translations and rotations of the simulated system.

Isothermal-Isobaric (NPT) ensemble

In the isothermal-isobaric ensemble, moles (N), pressure (P) and temperature (T) are conserved. In addition to a thermostat, a barostat is needed. It corresponds most closely to laboratory conditions with a flask open to ambient temperature and pressure.

In the simulation of biological membranes, isotropic pressure control is not appropriate. For lipid bilayers, pressure control occurs under constant membrane area (NPAT) or constant surface tension " γ " (NP γ T).

Generalized ensembles

The replica exchange method is a generalized ensemble. It was originally created to deal with the slow dynamics of disordered spin systems. It is also called parallel tempering. The replica exchange MD (REMD) formulation ^[9] tries to overcome the multiple-minima problem by exchanging the temperature of non-interacting replicas of the system running at several temperatures.

Potentials in MD simulations

A molecular dynamics simulation requires the definition of a potential function, or a description of the terms by which the particles in the simulation will interact. In chemistry and biology this is usually referred to as a force field. Potentials may be defined at many levels of physical accuracy; those most commonly used in chemistry are based on molecular mechanics and embody a classical treatment of particle-particle interactions that can reproduce structural and conformational changes but usually cannot reproduce chemical reactions.

The reduction from a fully quantum description to a classical potential entails two main approximations. The first one is the Born-Oppenheimer approximation, which states that the dynamics of electrons is so fast that they can be considered to react instantaneously to the motion of their nuclei. As a consequence, they may be treated separately. The second one treats the nuclei, which are much heavier than electrons, as point particles that follow classical Newtonian dynamics. In classical molecular dynamics the effect of the electrons is approximated as a single potential energy surface, usually representing the ground state.

When finer levels of detail are required, potentials based on quantum mechanics are used; some techniques attempt to create hybrid classical/quantum potentials where the bulk of the system is treated classically but a small region is treated as a quantum system, usually undergoing a chemical transformation.

Empirical potentials

Empirical potentials used in chemistry are frequently called force fields, while those used in materials physics are called just empirical or analytical potentials.

Most force fields in chemistry are empirical and consist of a summation of bonded forces associated with chemical bonds, bond angles, and bond dihedrals, and non-bonded forces associated with van der Waals forces and electrostatic charge. Empirical potentials represent quantum-mechanical effects in a limited way through ad-hoc functional approximations. These potentials contain free parameters such as atomic charge, van der Waals parameters reflecting estimates of atomic radius, and equilibrium bond length, angle, and dihedral; these are obtained by fitting against detailed electronic calculations

(quantum chemical simulations) or experimental physical properties such as elastic constants, lattice parameters and spectroscopic measurements.

Because of the non-local nature of non-bonded interactions, they involve at least weak interactions between all particles in the system. Its calculation is normally the bottleneck in the speed of MD simulations. To lower the computational cost, force fields employ numerical approximations such as shifted cutoff radii, reaction field algorithms, particle mesh Ewald summation, or the newer Particle-Particle Particle Mesh (P3M).

Chemistry force fields commonly employ preset bonding arrangements (an exception being *ab-initio* dynamics), and thus are unable to model the process of chemical bond breaking and reactions explicitly. On the other hand, many of the potentials used in physics, such as those based on the bond order formalism can describe several different coordinations of a system and bond breaking. Examples of such potentials include the Brenner potential^[10] for hydrocarbons and its further developments for the C-Si-H and C-O-H systems. The ReaxFF potential^[11] can be considered a fully reactive hybrid between bond order potentials and chemistry force fields.

Pair potentials vs. many-body potentials

The potential functions representing the non-bonded energy are formulated as a sum over interactions between the particles of the system. The simplest choice, employed in many popular force fields, is the "pair potential", in which the total potential energy can be calculated from the sum of energy contributions between pairs of atoms. An example of such a pair potential is the non-bonded Lennard-Jones potential (also known as the 6-12 potential), used for calculating van der Waals forces.

$$U(r) = 4\epsilon \left[\left(\frac{\sigma}{r} \right)^{12} - \left(\frac{\sigma}{r} \right)^6 \right]$$

Another example is the Born (ionic) model of the ionic lattice. The first term in the next equation is Coulomb's law for a pair of ions, the second term is the short-range repulsion explained by Pauli's exclusion principle and the final term is the dispersion interaction term. Usually, a simulation only includes the dipolar term, although sometimes the quadrupolar term is included as well.

$$U_{ij}(r_{ij}) = \sum \frac{z_i z_j}{4\pi\epsilon_0 r_{ij}} + \sum A_l \exp \frac{-r_{ij}}{p_l} + \sum C_l r_{ij}^{-n_l} + \dots$$

In many-body potentials, the potential energy includes the effects of three or more particles interacting with each other. In simulations with pairwise potentials, global interactions in the system also exist, but they occur only through pairwise terms. In many-body potentials, the potential energy cannot be found by a sum over pairs of atoms, as these interactions are calculated explicitly as a combination of higher-order terms. In the statistical view, the dependency between the variables cannot in general be expressed using only pairwise products of the degrees of freedom. For example, the Tersoff potential^[12], which was originally used to simulate carbon, silicon and germanium and has since been used for a wide range of other materials, involves a sum over groups of three atoms, with the angles between the atoms being an important factor in the potential. Other examples are the embedded-atom method (EAM)^[13] and the Tight-Binding Second Moment Approximation (TBSMA) potentials^[14], where the electron density of states in the region of an atom is calculated from a sum of contributions from surrounding atoms, and the potential energy contribution is then a function of this sum.

Semi-empirical potentials

Semi-empirical potentials make use of the matrix representation from quantum mechanics. However, the values of the matrix elements are found through empirical formulae that estimate the degree of overlap of specific atomic orbitals. The matrix is then diagonalized to determine the occupancy of the different atomic orbitals, and empirical formulae are used once again to determine the energy contributions of the orbitals.

There are a wide variety of semi-empirical potentials, known as tight-binding potentials, which vary according to the atoms being modeled.

Polarizable potentials

Most classical force fields implicitly include the effect of polarizability, e.g. by scaling up the partial charges obtained from quantum chemical calculations. These partial charges are stationary with respect to the mass of the atom. But molecular dynamics simulations can explicitly model polarizability with the introduction of induced dipoles through different methods, such as Drude particles or fluctuating charges. This allows for a dynamic redistribution of charge between atoms which responds to the local chemical environment.

For many years, polarizable MD simulations have been touted as the next generation. For homogenous liquids such as water, increased accuracy has been achieved through the inclusion of polarizability.^[15] Some promising results have also been achieved for proteins.^[16] However, it is still uncertain how to best approximate polarizability in a simulation.

Ab-initio methods

In classical molecular dynamics, a single potential energy surface (usually the ground state) is represented in the force field. This is a consequence of the Born-Oppenheimer approximation. If excited states, chemical reactions or a more accurate representation is needed, electronic behavior can be obtained from first principles by using a quantum mechanical method, such as Density Functional Theory. This is known as Ab Initio Molecular Dynamics (AIMD). Due to the cost of treating the electronic degrees of freedom, the computational cost of this simulations is much higher than classical molecular dynamics. This implies that AIMD is limited to smaller systems and shorter periods of time.

Ab-initio quantum-mechanical methods may be used to calculate the potential energy of a system on the fly, as needed for conformations in a trajectory. This calculation is usually made in the close neighborhood of the reaction coordinate. Although various approximations may be used, these are based on theoretical considerations, not on empirical fitting. *Ab-Initio* calculations produce a vast amount of information that is not available from empirical methods, such as density of electronic states or other electronic properties. A significant advantage of using *ab-initio* methods is the ability to study reactions that involve breaking or formation of covalent bonds, which correspond to multiple electronic states.

A popular software for *ab-initio* molecular dynamics is the Car-Parrinello Molecular Dynamics (CPMD) package based on the density functional theory.

Hybrid QM/MM

QM (quantum-mechanical) methods are very powerful. However, they are computationally expensive, while the MM (classical or molecular mechanics) methods are fast but suffer from several limitations (require extensive parameterization; energy estimates obtained are not very accurate; cannot be used to simulate reactions where covalent bonds are broken/formed; and are limited in their abilities for providing accurate details regarding the chemical environment). A new class of method has emerged that combines the good points of QM (accuracy) and MM (speed) calculations. These methods are known as mixed or hybrid quantum-mechanical and molecular mechanics methods (hybrid QM/MM). The methodology for such techniques was introduced by Warshel and coworkers. In the recent years have been pioneered by several groups including: Arieh Warshel (University of Southern California), Weitao Yang (Duke University), Sharon Hammes-Schiffer (The Pennsylvania State University), Donald Truhlar and Jiali Gao (University of Minnesota) and Kenneth Merz (University of Florida).

The most important advantage of hybrid QM/MM methods is the speed. The cost of doing classical molecular dynamics (MM) in the most straightforward case scales $O(n^2)$, where N is the number of atoms in the system. This is mainly due to electrostatic interactions term (every particle interacts with every other particle). However, use of cutoff radius, periodic pair-list updates and more recently the variations of the particle-mesh Ewald's (PME) method has reduced this between $O(N)$ to $O(n^2)$. In other words, if a system with twice many atoms is simulated then it would take between twice to four times as much computing power. On the other hand the simplest *ab-initio* calculations typically scale $O(n^3)$ or worse (Restricted Hartree-Fock calculations have been suggested to scale $\sim O(n^{2.7})$). To overcome the limitation, a small part of the system is treated quantum-mechanically (typically active-site of an enzyme) and the remaining system is treated classically.

In more sophisticated implementations, QM/MM methods exist to treat both light nuclei susceptible to quantum effects (such as hydrogens) and electronic states. This allows generation of hydrogen wave-functions (similar to electronic wave-functions). This methodology has been useful in investigating phenomenon such as hydrogen tunneling. One example where QM/MM methods have provided new discoveries is the calculation of hydride transfer in the enzyme liver alcohol dehydrogenase. In this case, tunneling is important for the hydrogen, as it determines the reaction rate.^[17]

Coarse-graining and reduced representations

At the other end of the detail scale are coarse-grained and lattice models. Instead of explicitly representing every atom of the system, one uses "pseudo-atoms" to represent groups of atoms. MD simulations on very large systems may require such large computer resources that they cannot easily be studied by traditional all-atom methods. Similarly, simulations of processes on long timescales (beyond about 1 microsecond) are prohibitively expensive, because they require so many timesteps. In these cases, one can sometimes tackle the problem by using reduced representations, which are also called coarse-grained models.

Examples for coarse graining (CG) methods are discontinuous molecular dynamics (CG-DMD)^{[18] [19]} and Go-models^[20]. Coarse-graining is done sometimes taking larger pseudo-atoms. Such united atom approximations have been used in MD simulations of biological membranes. The aliphatic tails of lipids are represented by a few pseudo-atoms

by gathering 2-4 methylene groups into each pseudo-atom.

The parameterization of these very coarse-grained models must be done empirically, by matching the behavior of the model to appropriate experimental data or all-atom simulations. Ideally, these parameters should account for both enthalpic and entropic contributions to free energy in an implicit way. When coarse-graining is done at higher levels, the accuracy of the dynamic description may be less reliable. But very coarse-grained models have been used successfully to examine a wide range of questions in structural biology.

Examples of applications of coarse-graining in biophysics:

- protein folding studies are often carried out using a single (or a few) pseudo-atoms per amino acid;
- DNA supercoiling has been investigated using 1-3 pseudo-atoms per basepair, and at even lower resolution;
- Packaging of double-helical DNA into bacteriophage has been investigated with models where one pseudo-atom represents one turn (about 10 basepairs) of the double helix;
- RNA structure in the ribosome and other large systems has been modeled with one pseudo-atom per nucleotide.

The simplest form of coarse-graining is the "united atom" (sometimes called "extended atom") and was used in most early MD simulations of proteins, lipids and nucleic acids. For example, instead of treating all four atoms of a CH_3 methyl group explicitly (or all three atoms of CH_2 methylene group), one represents the whole group with a single pseudo-atom. This pseudo-atom must, of course, be properly parameterized so that its van der Waals interactions with other groups have the proper distance-dependence. Similar considerations apply to the bonds, angles, and torsions in which the pseudo-atom participates. In this kind of united atom representation, one typically eliminates all explicit hydrogen atoms except those that have the capability to participate in hydrogen bonds ("polar hydrogens"). An example of this is the Charmm 19 force-field.

The polar hydrogens are usually retained in the model, because proper treatment of hydrogen bonds requires a reasonably accurate description of the directionality and the electrostatic interactions between the donor and acceptor groups. A hydroxyl group, for example, can be both a hydrogen bond donor and a hydrogen bond acceptor, and it would be impossible to treat this with a single OH pseudo-atom. Note that about half the atoms in a protein or nucleic acid are nonpolar hydrogens, so the use of united atoms can provide a substantial savings in computer time.

Examples of applications

Molecular dynamics is used in many fields of science.

- First macromolecular MD simulation published (1977, Size: 500 atoms, Simulation Time: 9.2 ps=0.0092 ns, Program: CHARMM precursor) Protein: Bovine Pancreatic Trypsine Inhibitor. This is one of the best studied proteins in terms of folding and kinetics. Its simulation published in Nature magazine paved the way for understanding protein motion as essential in function and not just accessory.^[21]
- MD is the standard method to treat collision cascades in the heat spike regime, i.e. the effects that energetic neutron and ion irradiation have on solids and solid surfaces.^{[22] [23]}

The following two biophysical examples are not run-of-the-mill MD simulations. They illustrate almost heroic efforts to produce simulations of a system of very large size (a complete virus) and very long simulation times (500 microseconds):

- MD simulation of the complete satellite tobacco mosaic virus (**STMV**) (2006, Size: 1 million atoms, Simulation time: 50 ns, program: NAMD) This virus is a small, icosahedral plant virus which worsens the symptoms of infection by Tobacco Mosaic Virus (TMV). Molecular dynamics simulations were used to probe the mechanisms of viral assembly. The entire STMV particle consists of 60 identical copies of a single protein that make up the viral capsid (coating), and a 1063 nucleotide single stranded RNA genome. One key finding is that the capsid is very unstable when there is no RNA inside. The simulation would take a single 2006 desktop computer around 35 years to complete. It was thus done in many processors in parallel with continuous communication between them.^[24]
- Folding Simulations of the Villin Headpiece in All-Atom Detail (2006, Size: 20,000 atoms; Simulation time: 500 μ s = 500,000 ns, Program: folding@home) This simulation was run in 200,000 CPU's of participating personal computers around the world. These computers had the folding@home program installed, a large-scale distributed computing effort coordinated by Vijay Pande at Stanford University. The kinetic properties of the Villin Headpiece protein were probed by using many independent, short trajectories run by CPU's without continuous real-time communication. One technique employed was the Pfold value analysis, which measures the probability of folding before unfolding of a specific starting conformation. Pfold gives information about transition state structures and an ordering of conformations along the folding pathway. Each trajectory in a Pfold calculation can be relatively short, but many independent trajectories are needed.^[25]

Molecular dynamics algorithms

Integrators

- Verlet-Stoermer integration
- Runge-Kutta integration
- Beeman's algorithm
- Gear predictor - corrector
- Constraint algorithms (for constrained systems)
- Symplectic integrator

Short-range interaction algorithms

- Cell lists
- Verlet list
- Bonded interactions

Long-range interaction algorithms

- Ewald summation
 - Particle Mesh Ewald (PME)
 - Particle-Particle Particle Mesh P3M
 - Reaction Field Method
-

Parallelization strategies

- Domain decomposition method (Distribution of system data for parallel computing)
- Molecular Dynamics - Parallel Algorithms ^[26]

Major software for MD simulations

- Abalone (classical, implicit water)
 - ABINIT (DFT)
 - ACEMD ^[27] (running on NVIDIA GPUs: heavily optimized with CUDA)
 - ADUN ^[28] (classical, P2P database for simulations)
 - AMBER (classical)
 - Ascalaph ^[29] (classical, GPU accelerated)
 - CASTEP (DFT)
 - CPMD (DFT)
 - CP2K ^[30] (DFT)
 - CHARMM (classical, the pioneer in MD simulation, extensive analysis tools)
 - COSMOS ^[31] (classical and hybrid QM/MM, quantum-mechanical atomic charges with BPT)
 - Desmond ^[32] (classical, parallelization with up to thousands of CPU's)
 - DL_POLY ^[33] (classical)
 - ESPResSo (classical, coarse-grained, parallel, extensible)
 - Fireball ^[34] (tight-binding DFT)
 - GROMACS (classical)
 - GROMOS (classical)
 - GULP (classical)
 - Hippo ^[35] (classical)
 - LAMMPS (classical, large-scale with spatial-decomposition of simulation domain for parallelism)
 - MDynaMix (classical, parallel)
 - MOLDY ^[36] (classical, parallel) latest release ^[37]
 - Materials Studio ^[38] (Forcite MD using COMPASS, Dreiding, Universal, cvff and pcff forcefields in serial or parallel, QMERA (QM+MD), ONESTEP (DFT), etc.)
 - MOSCITO (classical)
 - NAMD (classical, parallelization with up to thousands of CPU's)
 - NEWTON-X ^[39] (ab initio, surface-hopping dynamics)
 - ProtoMol ^[40] (classical, extensible, includes multigrid electrostatics)
 - PWscf (DFT)
 - S/PHI/nX ^[41] (DFT)
 - SIESTA (DFT)
 - VASP (DFT)
 - TINKER (classical)
 - YASARA ^[42] (classical)
 - ORAC ^[43] (classical)
 - XMD (classical)
-

Related software

- VMD - MD simulation trajectories can be visualized and analyzed.
- PyMol - Molecular Visualization software written in python
- Packmol ^[44] Package for building starting configurations for MD in an automated fashion
- Sirius - Molecular modeling, analysis and visualization of MD trajectories
- esra ^[45] - Lightweight molecular modeling and analysis library (Java/Jython/Mathematica).
- Molecular Workbench ^[46] - Interactive molecular dynamics simulations on your desktop
- BOSS - MC in OPLS

Specialized hardware for MD simulations

- Anton - A specialized, massively parallel supercomputer designed to execute MD simulations.
- MDGRAPE - A special purpose system built for molecular dynamics simulations, especially protein structure prediction.

See also

- Molecular graphics
 - Molecular modeling
 - Computational chemistry
 - Energy drift
 - Force field in Chemistry
 - Force field implementation
 - Monte Carlo method
 - Molecular Design software
 - Molecular mechanics
 - Molecular modeling on GPU
 - Protein dynamics
 - Implicit solvation
 - Car-Parrinello method
 - Symplectic numerical integration
 - Software for molecular mechanics modeling
 - Dynamical systems
 - Theoretical chemistry
 - Statistical mechanics
 - Quantum chemistry
 - Discrete element method
 - List of nucleic acid simulation software
-

References

- [1] Alder, B. J.; T. E. Wainwright (1959). "Studies in Molecular Dynamics. I. General Method". *J. Chem. Phys.* **31** (2): 459. doi: 10.1063/1.1730376 (<http://dx.doi.org/10.1063/1.1730376>).
- [2] A. Rahman (1964). "Correlations in the Motion of Atoms in Liquid Argon". *Phys Rev* **136**: A405-A411. doi: 10.1103/PhysRev.136.A405 (<http://dx.doi.org/10.1103/PhysRev.136.A405>).
- [3] Bernal, J.D. (1964). "The Bakerian lecture, 1962: The structure of liquids". *Proc. R. Soc.* **280**: 299-322. doi: 10.1098/rspa.1964.0147 (<http://dx.doi.org/10.1098/rspa.1964.0147>).
- [4] Schlick, T. (1996). "Pursuing Laplace's Vision on Modern Computers". in J. P. Mesirov, K. Schulten and D. W. Summers. *Mathematical Applications to Biomolecular Structure and Dynamics, IMA Volumes in Mathematics and Its Applications*. **82**. New York: Springer-Verlag. pp. 218-247. ISBN 978-0387948386.
- [5] de Laplace, P. S. (1820) (in French). *Oeuvres Complètes de Laplace, Théorie Analytique des Probabilités*. Paris, France: Gauthier-Villars.
- [6] Streett WB, Tildesley DJ, Saville G (1978). "Multiple time-step methods in molecular dynamics". *Mol Phys* **35** (3): 639-648. doi: 10.1080/00268977800100471 (<http://dx.doi.org/10.1080/00268977800100471>).
- [7] Tuckerman ME, Berne BJ, Martyna GJ (1991). "Molecular dynamics algorithm for multiple time scales: systems with long range forces". *J Chem Phys* **94** (10): 6811-6815.
- [8] Tuckerman ME, Berne BJ, Martyna GJ (1992). "Reversible multiple time scale molecular dynamics". *J Chem Phys* **97** (3): 1990-2001. doi: 10.1063/1.463137 (<http://dx.doi.org/10.1063/1.463137>).
- [9] Sugita, Yuji; Yuko Okamoto (1999). "Replica-exchange molecular dynamics method for protein folding". *Chem Phys Letters* **314**: 141-151. doi: 10.1016/S0009-2614(99)01123-9 ([http://dx.doi.org/10.1016/S0009-2614\(99\)01123-9](http://dx.doi.org/10.1016/S0009-2614(99)01123-9)).
- [10] Brenner, D. W. (1990). "Empirical potential for hydrocarbons for use in simulating the chemical vapor deposition of diamond films". *Phys. Rev. B* **42** (15): 9458. doi: 10.1103/PhysRevB.42.9458 (<http://dx.doi.org/10.1103/PhysRevB.42.9458>).
- [11] van Duin, A.; Siddharth Dasgupta, Francois Lorant and William A. Goddard III (2001). *J. Phys. Chem. A* **105**: 9398.
- [12] Tersoff, J. (1989). "Modeling solid-state chemistry: Interatomic potentials for multicomponent systems". *Phys. Rev. B* **39**: 5566. doi: 10.1103/PhysRevB.39.5566 (<http://dx.doi.org/10.1103/PhysRevB.39.5566>).
- [13] Daw, M. S.; S. M. Foiles and M. I. Baskes (1993). "The embedded-atom method: a review of theory and applications". *Mat. Sci. And Engr. Rep.* **9**: 251. doi: 10.1016/0920-2307(93)90001-U ([http://dx.doi.org/10.1016/0920-2307\(93\)90001-U](http://dx.doi.org/10.1016/0920-2307(93)90001-U)).
- [14] Cleri, F.; V. Rosato (1993). "Tight-binding potentials for transition metals and alloys". *Phys. Rev. B* **48**: 22. doi: 10.1103/PhysRevB.48.22 (<http://dx.doi.org/10.1103/PhysRevB.48.22>).
- [15] Lamoureux G, Harder E, Vorobyov IV, Roux B, MacKerell AD (2006). "A polarizable model of water for molecular dynamics simulations of biomolecules". *Chem Phys Lett* **418**: 245-249. doi: 10.1016/j.cplett.2005.10.135 (<http://dx.doi.org/10.1016/j.cplett.2005.10.135>).
- [16] Patel, S.; MacKerell, Jr. AD; Brooks III, Charles L (2004). "CHARMM fluctuating charge force field for proteins: II protein/solvent properties from molecular dynamics simulations using a nonadditive electrostatic model". *J Comput Chem* **25**: 1504-1514. doi: 10.1002/jcc.20077 (<http://dx.doi.org/10.1002/jcc.20077>).
- [17] Billeter, SR; SP Webb, PK Agarwal, T Iordanov, S Hammes-Schiffer (2001). "Hydride Transfer in Liver Alcohol Dehydrogenase: Quantum Dynamics, Kinetic Isotope Effects, and Role of Enzyme Motion". *J Am Chem Soc* **123**: 11262-11272. doi: 10.1021/ja011384b (<http://dx.doi.org/10.1021/ja011384b>).
- [18] Smith, A; CK Hall (2001). "Alpha-Helix Formation: Discontinuous Molecular Dynamics on an Intermediate-Resolution Protein Model". *Proteins* **44**: 344-360.
- [19] Ding, F; JM Borreguero, SV Buldyrey, HE Stanley, NV Dokholyan (2003). "Mechanism for the alpha-helix to beta-hairpin transition". *J Am Chem Soc* **53**: 220-228. doi: 10.1002/prot.10468 (<http://dx.doi.org/10.1002/prot.10468>).
- [20] Paci, E; M Vendruscolo, M Karplus (2002). "Validity of Go Models: Comparison with a Solvent-Shielded Empirical Energy Decomposition". *Biophys J* **83**: 3032-3038. doi: 10.1016/S0006-3495(02)75308-3 ([http://dx.doi.org/10.1016/S0006-3495\(02\)75308-3](http://dx.doi.org/10.1016/S0006-3495(02)75308-3)).
- [21] McCammon, J; JB Gelin, M Karplus (1977). "Dynamics of folded proteins". *Nature* **267**: 585-590. doi: 10.1038/267585a0 (<http://dx.doi.org/10.1038/267585a0>).
- [22] Averbach, R. S.; Diaz de la Rubia, T. (1998). "Displacement damage in irradiated metals and semiconductors". in H. Ehrenfest and F. Spaepen. *Solid State Physics*. **51**. New York: Academic Press. p. 281-402.
- [23] R. Smith, ed (1997). *Atomic & ion collisions in solids and at surfaces: theory, simulation and applications*. Cambridge, UK: Cambridge University Press.
- [24] Freddolino P, Arkhipov A, Larson SB, McPherson A, Schulten K. <http://www.ks.uiuc.edu/Research/STMV/> "Molecular dynamics simulation of the Satellite Tobacco Mosaic Virus

- (STMV)". *Theoretical and Computational Biophysics Group*. University of Illinois at Urbana Champaign. <http://www.ks.uiuc.edu/Research/STMV/>.
- [25] The Folding@Home Project (<http://folding.stanford.edu/>) and recent papers (<http://folding.stanford.edu/papers.html>) published using trajectories from it. Vijay Pande Group. Stanford University
- [26] <http://www.cs.sandia.gov/~sjplimp/md.html>
- [27] <http://www.acellera.com/index.php?arg=acemd>
- [28] <http://cbbli.imim.es/Adun>
- [29] <http://www.agilemolecule.com/Products.html>
- [30] <http://cp2k.berlios.de/>
- [31] http://www.cosmos-software.de/ce_intro.html
- [32] <http://www.DEShawResearch.com/resources.html>
- [33] http://www.ccp5.ac.uk/DL_POLY/
- [34] <http://fireball-dft.org>
- [35] <http://www.biowerkzeug.com/>
- [36] <http://www.ccp5.ac.uk/moldy/moldy.html>
- [37] http://ccpforge.cse.rl.ac.uk/frs/?group_id=34
- [38] <http://accelrys.com/products/materials-studio/>
- [39] <http://www.univie.ac.at/newtonx/>
- [40] <http://protomol.sourceforge.net/>
- [41] <http://www.sphinxlib.de>
- [42] <http://www.yasara.org>
- [43] <http://www.chim.unifi.it/orac/>
- [44] <http://www.ime.unicamp.br/~martinez/packmol>
- [45] <http://esra.sourceforge.net/cgi-bin/index.cgi>
- [46] <http://mw.concord.org/modeler/>

General references

- M. P. Allen, D. J. Tildesley (1989) *Computer simulation of liquids*. Oxford University Press. ISBN 0-19-855645-4.
- J. A. McCammon, S. C. Harvey (1987) *Dynamics of Proteins and Nucleic Acids*. Cambridge University Press. ISBN 0521307503 (hardback).
- D. C. Rapaport (1996) *The Art of Molecular Dynamics Simulation*. ISBN 0-521-44561-2.
- Frenkel, Daan; Smit, Berend (2002) [2001]. *Understanding Molecular Simulation : from algorithms to applications*. San Diego, California: Academic Press. ISBN 0-12-267351-4.
- J. M. Haile (2001) *Molecular Dynamics Simulation: Elementary Methods*. ISBN 0-471-18439-X
- R. J. Sadus, *Molecular Simulation of Fluids: Theory, Algorithms and Object-Orientation*, 2002, ISBN 0-444-51082-6
- Oren M. Becker, Alexander D. Mackerell Jr, Benoît Roux, Masakatsu Watanabe (2001) *Computational Biochemistry and Biophysics*. Marcel Dekker. ISBN 0-8247-0455-X.
- Andrew Leach (2001) *Molecular Modelling: Principles and Applications*. (2nd Edition) Prentice Hall. ISBN 978-0582382107.
- Tamar Schlick (2002) *Molecular Modeling and Simulation*. Springer. ISBN 0-387-95404-X.
- William Graham Hoover (1991) *Computational Statistical Mechanics*, Elsevier, ISBN 0-444-88192-1.

External links

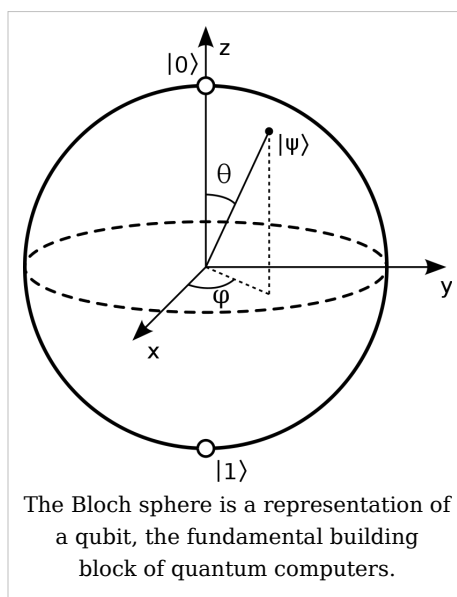
- The Blue Gene Project (<http://researchweb.watson.ibm.com/bluegene/>) (IBM)
- D. E. Shaw Research (<http://deshawresearch.com/>) (D. E. Shaw Research)
- Molecular Physics (<http://www.tandf.co.uk/journals/titles/00268976.asp>)
- Statistical mechanics of Nonequilibrium Liquids (<http://www.phys.unsw.edu.au/~gary/book.html>) Lecture Notes on non-equilibrium MD
- Introductory Lecture on Classical Molecular Dynamics (<http://www.fz-juelich.de/nic-series/volume10/sutmann.pdf>) by Dr. Godehard Sutmann, NIC, Forschungszentrum Jülich, Germany
- Introductory Lecture on Ab Initio Molecular Dynamics and Ab Initio Path Integrals (<http://www.fz-juelich.de/nic-series/volume10/tuckerman2.pdf>) by Mark E. Tuckerman, New York University, USA
- Introductory Lecture on Ab initio molecular dynamics: Theory and Implementation (<http://www.fz-juelich.de/nic-series/Volume1/marx.pdf>) by Dominik Marx, Ruhr-Universität Bochum and Jürg Hutter, Universität Zürich

Quantum computer

A **quantum computer** is a device for computation that makes direct use of quantum mechanical phenomena, such as superposition and entanglement, to perform operations on data. The basic principle behind quantum computation is that quantum properties can be used to represent data and perform operations on these data.^[1]

Although quantum computing is still in its infancy, experiments have been carried out in which quantum computational operations were executed on a very small number of qubits (**quantum binary digits**). Both practical and theoretical research continues with interest, and many national government and military funding agencies support quantum computing research to develop quantum computers for both civilian and national security purposes, such as cryptanalysis.^[2]

If large-scale quantum computers can be built, they will be able to solve certain problems much faster than any of our current classical computers (for example Shor's algorithm). Quantum computers are different from other computers such as DNA computers and traditional computers based on transistors. Some computing architectures such as optical computers^[3] may use classical superposition of electromagnetic waves. Without some specifically quantum mechanical resources such as entanglement, it is conjectured that an exponential advantage over classical computers is not possible.^[4]



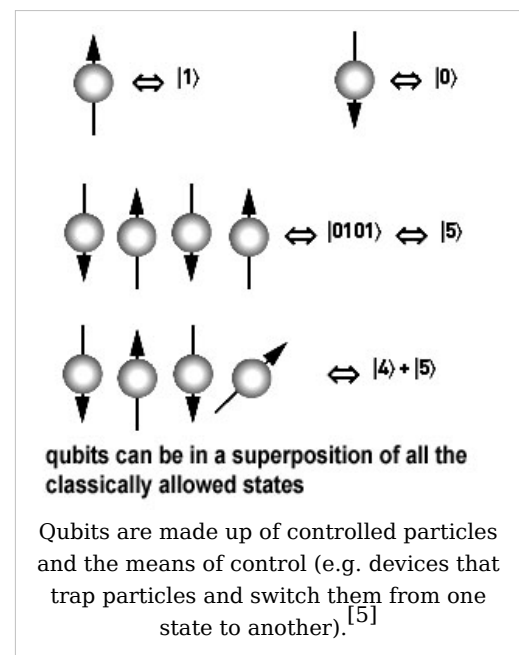
Basis

A classical computer has a memory made up of bits, where each bit holds either a one or a zero. A quantum computer maintains a sequence of qubits. A single qubit can hold a one, a zero, or, crucially, any quantum superposition of these; moreover, a pair of qubits can be in any quantum superposition of 4 states, and three qubits in any superposition of 8. In general a quantum computer with n qubits can be in an arbitrary superposition of up to 2^n different states simultaneously (this compares to a normal computer that can only be in *one* of these 2^n states at any one time). A quantum computer operates by manipulating those qubits with a fixed sequence of quantum logic gates. The sequence of gates to be applied is called a *quantum algorithm*.

An example of an implementation of qubits for a quantum computer could start with the use of particles with two spin states: "down" and "up" (typically written $|\downarrow\rangle$ and $|\uparrow\rangle$, or $|0\rangle$ and $|1\rangle$). But in fact any system possessing an observable quantity A which is *conserved* under time evolution and such that A has at least two discrete and sufficiently spaced consecutive eigenvalues, is a suitable candidate for implementing a qubit. This is true because any such system can be mapped onto an effective spin-1/2 system.

Bits vs. qubits

Consider first a classical computer that operates on a three-bit register. The state of the computer at any time is a probability distribution over the $2^3 = 8$ different three-bit strings 000, 001, ..., 111. If it is a deterministic computer, then it is in exactly one of these states with probability 1. However, if it is a probabilistic computer, then it may have a chance in being in a number of different states. We can describe this probabilistic state by eight nonnegative numbers a, b, c, d, e, f, g, h (where a = probability computer is in state 000, b = probability computer is in state 001, etc.). There is a restriction that these probabilities sum to 1.



The state of a three-qubit quantum computer is similarly described by an eight-dimensional vector (a, b, c, d, e, f, g, h) , called a wavefunction. However, instead of adding to one, the sum of the *squares* of the coefficient magnitudes, $|a|^2 + |b|^2 + \dots + |h|^2$, must equal one. Moreover, the coefficients are complex numbers. Since states are represented by complex wavefunctions, two states being added together will undergo interference. This is a key difference between quantum computing and probabilistic classical computing.^[6]

If you measure the three qubits, then you will observe a three-bit string. The probability of measuring a string will equal the squared magnitude of that string's coefficients (using our example, probability that we read state as 000 = $|a|^2$, probability that we read state as 001 = $|b|^2$, etc.). Thus a measurement of the quantum state with coefficients (a, b, \dots, h)

gives the classical probability distribution $(|a|^2, |b|^2, \dots, |h|^2)$. We say that the quantum state "collapses" classical state.

Note that an eight-dimensional vector can be specified in many different ways, depending on what basis you choose for the space. The basis of three-bit strings 000, 001, ..., 111 is known as the computational basis, and is often convenient, but other bases of unit-length, orthogonal vectors can also be used. Ket notation is often used to make explicit the choice of basis. For example, the state (a, b, c, d, e, f, g, h) in the computational basis can be written as $a|000\rangle + b|001\rangle + c|010\rangle + d|011\rangle + e|100\rangle + f|101\rangle + g|110\rangle + h|111\rangle$, where, e.g., $|010\rangle = (0, 0, 1, 0, 0, 0, 0, 0)$. The computational basis for a single qubit (two dimensions) is $|0\rangle = (1, 0)$, $|1\rangle = (0, 1)$, but another common basis is the Hadamard basis of $|+\rangle = \frac{1}{\sqrt{2}}(1, 1)$ and $|-\rangle = \frac{1}{\sqrt{2}}(1, -1)$.

Note that although recording a classical state of n bits, a 2^n -dimensional probability distribution, requires an exponential number of real numbers, practically we can always think of the system as being exactly one of the n -bit strings—we just don't know which one. Quantum mechanically, this is not the case, and all 2^n complex coefficients need to be kept track of to see how the quantum system evolves. For example, a 300-qubit quantum computer has a state described by 2^{300} (approximately 10^{90}) complex numbers, more than the number of atoms in the observable universe.

Operation

While a classical three-bit state and a quantum three-qubit state are both eight-dimensional vectors, they are manipulated quite differently for classical or quantum computation, respectively. For computing in either case, the system must be initialized, for example into the all-zeros string, $|000\rangle$, corresponding to the vector $(1, 0, 0, 0, 0, 0, 0, 0)$. In classical randomized computation, the system evolves according to the application of stochastic matrices, which preserve that the probabilities add up to one (i.e., preserve the L1 norm). In quantum computation, on the other hand, allowed operations are unitary matrices, which are effectively rotations (they preserve that the sum of the squares add up to one, the Euclidean or L2 norm). (Exactly what unitaries can be applied depend on the physics of the quantum device.) Consequently, since rotations can be undone by rotating backward, quantum computations are reversible. (Technically, quantum operations can be probabilistic combinations of unitaries, so quantum computation really does generalize classical computation. See quantum circuit for a more precise formulation.)

Finally, upon termination of the algorithm, the result needs to be read off. In the case of a classical computer, we *sample* from the probability distribution on the three-bit register to obtain one definite three-bit string, say 000. Quantum mechanically, we *measure* the three-qubit state, which is equivalent to collapsing the quantum state down to a classical distribution (with the coefficients in the classical state being the squared magnitudes of the coefficients for the quantum state, as described above) followed by sampling from that distribution. Note that this destroys the original quantum state. Many algorithms will only give the correct answer with a certain probability, however by repeatedly initializing, running and measuring the quantum computer, the probability of getting the correct answer can be increased.

For more details on the sequences of operations used for various algorithms, see universal quantum computer, Shor's algorithm, Grover's algorithm, Deutsch-Jozsa algorithm, quantum Fourier transform, quantum gate, quantum adiabatic algorithm and quantum

error correction.

Potential

Integer factorization is believed to be computationally infeasible with an ordinary computer for large integers that are the product of only a few prime numbers (e.g., products of two 300-digit primes).^[7] By comparison, a quantum computer could efficiently solve this problem using Shor's algorithm to find its factors. This ability would allow a quantum computer to "break" many of the cryptographic systems in use today, in the sense that there would be a polynomial time (in the number of digits of the integer) algorithm for solving the problem. In particular, most of the popular public key ciphers are based on the difficulty of factoring integers (or the related discrete logarithm problem which can also be solved by Shor's algorithm), including forms of RSA. These are used to protect secure Web pages, encrypted email, and many other types of data. Breaking these would have significant ramifications for electronic privacy and security. The only way to increase the security of an algorithm like RSA would be to increase the key size and hope that an adversary does not have the resources to build and use a powerful enough quantum computer.

A way out of this dilemma would be to use some kind of quantum cryptography. There are also some digital signature schemes that are believed to be secure against quantum computers. See for instance Lamport signatures.

Besides factorization and discrete logarithms, quantum algorithms offering a more than polynomial speedup over the best known classical algorithm have been found for several problems,^[8] including the simulation of quantum physical processes from chemistry and solid state physics, the approximation of Jones polynomials, and solving Pell's equation. No mathematical proof has been found that shows that an equally fast classical algorithm cannot be discovered, although this is considered unlikely. For some problems, quantum computers offer a polynomial speedup. The most well-known example of this is *quantum database search*, which can be solved by Grover's algorithm using quadratically fewer queries to the database than are required by classical algorithms. In this case the advantage is provable. Several other examples of provable quantum speedups for query problems have subsequently been discovered, such as for finding collisions in two-to-one functions and evaluating NAND trees.

Consider a problem that has these four properties:

1. The only way to solve it is to guess answers repeatedly and check them,
2. There are n possible answers to check,
3. Every possible answer takes the same amount of time to check, and
4. There are no clues about which answers might be better: generating possibilities randomly is just as good as checking them in some special order.

An example of this is a password cracker that attempts to guess the password for an encrypted file (assuming that the password has a maximum possible length).

For problems with all four properties, the time for a quantum computer to solve this will be proportional to the square root of n . That can be a very large speedup, reducing some problems from years to seconds. It can be used to attack symmetric ciphers such as Triple DES and AES by attempting to guess the secret key. Regardless of whether any of these problems can be shown to have an advantage on a quantum computer, they nonetheless will always have the advantage of being an excellent tool for studying quantum mechanical

interactions, which of itself is an enormous value to the scientific community.

Grover's algorithm can also be used to obtain a quadratic speed-up [over a brute-force search] for a class of problems known as NP-complete.

Since chemistry and nanotechnology rely on understanding quantum systems, and such systems are impossible to simulate in an efficient manner classically, many believe quantum simulation will be one of the most important applications of quantum computing.^[9]

There are a number of practical difficulties in building a quantum computer, and thus far quantum computers have only solved trivial problems. David DiVincenzo, of IBM, listed the following requirements for a practical quantum computer:^[10]

- scalable physically to increase the number of qubits;
- qubits can be initialized to arbitrary values;
- quantum gates faster than decoherence time;
- universal gate set;
- qubits can be read easily.

Quantum decoherence

One of the greatest challenges is controlling or removing decoherence. This usually means isolating the system from its environment as the slightest interaction with the external world would cause the system to decohere. This effect is irreversible, as it is non-unitary, and is usually something that should be avoided, if not highly controlled. Decoherence times for candidate systems, in particular the transverse relaxation time T_2 (for NMR and MRI technology, also called the *dephasing time*), typically range between nanoseconds and seconds at low temperature.^[6]

These issues are more difficult for optical approaches as the timescales are orders of magnitude lower and an often cited approach to overcoming them is optical pulse shaping. Error rates are typically proportional to the ratio of operating time to decoherence time, hence any operation must be completed much more quickly than the decoherence time.

If the error rate is small enough, it is thought to be possible to use quantum error correction, which corrects errors due to decoherence, thereby allowing the total calculation time to be longer than the decoherence time. An often cited figure for required error rate in each gate is 10^{-4} . This implies that each gate must be able to perform its task 10,000 times faster than the decoherence time of the system.

Meeting this scalability condition is possible for a wide range of systems. However, the use of error correction brings with it the cost of a greatly increased number of required qubits. The number required to factor integers using Shor's algorithm is still polynomial, and thought to be between L and L^2 , where L is the number of bits in the number to be factored; error correction algorithms would inflate this figure by an additional factor of L . For a 1000-bit number, this implies a need for about 10^4 qubits without error correction.^[11] With error correction, the figure would rise to about 10^7 qubits. Note that computation time is about L^2 or about 10^7 steps and on 1 MHz, about 10 seconds.

A very different approach to the stability-decoherence problem is to create a topological quantum computer with anyons, quasi-particles used as threads and relying on braid theory to form stable logic gates.^{[12] [13]}

Candidates

There are a number of quantum computing candidates, among those:

- Superconductor-based quantum computers (including SQUID-based quantum computers)^[14]
- Trapped ion quantum computer
- Optical lattices
- Topological quantum computer
- Quantum dot on surface (e.g. the Loss-DiVincenzo quantum computer)
- Nuclear magnetic resonance on molecules in solution (liquid NMR)
- Solid state NMR Kane quantum computers
- Electrons on helium quantum computers
- Cavity quantum electrodynamics (CQED)
- Molecular magnet
- Fullerene-based ESR quantum computer
- Optic-based quantum computers (Quantum optics)
- Diamond-based quantum computer^{[15] [16] [17]}
- Bose-Einstein condensate-based quantum computer^[18]
- Transistor-based quantum computer - string quantum computers with entrainment of positive holes using an electrostatic trap
- Spin-based quantum computer
- Adiabatic quantum computation^[19]
- Rare-earth-metal-ion-doped inorganic crystal based quantum computers^{[20] [21]}

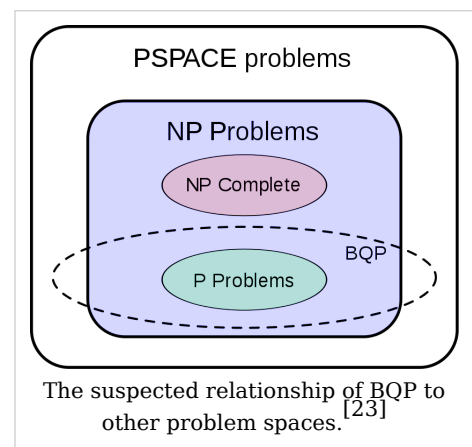
The large number of candidates shows explicitly that the topic, in spite of rapid progress, is still in its infancy. But at the same time there is also a vast amount of flexibility.

In 2005, researchers at the University of Michigan built a semiconductor chip which functioned as an ion trap. Such devices, produced by standard lithography techniques, may point the way to scalable quantum computing tools.^[22] An improved version was made in 2006.

Quantum computing in computational complexity theory

This section surveys what is currently known mathematically about the power of quantum computers. It describes the known results from computational complexity theory and the theory of computation dealing with quantum computers.

The class of problems that can be efficiently solved by quantum computers is called **BQP**, for "bounded error, quantum, polynomial time". Quantum computers only run **probabilistic** algorithms, so **BQP** on quantum computers is the counterpart of **BPP** on classical computers. It is defined as the set of problems solvable with a polynomial-time algorithm, whose probability of error is bounded away from one quarter.^[23] A quantum computer is said to "solve" a problem if, for every instance, its answer will be right with high probability. If that solution runs in polynomial time, then that problem is in **BQP**.



BQP is contained in the complexity class $\#P$ (or more precisely in the associated class of decision problems $P^{\#P}$),^[24] which is a subclass of PSPACE.

BQP is suspected to be disjoint from NP-complete and a strict superset of **P**, but that is not known. Both integer factorization and discrete log are in **BQP**. Both of these problems are **NP** problems suspected to be outside **BPP**, and hence outside **P**. Both are suspected to not be NP-complete. There is a common misconception that quantum computers can solve NP-complete problems in polynomial time. That is not known to be true, and is generally suspected to be false.^[24]

Quantum gates may be viewed as linear transformations. Daniel S. Abrams and Seth Lloyd have shown that if *nonlinear* transformations are permitted, then NP-complete problems could be solved in polynomial time. It could even do so for $\#P$ -complete problems. They do not believe that such a machine is possible.

Although quantum computers may be faster than classical computers, those described above can't solve any problems that classical computers can't solve, given enough time and memory (however, those amounts might be practically infeasible). A Turing machine can simulate these quantum computers, so such a quantum computer could never solve an undecidable problem like the halting problem. The existence of "standard" quantum computers does not disprove the Church–Turing thesis.^[23]

See also

- List of emerging technologies
- Quantum bus
- Timeline of quantum computing
- Chemical computer
- DNA computer
- Decoherence by transposons in evolution
- Mathematical biology
- Molecular computer

References

- [1] " Quantum Computing with Molecules (<http://www.media.mit.edu/physics/publications/papers/98.06.sciam/0698gershenfeld.html>)" article in Scientific American by Neil Gershenfeld and Isaac L. Chuang - a generally accessible overview of quantum computing and so on.
- [2] Quantum Information Science and Technology Roadmap (http://qist.lanl.gov/qcomp_map.shtml) for a sense of where the research is heading.
- [3] One photon Grover algorithm (<http://espace.library.uq.edu.au/eserv/UQ:10849/n9905086.pdf>)
- [4] Lieven M.K. Vandersypen et al. (1999). "Separability of Very Noisy Mixed States and Implications for NMR Quantum Computing". *Phys. Rev. Lett* **83**: 1054–1057. doi: 10.1103/PhysRevLett.83.1054 (<http://dx.doi.org/10.1103/PhysRevLett.83.1054>).
- [5] Waldner, Jean-Baptiste (2007). *Nanocomputers and Swarm Intelligence*. London: ISTE. pp. p157. ISBN 2746215160.
- [6] DiVincenzo (1995).
- [7] Integer Factoring (http://modular.fas.harvard.edu/edu/Fall2001/124/misc/arjen_lenstra_factoring.pdf)
By ARJEN K. LENSTRA - Designs, Codes and Cryptography, 19, 101–128 (2000) Kluwer Academic Publishers
- [8] Quantum Algorithm Zoo (<http://www.its.caltech.edu/~sjordan/zoo.html>) - Stephen Jordan's Homepage
- [9] The Father of Quantum Computing (<http://www.wired.com/science/discoveries/news/2007/02/72734>) By Quinn Norton 02.15.2007, Wired.com
- [10] David P. DiVincenzo, IBM (2000-04-13). <http://arxiv.org/abs/quant-ph/0002077>|"The Physical Implementation of Quantum Computation". <http://arxiv.org/abs/quant-ph/0002077>. Retrieved on 2006-11-17.

- [11] M. I. Dyakonov, Université Montpellier (2006-10-14). <http://arxiv.org/abs/quant-ph/0610117>|"Is Fault-Tolerant Quantum Computation Really Possible?". <http://arxiv.org/abs/quant-ph/0610117>. Retrieved on 2007-02-16.
- [12] Freedman, Michael; Alexei Kitaev, Michael Larsen, Zhenghan Wang (2002-10-20). "Topological Quantum Computation". *Bulletin of the American Mathematical Society* **40** (1): 31–38. doi: 10.1090/S0273-0979-02-00964-3 (<http://dx.doi.org/10.1090/S0273-0979-02-00964-3>).
- [13] Monroe, Don, *Anyons: The breakthrough quantum computing needs?* (<http://www.newscientist.com/channel/fundamentals/mg20026761.700-anyons-the-breakthrough-quantum-computing-needs.html>), New Scientist, 1 October 2008
- [14] Clarke, John; Wilhelm, Frank (June 19, 2008), "<http://www.nature.com/nature/journal/v453/n7198/full/nature07128.html>|Superconducting quantum bits", *Nature* **453**: 1031–1042, doi: 10.1038/nature07128 (<http://dx.doi.org/10.1038/nature07128>), <http://www.nature.com/nature/journal/v453/n7198/full/nature07128.html>
- [15] Nizovtsev, A. P.; Kilin, S. Ya.; Jelezko, F.; Gaebel, T.; Popa, I.; Gruber, A.; Wrachtrup, J. (October 19, 2004), "<http://www.springerlink.com/content/5p6554lg35716085/>|A quantum computer based on NV centers in diamond: Optically detected nutations of single electron and nuclear spins", *Optics and Spectroscopy* **99** (2): 248–260, doi: 10.1134/1.2034610 (<http://dx.doi.org/10.1134/1.2034610>), <http://www.springerlink.com/content/5p6554lg35716085/>
- [16] Wolfgang Gruener, TG Daily (2007-06-01). <http://www.tgdaily.com/content/view/32306/118/>|"Research indicates diamonds could be key to quantum storage". <http://www.tgdaily.com/content/view/32306/118/>. Retrieved on 2007-06-04.
- [17] Neumann, P.; Mizuochi, N.; Rempp, F.; Hemmer, P.; Watanabe, H.; Yamasaki, S.; Jacques, V.; Gaebel, T.; *et al.* (June 6, 2008), "<http://www.sciencemag.org/cgi/content/abstract/320/5881/1326>|Multipartite Entanglement Among Single Spins in Diamond", *Science* **320** (5881): 1326–1329, doi: 10.1126/science.1157233 (<http://dx.doi.org/10.1126/science.1157233>), PMID 18535240, <http://www.sciencemag.org/cgi/content/abstract/320/5881/1326>
- [18] Rene Millman, IT PRO (2007-08-03). <http://www.itpro.co.uk/news/121086/trapped-atoms-could-advance-quantum-computing.html>|"Trapped atoms could advance quantum computing". <http://www.itpro.co.uk/news/121086/trapped-atoms-could-advance-quantum-computing.html>. Retrieved on 2007-07-26.
- [19] William M Kaminsky, MIT (Date Unknown). <http://arxiv.org/pdf/quant-ph/0403090>|"Scalable Superconducting Architecture for Adiabatic Quantum Computation". <http://arxiv.org/pdf/quant-ph/0403090>. Retrieved on 2007-02-19.
- [20] Ohlsson, N.; Mohan, R. K.; Kröll, S. (January 1, 2002), "<http://www.sciencedirect.com/science/article/B6TVF-44J3RM9-J/2/307aab59d157ddd2ebb8281f76f89138>|Quantum computer hardware based on rare-earth-ion-doped inorganic crystals", *Opt. Commun.* **201** (1–3): 71–77, doi: 10.1016/S0030-4018(01)01666-2 ([http://dx.doi.org/10.1016/S0030-4018\(01\)01666-2](http://dx.doi.org/10.1016/S0030-4018(01)01666-2)), <http://www.sciencedirect.com/science/article/B6TVF-44J3RM9-J/2/307aab59d157ddd2ebb8281f76f89138>
- [21] Longdell, J. J.; Sellars, M. J.; Manson, N. B. (September 23, 2004), "<http://prola.aps.org/abstract/PRL/v93/i13/e130503>|Demonstration of conditional quantum phase shift between ions in a solid", *Phys. Rev. Lett.* **93** (13): 130503, doi: 10.1103/PhysRevLett.93.130503 (<http://dx.doi.org/10.1103/PhysRevLett.93.130503>), <http://prola.aps.org/abstract/PRL/v93/i13/e130503>
- [22] Ann Arbor (2005-12-12). <http://www.umich.edu/news/index.html?Releases/2005/Dec05/r121205b>|"U-M develops scalable and mass-producible quantum computer chip". <http://www.umich.edu/news/index.html?Releases/2005/Dec05/r121205b>. Retrieved on 2006-11-17.
- [23] Nielsen and Chuang (2000).
- [24] Bernstein and Vazirani, Quantum complexity theory, *SIAM Journal on Computing*, 26(5):1411-1473, 1997. (<http://www.cs.berkeley.edu/~vazirani/bv.ps>)

General references

- Derek Abbott, Charles R. Doering, Carlton M. Caves, Daniel M. Lidar, Howard E. Brandt, Alexander R. Hamilton, David K. Ferry, Julio Gea-Banacloche, Sergey M. Bezrukov, and Laszlo B. Kish (2003). "Dreams versus Reality: Plenary Debate Session on Quantum Computing". *Quantum Information Processing* **2** (6): 449–472. doi: 10.1023/B:QINP.0000042203.24782.9a (<http://dx.doi.org/10.1023/B:QINP.0000042203.24782.9a>). arXiv:quant-ph/0310130. (Alternative Location (free) at Michigan university's repository Deep Blue (<http://hdl.handle.net/2027.42/45526>))

- David P. DiVincenzo (2000). "The Physical Implementation of Quantum Computation". *Experimental Proposals for Quantum Computation*. arXiv:quant-ph/0002077
- David P. DiVincenzo (1995). "Quantum Computation". *Science* **270** (5234): 255–261. doi: 10.1126/science.270.5234.255 (<http://dx.doi.org/10.1126/science.270.5234.255>). Table 1 lists switching and dephasing times for various systems.
- Richard Feynman (1982). "Simulating physics with computers". *International Journal of Theoretical Physics* **21**: 467. doi: 10.1007/BF02650179 (<http://dx.doi.org/10.1007/BF02650179>).
- Gregg Jaeger (2006). *Quantum Information: An Overview*. Berlin: Springer. ISBN 0-387-35725-4. OCLC 255569451 (<http://worldcat.org/oclc/255569451>). <http://www.springer.com/west/home/physics?SGWID=4-10100-22-173664707-detailsPage=ppmmedia|toc>
- Michael Nielsen and Isaac Chuang (2000). *Quantum Computation and Quantum Information*. Cambridge: Cambridge University Press. ISBN 0-521-63503-9. OCLC 174527496 (<http://worldcat.org/oclc/174527496>).
- Stephanie Frank Singer (2005). *Linearity, Symmetry, and Prediction in the Hydrogen Atom*. New York: Springer. ISBN 0-387-24637-1. OCLC 253709076 (<http://worldcat.org/oclc/253709076>).
- Giuliano Benenti (2004). *Principles of Quantum Computation and Information Volume 1*. New Jersey: World Scientific. ISBN 9-812-38830-3. OCLC 179950736 (<http://worldcat.org/oclc/179950736>).
- David P. DiVincenzo (2000). "The Physical Implementation of Quantum Computation". *Experimental Proposals for Quantum Computation*. arXiv:quant-ph/0002077.
- C. Adami, N.J. Cerf. (1998). "Quantum computation with linear optics". arXiv:quant-ph/9806048v1.
- Joachim Stolze,; Dieter Suter, (2004). *Quantum Computing*. Wiley-VCH. ISBN 3527404384.
- Ian Mitchell, (1998). <http://citeseer.ist.psu.edu/mitchell98computing.html>|"Computing Power into the 21st Century: Moore's Law and Beyond". <http://citeseer.ist.psu.edu/mitchell98computing.html>.
- Rolf Landauer, (1961). <http://www.research.ibm.com/journal/rd/053/ibmrd0503C.pdf>|"Irreversibility and heat generation in the computing process". <http://www.research.ibm.com/journal/rd/053/ibmrd0503C.pdf>.
- Gordon E. Moore (1965). *Cramming more components onto integrated circuits*.
- R.W. Keyes, (1988). *Miniaturization of electronics and its limits*.
- M. A. Nielsen,; E. Knill, ; R. Laamme,. <http://citeseer.ist.psu.edu/595490.html>|"Complete Quantum Teleportation By Nuclear Magnetic Resonance". <http://citeseer.ist.psu.edu/595490.html>.
- Lieven M.K. Vandersypen,; Constantino S. Yannoni, ; Isaac L. Chuang, (2000). *Liquid state NMR Quantum Computing*.
- Imai Hiroshi,; Hayashi Masahito, (2006). *Quantum Computation and Information*. Berlin: Springer. ISBN 3540331328.
- Andre Berthiaume, (1997). <http://citeseer.ist.psu.edu/article/berthiaume97quantum.html>|"Quantum Computation".

<http://citeseer.ist.psu.edu/article/berthiaume97quantum.html>.

- David R. Simon, (1994). <http://citeseer.ist.psu.edu/simon94power.html>|"On the Power of Quantum Computation". Institute of Electrical and Electronic Engineers Computer Society Press. <http://citeseer.ist.psu.edu/simon94power.html>.
- http://www.crypto.rub.de/its_seminar_ss08.html|"Seminar Post Quantum Cryptology". Chair for communication security at the Ruhr-University Bochum. http://www.crypto.rub.de/its_seminar_ss08.html.

Further reading

- Weinberger, Sharon, "Spooky research cuts: US intelligence agency axes funding for work on quantum computing" (<http://www.nature.com/news/2009/090603/full/459625a.html>), Nature 459, 625 (2009), 3 June 2009

External links

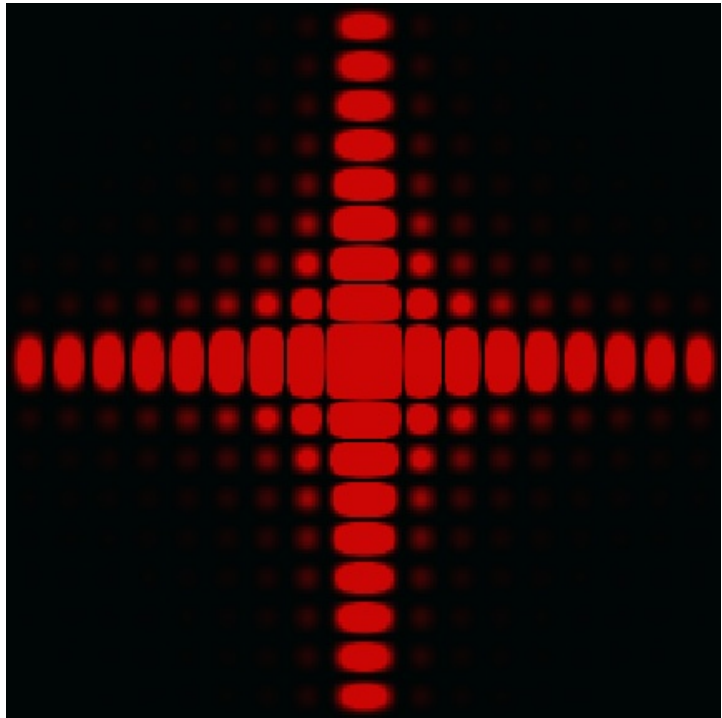
- jQuantum: Java quantum circuit simulator (<http://jqquantum.sourceforge.net/jQuantumApplet.html>)
 - QCAD: Quantum circuit emulator (<http://www.phys.cs.is.nagoya-u.ac.jp/~watanabe/qcad/index.html>)
 - C++ Quantum Library (<https://gna.org/projects/quantumlibrary>)
 - Haskell Library for Quantum computations (<http://hackage.haskell.org/cgi-bin/hackage-scripts/package/quantum-arrow>)
 - Video Lectures by David Deutsch (http://www.quiprocone.org/Protected/DD_lectures.htm)
 - Quasi quantum computer. (<http://x-machines.comoj.com/hyper-electromagnetics/index.html>)
-

Theory

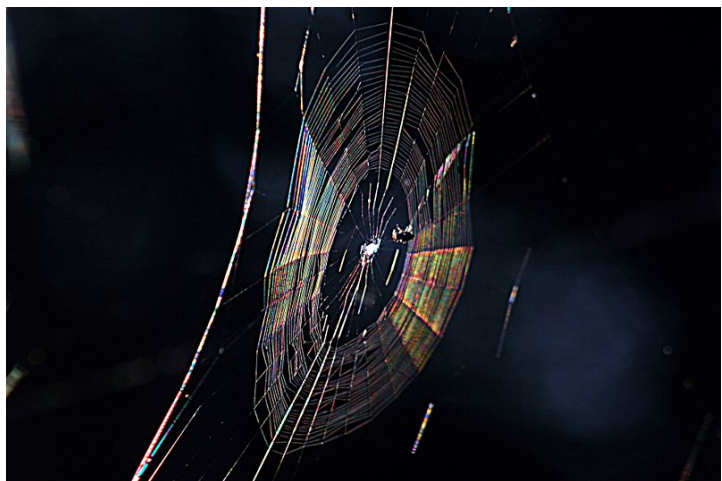
Diffraction

Diffraction is normally taken to refer to various phenomena which occur when a wave encounters an obstacle. It is described as the apparent bending of waves around small obstacles and the spreading out of waves past small openings.^[2] Very similar effects are observed when there is an alteration in the properties of the medium in which the wave is travelling, for example a variation in refractive index for light waves or in acoustic impedance for sound waves and these can also be referred to as diffraction effects. Diffraction occurs with all waves, including sound waves, water waves, and electromagnetic waves such as visible light, x-rays and radio waves. As physical objects have wave-like properties (at the atomic level), diffraction also occurs with matter and can be studied according to the principles of quantum mechanics.

While diffraction occurs whenever propagating waves encounter such changes, its effects are generally most pronounced for waves where the wavelength is on the order of the size of the diffracting objects. If the obstructing object provides multiple, closely-spaced openings, a complex pattern of varying intensity can result. This is due to the superposition, or interference, of different parts of a wave that traveled to the observer by different paths (see diffraction grating).



The intensity pattern formed on a screen by diffraction from a square aperture



Colors seen in a spider web are partially due to diffraction, according to some analyses.^[1]

The formalism of diffraction can also describe the way in which waves of finite extent propagate in free space. For example, the expanding profile of a laser beam, the beam shape of a radar antenna and the field of view of an ultrasonic transducer are all explained by diffraction theory.

Examples of diffraction in everyday life

The effects of diffraction can be regularly seen in everyday life. The most colorful examples of diffraction are those involving light; for example, the closely spaced tracks on a CD or DVD act as a diffraction grating to form the familiar rainbow pattern we see when looking at a disk. This principle can be extended to engineer a grating with a structure such that it will produce any diffraction pattern desired; the hologram on a credit card is an example. Diffraction in the atmosphere by small particles can cause a bright ring to be visible around a bright light source like the sun or the moon. A shadow of a solid object, using light from a compact source, shows small fringes near its edges. The speckle pattern which is observed when laser light falls on an optically rough surface is also a diffraction phenomenon. All these effects are a consequence of the fact that light is a wave.



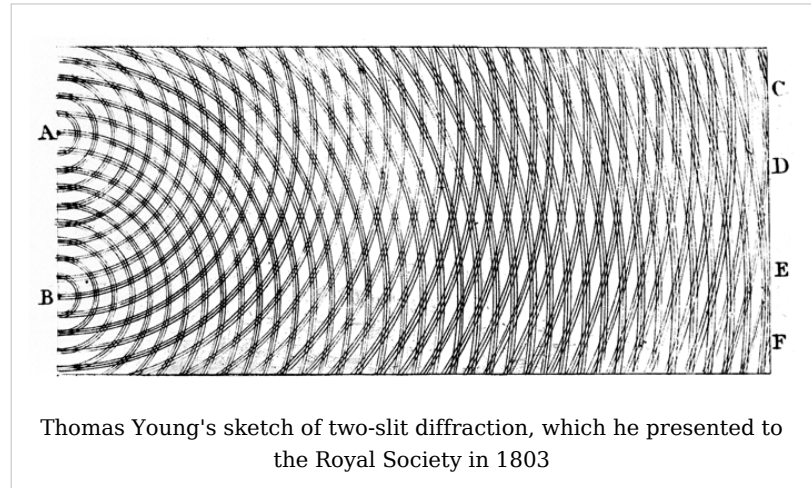
Solar glory at the steam from hot springs. A **glory** is an optical phenomenon produced by light backscattered (a combination of diffraction, reflection and refraction) towards its source by a cloud of uniformly-sized water droplets.

Diffraction can occur with any kind of wave. Ocean waves diffract around jetties and other obstacles. Sound waves can diffract around objects, which is why one can still hear someone calling even when hiding behind a tree.^[3] Diffraction can also be a concern in some technical applications; it sets a fundamental limit to the resolution of a camera, telescope, or microscope.

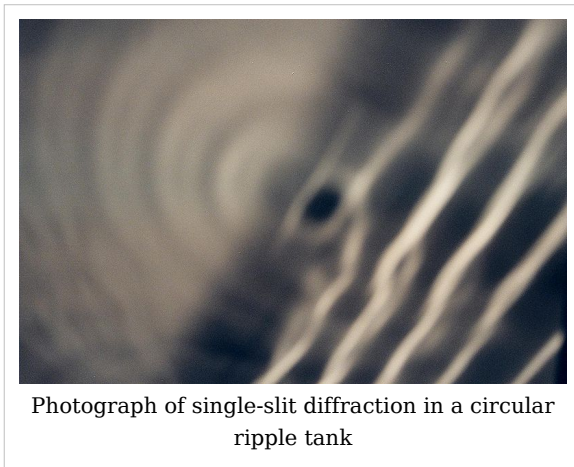
History

The effects of diffraction of light were first carefully observed and characterized by Francesco Maria Grimaldi, who also coined the term *diffraction*, from the Latin *diffringere*, 'to break into pieces', referring to light breaking up into different directions. The results of Grimaldi's observations were published posthumously in 1665.^[4] ^[5] Isaac Newton

studied these effects and attributed them to *inflexion* of light rays. James Gregory (1638-1675) observed the diffraction patterns caused by a bird feather, which was effectively the first diffraction grating. In 1803 Thomas Young did his famous experiment observing interference from two closely spaced slits. Explaining his results by interference of the waves emanating from the two different slits, he deduced that light must propagate as waves. Augustin-Jean Fresnel did more definitive studies and calculations of diffraction, published in 1815 and 1818, and thereby gave great support to the wave theory of light that had been advanced by Christiaan Huygens and reinvigorated by Young, against Newton's particle theory. In addition, Young's experiment was one of the experiments used to prove that light acts as both a particle and a wave.



The mechanism of diffraction



Diffraction arises because of the way in which waves propagate; this is described by the Huygens-Fresnel principle. The propagation of a wave can be visualized by considering every point on a wavefront as a point source for a secondary radial wave. The subsequent propagation and addition of all these radial waves form the new wavefront. When waves are added together, their sum is determined by the relative phases as well as the amplitudes of the individual waves, an effect which is often known as wave interference. The summed amplitude of the waves can have any value

between zero and the sum of the individual amplitudes. Hence, diffraction patterns usually have a series of maxima and minima.

To determine the form of a diffraction pattern, we must determine the phase and amplitude of each of the Huygens wavelets at each point in space and then find the sum of these waves. There are various analytical models which can be used to do this including the Fraunhofer diffraction equation for the far field and the Fresnel Diffraction equation for the

near-field. Most configurations cannot be solved analytically; solutions can be found using various numerical analytical methods including Finite element and boundary element methods

Diffraction systems

It is possible to obtain a qualitative understanding of many diffraction phenomena by considering how the relative phases of the individual secondary wave sources vary, and in particular, the conditions in which the phase difference equals half a cycle in which case waves will cancel one another out.

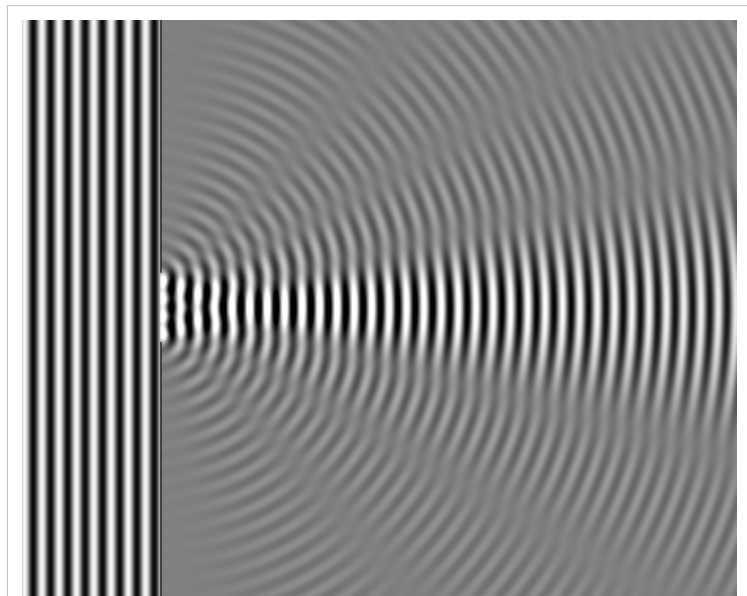
The simplest descriptions of diffraction are those in which the situation can be reduced to a two dimensional problem. For water waves, this is already the case, water waves propagate only on the surface of the water. For light, we can often neglect one direction if the diffracting object extends in that direction over a distance far greater than the wavelength. In the case of light shining through small circular holes we will have to take into account the full three dimensional nature of the problem.

Some of the simpler cases of diffraction are considered below.

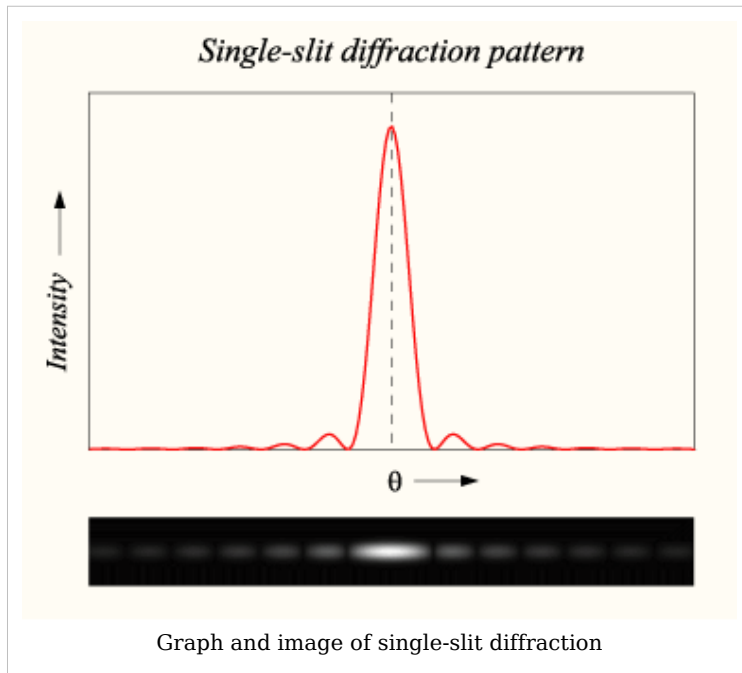
Single-slit diffraction

A long slit of infinitesimal width which is illuminated by light diffracts the light into a series of circular waves and the wavefront which emerges from the slit is a cylindrical wave of uniform intensity.

A slit which is wider than a wavelength has a large number of point sources spaced evenly across the width of the slit. The light at a given angle is made up of contributions from each of these point sources and if the relative phases of these contributions vary by more than 2π , we expect to find minima and maxima in the diffracted light.



Numerical approximation of diffraction pattern from a slit of width four wavelengths with an incident plane wave. The main central beam, nulls, and phase reversals are apparent.



We can find the angle at which a first minimum is obtained in the diffracted light by the following reasoning. The light from a source located at the top edge of the slit interferes destructively with a source located at the middle of the slit, when the path difference between them is equal to $\lambda/2$. Similarly, the source just below the top of the slit will interfere destructively with the source located just below the middle of the slit at the same angle. We can continue this reasoning along the entire height of the slit to conclude that the condition for destructive interference for the entire slit is the same as the condition for destructive interference between two narrow slits a distance apart that is half the width of the slit. The path difference is given by $\frac{d \sin(\theta)}{2}$ so that the minimum intensity occurs at an angle θ_{\min} given by

$$d \sin \theta_{\min} = \lambda$$

where d is the width of the slit.

A similar argument can be used to show that if we imagine the slit to be divided into four, six, eight parts, etc, minima are obtained at angles θ_n given by

$$d \sin \theta_n = n\lambda$$

where n is an integer greater than zero.

There is no such simple argument to enable us to find the maxima of the diffraction pattern. The intensity profile can be calculated using the Fraunhofer diffraction integral as

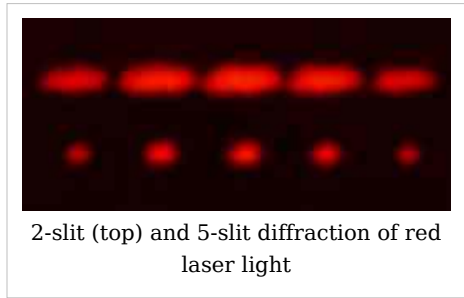
$$I(\theta) = I_0 \text{sinc}^2(d \sin \theta / \lambda)$$

where the sinc function is given by $\text{sinc}(x) = \sin(\pi x) / (\pi x)$ if $x \neq 0$, and $\text{sinc}(0) = 1$.

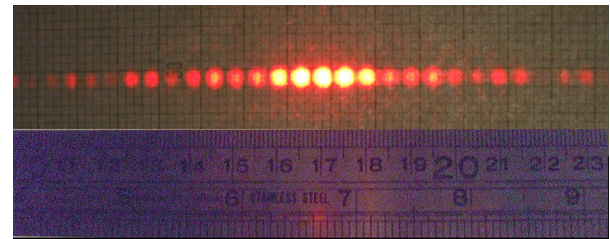
It should be noted that this analysis applies only to the far field, that is at a distance much larger than the width of the slit.

Diffraction grating

A diffraction grating is an optical component with a regular pattern. The form of the light diffracted by a grating depends on the structure of the elements and the number of elements present, but all gratings have intensity maxima at angles θ_m which are given by the grating equation



2-slit (top) and 5-slit diffraction of red laser light



A diffraction pattern of a 633 nm laser through a grid of 150 slits

$$d(\sin \theta_m + \sin \theta_i) = m\lambda.$$

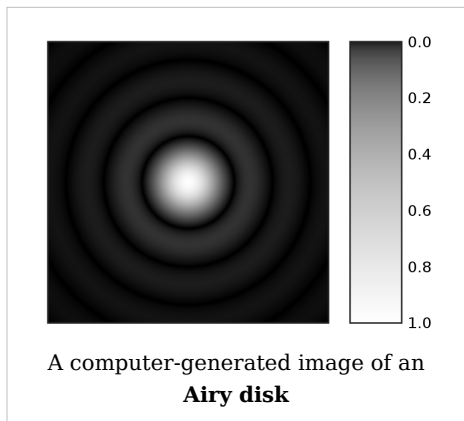
where θ_i is the angle at which the light is incident, d is the separation of grating elements and m is an integer which can be positive or negative.

The light diffracted by a grating is found by summing the light diffracted from each of the elements, and is essentially a convolution of diffraction and interference patterns.

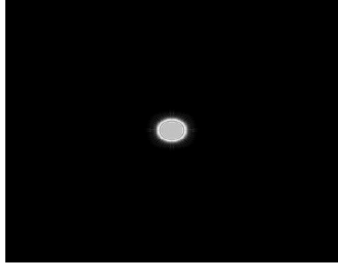
The figure shows the light diffracted by 2-element and 5-element gratings where the grating spacings are the same; it can be seen that the maxima are in the same position, but the detailed structures of the intensities are different.

Diffraction by a circular aperture

The far-field diffraction of a plane wave incident on a circular aperture is often referred to as the Airy Disk. The variation in intensity with angle is given by



A computer-generated image of an **Airy disk**



Computer generated light diffraction pattern from a circular aperture of diameter 0.5micron at a wavelength of 0.6micron (red-light) at distances of 0.1cm - 1cm in steps of 0.1cm. One can see the image moving from Fresnel region into the Fraunhofer region where the Airy pattern is seen.

$$I(\theta) = I_0 \left(\frac{2J_1(ka \sin \theta)}{ka \sin \theta} \right)^2$$

where a is the radius of the circular aperture, k is equal to $2\pi/\lambda$ and J_1 is a Bessel function. The smaller the aperture, the larger the spot size at a given distance, and the greater the divergence of the diffracted beams.

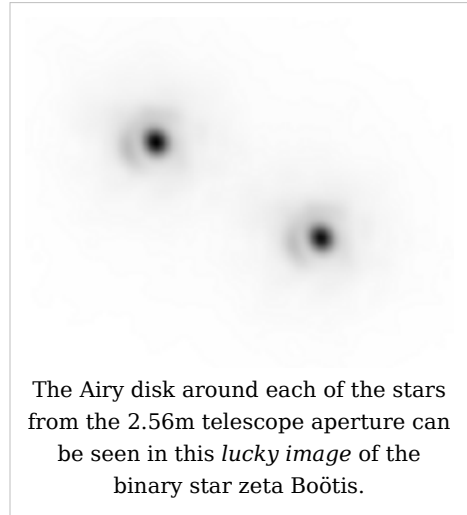
Propagation of a laser beam

The way in which the profile of a laser beam changes as it propagates is determined by diffraction. The output mirror of the laser is an aperture, and the subsequent beam shape is determined by that aperture. Hence, the smaller the output beam, the quicker it diverges. Diode lasers have much greater divergence than He-Ne lasers for this reason.

Paradoxically, it is possible to reduce the divergence of a laser beam by first expanding it with one convex lens, and then collimating it with a second convex lens whose focal point is coincident with that of the first lens. The resulting beam has a larger aperture, and hence a lower divergence.

Diffraction-limited imaging

The ability of an imaging system to resolve detail is ultimately limited by diffraction. This is because a plane wave incident on a circular lens or mirror is diffracted as described above. The light is not focused to a point but forms an Airy disk having a central spot in the focal plane with radius to first null of



$$d = 1.22\lambda N,$$

where λ is the wavelength of the light and N is the f-number (focal length divided by diameter) of the imaging optics. In object space, the corresponding angular resolution is

$$\sin \theta = 1.22 \frac{\lambda}{D},$$

where D is the diameter of the entrance pupil of the imaging lens (e.g., of a telescope's main mirror).

Two point sources will each produce an Airy pattern – see the photo of a binary star. As the point sources move closer together, the patterns will start to overlap, and ultimately they will merge to form a single pattern, in which case the two point sources cannot be resolved in the image. The Rayleigh criterion specifies that two point sources can be considered to be resolvable if the separation of the two images is at least the radius of the Airy disk, i.e. if the first minimum of one coincides with the maximum of the other.

Thus, the larger the aperture of the lens, and the smaller the wavelength, the finer the resolution of an imaging system. This is why telescopes have very large lenses or mirrors, and why optical microscopes are limited in the detail which they can see.

Speckle patterns

The speckle pattern which is seen when using a laser pointer is another diffraction phenomenon. It is a result of the superposition of many waves with different phases, which are produced when a laser beam illuminates a rough surface. They add together to give a resultant wave whose amplitude, and therefore intensity varies randomly.

Common features of diffraction patterns

Several qualitative observations can be made of diffraction in general:

- The angular spacing of the features in the diffraction pattern is inversely proportional to the dimensions of the object causing the diffraction. In other words: The smaller the diffracting object, the 'wider' the resulting diffraction pattern, and vice versa. (More precisely, this is true of the sines of the angles.)

- The diffraction angles are invariant under scaling; that is, they depend only on the ratio of the wavelength to the size of the diffracting object.
- When the diffracting object has a periodic structure, for example in a diffraction grating, the features generally become sharper. The third figure, for example, shows a comparison of a double-slit pattern with a pattern formed by five slits, both sets of slits having the same spacing, between the center of one slit and the next.

Particle diffraction

Quantum theory tells us that every particle exhibits wave properties. In particular, massive particles can interfere and therefore diffract. Diffraction of electrons and neutrons stood as one of the powerful arguments in favor of quantum mechanics. The wavelength associated with a particle is the de Broglie wavelength

$$\lambda = \frac{h}{p}$$

where h is Planck's constant and p is the momentum of the particle (mass \times velocity for slow-moving particles). For most macroscopic objects, this wavelength is so short that it is not meaningful to assign a wavelength to them. A sodium atom traveling at about 3000 m/s would have a De Broglie wavelength of about 5 pico meters.

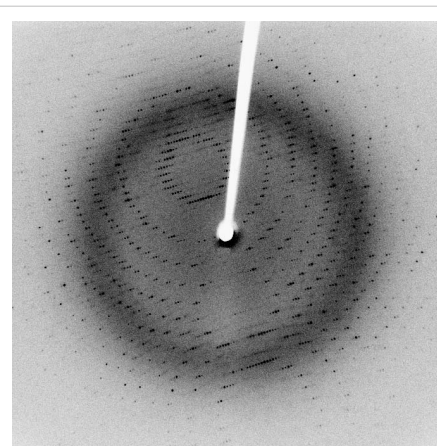
Because the wavelength for even the smallest of macroscopic objects is extremely small, diffraction of matter waves is only visible for small particles, like electrons, neutrons, atoms and small molecules. The short wavelength of these matter waves makes them ideally suited to study the atomic crystal structure of solids and large molecules like proteins.

Relatively recently, larger molecules like buckyballs were also shown to diffract.^[6]

Bragg diffraction

Diffraction from a three dimensional periodic structure such as atoms in a crystal is called Bragg diffraction. It is similar to what occurs when waves are scattered from a diffraction grating. Bragg diffraction is a consequence of interference between waves reflecting from different crystal planes. The condition of constructive interference is given by *Bragg's law*:

$$m\lambda = 2d \sin \theta$$



Following Bragg's law, each dot (or reflection), in this diffraction pattern forms from the constructive interference of X-rays passing through a crystal. The data can be used to determine the crystal's atomic structure.

where

λ is the wavelength,

d is the distance between crystal planes,

θ is the angle of the diffracted wave.

and m is an integer known as the *order* of the diffracted beam.

Bragg diffraction may be carried out using either light of very short wavelength like x-rays or matter waves like neutrons (and electrons) whose wavelength is on the order of (or much smaller than) the atomic spacing^[7]. The pattern produced gives information of the separations of crystallographic planes d , allowing one to deduce the crystal structure. Diffraction contrast, in electron microscopes and x-topography devices in particular, is also a powerful tool for examining individual defects and local strain fields in crystals.

Coherence

The description of diffraction relies on the interference of waves emanating from the same source taking different paths to the same point on a screen. In this description, the difference in phase between waves that took different paths is only dependent on the effective path length. This does not take into account the fact that waves that arrive at the screen at the same time were emitted by the source at different times. The initial phase with which the source emits waves can change over time in an unpredictable way. This means that waves emitted by the source at times that are too far apart can no longer form a constant interference pattern since the relation between their phases is no longer time independent.

The length over which the phase in a beam of light is correlated, is called the Coherence length. In order for interference to occur, the path length difference must be smaller than the coherence length. This is sometimes referred to as spectral coherence, as it is related to the presence of different frequency components in the wave. In the case of light emitted by an atomic transition, the coherence length is related to the lifetime of the excited state from which the atom made its transition.

If waves are emitted from an extended source, this can lead to incoherence in the transversal direction. When looking at a cross section of a beam of light, the length over which the phase is correlated is called the transverse coherence length. In the case of Young's double slit experiment, this would mean that if the transverse coherence length is smaller than the spacing between the two slits, the resulting pattern on a screen would look like two single slit diffraction patterns.

In the case of particles like electrons, neutrons and atoms, the coherence length is related to the spatial extent of the wave function that describes the particle.

See also

- Atmospheric diffraction
- Bragg diffraction
- Cloud iridescence
- Diffraction formalism
- Diffractometer
- Dynamical theory of diffraction
- Diffraction grating
- Electron diffraction
- Fraunhofer diffraction
- Fresnel diffraction
- Fresnel number
- Fresnel zone
- Neutron diffraction
- Prism
- Powder diffraction
- Refraction
- Schaefer-Bergmann diffraction
- Thinned array curse
- X-ray scattering techniques

References

- [1] Dietrich Zawischa. <http://www.itp.uni-hannover.de/~zawischa/ITP/spiderweb.html>|"Optical effects on spider webs". <http://www.itp.uni-hannover.de/%7Ezawischa/ITP/spiderweb.html>. Retrieved on 2007-09-21.
- [2] Diffraction concepts (<http://hyperphysics.phy-astr.gsu.edu/Hbase/phyopt/diffracn.html#c1>)
- [3] Andrew Norton (2000). http://books.google.com/books?id=XRRMxjr24pwC&pg=PA102&dq=sound+wave+diffraction+behind+tree&lr=&as_drrb_is=q&as_minm_is=1&as_miny_is=2009&as_maxm_is=12&as_maxy_is=2009&as_brr=3&as_pt=ALLTYPES&ei=EjjDSbulDJG4kwSBY6yADg *fields and waves*. CRC Press. p. 102. ISBN 9780750307192. http://books.google.com/books?id=XRRMxjr24pwC&pg=PA102&dq=sound+wave+diffraction+behind+tree&lr=&as_drrb_is=q&as_minm_is=1&as_miny_is=2009&as_maxm_is=12&as_maxy_is=2009&as_brr=3&as_pt=ALLTYPES&ei=EjjDSbulDJG4kwSBY6yADg
- [4] Jean Louis Aubert (1760). <http://books.google.com/books?vid=OCLC58901501&id=3OgDAAAAMAAJ&pg=PP151&lpg=PP151&dq=grimaldi+diffraction+pour+l'histoire+des+sciences+et+des+beaux+arts>. Paris: Impr. de S. A. S.; Chez E. Ganeau. pp. 149. http://books.google.com/books?vid=OCLC58901501&id=3OgDAAAAMAAJ&pg=PP151&lpg=PP151&dq=grimaldi+diffraction+date:0-1800&as_brr=1.
- [5] Sir David Brewster (1831). <http://books.google.com/books?vid=OCLC03255091&id=opYAAAAAMAAJ&pg=RA1-PA95&lpg=RA1-PA95&dq=grimaldi+diffraction+treatise+on+optics> *Treatise on Optics*. London: Longman, Rees, Orme, Brown & Green and John Taylor. pp. 95. http://books.google.com/books?vid=OCLC03255091&id=opYAAAAAMAAJ&pg=RA1-PA95&lpg=RA1-PA95&dq=grimaldi+diffraction+date:0-1840&as_brr=1.
- [6] Brezger, B.; Hackermüller, L.; Uttenthaler, S.; Petschinka, J.; Arndt, M.; Zeilinger, A. (February 2002). "http://homepage.univie.ac.at/Lucia.Hackermueller/unsereArtikel/Brezger2002a.pdf|Matter-Wave Interferometer for Large Molecules" (reprint). *Physical Review Letters* **88** (10): 100404. doi: 10.1103/PhysRevLett.88.100404 (<http://dx.doi.org/10.1103/PhysRevLett.88.100404>). <http://homepage.univie.ac.at/Lucia.Hackermueller/unsereArtikel/Brezger2002a.pdf>. Retrieved on 2007-04-30.
- [7] John M. Cowley (1975) *Diffraction physics* (North-Holland, Amsterdam) ISBN 0 444 10791 6

External links

- Do Sensors “Outresolve” Lenses? (<http://luminous-landscape.com/tutorials/resolution.shtml>); on lens and sensor resolution interaction.
- Diffraction and acoustics. (<http://www.acoustics.salford.ac.uk/feschools/waves/diffract.htm>)
- Diffraction in photography. (<http://sankey.ws/diffraction.html>)
- On Diffraction (<http://www.mathpages.com/home/kmath636/kmath636.htm>) at MathPages.
- Diffraction pattern calculators (<http://demonstrations.wolfram.com/search.html?query=diffraction>) at The Wolfram Demonstrations Project
- Wave Optics (http://www.lightandmatter.com/html_books/5op/ch05/ch05.html) – A chapter of an online textbook.
- 2-D wave Java applet (<http://www.falstad.com/wave2d/>) – Displays diffraction patterns of various slit configurations.
- Diffraction Java applet (<http://www.falstad.com/diffraction/>) – Displays diffraction patterns of various 2-D apertures.
- Diffraction approximations illustrated (<http://www.mit.edu/~birge/diffraction/>) – MIT site that illustrates the various approximations in diffraction and intuitively explains the Fraunhofer regime from the perspective of linear system theory.
- Gap (<http://www.phy.hk/wiki/englishhtm/Diffraction.htm>) Obstacle (<http://www.phy.hk/wiki/englishhtm/Diffraction2.htm>) Corner (<http://www.phy.hk/wiki/englishhtm/Diffraction3.htm>) – Java simulation of diffraction of water wave.
- Google Maps (<http://maps.google.com/maps?q=Panama+canal&hl=en&ie=UTF8&om=1&z=16&ll=9.385048,-79.918799&spn=0.015539,0.027122&t=k&iwloc=addr>) – Satellite image of Panama Canal entry ocean wave diffraction.

Quantum Mechanics

1. REDIRECT Quantum mechanics

This is a redirect from a title with another method of capitalisation. It leads to the title in accordance with the Wikipedia naming conventions for capitalisation, and can help writing, searching, and international language issues.

Pages linking to any of these redirects may be updated to link directly to the target page. However, do not replace these redirected links with a piped link unless the page is updated for another reason.

For more information, see Category:Redirects from other capitalisations.

S-matrix

***Scattering matrix** redirects here. For the meaning in linear electrical networks, see scattering parameters.*

For the 1960's approach to particle physics, see *S-matrix theory*.

In physics, the **scattering matrix** (or **S-matrix**) relates the initial state and the final state for an interaction of particles. It is used in quantum mechanics, scattering theory and quantum field theory.

More formally, the S-matrix is defined as the unitary matrix connecting asymptotic particle states in the Hilbert space of physical states (scattering channels). While the S-matrix may be defined for any background (spacetime) that is asymptotically solvable and has no horizons, it has a simple form in the case of the Minkowski space. In this special case, the Hilbert space is a space of irreducible unitary representations of the inhomogeneous Lorentz group; the S-matrix is the evolution operator between time equal to minus infinity, and time equal to plus infinity. It can be shown that if a quantum field theory in Minkowski space has a mass gap, the state in the asymptotic past and in the asymptotic future are both described by Fock spaces.

History

The S-matrix was first introduced by John Archibald Wheeler in the 1937 paper "'On the Mathematical Description of Light Nuclei by the Method of Resonating Group Structure'" ^[1]. In this paper Wheeler introduced a *scattering matrix* - a unitary matrix of coefficients connecting "the asymptotic behaviour of an arbitrary particular solution [of the integral equations] with that of solutions of a standard form" ^[2].

In the 1940s Werner Heisenberg developed, independently, the idea of the S-matrix. Due to the problematic divergences present in quantum field theory at that time Heisenberg was motivated to isolate the essential features of the theory that would not be affected by future changes as the theory developed. In doing so he was led to introduce a unitary "characteristic" S-matrix ^[2].

Motivation

In high-energy particle physics we are interested in computing the probability for different outcomes in scattering experiments. These experiments can be broken down into three stages:

1. Collide together a collection of incoming particles (usually *two* particles with high energies).
2. Allowing the incoming particles to interact. These interactions may change the types of particles present (e.g. if an electron and a positron annihilate they may produce two photons).
3. Measuring the resulting outgoing particles.

The process by which the incoming particles are transformed (through their interaction) into the outgoing particles is called scattering. For particle physics a physical theory of these processes must be able to compute the probability for different outgoing particles when we collide different incoming particles with different energies. The S-matrix in quantum field theory is used to do exactly this.

Use of S-matrices

The S-matrix is closely related to the transition probability amplitude in quantum mechanics and to cross sections of various interactions; the elements (individual numerical entries) in the S-matrix are known as **scattering amplitudes**. Poles of the S-matrix in the complex-energy plane are identified with bound states, virtual states or resonances. Branch cuts of the S-matrix in the complex-energy plane are associated to the opening of a scattering channel.

In the Hamiltonian approach to quantum field theory, the S-matrix may be calculated as a time-ordered exponential of the integrated Hamiltonian in the interaction picture; it may be also expressed using Feynman's path integrals. In both cases, the perturbative calculation of the S-matrix leads to Feynman diagrams.

In scattering theory, the **S-matrix** is an operator mapping free particle *in-states* to free particle *out-states* (scattering channels) in the Heisenberg picture. This is very useful because we cannot describe exactly the interaction (at least, the most interesting ones).

Mathematical definition

In Dirac notation, we define $|0\rangle$ as the vacuum quantum state. If $a^\dagger(k)$ is a creation operator, its hermitian conjugate (destruction or annihilation operator) acts on the vacuum as follows:

$$a(k)|0\rangle = 0$$

Now, we define two kinds of creation/destruction operators, acting on different Hilbert spaces (IN space i , OUT space f), $a_i^\dagger(k)$ and $a_f^\dagger(k)$.

So now

$$\begin{aligned}\mathcal{H}_{\text{IN}} &= \text{span}\{|I, k_1 \dots k_n\rangle = a_i^\dagger(k_1) \dots a_i^\dagger(k_n) |I, 0\rangle\}, \\ \mathcal{H}_{\text{OUT}} &= \text{span}\{|F, p_1 \dots p_n\rangle = a_f^\dagger(p_1) \dots a_f^\dagger(p_n) |F, 0\rangle\}.\end{aligned}$$

It is possible to prove that $|I, 0\rangle$ and $|F, 0\rangle$ are both invariant under translation and that the states $|I, k_1 \dots k_n\rangle$ and $|F, p_1 \dots p_n\rangle$ are eigenstates of the momentum operator \mathcal{P}^μ .

In the Heisenberg picture the states are time-independent, so we can expand initial states on a basis of final states (or vice versa) as follows:

$$|I, k_1 \dots k_n\rangle = C_0 + \sum_{m=1}^{\infty} \int d^4 p_1 \dots d^4 p_m C_m(p_1 \dots p_m) |F, p_1 \dots p_n\rangle$$

Where $|C_m|^2$ is the probability that the interaction transforms $|I, k_1 \dots k_n\rangle$ into $|F, p_1 \dots p_n\rangle$

According to Wigner's theorem, S must be a unitary operator such that $\langle I, \beta | S | I, \alpha \rangle = S_{\alpha\beta} = \langle F, \beta | I, \alpha \rangle$. Moreover, S leaves the vacuum state invariant and transforms IN-space fields in OUT-space fields:

$$S |0\rangle = |0\rangle$$

$$\phi_f = S^{-1} \phi_i S$$

If S describes an interaction correctly, these properties must be also true:

If the system is made up with a single particle in momentum eigenstate $|k\rangle$, then $S |k\rangle = |k\rangle$

The S-matrix element must be nonzero if and only if momentum is conserved.

S-matrix and evolution operator U

$$a(k, t) = U^{-1}(t) a_i(k) U(t)$$

$$\phi_f = U^{-1}(\infty) \phi_i U(\infty) = S^{-1} \phi_i S$$

Therefore $S = e^{i\alpha} U(\infty)$ where

$$e^{i\alpha} = \langle 0 | U(\infty) | 0 \rangle^{-1}$$

because

$$S |0\rangle = |0\rangle.$$

Substituting the explicit expression for U we obtain:

$$S = \frac{1}{\langle 0 | U(\infty) | 0 \rangle} T e^{-i \int d\tau V_i(\tau)}$$

By inspection it can be seen that this formula is not explicitly covariant.

Dyson series

The most widely used expression for the S-matrix is the Dyson series. This expresses the S-matrix operator as the series:

$$S = \sum_{n=0}^{\infty} \frac{(-i)^n}{n!} \int \dots \int d^4 x_1 d^4 x_2 \dots d^4 x_n T[H_{int}(x_1) H_{int}(x_2) \dots H_{int}(x_n)]$$

where:

- $T[\dots]$ denotes time-ordering,
- $H_{int}(x)$ denotes the interaction Hamiltonian which describes the interactions in the theory.

See also

- Feynman diagram
- LSZ reduction formula
- Wick's theorem

References and Bibliography

- [1] John A. Wheeler, 'On the Mathematical Description of Light Nuclei by the Method. of Resonating Group Structure (<http://link.aps.org/abstract/PR/v52/p1107>)' Phys. Rev. 52, 1107 - 1122 (1937)
- [2] Jagdish Mehra, Helmut Rechenberg, *The Historical Development of Quantum Theory* (Pages 990 and 1031) Springer, 2001 ISBN 0387950869, 9780387950860

Barut, A.O. (1967). *The Theory of the Scattering Matrix*.

Tony Philips (11 2001). <http://www.math.sunysb.edu/~tony/whatsnew/column/feynman-1101/feynman1.html>|"Finite-dimensional Feynman Diagrams". *What's New In Math. American Mathematical Society*. <http://www.math.sunysb.edu/~tony/whatsnew/column/feynman-1101/feynman1.html>. Retrieved on 2007-10-23.

Quantum logic

In quantum mechanics, **quantum logic** is a set of rules for reasoning about propositions which takes the principles of quantum theory into account. This research area and its name originated in the 1936 paper by Garrett Birkhoff and John von Neumann, who were attempting to reconcile the apparent inconsistency of classical boolean logic with the facts concerning the measurement of complementary variables in quantum mechanics, such as position and momentum.

Quantum logic can be formulated either as a modified version of propositional logic or as a non-commutative and non-associative many-valued (MV) logic^{[1] [2] [3] [4] [5]}. It has some properties which clearly distinguish it from classical logic, most notably, the failure of the distributive law of propositional logic:

$$p \text{ and } (q \text{ or } r) = (p \text{ and } q) \text{ or } (p \text{ and } r),$$

where the symbols p , q and r are propositional variables. To illustrate why the distributive law fails, consider a particle moving on a line and let

$$p = \text{"the particle is moving to the right"}$$

$$q = \text{"the particle is in the interval } [-1,1]\text{"}$$

$$r = \text{"the particle is not in the interval } [-1,1]\text{"}$$

then the proposition " q or r " is true, so

$$p \text{ and } (q \text{ or } r) = p$$

On the other hand, the propositions " p and q " and " p and r " are both false, since they assert tighter restrictions on simultaneous values of position and momentum than is allowed by the uncertainty principle. So,

$$(p \text{ and } q) \text{ or } (p \text{ and } r) = \text{false}$$

Thus the distributive law fails.

Quantum logic has been proposed as the correct logic for propositional inference generally, most notably by the philosopher Hilary Putnam, at least at one point in his career. This thesis was an important ingredient in Putnam's paper *Is Logic Empirical?* in which he analysed the epistemological status of the rules of propositional logic. Putnam attributes the idea that anomalies associated to quantum measurements originate with anomalies in the logic of physics itself to the physicist David Finkelstein. It should be noted, however, that this idea had been around for some time and had been revived several years earlier by George Mackey's work on group representations and symmetry.

The more common view regarding quantum logic, however, is that it provides a formalism for relating observables, system preparation filters and states. In this view, the quantum logic approach resembles more closely the C*-algebraic approach to quantum mechanics; in fact with some minor technical assumptions it can be subsumed by it. The similarities of the quantum logic formalism to a system of deductive logic may then be regarded more as a curiosity than as a fact of fundamental philosophical importance.

Introduction

In his classic treatise *Mathematical Foundations of Quantum Mechanics*, John von Neumann noted that projections on a Hilbert space can be viewed as propositions about physical observables. The set of principles for manipulating these quantum propositions was called *quantum logic* by von Neumann and Birkhoff. In his book (also called *Mathematical Foundations of Quantum Mechanics*) G. Mackey attempted to provide a set of axioms for this propositional system as an orthocomplemented lattice. Mackey viewed elements of this set as potential *yes or no questions* an observer might ask about the state of a physical system, questions that would be settled by some measurement. Moreover Mackey defined a physical observable in terms of these basic questions. Mackey's axiom system is somewhat unsatisfactory though, since it assumes that the partially ordered set is actually given as the orthocomplemented closed subspace lattice of a separable Hilbert space. Piron, Ludwig and others have attempted to give axiomatizations which do not require such explicit relations to the lattice of subspaces.

The remainder of this article assumes the reader is familiar with the spectral theory of self-adjoint operators on a Hilbert space. However, the main ideas can be understood using the finite-dimensional spectral theorem.

Projections as propositions

The so-called *Hamiltonian* formulations of classical mechanics have three ingredients: *states*, *observables* and *dynamics*. In the simplest case of a single particle moving in \mathbf{R}^3 , the state space is the position-momentum space \mathbf{R}^6 . We will merely note here that an observable is some real-valued function f on the state space. Examples of observables are position, momentum or energy of a particle. For classical systems, the value $f(x)$, that is the value of f for some particular system state x , is obtained by a process of measurement of f . The propositions concerning a classical system are generated from basic statements of the form

- Measurement of f yields a value in the interval $[a, b]$ for some real numbers a, b .

It follows easily from this characterization of propositions in classical systems that the corresponding logic is identical to that of some Boolean algebra of subsets of the state

space. By logic in this context we mean the rules that relate set operations and ordering relations, such as de Morgan's laws. These are analogous to the rules relating boolean conjunctives and material implication in classical propositional logic. For technical reasons, we will also assume that the algebra of subsets of the state space is that of all Borel sets. The set of propositions is ordered by the natural ordering of sets and has a complementation operation. In terms of observables, the complement of the proposition $\{f \geq a\}$ is $\{f < a\}$.

We summarize these remarks as follows:

- The proposition system of a classical system is a lattice with a distinguished *orthocomplementation* operation: The lattice operations of *meet* and *join* are respectively set intersection and set union. The orthocomplementation operation is set complement. Moreover this lattice is *sequentially complete*, in the sense that any sequence $\{E_i\}_i$ of elements of the lattice has a least upper bound, specifically the set-theoretic union:

$$\text{LUB}(\{E_i\}) = \bigcup_{i=1}^{\infty} E_i.$$

In the Hilbert space formulation of quantum mechanics as presented by von Neumann, a physical observable is represented by some (possibly unbounded) densely-defined self-adjoint operator A on a Hilbert space H . A has a spectral decomposition, which is a projection-valued measure E defined on the Borel subsets of \mathbf{R} . In particular, for any bounded Borel function f , the following equation holds:

$$f(A) = \int_{\mathbf{R}} f(\lambda) dE(\lambda).$$

In case f is the indicator function of an interval $[a, b]$, the operator $f(A)$ is a self-adjoint projection, and can be interpreted as the quantum analogue of the classical proposition

- Measurement of A yields a value in the interval $[a, b]$.

The propositional lattice of a quantum mechanical system

This suggests the following quantum mechanical replacement for the orthocomplemented lattice of propositions in classical mechanics. This is essentially Mackey's *Axiom VII*:

- The orthocomplemented lattice Q of propositions of a quantum mechanical system is the lattice of closed subspaces of a complex Hilbert space H where orthocomplementation of V is the orthogonal complement V^\perp .

Q is also sequentially complete: any pairwise disjoint sequence $\{V_i\}_i$ of elements of Q has a least upper bound. Here disjointness of W_1 and W_2 means W_2 is a subspace of W_1^\perp . The least upper bound of $\{V_i\}_i$ is the closed internal direct sum.

Henceforth we identify elements of Q with self-adjoint projections on the Hilbert space H .

The structure of Q immediately points to a difference with the partial order structure of a classical proposition system. In the classical case, given a proposition p , the equations

$$I = p \vee q$$

$$0 = p \wedge q$$

have exactly one solution, namely the set-theoretic complement of p . In these equations I refers to the atomic proposition which is identically true and 0 the atomic proposition which is identically false. In the case of the lattice of projections there are infinitely many solutions to the above equations.

Having made these preliminary remarks, we turn everything around and attempt to define observables within the projection lattice framework and using this definition establish the correspondence between self-adjoint operators and observables : A *Mackey observable* is a countably additive homomorphism from the orthocomplemented lattice of the Borel subsets of \mathbf{R} to Q . To say the mapping φ is a countably additive homomorphism means that for any sequence $\{S_i\}_i$ of pairwise disjoint Borel subsets of \mathbf{R} , $\{\varphi(S_i)\}_i$ are pairwise orthogonal projections and

$$\varphi\left(\bigcup_{i=1}^{\infty} S_i\right) = \sum_{i=1}^{\infty} \varphi(S_i).$$

Theorem. There is a bijective correspondence between Mackey observables and densely-defined self-adjoint operators on H .

This is the content of the spectral theorem as stated in terms of spectral measures.

Statistical structure

Imagine a forensics lab which has some apparatus to measure the speed of a bullet fired from a gun. Under carefully controlled conditions of temperature, humidity, pressure and so on the same gun is fired repeatedly and speed measurements taken. This produces some distribution of speeds. Though we will not get exactly the same value for each individual measurement, for each cluster of measurements, we would expect the experiment to lead to the same distribution of speeds. In particular, we can expect to assign probability distributions to propositions such as $\{a \leq \text{speed} \leq b\}$. This leads naturally to propose that under controlled conditions of preparation, the measurement of a classical system can be described by a probability measure on the state space. This same statistical structure is also present in quantum mechanics.

A *quantum probability measure* is a function P defined on Q with values in $[0,1]$ such that $P(0)=0$, $P(I)=1$ and if $\{E_i\}_i$ is a sequence of pairwise orthogonal elements of Q then

$$P\left(\sum_{i=1}^{\infty} E_i\right) = \sum_{i=1}^{\infty} P(E_i).$$

The following highly non-trivial theorem is due to Andrew Gleason:

Theorem. Suppose H is a separable Hilbert space of complex dimension at least 3. Then for any quantum probability measure on Q there exists a unique trace class operator S such that

$$P(E) = \text{Tr}(SE)$$

for any self-adjoint projection E .

The operator S is necessarily non-negative (that is all eigenvalues are non-negative) and of trace 1. Such an operator is often called a *density operator*.

Physicists commonly regard a density operator as being represented by a (possibly infinite) density matrix relative to some orthonormal basis.

For more information on statistics of quantum systems, see quantum statistical mechanics.

Automorphisms

An *automorphism* of Q is a bijective mapping $\alpha: Q \rightarrow Q$ which preserves the orthocomplemented structure of Q , that is

$$\alpha\left(\sum_{i=1}^{\infty} E_i\right) = \sum_{i=1}^{\infty} \alpha(E_i)$$

for any sequence $\{E_i\}_i$ of pairwise orthogonal self-adjoint projections. Note that this property implies monotonicity of α . If P is a quantum probability measure on Q , then $E \rightarrow \alpha(E)$ is also a quantum probability measure on Q . By the Gleason theorem characterizing quantum probability measures quoted above, any automorphism α induces a mapping α^* on the density operators by the following formula:

$$\text{Tr}(\alpha^*(S)E) = \text{Tr}(S\alpha(E)).$$

The mapping α^* is bijective and preserves convex combinations of density operators. This means

$$\alpha^*(r_1 S_1 + r_2 S_2) = r_1 \alpha^*(S_1) + r_2 \alpha^*(S_2)$$

whenever $1 = r_1 + r_2$ and r_1, r_2 are non-negative real numbers. Now we use a theorem of Richard Kadison:

Theorem. Suppose β is a bijective map from density operators to density operators which is convexity preserving. Then there is an operator U on the Hilbert space which is either linear or conjugate-linear, preserves the inner product and is such that

$$\beta(S) = USU^*$$

for every density operator S . In the first case we say U is unitary, in the second case U is anti-unitary.

Remark. This note is included for technical accuracy only, and should not concern most readers. The result quoted above is not directly stated in Kadison's paper, but can be reduced to it by noting first that β extends to a positive trace preserving map on the trace class operators, then applying duality and finally applying a result of Kadison's paper.

The operator U is not quite unique; if r is a complex scalar of modulus 1, then rU will be unitary or anti-unitary if U is and will implement the same automorphism. In fact, this is the only ambiguity possible.

It follows that automorphisms of Q are in bijective correspondence to unitary or anti-unitary operators modulo multiplication by scalars of modulus 1. Moreover, we can regard automorphisms in two equivalent ways: as operating on states (represented as density operators) or as operating on Q .

Non-relativistic dynamics

In non-relativistic physical systems, there is no ambiguity in referring to time evolution since there is a global time parameter. Moreover an isolated quantum system evolves in a deterministic way: if the system is in a state S at time t then at time $s > t$, the system is in a state $F_{s,t}(S)$. Moreover, we assume

- The dependence is reversible: The operators $F_{s,t}$ are bijective.
- The dependence is homogeneous: $F_{s,t} = F_{s-t,0}$.
- The dependence is convexity preserving: That is, each $F_{s,t}(S)$ is convexity preserving.
- The dependence is weakly continuous: The mapping $\mathbf{R} \rightarrow \mathbf{R}$ given by $t \rightarrow \text{Tr}(F_{s,t}(S) E)$ is continuous for every E in Q .

By Kadison's theorem, there is a 1-parameter family of unitary or anti-unitary operators $\{U_t\}_t$ such that

$$F_{s,t}(S) = U_{s-t} S U_{s-t}^*$$

In fact,

Theorem. Under the above assumptions, there is a strongly continuous 1-parameter group of unitary operators $\{U_t\}_t$ such that the above equation holds.

Note that it easily follows from uniqueness from Kadison's theorem that

$$U_{t+s} = \sigma(t, s) U_t U_s$$

where $\sigma(t, s)$ has modulus 1. Now the square of an anti-unitary is a unitary, so that all the U_t are unitary. The remainder of the argument shows that $\sigma(t, s)$ can be chosen to be 1 (by modifying each U_t by a scalar of modulus 1.)

Pure states

A convex combinations of statistical states S_1 and S_2 is a state of the form $S = p_1 S_1 + p_2 S_2$ where p_1, p_2 are non-negative and $p_1 + p_2 = 1$. Considering the statistical state of system as specified by lab conditions used for its preparation, the convex combination S can be regarded as the state formed in the following way: toss a biased coin with outcome probabilities p_1, p_2 and depending on outcome choose system prepared to S_1 or S_2 .

Density operators form a convex set. The convex set of density operators has extreme points; these are the density operators given by a projection onto a one-dimensional space. To see that any extreme point is such a projection, note that by the spectral theorem S can be represented by a diagonal matrix; since S is non-negative all the entries are non-negative and since S has trace 1, the diagonal entries must add up to 1. Now if it happens that the diagonal matrix has more than one non-zero entry it is clear that we can express it as a convex combination of other density operators.

The extreme points of the set of density operators are called pure states. If S is the projection on the 1-dimensional space generated by a vector ψ of norm 1 then

$$\text{Tr}(SE) = \langle E\psi | \psi \rangle$$

for any E in Q . In physics jargon, if

$$S = |\psi\rangle\langle\psi|,$$

where ψ has norm 1, then

$$\text{Tr}(SE) = \langle \psi | E | \psi \rangle.$$

Thus pure states can be identified with *rays* in the Hilbert space H .

The measurement process

Consider a quantum mechanical system with lattice Q which is in some statistical state given by a density operator S . This essentially means an ensemble of systems specified by a repeatable lab preparation process. The result of a cluster of measurements intended to determine the truth value of proposition E , is just as in the classical case, a probability distribution of truth values **T** and **F**. Say the probabilities are p for **T** and $q = 1 - p$ for **F**. By the previous section $p = \text{Tr}(S E)$ and $q = \text{Tr}(S (I-E))$.

Perhaps the most fundamental difference between classical and quantum systems is the following: regardless of what process is used to determine E immediately after the measurement the system will be in one of two statistical states:

- If the result of the measurement is **T**

$$\frac{1}{\text{Tr}(ES)} ESE.$$

- If the result of the measurement is **F**

$$\frac{1}{\text{Tr}((I-E)S)} (I-E)S(I-E).$$

(We leave to the reader the handling of the degenerate cases in which the denominators may be 0.) We now form the convex combination of these two ensembles using the relative frequencies p and q . We thus obtain the result that the measurement process applied to a statistical ensemble in state S yields another ensemble in statistical state:

$$M_E(S) = ESE + (I-E)S(I-E).$$

We see that a pure ensemble becomes a mixed ensemble after measurement. Measurement, as described above, is a special case of quantum operations.

Limitations

Quantum logic derived from propositional logic provides a satisfactory foundation for a theory of reversible quantum processes. Examples of such processes are the covariance transformations relating two frames of reference, such as change of time parameter or the transformations of special relativity. Quantum logic also provides a satisfactory understanding of density matrices. Quantum logic can be stretched to account for some kinds of measurement processes corresponding to answering yes-no questions about the state of a quantum system. However, for more general kinds of measurement operations (that is quantum operations), a more complete theory of filtering processes is necessary. Such an approach is provided by the consistent histories formalism. On the other hand, quantum logics derived from MV-logic extend its range of applicability to irreversible quantum processes and/or 'open' quantum systems.

In any case, these quantum logic formalisms must be generalized in order to deal with super-geometry (which is needed to handle Fermi-fields) and non-commutative geometry (which is needed in string theory and quantum gravity theory). Both of these theories use a partial algebra with an "integral" or "trace". The elements of the partial algebra are not observables; instead the "trace" yields "greens functions" which generate scattering amplitudes. One thus obtains a local S-matrix theory (see D. Edwards).

Since around 1978 the Flato school (see F. Bayen) has been developing an alternative to the quantum logics approach called deformation quantization (see Weyl quantization).

In 2004, Prakash Panangaden described how to capture the kinematics of quantum causal evolution using System BV, a deep inference logic originally developed for use in structural proof theory.[6] Alessio Guglielmi, Lutz Straßburger, and Richard Blute have also done work in this area.[7]

Cited references

- [1] http://arxiv.org/PS_cache/quant-ph/pdf/0101/0101028v2.pdf Maria Luisa Dalla Chiara and Roberto Giuntini. 2008. *Quantum Logic.*, 102 pages PDF
- [2] Dalla Chiara, M. L. and Giuntini, R.: 1994, Unsharp quantum logics, *Foundations of Physics.*, **24**, 1161-1177.
- [3] <http://planetphysics.org/encyclopedia/QuantumLMAlgebraicLogic.html> I. C. Baianu. 2009. Quantum LMn Algebraic Logic.
- [4] Georgescu, G. and C. Vraciu. 1970, On the characterization of centered Łukasiewicz algebras., *J. Algebra*, **16**: 486-495.
- [5] Georgescu, G. 2006, N-valued Logics and Łukasiewicz-Moisil Algebras, *Axiomathes*, **16** (1-2): 123-
- [6] <http://cs.bath.ac.uk/ag/p/BVQuantCausEvol.pdf>
- [7] <http://alessio.guglielmi.name/res/cos/crt.html#CQE>

See also

- Mathematical formulation of quantum mechanics
- Multi-valued logic
- Quasi-set theory
- HPO formalism (An approach to temporal quantum logic)
- Quantum field theory

Literature

- S. Auyang, *How is Quantum Field Theory Possible?*, Oxford University Press, 1995.
- F.Bayen,M.Flato,C.Fronsdal,A.Lichnerowicz and D.Sternheimer, *Deformation theory and quantization I,II*,Ann. Phys. (N.Y.),111 (1978) pp. 61-110,111-151.
- G. Birkhoff and J. von Neumann, *The Logic of Quantum Mechanics*, Annals of Mathematics, vol 37 pp 823-843, 1936.
- D. Cohen, *An Introduction to Hilbert Space and Quantum Logic*, Springer-Verlag, 1989. This is a thorough but elementary and well-illustrated introduction, suitable for advanced undergraduates.
- D. Edwards, *The Mathematical Foundations of Quantum Field Theory: Fermions, Gauge Fields, and Super-symmetry, Part I: Lattice Field Theories*, International J. of Theor. Phys., Vol. 20, No. 7 (1981).
- D. Finkelstein, *Matter, Space and Logic*, Boston Studies in the Philosophy of Science vol V, 1969
- A. Gleason, *Measures on the Closed Subspaces of a Hilbert Space*, Journal of Mathematics and Mechanics, 1957.
- R. Kadison, *Isometries of Operator Algebras*, Annals of Mathematics, vol 54 pp 325-338, 1951
- G. Ludwig, *Foundations of Quantum Mechanics*, Springer-Verlag, 1983.
- G. Mackey, *Mathematical Foundations of Quantum Mechanics*, W. A. Benjamin, 1963 (paperback reprint by Dover 2004).

- J. von Neumann, *Mathematical Foundations of Quantum Mechanics*, Princeton University Press, 1955. Reprinted in paperback form.
- R. Omnès, *Understanding Quantum Mechanics*, Princeton University Press, 1999. An extraordinarily lucid discussion of some logical and philosophical issues of quantum mechanics, with careful attention to the history of the subject. Also discusses consistent histories.
- N. Papanikolaou, *Reasoning Formally About Quantum Systems: An Overview*, ACM SIGACT News, 36(3), pp. 51-66, 2005.
- C. Piron, *Foundations of Quantum Physics*, W. A. Benjamin, 1976.
- H. Putnam, *Is Logic Empirical?*, Boston Studies in the Philosophy of Science vol. V, 1969
- H. Weyl, *The Theory of Groups and Quantum Mechanics*, Dover Publications, 1950.

External links

- Stanford Encyclopedia of Philosophy entry on Quantum Logic and Probability Theory (<http://plato.stanford.edu/entries/qt-quantlog/>)

Spin

Spin may refer to:

- Rotation or spin, a movement of an object in a circular motion
- Spin (physics) or particle spin, a fundamental property of elementary particles
- Spin (flight), a special and often intense case of a stall
- Spin (public relations), a heavily biased portrayal of an event or situation
- Spin (breakdance move)
- Spinning (textiles), the process of creating yarn from various raw fiber materials
- Spinning (polymers), a process for creating polymer fibers
- Spins, a state of dizziness and disorientation due to intoxication ("the spins")

In **media**:

- *Spin* (film), a 1995 documentary film of politicians' behind-the-scenes conversations
- *Spin* (2003 film)
- *Spin* (novel), a novel by Robert Charles Wilson
- *Spin* (magazine), a pop music magazine
- "Spin" (*House* episode)

In **music**:

- Spin (radio), a single play of a song
- SPiN (U.S. band), an American rock band
- Spin (band), a band from the Maltese Islands
- *Spin* (album), the first solo album by Darren Hayes
- "Spin" (Lifehouse song), a song by Lifehouse from *Stanley Climbfall*
- "Spin", a song by Taking Back Sunday from *Louder Now*
- "Spinnin'", a song by Soul Asylum from *And the Horse They Rode in On*
- "Spinning", a song by Christopher Cross from *Christopher Cross*
- "Spinning", a song by Jack's Mannequin from *The Glass Passenger*
- *Spin* (Eric Roche album), an album by Eric Roche

In **sports**:

- Spin bowling, a type of bowling technique in cricket
- Spinning, a form of high-intensity exercise using a stationary exercise bicycle
- Poi spinning, a form of juggling
- Figure-skating spin, a skating move
- Wheelspin, spinning the wheels of a vehicle in place

In **computing**:

- SPIN (software) or Secure Peered Internet
- Spin (programming language), a high-level programming language
- SPIN (operating system), an OS based on Mach
- SPIN (software process), a Software Process Improvement Network
- SPIN model checker, a software tool
- Busy spin, a technique in which a process continually checks whether a condition is true

In **other uses**:

- Spin group, a particular double cover of the special orthogonal group $SO(n)$
- Metal spinning, the process of forming metal over a mandrel while spinning around a lathe
- Sufi spinning, a twirling meditation
- Fokker Spin, an airplane built by Anthony Fokker

See also

- *Spinning Around*, a song by Kylie Minogue
-

Fermion

In particle physics, **fermions** are particles which obey Fermi-Dirac statistics; they are named after Enrico Fermi. In contrast to bosons, which have Bose-Einstein statistics, only one fermion can occupy a quantum state at a given time; this is the Pauli Exclusion Principle. Thus, if more than one fermion occupies the same place in space, the properties of each fermion (e.g. its spin) must be different from the rest. Therefore, fermions are usually associated with matter while bosons are often force carrier particles, though the distinction between the two concepts is not clear cut in quantum physics.

Fermions can be elementary, like the electron, or composite, like the proton. All observed fermions have half-integer spin, as opposed to bosons, which have integer spin. This is in accordance with the spin-statistics theorem which states that in any reasonable relativistic quantum field theory, particles with integer spin are bosons, while particles with half-integer spin are fermions.

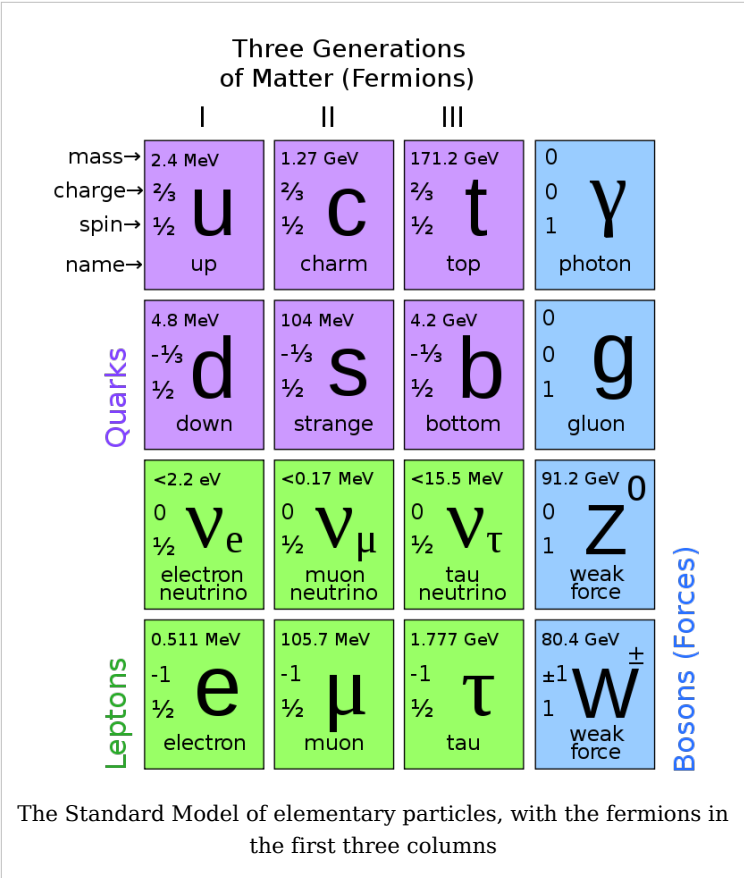
In the Standard Model there are two types of elementary fermions: quarks and leptons. In total, there are 24 different fermions; 6 quarks and 6 leptons, each with a corresponding antiparticle:

- 12 quarks - 6 particles (u · d · s · c · b · t) with 6 corresponding antiparticles (u · d · s · c · b · t);
- 12 leptons - 6 particles (e⁻ · μ⁻ · τ⁻ · ν_e · ν_μ · ν_τ) with 6 corresponding antiparticles (e⁺ · μ⁺ · τ⁺ · ν_e · ν_μ · ν_τ).

Composite fermions, such as protons and neutrons, are essential building blocks of matter. Weakly interacting fermions can also display bosonic behaviour, as in superconductivity.

Definition and basic properties

By definition, fermions are particles which obey Fermi-Dirac statistics: when one swaps two fermions, the wavefunction of the system changes sign.^[1] This "antisymmetric wavefunction" behavior implies that fermions are subject to the Pauli exclusion principle — no two fermions can occupy the same quantum state at the same time. This results in "rigidity" or "stiffness" of states which include fermions (atomic nuclei, atoms, molecules,



etc.), so fermions are sometimes said to be the constituents of matter, while bosons are said to be the particles that transmit interactions (force carriers), or the constituents of radiation. The quantum fields of fermions are fermionic fields, obeying canonical anticommutation relations.

The Pauli exclusion principle for fermions and the associated rigidity of matter is responsible for the stability of the electron shells of atoms (thus for stability of atomic matter) and the complexity of atoms (making it impossible for all atomic electrons to occupy the same energy level), thus making complex chemistry possible. It is also responsible for the pressure within degenerate matter which largely governs the equilibrium state of white dwarfs and neutron stars. On a more everyday scale, the Pauli exclusion principle is a major contributor to the Young modulus of matter.

All known fermions are particles with half-integer spin: as an observer circles a fermion (or as the fermion rotates 360° about its axis) the wavefunction of the fermion changes sign. In the framework of nonrelativistic quantum mechanics, this is a purely empirical observation. However, in relativistic quantum field theory, the spin-statistics theorem shows that half-integer spin particles cannot be bosons and integer spin particles cannot be fermions.^[2]

In large systems, the difference between bosonic and fermionic statistics is only apparent at large densities when their wave functions overlap. At low densities, both types of statistics are well approximated by Maxwell-Boltzmann statistics, which is described by classical mechanics.

Elementary fermions

All observed elementary particles are either fermions or bosons. The known elementary fermions are divided into two groups: quarks and leptons.

- Quarks make up protons, neutrons and other baryons, which are composite fermions; they also comprise mesons, which are composite bosons.
- Leptons include the electron and similar, heavier particles (the muon and tauon); they also include neutrinos.

The known fermions of left-handed helicity experience weak interactions while the known right-handed fermions do not. Or put another way, only left-handed fermions and right-handed antifermions interact with the W boson.

Composite fermions

Composite particles (such as hadrons, nuclei, and atoms) can be bosons or fermions depending on their constituents. More precisely, because of the relation between spin and statistics, a particle containing an odd number of fermions is itself a fermion: it will have half-integer spin.

Examples include the following:

- A baryon, such as the proton or neutron, contains three fermionic quarks and is therefore a fermion;
 - The nucleus of a carbon-13 atom contains 6 protons and 7 neutrons and is therefore a fermion;
 - The atom helium-3 (^3He) is made of 2 protons, a neutron and 2 electrons and is therefore a fermion.
-

The number of bosons within a composite particle made up of simple particles bound with a potential has no effect on whether it is a boson or a fermion.

Fermionic or bosonic behavior of a composite particle (or system) is only seen at large (compared to size of the system) distance. At proximity, where spatial structure begins to be important, a composite particle (or system) behaves according to its constituent makeup.

Fermions can exhibit bosonic behavior when they become loosely bound in pairs. This is the origin of superconductivity and the superfluidity of helium-3: in superconducting materials, electrons interact through the exchange of phonons, forming Cooper pairs, while in helium-3, Cooper pairs are formed via spin fluctuations.

The fundamental building blocks of the fractional quantum Hall effect are also particles known as composite fermions, which are electrons with an even number of quantized vortices attached to them.

Skymions

In a quantum field theory, there can be field configurations of bosons which are topologically twisted. These are coherent states (or solitons) which behave like a particle, and they can be fermionic even if all the elementary particles are bosons. This was discovered by Tony Skyrme in the early 1960s, so fermions made of bosons are named Skymions after him.

Skyrme's original example involves fields which take values on a three dimensional sphere, the original nonlinear sigma model that describes the large distance behavior of pions. In Skyrme's model, which is reproduced in the large N or string approximation to QCD, the proton and neutron are fermionic topological solitons of the pion field. While Skyrme's example involves pion physics, there is a much more familiar example in quantum electrodynamics with a magnetic monopole. A bosonic monopole with the smallest possible magnetic charge and a bosonic version of the electron would form a fermionic dyon.

See also

- Fermionic field
 - Identical particles
 - Parastatistics
 - Anyon
 - Fermionic condensate
 - Superconductivity
 - Fractional quantum Hall effect
-

Notes

[1] Srednicki (2007), pages 28-29
[2] Sakurai (1994), page 362

References

- Sakurai, J.J. (1994). *Modern Quantum Mechanics* (Revised Edition), pp 361-363. Addison-Wesley Publishing Company, ISBN 0-201-53929-2.
- Srednicki, Mark (2007). *Quantum Field Theory* (<http://www.physics.ucsb.edu/~mark/qft.html>), Cambridge University Press, ISBN 978-0521864497.

Boson

For other meanings, see Boson (disambiguation).

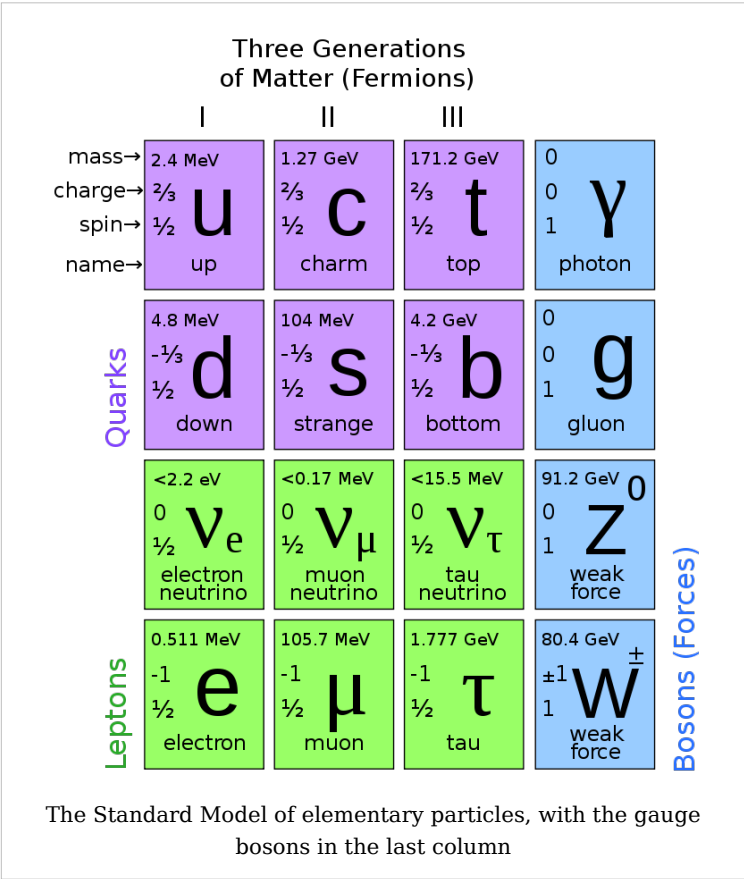
In particle physics, **bosons** are particles which obey Bose-Einstein statistics; they are named after Satyendra Nath Bose and Albert Einstein. In contrast to fermions, which obey Fermi-Dirac statistics, several bosons can occupy the same quantum state. Thus, bosons with the same energy can occupy the same place in space. Therefore bosons are often force carrier particles while fermions are usually associated with matter, though the distinction between the two concepts is not clear cut in quantum physics.

Bosons may be either elementary, like the photon, or composite, like mesons. All observed bosons have integer spin, as opposed to fermions, which have half-integer spin. This is in accordance with the spin-statistics theorem which states that in any reasonable relativistic quantum field theory, particles with integer spin are bosons, while particles with half-integer spin are fermions.

While most bosons are composite particles, in the Standard Model, there are five bosons which are elementary:

- the gauge bosons ($\gamma \cdot g \cdot W^\pm \cdot Z$);
- the Higgs boson (H^0).

Unlike the gauge bosons, the Higgs boson has not yet been observed experimentally.^[1]



The Standard Model of elementary particles, with the gauge bosons in the last column

Composite bosons are important in superfluidity and other applications of Bose-Einstein condensates.

Definition and basic properties

By definition, bosons are particles which obey Bose-Einstein statistics: when one swaps two bosons, the wavefunction of the system is unchanged.^[2] Fermions, on the other hand, obey Fermi-Dirac statistics and the Pauli exclusion principle: two fermions cannot occupy the same quantum state as each other, resulting in a "rigidity" or "stiffness" of matter which includes fermions. Thus fermions are sometimes said to be the constituents of matter, while bosons are said to be the particles that transmit interactions (force carriers), or the constituents of radiation. The quantum fields of bosons are bosonic fields, obeying canonical commutation relations.

The properties of lasers and masers, superfluid helium-4 and Bose-Einstein condensates are all consequences of statistics of bosons. Another result is that the spectrum of a photon gas in thermal equilibrium is a Planck spectrum, one example of which is black-body radiation; another is the thermal radiation of the opaque early Universe seen today as microwave background radiation. Interaction of virtual bosons with real fermions are called fundamental interactions, and these result in all forces we know. The bosons involved in these interactions are called gauge bosons.

All known elementary and composite particles are bosons or fermions, depending on their spin: particles with half-integer spin are fermions; particles with integer spin are bosons. In the framework of nonrelativistic quantum mechanics, this is a purely empirical observation. However, in relativistic quantum field theory, the spin-statistics theorem shows that half-integer spin particles cannot be bosons and integer spin particles cannot be fermions.^[3]

In large systems, the difference between bosonic and fermionic statistics is only apparent at large densities—when their wave functions overlap. At low densities, both types of statistics are well approximated by Maxwell-Boltzmann statistics, which is described by classical mechanics.

Elementary bosons

All observed elementary particles are either fermions or bosons. The observed elementary bosons are all gauge bosons: photons, W and Z bosons and gluons.

- Photons are the force carriers of the electromagnetic field.
- W and Z bosons are the force carriers which mediate the weak nuclear force.
- Gluons are the fundamental force carriers underlying the strong nuclear force.

In addition, the standard model postulates the existence of Higgs bosons, which give other particles their mass via the Higgs mechanism.

Finally, many approaches to quantum gravity postulate a force carrier for gravity, the graviton, which is a boson of spin 2.

Composite bosons

Composite particles (such as hadrons, nuclei, and atoms) can be bosons or fermions depending on their constituents. More precisely, because of the relation between spin and statistics, a particle containing an even number of fermions is a boson, since it has integer spin.

Examples include the following:

- A meson contains two fermionic quarks and is therefore a boson;
- The nucleus of a carbon-12 atom contains 6 protons and 6 neutrons (all fermions) and is therefore a boson;
- The atom helium-4 (${}^4\text{He}$) is made of 2 protons, 2 neutrons and 2 electrons and is therefore a boson.

The number of bosons within a composite particle made up of simple particles bound with a potential has no effect on whether it is a boson or a fermion.

Fermionic or bosonic behavior of a composite particle (or system) is only seen at large (compared to size of the system) distance. At proximity, where spatial structure begins to be important, a composite particle (or system) behaves according to its constituent makeup. For example, two atoms of helium-4 cannot share the same space if it is comparable by size to the size of the inner structure of the helium atom itself ($\sim 10^{-10}$ m)—despite bosonic properties of the helium-4 atoms. Thus, liquid helium has finite density comparable to the density of ordinary liquid matter.

See also

- Bosonic field
- Identical particles
- Parastatistics
- Anyon
- Bose gas
- Superfluid

Notes

- [1] Standard Model of Particle Physics (http://www.sldnt.slac.stanford.edu/alr/standard_model.htm), SLAC Large Detector (SLD) group (<http://www-sld.slac.stanford.edu/sldwww/sld.html>), Stanford Linear Accelerator Center (<http://www.slac.stanford.edu>).
- [2] Srednicki (2007), pages 28-29
- [3] Sakurai (1994), page 362

References

- Sakurai, J.J. (1994). *Modern Quantum Mechanics* (Revised Edition), pp 361-363. Addison-Wesley Publishing Company, ISBN 0-201-53929-2.
- Srednicki, Mark (2007). *Quantum Field Theory* (<http://www.physics.ucsb.edu/~mark/qft.html>), Cambridge University Press, ISBN 978-0521864497.

Standard Model

The **Standard Model** of particle physics is a theory of three of the four known fundamental interactions and the elementary particles that take part in these interactions. These particles make up all visible matter in the universe. The standard model is a gauge theory of the electroweak and strong interactions with the gauge group $SU(3)\times SU(2)\times U(1)$.

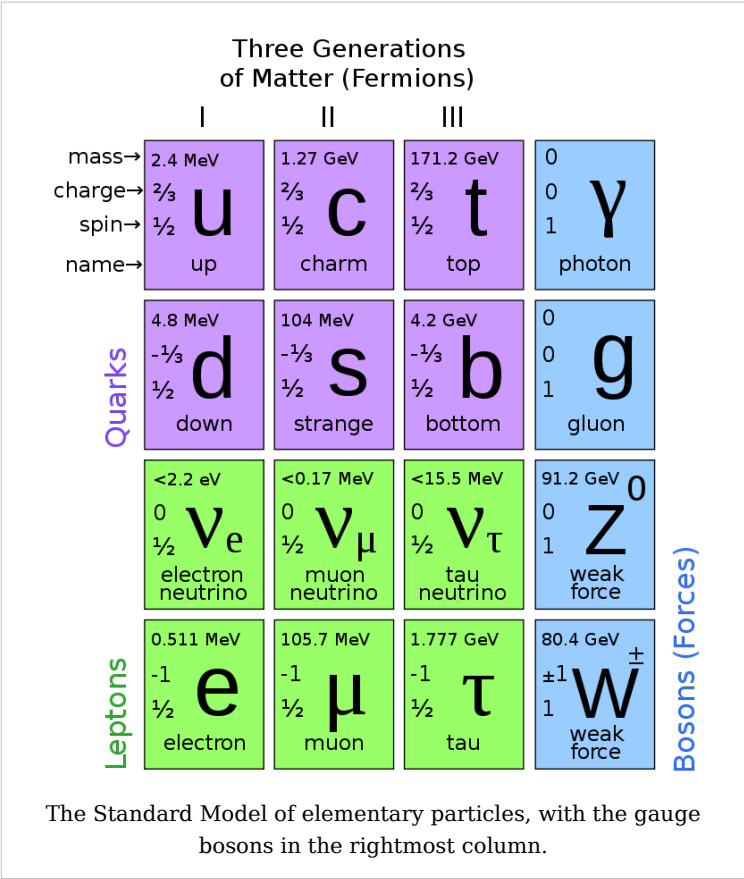
Every high energy physics experiment carried out since the mid-20th century has eventually yielded findings consistent with the Standard Model. Still, the Standard Model falls short of being a complete theory of fundamental interactions because it does not include gravity or dark matter. It isn't quite a complete description of leptons either, because it does not describe nonzero neutrino masses, although simple natural extensions do.

Historical background

The first step towards the Standard Model was Sheldon Glashow's discovery, in 1963, of a way to combine the electromagnetic and weak interactions. In 1967, Steven Weinberg and Abdus Salam incorporated the Higgs mechanism into Glashow's electroweak theory, giving it its modern form.^{[1] [2]} The Higgs mechanism is also believed to give rise to the rest masses of all the elementary particles the Standard Model accounts for, the W and Z bosons, and the fermions, the latter broken down into quarks and leptons.

After the discovery at CERN of neutral weak currents,^{[3] [4] [5] [6]} caused by Z boson exchange, the electroweak theory became widely accepted. Glashow, Salam, and Weinberg shared the 1979 Nobel Prize in Physics for discovering the electroweak theory. The W and Z bosons were discovered experimentally in 1981, and their masses were found to be as the Standard Model predicted.

The theory of the strong interaction, to which many contributed, acquired its modern form around 1973-74, when experiments confirmed that the hadrons were composed of fractionally charged quarks.



Overview

At present, matter and energy are best understood in terms of the kinematics and interactions of elementary particles. To date, physics has reduced the laws governing the behavior and interaction of all known forms of matter and energy, to a small set of fundamental laws and theories. A major goal of physics is to find the "common ground" that would unite all of these theories into one integrated theory of everything, of which all the other known laws would be special cases, and from which the behavior of all matter and energy could be derived (at least in principle). "Details can be worked out if the situation is simple enough for us to make an approximation, which is almost never, but often we can understand more or less what is happening." (The Feynman Lectures on Physics, Vol 1. 2-7)

The Standard Model groups two major extant theories — quantum electroweak and quantum chromodynamics — into an internally consistent theory describing the interactions between all experimentally observed particles. The Standard Model describes each type of particle in terms of a mathematical field, via quantum field theory. For a technical description of these fields and their interactions, see Standard Model (mathematical formulation).

Particle content

Elementary particles: fermions

In the Standard Model, fermions are defined as elementary particles having spin- $\frac{1}{2}$, and that respect the Pauli Exclusion Principle in accordance with the spin-statistics theorem. There are 12 known fermions, each with a corresponding antiparticle. They are classified according to how they interact (or equivalently, by what charges they carry). There are six quarks (up, down, charm, strange, top, bottom), and six leptons (electron, muon, tauon, and their corresponding neutrinos).

Organization of Fermions

	Charge	First generation		Second generation		Third generation	
Quarks	$+\frac{2}{3}$	Up	u	Charm	c	Top	t
	$-\frac{1}{3}$	Down	d	Strange	s	Bottom	b
Leptons	-1	Electron	e^-	Muon	μ^-	Tauon	τ^-
	0	Electron neutrino	ν_e	Muon neutrino	ν_μ	Tauon neutrino	ν_τ

Pairs from each classification are grouped together to form a generation, with corresponding particles exhibiting similar physical behavior (see table at right).

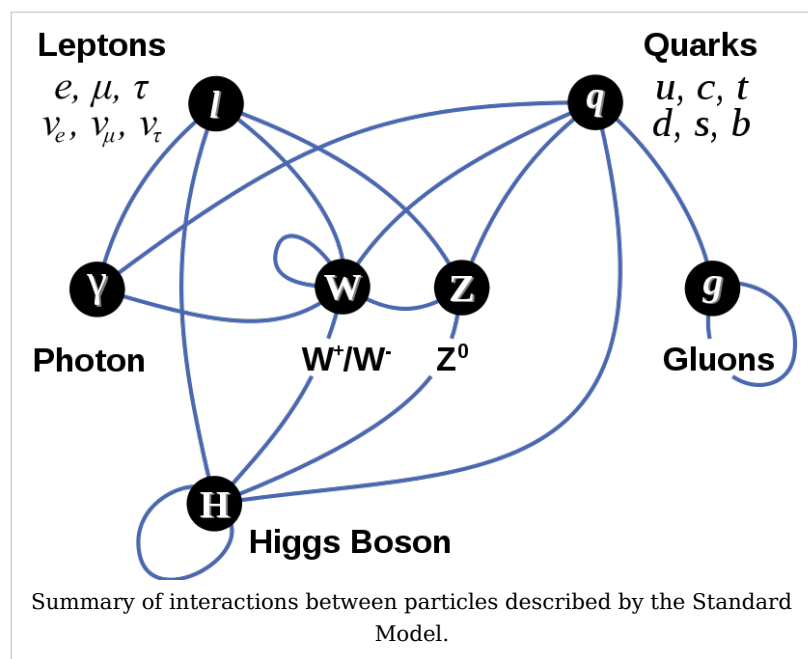
The defining property of the quarks is that they carry color charge, and hence, interact via the strong force. The infrared confining behavior of the strong force results in quarks being perpetually (or at least since very soon after the start of the big bang) bound to one another, forming color-neutral composite particles (hadrons) containing either a quark and an antiquark (mesons) or three quarks (baryons). The familiar proton and the neutron are the two baryons having the smallest mass. Quarks also carry electric charge and weak isospin. Hence they interact with other fermions both electromagnetically and via the weak nuclear interaction.

The remaining six fermions do not carry color charge and are called leptons. The three neutrinos do not carry electric charge either, so their motion is directly influenced only by the weak nuclear force, which makes them notoriously difficult to detect. However, by virtue of carrying an electric charge, the electron, muon and the tauon interact electromagnetically.

Each member of a generation has greater mass than the corresponding particles of lower generations. The first generation charged particles do not decay; hence all ordinary (baryonic) matter is made of such particles. Specifically, all atoms consist of electrons orbiting atomic nuclei ultimately constituted of up and down quarks. Second and third generations charged particles, on the other hand, decay with very short half lives, and are observed only in very high-energy environments. Neutrinos of all generations also do not decay and pervade the universe, but rarely interact with baryonic matter.

Force mediating particles

Forces in physics are the ways that particles interact and influence each other. At a macro level, the electromagnetic force allows particles to interact with one another via electric and magnetic fields, and the force of gravitation allows two particles with mass to attract one another in accordance with Newton's Law of Gravitation. The standard model explains such forces as resulting from matter particles exchanging other particles, known as *force mediating*



particles. When a force mediating particle is exchanged, at a macro level the effect is equivalent to a force influencing both of them, and the particle is therefore said to have *mediated* (i.e., been the agent of) that force. Force mediating particles are believed to be the reason why the forces and interactions between particles observed in the laboratory and in the universe exist.

The known force mediating particles described by the Standard Model also all have spin (as do matter particles), but in their case, the value of the spin is 1, meaning that all force mediating particles are bosons. As a result, they do not follow the Pauli Exclusion Principle. The different types of force mediating particles are described below.

- Photons mediate the electromagnetic force between electrically charged particles. The photon is massless and is well-described by the theory of quantum electrodynamics.
- The W^+ , W^- , and Z gauge bosons mediate the weak interactions between particles of different flavors (all quarks and leptons). They are massive, with the Z being more massive than the W^\pm . The weak interactions involving the W^\pm act on exclusively

left-handed particles and *right-handed* antiparticles. Furthermore, the W^\pm carry an electric charge of +1 and -1 and couple to the electromagnetic interactions. The electrically neutral Z boson interacts with both left-handed particles and antiparticles. These three gauge bosons along with the photons are grouped together which collectively mediate the electroweak interactions.

- The eight gluons mediate the strong interactions between color charged particles (the quarks). Gluons are massless. The eightfold multiplicity of gluons is labeled by a combination of color and an anticolor charge (e.g., red-antigreen).^[7] Because the gluon has an effective color charge, they can interact among themselves. The gluons and their interactions are described by the theory of quantum chromodynamics.

The interactions between all the particles described by the Standard Model are summarized by the diagram at the top of this section.

Force Mediating Particles

Electromagnetic Force		Weak Nuclear Force		Strong Nuclear Force	
Photon	γ	W^+ , W^- , and Z Gauge Bosons	W^+ , W^- , Z	8 Gluons	g

The Higgs boson

The Higgs particle is a massive scalar elementary particle predicted by the Standard Model. It has no intrinsic spin, and for that reason is classified as a boson (like the force mediating particles, which have integer spin). Because an exceptionally large amount of energy and beam luminosity are required to create a Higgs boson in high energy colliders, it is the only fundamental particle predicted by the Standard Model that has yet to be observed.

The Higgs boson plays a unique role in the Standard Model, by explaining why the other elementary particles, the photon and gluon excepted, are massive. In particular, the Higgs boson would explain why the photon has no mass, while the W and Z bosons are very heavy. Elementary particle masses, and the differences between electromagnetism (mediated by the photon) and the weak force (mediated by the W and Z bosons), are critical to many aspects of the structure of microscopic (and hence macroscopic) matter. In electroweak theory, the Higgs boson generates the masses of the leptons (electron, muon, and tauon) and quarks.

As yet, no experiment has directly detected the existence of the Higgs boson, but there is some indirect evidence for it. It is hoped that the Large Hadron Collider at CERN will confirm the existence of this particle.

Chien-Peng Yuan et al. believe that the Higgs boson may have been produced but overlooked:

"...experimenters may have already overlooked a Higgs particle, argues theorist Chien-Peng Yuan of Michigan State University in East Lansing and his colleagues. They considered the simplest possible supersymmetric theory. Ordinarily, theorists assume that the lightest of theory's five Higgses is the one that drags on the W and Z. Those interactions then feed back on Higgs and push its mass above 121 times the mass of the proton, the highest mass searched for at CERN's Large Electron-Positron (LEP) collider, which ran from 1989 to 2000. But it's possible that the lightest Higgs weighs as little as 65 times the mass of a proton and has

been missed, Yuan and colleagues argue in a paper to be published in *Physical Review Letters*.^[8]

Field content

The standard model has the following fields:

Spin 1

1. A U(1) gauge field $B_{\mu\nu}$ with coupling g' (weak U(1) or weak hypercharge)
2. An SU(2) gauge field $W_{\mu\nu}$ with coupling g (weak SU(2) or weak isospin)
3. An SU(3) gauge field $G_{\mu\nu}$ with coupling g_s (strong SU(3) or color)

Spin 1/2

The spin 1/2 particles are in representations of the gauge groups. For the U(1) group, we list the value of the weak hypercharge instead.

The left-handed fermionic fields are:

1. An SU(3) singlet, SU(2) doublet with U(1) weak hypercharge -1 (left-handed lepton)
2. An SU(3) singlet, SU(2) singlet with U(1) weak hypercharge 2 (left-handed antilepton)
3. An SU(3) triplet, SU(2) doublet, with U(1) weak hypercharge $\frac{1}{3}$ (left-handed quarks)
4. An SU(3) triplet, SU(2) singlet, with U(1) weak hypercharge $-\frac{4}{3}$ (left-handed up-type antiquark)
5. An SU(3) triplet, SU(2) singlet, with U(1) weak hypercharge $\frac{2}{3}$ (left-handed down-type antiquark)

By CPT symmetry, there is a set of right-handed fermions with the opposite quantum numbers.

This describes one *generation* of leptons and quarks, and there are three generations, so there are three copies of each field. Note that there are twice as many left-handed lepton field components as left-handed antilepton field components in each generation, but an equal number of left-handed quark and antiquark fields.

Spin 0

1. An SU(2) doublet H with U(1) hyper-charge -1 (Higgs field)

note that $|H|^2$, summed over the two SU(2) components, is invariant under both SU(2) and under U(1), and so it can appear as a renormalizable term in the Lagrangian, as can its square.

This field acquires a vacuum expectation value, leaving a combination of the weak isospin and hypercharge unbroken. This is the electromagnetic gauge group, and the photon remains massless. The standard formula for the electric charge (which defines the normalization of the weak hypercharge, which would otherwise be somewhat arbitrary) is:

$$q = I_z + \frac{Y}{2}$$

Beware that the normalization $q = I_z + Y$ sometimes is also used.

Lagrangian

The Lagrangian for the spin 1 and spin 1/2 fields is the most general renormalizable gauge field Lagrangian with no fine tunings:

$$\text{Spin 1: } \int -\frac{1}{4}B_{\mu\nu}B^{\mu\nu} - \frac{1}{4}\text{tr}W_{\mu\nu}W^{\mu\nu} - \frac{1}{4}\text{tr}G_{\mu\nu}G^{\mu\nu}$$

where the traces are over the SU(2) and SU(3) indices hidden in W and G respectively. The two-index objects are the field strengths derived from W and G the vector fields. There are also two extra hidden parameters: the theta angles for SU(2) and SU(3).

Note that the spin 1/2 particles can have no mass terms, because there is no right/left helicity pair with the same SU(2) and SU(3) representation and the same weak hypercharge. This means that if the gauge charges were conserved in the vacuum, none of the spin 1/2 particles could ever swap helicity, and they would all be massless.

For a neutral fermion, for example, a hypothetical right-handed lepton N, or N^α in relativistic two-spinor notation, with no SU(3),SU(2) representation and zero charge, it is possible to add the term:

$$\int MN^\alpha N^\beta \epsilon_{\alpha\beta} + \bar{N}_{\dot{\alpha}} \bar{N}_{\dot{\beta}} \epsilon^{\dot{\alpha}\dot{\beta}}$$

and this term gives the neutral fermion a Majorana mass. Since the generic value for M will be of order 1, such a particle would generically be unacceptably heavy.

Note that the interactions are completely determined by the theory - the leptons introduce no extra parameters.

Higgs mechanism

The Lagrangian for the Higgs includes the most general renormalizable self interaction:

$$S_{\text{Higgs}} = \int d^4x [(D_\mu H)^*(D^\mu H) + \lambda(|H|^2 - v^2)^2]$$

The parameter v^2 has dimensions of mass squared, and it gives the location where the classical Lagrangian is at a minimum. In order for the Higgs mechanism to work, v^2 must be a positive number. v has units of mass, and it is the only parameter in the standard model which is not dimensionless. It is also much smaller than the Planck scale, it is approximately equal to the Higgs mass and sets the scale for the mass of everything else. This is the only real fine-tuning to a small nonzero value in the standard model, and it is called the Hierarchy problem.

It is traditional to choose the SU(2) gauge so that the Higgs doublet in the vacuum has expectation value $(v,0)$.

Masses and CKM matrix

The rest of the interactions are the most general spin-0 spin-^1_2 Yukawa interactions, and there are many of these. These constitute most of the free parameters in the model. The Yukawa couplings generate the masses and mixings once the Higgs gets its vacuum expectation value.

The terms $L^* H R$ generate a mass term for each of the three generations of leptons. There are 9 of these terms, but by relabeling L and R, the matrix can be diagonalized. Since only the upper component of H is nonzero, the upper SU(2) component of L mixes with R to make the electron, the muon, and the tauon, leaving over a lower massless component, the neutrino.

The terms QHU generate up masses, while QHD generate down masses. But since there is more than one right-handed singlet in each generation, it is not possible to diagonalize both with a good basis for the fields, and there is an extra CKM matrix.

Theoretical aspects

Construction of the Standard Model Lagrangian

Parameters of the Standard Model

Symbol	Description	Renormalization scheme (point)	Value
m_e	Electron mass		511 keV
m_μ	Muon mass		106 MeV
m_τ	Tauon mass		1.78 GeV
m_u	Up quark mass	($\mu_{\overline{\text{MS}}} = 2 \text{ GeV}$)	1.9 MeV
m_d	Down quark mass	($\mu_{\overline{\text{MS}}} = 2 \text{ GeV}$)	4.4 MeV
m_s	Strange quark mass	($\mu_{\overline{\text{MS}}} = 2 \text{ GeV}$)	87 MeV
m_c	Charm quark mass	($\mu_{\overline{\text{MS}}} = m_c$)	1.32 GeV
m_b	Bottom quark mass	($\mu_{\overline{\text{MS}}} = m_b$)	4.24 GeV
m_t	Top quark mass	(on-shell scheme)	172.7 GeV
θ_{12}	CKM 12-mixing angle		0.229
θ_{23}	CKM 23-mixing angle		0.042
θ_{13}	CKM 13-mixing angle		0.004
δ	CKM CP-violating Phase		0.995
g_1	U(1) gauge coupling	($\mu_{\overline{\text{MS}}} = M_Z$)	0.357
g_2	SU(2) gauge coupling	($\mu_{\overline{\text{MS}}} = M_Z$)	0.652
g_3	SU(3) gauge coupling	($\mu_{\overline{\text{MS}}} = M_Z$)	1.221
θ_{QCD}	QCD Vacuum Angle		~ 0
μ	Higgs quadratic coupling		Unknown
λ	Higgs self-coupling strength		Unknown

Technically, quantum field theory provides the mathematical framework for the standard model, in which a Lagrangian controls the dynamics and kinematics of the theory. Each

kind of particle is described in terms of a dynamical field that pervades space-time. The construction of the standard model proceeds following the modern method of constructing most field theories: by first postulating a set of symmetries of the system, and then by writing down the most general renormalizable Lagrangian from its particle (field) content that observes these symmetries.

The global Poincaré symmetry is postulated for all relativistic quantum field theories. It consists of the familiar translational symmetry, rotational symmetry and the inertial reference frame invariance central to the theory of special relativity. The local $SU(3) \times SU(2) \times U(1)$ gauge symmetry is an internal symmetry that essentially defines the standard model. Roughly, the three factors of the gauge symmetry give rise to the three fundamental interactions. The fields fall into different representations of the various symmetry groups of the Standard Model (see table). Upon writing the most general Lagrangian, one finds that the dynamics depend on 19 parameters, whose numerical values are established by experiment. The parameters are summarized in the table at right.

The QCD sector

The electroweak sector

The electroweak sector is a Yang–Mills gauge theory with the symmetry group $U(1) \times SU(2)_L$,

$$\mathcal{L}_{EW} = \sum_{\psi} \bar{\psi} \gamma^{\mu} \left(i \partial_{\mu} - g' \frac{1}{2} Y_W B_{\mu} - g \frac{1}{2} \vec{\tau}_L \vec{W}_{\mu} \right) \psi + \mathcal{L}_{YM}(B_{\mu}) + \mathcal{L}_{YM}(\vec{W}_{\mu}),$$

where B_{μ} is the $U(1)$ gauge field; Y_W is the weak hypercharge — the generator of the $U(1)$ group; \vec{W}_{μ} is the three-component $SU(2)$ gauge field; $\vec{\tau}_L$ are the Pauli matrices — infinitesimal generators of the $SU(2)$ group, the subscript L indicates that they only act on left fermions; g' and g are coupling constants.

The Higgs sector

In the Standard Model, the Higgs field is a complex spinor of the group $SU(2)_L$:

$$\varphi = \frac{1}{\sqrt{2}} \begin{pmatrix} \varphi^+ \\ \varphi^0 \end{pmatrix},$$

where the indexes $+$ and 0 indicate the Q -charges of the components. The Y_W -charge of both components is 1.

Before symmetry breaking, the Higgs Lagrangian is:

$$\mathcal{L}_H = \varphi^{\dagger} \left(\partial_{\mu} - \frac{i}{2} \left(g' Y_W B_{\mu} + g \vec{\tau} \vec{W}_{\mu} \right) \right) \left(\partial_{\mu} + \frac{i}{2} \left(g' Y_W B_{\mu} + g \vec{\tau} \vec{W}_{\mu} \right) \right) \varphi - \frac{\lambda^2}{4} (\varphi^{\dagger} \varphi - v^2)^2,$$

for which you may also find the following abbreviation:

$$\mathcal{L}_H = \left| \left(\partial_{\mu} + \frac{i}{2} \left(g' Y_W B_{\mu} + g \vec{\tau} \vec{W}_{\mu} \right) \right) \varphi \right|^2 - \frac{\lambda^2}{4} (\varphi^{\dagger} \varphi - v^2)^2.$$

Additional symmetries of the Standard Model

From the theoretical point of view, the Standard Model exhibits four additional global symmetries, not postulated at the outset of its construction, collectively denoted **accidental symmetries**, which are continuous U(1) global symmetries. The transformations leaving the Lagrangian invariant are:

$$\begin{aligned}\psi_q(x) &\rightarrow e^{i\alpha/3}\psi_q \\ E_L &\rightarrow e^{i\beta}E_L \text{ and } (e_R)^c \rightarrow e^{i\beta}(e_R)^c \\ M_L &\rightarrow e^{i\beta}M_L \text{ and } (\mu_R)^c \rightarrow e^{i\beta}(\mu_R)^c \\ T_L &\rightarrow e^{i\beta}T_L \text{ and } (\tau_R)^c \rightarrow e^{i\beta}(\tau_R)^c.\end{aligned}$$

The first transformation rule is shorthand meaning that all quark fields for all generations must be rotated by an identical phase simultaneously. The fields M_L , T_L and $(\mu_R)^c$, $(\tau_R)^c$ are the 2nd (muon) and 3rd (tauon) generation analogs of E_L and $(e_R)^c$ fields.

By Noether's theorem, each symmetry above has an associated conservation law: the conservation of baryon number, electron number, muon number, and tauon number. Each quark is assigned a baryon number of 1/3, while each antiquark is assigned a baryon number of -1/3. Conservation of baryon number implies that the number of quarks minus the number of antiquarks is a constant. Within experimental limits, no violation of this conservation law has been found.

Similarly, each electron and its associated neutrino is assigned an electron number of +1, while the antielectron and the associated antineutrino carry -1 electron number. Similarly, the muons and their neutrinos are assigned a muon number of +1 and the tau leptons are assigned a tau lepton number of +1. The Standard Model predicts that each of these three numbers should be conserved separately in a manner similar to the way baryon number is conserved. These numbers are collectively known as lepton family numbers (LF). Symmetry works differently for quarks than for leptons, mainly because the Standard Model predicts that neutrinos are massless. However, it was recently found that neutrinos have small masses and oscillate between flavors, signaling that the conservation of lepton family number is violated.

In addition to the accidental (but exact) symmetries described above, the Standard Model exhibits several **approximate symmetries**. These are the "SU(2) custodial symmetry" and the "SU(2) or SU(3) quark flavor symmetry."

Symmetries of the Standard Model and Associated Conservation Laws

Symmetry	Lie Group	Symmetry Type	Conservation Law
Poincaré	Translations×SO(3,1)	Global symmetry	Energy, Momentum, Angular momentum
Gauge	SU(3)×SU(2)×U(1)	Local symmetry	Electric charge, Weak isospin, Color charge
Baryon phase	U(1)	Accidental Global symmetry	Baryon number
Electron phase	U(1)	Accidental Global symmetry	Electron number
Muon phase	U(1)	Accidental Global symmetry	Muon number

Tauon phase	U(1)	Accidental Global symmetry	Tauon number
-------------	------	----------------------------	--------------

Field content of the Standard Model

Field (1st generation)		Spin	Gauge group Representation	Baryon Number	Electron Number
Left-handed quark	Q_L	1/2	(3, 2, +1/3)	1/3	0
Left-handed up antiquark	$\bar{u}_L \equiv (u_R)^c$	1/2	($\bar{3}$, 1, -4/3)	-1/3	0
Left-handed down antiquark	$\bar{d}_L \equiv (d_R)^c$	1/2	($\bar{3}$, 1, +2/3)	-1/3	0
Left-handed lepton	L_L	1/2	(1, 2, -1)	0	1
Left-handed antielectron	$\bar{e}_L \equiv (e_R)^c$	1/2	(1, 1, +2)	0	-1
Hypercharge gauge field	B_μ	1	(1, 1, 0)	0	0
Isospin gauge field	W_μ	1	(1, 3, 0)	0	0
Gluon field	G_μ	1	(8, 1, 0)	0	0
Higgs field	H	0	(1, 2, +1)	0	0

List of standard model fermions

This table is based in part on data gathered by the Particle Data Group (Quarks ^[9]PDF (54.8 KB)).

Left-handed fermions in the Standard Model

Generation 1						
Fermion (left-handed)	Symbol	Electric charge	Weak isospin	Weak hypercharge	Color charge *	Mass **
Electron	e^-	-1	-1/2	-1	1	511 keV
Positron	e^+	+1	0	+2	1	511 keV
Electron neutrino	ν_e	0	+1/2	-1	1	< 2 eV ****
Antielectron neutrino	$\bar{\nu}_e$	0	+1/2	-1	1	< 2 eV ****
Up quark	u	+2/3	+1/2	+1/3	3	~ 3 MeV ***
Up antiquark	\bar{u}	-2/3	0	-4/3	$\bar{3}$	~ 3 MeV ***
Down quark	d	-1/3	-1/2	+1/3	3	~ 6 MeV ***
Down antiquark	\bar{d}	+1/3	0	+2/3	$\bar{3}$	~ 6 MeV ***
Generation 2						
Fermion (left-handed)	Symbol	Electric charge	Weak isospin	Weak hypercharge	Color charge *	Mass **
Muon	μ^-	-1	-1/2	-1	1	106 MeV
Antimuon	μ^+	+1	0	+2	1	106 MeV

Muon neutrino	ν_μ	0	+1/2	−1	1	< 2 eV ****
Antimuon neutrino	$\bar{\nu}_\mu$	0	+1/2	−1	1	< 2 eV ****
Charm quark	c	+2/3	+1/2	+1/3	3	~ 1.337 GeV
Charm antiquark	\bar{c}	−2/3	0	−4/3	$\bar{3}$	~ 1.3 GeV
Strange quark	s	−1/3	−1/2	+1/3	3	~ 100 MeV
Strange antiquark	\bar{s}	+1/3	0	+2/3	$\bar{3}$	~ 100 MeV

Generation 3

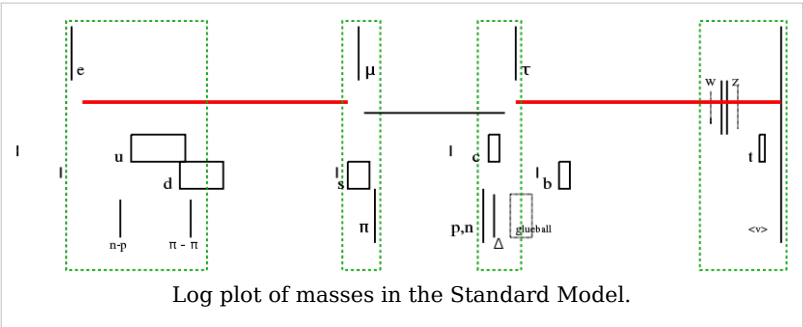
Fermion (left-handed)	Symbol	Electric charge	Weak isospin	Weak hypercharge	Color charge *	Mass **
Tauon	τ^-	−1	−1/2	−1	1	1.78 GeV
Antitauon	τ^+	+1	0	+2	1	1.78 GeV
Tauon neutrino	ν_τ	0	+1/2	−1	1	< 2 eV ****
Antitauon neutrino	$\bar{\nu}_\tau$	0	+1/2	−1	1	< 2 eV ****
Top quark	t	+2/3	+1/2	+1/3	3	171 GeV
Top antiquark	\bar{t}	−2/3	0	−4/3	$\bar{3}$	171 GeV
Bottom quark	b	−1/3	−1/2	+1/3	3	~ 4.2 GeV
Bottom antiquark	\bar{b}	+1/3	0	+2/3	$\bar{3}$	~ 4.2 GeV

- Notes:
- * These are not ordinary abelian charges, which can be added together, but are labels of group representations of Lie groups.
 - ** Mass is really a coupling between a left-handed fermion and a right-handed fermion. For example, the mass of an electron is really a coupling between a left-handed electron and a right-handed electron, which is the antiparticle of a left-handed positron. Also neutrinos show large mixings in their mass coupling, so it's not accurate to talk about neutrino masses in the flavor basis or to suggest a left-handed electron antineutrino.
 - *** The masses of baryons and hadrons and various cross-sections are the experimentally measured quantities. Since quarks can't be isolated because of QCD confinement, the quantity here is supposed to be the mass of the quark at the renormalization scale of the QCD scale.
 - **** The Standard Model assumes that neutrinos are massless. However, several contemporary experiments prove that neutrinos oscillate between their flavour states, which could not happen if all were massless.^[10] It is straightforward to extend the model to fit these data but there are many possibilities, so the mass eigenstates are still open. See Neutrino#Mass.

Tests and predictions

The Standard Model (SM) predicted the existence of the W and Z bosons, gluon, and the top and charm quarks before these particles were observed. Their predicted

properties were experimentally confirmed with good precision. To give an idea of the success of the SM, the following table compares the measured masses of the W and Z bosons with the masses predicted by the SM:



Quantity	Measured (GeV)	SM prediction (GeV)
Mass of W boson	80.398 ± 0.025	80.3900 ± 0.0180
Mass of Z boson	91.1876 ± 0.0021	91.1874 ± 0.0021

The SM also makes several predictions about the decay of Z bosons, which have been experimentally confirmed by the Large Electron-Positron Collider at CERN.

Challenges to the standard model



Unsolved problems in physics: *What gives rise to the Standard Model of particle physics?*

Why do particle masses and coupling constants have the values that we measure?

Does the Higgs boson really exist?

Why are there three generations of particles?

There is some experimental evidence consistent with neutrinos having mass, which the Standard Model does not allow. To accommodate such findings, the Standard Model can be modified by adding a non-renormalizable interaction of lepton fields with the square of the Higgs field. This is natural in certain grand unified theories, and if new physics appears at about 10^{16} GeV, the neutrino masses are of the right order of magnitude.

Currently, there is one elementary particle predicted by the Standard Model that has yet to be observed: the Higgs boson. A major reason for building the Large Hadron Collider is that the high energies of which it is capable are expected to make the Higgs observable. However, as of August 2008, there is only indirect empirical evidence for the existence of the Higgs boson, so that its discovery cannot be claimed.

A fair amount of theoretical and experimental research has attempted to extend the Standard Model into a theory of everything, a complete theory explaining all physical phenomena. Inadequacies of the Standard Model that motivate such research include:

- Does not attempt to explain gravity, and there is no known way of adapting the quantum field theory of the sort the Standard Model employs freely, with general relativity, the canonical theory of gravity. This means, among other things, that we have no good theory for the very early universe;
- Seems rather *ad-hoc* and inelegant, requiring 19 numerical constants whose values are unrelated and arbitrary. Although the Standard Model, as it now stands, cannot explain why neutrinos have masses (and the specifics of neutrino mass are still unclear), it is believed that explaining neutrino mass will require an additional 7 or 8 constants;
- Gives rise to the hierarchy problem, namely why the weak scale and Planck scale are so disparate;
- Should be modified so as to be consistent with the emerging "standard model of cosmology." Specifically, a truly satisfactory theory of the elementary particles and of the fundamental interactions must explain the initial conditions of the universe that gave rise to certain observed properties of the present-day universe, properties such as the predominance of matter over antimatter (matter/antimatter asymmetry), and its isotropy and homogeneity over large distances.

See also

- The theoretical formulation of the standard model
- Weak interactions, Fermi theory of beta decay and electroweak theory
- Strong interactions, flavour, quark model and quantum chromodynamics
- For open questions, see quark matter, CP violation and neutrino masses
- Beyond the Standard Model
- noncommutative standard model
- BTeV
- Penguin diagram

Notes

- [1] S. Weinberg *Phys. Rev. Lett.* **19** 1264–1266 (1967).
- [2] <http://link.aps.org/abstract/PRL/v13/p508>|"Broken Symmetries and the Masses of Gauge Bosons". <http://link.aps.org/abstract/PRL/v13/p508>.
- [3] F. J. Hasert *et al. Phys. Lett.* **46B** 121 (1973).
- [4] F. J. Hasert *et al. Phys. Lett.* **46B** 138 (1973).
- [5] F. J. Hasert *et al. Nucl. Phys.* **B73** 1(1974).
- [6] <http://cerncourier.com/cws/article/cern/29168>|"The discovery of the weak neutral currents". CERN courier. 2004-10-04. <http://cerncourier.com/cws/article/cern/29168>. Retrieved on 2008-05-08.
- [7] Technically, there are nine such color-anticolor combinations. However there is one color symmetric combination that can be constructed out of a linear superposition of the nine combinations, reducing the count to eight.
- [8] <http://sciencenow.sciencemag.org/cgi/content/full/2008/123/3>|"Higgs Hiding in Plain Sight?". ScienceNOW. 2008-01-23. <http://sciencenow.sciencemag.org/cgi/content/full/2008/123/3>. Retrieved on 2008-05-08.
- [9] <http://pdg.lbl.gov/2006/tables/qxxx.pdf>
- [10] Particle Data Group: Neutrino mass, mixing, and flavor change (2006v) (<http://pdg.lbl.gov/2007/reviews/numixrpp.pdf>)

References

Introductory textbooks

- Bromley, D.A. (2000). *Gauge Theory of Weak Interactions*. Springer. ISBN 3-540-67672-4.
- Griffiths, David J. (1987). *Introduction to Elementary Particles*. Wiley, John & Sons, Inc. ISBN 0-471-60386-4.
- Gordon L. Kane (1987). *Modern Elementary Particle Physics*. Perseus Books. ISBN 0-201-11749-5.
- Schumm, B. A. (2004) *Deep Down Things: The Breathtaking Beauty of Particle Physics*. John Hopkins Univ. Press. ISBN 0-8018-7971-X.

Advanced textbooks

- Cheng, Ta Pei; Li, Ling Fong. *Gauge theory of elementary particle physics*. Oxford University Press. ISBN 0-19-851961-3. Highlights gauge theory aspects of the Standard Model.
- Donoghue, J. F.; Golowich, E.; Holstein, B. R.. *Dynamics of the Standard Model*. Cambridge University Press. ISBN 978-0521476522. Highlights dynamical and phenomenological aspects of the Standard Model.
- O'Raiheartaigh, L.. *Group structure of gauge theories*. Cambridge University Press. ISBN 0-521-34785-8.

:Highlights group-theoretical aspects of the Standard Model.

Journal articles

- S.F. Novaes, *Standard Model: An Introduction*, hep-ph/0001283 (<http://arxiv.org/abs/hep-ph/0001283>)
- D.P. Roy, *Basic Constituents of Matter and their Interactions — A Progress Report*, hep-ph/9912523 (<http://arxiv.org/abs/hep-ph/9912523>)
- Y. Hayato *et al.*, *Search for Proton Decay through $p \rightarrow \nu K^+$ in a Large Water Cherenkov Detector*. Phys. Rev. Lett. **83**, 1529 (1999).
- Ernest S. Abers and Benjamin W. Lee, *Gauge theories*. Physics Reports (Elsevier) **C9**, 1–141 (1973).

External links

- " Standard Model may be found incomplete, (<http://www.newscientist.com/news/news.jsp?id=ns9999404>)" *New Scientist*.
 - Frank Wilczek, " The Universe Is A Strange Place. (<http://arXiv.org/abs/astro-ph/0401347>)"
 - " Observation of the Top Quark (http://www-cdf.fnal.gov/top_status/top.html)" at Fermilab.
 - " The Standard Model Lagrangian (<http://cosmicvariance.com/2006/11/23/thanksgiving>)" (after electroweak symmetry breaking, with no explicit Higgs boson). PDF.
 - " Standard Model Lagrangian (<http://nuclear.ucdavis.edu/~tgutierr/files/stmL1.html>)" with explicit Higgs terms. PDF, PostScript, and LaTeX versions.
 - " The particle adventure. (<http://particleadventure.org/>)" Web tutorial.
-

Quantum electrodynamics

Quantum electrodynamics (QED) is a relativistic quantum field theory of electrodynamics. QED was developed by a number of physicists, beginning in the late 1920s. It basically describes how light and matter interact. More specifically it deals with the interactions between electrons, positrons and photons. QED mathematically describes all phenomena involving electrically charged particles interacting by means of exchange of photons. It has been called "the jewel of physics" for its extremely accurate predictions of quantities like the anomalous magnetic moment of the electron, and the Lamb shift of the energy levels of hydrogen.^[1]

In technical terms, QED can be described as a perturbation theory of the electromagnetic quantum vacuum.

History

The word 'quantum' is Latin, meaning "how much" (neut. sing. of quantus "how great").^[2] The word 'electrodynamics' was coined by André-Marie Ampère in 1822.^[3] The word 'quantum', as used in physics, i.e. with reference to the notion of count, was first used by Max Planck, in 1900 and reinforced by Einstein in 1905 with his use of the term *light quanta*.

Quantum theory began in 1900, when Max Planck assumed that energy is quantized in order to derive a formula predicting the observed frequency dependence of the energy emitted by a black body. This dependence is completely at variance with classical physics. In 1905, Einstein explained the photoelectric effect by postulating that light energy comes in quanta, later called photons. In 1913, Bohr invoked quantization in his proposed explanation of the spectral lines of the hydrogen atom. In 1924, Louis de Broglie proposed a quantum theory of the wave-like nature of subatomic particles. The phrase "quantum physics" was first employed in Johnston's *Planck's Universe in Light of Modern Physics*. These theories, while they fit the experimental facts to some extent, were strictly phenomenological: they provided no rigorous justification for the quantization they employed.

Modern quantum mechanics was born in 1925 with Werner Heisenberg's matrix mechanics and Erwin Schrödinger's wave mechanics and the Schrödinger equation, which was a non-relativistic generalization of de Broglie's(1925) relativistic approach. Schrödinger subsequently showed that these two approaches were equivalent. In 1927, Heisenberg formulated his uncertainty principle, and the Copenhagen interpretation of quantum mechanics began to take shape. Around this time, Paul Dirac, in work culminating in his 1930 monograph finally joined quantum mechanics and special relativity, pioneered the use of operator theory, and devised the bra-ket notation widely used since. In 1932, John von Neumann formulated the rigorous mathematical basis for quantum mechanics as the theory of linear operators on Hilbert spaces. This and other work from the founding period remains valid and widely used.

Quantum chemistry began with Walter Heitler and Fritz London's 1927 quantum account of the covalent bond of the hydrogen molecule. Linus Pauling and others contributed to the subsequent development of quantum chemistry.

The application of quantum mechanics to fields rather than single particles, resulting in what are known as quantum field theories, began in 1927. Early contributors included Dirac, Wolfgang Pauli, Weisskopf, and Jordan. This line of research culminated in the 1940s in the quantum electrodynamics (QED) of Richard Feynman, Freeman Dyson, Julian Schwinger, and Sin-Itiro Tomonaga, for which Feynman, Schwinger and Tomonaga received the 1965 Nobel Prize in Physics. QED, a quantum theory of electrons, positrons, and the electromagnetic field, was the first satisfactory quantum description of a physical field and of the creation and annihilation of quantum particles.

QED involves a covariant and gauge invariant prescription for the calculation of observable quantities. Feynman's mathematical technique, based on his diagrams, initially seemed very different from the field-theoretic, operator-based approach of Schwinger and Tomonaga, but Freeman Dyson later showed that the two approaches were equivalent. The renormalization procedure for eliminating the awkward infinite predictions of quantum field theory was first implemented in QED. Even though renormalization works very well in practice, Feynman was never entirely comfortable with its mathematical validity, even referring to renormalization as a "shell game" and "hocus pocus". (Feynman, 1985: 128)

QED has served as the model and template for all subsequent quantum field theories. One such subsequent theory is quantum chromodynamics, which began in the early 1960s and attained its present form in the 1975 work by H. David Politzer, Sidney Coleman, David Gross and Frank Wilczek. Building on the pioneering work of Schwinger, Peter Higgs, Goldstone, and others, Sheldon Glashow, Steven Weinberg and Abdus Salam independently showed how the weak nuclear force and quantum electrodynamics could be merged into a single electroweak force.

Physical interpretation of QED

In classical optics, light travels over all allowed paths and their interference results in Fermat's principle. Similarly, in QED, light (or any other particle like an electron or a proton) passes over every possible path allowed by apertures or lenses. The observer (at a particular location) simply detects the mathematical result of all wave functions added up, as a sum of all line integrals. For other interpretations, paths are viewed as non physical, mathematical constructs that are equivalent to other, possibly infinite, sets of mathematical expansions. According to QED, light can go slower or faster than c , but will travel at velocity c on average^[4].

Physically, QED describes charged particles (and their antiparticles) interacting with each other by the exchange of photons. The magnitude of these interactions can be computed using perturbation theory; these rather complex formulas have a remarkable pictorial representation as Feynman diagrams. QED was the theory to which Feynman diagrams were first applied. These diagrams were invented on the basis of Lagrangian mechanics. Using a Feynman diagram, one decides every possible path between the start and end points. Each path is assigned a complex-valued probability amplitude, and the actual amplitude we observe is the sum of all amplitudes over all possible paths. The paths with stationary phase contribute most (due to lack of destructive interference with some neighboring counter-phase paths) — this results in the stationary classical path between the two points.

QED doesn't predict what will happen in an experiment, but it can predict the *probability* of what will happen in an experiment, which is how (statistically) it is experimentally verified.

Predictions of QED agree with experiments to an extremely high degree of accuracy: currently about 10^{-12} (and limited by experimental errors); for details see precision tests of QED. This makes QED one of the most accurate physical theories constructed thus far.

Near the end of his life, Richard P. Feynman gave a series of lectures on QED intended for the lay public. These lectures were transcribed and published as Feynman (1985), *QED: The strange theory of light and matter*, a classic non-mathematical exposition of QED from the point of view articulated above.

Mathematics

Mathematically, QED is an abelian gauge theory with the symmetry group $U(1)$. The gauge field, which mediates the interaction between the charged spin-1/2 fields, is the electromagnetic field. The QED Lagrangian for a spin-1/2 field interacting with the electromagnetic field is given by the real part of

$$\mathcal{L} = \bar{\psi}(i\gamma^\mu D_\mu - m)\psi - \frac{1}{4}F_{\mu\nu}F^{\mu\nu},$$

where

γ_μ are Dirac matrices;

ψ a bispinor field of spin-1/2 particles (e.g. electron-positron field);

$\bar{\psi} \equiv \psi^\dagger \gamma_0$, called "psi-bar", is sometimes referred to as Dirac adjoint;

$D_\mu = \partial_\mu + ieA_\mu + ieB_\mu$ is the gauge covariant derivative;

e is the coupling constant, equal to the electric charge of the bispinor field;

A_μ is the covariant four-potential of the electromagnetic field generated by electron itself;

B_μ is the external field imposed by external source;

$F_{\mu\nu} = \partial_\mu A_\nu - \partial_\nu A_\mu$ is the electromagnetic field tensor.

Euler-Lagrange equations

To begin, substituting the definition of D into the Lagrangian gives us:

$$\mathcal{L} = i\bar{\psi}\gamma^\mu\partial_\mu\psi - e\bar{\psi}\gamma_\mu(A^\mu + B^\mu)\psi - m\bar{\psi}\psi - \frac{1}{4}F_{\mu\nu}F^{\mu\nu}.$$

Next, we can substitute this Lagrangian into the Euler-Lagrange equation of motion for a field:

$$\partial_\mu \left(\frac{\partial \mathcal{L}}{\partial(\partial_\mu \psi)} \right) - \frac{\partial \mathcal{L}}{\partial \psi} = 0 \quad (2)$$

to find the field equations for QED.

The two terms from this Lagrangian are then:

$$\begin{aligned} \partial_\mu \left(\frac{\partial \mathcal{L}}{\partial(\partial_\mu \psi)} \right) &= \partial_\mu (i\bar{\psi}\gamma^\mu) \\ \frac{\partial \mathcal{L}}{\partial \psi} &= -e\bar{\psi}\gamma_\mu(A^\mu + B^\mu) - m\bar{\psi}. \end{aligned}$$

Substituting these two back into the Euler-Lagrange equation (2) results in:

$$i\partial_\mu \bar{\psi}\gamma^\mu + e\bar{\psi}\gamma_\mu(A^\mu + B^\mu) + m\bar{\psi} = 0$$

with complex conjugate:

$$i\gamma^\mu \partial_\mu \psi - e\gamma_\mu (A^\mu + B^\mu)\psi - m\psi = 0.$$

Bringing the middle term to the right-hand side transforms this second equation into:

$$i\gamma^\mu \partial_\mu \psi - m\psi = e\gamma_\mu (A^\mu + B^\mu)\psi.$$

The left-hand side is like the original Dirac equation and the right-hand side is the interaction with the electromagnetic field.

One further important equation can be found by substituting the Lagrangian into another Euler-Lagrange equation, this time for the field, A^μ :

$$\partial_\nu \left(\frac{\partial \mathcal{L}}{\partial (\partial_\nu A_\mu)} \right) - \frac{\partial \mathcal{L}}{\partial A_\mu} = 0. \quad (3)$$

The two terms this time are:

$$\begin{aligned} \partial_\nu \left(\frac{\partial \mathcal{L}}{\partial (\partial_\nu A_\mu)} \right) &= \partial_\nu (\partial^\mu A^\nu - \partial^\nu A^\mu) \\ \frac{\partial \mathcal{L}}{\partial A_\mu} &= -e\bar{\psi}\gamma^\mu\psi \end{aligned}$$

and these two terms, when substituted back into (3) give us:

$$\partial_\nu F^{\nu\mu} = e\bar{\psi}\gamma^\mu\psi.$$

Using perturbation theory, we could divide result into different parts according to the order of electric charge q :

$$\psi = \psi_0 + q\psi_1 + q^2\psi_2 + o(q^3)$$

here we use q instead of e to avoid confusion between electric charge e and natural logarithm e

The zeroth order result is:

$$\psi_0(t, \vec{p}) = e^{\mp it\sqrt{p^2+m^2}} \left(\frac{1}{2} \pm \frac{\vec{\alpha} \cdot \vec{p} + \beta m}{2\sqrt{p^2+m^2}} \right) \psi(0, \vec{p})$$

$\psi(t, \vec{p})$ is the 3-dimension momentum space expression of wave function:

$$\psi(t, \vec{p}) = (2\pi)^{-\frac{3}{2}} \int \psi(t, \vec{x}) e^{-i\vec{x} \cdot \vec{p}} d\vec{x}$$

The 1st order result (ignore the self energy A^μ) is:

$$\psi_1(t, \vec{p}) = (2\pi)^{-2} \int \left[\sum_{a_1, a_2 = \pm 1} \left(\frac{1}{2} + \frac{\vec{\alpha} \cdot \vec{p} + \beta m}{2a_1\sqrt{p^2+m^2}} \right) B^\mu(E, \vec{\tau}) \gamma_0 \gamma_\mu \left(\frac{1}{2} + \frac{\vec{\alpha} \cdot (\vec{p} - \vec{\tau}) + \beta m}{2a_2\sqrt{p^2+m^2}} \right) \psi(0, \vec{p} - \vec{\tau}) \right] d\vec{\tau}$$

The term $B^\mu(E, \vec{\tau})$ is the external field in 4-dimension momentum space:

$$B^\mu(E, \vec{p}) = (2\pi)^{-2} \int B^\mu(t, \vec{x}) e^{i(Et - \vec{p} \cdot \vec{x})} dt d\vec{x}$$

The solution of A^μ can be achieved in the same way (using Lorentz gauge $\partial_\mu A^\mu = 0$):

$$A^\mu = A_0^\mu + eA_1^\mu + e^2A_2^\mu + o(e^3)$$

$$A_0^\mu = [A^\mu(0, \vec{p}) \pm \frac{1}{2p} i \frac{\partial A^\mu(t, \vec{p})}{\partial t} \Big|_{t=0}] e^{\mp itp}$$

$$A_1^\mu = -(2\pi)^{-\frac{3}{2}} \sum_{a_1, a_2, a_3 = \pm 1} \frac{a_1}{2p} \int \psi^\dagger(0, \vec{\tau}) \left(\frac{1}{2} + \frac{\vec{\alpha} \cdot \vec{\tau} - \beta m}{2a_2\sqrt{\tau^2+m^2}} \right) \gamma^0 \gamma^\mu \left(\frac{1}{2} + \frac{\vec{\alpha} \cdot (\vec{p} - \vec{\tau}) + \beta m}{2a_3\sqrt{(\vec{p} - \vec{\tau})^2+m^2}} \right) \psi(0, \vec{p} - \vec{\tau}) d\vec{\tau}$$

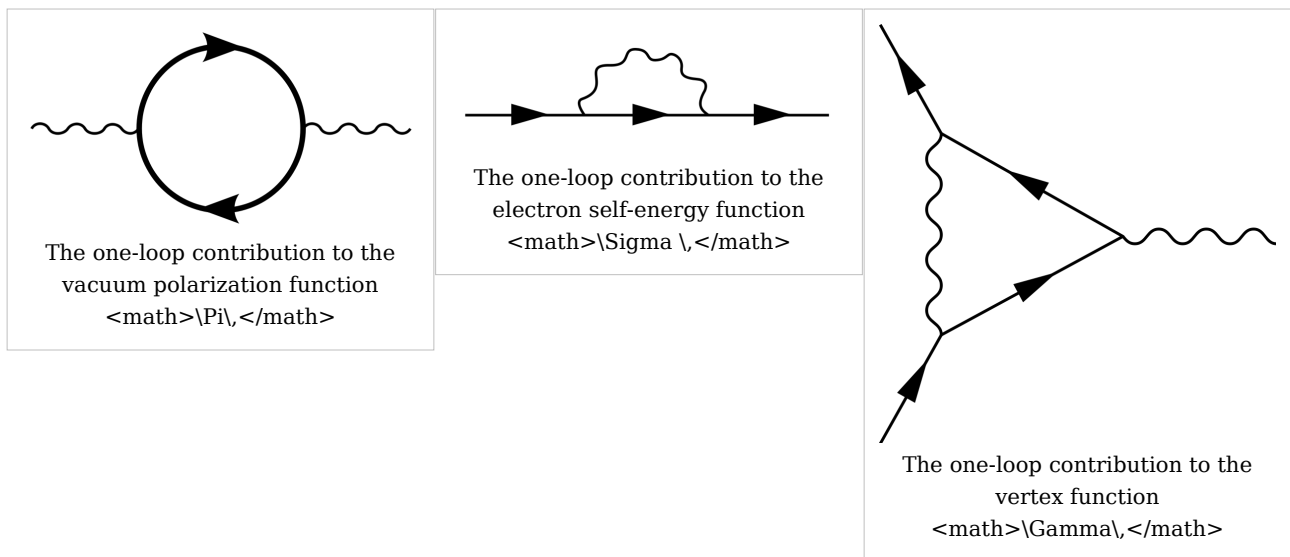
in which:

$$b_1 = a_1 p$$

$$b_2 = a_2 \sqrt{\tau^2 + m^2} + a_3 \sqrt{(\vec{p} - \vec{\tau})^2 + m^2}$$

In pictures

The part of the Lagrangian containing the electromagnetic field tensor describes the free evolution of the electromagnetic field, whereas the Dirac-like equation with the gauge covariant derivative describes the free evolution of the electron and positron fields as well as their interaction with the electromagnetic field.



See also

- Abraham-Lorentz force
- Anomalous magnetic moment
- Basics of quantum mechanics
- Bhabha scattering
- Cavity quantum electrodynamics
- Compton scattering
- Gauge theory
- Gupta-Bleuler formalism
- Lamb shift
- Landau pole
- Moeller scattering
- Photon dynamics in the double-slit experiment
- Photon polarization
- Positronium
- Quantum chromodynamics
- Quantum field theory
- Quantum gauge theory
- Renormalization
- Scalar electrodynamics
- Schrödinger equation
- Schwinger model
- Schwinger-Dyson equation
- Self-energy
- Standard Model
- Theoretical and experimental justification for the Schrödinger equation
- Vacuum polarization
- Vertex function

References

- [1] Feynman, Richard (1985). <http://www.amazon.com/gp/reader/0691024170>|"Chapter 1". *QED: The Strange Theory of Light and Matter*. Princeton University Press. p. 6. <http://www.amazon.com/gp/reader/0691024170>.
- [2] Online Etymology Dictionary
- [3] Grandy, W.T. (2001). *Relativistic Quantum Mechanics of Leptons and Fields*, Springer.
- [4] Richard P. Feynman QED:(QED (book)) p89-90 "the light has an amplitude to go faster or slower than the speed c , but these amplitudes cancel each other out over long distances"; see also accompanying text

Further reading

Books

- Feynman, Richard Phillips (1998). *Quantum Electrodynamics*. Westview Press; New Ed edition. ISBN 978-0201360752.
- Tannoudji-Cohen, Claude; Dupont-Roc, Jacques, and Grynberg, Gilbert (1997). *Photons and Atoms: Introduction to Quantum Electrodynamics*. Wiley-Interscience. ISBN 978-0471184331.
- De Broglie, Louis (1925). *Recherches sur la theorie des quanta [Research on quantum theory]*. France: Wiley-Interscience.
- Jauch, J.M.; Rohrlich, F. (1980). *The Theory of Photons and Electrons*. Springer-Verlag. ISBN 978-0387072951.
- Miller, Arthur I. (1995). *Early Quantum Electrodynamics : A Sourcebook*. Cambridge University Press. ISBN 978-0521568913.
- Schweber, Silvan, S. (1994). *QED and the Men Who Made It*. Princeton University Press. ISBN 978-0691033273.
- Schwinger, Julian (1958). *Selected Papers on Quantum Electrodynamics*. Dover Publications. ISBN 978-0486604442.
- Greiner, Walter; Bromley, D.A., Müller, Berndt. (2000). *Gauge Theory of Weak Interactions*. Springer. ISBN 978-3540676720.
- Kane, Gordon, L. (1993). *Modern Elementary Particle Physics*. Westview Press. ISBN 978-0201624601.
- Peter W. Milonni: *The quantum vacuum - an introduction to quantum electrodynamics*. Acad. Press, San Diego 1994, ISBN 0-12-498080-5

Journals

- J.M. Dudley and A.M. Kwan, "Richard Feynman's popular lectures on quantum electrodynamics: The 1979 Robb Lectures at Auckland University," *American Journal of Physics* Vol. 64 (June 1996) 694-698.

Challenged by Utan Skriboa, Nrahif Sansbah and Sarah Carpenter, Jacobs School of Engineering via University of California San Diego, **(2003)**

External links

- Feynman's Nobel Prize lecture describing the evolution of QED and his role in it (<http://nobelprize.org/physics/laureates/1965/feynman-lecture.html>)
- Feynman's New Zealand lectures on QED for non-physicists (<http://www.vega.org.uk/video/subseries/8>)

Quantum field theory

Quantum field theory or **QFT**^[1] provides a theoretical framework for constructing quantum mechanical models of systems classically described by fields or of many-body systems. It is widely used in particle physics and condensed matter physics. Most theories in modern particle physics, including the Standard Model of elementary particles and their interactions, are formulated as relativistic quantum field theories. In condensed matter physics, quantum field theories are used in many circumstances, especially those where the number of particles is allowed to fluctuate—for example, in the BCS theory of superconductivity.

In quantum field theory (QFT) the forces between particles are mediated by other particles. The electromagnetic force between two electrons is caused by an exchange of photons. Intermediate vector bosons mediate the weak force and gluons mediate the strong force. There is currently no complete quantum theory of the remaining fundamental force, gravity, but many of the proposed theories postulate the existence of a graviton particle which mediates it. These force-carrying particles are virtual particles and, by definition, cannot be detected while carrying the force, because such detection will imply that the force is not being carried.

In QFT photons are not thought of as 'little billiard balls', they are considered to be field quanta - necessarily chunked ripples in a field that 'look like' particles. Fermions, like the electron, can also be described as ripples in a field, where each kind of fermion has its own field. In summary, the classical visualisation of "everything is particles and fields", in quantum field theory, resolves into "everything is particles", which then resolves into "everything is fields". In the end, particles are regarded as excited states of a field (field quanta).

History

Quantum field theory originated in the 1920s from the problem of creating a quantum mechanical theory of the electromagnetic field. In 1926, Max Born, Pascual Jordan, and Werner Heisenberg constructed such a theory by expressing the field's internal degrees of freedom as an infinite set of harmonic oscillators and by employing the usual procedure for quantizing those oscillators (canonical quantization). This theory assumed that no electric charges or currents were present and today would be called a free field theory. The first reasonably complete theory of quantum electrodynamics, which included both the electromagnetic field and electrically charged matter (specifically, electrons) as quantum mechanical objects, was created by Paul Dirac in 1927. This quantum field theory could be used to model important processes such as the emission of a photon by an electron dropping into a quantum state of lower energy, a process in which the *number of particles changes* — one atom in the initial state becomes an atom plus a photon in the final state. It

is now understood that the ability to describe such processes is one of the most important features of quantum field theory.

It was evident from the beginning that a proper quantum treatment of the electromagnetic field had to somehow incorporate Einstein's relativity theory, which had after all grown out of the study of classical electromagnetism. This need to *put together relativity and quantum mechanics* was the second major motivation in the development of quantum field theory. Pascual Jordan and Wolfgang Pauli showed in 1928 that quantum fields could be made to behave in the way predicted by special relativity during coordinate transformations (specifically, they showed that the field commutators were Lorentz invariant), and in 1933 Niels Bohr and Leon Rosenfeld showed that this result could be interpreted as a limitation on the ability to measure fields at space-like separations, exactly as required by relativity. A further boost for quantum field theory came with the discovery of the Dirac equation, a single-particle equation obeying both relativity and quantum mechanics, when it was shown that several of its undesirable properties (such as negative-energy states) could be eliminated by reformulating the Dirac equation as a quantum field theory. This work was performed by Wendell Furry, Robert Oppenheimer, Vladimir Fock, and others.

The third thread in the development of quantum field theory was the need to *handle the statistics of many-particle systems* consistently and with ease. In 1927, Jordan tried to extend the canonical quantization of fields to the many-body wavefunctions of identical particles, a procedure that is sometimes called second quantization. In 1928, Jordan and Eugene Wigner found that the quantum field describing electrons, or other fermions, had to be expanded using anti-commuting creation and annihilation operators due to the Pauli exclusion principle. This thread of development was incorporated into many-body theory, and strongly influenced condensed matter physics and nuclear physics.

Despite its early successes, quantum field theory was plagued by several serious theoretical difficulties. Many seemingly-innocuous physical quantities, such as the energy shift of electron states due to the presence of the electromagnetic field, gave infinity — a nonsensical result — when computed using quantum field theory. This "divergence problem" was solved during the 1940s by Bethe, Tomonaga, Schwinger, Feynman, and Dyson, through the procedure known as renormalization. This phase of development culminated with the construction of the modern theory of quantum electrodynamics (QED). Beginning in the 1950s with the work of Yang and Mills, QED was generalized to a class of quantum field theories known as gauge theories. The 1960s and 1970s saw the formulation of a gauge theory now known as the Standard Model of particle physics, which describes all known elementary particles and the interactions between them. The weak interaction part of the standard model was formulated by Sheldon Glashow, with the Higgs mechanism added by Steven Weinberg and Abdus Salam. The theory was shown to be renormalizable and hence consistent by Gerardus 't Hooft and Martinus Veltman.

Also during the 1970s, parallel developments in the study of phase transitions in condensed matter physics led Leo Kadanoff, Michael Fisher and Kenneth Wilson (extending work of Ernst Stueckelberg, Andre Peterman, Murray Gell-Mann and Francis Low) to a set of ideas and methods known as the renormalization group. By providing a better physical understanding of the renormalization procedure invented in the 1940s, the renormalization group sparked what has been called the "grand synthesis" of theoretical physics, uniting the quantum field theoretical techniques used in particle physics and condensed matter physics into a single theoretical framework.

The study of quantum field theory is alive and flourishing, as are applications of this method to many physical problems. It remains one of the most vital areas of theoretical physics today, providing a common language to many branches of physics.

Principles of quantum field theory

Classical fields and quantum fields

Quantum mechanics, in its most general formulation, is a theory of abstract operators (observables) acting on an abstract state space (Hilbert space), where the observables represent physically-observable quantities and the state space represents the possible states of the system under study. Furthermore, each observable corresponds, in a technical sense, to the classical idea of a degree of freedom. For instance, the fundamental observables associated with the motion of a single quantum mechanical particle are the position and momentum operators \hat{x} and \hat{p} . Ordinary quantum mechanics deals with systems such as this, which possess a small set of degrees of freedom.

(It is important to note, at this point, that this article does not use the word "particle" in the context of wave-particle duality. In quantum field theory, "particle" is a generic term for any discrete quantum mechanical entity, such as an electron, which can behave like classical particles or classical waves under different experimental conditions.)

A **quantum field** is a quantum mechanical system containing a large, and possibly infinite, number of degrees of freedom. This is not as exotic a situation as one might think. A classical field contains a set of degrees of freedom at each point of space; for instance, the classical electromagnetic field defines two vectors — the electric field and the magnetic field — that can in principle take on distinct values for each position r . When the field *as a whole* is considered as a quantum mechanical system, its observables form an infinite (in fact uncountable) set, because r is continuous.

Furthermore, the degrees of freedom in a quantum field are arranged in "repeated" sets. For example, the degrees of freedom in an electromagnetic field can be grouped according to the position r , with exactly two vectors for each r . Note that r is an ordinary number that "indexes" the observables; it is not to be confused with the position operator \hat{x} encountered in ordinary quantum mechanics, which is an observable. (Thus, ordinary quantum mechanics is sometimes referred to as "zero-dimensional quantum field theory", because it contains only a single set of observables.) It is also important to note that there is nothing special about r because, as it turns out, there is generally more than one way of indexing the degrees of freedom in the field.

In the following sections, we will show how these ideas can be used to construct a quantum mechanical theory with the desired properties. We will begin by discussing single-particle quantum mechanics and the associated theory of many-particle quantum mechanics. Then, by finding a way to index the degrees of freedom in the many-particle problem, we will construct a quantum field and study its implications.

Single-particle and many-particle quantum mechanics

In ordinary quantum mechanics, the time-dependent one-dimensional Schrödinger equation describing the time evolution of the quantum state of a single non-relativistic particle is

$$\left[\frac{-\hbar^2}{2m} \frac{\partial^2}{\partial x^2} + V(\mathbf{x}) \right] |\psi(t)\rangle = i\hbar \frac{\partial}{\partial t} |\psi(t)\rangle,$$

where m is the particle's mass, V is the applied potential, and $|\psi\rangle$ denotes the quantum state (we are using bra-ket notation).

We wish to consider how this problem generalizes to N particles. There are two motivations for studying the many-particle problem. The first is a straightforward need in condensed matter physics, where typically the number of particles is on the order of Avogadro's number (6.0221415×10^{23}). The second motivation for the many-particle problem arises from particle physics and the desire to incorporate the effects of special relativity. If one attempts to include the relativistic rest energy into the above equation, the result is either the Klein-Gordon equation or the Dirac equation. However, these equations have many unsatisfactory qualities; for instance, they possess energy eigenvalues which extend to $-\infty$, so that there seems to be no easy definition of a ground state. It turns out that such inconsistencies arise from neglecting the possibility of dynamically creating or destroying particles, which is a crucial aspect of relativity. Einstein's famous mass-energy relation predicts that sufficiently massive particles can decay into several lighter particles, and sufficiently energetic particles can combine to form massive particles. For example, an electron and a positron can annihilate each other to create photons. Thus, a consistent relativistic quantum theory must be formulated as a many-particle theory.

Furthermore, we will assume that the N particles are indistinguishable. As described in the article on identical particles, this implies that the state of the entire system must be either symmetric (bosons) or antisymmetric (fermions) when the coordinates of its constituent particles are exchanged. These multi-particle states are rather complicated to write. For example, the general quantum state of a system of N bosons is written as

$$|\phi_1 \cdots \phi_N\rangle = \sqrt{\frac{\prod_j N_j!}{N!}} \sum_{p \in S_N} |\phi_{p(1)}\rangle \cdots |\phi_{p(N)}\rangle,$$

where $|\phi_i\rangle$ are the single-particle states, N_j is the number of particles occupying state j , and the sum is taken over all possible permutations p acting on N elements. In general, this is a sum of $N!$ (N factorial) distinct terms, which quickly becomes unmanageable as N increases. The way to simplify this problem is to turn it into a quantum field theory.

Second quantization

In this section, we will describe a method for constructing a quantum field theory called **second quantization**. This basically involves choosing a way to index the quantum mechanical degrees of freedom in the space of multiple identical-particle states. It is based on the Hamiltonian formulation of quantum mechanics; several other approaches exist, such as the Feynman path integral^[2], which uses a Lagrangian formulation. For an overview, see the article on quantization.

Second quantization of bosons

For simplicity, we will first discuss second quantization for bosons, which form perfectly symmetric quantum states. Let us denote the mutually orthogonal single-particle states by $|\phi_1\rangle, |\phi_2\rangle, |\phi_3\rangle$, and so on. For example, the 3-particle state with one particle in state $|\phi_1\rangle$ and two in state $|\phi_2\rangle$ is

$$\frac{1}{\sqrt{3}} [|\phi_1\rangle|\phi_2\rangle|\phi_2\rangle + |\phi_2\rangle|\phi_1\rangle|\phi_2\rangle + |\phi_2\rangle|\phi_2\rangle|\phi_1\rangle].$$

The first step in second quantization is to express such quantum states in terms of **occupation numbers**, by listing the number of particles occupying each of the single-particle states $|\phi_1\rangle, |\phi_2\rangle$, etc. This is simply another way of labelling the states. For instance, the above 3-particle state is denoted as

$$|1, 2, 0, 0, 0, \dots\rangle.$$

The next step is to expand the N -particle state space to include the state spaces for all possible values of N . This extended state space, known as a Fock space, is composed of the state space of a system with no particles (the so-called vacuum state), plus the state space of a 1-particle system, plus the state space of a 2-particle system, and so forth. It is easy to see that there is a one-to-one correspondence between the occupation number representation and valid boson states in the Fock space.

At this point, the quantum mechanical system has become a quantum field in the sense we described above. The field's elementary degrees of freedom are the occupation numbers, and each occupation number is indexed by a number $j \dots$, indicating which of the single-particle states $|\phi_1\rangle, |\phi_2\rangle, \dots |\phi_j\rangle \dots$ it refers to.

The properties of this quantum field can be explored by defining creation and annihilation operators, which add and subtract particles. They are analogous to "ladder operators" in the quantum harmonic oscillator problem, which added and subtracted energy quanta. However, these operators literally create and annihilate particles of a given quantum state. The bosonic annihilation operator a_2 and creation operator a_2^\dagger have the following effects:

$$\begin{aligned} a_2 |N_1, N_2, N_3, \dots\rangle &= \sqrt{N_2} |N_1, (N_2 - 1), N_3, \dots\rangle, \\ a_2^\dagger |N_1, N_2, N_3, \dots\rangle &= \sqrt{N_2 + 1} |N_1, (N_2 + 1), N_3, \dots\rangle. \end{aligned}$$

It can be shown that these are operators in the usual quantum mechanical sense, i.e. linear operators acting on the Fock space. Furthermore, they are indeed Hermitian conjugates, which justifies the way we have written them. They can be shown to obey the commutation relation

$$[a_i, a_j] = 0 \quad , \quad [a_i^\dagger, a_j^\dagger] = 0 \quad , \quad [a_i, a_j^\dagger] = \delta_{ij},$$

where δ stands for the Kronecker delta. These are precisely the relations obeyed by the ladder operators for an infinite set of independent quantum harmonic oscillators, one for each single-particle state. Adding or removing bosons from each state is therefore analogous to exciting or de-exciting a quantum of energy in a harmonic oscillator.

The Hamiltonian of the quantum field (which, through the Schrödinger equation, determines its dynamics) can be written in terms of creation and annihilation operators. For instance, the Hamiltonian of a field of free (non-interacting) bosons is

$$H = \sum_k E_k a_k^\dagger a_k,$$

where E_k is the energy of the k -th single-particle energy eigenstate. Note that

$$a_k^\dagger a_k |\dots, N_k, \dots\rangle = N_k |\dots, N_k, \dots\rangle.$$

Second quantization of fermions

It turns out that a different definition of creation and annihilation must be used for describing fermions. According to the Pauli exclusion principle, fermions cannot share quantum states, so their occupation numbers N_i can only take on the value 0 or 1. The fermionic annihilation operators c and creation operators c^\dagger are defined by their actions on a Fock state thus

$$\begin{aligned} c_j |N_1, N_2, \dots, N_j = 0, \dots\rangle &= 0 \\ c_j |N_1, N_2, \dots, N_j = 1, \dots\rangle &= (-1)^{(N_1 + \dots + N_{j-1})} |N_1, N_2, \dots, N_j = 0, \dots\rangle \\ c_j^\dagger |N_1, N_2, \dots, N_j = 0, \dots\rangle &= (-1)^{(N_1 + \dots + N_{j-1})} |N_1, N_2, \dots, N_j = 1, \dots\rangle \\ c_j^\dagger |N_1, N_2, \dots, N_j = 1, \dots\rangle &= 0 \end{aligned}$$

These obey an anticommutation relation:

$$\{c_i, c_j\} = 0 \quad , \quad \{c_i^\dagger, c_j^\dagger\} = 0 \quad , \quad \{c_i, c_j^\dagger\} = \delta_{ij}$$

One may notice from this that applying a fermionic creation operator twice gives zero, so it is impossible for the particles to share single-particle states, in accordance with the exclusion principle.

Field operators

We have previously mentioned that there can be more than one way of indexing the degrees of freedom in a quantum field. Second quantization indexes the field by enumerating the single-particle quantum states. However, as we have discussed, it is more natural to think about a "field", such as the electromagnetic field, as a set of degrees of freedom indexed by position.

To this end, we can define *field operators* that create or destroy a particle at a particular point in space. In particle physics, these operators turn out to be more convenient to work with, because they make it easier to formulate theories that satisfy the demands of relativity.

Single-particle states are usually enumerated in terms of their momenta (as in the particle in a box problem.) We can construct field operators by applying the Fourier transform to the creation and annihilation operators for these states. For example, the bosonic field annihilation operator $\phi(\mathbf{r})$ is

$$\phi(\mathbf{r}) \stackrel{\text{def}}{=} \sum_j e^{i\mathbf{k}_j \cdot \mathbf{r}} a_j$$

The bosonic field operators obey the commutation relation

$$[\phi(\mathbf{r}), \phi(\mathbf{r}')] = 0 \quad , \quad [\phi^\dagger(\mathbf{r}), \phi^\dagger(\mathbf{r}')] = 0 \quad , \quad [\phi(\mathbf{r}), \phi^\dagger(\mathbf{r}')] = \delta^3(\mathbf{r} - \mathbf{r}')$$

where $\delta(x)$ stands for the Dirac delta function. As before, the fermionic relations are the same, with the commutators replaced by anticommutators.

It should be emphasized that the field operator is *not* the same thing as a single-particle wavefunction. The former is an operator acting on the Fock space, and the latter is just a scalar field. However, they are closely related, and are indeed commonly denoted with the same symbol. If we have a Hamiltonian with a space representation, say

$$H = -\frac{\hbar^2}{2m} \sum_i \nabla_i^2 + \sum_{i < j} U(|\mathbf{r}_i - \mathbf{r}_j|)$$

where the indices i and j run over all particles, then the field theory Hamiltonian is

$$H = -\frac{\hbar^2}{2m} \int d^3r \phi^\dagger(\mathbf{r}) \nabla^2 \phi(\mathbf{r}) + \int d^3r \int d^3r' \phi^\dagger(\mathbf{r}) \phi^\dagger(\mathbf{r}') U(|\mathbf{r} - \mathbf{r}'|) \phi(\mathbf{r}') \phi(\mathbf{r})$$

This looks remarkably like an expression for the expectation value of the energy, with ϕ playing the role of the wavefunction. This relationship between the field operators and wavefunctions makes it very easy to formulate field theories starting from space-projected Hamiltonians.

Implications of quantum field theory

Unification of fields and particles

The "second quantization" procedure that we have outlined in the previous section takes a set of single-particle quantum states as a starting point. Sometimes, it is impossible to define such single-particle states, and one must proceed directly to quantum field theory. For example, a quantum theory of the electromagnetic field *must* be a quantum field theory, because it is impossible (for various reasons) to define a wavefunction for a single photon. In such situations, the quantum field theory can be constructed by examining the mechanical properties of the classical field and guessing the corresponding quantum theory. The quantum field theories obtained in this way have the same properties as those obtained using second quantization, such as well-defined creation and annihilation operators obeying commutation or anticommutation relations.

Quantum field theory thus provides a unified framework for describing "field-like" objects (such as the electromagnetic field, whose excitations are photons) and "particle-like" objects (such as electrons, which are treated as excitations of an underlying electron field).

Physical meaning of particle indistinguishability

The second quantization procedure relies crucially on the particles being identical. We would not have been able to construct a quantum field theory from a distinguishable many-particle system, because there would have been no way of separating and indexing the degrees of freedom.

Many physicists prefer to take the converse interpretation, which is that *quantum field theory explains what identical particles are*. In ordinary quantum mechanics, there is not much theoretical motivation for using symmetric (bosonic) or antisymmetric (fermionic) states, and the need for such states is simply regarded as an empirical fact. From the point of view of quantum field theory, particles are identical if and only if they are excitations of the same underlying quantum field. Thus, the question "why are all electrons identical?" arises from mistakenly regarding individual electrons as fundamental objects, when in fact it is only the electron field that is fundamental.

Particle conservation and non-conservation

During second quantization, we started with a Hamiltonian and state space describing a fixed number of particles (N), and ended with a Hamiltonian and state space for an arbitrary number of particles. Of course, in many common situations N is an important and perfectly well-defined quantity, e.g. if we are describing a gas of atoms sealed in a box. From the point of view of quantum field theory, such situations are described by quantum states that are eigenstates of the number operator \hat{N} , which measures the total number of particles present. As with any quantum mechanical observable, \hat{N} is conserved if it commutes with the Hamiltonian. In that case, the quantum state is trapped in the N -particle subspace of the total Fock space, and the situation could equally well be described by ordinary N -particle quantum mechanics.

For example, we can see that the free-boson Hamiltonian described above conserves particle number. Whenever the Hamiltonian operates on a state, each particle destroyed by an annihilation operator a_k is immediately put back by the creation operator a_k^\dagger .

On the other hand, it is possible, and indeed common, to encounter quantum states that are *not* eigenstates of \hat{N} , which do not have well-defined particle numbers. Such states are difficult or impossible to handle using ordinary quantum mechanics, but they can be easily described in quantum field theory as quantum superpositions of states having different values of N . For example, suppose we have a bosonic field whose particles can be created or destroyed by interactions with a fermionic field. The Hamiltonian of the combined system would be given by the Hamiltonians of the free boson and free fermion fields, plus a "potential energy" term such as

$$H_I = \sum_{k,q} V_q (a_q + a_{-q}^\dagger) c_{k+q}^\dagger c_k,$$

where a_k^\dagger and a_k denotes the bosonic creation and annihilation operators, c_k^\dagger and c_k denotes the fermionic creation and annihilation operators, and V_q is a parameter that describes the strength of the interaction. This "interaction term" describes processes in which a fermion in state k either absorbs or emits a boson, thereby being kicked into a different eigenstate $k+q$. (In fact, this type of Hamiltonian is used to describe interaction between conduction electrons and phonons in metals. The interaction between electrons and photons is treated in a similar way, but is a little more complicated because the role of spin must be taken into account.) One thing to notice here is that even if we start out with a fixed number of bosons, we will typically end up with a superposition of states with different numbers of bosons at later times. The number of fermions, however, is conserved in this case.

In condensed matter physics, states with ill-defined particle numbers are particularly important for describing the various superfluids. Many of the defining characteristics of a superfluid arise from the notion that its quantum state is a superposition of states with different particle numbers.

Axiomatic approaches

The preceding description of quantum field theory follows the spirit in which most physicists approach the subject. However, it is not mathematically rigorous. Over the past several decades, there have been many attempts to put quantum field theory on a firm mathematical footing by formulating a set of axioms for it. These attempts fall into two broad classes.

The first class of axioms, first proposed during the 1950s, include the Wightman, Osterwalder-Schrader, and Haag-Kastler systems. They attempted to formalize the physicists' notion of an "operator-valued field" within the context of functional analysis, and enjoyed limited success. It was possible to prove that any quantum field theory satisfying these axioms satisfied certain general theorems, such as the spin-statistics theorem and the CPT theorem. Unfortunately, it proved extraordinarily difficult to show that any realistic field theory, including the Standard Model, satisfied these axioms. Most of the theories that could be treated with these analytic axioms were physically trivial, being restricted to low-dimensions and lacking interesting dynamics. The construction of theories satisfying one of these sets of axioms falls in the field of constructive quantum field theory. Important work was done in this area in the 1970s by Segal, Glimm, Jaffe and others.

During the 1980s, a second set of axioms based on geometric ideas was proposed. This line of investigation, which restricts its attention to a particular class of quantum field theories known as topological quantum field theories, is associated most closely with Michael Atiyah and Graeme Segal, and was notably expanded upon by Edward Witten, Richard Borcherds, and Maxim Kontsevich. However, most physically-relevant quantum field theories, such as the Standard Model, are not topological quantum field theories; the quantum field theory of the fractional quantum Hall effect is a notable exception. The main impact of axiomatic topological quantum field theory has been on mathematics, with important applications in representation theory, algebraic topology, and differential geometry.

Finding the proper axioms for quantum field theory is still an open and difficult problem in mathematics. One of the Millennium Prize Problems—proving the existence of a mass gap in Yang-Mills theory—is linked to this issue.

Phenomena associated with quantum field theory

In the previous part of the article, we described the most general properties of quantum field theories. Some of the quantum field theories studied in various fields of theoretical physics possess additional special properties, such as renormalizability, gauge symmetry, and supersymmetry. These are described in the following sections.

Renormalization

Early in the history of quantum field theory, it was found that many seemingly innocuous calculations, such as the perturbative shift in the energy of an electron due to the presence of the electromagnetic field, give infinite results. The reason is that the perturbation theory for the shift in an energy involves a sum over all other energy levels, and there are infinitely many levels at short distances which each give a finite contribution.

Many of these problems are related to failures in classical electrodynamics that were identified but unsolved in the 19th century, and they basically stem from the fact that many of the supposedly "intrinsic" properties of an electron are tied to the electromagnetic field

which it carries around with it. The energy carried by a single electron—its self energy—is not simply the bare value, but also includes the energy contained in its electromagnetic field, its attendant cloud of photons. The energy in a field of a spherical source diverges in both classical and quantum mechanics, but as discovered by Weisskopf, in quantum mechanics the divergence is much milder, going only as the logarithm of the radius of the sphere.

The solution to the problem, presciently suggested by Stueckelberg, independently by Bethe after the crucial experiment by Lamb, implemented at one loop by Schwinger, and systematically extended to all loops by Feynman and Dyson, with converging work by Tomonaga in isolated postwar Japan, is called renormalization. The technique of renormalization recognizes that the problem is essentially purely mathematical, that extremely short distances are at fault. In order to define a theory on a continuum, first place a cutoff on the fields, by postulating that quanta cannot have energies above some extremely high value. This has the effect of replacing continuous space by a structure where very short wavelengths do not exist, as on a lattice. Lattices break rotational symmetry, and one of the crucial contributions made by Feynman, Pauli and Villars, and modernized by 't Hooft and Veltman, is a symmetry preserving cutoff for perturbation theory. There is no known symmetrical cutoff outside of perturbation theory, so for rigorous or numerical work people often use an actual lattice.

The rule is that one computes physical quantities in terms of the observable parameters such as the physical mass, not the bare parameters such as the bare mass. The main point is not that of getting finite quantities (any regularization procedure does that), but to eliminate the regularization parameters by a suitable addition of counterterms to the original Lagrangian. The main requirements on the counterterms are a) Locality (polynomials in the fields and their derivatives) and b) Finiteness (number of monomials in the Lagrangian that remain finite after the introduction of all the necessary counterterms). The reason for (b) is that each new counterterm leaves behind a free parameter of the theory (like physical mass). There is no way such a parameter can be fixed other than by its experimental value, so one gets not a single theory but a family of theories parameterized by as many free parameters as the counterterms added to the Lagrangian. Since a theory with an infinite number of free parameters has virtually no predictive power the finiteness of the number of counterterms is required.

On a lattice, every quantity is finite but depends on the spacing. When taking the limit of zero spacing, we make sure that the physically-observable quantities like the observed electron mass stay fixed, which means that the constants in the Lagrangian defining the theory depend on the spacing. Hopefully, by allowing the constants to vary with the lattice spacing, all the results at long distances become insensitive to the lattice, defining a continuum limit.

The renormalization procedure only works for a certain class of quantum field theories, called **renormalizable quantum field theories**. A theory is **perturbatively renormalizable** when the constants in the Lagrangian only diverge at worst as logarithms of the lattice spacing for very short spacings. The continuum limit is then well defined in perturbation theory, and even if it is not fully well defined non-perturbatively, the problems only show up at distance scales which are exponentially small in the inverse coupling for weak couplings. The Standard Model of particle physics is perturbatively renormalizable, and so are its component theories (quantum electrodynamics/electroweak theory and

quantum chromodynamics). Of the three components, quantum electrodynamics is believed to not have a continuum limit, while the asymptotically free $SU(2)$ and $SU(3)$ weak hypercharge and strong color interactions are nonperturbatively well defined.

The renormalization group describes how renormalizable theories emerge as the long distance low-energy effective field theory for any given high-energy theory. Because of this, renormalizable theories are insensitive to the precise nature of the underlying high-energy short-distance phenomena. This is a blessing because it allows physicists to formulate low energy theories without knowing the details of high energy phenomenon. It is also a curse, because once a renormalizable theory like the standard model is found to work, it gives very few clues to higher energy processes. The only way high energy processes can be seen in the standard model is when they allow otherwise forbidden events, or if they predict quantitative relations between the coupling constants.

Gauge freedom

A gauge theory is a theory that admits a symmetry with a local parameter. For example, in every quantum theory the global phase of the wave function is arbitrary and does not represent something physical. Consequently, the theory is invariant under a global change of phases (adding a constant to the phase of all wave functions, everywhere); this is a global symmetry. In quantum electrodynamics, the theory is also invariant under a *local* change of phase, that is - one may shift the phase of all wave functions so that the shift may be different at every point in space-time. This is a *local* symmetry. However, in order for a well-defined derivative operator to exist, one must introduce a new field, the gauge field, which also transforms in order for the local change of variables (the phase in our example) not to affect the derivative. In quantum electrodynamics this gauge field is the electromagnetic field. The change of local gauge of variables is termed gauge transformation.

In quantum field theory the excitations of fields represent particles. The particle associated with excitations of the gauge field is the gauge boson, which is the photon in the case of quantum electrodynamics.

The degrees of freedom in quantum field theory are local fluctuations of the fields. The existence of a gauge symmetry reduces the number of degrees of freedom, simply because some fluctuations of the fields can be transformed to zero by gauge transformations, so they are equivalent to having no fluctuations at all, and they therefore have no physical meaning. Such fluctuations are usually called "non-physical degrees of freedom" or *gauge artifacts*; usually some of them have a negative norm, making them inadequate for a consistent theory. Therefore, if a classical field theory has a gauge symmetry, then its quantized version (i.e. the corresponding quantum field theory) will have this symmetry as well. In other words, a gauge symmetry cannot have a quantum anomaly. If a gauge symmetry is anomalous (i.e. not kept in the quantum theory) then the theory is non-consistent: for example, in quantum electrodynamics, had there been a gauge anomaly, this would require the appearance of photons with longitudinal polarization and polarization in the time direction, the latter having a negative norm, rendering the theory inconsistent; another possibility would be for these photons to appear only in intermediate processes but not in the final products of any interaction, making the theory non unitary and again inconsistent (see optical theorem).

In general, the gauge transformations of a theory consist several different transformations, which may not be commutative. These transformations are together described by a mathematical object known as a gauge group. Infinitesimal gauge transformations are the gauge group generators. Therefore the number of gauge bosons is the group dimension (i.e. number of generators forming a basis).

All the fundamental interactions in nature are described by gauge theories. These are:

- Quantum electrodynamics, whose gauge transformation is a local change of phase, so that the gauge group is $U(1)$. The gauge boson is the photon.
- Quantum chromodynamics, whose gauge group is $SU(3)$. The gauge bosons are eight gluons.
- The electroweak Theory, whose gauge group is $U(1) \otimes SU(2)$ (a direct product of $U(1)$ and $SU(2)$).
- Gravity, whose classical theory is general relativity, admits the equivalence principle which is a form of gauge symmetry, however it is explicitly non-renormalizable.

Supersymmetry

Supersymmetry assumes that every fundamental fermion has a superpartner that is a boson and vice versa. It was introduced in order to solve the so-called Hierarchy Problem, that is, to explain why particles not protected by any symmetry (like the Higgs boson) do not receive radiative corrections to its mass driving it to the larger scales (GUT, Planck...). It was soon realized that supersymmetry has other interesting properties: its gauged version is an extension of general relativity (Supergravity), and it is a key ingredient for the consistency of string theory.

The way supersymmetry protects the hierarchies is the following: since for every particle there is a superpartner with the same mass, any loop in a radiative correction is cancelled by the loop corresponding to its superpartner, rendering the theory UV finite.

Since no superpartners have yet been observed, if supersymmetry exists it must be broken (through a so-called soft term, which breaks supersymmetry without ruining its helpful features). The simplest models of this breaking require that the energy of the superpartners not be too high; in these cases, supersymmetry is expected to be observed by experiments at the Large Hadron Collider.

See also

- | | |
|--|---|
| <ul style="list-style-type: none"> • List of quantum field theories • Feynman path integral • Quantum chromodynamics • Quantum electrodynamics • Quantum flavordynamics • Quantum geometrodynamics • Quantum hydrodynamics • Quantum magnetodynamics • Quantum triviality | <ul style="list-style-type: none"> • Basic concepts of quantum mechanics • Relationship between string theory and quantum field theory • Abraham-Lorentz force • Form factor • Photon polarization • Theoretical and experimental justification for the Schrödinger equation • Invariance mechanics • Green-Kubo relations • Green's function (many-body theory) |
|--|---|

- Schwinger-Dyson equation
- Relation between Schrödinger's equation and the path integral formulation of quantum mechanics
- Common integrals in quantum field theory

Notes

- [1] Weinberg, S. *Quantum Field Theory*, Vols. I to III, 2000, Cambridge University Press: Cambridge, UK.
- [2] Abraham Pais, *Inward Bound: Of Matter and Forces in the Physical World* ISBN 0198519974. Pais recounts how his astonishment at the rapidity with which Feynman could calculate using his method. Feynman's method is now part of the standard methods for physicists.

Suggested reading for the layman

- Gribbin, John ; *Q is for Quantum: Particle Physics from A to Z*, Weidenfeld & Nicolson (1998) [ISBN 0297817523] (<http://www.amazon.com/Q-QUANTUM-Encyclopedia-Particle-Physics/dp/0684863154/>)
- Feynman, Richard ; *The Character of Physical Law* (<http://www.amazon.com/Character-Physical-Messenger-Lectures-1964/dp/0262560038/>)
- Feynman, Richard ; *QED* (<http://www.amazon.com/QED-Strange-Princeton-Science-Library/dp/0691125759/>)

Suggested reading

- Wilczek, Frank ; *Quantum Field Theory*, Review of Modern Physics 71 (1999) S85-S95. Review article written by a master of Q.C.D., *Nobel laureate 2003* (<http://nobelprize.org/physics/laureates/2004/wilczek-autobio.html>). Full text available at : [hep-th/9803075](http://fr.arxiv.org/abs/hep-th/9803075) (<http://fr.arxiv.org/abs/hep-th/9803075>)
- Ryder, Lewis H. ; *Quantum Field Theory* (Cambridge University Press, 1985), ISBN 0-521-33859-X. Introduction to relativistic Q.F.T. for particle physics.
- Zee, Anthony ; *Quantum Field Theory in a Nutshell*, Princeton University Press (2003) ISBN 0-691-01019-6.
- Peskin, M and Schroeder, D. ; *An Introduction to Quantum Field Theory* (Westview Press, 1995) ISBN 0-201-50397-2
- Weinberg, Steven ; *The Quantum Theory of Fields* (3 volumes) Cambridge University Press (1995). A monumental treatise on Q.F.T. written by a leading expert, *Nobel laureate 1979* (<http://nobelprize.org/physics/laureates/1979/weinberg-lecture.html>).
- Loudon, Rodney ; *The Quantum Theory of Light* (Oxford University Press, 1983), ISBN 0-19-851155-8
- Greiner, Walter and Müller, Berndt (2000). *Gauge Theory of Weak Interactions*. Springer. ISBN 3-540-67672-4.
- Paul H. Frampton, *Gauge Field Theories*, Frontiers in Physics, Addison-Wesley (1986), Second Edition, Wiley (2000).
- Gordon L. Kane (1987). *Modern Elementary Particle Physics*. Perseus Books. ISBN 0-201-11749-5.
- Yndurain, Francisco Jose; *Relativistic Quantum Mechanics and Introduction to Field Theory* (Springer, 1 edition 1996), ISBN 978-3540604532

- Kleinert, Hagen and Verena Schulte-Frohlinde, *Critical Properties of φ^4 -Theories*, World Scientific (Singapur, 2001) (<http://www.worldscibooks.com/physics/4733.html>); Paperback ISBN 981-02-4658-7 (also available online (<http://www.physik.fu-berlin.de/~kleinert/re.html#B6>))
- Kleinert, Hagen, *Multivalued Fields in in Condensed Matter, Electrodynamics, and Gravitation*, World Scientific (Singapore, 2008) (<http://www.worldscibooks.com/physics/6742.html>) (also available online (<http://www.physik.fu-berlin.de/~kleinert/re.html#B9>))
- Itzykson, Claude and Zuber, Jean Bernard (1980). *Quantum Field Theory*. McGraw-Hill International Book Co.,. ISBN 0-07-032071-3.
- Bogoliubov, Nikolay, Shirkov, Dmitry (1982). *Quantum Fields*. Benjamin-Cummings Pub. Co. ISBN 0805309837.

Advanced reading

- N. N. Bogoliubov, A. A. Logunov, A. I. Oksak, I. T. Todorov (1990): *General Principles of Quantum Field Theory*. Dordrecht; Boston, Kluwer Academic Publishers. ISBN 079230540X. ISBN 978-0792305408.

External links

- Free condensed matter books and notes (<http://www.freebookcentre.net/Physics/Condensed-Matter-Books.html>).
- Siegel, Warren ; *Fields* (<http://insti.physics.sunysb.edu/~siegel/errata.html>) (also available from arXiv:hep-th/9912205)
- 't Hooft, Gerard ; *The Conceptual Basis of Quantum Field Theory*, Handbook of the Philosophy of Science, Elsevier (to be published). Review article written by a master of gauge theories, laureate 1999 (<http://nobelprize.org/physics/laureates/1999/thooft-autobio.html>"Nobel). Full text available in (<http://www.phys.uu.nl/~thooft/lectures/basisqft.pdf>"here").
- Srednicki, Mark ; *Quantum Field Theory* (<http://gabriel.physics.ucsb.edu/~mark/qft.html>)
- Kuhlmann, Meinard ; *Quantum Field Theory* (<http://plato.stanford.edu/entries/quantum-field-theory/>), Stanford Encyclopedia of Philosophy
- Quantum field theory textbooks: a list with links to amazon.com (<http://motls.blogspot.com/2006/01/qft-didactics.html>)
- Pedagogic Aids to Quantum Field Theory (<http://quantumfieldtheory.info>). Click on the link "Introduction" for a simplified introduction to QFT suitable for someone familiar with quantum mechanics.

Quantum chromodynamics

Quantum chromodynamics (abbreviated as QCD) is a theory of the strong interaction (color force), a fundamental force describing the interactions of the quarks and gluons making up hadrons (such as the proton, neutron or pion). It is the study of the SU(3) Yang–Mills theory of color-charged fermions (the quarks). QCD is a quantum field theory of a special kind called a non-abelian gauge theory. It is an important part of the Standard Model of particle physics. A huge body of experimental evidence for QCD has been gathered over the years.

QCD enjoys two peculiar properties:

- **Asymptotic freedom**, which means that in very high-energy reactions, quarks and gluons interact very weakly. This prediction of QCD was first discovered in the early 1970s by David Politzer and by Frank Wilczek and David Gross. For this work they were awarded the 2004 Nobel Prize in Physics.
- **Confinement**, which means that the force between quarks does not diminish as they are separated. Because of this, it would take an infinite amount of energy to separate two quarks; they are forever bound into hadrons such as the proton and the neutron. Although analytically unproven, confinement is widely believed to be true because it explains the consistent failure of free quark searches, and it is easy to demonstrate in lattice QCD.

Moreover: the above-mentioned two properties are *continuous* all the way, i.e. there is no phase-transition line separating them.

Terminology

The word *quark* was coined by American physicist Murray Gell-Mann (b. 1929) in its present sense, the word having been taken from the phrase "Three quarks for Muster Mark" in *Finnegans Wake* by James Joyce. Gell-Mann wrote in a private letter of June 27, 1978, to the editor of the Oxford English Dictionary that he had been influenced by Joyce's words: "The allusion to three quarks seemed perfect" (originally there were only three subatomic quarks.) Gell-Mann, however, wanted to pronounce the word with (ô) not (ä), as Joyce seemed to indicate by rhyming words in the vicinity such as *Mark*. Gell-Mann got around that "by supposing that one ingredient of the line 'Three quarks for Muster Mark' was a cry of 'Three quarts for Mister . . . ' heard in H.C. Earwicker's pub," a plausible suggestion given the complex punning in Joyce's novel. ^[1]

The three kinds of charge in QCD (as opposed to one in Quantum electrodynamics or QED) are usually referred to as "color charge" by loose analogy to the three kinds of color (red, green and blue) perceived by humans. Since the theory of electric charge is dubbed "electrodynamics", the Greek word "chroma" Χρώμα (meaning color) is applied to the theory of color charge, "chromodynamics".

Lagrangian

The dynamics of the quarks and gluons are controlled by the quantum chromodynamics Lagrangian. The gauge invariant QCD Lagrangian is

$$\begin{aligned}\mathcal{L}_{\text{QCD}} &= \bar{\psi}_i (i\gamma^\mu (D_\mu)_{ij} - m \delta_{ij}) \psi_j - \frac{1}{4} G_{\mu\nu}^a G_a^{\mu\nu} \\ &= \bar{\psi}_i (i\gamma^\mu \partial_\mu - m) \psi_i - g G_\mu^a \bar{\psi}_i \gamma^\mu T_{ij}^a \psi_j - \frac{1}{4} G_{\mu\nu}^a G_a^{\mu\nu},\end{aligned}$$

where $\psi_i(x)$ is the quark field, a dynamical function of space-time, in the fundamental representation of the SU(3) gauge group, indexed by i, j, \dots ; $G_\mu^a(x)$ are the gluon fields, also a dynamical function of space-time, in the adjoint representation of the SU(3) gauge group, indexed by a, b, \dots ; γ^μ are the Dirac matrices, connecting the spinor representation to the vector representation of the Lorentz group; and T_{ij}^a are the generators, connecting the fundamental, antifundamental and adjoint representations of the SU(3) gauge group. The Gell-Mann matrices provide one such representation for the generators.

The symbol $G_{\mu\nu}^a$ represents the gauge invariant gluonic field strength tensor, analogous to the electromagnetic field strength tensor, $F^{\mu\nu}$, in Electrodynamics. It is given by

$$G_{\mu\nu}^a = \partial_\mu G_\nu^a - \partial_\nu G_\mu^a - gf^{abc} G_\mu^b G_\nu^c,$$

where f^{abc} are the structure constants of SU(3). Note that the rules to move-up or pull-down the a, b , or c indexes are *trivial*, (+.....+), so that $f^{abc} = f_{abc}$, whereas for the μ or ν indexes one has the non-trivial *relativistic* rules, corresponding e.g. to the signature (+---). Furthermore, for mathematicians, according to this formula the gluon colour field can be represented by a SU(3)-Lie algebra-valued "curvature"-2-form $\mathbf{G} = d\tilde{\mathbf{G}} - g \tilde{\mathbf{G}} \wedge \tilde{\mathbf{G}}$, where $\tilde{\mathbf{G}}$ is a "vector potential"-1-form corresponding to \mathbf{G} and \wedge is the (antisymmetric) "wedge product" of this algebra, producing the "structure constants" f^{abc} .

The constants m and g control the quark mass and coupling constants of the theory, subject to renormalization in the full quantum theory.

An important theoretical notion concerning the final term of the above Lagrangian is the *Wilson loop* variable. This loop variable plays a most-important role in discretized forms of the QCD (see lattice QCD), and more generally, it distinguishes confined and deconfined states of a gauge theory. It was introduced by the Noble-prize winner Kenneth G. Wilson and is treated in a separate article.

History

With the invention of bubble chambers and spark chambers in the 1950s, experimental particle physics discovered a large and ever-growing number of particles called hadrons. It seemed that such a large number of particles could not all be fundamental. First, the particles were classified by charge and isospin by Eugene Wigner and Werner Heisenberg; then, in 1953, according to strangeness by Murray Gell-Mann and Kazuhiko Nishijima. To gain greater insight, the hadrons were sorted into groups having similar properties and masses using the *eightfold way*, invented in 1961 by Gell-Mann and Yuval Ne'eman. Gell-Mann and George Zweig, correcting an earlier approach of Shoichi Sakata, went on to propose in 1963 that the structure of the groups could be explained by the existence of three flavours of smaller particles inside the hadrons: the quarks.

Perhaps the first remark that quarks should possess an additional quantum number was made^[2] as a short footnote in the preprint of Boris Struminsky^[3] in connection with Ω^- hyperon composed of three strange quarks with parallel spins (this situation was strange, because since quarks are fermions, such combination is forbidden by the Pauli exclusion principle):

Three identical quarks cannot form an antisymmetric S-state. In order to realize an antisymmetric orbital S-state, it is necessary for the quark to have an additional quantum number.

- B. V. Struminsky, *Magnetic moments of barions in the quark model*, JINR-Preprint P-1939, Dubna, Submitted on January 7, 1965

Boris Stryminsky was a PhD student of Nikolay Bogolyubov and the problem considered in his preprint was formulated by Nikolay Bogolyubov, who advised Boris Struminsky in this research. In the beginning of 1965, Nikolay Bogolyubov, Boris Struminsky and Albert Tavchelimidze wrote a preprint with a more detailed discussion of the additional quark quantum degree of freedom^[4]. This work was also presented by Albert Tavchelimidze at an international conference in Trieste (Italy), in May 1965^[5] [6].

Similar mysterious situation was with the Δ^{++} baryon; in the quark model, it is composed of three up quarks with parallel spins. However, since quarks are fermions, this combination is forbidden by the Pauli exclusion principle. In 1965, Moo-Young Han with Yoichiro Nambu and Oscar W. Greenberg independently resolved the problem by proposing that quarks possess an additional SU(3) gauge degree of freedom, later called colour charge. Han and Nambu noted that quarks might interact via an octet of vector gauge bosons: the gluons.

Since free quark searches consistently failed to turn up any evidence for the new particles, and because an elementary particle back then was *defined* as a particle which could be separated and isolated, Gell-Mann often said that quarks were merely convenient mathematical constructs, not real particles. The meaning of this statement was usually clear in context: he meant quarks are confined. But he also was implying that the strong interactions could probably not be fully described by quantum field theory.

Richard Feynman argued that high energy experiments showed quarks are real particles: he called them *partons* (since they were parts of hadrons). By particles, Feynman meant objects which travel along paths, elementary particles in a field theory.

The difference between Feynman's and Gell-Mann's approaches reflected a deep split in the theoretical physics community. Feynman thought the quarks have a distribution of position or momentum, like any other particle, and he (correctly) believed that the diffusion of parton momentum explained diffractive scattering. Although Gell-Mann believed that certain quark charges could be localized, he was open to the possibility that the quarks themselves could not be localized because space and time break down. This was the more radical approach of S-matrix theory.

James Bjorken proposed that pointlike partons would imply certain relations should hold in deep inelastic scattering of electrons and protons, which were spectacularly verified in experiments at SLAC in 1969. This led physicists to abandon the S-matrix approach for the strong interactions.

The discovery of asymptotic freedom in the strong interactions by David Gross, David Politzer and Frank Wilczek allowed physicists to make precise predictions of the results of many high energy experiments using the quantum field theory technique of perturbation

theory. Evidence of gluons was discovered in three jet events at PETRA in 1979. These experiments became more and more precise, culminating in the verification of perturbative QCD at the level of a few percent at the LEP in CERN.

The other side of asymptotic freedom is confinement. Since the force between color charges does not decrease with distance, it is believed that quarks and gluons can never be liberated from hadrons. This aspect of the theory is verified within lattice QCD computations, but is not mathematically proven. One of the Millennium Prize Problems announced by the Clay Mathematics Institute requires a claimant to produce such a proof. Other aspects of non-perturbative QCD are the exploration of phases of quark matter, including the quark-gluon plasma.

The relation between the short-distance particle limit and the confining long-distance limit is one of the topics recently explored using string theory, the modern form of S-matrix theory.^{[7] [8]}

The theory



Unsolved problems in physics: *QCD in the non-perturbative regime*:

- **Confinement**: the equations of QCD remain unsolved at energy scales relevant for describing atomic nuclei. How does QCD give rise to the physics of nuclei and nuclear constituents?
- **Quark matter**: the equations of QCD predict that a sea of quarks and gluons should be formed at high temperature and density. What are the properties of this phase of matter?

Some definitions

Every field theory of particle physics is based on certain symmetries of nature whose existence is deduced from observations. These can be

- local symmetries, that is the symmetry acts independently at each point in space-time. Each such symmetry is the basis of a gauge theory and requires the introduction of its own gauge bosons.
- global symmetries, which are symmetries whose operations must be simultaneously applied to all points of space-time.

QCD is a gauge theory of the SU(3) gauge group obtained by taking the color charge to define a local symmetry.

Since the strong interaction does not discriminate between different flavors of quark, QCD has approximate **flavor symmetry**, which is broken by the differing masses of the quarks.

There are additional global symmetries whose definitions require the notion of chirality, discrimination between left and right-handed. If the spin of a particle has a positive projection on its direction of motion then it is called left-handed; otherwise, it is right-handed. Chirality and handedness are not the same, but become approximately equivalent at high energies.

- **Chiral** symmetries involve independent transformations of these two types of particle.
- **Vector** symmetries (also called diagonal symmetries) mean the same transformation is applied on the two chiralities.

- **Axial** symmetries are those in which one transformation is applied on left-handed particles and the inverse on the right-handed particles.

The symmetry groups

The color group $SU(3)$ corresponds to the local symmetry whose gauging gives rise to QCD. The electric charge labels a representation of the local symmetry group $U(1)$ which is gauged to give QED: this is an abelian group. If one considers a version of QCD with N_f flavors of massless quarks, then there is a global (chiral) flavor symmetry group $SU_L(N_f) \times SU_R(N_f) \times U_B(1) \times U_A(1)$. The chiral symmetry is spontaneously broken by the QCD vacuum to the vector (L+R) $SU_V(N_f)$ with the formation of a chiral condensate. The vector symmetry, $U_B(1)$ corresponds to the baryon number of quarks and is an exact symmetry. The axial symmetry $U_A(1)$ is exact in the classical theory, but broken in the quantum theory, an occurrence called an anomaly. Gluon field configurations called instantons are closely related to this anomaly.

There are two different types of $SU(3)$ symmetry: there is the symmetry that acts on the different colors of quarks, and this is an exact gauge symmetry mediated by the gluons, and there is also a flavor symmetry which rotates different flavors of quarks to each other, or *flavor* $SU(3)$. Flavor $SU(3)$ is an approximate symmetry of the vacuum of QCD, and is not a fundamental symmetry at all. It is an accidental consequence of the small mass of the three lightest quarks.

In the QCD vacuum there are vacuum condensates of all the quarks whose mass is less than the QCD scale. This includes the up and down quarks, and to a lesser extent the strange quark, but not any of the others. The vacuum is symmetric under $SU(2)$ isospin rotations of up and down, and to a lesser extent under rotations of up, down and strange, or full flavor group $SU(3)$, and the observed particles make isospin and $SU(3)$ multiplets.

The approximate flavor symmetries do have associated gauge bosons, observed particles like the rho and the omega, but these particles are nothing like the gluons and they are not massless. They are emergent gauge bosons in an approximate string description of QCD.

The fields

Quarks are massive spin-1/2 fermions which carry a color charge whose gauging is the content of QCD. Quarks are represented by Dirac fields in the fundamental representation **3** of the gauge group $SU(3)$. They also carry electric charge (either -1/3 or 2/3) and participate in weak interactions as part of weak isospin doublets. They carry global quantum numbers including the baryon number, which is 1/3 for each quark, hypercharge and one of the flavor quantum numbers.

Gluons are spin-1 bosons which also carry color charges, since they lie in the adjoint representation **8** of $SU(3)$. They have no electric charge, do not participate in the weak interactions, and have no flavor. They lie in the singlet representation **1** of all these symmetry groups.

Every quark has its own antiquark. The charge of each antiquark is exactly the opposite of the corresponding quark.

The dynamics

According to the rules of quantum field theory, and the associated Feynman diagrams, the above theory gives rise to three basic interactions: a quark may emit (or absorb) a gluon, a gluon may emit (or absorb) a gluon, and two gluons may directly interact. This contrasts with QED, in which only the first kind of interaction occurs, since photons have no charge. Diagrams involving Faddeev-Popov ghosts must be considered too.

Methods

Further analysis of the content of the theory is complicated. Various techniques have been developed to work with QCD. Some of them are discussed briefly below.

Perturbative QCD

This approach is based on asymptotic freedom, which allows perturbation theory to be used accurately in experiments performed at very high energies. Although limited in scope, this approach has resulted in the most precise tests of QCD to date.

Lattice QCD

Among non-perturbative approaches to QCD, the most well established one is lattice QCD. This approach uses a discrete set of space-time points (called the lattice) to reduce the analytically intractable path integrals of the continuum theory to a very difficult numerical computation which is then carried out on supercomputers like the QCDOC which was constructed for precisely this purpose. While it is a slow and resource-intensive approach, it has wide applicability, giving insight into parts of the theory inaccessible by other means. Lattice QCD is not, however, useful at high density and low temperature (e.g. nuclear matter or the interior of neutron stars).

$1/N$ expansion

A well-known approximation scheme, the $1/N$ expansion, starts from the premise that the number of colors is infinite, and makes a series of corrections to account for the fact that it is not. Until now it has been the source of qualitative insight rather than a method for quantitative predictions. Modern variants include the AdS/CFT approach.

Effective theories

For specific problems some theories may be written down which seem to give qualitatively correct results. In the best of cases, these may then be obtained as systematic expansions in some parameter of the QCD Lagrangian. Among the best such effective models one should now count chiral perturbation theory (which expands around light quark masses near zero), heavy quark effective theory (which expands around heavy quark mass near infinity), and soft-collinear effective theory (which expands around large ratios of energy scales). Other less accurate models are the Nambu-Jona-Lasinio model and the chiral model.

Experimental tests

The notion of quark flavours was prompted by the necessity of explaining the properties of hadrons during the development of the quark model. The notion of colour was necessitated by the puzzle of the Δ^{++} . This has been dealt with in the section on the history of QCD.

The first evidence for quarks as real constituent elements of hadrons was obtained in deep inelastic scattering experiments at SLAC. The first evidence for gluons came in three jet events at PETRA.

Good quantitative tests of perturbative QCD are

- the running of the QCD coupling as deduced from many observations
- scaling violation in polarized and unpolarized deep inelastic scattering
- vector boson production at colliders (this includes the Drell-Yan process)
- jet cross sections in colliders
- event shape observables at the LEP
- heavy-quark production in colliders

Quantitative tests of non-perturbative QCD are fewer, because the predictions are harder to make. The best is probably the running of the QCD coupling as probed through lattice computations of heavy-quarkonium spectra. There is a recent claim about the mass of the heavy meson B_c [9]. Other non-perturbative tests are currently at the level of 5% at best. Continuing work on masses and form factors of hadrons and their weak matrix elements are promising candidates for future quantitative tests. The whole subject of quark matter and the quark-gluon plasma is a non-perturbative test bed for QCD which still remains to be properly exploited.

See also

- For overviews, see Standard Model, its field theoretical formulation, strong interactions, quarks and gluons, hadrons, confinement, QCD matter, or quark-gluon plasma.
- For details, see gauge theory, quantization procedure including BRST and Faddeev-Popov ghosts. A more general category is quantum field theory.
- For techniques, see Lattice QCD, $1/N$ expansion, perturbative QCD, heavy quark effective theory, chiral models, and the Nambu and Jona-Lasinio model.
- For experiments, see quark search experiments, deep inelastic scattering, jet physics, quark-gluon plasma.

Footnotes

- [1] Gell-Mann, Murray (1995). *The Quark and the Jaguar*. Owl Books. ISBN 978-0805072532.
- [2] F. Tkachov, A contribution to the history of quarks: Boris Struminsky's 1965 JINR publication (<http://arxiv.org/abs/0904.0343>)
- [3] B. V. Struminsky, Magnetic moments of baryons in the quark model. JINR-Preprint P-1939, Dubna, Russia. Submitted on January 7, 1965.
- [4] N. Bogolubov, B. Struminsky, A. Tavkhelidze. On composite models in the theory of elementary particles. JINR Preprint D-1968, Dubna 1965.
- [5] A. Tavkhelidze. Proc. Seminar on High Energy Physics and Elementary Particles, Trieste, 1965, Vienna IAEA, 1965, p. 763.
- [6] V. A. Matveev and A. N. Tavkhelidze (INR, RAS, Moscow) The quantum number color, colored quarks and QCD (<http://www.inr.ru/quantum.html>) (Dedicated to the 40th Anniversary of the Discovery of the Quantum Number Color). Report presented at the 99th Session of the JINR Scientific Council, Dubna, 19-20 January 2006.

- [7] J. Polchinski, M. Strassler (2002). "Hard Scattering and Gauge/String duality". *Physical Review Letters* **88**: 31601. doi: 10.1103/PhysRevLett.88.031601 (<http://dx.doi.org/10.1103/PhysRevLett.88.031601>).
- [8] Brower, Mathur, Tan, *Glueball Spectrum for QCD from AdS Supergravity duality*, arXiv:hep-th/0003115.
- [9] <http://www.aip.org/pnu/2005/split/731-1.html>

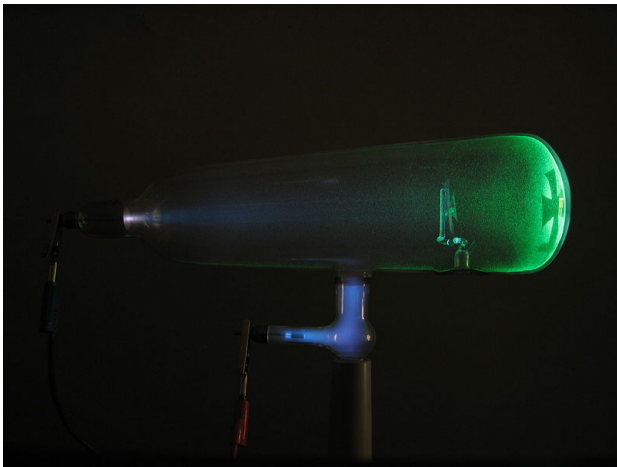
References

- Greiner, Walter; Schäfer, Andreas (1994). *Quantum Chromodynamics*. Springer. ISBN 0-387-57103-5.
- Halzen, Francis; Martin, Alan (1984). *Quarks & Leptons: An Introductory Course in Modern Particle Physics*. John Wiley & Sons. ISBN 0-471-88741-2.
- Creutz, Michael (1985). *Quarks, Gluons and Lattices*. Cambridge University Press. ISBN 978-0521315357.

External links

- Particle data group (<http://pdg.lbl.gov/>)
 - The millennium prize (<http://www.claymath.org/millennium/>) for proving confinement (<http://www.claymath.org/millennium/>)
 - Ab Initio Determination of Light Hadron Masses (<http://www.sciencemag.org/cgi/content/abstract/322/5905/1224>)
 - Andreas S Kronfeld (<http://www.sciencemag.org/cgi/content/summary/322/5905/1198>) *The Weight of the World Is Quantum Chromodynamics*
 - Andreas S Kronfeld (http://www.iop.org/EJ/article/1742-6596/125/1/012067/jpconf8_125_012067.pdf?request-id=f9ccdf0d-ee26-4856-99fb-ce5bfef07c4c) *Quantum chromodynamics with advanced computing*
 - Standard model gets right answer (http://www.sciencenews.org/view/generic/id/38788/title/Standard_model_gets_right_answer_for_proton,_neutron_masses)
-

Electron

Electron	
	
Experiments with Crookes tube first demonstrated the particle nature of electrons. In this illustration, the profile of the cross-shaped target is projected against the tube face at right by a beam of electrons. ^[1]	
Composition:	Elementary particle ^[2]
Family:	Fermion
Group:	Lepton
Generation:	First
Interaction:	Gravity, Electromagnetic, Weak
Antiparticle:	Positron (also called antielectron)
Theorized:	Richard Laming (1838-51), ^[3] G. Johnstone Stoney (1874) and others. ^{[4] [5]}
Discovered:	J. J. Thomson (1897) ^[6]
Symbol(s):	e^- , β^-
Mass:	$9.10938215(45)\times 10^{-31}\text{ kg}$ ^[7] $5.4857990943(23)\times 10^{-4}\text{ u}$ ^[7] $[1822.88850204(77)]^{-1}\text{ u}$ ^[8] $0.510998910(13)\text{ MeV}/c^2$ ^[7]
Electric charge:	-1 e ^[9] $-1.602176487(40)\times 10^{-19}\text{ C}$ ^[7]
Magnetic moment:	$-1.00115965218111\text{ }\mu_{\text{B}}$ ^[7]
Spin:	$\frac{1}{2}$

The **electron** is a subatomic particle that carries a negative electric charge. It has no known substructure and is believed to be a point particle.^[2] Electrons participate in gravitational, electromagnetic and weak interactions. Like its rest mass and elementary charge, the intrinsic angular momentum (or spin) of an electron has a constant value. In the collision of an electron and a positron, the electron's antiparticle, both are annihilated. An

electron-positron pair can be produced from gamma ray photons with sufficient energy.^[10]

The concept of an indivisible amount of electric charge was theorized to explain the chemical properties of atoms, beginning in 1838 by British natural philosopher Richard Laming;^[4] the name *electron* was introduced for this charge in 1894 by Irish physicist George Johnstone Stoney. The electron was identified as a particle in 1897 by J. J. Thomson and his team of British physicists.^{[6] [11]} Electrons are identical particles that belong to the first generation of the lepton particle family. Electrons have quantum mechanical properties of both a particle and a wave, so they can collide with other particles and be diffracted like light. Each electron occupies a quantum state that describes its random behavior upon measuring a physical parameter, such as its energy or spin orientation. Because an electron is a type of fermion, no two electrons can occupy the same quantum state; this property is known as the Pauli exclusion principle.^[12]

In many physical phenomena, such as electricity, magnetism, and thermal conductivity, electrons play an essential role. An electron generates a magnetic field while moving, and it is deflected by external magnetic fields. When an electron is accelerated, it can absorb or radiate energy in the form of photons. Electrons, together with atomic nuclei made of protons and neutrons, make up atoms. However, electrons contribute less than 0.06% to an atom's total mass. The attractive Coulomb force between an electron and a proton causes electrons to be bound into atoms. The exchange or sharing of the electrons between two or more atoms is the main cause of chemical bonding.^[13]

Electrons were created by the Big Bang, and they can be annihilated during stellar nucleosynthesis. Electrons are produced by cosmic rays entering the atmosphere and are predicted to be created by Hawking radiation at the event horizon of a black hole. Radioactive isotopes can release an electron from an atomic nucleus as a result of negative beta decay. Laboratory instruments are capable of containing and observing individual electrons, while telescopes can detect electron plasma by its energy emission. Electron plasma has multiple applications, including welding, cathode ray tubes, electron microscopes, radiation therapy, lasers and particle accelerators.

History

The ancient Greeks noticed that amber, a gemstone that is formed from the hardened sap of trees, attracted small objects when rubbed with fur; apart from lightning, this phenomenon was man's earliest known experience of electricity.^[14] In his 1600 treatise *De Magnete*, the English physician William Gilbert coined the New Latin term *electricus*, to refer to this property of attracting small objects after being rubbed.^[15] Both *electric* and *electricity* are derived from the Latin *ēlectrum*, which came from the Greek word *ēlektron* (ἤλεκτρον) for amber.

During the period 1838–51, British natural philosopher Richard Laming conceived the idea that an atom is composed of a core of matter surrounded by subatomic particles that had unit electric charges.^[3] Beginning in 1846, German physicist William Weber theorized that electricity was composed of positively and negatively charged fluids, and their interaction was governed by the inverse square law. After studying the phenomenon of electrolysis in 1874, Irish physicist George Johnstone Stoney suggested that there existed a "single definite quantity of electricity", the charge of a monovalent ion. He was able to estimate the value of this elementary charge *e* by means of Faraday's laws of electrolysis.^[16] However, Stoney believed these charges were permanently attached to atoms and could not be

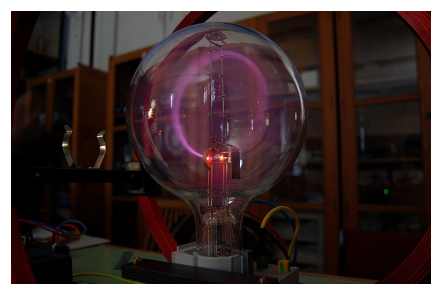
removed. In 1881, German physicist Hermann von Helmholtz argued that both positive and negative charges were divided into elementary parts, each of which "behaves like atoms of electricity".^[4]

In 1894, Stoney coined the term *electron* to represent these elementary charges, saying, "...an estimate was made of the actual amount of this most remarkable fundamental unit of electricity, for which I have since ventured to suggest the name *electron*."^[17] The English name *electron* is a combination of the word *electric* and the suffix *-on*, with the latter now used to designate a subatomic particle, such as a proton or neutron.^{[18] [19]}

At the end of the nineteenth century, the various scientific concepts came together to form a unified theory based upon the electron as a fundamental component of matter.^[5]

Discovery

The German physicist Johann Wilhelm Hittorf undertook the study of electrical conductivity in rarified gases. In 1869, he discovered a glow emitted from the cathode that increased in size with decrease in gas pressure. In 1876, the German physicist Eugen Goldstein showed that the rays from this glow cast a shadow, and he dubbed them cathode rays.^[21] During the 1870s, the English chemist and physicist Sir William Crookes developed the first cathode ray tube to have a high vacuum inside.^[22] He then showed that the



A beam of electrons is being deflected in a circle by a magnetic field.^[20]

luminescence rays appearing within the tube carried energy and moved from the cathode to the anode. Furthermore, by applying a magnetic field, he was able to deflect the rays, thereby demonstrating that the beam behaved as though it were negatively charged.^{[23] [24]} In 1879, he proposed that these properties could be explained by what he termed 'radiant matter'. He suggested that this was a fourth state of matter, consisting of negatively charged molecules that were being projected with high velocity from the cathode.^[25]

The German-born British physicist Arthur Schuster expanded upon Crookes's experiments by placing metal plates in parallel to the cathode rays and applying an electrical potential between the plates. The field deflected the rays toward the positive plate, providing further evidence that the rays carried negative charge. By measuring the amount of deflection for a given level of current, in 1890 Schuster was able to estimate the charge-to-mass ratio of the ray components. However, this produced such an unexpectedly large value that little credence was given to his calculations at the time.^[23]

In 1896, the British physicist J. J. Thomson, with his colleagues John S. Townsend and H. A. Wilson,^[6] performed experiments indicating that cathode rays really were unique particles, rather than waves, atoms or molecules as was believed earlier. Thomson made good estimates of both the charge e and the mass m , finding that cathode ray particles, which he called "corpuscles," had perhaps one thousandth of the mass of the least massive ion known: hydrogen. He showed that their charge to mass ratio, e/m , was independent of cathode material. He further showed that the negatively charged particles produced by radioactive materials, by heated materials and by illuminated materials were universal.^[26] The name electron was again proposed for these particles by the Irish physicist George F. Fitzgerald, and the name has since gained universal acceptance.^[23]

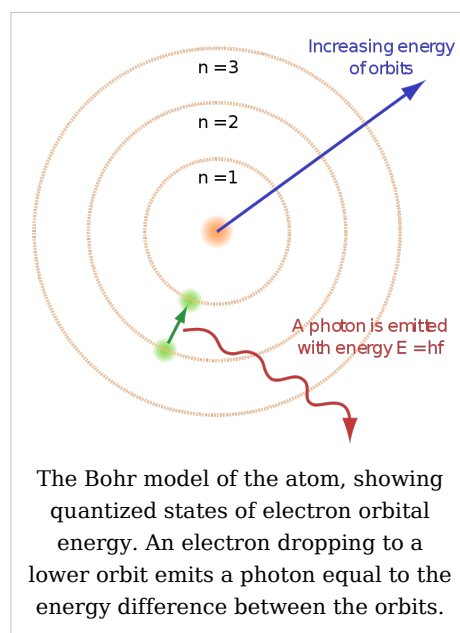
While studying naturally fluorescing minerals in 1896, the French physicist Henri Becquerel discovered that they emitted radiation without any exposure to an external energy source. These radioactive materials became the subject of much interest by scientists, including the New Zealander physicist Ernest Rutherford who discovered they emitted particles. He designated these particles alpha and beta, based on their ability to penetrate matter.^[27] In 1900, Becquerel showed that the beta rays emitted by radium could be deflected by an electric field, and that their mass-to-charge ratio was the same as for cathode rays.^[28] This evidence strengthened the view that electrons existed as components of atoms.^{[29] [30]}

The electron's charge was more carefully measured by the American physicist Robert Millikan in his oil-drop experiment of 1909, which was published in 1911. This experiment used an electric field to prevent a charged droplet of oil from falling as a result of gravity. This device could measure the electric charge from as few as 1-150 ions with an error margin of less than 0.3%. Comparable experiments had been done earlier by Thomson's team, using clouds of charged water droplets generated by electrolysis,^[6] and in 1911 by Abram Ioffe, who independently obtained the same result as Millikan using charged microparticles of metals, then published his results in 1913.^{[31] [32]} However, oil drops were more stable than water drops due to their slower evaporation rate, and thus more suited to precise experimentation over longer periods of time.^[33]

Around the beginning of the twentieth century, it was found that under certain conditions a fast moving charged particle caused a condensation of supersaturated water vapor along its path. In 1911, Charles Wilson used this principle to devise his cloud chamber, allowing the tracks of charged particles, such as fast-moving electrons, to be photographed. This and subsequent particle detectors allowed electrons to be studied individually, rather than in bulk as had been the case before.^[34]

Atomic theory

By 1914, experiments by physicists Ernest Rutherford, Henry Moseley, James Franck and Gustav Hertz had largely established the structure of an atom as a dense nucleus of positive charge surrounded by lower-mass electrons.^[35] In 1913, Danish physicist Niels Bohr postulated that electrons resided in quantized energy states, with the energy determined by the angular momentum of the electron's orbits about the nucleus. The electrons could move between these states, or orbits, by the emission or absorption of photons at specific frequencies. By means of these quantized orbits, he accurately explained the spectral lines of hydrogen that were formed when the gas is energized by heat or electricity.^[36] However, Bohr's model failed to account for the relative intensities of the spectral lines and it was unsuccessful in explaining the spectrum of more complex atoms.^[35]



Chemical bonds between atoms were explained by Gilbert Newton Lewis, who in 1916 proposed that a covalent bond between two atoms is maintained by a pair of electrons

shared by them.^[37] Later, in 1923, Walter Heitler and Fritz London gave the full explanation of the electron-pair formation and chemical bonding in terms of the then-recently developed quantum mechanics.^[38] In 1919, the American chemist Irving Langmuir elaborated on the Lewis' static model of the atom and suggested that all electrons were distributed in successive "concentric (nearly) spherical shells, all of equal thickness".^[39] The shells were, in turn, divided by him in a number of cells each containing one pair of electrons. With this model Langmuir was able to qualitatively explain the chemical properties of all elements in the periodic table,^[38] which were known to largely repeat themselves according to the periodic law.^[40]

In 1924, Austrian physicist Wolfgang Pauli observed that the shell-like structure of the atom could be explained by a set of four parameters that defined every quantum energy state, as long as each state was inhabited by no more than a single electron. (This prohibition against more than one electron occupying the same quantum energy state became known as the Pauli exclusion principle.)^[41] However, what physicists lacked was a physical mechanism to explain the fourth parameter, which had two possible values. This was provided by the Dutch physicists Abraham Goudsmith and George Uhlenbeck when they suggested that an electron, in addition to the angular momentum of its orbit, could possess an intrinsic angular momentum.^[35] ^[42] This property became known as spin, and it explained the previously mysterious splitting of spectral lines observed with a high-resolution spectrograph; this phenomenon is known as fine structure splitting.^[43]

Quantum mechanics

In his 1924 dissertation *Recherches sur la théorie des quanta*, French physicist Louis de Broglie hypothesized that all matter possesses a wave-particle duality similar to light.^[44] the de Broglie hypothesis. That is, under the appropriate conditions, electrons and other matter would show properties of either particles or waves. The corpuscular properties of a particle are demonstrated when it is shown to have a localized position in space at each moment in time and a trajectory that is subject to modification by external forces.^[45] The wave-like nature is observed, for example, when a beam of light is passed through parallel slits and creates interference patterns. In 1927, the interference effect was demonstrated with a beam of electrons by English physicist George Paget Thomson with a thin metal film and by American physicists Clinton Davisson and Lester Germer using a crystal of nickel.^[46]

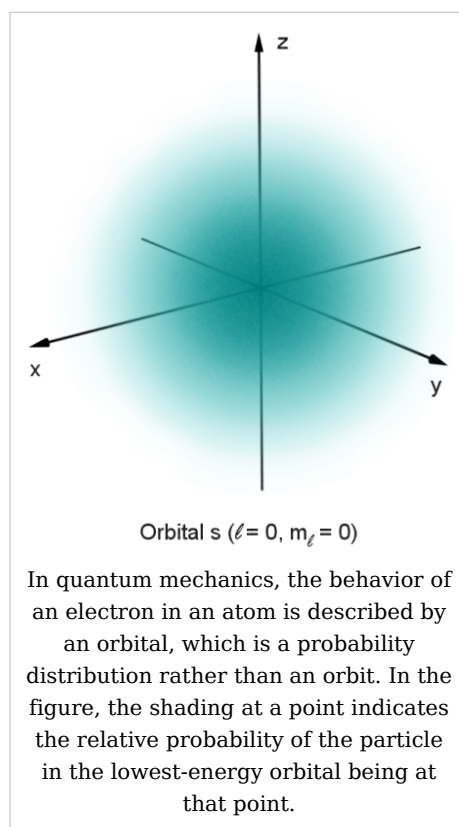
The success of de Broglie's prediction led to the publication, by Erwin Schrödinger in 1926, of the equation named after him that successfully describes how electron waves propagated.^[47] Rather than yielding a solution that determines the location of an electron over time, this wave equation can be used to predict the probability of finding an electron near a position. This approach was later called quantum mechanics, which provided an almost exact derivation to the energy states of an electron in a hydrogen atom.^[48] Once spin and the interaction between multiple electrons were considered, the quantum mechanics allowed the configuration of electrons in atoms with higher atomic numbers than hydrogen to be successfully predicted. However, for atoms with multiple electrons, the exact solution to the wave equation is much more complicated, so approximations are necessary.^[49]

In 1928, building on Wolfgang Pauli's work, Paul Dirac formulated the Dirac equation, which for the first time correctly described an electron moving at velocities close to the speed of light.^[50] In order to resolve some problems with in his relativistic equation, in 1930 Dirac developed a model of the vacuum as an infinite sea of particles having negative energy, which was dubbed the Dirac sea. This led him to predict the existence of a positron, the antimatter counterpart of the electron.^[51] This particle was discovered in 1932 by Carl D. Anderson, who proposed calling standard electrons *negatrons*, and using *electron* as a generic term to describe both the positively and negatively charged variants. This usage of the term 'negatron' is still occasionally encountered today, and it may be shortened to 'negaton'.^[52] ^[53]

The first experimental discrepancy in Dirac's theory was discovered in 1947 by Willis Lamb, working in collaboration with graduate student Robert Retherford. They found that certain quantum states of hydrogen atom, which should have the same energy, were shifted in relation to each other, the difference being the Lamb shift. About the same time, Polykarp Kusch, working with Henry M. Foley, discovered the magnetic moment of the electron is slightly larger than predicted by Dirac's theory. This small difference was later called anomalous magnetic dipole moment of the electron. To resolve these issues, a refined version of the quantum electrodynamics theory was developed by Sin-Itiro Tomonaga, Julian Schwinger and Richard P. Feynman.^[54]

Particle accelerators

With the development of the particle accelerator during the first half of the twentieth century, physicists began to delve deeper into the properties of subatomic particles.^[55] The first successful attempt to accelerate electrons using magnetic induction was made in 1942 by Donald Kerst. His initial betatron reached energies of 2.3 MeV (million electron volts), while subsequent betatrons achieved 300 MeV. In 1947, synchrotron radiation was discovered with a 70 MeV electron synchrotron at General Electric. This radiation was



caused by the acceleration of electrons, moving near the speed of light, through a magnetic field.^[56]

With a beam energy of 1.5 GeV, the first high-energy particle collider was ADONE, which began operations in 1968.^[57] This device accelerated electrons and positrons—the antiparticles of electrons—in opposite directions, effectively doubling the energy of their collision when compared to striking a static target with an electron.^[58] The Large Electron-Positron Collider (LEP) at CERN, which was operational from 1989 to 2000, achieved collision energies of 209 GeV and made important measurements for the Standard Model of particle physics.^{[59] [60]}

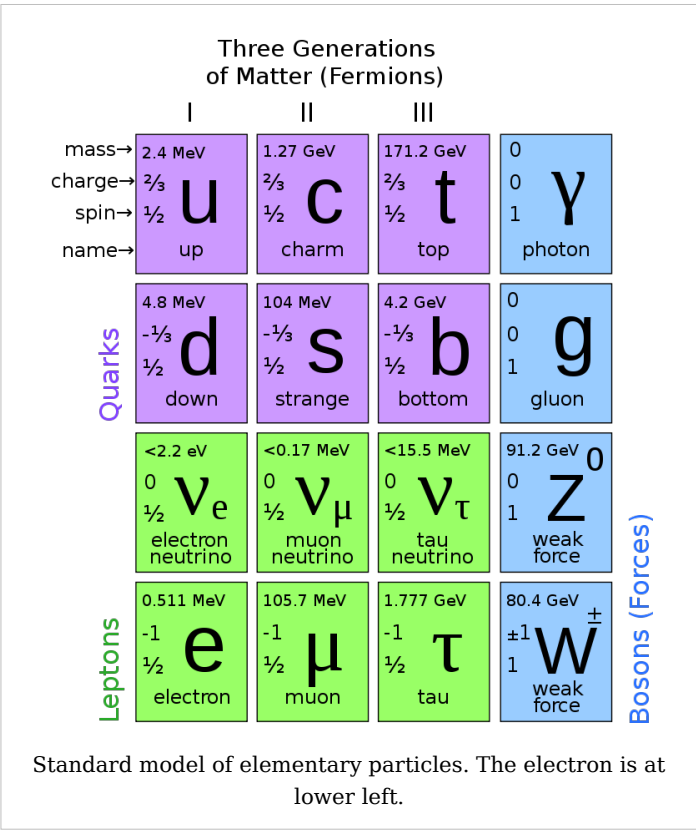
Characteristics

Classification

In the Standard Model of particle physics, electrons belong to the group of subatomic particles called leptons, which are believed to be elementary or fundamental particles. Electrons have the lowest mass of any electrically charged lepton and belong to the first-generation of fundamental particles.^[61]

The electron is an analog of the two charged leptons of the second and third generations, the muon and the tauon, respectively, which are identical in charge, spin, and interaction, but are more massive. All members of the lepton group belong to the family of fermions. This family includes all elementary particles with half-odd integer spin; the electron has spin $1/2$. Leptons differ from the other basic constituent of matter, the quarks, by their lack of strong interaction.^[62]

If the spin of the electron is oriented in the same direction as its momentum, it is called a right-handed spin; otherwise it is left-handed. Thus the same electron can have left- or right-handed spin, depending on its velocity with respect to an observer. The left-handed spin component of the electron forms a weak isospin doublet with the electron neutrino, which is an uncharged, first-generation lepton with little or no mass.^[63] The right-handed component of the electron spin is an isospin singlet.^[64]



Fundamental properties

The mass of an electron is approximately 9.109×10^{-31} kilograms,^[7] or 5.489×10^{-4} atomic mass units. Based on Einstein's principle of mass-energy equivalence, this mass corresponds to a rest energy of 0.511 MeV. The ratio between the mass of a proton and that of an electron is about 1836.^[65] This ratio is one of the fundamental constants of physics, and the Standard Model of particle physics assumes this and other constants are unchanging. Astronomical measurements show that the ratio has held the same value for at least half the age of the universe.^[66]

Electrons have an electric charge of -1.602×10^{-19} Coulomb,^[7] which is used as a standard unit of elementary charge for subatomic particles. Within the limits of experimental accuracy, the electron charge is identical to the charge of a proton, but with the opposite sign.^[67] As the symbol e is used for the constant of electric charge, the electron is commonly symbolized by e^- , where the minus sign indicates the negative charge. The positron is symbolized by e^+ because it has the same properties as the electron but with a positive rather than negative charge.^[7] ^[62]

The electron has no known substructure.^[2] ^[68] Hence, it is defined or assumed to be a point charge with no spatial extent—a point particle.^[12] Observation of a single electron in a Penning trap shows the upper limit of the particle's radius is 10^{-22} meters.^[69] The classical electron radius is 2.8179×10^{-15} m. This is the radius that is inferred from the electron's electric charge, by assuming that its mass has exclusively electrostatic origin and using the classical theory of electrodynamics alone, while ignoring quantum mechanics.^[70]

[71]

[72]

[73]

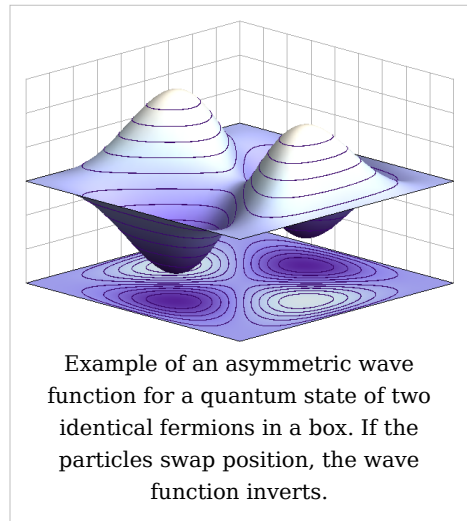
[74]

There are elementary particles that spontaneously decay into different particles. An example is the muon, which decays into an electron, a neutrino and an antineutrino, with a half life of 2.2×10^{-6} seconds. However, the electron is thought to be stable on theoretical grounds; an electron decaying into a neutrino and photon would mean that electric charge is not conserved.^[75] The experimental lower bound for the electron's mean lifetime is 4.6×10^{26} years, with a 90% confidence interval.^[76]

Quantum properties

As with all particles, electrons can act as waves. This is called the wave-particle duality and can be demonstrated using the double-slit experiment. The wave-like nature of the electron allows it to pass through two parallel slits simultaneously, rather than just one slit as would be the case for a classical particle. In quantum mechanics, the wave-like property of an electron is described mathematically by a complex-valued function, the wave function, commonly denoted by the Greek letter psi (ψ). When the absolute value of this function is squared, it gives the probability that an electron will be observed near a location—the electron density.^[77]

Electrons are identical particles because they can not be distinguished from each other by their intrinsic physical properties. In the quantum mechanics, this means that a pair of interacting electrons must be able to swap positions without an observable change to the state of the system. The wave function of fermions, including electrons, is antisymmetric, meaning that it changes sign when two electrons are swapped; that is, $\psi(r_1, r_2) = -\psi(r_2, r_1)$, where the variables r_1 and r_2 correspond to the first and second electrons, respectively. Since the absolute value is not changed by a sign swap, this corresponds to equal probabilities. Bosons, such as the photon, have symmetric wave functions instead.^[77]

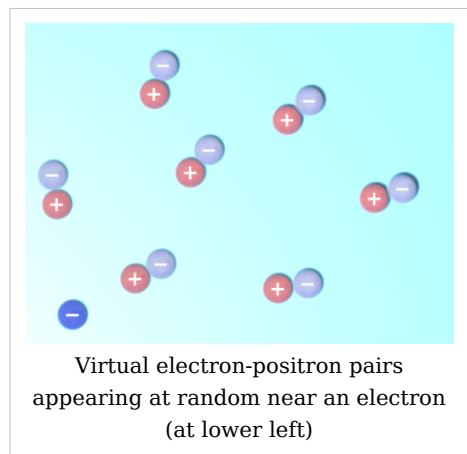


In the case of antisymmetry, solutions of the wave equation for interacting electrons result in a zero probability that each pair will occupy the same location or state. This is responsible for the Pauli exclusion principle, which precludes any two electrons from occupying the same quantum state. This principle explains many of the properties of electrons. For example, it causes groups of bound electrons to occupy different orbitals in an atom, rather than all overlapping each other in the same orbit.^[77]

Virtual particles

Physicists believe that empty space may be continually creating pairs of virtual particles, such as a positron and electron, which rapidly annihilate each other shortly thereafter.^[78] The net energy from this reaction is zero. The combination of the energy variation needed to create these particles, and the time during which they exist, fall under the threshold of detectability expressed by the Heisenberg uncertainty relation, $\Delta E \cdot \Delta t \geq \hbar$. In effect, the energy needed to create these virtual particles, ΔE , can be "borrowed" from the vacuum for a period of time, Δt , so that their product is no more than the reduced Planck constant, $\hbar \approx 6.6 \times 10^{-16}$ eV·s. Thus, for a virtual electron, Δt is at most 1.3×10^{-21} s.^[79]

While an electron-positron virtual pair is in existence, the coulomb force from the ambient electric field surrounding an electron causes a created positron to be attracted to the original electron, while a created electron experiences a repulsion. This causes the two charged virtual particles to physically separate for a brief period before merging back together, and during this period they behave like an electric dipole. The combined effect of many such pair creations is to partially shield the charge of the electron, in a process called vacuum polarization. Thus the effective charge of an electron is actually smaller than its true value, and the charge increases with decreasing distance from the electron.^{[80] [81]}



This polarization was confirmed experimentally in 1997 using the Japanese TRISTAN particle accelerator.^[82]

A comparable shielding effect is seen for the mass of the electron. The equivalent rest energy consists of the mass-energy of the "bare" particle plus the energy of the surrounding electric field. In classical physics, the energy of the electric field is dependent upon the size of the charged object, which, for a dimensionless particle, results in an infinite energy. Instead, because of vacuum fluctuations, allowance must be made for an electron-positron pair appearing in the electric field and the positron annihilating the original electron, causing the virtual electron to become a real electron. This interaction creates a negative energy imbalance that counteracts the radius-dependency of the electric field.^[83] The total mass is referred to as the renormalized mass, because a mathematical technique called renormalization is used by physicists to relate the observed mass and bare mass of the electron. This method replaces the terms used to compute the mass with the actual mass found experimentally, thereby avoiding problems with divergences in the formulas.^[84]

The electron has an intrinsic angular momentum or spin, which equals $\frac{1}{2}\hbar$ in units of \hbar , and an intrinsic magnetic moment along its spin axis.^[7] The magnitude of the spin is $\sqrt{3}\frac{1}{2}\hbar$.^[85]
[86]

^[87] A projection of the spin on any axis can only be $\pm\frac{1}{2}\hbar$; this property is usually stated by referring to the electron as a spin- $\frac{1}{2}$ particle.

The magnetic moment associated with the orbital motion of an electron in an atom is expressed in terms of the Bohr magneton,^[88]

[89]

^[90] which is a physical constant equal to $9.274\,009\,15(23) \times 10^{-24}$ joules per tesla.^[7] The intrinsic angular momentum of an electron is almost equal to one Bohr magneton, with the 0.1% difference (anomalous magnetic moment) being explained by interaction with virtual particles and antiparticles.^[91] ^[92] The extraordinarily precise agreement of this predicted difference with the experimentally determined value is viewed as one of the great achievements of the quantum electrodynamics.^[93]

In classical physics, the angular momentum and magnetic moment of an object depend upon its physical dimensions. Hence, the concept of a dimensionless electron possessing these properties is unclear. A possible explanation lies in the formation of virtual photons in the electric field generated by the electron. These photons cause the electron to shift about in a jittery fashion (known as *zitterbewegung*),^[94] which results in a net circular motion with precession. This motion produces both the spin and the magnetic moment of the electron.^[12] ^[95] In atoms, this creation of virtual photons explains the Lamb shift observed in spectral lines.^[80]

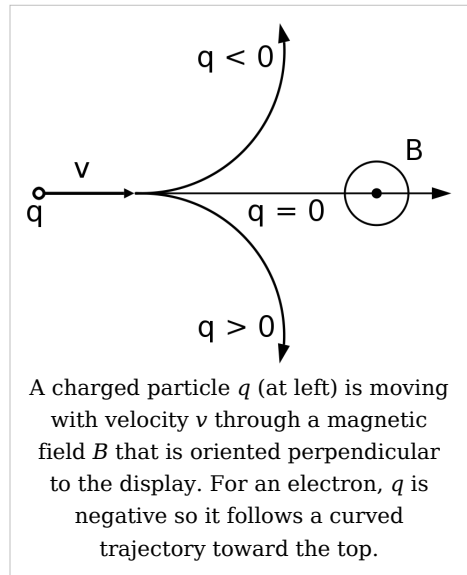
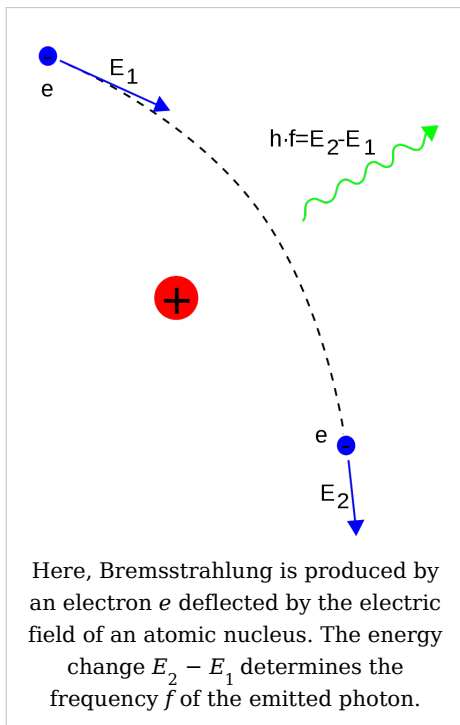
Interaction

An electron generates an electric field that exerts an attractive force on a particle with a positive charge, such as the proton, and a repulsive force on a particle with a negative charge. The strength of this force is determined by Coulomb's inverse square law.^[96] When an electron is in motion, it generates a magnetic field,^[97] which is related to the motion of electrons (the current) with respect to an observer by the Ampère-Maxwell law. It is this property of induction which supplies the magnetic field that drives an electric motor.^[98] The electromagnetic field of an arbitrary moving charged particle is expressed by the Liénard-Wiechert potentials, which are valid even when the particle's speed is close to that of light (or relativistic velocities).

When an electron is moving through a magnetic field, it is subject to the Lorentz force that exerts an influence in a direction perpendicular to the plane defined by the magnetic field and the electron velocity. This centripetal force causes the electron to follow a helical trajectory through the field at a radius equal to the gyroradius. The acceleration from this curving motion induces the electron to radiate energy in the form of synchrotron radiation.^{[99] [100] [101]} The energy emission in turn causes a recoil of the electron, known as the Abraham-Lorentz-Dirac force, which creates a friction that slows the electron. This force is caused by a back-reaction of the electron's own field upon itself.^[102]

In the quantum electrodynamics the electromagnetic interaction between particles is mediated by photons.

An isolated electron that is not undergoing acceleration is unable to emit or absorb a real photon; doing so would violate conservation of energy and momentum. Instead, virtual photons can transfer momentum between two charged particles. It is this exchange of virtual photons that, for example, generates the Coulomb force.^[103] Energy emission can occur when a moving electron is deflected by a charged particle, such as a proton. The acceleration of the electron results in the emission of Bremsstrahlung radiation.^[104]



The relative strength of the electromagnetic interaction between two charged particles, such as an electron and a proton, is given by the fine-structure constant. This value is a dimensionless quantity formed by the ratio of two energies: the electrostatic energy of attraction (or repulsion) at a separation of one Compton wavelength, and the rest energy of the charge. It is given by $\alpha \approx 7.297353 \times 10^{-3}$, which is approximately equal to $1/137$.^[7]

The outcome of an elastic collision between a photon and a solitary electron is called Compton scattering. This collision results in a transfer of momentum between the particles, which modifies the wavelength of the photon by an amount called the Compton shift.^[105]

[106]

[107] The maximum magnitude of this wavelength shift is h/mc , which is known as the Compton wavelength.^[108] For an electron, it has a value of 2.43×10^{-12} m.^[7]

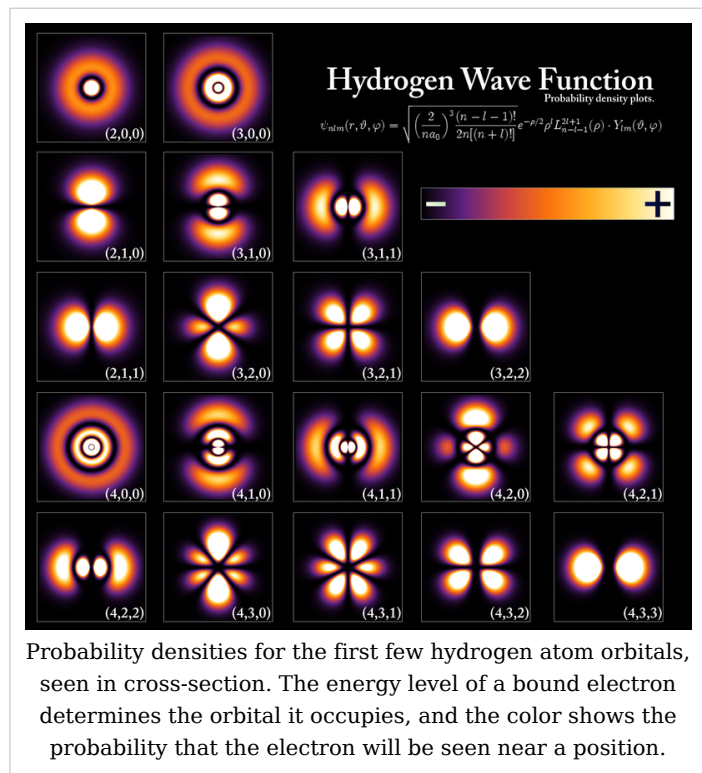
When electrons and positrons collide, they annihilate each other, giving rise to two or more gamma ray photons emitted at roughly 180° to each other. If the electron and positron have

negligible momentum, a positronium atom can form before annihilation results in two 0.511 MeV gamma ray photons.^{[109] [110]} On the other hand, high-energy photons may transform into an electron and a positron by a process called pair production, but only in the presence of a nearby charged particle, such as a nucleus.^{[111] [112]}

In the theory of electroweak interaction, the left-handed spin component of the electron forms a weak isospin doublet with the electron neutrino. This means that during weak interactions, electron neutrinos behave like electrons. Either member of this doublet can undergo a charged current interaction by emitting or absorbing a W boson and be converted into the other member. Charge is conserved during this reaction because the W boson also carries a charge, cancelling out any net change during the transmutation. Charged current interactions are responsible for the phenomenon of beta decay in a radioactive atom. Both the electron and electron neutrino can undergo a neutral current interaction via a Z^0 boson exchange, and this is responsible for neutrino-electron elastic scattering.^[63]

Atoms and molecules

An electron can be *bound* to the nucleus of an atom by the attractive Coulomb force. The wave-like behavior of a bound electron is described by a function called an atomic orbital. Each orbital has its own set of quantum numbers such as energy, angular momentum and projection of angular momentum, and only a discrete set of these orbitals exist around the nucleus. Electrons can transfer between different orbitals by the emission or absorption of photons with an energy that matches the difference in potential.^[113] Other methods of orbital transfer include collisions with particles, such as electrons, and the Auger effect.^[114] In order to escape the atom, the energy of the electron must be increased above its binding energy to the atom. This occurs, for example, with the photoelectric effect, where an incident photon exceeding the atom's ionization energy is absorbed by the electron.^[115]



The orbital angular momentum of electrons is quantized. Because the electron is charged, it produces a magnetic moment that is proportional to the angular momentum. The net magnetic moment of an atom is equal to the vector sum of all its component orbital and spin magnetic moments. Pairs of electrons in an atom align their spins in opposite directions, giving them different spin quantum numbers that satisfy the Pauli exclusion principle. Thus the magnetic moments of an atom's paired electrons cancel each other out. The nucleus contributes a magnetic moment, but this is negligible in comparison to the

effect from the electrons.^[116]

The chemical bond between atoms occurs as a result of electromagnetic interactions, as described by the laws of quantum mechanics.^[117] The strongest bonds are formed by the sharing or transfer of electrons between atoms, allowing the formation of molecules.^[118] Within a molecule, electrons move under the influence of several nuclei, and occupy molecular orbitals; much as they can occupy atomic orbitals in isolated atoms.^[119] A fundamental factor in these molecular structures is the existence of electron pairs. These are electrons with opposed spins, allowing them to occupy the same molecular orbital without violating the Pauli exclusion principle (much like in atoms). Different molecular orbitals have different spatial distribution of the electron density. For instance, in bonded pairs (i.e. in the pairs that actually bind atoms together) electrons can be found with the maximal probability in a relatively small volume between the nuclei. On the contrary, in non-bonded pairs electrons are distributed in a large volume around nuclei.^[120]

Conductivity

If a body has more or fewer electrons than are required to balance the positive charge of the nuclei, then that object has an electric charge. (For a single atom or molecule, the object is termed an ion.) When there is an excess of electrons, the object is said to be negatively charged. When there are fewer electrons than the number of protons in nuclei, the object is said to be positively charged. When the number of electrons and the number of protons are equal, their charges cancel each other and the object is said to be electrically neutral. A macroscopic body can develop an electric charge through rubbing, by the triboelectric effect.^[122]

Independent electrons moving in vacuum or certain media are termed *free* electrons. When free electrons move, they produce a net flow of charge called an electric current, which generates a magnetic field. Likewise a current can be created by a changing magnetic field. These interactions are described mathematically by Maxwell's equations.^[123]

At a given temperature, each material has an electrical conductivity that determines the value of electric current when an electric potential is applied. Examples of good conductors include metals such as copper and gold, whereas glass and Teflon are poor conductors. In any dielectric material, the electrons remain bound to their respective atoms and the material behaves as an insulator. Any semiconductor has a variable level of conductivity that lies between the extremes of conduction and insulation.^[124] On the other hand, metals have an electronic band structure that allows for delocalized electrons. These electrons are not associated with specific atoms, so when an electric field is applied, they are free to move like a gas (called Fermi gas)^[125] through the material much like free electrons.

Because of collisions between electrons and atoms, the drift velocity of electrons in a conductor is on the order of millimetres per second. However, the speed at which a change of current at one point in the material causes changes in currents in other parts of the material, the velocity of propagation, is typically about 75% of light speed.^[126] This occurs



Lightning is an example of the phenomena produced by triboelectricity.^[121]

because electrical signals propagate as a wave, with the velocity dependent on the dielectric constant of the material.^[127]

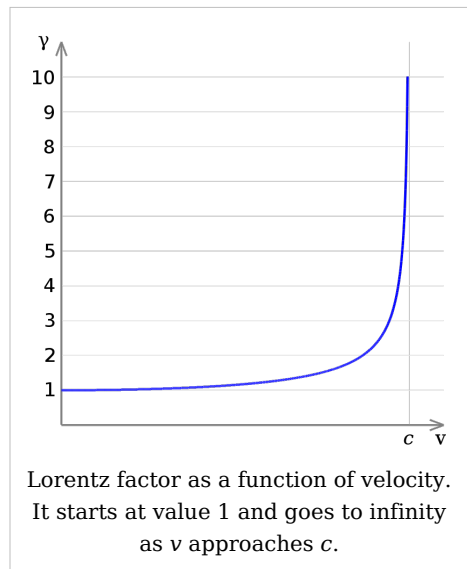
Metals make relatively good conductors of heat, primarily because the delocalized electrons are free to transport thermal energy between atoms. However, unlike electrical conductivity, the thermal conductivity of a metal is nearly independent of temperature. This is expressed mathematically by the Wiedemann-Franz law,^[125] which states that the ratio of thermal conductivity to the electrical conductivity is proportional to the temperature. The thermal disorder in the metallic lattice increases the electrical resistivity of the material, producing a temperature dependence for electrical current.^[128]

When cooled below a point called the critical temperature, materials can undergo a phase transition in which they lose all resistivity to electrical current, in a process known as superconductivity. In BCS theory, this behavior is modeled by pairs of electrons entering a quantum state known as a Bose-Einstein condensate. These Cooper pairs have their motion coupled to nearby matter via lattice vibrations called phonons, thereby avoiding the collisions with atoms that normally create electrical resistance.^[129] (Cooper pairs have a radius of roughly 100 nm, so they can overlap each other.)^[130] However, the mechanism by which higher temperature superconductors operate remains uncertain.

Motion and energy

According to Einstein's theory of special relativity, as an electron's speed approaches the speed of light, from an observer's point of view its relativistic mass increases, thereby making it more and more difficult to accelerate it from within the observer's frame of reference. The speed of an electron can approach, but never reach, the speed of light in a vacuum, c . However, when relativistic electrons—that is, electrons moving at a speed close to c —are injected into a dielectric medium such as water, where the local speed of light is significantly less than c , the electrons temporarily travel faster than light in the medium. As they interact with the medium, they generate a faint light called Cherenkov radiation.^[131]

The effects of special relativity are based on a quantity known as the Lorentz factor, defined as $\gamma = 1/\sqrt{1 - v^2/c^2}$ where v is the speed of the particle. The kinetic energy K_e of an electron moving with velocity v is:



$$K_e = (\gamma - 1)m_e c^2$$

where m_e is the mass of electron. For example, the Stanford linear accelerator can accelerate an electron to roughly 51 GeV.^[132] This gives a value of 100,000 for γ , since the

mass of an electron is $0.51 \text{ MeV}/c^2$. The relativistic momentum of this electron is 100,000 times the momentum that classical mechanics would predict for an electron at the same speed.^[133]

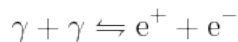
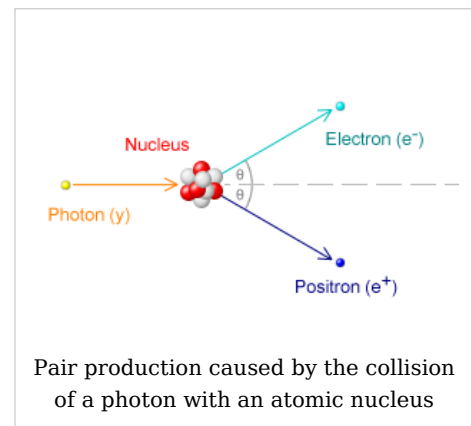
[134]

[135]

Since an electron behaves as a wave, at a given velocity it has a characteristic de Broglie wavelength. This is given by $\lambda_e = h/p$ where h is Planck's constant and p is the momentum.^[44] For the 51 GeV electron above, the wavelength is about $2.4 \times 10^{-17} \text{ m}$, small enough to explore structures well below the size of an atomic nucleus.^[136]

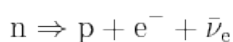
Formation

The Big Bang theory is the most widely accepted scientific theory to explain the early stages in the evolution of the Universe.^[137] For the first millisecond of the Big Bang, the temperatures were over 10 billion kelvins and photons had mean energies over a million electron volts. These photons were sufficiently energetic that they could react with each other to form pairs of electrons and positrons,



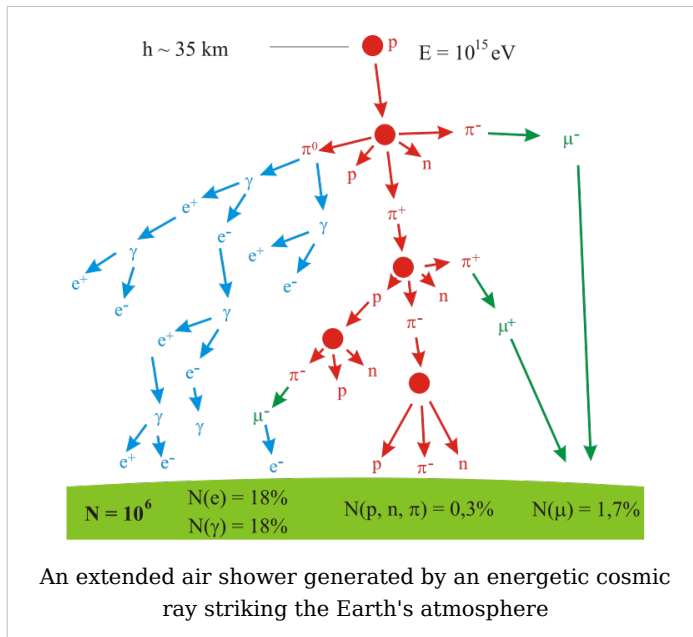
where γ is a photon, e^+ is a positron and e^- is an electron. Likewise, positron-electron pairs annihilated each other and emitted energetic photons. An equilibrium between electrons, positrons and protons was maintained during this phase of the evolution of the Universe. After 15 seconds had passed, however, the temperature of the universe dropped below the threshold where electron-positron formation could occur. Most of the surviving electrons and positrons annihilated each other, releasing gamma radiation that briefly reheated the universe.^[138]

For reasons that remain uncertain, during the process of leptogenesis there was an excess in the number of electrons over positrons.^[139] Hence, about one electron in every billion survived the annihilation process. This excess matched the excess of protons over anti-protons, in a condition known as baryon asymmetry, resulting in a net charge of zero for the universe.^{[140] [141]} The surviving protons and neutrons began to participate in reactions with each other—in the process known as nucleosynthesis, forming isotopes of hydrogen and helium, with trace amounts of lithium. This process peaked after about five minutes.^[142] Any leftover neutrons underwent negative beta decay with a half-life of about a thousand seconds, releasing a proton and electron in the process,



where n is a neutron, p is a proton and $\bar{\nu}_e$ is an electron antineutrino. For about the next 300,000–400,000 years, the excess electrons remained too energetic to bind with atomic nuclei.^[143] What followed is a period known as recombination, when neutral atoms were formed and the expanding universe became transparent to radiation.^[144]

Roughly one million years after the big bang, the first generation of stars began to form.^[144] Within a star, stellar nucleosynthesis results in the production of positrons from the fusion of atomic nuclei. These antimatter particles immediately annihilate with electrons, releasing gamma rays. The net result is a steady reduction in the number of electrons, and a matching increase in the number of neutrons. However, the process of stellar evolution can result in the synthesis of radioactive isotopes. Selected isotopes can subsequently undergo negative beta decay, emitting an electron and antineutrino from the nucleus.^[145] An example is the cobalt-60 (^{60}Co) isotope, which decays to form nickel-60 (^{60}Ni).^[146]



At the end of their lifetime, a star with more than about 20 solar masses can undergo gravitational collapse to form a black hole.^[147] According to classical physics, these massive stellar objects exert a gravitational attraction that is strong enough to prevent anything, even radiation, from escaping past the Schwarzschild radius. However, it is believed that quantum mechanical effects may allow Hawking radiation to be emitted at this distance. Electrons (and positrons) are thought to be created at the event horizon of these stellar remnants.

When pairs of virtual particles (such as an electron and positron) are created in the vicinity of the event horizon, the random spacial distribution of these particles may permit one of them to appear on the exterior; this process is called quantum tunneling. The gravitational potential of the black hole can then supply the energy that transforms this virtual particle into a real particle, allowing it to radiate away into space.^[148] In exchange, the other member of the pair is given negative energy, which results in a net loss of mass-energy by the black hole. The rate of Hawking radiation increases with decreasing mass, eventually causing the black hole to evaporate away until, finally, it explodes.^[149]

Cosmic rays are particles travelling through space with high energies. Energy events as high as 3.0×10^{20} eV have been recorded.^[150] When these particles collide with nucleons in the Earth's atmosphere, a shower of particles is generated, including pions.^[151] More than half of the cosmic radiation observed from the Earth's surface consists of muons. The particle called a muon is a lepton which is produced in the upper atmosphere by the decay of a pion. A muon, in turn, can decay to form an electron or positron. Thus, for the negatively charged pion π^- ,^[152]

$$\pi^- \Rightarrow \mu^- + \nu_\mu$$

$$\mu^- \Rightarrow e^- + \bar{\nu}_e + \nu_\mu$$

where μ^- is a muon and ν_μ is a muon neutrino.

Observation

Remote observation of electrons requires the detection of their radiated energy. For example, in high-energy environments such as the corona of a star, free electrons form a plasma that radiates energy due to Bremsstrahlung. Electron gas can undergo plasma oscillation, which is waves caused by synchronized variations in electron density, and these produce energy emissions that can be detected by the use of radio telescopes.^[154]

The frequency of a photon is proportional to its energy. As a bound electron transitions between different energy levels of an atom, it will absorb or emit photons at characteristic frequencies called absorption and emission lines, respectively. For instance, when atoms are irradiated by a source with a broad spectrum, distinct absorption lines will appear in the spectrum of transmitted radiation. Each element or molecule displays a characteristic set of spectral lines, such as the hydrogen spectral series. Spectroscopic measurements of the strength and width of these lines allow the composition and physical properties of a substance to be determined.^{[155] [156]}

In laboratory conditions, the interactions of individual electrons can be observed by means of particle detectors, which allow measurement of specific properties such as energy, spin and charge.^[115] The development of the Paul trap and Penning trap allows charged particles to be contained within a small region for long durations. This enables very precise measurements of the particle properties. For example, in one instance the Penning trap was used to contain a single electron for a period of 10 months.^[157] Measurements allowed the magnetic moment of the electron to be measured to a precision of eleven digits, which, in 1980, was a greater accuracy than for any other physical constant.^[158]

The first video images of an electron's energy distribution were captured by a team at Lund University in Sweden, February 2008. To capture this phenomenon, the scientists used extremely short flashes of light, called attosecond pulses, which allowed the team at the university's Faculty of Engineering to capture the electron's motion for the first time.^{[159] [160]}

The distribution of the electrons in solid materials can be visualized by angle resolved photoemission spectroscopy (ARPES). This technique uses the photoelectric effect to measure the reciprocal space, a mathematical representation of periodic structures, used to infer the original structure. ARPES can be used to determine the direction, speed and scattering of electrons within the material.^[161]

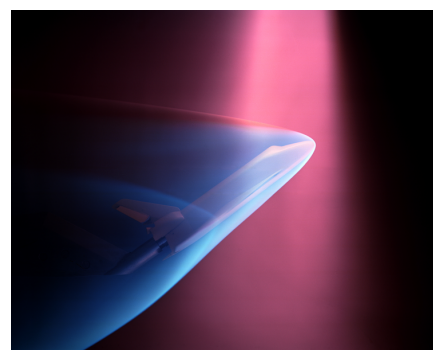


Aurorae are typically caused by energetic electrons precipitating into the atmosphere.^[153]

Plasma applications

Particle beams

Electron beams are used in welding^[163] and lithography.^[164] Electron beam processing is used to irradiate materials in order to change their material properties or sterilize medical and food products.^[165] In radiation therapy, electron beams are generated by linear accelerators for treatment of superficial tumors. Because an electron beam only penetrates to a limited depth before being absorbed, typically up to 5 cm for beams in the range 5–20 MeV, electron therapy is useful for treating skin lesions such as basal cell carcinomas. An electron beam can be used to supplement the treatment of areas that have been irradiated by X-rays.^{[166] [167]}



During a NASA wind tunnel test, a model of the Space Shuttle is targeted by a beam of electrons, simulating the effect of ionizing gases during re-entry.^[162]

Particle accelerators use electric fields to propel electrons and their antiparticles to high energies. As these particles pass through magnetic fields, they emit synchrotron radiation. The intensity of this radiation is spin dependent, which causes polarization of the electron beam—a process known as the Sokolov-Ternov effect.^[168] The polarized electron beams can be useful for various experiments. Synchrotron radiation can also be used for cooling the electron beams, which reduces the momentum spread of the particles. Once the particles have accelerated to the required energies, separate electron and positron beams are brought into collision. The resulting energy emissions are observed with particle detectors and used to study particle physics.^[169]

Imaging

Low-energy electron diffraction (LEED) is a method of bombarding a crystalline material with a collimated beam of electrons, then observing the resulting diffraction patterns to determine the structure of the material. The required energy of the electrons is typically in the range of 20–200-eV.^[170] The reflection high energy electron diffraction (RHEED) technique uses the reflection of a beam of electrons fired at various low angles to characterize the surface of crystalline materials. The beam energy is typically in the range of 8–20 keV and the grazing angle is 1–4°.^{[171] [172]}

The electron microscope directs a focused beam of electrons at a specimen. As the beam interacts with the material, the electrons are scattered and lose energy. By recording the changes in the electron beam, investigators can produce an image of the material.^[173] In blue light, conventional optical microscopes have a diffraction-limited resolution of about 100 nm. By comparison, electron microscopes are limited by the de Broglie wavelength of the electron. This is equal to 0.0037 nm for electrons accelerated across a 100,000-volt potential.^[174] For example, the TEAM electron microscope is capable of 0.05 nm resolution: small enough to resolve individual atoms.^[175] This makes the electron microscope a useful laboratory instrument for high resolution imaging. However, electron microscopes are expensive instruments that are costly to maintain. The high vacuum required to operate an electron microscope also prevents them from being used to observe living organisms.^[176]

There exist two main types of electron microscopes: transmission and scanning. Transmission electron microscopes function in a manner similar to optical microscopes, with a beam of electrons passing through a material. The magnifications range from 1,000× to 1,000,000× or better. Quantum effects of electrons are used in the scanning tunneling microscope to study features on solid surfaces with lateral resolution at the atomic scale of around 0.2 nm.^{[176] [177]}

Other

In the free electron laser (FEL), a relativistic electron beam is passed through a pair of undulators containing arrays of dipole magnets, whose fields are oriented in alternating directions. The electrons emit synchrotron radiation, which, in turn, coherently interacts with the electrons. This leads to the strong amplification of the radiation field at the resonance frequency. FEL can emit a coherent high-brilliance electromagnetic radiation with a wide range of frequencies, from microwaves to soft X-rays. These devices can be used in the future for manufacturing, communication and various medical applications, such as soft tissue surgery.^[178]

Electrons are at the heart of cathode ray tubes, which are used extensively as display devices in laboratory instruments, computer monitors and television sets.^[179] In a photomultiplier tube, one photon strikes the photocathode, initiating an avalanche of electrons that produces a detectable current.^[180] Vacuum tubes used the flow of electrons in a near vacuum to manipulate electrical signals, and they played a critical role in the development of electronics technology. However, vacuum tubes have been largely supplanted by solid-state devices such as the transistor.^[181]

See also

- Covalent bonding
- Electron bubble
- Exoelectron emission
- G-factor
- One-electron universe
- Spintronics
- Stern-Gerlach experiment

Notes

- [1] Dahl, Per F. (1997). *Flash of the Cathode Rays: A History of J J Thomson's Electron*. CRC Press. p. 72. ISBN 0750304537.
- [2] Eichten, Estia J.; Lane, Kenneth D.; Peskin, Michael E. (1983). "New Tests for Quark and Lepton Substructure". *Physical Review Letters* **50**: 030802(1-4). doi: 10.1103/PhysRevLett.97.030802 (<http://dx.doi.org/10.1103/PhysRevLett.97.030802>).
- [3] Farrar, W. V. (1969). "Richard Laming and the Coal-Gas Industry, with His Views on the Structure of Matter". *Annals of Science* **25**: 243-254. doi: 10.1080/00033796900200141 (<http://dx.doi.org/10.1080/00033796900200141>).
- [4] Arabatzis, Theodore (2006). *Representing Electrons: A Biographical Approach to Theoretical Entities*. University of Chicago Press. pp. 70-74. ISBN 0226024210.
- [5] Buchwald, Jed Z.; Warwick, Andrew (2001). *Histories of the Electron: The Birth of Microphysics*. MIT Press. pp. 195-203. ISBN 0262524244.
- [6] Dahl (1997:122-185).
- [7] The original source for CODATA is:
Mohr, Peter J.; Taylor, Barry N.; Newell, David B. (2006-06-06). "CODATA recommended values of the fundamental physical constants". *Reviews of Modern*

Physics **80**: 633–730. doi: 10.1103/RevModPhys.80.633 (<http://dx.doi.org/10.1103/RevModPhys.80.633>).

Individual physical constants from the CODATA are available at:

<http://physics.nist.gov/cuu/>|"The NIST Reference on Constants, Units and Uncertainty". National Institute of Standards and Technology. <http://physics.nist.gov/cuu/>. Retrieved on 2009-01-15.

- [8] The fractional version's denominator is the inverse of the decimal value (along with its relative standard uncertainty of 4.2×10^{-10}).
- [9] The electron's charge is the negative of elementary charge, which is a positive value for the proton.
- [10] Anastopoulos, Charis (2008). *Particle Or Wave: The Evolution of the Concept of Matter in Modern Physics*. Princeton University Press. pp. 236–237. ISBN 0691135126.
- [11] Wilson, Robert (1997). *Astronomy Through the Ages: The Story of the Human Attempt to Understand the Universe*. CRC Press. p. 138. ISBN 0748407480.
- [12] Curtis, Lorenzo J. (2003). *Atomic Structure and Lifetimes: A Conceptual Approach*. Cambridge University Press. p. 74. ISBN 0521536359.
- [13] Pauling, Linus C. (1960), <http://books.google.co.uk/books?id=L-1K9HmKmUUC>|*The Nature of the Chemical Bond and the Structure of Molecules and Crystals* (3rd ed.), Cornell University Press, pp. 4–5, ISBN 0801403332, <http://books.google.co.uk/books?id=L-1K9HmKmUUC>
- [14] Shipley, Joseph T. (1945). *Dictionary of Word Origins*. New York, N. Y.: The Philosophical Library. p. 133.
- [15] Baigrie, Brian (2006). *Electricity and Magnetism: A Historical Perspective*. Greenwood Press. pp. 7–8. ISBN 0-3133-3358-0.
- [16] Barrow, J. D. (1983). "<http://adsabs.harvard.edu/abs/1983QJRAS..24...24B>|Natural Units Before Planck". *Royal Astronomical Society Quarterly Journal* **24**: 24–26. <http://adsabs.harvard.edu/abs/1983QJRAS..24...24B>. Retrieved on 2008-08-30.
- [17] Stoney, George Johnstone (October 1894). "Of the "Electron," or Atom of Electricity". *Philosophical Magazine* **38** (5): 418–420.
- [18] Soukhanov, Anne H. ed. (1986). *Word Mysteries & Histories*. Boston, MA: Houghton Mifflin Company. p. 73. ISBN 0-395-40265-4.
- [19] Guralnik, David B. ed. (1970). *Webster's New World Dictionary*. Englewood Cliffs, N. J.: Prentice-Hall, Incorporated. p. 450.
- [20] Born, Max; Blin-Stoyle, Roger John; Radcliffe, J. M. (1989). *Atomic Physics*. Courier Dover Publications. p. 26. ISBN 0486659844.
- [21] Dahl (1997:55–58).
- [22] DeKosky, Robert (1983). "William Crookes and the quest for absolute vacuum in the 1870s". *Annals of Science* **40** (1): 1–18. doi: 10.1080/00033798300200101 (<http://dx.doi.org/10.1080/00033798300200101>).
- [23] Leicester, Henry M. (1971). *The Historical Background of Chemistry*. Courier Dover Publications. pp. 221–222. ISBN 0486610535.
- [24] Dahl (1997:64–78).
- [25] Zekman, P. (1907). "<http://books.google.com/books?id=UtYRAAAAYAAJ>|Sir William Crookes, F.R.S.". *Nature* **77** (1984): 1–3. doi: 10.1038/077001a0 (<http://dx.doi.org/10.1038/077001a0>). <http://books.google.com/books?id=UtYRAAAAYAAJ>. Retrieved on 2008-08-25.
- [26] Thomson, J. J. (1906-12-11). http://nobelprize.org/nobel_prizes/physics/laureates/1906/thomson-lecture.html|"Lecture, The Nobel Prize in Physics 1906". The Nobel Foundation. http://nobelprize.org/nobel_prizes/physics/laureates/1906/thomson-lecture.html. Retrieved on 2008-08-25.
- [27] Trenn, Thaddeus J. (March 1976). "<http://www.jstor.org/pss/231134>|Rutherford on the Alpha-Beta-Gamma Classification of Radioactive Rays". *Isis* **67** (1): 61–75. doi: 10.1086/351545 (<http://dx.doi.org/10.1086/351545>). <http://www.jstor.org/pss/231134>. Retrieved on 2008-09-04.
- [28] Becquerel, Henri (1900). "Déviation du Rayonnement du Radium dans un Champ Électrique" (in French). *Comptes Rendus de l'Académie des Sciences* **130**: 809–815.
- [29] Buchwald and Warwick (2001:90-91).
- [30] Myers, William G. (1976-07-01). "<http://jnm.snmjournals.org/cgi/content/abstract/17/7/579>|Becquerel's Discovery of Radioactivity in 1896". *Journal of Nuclear Medicine* **17** (7): 579–582. PMID 775027. <http://jnm.snmjournals.org/cgi/content/abstract/17/7/579>. Retrieved on 2008-09-04.
- [31] Kikoin, I. K.; Sominskiĭ, M. S. (1961). "Abram Fedorovich Ioffe (on his eightieth birthday)". *Soviet Physics Uspekhi* **3**: 798–809. doi: 10.1070/PU1961v003n05ABEH005812 (<http://dx.doi.org/10.1070/PU1961v003n05ABEH005812>).

- [32] Kizilova, Anna. http://www.russia-ic.com/people/education_science/i/261/|"Abram Ioffe (biography)". Russia-InfoCentre. http://www.russia-ic.com/people/education_science/i/261/. Retrieved on 2006-09-22.
- [33] Millikan, R. A. (1911). "The Isolation of an Ion, a Precision Measurement of its Charge, and the Correction of Stokes's Law". *Physical Review* **32** (2): 349–397. doi: 10.1103/PhysRevSeriesI.32.349 (<http://dx.doi.org/10.1103/PhysRevSeriesI.32.349>).
- [34] Das Gupta, N. N.; Ghosh, S. K. (1999). "A Report on the Wilson Cloud Chamber and Its Applications in Physics". *Reviews of Modern Physics* **18**: 225–290. doi: 10.1103/RevModPhys.18.225 (<http://dx.doi.org/10.1103/RevModPhys.18.225>).
- [35] Smirnov, Boris M. (2003). *Physics of Atoms and Ions*. Springer. pp. 14–21. ISBN 038795550X.
- [36] Bohr, Niels (1922-12-11). http://nobelprize.org/nobel_prizes/physics/laureates/1922/bohr-lecture.html|"Nobel Lecture: The Structure of the Atom". The Nobel Foundation. http://nobelprize.org/nobel_prizes/physics/laureates/1922/bohr-lecture.html. Retrieved on 2008-12-03.
- [37] Lewis, Gilbert N. (April 1916). "The Atom and the Molecule". *Journal of the American Chemical Society* **38** (4): 762–786. doi: 10.1021/ja02261a002 (<http://dx.doi.org/10.1021/ja02261a002>).
- [38] Arabatzis, Theodore; Gavroglu, Kostas (1997). "<http://www.iop.org/EJ/abstract/0143-0807/18/3/005>|The chemists' electron". *European Journal of Physics* **18**: 150–163. doi: 10.1088/0143-0807/18/3/005 (<http://dx.doi.org/10.1088/0143-0807/18/3/005>). <http://www.iop.org/EJ/abstract/0143-0807/18/3/005>.
- [39] Langmuir, Irving (1919). "The Arrangement of Electrons in Atoms and Molecules". *Journal of the American Chemical Society* **41** (6): 868–934. doi: 10.1021/ja02227a002 (<http://dx.doi.org/10.1021/ja02227a002>).
- [40] Scerri, Eric R. (2007). *The Periodic Table*. Oxford University Press US. pp. 205–226. ISBN 0195305736.
- [41] Massimi, Michela (2005). *Pauli's Exclusion Principle, The Origin and Validation of a Scientific Principle*. Cambridge University Press. pp. 7–8. ISBN 0521839114.
- [42] Uhlenbeck, G. E.; Goudsmith, S. (1925). "<http://adsabs.harvard.edu/abs/1925NW.....13..953E>|Ersetzung der Hypothese vom unmechanischen Zwang durch eine Forderung bezüglich des inneren Verhaltens jedes einzelnen Elektrons" (in German). *Die Naturwissenschaften* **13** (47). <http://adsabs.harvard.edu/abs/1925NW.....13..953E>. Retrieved on 2008-09-02.
- [43] W., Pauli (1923). "<http://adsabs.harvard.edu/abs/1923ZPhy...16..155P>|Über die Gesetzmäßigkeiten des anomalen Zeemaneffektes" (in German). *Zeitschrift für Physik* **16** (1): 155–164. doi: 10.1007/BF01327386 (<http://dx.doi.org/10.1007/BF01327386>). <http://adsabs.harvard.edu/abs/1923ZPhy...16..155P>. Retrieved on 2008-09-02.
- [44] de Broglie, Louis (1929-12-12). http://nobelprize.org/nobel_prizes/physics/laureates/1929/broglie-lecture.html|"Lecture, The Nobel Prize in Physics 1929". Nobel Foundation. http://nobelprize.org/nobel_prizes/physics/laureates/1929/broglie-lecture.html. Retrieved on 2008-08-30.
- [45] Falkenburg, Brigitte (2007). *Particle Metaphysics: A Critical Account of Subatomic Reality*. Springer. p. 85. ISBN 3540337318.
- [46] Davisson, Clinton (1937-12-13). http://nobelprize.org/nobel_prizes/physics/laureates/1937/davisson-lecture.html|"Lecture, The Nobel Prize in Physics 1937". Nobel Foundation. http://nobelprize.org/nobel_prizes/physics/laureates/1937/davisson-lecture.html. Retrieved on 2008-08-30.
- [47] Schrödinger, Erwin (1926). "<http://adsabs.harvard.edu/abs/1926AnP...385..437S>|Quantisierung als Eigenwertproblem" (in German). *Annalen der Physik* **385** (13): 437–490. doi: 10.1002/andp.19263851302 (<http://dx.doi.org/10.1002/andp.19263851302>). <http://adsabs.harvard.edu/abs/1926AnP...385..437S>. Retrieved on 2008-08-31.
- [48] Rigden, John S. (2003). *Hydrogen*. Harvard University Press. pp. 59–86. ISBN 0674012526.
- [49] Reed, Bruce Cameron (2007). *Quantum Mechanics*. Jones & Bartlett Publishers. pp. 275–350. ISBN 0763744514.
- [50] Dirac, P. A. M. (1928-02-01). "The Quantum Theory of the Electron". *Proceedings of the Royal Society of London. Series A* **117** (778): 610–624. doi: 10.1098/rspa.1928.0023 (<http://dx.doi.org/10.1098/rspa.1928.0023>).
- [51] Dirac, Paul A. M. (1933-12-12). http://nobelprize.org/nobel_prizes/physics/laureates/1933/dirac-lecture.html|"Theory of Electrons and Positrons". The Nobel Foundation. http://nobelprize.org/nobel_prizes/physics/laureates/1933/dirac-lecture.html. Retrieved on 2008-11-01.
- [52] Kragh, Helge (2002). *Quantum Generations: A History of Physics in the Twentieth Century*. Princeton University Press. p. 132. ISBN 0691095523.
- [53] Gaynor, Frank (1950). *Concise Encyclopedia of Atomic Energy*. New York: Philosophical Library. pp. 117.
- [54] http://nobelprize.org/nobel_prizes/physics/laureates/1965/|"The Nobel Prize in Physics 1965". The Nobel Foundation. http://nobelprize.org/nobel_prizes/physics/laureates/1965/. Retrieved on 2008-11-04.

- [55] Panofsky, Wolfgang K. H. (1997). <http://www.slac.stanford.edu/pubs/beamline/27/1/27-1-panofsky.pdf> "The Evolution of Particle Accelerators & Colliders" (PDF). Stanford University. <http://www.slac.stanford.edu/pubs/beamline/27/1/27-1-panofsky.pdf>. Retrieved on 2008-09-15.
- [56] Elder, F. R.; Gurewitsch, A. M.; Langmuir, R. V.; Pollock, H. C. (1947). "Radiation from Electrons in a Synchrotron". *Physical Review* **71** (11): 829–830. doi: 10.1103/PhysRev.71.829.5 (<http://dx.doi.org/10.1103/PhysRev.71.829.5>).
- [57] Hoddeson, Lillian; Brown, Laurie; Riordan, Michael; Dresden, Max (1997). *The Rise of the Standard Model: Particle Physics in the 1960s and 1970s*. Cambridge University Press. pp. 25–26. ISBN 0521578167.
- [58] Bernardini, Carlo (2004). "<http://ads.ari.uni-heidelberg.de/abs/2004PhP.....6..156B|AdA:The First Electron-Positron Collider>". *Physics in Perspective* **6** (2): 156–183. doi: 10.1007/s00016-003-0202-y (<http://dx.doi.org/10.1007/s00016-003-0202-y>). <http://ads.ari.uni-heidelberg.de/abs/2004PhP.....6..156B>. Retrieved on 2008-09-15.
- [59] Staff (2008). <http://public.web.cern.ch/PUBLIC/en/Research/LEPExp-en.html> "Testing the Standard Model: The LEP experiments". CERN. <http://public.web.cern.ch/PUBLIC/en/Research/LEPExp-en.html>. Retrieved on 2008-09-15.
- [60] Staff (2000-12-01). <http://cerncourier.com/cws/article/cern/28335> "LEP reaps a final harvest". CERN Courier. <http://cerncourier.com/cws/article/cern/28335>. Retrieved on 2008-11-01.
- [61] Frampton, Paul H.; Hung, P. Q.; Sher, Marc (June 2000). "Quarks and Leptons Beyond the Third Generation". *Physics Reports* **330**: 263–3485. doi: 10.1016/S0370-1573(99)00095-2 ([http://dx.doi.org/10.1016/S0370-1573\(99\)00095-2](http://dx.doi.org/10.1016/S0370-1573(99)00095-2)).
- [62] Raith, Wilhelm; Mulvey, Thomas (2001). *Constituents of Matter: Atoms, Molecules, Nuclei and Particles*. CRC Press. pp. 777–781. ISBN 0849312027.
- [63] Quigg, Chris (June 4–30, 2000). "The Electroweak Theory (<http://arxiv.org/abs/hep-ph/0204104v1>)". *TASI 2000: Flavor Physics for the Millennium*: 80, Boulder, Colorado: arXiv. Retrieved on 2008-09-21.
- [64] Rosen, S. P. (1978). "Universality and the weak isospin of leptons, nucleons, and quarks". *Physical Review D* **17**: 2471–2474. doi: 10.1103/PhysRevD.17.2471 (<http://dx.doi.org/10.1103/PhysRevD.17.2471>).
- [65] Zombeck, Martin V. (2007). *Handbook of Space Astronomy and Astrophysics* (Third ed.). Cambridge University Press. p. 14. ISBN 0521782422.
- [66] Murphy, Michael T.; Flambaum, Victor V.; Muller, Sébastien; Henkel, Christian (2008-06-20). "<http://www.sciencemag.org/cgi/content/abstract/320/5883/1611> | Strong Limit on a Variable Proton-to-Electron Mass Ratio from Molecules in the Distant Universe". *Science* **320** (5883): 1611–1613. doi: 10.1126/science.1156352 (<http://dx.doi.org/10.1126/science.1156352>). PMID 18566280. <http://www.sciencemag.org/cgi/content/abstract/320/5883/1611>. Retrieved on 2008-09-03.
- [67] Zorn, Jens C.; Chamberlain, George E.; Hughes, Vernon W. (1963). "Experimental Limits for the Electron-Proton Charge Difference and for the Charge of the Neutron". *Physical Review* **129** (6): 2566–2576. doi: 10.1103/PhysRev.129.2566 (<http://dx.doi.org/10.1103/PhysRev.129.2566>).
- [68] Gabrielse, G.; Hanneke, D.; Kinoshita, T.; Nio, M.; Odom, B. (2006). "New Determination of the Fine Structure Constant from the Electron g Value and QED". *Physical Review Letters* **97**: 811–814. doi: 10.1103/PhysRevLett.97.811 (<http://dx.doi.org/10.1103/PhysRevLett.97.811>).
- [69] Dehmelt, Hans (1988). "A Single Atomic Particle Forever Floating at Rest in Free Space: New Value for Electron Radius". *Physica Scripta* **T22**: 102–110. doi: 10.1088/0031-8949/1988/T22/016 (<http://dx.doi.org/10.1088/0031-8949/1988/T22/016>).
- [70] From electrostatics theory, the potential energy of a sphere with radius r and charge e is given by:

$$E_p = \frac{e^2}{8\pi\epsilon_0 r}$$

- [72] where ϵ_0 is the vacuum permittivity. For an electron with rest mass m_0 , the rest energy is equal to:

$$E_p = m_0 c^2$$

- [74] where c is the speed of light in a vacuum. Setting them equal and solving for r gives the classical electron radius.

See: Haken, Hermann; Wolf, Hans Christoph; Brewer, W. D. (2005). *The Physics of Atoms and Quanta: Introduction to Experiments and Theory*. Springer. p. 70. ISBN 3540208070.

- [75] Steinberg, R. I.; Kwiatkowski, K.; Maenhaut, W.; Wall, N. S. (1999). "Experimental test of charge conservation and the stability of the electron". *Physical Review D* **61** (2): 2582–2586. doi: 10.1103/PhysRevD.61.2582 (<http://dx.doi.org/10.1103/PhysRevD.61.2582>).
- [76] Yao, W.-M.; Particle Data Group (July 2006). "Review of Particle Physics". *Journal of Physics G: Nuclear and Particle Physics* **33** (1): 77–115. doi: 10.1088/0954-3899/33/1/001 (<http://dx.doi.org/10.1088/0954-3899/33/1/001>).
- [77] Munowitz, Michael (2005). *Knowing, The Nature of Physical Law*. Oxford University Press. pp. 162–218. ISBN 0195167376.

- [78] Kane, Gordon (2006-10-09). <http://www.sciam.com/article.cfm?id=are-virtual-particles-rea&topicID=13>|"Are virtual particles really constantly popping in and out of existence? Or are they merely a mathematical bookkeeping device for quantum mechanics?". Scientific American. <http://www.sciam.com/article.cfm?id=are-virtual-particles-rea&topicID=13>. Retrieved on 2008-09-19.
- [79] Taylor, John (1989). Davies, Paul. ed. *The New Physics*. Cambridge University Press. p. 464. ISBN 0521438314.
- [80] Genz, Henning (2001). *Nothingness: The Science of Empty Space*. Da Capo Press. pp. 241–243, 245–247. ISBN 0738206105.
- [81] Gribbin, John (1997-01-25). <http://www.newscientist.com/article/mg15320662.300-science--more-to-electrons-than-meets-the-eye.html>|"More to electrons than meets the eye". New Scientist. <http://www.newscientist.com/article/mg15320662.300-science--more-to-electrons-than-meets-the-eye.html>. Retrieved on 2008-09-17.
- [82] Levine, I.; TOPAZ Collaboration (1997). "Measurement of the Electromagnetic Coupling at Large Momentum Transfer". *Physical Review Letters* **78**: 424–427. doi: 10.1103/PhysRevLett.78.424 (<http://dx.doi.org/10.1103/PhysRevLett.78.424>).
- [83] Murayama, Hitoshi (March 10–17, 2006). "Supersymmetry Breaking Made Easy, Viable and Generic (<http://arxiv.org/abs/0709.3041>)". *Proceedings of the XLIIInd Rencontres de Moriond on Electroweak Interactions and Unified Theories*. Retrieved on 2008-09-30.—lists a 9% mass difference for an electron that is the size of the Planck distance.
- [84] Modanese, Giovanni (2003). "<http://arxiv.org/abs/hep-th/0009046>|Inertial Mass and Vacuum Fluctuations in Quantum Field Theory". *Foundations of Physics Letters* **16**: 135–141. doi: 10.1023/A:1024118627357 (<http://dx.doi.org/10.1023/A:1024118627357>). <http://arxiv.org/abs/hep-th/0009046>. Retrieved on 2008-09-30.
- [85] This magnitude is given by the spin angular momentum,
- $$S = \sqrt{s(s+1)} \cdot \frac{h}{2\pi} = \frac{\sqrt{3}}{2} \hbar$$
- [87] for quantum number $s = \frac{1}{2}$.
- See: Gupta, M. C. (2001). *Atomic and Molecular Spectroscopy*. New Age Publishers. p. 81. ISBN 8122413005.
- [88] Bohr magneton
- $$\mu_B = \frac{e\hbar}{2m_e} = 9.27400915(23) \times 10^{-24} \text{ J/T}$$
- [91] Schwinger, Julian (1948). "On Quantum-Electrodynamics and the Magnetic Moment of the Electron". *Physical Review* **73** (4): 416–417. doi: 10.1103/PhysRev.73.416 (<http://dx.doi.org/10.1103/PhysRev.73.416>).
- [92] Odom, B.; Hanneke, D.; D'Urso, B.; Gabrielse, G. (2006). "New Measurement of the Electron Magnetic Moment Using a One-Electron Quantum Cyclotron". *Physical Review Letters* **97**: 030801(1–4). doi: 10.1103/PhysRevLett.97.030801 (<http://dx.doi.org/10.1103/PhysRevLett.97.030801>).
- [93] Huang, Kerson (2007). *Fundamental Forces of Nature: The Story of Gauge Fields*. World Scientific. pp. 123–125. ISBN 9812706453.
- [94] Foldy, Leslie L.; Wouthuysen, Siegfried A. (1950). "On the Dirac Theory of Spin 1/2 Particles and Its Non-Relativistic Limit". *Physical Review* **78**: 29–36. doi: 10.1103/PhysRev.78.29 (<http://dx.doi.org/10.1103/PhysRev.78.29>).
- [95] Sidharth, Burra G. (August 2008). "<http://arxiv.org/abs/0806.0985>|Revisiting Zitterbewegung". *International Journal of Theoretical Physics* **48**: 497. doi: 10.1007/s10773-008-9825-8 (<http://dx.doi.org/10.1007/s10773-008-9825-8>). <http://arxiv.org/abs/0806.0985>. Retrieved on 2008-11-10.
- [96] Elliott, R. S. (1978). "http://ieeexplore.ieee.org/xpls/abs_all.jsp?arnumber=3600|The history of electromagnetics as Hertz would have known it". *IEEE Transactions on Microwave Theory and Techniques* **36** (5): 806–823. doi: 10.1109/22.3600 (<http://dx.doi.org/10.1109/22.3600>). http://ieeexplore.ieee.org/xpls/abs_all.jsp?arnumber=3600. Retrieved on 2008-09-22. A subscription required for access.
- [97] Munowitz (2005:140).
- [98] Crowell, Benjamin (2000). *Electricity and Magnetism*. Light and Matter. pp. 129–152. ISBN 0970467044.
- [99] Munowitz (2005:160).
- [100] Mahadevan, Rohan; Narayan, Ramesh; Yi, Insu (1996). "<http://arxiv.org/abs/astro-ph/9601073v1>|Harmony in Electrons: Cyclotron and Synchrotron Emission by Thermal Electrons in a Magnetic Field". *Astrophysical Journal* **465**: 327–. doi: 10.1086/177422 (<http://dx.doi.org/10.1086/177422>). <http://arxiv.org/abs/astro-ph/9601073v1>. Retrieved on 2008-09-28.
- [101] Radiation from non-relativistic electrons is sometimes termed cyclotron radiation.
- [102] Rohrlich, F. (December 1999). "The self-force and radiation reaction". *American Journal of Physics* **68** (12): 1109–1112. doi: 10.1119/1.1286430 (<http://dx.doi.org/10.1119/1.1286430>).
- [103] Georgi, Howard (1989). Davies, Paul. ed. *The New Physics*. Cambridge University Press. p. 427. ISBN 0521438314.

- [104] Blumenthal, George J.; Gould, Robert J. (1970). "Bremsstrahlung, Synchrotron Radiation, and Compton Scattering of High-Energy Electrons Traversing Dilute Gases". *Reviews of Modern Physics* **42**: 237–270. doi: 10.1103/RevModPhys.42.237 (<http://dx.doi.org/10.1103/RevModPhys.42.237>).
- [105] The change in wavelength, $\Delta\lambda$, depends on the angle of the recoil, θ , as follows,
- $$\Delta\lambda = \frac{h}{mc}(1 - \cos\theta)$$
- [107] where c is the speed of light in a vacuum and m is the electron mass. See Zombeck (2007:393,396).
- [108] Staff (2008). http://nobelprize.org/nobel_prizes/physics/laureates/1927/|"The Nobel Prize in Physics 1927". The Nobel Foundation. http://nobelprize.org/nobel_prizes/physics/laureates/1927/. Retrieved on 2008-09-28.
- [109] Beringer, Robert; Montgomery, C. G. (1942). "The Angular Distribution of Positron Annihilation Radiation". *Physical Review* **61** (5–6): 222–224. doi: 10.1103/PhysRev.61.222 (<http://dx.doi.org/10.1103/PhysRev.61.222>).
- [110] Wilson, Jerry; Buffa, Anthony (2000). *College Physics* (4th ed.). Prentice Hall. pp. 888. ISBN 0130824445.
- [111] Eichler, Jörg (2005-11-14). "Electron-positron pair production in relativistic ion-atom collisions". *Physics Letters A* **347** (1–3): 67–72. doi: 10.1016/j.physleta.2005.06.105 (<http://dx.doi.org/10.1016/j.physleta.2005.06.105>).
- [112] Hubbell, J. H. (June 2006). "Electron positron pair production by photons: A historical overview". *Radiation Physics and Chemistry* **75** (6): 614–623. doi: 10.1016/j.radphyschem.2005.10.008 (<http://dx.doi.org/10.1016/j.radphyschem.2005.10.008>). Bibcode: 2006RaPC...75..614H (<http://adsabs.harvard.edu/abs/2006RaPC...75..614H>).
- [113] Mulliken, Robert S. (1967). "Spectroscopy, Molecular Orbitals, and Chemical Bonding". *Science* **157** (3784): 13–24. doi: 10.1126/science.157.3784.13 (<http://dx.doi.org/10.1126/science.157.3784.13>). PMID 5338306.
- [114] Burhop, Eric H. S. (1952). *The Auger Effect and Other Radiationless Transitions*. New York: Cambridge University Press. pp. 2–3.
- [115] Grupen, C. (June 28–July 10 1999). "Physics of Particle Detection". *AIP Conference Proceedings, Instrumentation in Elementary Particle Physics, VIII* **536**: 3–34, Istanbul: Dordrecht, D. Reidel Publishing Company. doi: 10.1063/1.1361756 (<http://dx.doi.org/10.1063/1.1361756>).
- [116] Jiles, David (1998). *Introduction to Magnetism and Magnetic Materials*. CRC Press. pp. 280–287. ISBN 0412798603.
- [117] Löwdin, Per Olov; Erkki Brändas, Erkki; Kryachko, Eugene S. (2003). *Fundamental World of Quantum Chemistry: A Tribute to the Memory of Per- Olov Löwdin*. Springer. pp. 393–394. ISBN 140201290X.
- [118] Pauling, Linus (1960). *The Nature of the Chemical Bond and the Structure of Molecules and Crystals: An Introduction to Modern Structural Chemistry*. Cornell University Press. pp. 5–10. ISBN 0801403332.
- [119] McQuarrie, Donald Allan; Simon, John Douglas (1997). *Physical Chemistry: A Molecular Approach*. University Science Books. pp. 325–361. ISBN 0935702997.
- [120] Daudel, R.; Bader, R. F. W.; Stephens, M. E.; Borrett, D. S. (1973-10-11). "<http://article.pubs.nrc-cnrc.gc.ca/ppv/RPViewDoc?issn=1480-3291&volume=52&issue=8&startPage=1310>|The Electron Pair in Chemistry". *Canadian Journal of Chemistry* **52**: 1310–1320. doi: 10.1139/v74-201 (<http://dx.doi.org/10.1139/v74-201>). <http://article.pubs.nrc-cnrc.gc.ca/ppv/RPViewDoc?issn=1480-3291&volume=52&issue=8&startPage=1310>. Retrieved on 2008-10-12.
- [121] Freeman, G. R.; March, N. H. (1999). "Triboelectricity and some associated phenomena". *Materials science and technology* **15** (12): 1454–1458.
- [122] Weinberg, Steven (2003). *The Discovery of Subatomic Particles*. Cambridge University Press. pp. 15–16. ISBN 052182351X.
- [123] Guru, Bhag S.; Hızıroğlu, Hüseyin R. (2004). *Electromagnetic Field Theory*. Cambridge University Press. pp. 138, 276. ISBN 0521830168.
- [124] Achuthan, M. K.; Bhat, K. N. (2007). *Fundamentals of Semiconductor Devices*. Tata McGraw-Hill. pp. 49–67. ISBN 007061220X.
- [125] Ziman, J. M. (2001). *Electrons and Phonons: The Theory of Transport Phenomena in Solids*. Oxford University Press. p. 260. ISBN 0198507798.
- [126] Main, Peter (1993-06-12). "<http://www.newscientist.com/article/mg13818774.500-when-electrons-go-with-the-flow-remove-the-obstacles-thatcreate-electri> electrons go with the flow: Remove the obstacles that create electrical resistance, and you get ballistic electrons and a quantum surprise". *New Scientist* **1887**: 30. <http://www.newscientist.com/article/mg13818774.500-when-electrons-go-with-the-flow-remove-the-obstacles-thatcreate-electrical-resistance-and-you-get-ballistic-electrons-and-a->html. Retrieved on 2008-10-09.
- [127] Blackwell, Glenn R. (2000). *The Electronic Packaging Handbook*. CRC Press. pp. 6.39–6.40. ISBN 0849385911.

- [128] Durrant, Alan (2000). *Quantum Physics of Matter: The Physical World*. CRC Press. pp. 43, 71–78. ISBN 0750307218.
- [129] Staff (2008). http://nobelprize.org/nobel_prizes/physics/laureates/1972/|"The Nobel Prize in Physics 1972". The Nobel Foundation. http://nobelprize.org/nobel_prizes/physics/laureates/1972/. Retrieved on 2008-10-13.
- [130] Kadin, Alan M. (2007). "<http://arxiv.org/abs/cond-mat/0510279>|Spatial Structure of the Cooper Pair". *Journal of Superconductivity and Novel Magnetism* **20** (4): 285–292. doi: 10.1007/s10948-006-0198-z (<http://dx.doi.org/10.1007/s10948-006-0198-z>). <http://arxiv.org/abs/cond-mat/0510279>. Retrieved on 2008-10-13.
- [131] Staff (2008). http://nobelprize.org/nobel_prizes/physics/laureates/1958/|"The Nobel Prize in Physics 1958, for the discovery and the interpretation of the Cherenkov effect". The Nobel Foundation. http://nobelprize.org/nobel_prizes/physics/laureates/1958/. Retrieved on 2008-09-25.
- [132] Staff (2008-08-26). <http://www2.slac.stanford.edu/vvc/theory/relativity.html>|"Special Relativity". Stanford Linear Accelerator Center. <http://www2.slac.stanford.edu/vvc/theory/relativity.html>. Retrieved on 2008-09-25.
- [133] Solving for the velocity of the electron, and using an approximation for large γ , gives:
- $$v = c\sqrt{1 - \frac{1}{\gamma^2}} \approx \left(1 - \frac{1}{2}\gamma^{-2}\right)c = 0.999\,999\,999\,95\,c.$$
- [136] Adams, Steve (2000). *Frontiers: Twentieth Century Physics*. CRC Press. p. 215. ISBN 0748408401.
- [137] Lurquin, Paul F. (2003). *The Origins of Life and the Universe*. Columbia University Press. p. 2. ISBN 0231126557.
- [138] Silk, Joseph (2000). *The Big Bang: The Creation and Evolution of the Universe* (3rd ed.). Macmillan. pp. 110–112, 134–137. ISBN 080507256X.
- [139] Christianto, Vic; Smarandache, Florentin (October 2007). "http://www.ptep-online.com/index_files/2007/PP-11-16.PDF|Thirty Unsolved Problems in the Physics of Elementary Particles" (PDF). *Progress in Physics* **4**: 112–114. http://www.ptep-online.com/index_files/2007/PP-11-16.PDF. Retrieved on 2008-09-04.
- [140] Kolb, Edward W.; Wolfram, Stephen (1980-04-07). "The Development of Baryon Asymmetry in the Early Universe". *Physics Letters B* **91** (2): 217–221. doi: 10.1016/0370-2693(80)90435-9 ([http://dx.doi.org/10.1016/0370-2693\(80\)90435-9](http://dx.doi.org/10.1016/0370-2693(80)90435-9)).
- [141] Sather, Eric (Spring/Summer 1996). <http://www.slac.stanford.edu/pubs/beamline/26/1/26-1-sather.pdf>|"The Mystery of Matter Asymmetry" (PDF). *Beam Line*. University of Stanford. <http://www.slac.stanford.edu/pubs/beamline/26/1/26-1-sather.pdf>. Retrieved on 2008-11-01.
- [142] Burles, Scott; Nollett, Kenneth M.; Turner, Michael S. (1999-03-19). <http://arxiv.org/abs/astro-ph/9903300>"Big-Bang Nucleosynthesis: Linking Inner Space and Outer Space". arXiv, University of Chicago. <http://arxiv.org/abs/astro-ph/9903300>. Retrieved on 2008-10-15.
- [143] Boesgaard, A. M.; Steigman, G. (1985). "http://adsabs.harvard.edu/cgi-bin/bib_query?1985ARA&A..23..319B|Big bang nucleosynthesis - Theories and observations". *Annual review of astronomy and astrophysics* **23** (2): 319–378. doi: 10.1146/annurev.aa.23.090185.001535 (<http://dx.doi.org/10.1146/annurev.aa.23.090185.001535>). http://adsabs.harvard.edu/cgi-bin/bib_query?1985ARA%26A..23..319B. Retrieved on 2008-08-28.
- [144] Barkana, Rennan (2006-08-18). "<http://www.sciencemag.org/cgi/content/full/313/5789/931>|The First Stars in the Universe and Cosmic Reionization". *Science* **313** (5789): 931–934. doi: 10.1126/science.1125644 (<http://dx.doi.org/10.1126/science.1125644>). PMID 16917052. <http://www.sciencemag.org/cgi/content/full/313/5789/931>. Retrieved on 2008-11-01.
- [145] Burbidge, E. Margaret; Burbidge, G. R.; Fowler, William A.; Hoyle, F. (1957). "Synthesis of Elements in Stars". *Reviews of Modern Physics* **29** (4): 548–647. doi: 10.1103/RevModPhys.29.547 (<http://dx.doi.org/10.1103/RevModPhys.29.547>).
- [146] Rodberg, L. S.; Weisskopf, V. F. (1957). "Fall of Parity: Recent Discoveries Related to Symmetry of Laws of Nature". *Science* **125** (3249): 627–633. doi: 10.1126/science.125.3249.627 (<http://dx.doi.org/10.1126/science.125.3249.627>). PMID 17810563.
- [147] Fryer, Chris L. (September 1999). "Mass Limits For Black Hole Formation". *The Astrophysical Journal* **522** (1): 413–418. doi: 10.1086/307647 (<http://dx.doi.org/10.1086/307647>). Bibcode: 1999ApJ...522..413F (<http://adsabs.harvard.edu/abs/1999ApJ...522..413F>).
- [148] Parikh, Maulik K.; Wilczek, Frank (2000). "Hawking Radiation As Tunneling". *Physical Review Letters* **85** (24): 5042–5045. doi: 10.1103/PhysRevLett.85.5042 (<http://dx.doi.org/10.1103/PhysRevLett.85.5042>).
- [149] Hawking, S. W. (1974-03-01). "Black hole explosions?". *Nature* **248**: 30–31. doi: 10.1038/248030a0 (<http://dx.doi.org/10.1038/248030a0>).
- [150] Halzen, F.; Hooper, D. (2002). "<http://adsabs.harvard.edu/abs/2002astro.ph..4527H>|High-energy neutrino astronomy: the cosmic ray connection". *Reports on Progress in Physics* **66**: 1025–1078. doi:

- 10.1088/0034-4885/65/7/201 (<http://dx.doi.org/10.1088/0034-4885/65/7/201>). <http://adsabs.harvard.edu/abs/2002astro.ph..4527H>. Retrieved on 2008-08-28.
- [151] Ziegler, J. F.. "Terrestrial cosmic ray intensities". *IBM Journal of Research and Development* **42** (1): 117–139. doi: 10.1147/rd.421.0117 (<http://dx.doi.org/10.1147/rd.421.0117>).
- [152] Sutton, Christine (1990-08-04). <http://www.newscientist.com/article/mg12717284.700-muons-pions-and-other-strange-particles-.html>"Muons, pions and other strange particles". New Scientist. <http://www.newscientist.com/article/mg12717284.700-muons-pions-and-other-strange-particles-.html>. Retrieved on 2008-08-28.
- [153] Wolpert, Stuart (2008-07-24). <http://www.universityofcalifornia.edu/news/article/18277>"Scientists solve 30-year-old aurora borealis mystery". University of California. <http://www.universityofcalifornia.edu/news/article/18277>. Retrieved on 2008-10-11.
- [154] Gurnett, Donald A.; Anderson, Roger R. (1976-12-10). "Electron Plasma Oscillations Associated with Type III Radio Bursts". *Science* **194** (4270): 1159–1162. doi: 10.1126/science.194.4270.1159 (<http://dx.doi.org/10.1126/science.194.4270.1159>). PMID 17790910.
- [155] Martin, W. C.; Wiese, W. L. (May 2007). <http://physics.nist.gov/Pubs/AtSpec/>"Atomic Spectroscopy: A Compendium of Basic Ideas, Notation, Data, and Formulas". National Institute of Standards and Technology. <http://physics.nist.gov/Pubs/AtSpec/>. Retrieved on 2007-01-08.
- [156] Fowles, Grant R. (1989). *Introduction to Modern Optics*. Courier Dover Publications. pp. 227–233. ISBN 0486659577.
- [157] Staff (2008). http://nobelprize.org/nobel_prizes/physics/laureates/1989/illpres/"The Nobel Prize in Physics 1989". The Nobel Foundation. http://nobelprize.org/nobel_prizes/physics/laureates/1989/illpres/. Retrieved on 2008-09-24.
- [158] Ekstrom, Philip; Wineland, David (1980). "<http://tf.nist.gov/general/pdf/166.pdf>The isolated Electron" (PDF). *Scientific American* **243** (2): 91–101. <http://tf.nist.gov/general/pdf/166.pdf>. Retrieved on 2008-09-24.
- [159] Mauritsson, Johan. <http://www.atto.fysik.lth.se/video/pressrelen.pdf>"Electron filmed for the first time ever" (PDF). Lunds Universitet. <http://www.atto.fysik.lth.se/video/pressrelen.pdf>. Retrieved on 2008-09-17.
- [160] Mauritsson, J.; Johnsson, P.; Mansten, E. *et al* (2008). "<http://www.atto.fysik.lth.se/publications/papers/MauritssonPRL2008.pdf>Coherent Electron Scattering Captured by an Attosecond Quantum Stroboscope" (pdf). *Physical Review Letters* **100**: 073003. doi: 10.1103/PhysRevLett.100.073003 (<http://dx.doi.org/10.1103/PhysRevLett.100.073003>). <http://www.atto.fysik.lth.se/publications/papers/MauritssonPRL2008.pdf>.
- [161] Damascelli, Andrea (2004). "Probing the Electronic Structure of Complex Systems by ARPES". *Physica Scripta* **T109**: 61–74. doi: 10.1238/Physica.Topical.109a00061 (<http://dx.doi.org/10.1238/Physica.Topical.109a00061>).
- [162] Staff (1975-04-14). <http://grin.hq.nasa.gov/ABSTRACTS/GPN-2000-003012.html>"Image # L-1975-02972". Langley Research Center, NASA. <http://grin.hq.nasa.gov/ABSTRACTS/GPN-2000-003012.html>. Retrieved on 2008-09-20.
- [163] Elmer, John (2008-03-03). <https://www.llnl.gov/str/MarApr08/elmer.html>"Standardizing the Art of Electron-Beam Welding". Lawrence Livermore National Laboratory. <https://www.llnl.gov/str/MarApr08/elmer.html>. Retrieved on 2008-10-16.
- [164] Ozdemir, Faik S. (June 25–27, 1979). "Electron beam lithography (<http://portal.acm.org/citation.cfm?id=800292.811744>)". *Proceedings of the 16th Conference on Design automation*: 383–391, San Diego, CA, USA: IEEE Press. Retrieved on 2008-10-16.
- [165] Jongen, Yves; Herer, Arnold (May 2-5, 1996). "Electron Beam Scanning in Industrial Applications (<http://adsabs.harvard.edu/abs/1996APS..MAY.H9902J>)". *APS/AAPT Joint Meeting*, American Physical Society. Retrieved on 2008-10-16.
- [166] Beddar, A. S.; Domanovic, M. A.; Kubu, M. L.; Ellis, R. J.; Sibata, C. H.; Kinsella, T. J. (November 2001). "http://findarticles.com/p/articles/mi_m0FSL/is_ai_81161386Mobile linear accelerators for intraoperative radiation therapy". *AORN Journal* **74**: 700. doi: 10.1016/S0001-2092(06)61769-9 ([http://dx.doi.org/10.1016/S0001-2092\(06\)61769-9](http://dx.doi.org/10.1016/S0001-2092(06)61769-9)). http://findarticles.com/p/articles/mi_m0FSL/is_ai_81161386. Retrieved on 2008-10-26.
- [167] Gazda, Michael J.; Coia, Lawrence R. (2007-06-01). <http://www.cancernetwork.com/cancer-management/chapter02/article/10165/1165822>"Principles of Radiation Therapy". Cancer Network. <http://www.cancernetwork.com/cancer-management/chapter02/article/10165/1165822>. Retrieved on 2008-10-26.
- [168] The polarization of an electron beam means that the spins of all electrons point into one direction. In other words, the projections of the spins of all electrons onto the their momentum vector have the same sign.
- [169] Chao, Alexander W.; Tigner, Maury (1999). *Handbook of Accelerator Physics and Engineering*. World Scientific Publishing Company. pp. 155, 188. ISBN 9810235003.

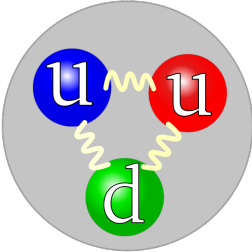
- [170] Oura, K.; Lifshits, V. G.; Saranin, A. A.; Zotov, A. V.; Katayama, M. (2003). *Surface Science: An Introduction*. Springer-Verlag. pp. 1–45. ISBN 3540005455.
- [171] Ichimiya, Ayahiko; Cohen, Philip I. (2004). *Reflection High-energy Electron Diffraction*. Cambridge University Press. p. 1. ISBN 0521453739.
- [172] Heppell, T. A. (1967). "A combined low energy and reflection high energy electron diffraction apparatus". *Journal of Scientific Instruments* **44**: 686–688. doi: 10.1088/0950-7671/44/9/311 (<http://dx.doi.org/10.1088/0950-7671/44/9/311>).
- [173] McMullan, D. (August 1993). <http://www-g.eng.cam.ac.uk/125/achievements/mcmullan/mcm.html>|"Scanning Electron Microscopy: 1928–1965". University of Cambridge. <http://www-g.eng.cam.ac.uk/125/achievements/mcmullan/mcm.htm>. Retrieved on 2009-03-23.
- [174] Cember, Herman (1996). *Introduction to Health Physics*. McGraw-Hill Professional. pp. 42–43. ISBN 0071054618.
- [175] Staff (2008-01-22). <http://www.physorg.com/news120231316.html>|"Debut of TEAM 0.5, the World's Best Microscope". PhysOrg. <http://www.physorg.com/news120231316.html>. Retrieved on 2008-10-21.
- [176] Bozzola, John J.; Russell, Lonnie D. (1999). *Electron Microscopy: Principles and Techniques for Biologists*. Jones & Bartlett Publishers. pp. 12, 197–199. ISBN 0763701920.
- [177] Flegler, Stanley L.; Heckman Jr., John W.; Klomparens, Karen L. (1995-10-01). *Scanning and Transmission Electron Microscopy: An Introduction* (Reprint ed.). Oxford University Press. pp. 43–45. ISBN 0195107519.
- [178] Freund, Henry P.; Antonsen, Thomas (1996). *Principles of Free-Electron Lasers*. Springer. pp. 1–30. ISBN 0412725401.
- [179] Kitzmiller, John W. (1995). *Television Picture Tubes and Other Cathode-Ray Tubes: Industry and Trade Summary*. DIANE Publishing. pp. 3–5. ISBN 0788121006.
- [180] Sclater, Neil (1999). *Electronic Technology Handbook*. McGraw-Hill Professional. pp. 227–228. ISBN 0070580480.
- [181] Staff (2008). http://nobelprize.org/educational_games/physics/integrated_circuit/history/|"The History of the Integrated Circuit". The Nobel Foundation. http://nobelprize.org/educational_games/physics/integrated_circuit/history/. Retrieved on 2008-10-18.

References

External links

- <http://www.aip.org/history/electron/>|"The Discovery of the Electron". American Institute of Physics, Center for History of Physics. <http://www.aip.org/history/electron/>. Retrieved on 2006-08-10.
- <http://pdg.lbl.gov/>|"Particle Data Group". University of California. <http://pdg.lbl.gov/>. Retrieved on 2008-11-17.
- Bock, Rudolf K.; Vasilescu, Angela (1998). <http://physics.web.cern.ch/Physics/ParticleDetector/BriefBook/>|*The Particle Detector BriefBook* (14th ed.). Springer. ISBN 3540641203. <http://physics.web.cern.ch/Physics/ParticleDetector/BriefBook/>. Retrieved on 2008-10-02.
- Brown University. <http://www.educatedearth.net/video.php?id=3573>|*Single Electron on Video*. [Shockwave/Flash]. Educated Earth. <http://www.educatedearth.net/video.php?id=3573>. Retrieved on 2009-01-23.

Proton

Proton	
	
The quark structure of the proton.	
Classification:	Baryon
Composition:	2 up, 1 down
Family:	Fermion
Group:	Hadron
Interaction:	Gravity, Electromagnetic, Weak, Strong
Antiparticle:	Antiproton
Theorized:	William Prout (1815)
Discovered:	Ernest Rutherford (1919)
Symbol(s):	p, p ⁺ , N ⁺
Mass:	1.672621637(83)×10 ⁻²⁷ kg 938.272013(23) MeV/c ² 1.00727646677(10) u ^[1]
Mean lifetime:	>2.1×10 ²⁹ years (stable)
Electric charge:	+1 e. 1.602176487(40) × 10 ⁻¹⁹ C ^[1]
Charge radius:	0.875(7) fm
Electric dipole moment:	<5.4×10 ⁻²⁴ e cm
Electric polarizability:	1.20(6)×10 ⁻³ fm ³
Magnetic moment:	2.792847351(28) μ _N
Magnetic polarizability:	1.9(5)×10 ⁻⁴ fm ³
Spin:	¹ □ ₂
Isospin:	¹ □ ₂
Parity:	+1
Condensed:	I(J ^P) = ¹ □ ₂ (¹ □ ₂ ⁺)

The **proton** is a subatomic particle with an electric charge of +1 elementary charge. It is found in the nucleus of each atom but is also stable by itself and has a second identity as the hydrogen ion, ¹H⁺. It is composed of 3 even more fundamental particles comprising two

up quarks and one down quark.^[2]

Description

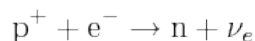
Protons are spin-1/2 fermions and are composed of three quarks^[3], making them baryons. The two up quarks and one down quark of the proton are held together by the strong force, mediated by gluons.^[2]

Protons and neutrons are both nucleons, which may be bound by the nuclear force into atomic nuclei. The nucleus of the most common isotope of the hydrogen atom is a single proton (it contains no neutrons). The nuclei of heavy hydrogen (deuterium and tritium) contain neutrons. All other types of atoms are composed of two or more protons and various numbers of neutrons. The number of protons in the nucleus determines the chemical properties of the atom and thus which chemical element is represented; it is the number of both neutrons and protons in a nuclide which determine the particular isotope of an element. Protons have a positive charge.

Stability

Protons are observed to be stable and their theoretical minimum half-life is 1×10^{36} years. Grand unified theories generally predict that proton decay should take place, although experiments so far have only resulted in a lower limit of 10^{35} years for the proton's lifetime. In other words, proton decay has never been witnessed and the experimental lower bound on the mean proton lifetime (2.1×10^{29} years) is put by the Sudbury Neutrino Observatory^[4].

However, protons are known to transform into neutrons through the process of electron capture. This process does not occur spontaneously but only when energy is supplied. The equation is:



where

p is a proton,

e is an electron,

n is a neutron, and

ν_e is an electron neutrino

The process is reversible: neutrons can convert back to protons through beta decay, a common form of radioactive decay. In fact, a free neutron decays this way with a mean lifetime of about 15 minutes.

The proton in chemistry

Atomic number

In chemistry the number of protons in the nucleus of an atom is known as the atomic number, which determines the chemical element to which the atom belongs. For example, the atomic number of chlorine is 17; this means that each chlorine atom has 17 protons and that all atoms with 17 protons are chlorine atoms. The chemical properties of each atom are determined by the number of (negatively charged) electrons, which for neutral atoms is equal to the number of (positive) protons so that the total charge is zero. For example, a

neutral chlorine atom has 17 protons and 17 electrons, while a negative Cl^- ion has 17 protons and 18 electrons for a total charge of -1.

All atoms of a given element are not necessarily identical, however, as the number of neutrons may vary to form different isotopes. Again for chlorine as an example, there are two stable isotopes - ^{35}Cl with 35 nucleons which are 17 protons and $35-17 = 18$ neutrons, and ^{37}Cl with 17 protons and $37-17 = 20$ neutrons. Other isotopes of chlorine are radioactive.

Hydrogen as proton

Since the atomic number of hydrogen is 1, a positive hydrogen ion (H^+) has no electrons and corresponds to a bare nucleus with 1 proton (and 0 neutrons for the most abundant isotope ^1H). In chemistry therefore, the word "proton" is commonly used as a synonym for hydrogen ion (H^+) or hydrogen nucleus in several contexts:

1. The transfer of H^+ in an acid-base reaction is referred to "proton transfer". The acid is referred to as a proton donor and the base as a proton acceptor.
2. The hydronium ion (H_3O^+) in aqueous solution corresponds to a hydrated hydrogen ion. Often the water molecule is ignored and the ion written as simply $\text{H}^+(\text{aq})$ or just H^+ , and referred to as a "proton". This is the usual meaning in biochemistry, as in the term proton pump which refers to a protein or enzyme which controls the movement of H^+ ions across cell membranes.
3. Proton NMR refers to the observation of hydrogen nuclei in (mostly organic) molecules by nuclear magnetic resonance. This method uses the spin of the proton, which has the value one-half.

History

Ernest Rutherford is generally credited with the discovery of the proton. In 1918 Rutherford noticed that when alpha particles were shot into nitrogen gas, his scintillation detectors showed the signatures of hydrogen nuclei. Rutherford determined that the only place this hydrogen could have come from was the nitrogen, and therefore nitrogen must contain hydrogen nuclei. He thus suggested that the hydrogen nucleus, which was known to have an atomic number of 1, was an elementary particle.

Prior to Rutherford, Eugen Goldstein had observed canal rays, which were composed of positively charged ions. After the discovery of the electron by J.J. Thomson, Goldstein suggested that since the atom is electrically neutral there must be a positively charged particle in the atom and tried to discover it. He used the "canal rays" observed to be moving against the electron flow in cathode ray tubes. After the electron had been removed from particles inside the cathode ray tube they became positively charged and moved towards the cathode. Most of the charged particles passed through the cathode, it being perforated, and produced a glow on the glass. At this point, Goldstein believed that he had discovered the proton.^[5] When he calculated the ratio of charge to mass of this new particle (which in case of the electron was found to be the same for every gas that was used in the cathode ray tube) was found to be different when the gases used were changed. The reason was simple. What Goldstein assumed to be a proton was actually an ion. He gave up his work there, but promised that "he would return." However, he was widely ignored.

The proton is named after the neuter singular of the Greek word for "first", *πρῶτον*.

Exposure

The Apollo Lunar Surface Experiments Packages (ALSEP) determined that more than 95% of the particles in the solar wind are electrons and protons, in approximately equal numbers.^{[6] [7]}

"Because the Solar Wind Spectrometer made continuous measurements, it was possible to measure how the Earth's magnetic field affects arriving solar wind particles. For about two-thirds of each orbit, the Moon is outside of the Earth's magnetic field. At these times, a typical proton density was 10 to 20 per cubic centimeter, with most protons having velocities between 400 and 650 kilometers per second. For about five days of each month, the Moon is inside the Earth's geomagnetic tail, and typically no solar wind particles were detectable. For the remainder of each lunar orbit, the Moon is in a transitional region known as the magnetosheath, where the Earth's magnetic field affects the solar wind but does not completely exclude it. In this region, the particle flux is reduced, with typical proton velocities of 250 to 450 kilometers per second. During the lunar night, the spectrometer was shielded from the solar wind by the Moon and no solar wind particles were measured."^[6]

Research has been performed on the dose-rate effects of protons, as typically found in space travel, on human health.^{[7] [8]} More specifically, there are hopes to identify what specific chromosomes are damaged, and to define the damage, during cancer development from proton exposure.^[7] Another study looks into determining "the effects of exposure to proton irradiation on neurochemical and behavioral endpoints, including dopaminergic functioning, amphetamine-induced conditioned taste aversion learning, and spatial learning and memory as measured by the Morris water maze."^[8] Electrical charging of spacecraft by exposure to interplanetary protons has also been studied.^[9] There are many more studies which pertain to space travel, including galactic cosmic rays and their possible health effects, and solar proton event exposure.

Antiproton

CPT-symmetry puts strong constraints on the relative properties of particles and antiparticles and, therefore, is open to stringent tests. For example, the charges of the proton and antiproton must sum to exactly zero. This equality has been tested to one part in 10^8 . The equality of their masses has also been tested to better than one part in 10^8 . By holding antiprotons in a Penning trap, the equality of the charge to mass ratio of the proton and the antiproton has been tested to one part in 9×10^{11} . The magnetic moment of the antiproton has been measured with error of 8×10^{-3} nuclear Bohr magnetons, and is found to be equal and opposite to that of the proton.

See also

- Electron
- Fermion field
- Hydrogen
- Hydron (chemistry)
- List of particles
- Neutron
- Particle physics
- Proton decay
- Proton-proton chain reaction
- Proton therapy
- Quark model
- Subatomic particle
- Space colonization

References

- [1] C. Amsler *et al.*, "Review of Particle Physics" Physics Letters **B667**, 1 (2008)
- [2] W.N.Cottingham and D.A.Greenwood "An Introduction to Nuclear Physics", Cambridge University Press (1986), p.19
- [3] Adair, Robert K.: "The Great Design: Particles, Fields, and Creation.", page 214. New York: Oxford University Press, 1989.
- [4] SNO Collaboration, S.N. Ahmed *et al.*, "Constraints on nucleon decay via *invisible* modes from the Sudbury Neutrino Observatory", Phys. Rev. Lett. **92** (2004) 102004
- [5] Gilreath, Esmarch S.: "Fundamental Concepts of Inorganic Chemistry.", page 5. New York: McGraw-Hill, 1958.
- [6] " *Apollo 11 Mission* (http://www.lpi.usra.edu/lunar/missions/apollo/apollo_11/experiments/swc/)" Lunar and Planetary Institute, 2009. Accessed 12 June 2009.
- [7] " *Space Travel and Cancer Linked? Stony Brook Researcher Secures NASA Grant to Study Effects of Space Radiation* (http://www.bnl.gov/bnlweb/pubaf/pr/PR_display.asp?prID=07-X17)" December 12, 2007. Brookhaven National Laboratory News. Stony Brook, N.Y., Accessed 12 June 2009
- [8] Shukitt-Hale, B., Szprengiel, A., Pluhar, J., Rabin, B. M. & Joseph, J. A. " *The effects of proton exposure on neurochemistry and behavior* (<http://biblioteca.universia.net/ficha.do?id=43176300>)". Elsevier Ltd on behalf of COSPAR. Article summary published by biblioteca.net. Accessed 12 June 2009.
- [9] N. W. Green and A. R. Frederickson. " *A Study of Spacecraft Charging due to Exposure to Interplanetary Protons* (<http://trs-new.jpl.nasa.gov/dspace/bitstream/2014/39501/1/05-0657.pdf>)". Jet Propulsion Laboratory, California Institute of Technology. Accessed 12 June 2009.

External links

- Particle Data Group (<http://pdg.lbl.gov>)
 - Large Hadron Collider (<http://www.cern.ch/lhc/>)
-

Hadrons

1. REDIRECT Hadron

This is a redirect from a plural word to the singular equivalent.

You may use the aliased template {{R to singular}} to accomplish the same end.

This redirect link is used for convenience, usually for plurals that do not follow simple conventions. In many cases, it is preferable to add the plural directly after the link (that is, [[link]]s). However, do not replace these redirected links with a simpler link unless the page is updated for another reason (see Wikipedia:Redirect#Do not "fix" links to redirects that are not broken).

For more information, follow the category link.

Quarks

1. REDIRECT Quark

Gluons

1. REDIRECT Gluon

Higgs boson

<i>Higgs boson</i>	
Composition:	Elementary particle
Family:	Boson
Status:	Hypothetical
Theorized:	F. Englert, R. Brout, P. Higgs, G. S. Guralnik, C. R. Hagen, and T. W. B. Kibble 1964
Spin:	0

The **Higgs boson** is a massive scalar elementary particle predicted to exist by the Standard Model in particle physics. At present there are no known fundamental scalar particles in nature.

The Higgs boson is the only Standard Model particle that has not yet been observed. Experimental detection of the Higgs boson would help explain the origin of mass in the universe. More specifically, the Higgs boson would explain the difference between the massless photon, which mediates electromagnetism, and the massive W and Z bosons, which mediate the weak force. If the Higgs boson exists, it is an integral and pervasive component of the material world.

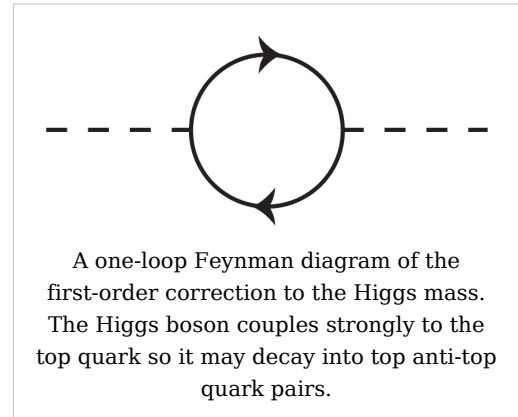
The Large Hadron Collider (LHC) at CERN in Geneva, which came online on September 10, 2008 is scheduled to become fully operational by late 2009, and is expected to provide experimental evidence either confirming or refuting the Higgs boson's existence. An accident in September 2008 has the LHC temporarily out of commission; ongoing experiments at Fermilab continue previous attempts at detection (although hindered by the lower energy of the Fermilab Tevatron accelerator). It has been reported that Fermilab physicists suggest the odds of Tevatron detecting the Higgs boson are between 50% and 96%, depending on its precise mass.^[1]

Origin

The Higgs mechanism, which gives mass to vector bosons, was theorized in 1964 by François Englert and Robert Brout ("boson scalaire");^[2] in October of the same year by Peter Higgs,^[3] working from the ideas of Philip Anderson; and independently by Gerald Guralnik, C. R. Hagen, and Tom Kibble,^[4] who worked out the results by the spring of 1963.^[5] The three papers written on this discovery by Guralnik, Hagen, Kibble, Higgs, Brout, and Englert were each recognized as milestone papers during *Physical Review Letters* 50th anniversary celebration.^[6] Steven Weinberg and Abdus Salam were the first to apply the Higgs mechanism to the electroweak symmetry breaking. The electroweak theory predicts a neutral particle whose mass is not far from that of the W and Z bosons.

Theoretical overview

The Higgs boson particle is one quantum component of the theoretical Higgs field. In empty space, the Higgs field has an amplitude different from zero, i.e., a non-zero vacuum expectation value. The existence of this non-zero vacuum expectation plays a fundamental role: it gives mass to every elementary particle which should have mass, including the Higgs boson itself. In particular, the acquisition of a non-zero vacuum expectation value spontaneously breaks electroweak gauge symmetry, which scientists often refer to as the Higgs mechanism. This is the simplest mechanism capable of giving mass to the gauge bosons while remaining compatible with gauge theories. In essence, this field is analogous to a pool of molasses that "sticks" to the otherwise massless fundamental particles which travel through the field, converting them into particles with mass which form, for example, the components of atoms.

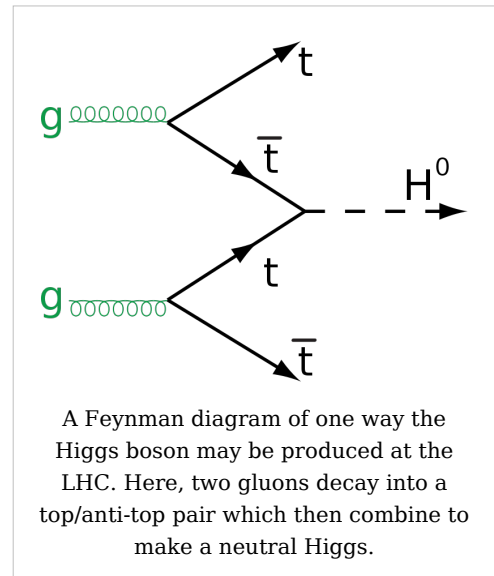


In the Standard Model, the Higgs field consists of two neutral and two charged component fields. Both of the charged components and one of the neutral fields are Goldstone bosons, which act as the longitudinal third-polarization components of the massive W^+ , W^- , and Z bosons. The quantum of the remaining neutral component corresponds to the massive Higgs boson. Since the Higgs field is a scalar field, the Higgs boson has no spin, hence no intrinsic angular momentum. The Higgs boson is also its own antiparticle and is CP-even.

The Standard Model does not predict the mass of the Higgs boson. If that mass is between 115 and 180 GeV/c^2 , then the Standard Model can be valid at energy scales all the way up to the Planck scale (10^{16} TeV). Many theorists expect new physics beyond the Standard Model to emerge at the TeV-scale, based on unsatisfactory properties of the Standard Model. The highest possible mass scale allowed for the Higgs boson (or some other electroweak symmetry breaking mechanism) is 1.4 TeV; beyond this point, the Standard Model becomes inconsistent without such a mechanism because unitarity is violated in certain scattering processes. Many models of supersymmetry predict that the lightest Higgs boson (of several) will have a mass only slightly above the current experimental limits, at around 120 GeV or less.

Experimental search

As of June 2009[7], the Higgs boson has yet to be observed experimentally, despite large efforts invested in accelerator experiments at CERN and Fermilab. The data gathered at the LEP collider at CERN allowed an experimental lower bound to be set for the mass of the Standard Model Higgs boson of $114.4 \text{ GeV}/c^2$ at 95% confidence level. The same experiment has produced a small number of events that could be interpreted as resulting from Higgs bosons with mass just above said cutoff - around 115 GeV - but the number of events was insufficient to draw definite conclusions.^[8] The LEP was shut down in 2000 due to construction of its successor - the Large Hadron Collider (LHC). The LHC, due to begin proper experimentation in 2009 after initial calibration, is expected to be able to confirm or reject the existence of the Higgs boson. Full operational mode has been delayed until late September 2009, because of problems discovered with a number of magnets during the calibration and startup phase.



At the Fermilab Tevatron, there are ongoing experiments searching for the Higgs boson. As of March 2009[7], combined data from CDF and D0 experiments at the Tevatron were sufficient to exclude the Higgs boson in the range between $160 \text{ GeV}/c^2$ and $170 \text{ GeV}/c^2$ at the 95% confidence level.^[9] Continued data collection is aimed at raising this lower bound.

It may be possible to estimate the mass of the Higgs Boson indirectly. In the Standard Model, the Higgs has a number of indirect effects; most notably, Higgs loops result in tiny corrections to W and Z masses. Precision measurements of electroweak parameters, such as the Fermi constant and masses of W/Z bosons, can be used to constrain the mass of the Higgs. As of 2006, measurements of electroweak observables allowed the exclusion of a Standard Model Higgs boson having a mass greater than $285 \text{ GeV}/c^2$ at 95% CL, and estimated its mass to be $129+74-49 \text{ GeV}/c^2$ (approximately 138 proton masses).^[10] As of early 2009, Standard Model Higgs is excluded by electroweak measurements above 185 GeV at 95% CL. However, it should be noted that these indirect constraints make assumptions about post-SM physics (or, more specifically, lack thereof). One may still discover a Higgs above 185 GeV if it's accompanied by other particles between Standard Model and GUT scale.

Some have argued that there exists potential evidence of the Higgs Boson,^{[11] [12]} but to date no such evidence has convinced the physics community.

Alternatives to the Higgs mechanism for electroweak symmetry breaking

In the years since the Higgs boson was proposed, several alternatives to the Higgs mechanism have been proposed. All of the alternative mechanisms use strongly interacting dynamics to produce a vacuum expectation value that breaks electroweak symmetry. A partial list of these alternative mechanisms are:

- Technicolor^[13] is a class of models that attempts to mimic the dynamics of the strong force as a way of breaking electroweak symmetry.
- Extra dimensional Higgsless models where the role of the Higgs field is played by the fifth component of the gauge field.^[14]
- Abbott-Farhi models of composite W and Z vector bosons.^[15]
- Top quark condensate

In popular culture

The Higgs boson is sometimes referred to as "the God particle," after the title of Leon Lederman's book for lay readers.^[16] The term mistakenly implies that the Higgs boson would complete our understanding of physics. In fact, while the discovery of the Higgs boson would be a groundbreaking stage in the story of electroweak unification, it would leave remaining the question of unification with Quantum Chromodynamics (QCD), gravity, and the ultimate origins and early evolution of the universe. Being an atheist, Peter Higgs dislikes the epithet "God particle".^[17] The term is rarely used by particle physicists when discussing the Higgs Boson; its prevalence is primarily due to its usage in popular media.

See also

- List of particles
- Yukawa interaction
- ZZ diboson
- Quantum triviality

Notes

- [1] <http://news.bbc.co.uk/2/hi/science/nature/7893689.stm>|"Race for 'God particle' heats up". <http://news.bbc.co.uk/2/hi/science/nature/7893689.stm>.
- [2] François Englert and Robert Brout, 1964, " Broken Symmetry and the Mass of Gauge Vector Mesons, (<http://link.aps.org/abstract/PRL/v13/p321>)" *Phys. Rev. Lett.* 13: 321-23.
- [3] Peter Higgs, 1964, " Broken Symmetries and the Masses of Gauge Bosons, (<http://link.aps.org/abstract/PRL/v13/p508>)" *Phys. Rev. Lett.* 13: 508-09.
- [4] Gerald Guralnik, C. R. Hagen, and T. W. B. Kibble, 1964, " Global Conservation Laws and Massless Particles, (http://prola.aps.org/abstract/PRL/v13/i20/p585_1)" *Phys. Rev. Let.* 13: 585-87.
- [5] Gerald Guralnik, 2001, " A Physics History of My Part in the Theory of Spontaneous Symmetry Breaking and Gauge particles, (<http://chep.het.brown.edu/stlouis-v4.pdf>)" Text of talk presented at a Colloquium at Washington University in St. Louis.
- [6] Physical Review Letters - 50th Anniversary Milestone Papers (<http://prl.aps.org/50years/milestones#1964>)
- [7] http://en.wikipedia.org/wiki/Higgs_boson
- [8] " Searches for Higgs Bosons (http://pdg.lbl.gov/2006/reviews/higgs_s055.pdf) (pdf)]" from W.-M. Yao *et al.* (2006). "<http://pdg.lbl.gov/Review of Particle Physics>". *J Phys. G* **33**: 1. doi: 10.1088/0954-3899/33/1/001 (<http://dx.doi.org/10.1088/0954-3899/33/1/001>). <http://pdg.lbl.gov>.
- [9] http://www.fnal.gov/pub/presspass/press_releases/Higgs-mass-constraints-20090313.html|"Fermilab experiments constrain Higgs mass". http://www.fnal.gov/pub/presspass/press_releases/Higgs-mass-constraints-20090313.html.

- [10] " H^0 Indirect Mass Limits from Electroweak Analysis. (<http://pdglive.lbl.gov/popubblockdata.brl?nodein=S055HEW&inscript=Y&sizein=1>)"
- [11] Potential Higgs Boson discovery: " Higgs Boson: Glimpses of the God particle. (<http://www.newscientist.com/channel/fundamentals/mg19325934.600-higgs-boson-glimpses-of-the-god-particle.html>)"
- [12] " 'God particle' may have been seen, (<http://news.bbc.co.uk/2/hi/science/nature/3546973.stm>)" BBC news.
- [13] S. Dimopoulos and Leonard Susskind (1979). "Mass Without Scalars". *Nucl.Phys.B* **155**: 237–252. doi: 10.1016/0550-3213(79)90364-X ([http://dx.doi.org/10.1016/0550-3213\(79\)90364-X](http://dx.doi.org/10.1016/0550-3213(79)90364-X)).
- [14] C. Csaki and C. Grojean and L. Pilo and J. Terning (2004). "<http://arXiv.org/abs/hep-ph/0308038>|Towards a realistic model of Higgsless electroweak symmetry breaking". *Physical Review Letters* **92**: 101802. doi: 10.1103/PhysRevLett.92.101802 (<http://dx.doi.org/10.1103/PhysRevLett.92.101802>). <http://arXiv.org/abs/hep-ph/0308038>.
- [15] L. F. Abbott and E. Farhi (1981). "Are the Weak Interactions Strong?". *Phys.Lett.B* **101**: 69. doi: 10.1016/0370-2693(81)90492-5 ([http://dx.doi.org/10.1016/0370-2693\(81\)90492-5](http://dx.doi.org/10.1016/0370-2693(81)90492-5)).
- [16] Leon Lederman, 1993. *The God Particle: If the Universe Is the Answer, What Is the Question?* New York: Dell.
- [17] (<http://www.reuters.com/article/scienceNews/idUSL0765287220080407?sp=true>)

References

- " The LEP Electroweak Working Group. (<http://lepewwg.web.cern.ch/LEPEWWG/>)"
- " Particle Data Group: Review of searches for Higgs bosons. (http://pdg.lbl.gov/2005/reviews/contents_sports.html#hyppartetc)"
- Leon Lederman and Dick Teresi, 1993. *The God Particle: If the Universe Is the Answer, What Is the Question?* Houghton Mifflin Co.. ISBN 0-395-55849-2, paperback ISBN 0-385-31211-3.
- " Fermilab Results Change Estimated Mass Of Postulated Higgs boson. (<http://www.spacedaily.com/news/physics-04s.html>)"
- " Higgs boson on the horizon. (<http://physicsweb.org/article/news/4/9/2/1>)"
- " Signs of mass-giving particle get stronger. (<http://www.sciencenews.org/articles/20001104/fob6.asp>)"
- " Higgs boson: One page explanation. (<http://pprc.qmul.ac.uk/~lloyd/epp/higgs3.html>)" In 1993, the UK Science Minister, William Waldegrave, challenged physicists to produce a one page answer to the question "What is the Higgs boson, and why do we want to find it?"
- " Higgs mechanism/boson simple explanation via cartoon. (http://www.pparc.ac.uk/ps/bbs/bbs_mass_hm.asp)"
- " Higgs physics at the LHC. (<http://www.quark.lu.se/~atlas/thesis/egede/thesis-node6.html>)"
- " Quark experiment predicts heavier Higgs. (<http://www.newscientist.com/news/news.jsp?id=ns99995095>)"
- Martin, Richard, " The God Particle and the Grid. (http://www.wired.com/wired/archive/12.04/grid_pr.html)"
- " The Higgs boson (<http://www.exploratorium.edu/origins/cern/ideas/higgs.html>)" by the CERN exploratorium.
- " Higgs Boson - the search for the God particle. (http://www.bbc.co.uk/radio4/history/inourtime/inourtime_20041118.shtml)" BBC Radio 4: "In Our Time"

Further reading

- G S Guralnik, C R Hagen and T W B Kibble (1964).
"http://link.aps.org/abstract/PRL/v13/p585|Global Conservation Laws and Massless Particles". *Physical Review Letters* **13**: 585. doi: 10.1103/PhysRevLett.13.585 (<http://dx.doi.org/10.1103/PhysRevLett.13.585>). <http://link.aps.org/abstract/PRL/v13/p585>.
- F Englert and R Brout (1964). "http://link.aps.org/abstract/PRL/v13/p321|Broken Symmetry and the Mass of Gauge Vector Mesons". *Physical Review Letters* **13**: 321. doi: 10.1103/PhysRevLett.13.321 (<http://dx.doi.org/10.1103/PhysRevLett.13.321>). <http://link.aps.org/abstract/PRL/v13/p321>.
- Peter Higgs (1964). "Broken Symmetries, Massless Particles and Gauge Fields". *Physics Letters* **12**: 132. doi: 10.1016/0031-9163(64)91136-9 ([http://dx.doi.org/10.1016/0031-9163\(64\)91136-9](http://dx.doi.org/10.1016/0031-9163(64)91136-9)).
- Peter Higgs (1964). "http://link.aps.org/abstract/PRL/v13/p508|Broken Symmetries and the Masses of Gauge Bosons". *Physical Review Letters* **13**: 508. doi: 10.1103/PhysRevLett.13.508 (<http://dx.doi.org/10.1103/PhysRevLett.13.508>). <http://link.aps.org/abstract/PRL/v13/p508>.
- Peter Higgs (1966). "http://prola.aps.org/abstract/PR/v145/i4/p1156_1|Spontaneous Symmetry Breakdown without Massless Bosons". *Physical Review* **145**: 1156. doi: 10.1103/PhysRev.145.1156 (<http://dx.doi.org/10.1103/PhysRev.145.1156>). http://prola.aps.org/abstract/PR/v145/i4/p1156_1.
- Y Nambu; G Jona-Lasinio (1961).
"http://prola.aps.org/abstract/PR/v122/i1/p345_1|Dynamical Model of Elementary Particles Based on an Analogy with Superconductivity". *I Phys. Rev.* **122**: 345–358. doi: 10.1103/PhysRev.122.345 (<http://dx.doi.org/10.1103/PhysRev.122.345>). http://prola.aps.org/abstract/PR/v122/i1/p345_1.
- J Goldstone, A Salam and S Weinberg (1962).
"http://prola.aps.org/abstract/PR/v127/i3/p965_1|Broken Symmetries". *Physical Review* **127**: 965. doi: 10.1103/PhysRev.127.965 (<http://dx.doi.org/10.1103/PhysRev.127.965>). http://prola.aps.org/abstract/PR/v127/i3/p965_1.
- P W Anderson (1963). "http://prola.aps.org/abstract/PR/v130/i1/p439_1|Plasmons, Gauge Invariance, and Mass". *Physical Review* **130**: 439. doi: 10.1103/PhysRev.130.439 (<http://dx.doi.org/10.1103/PhysRev.130.439>). http://prola.aps.org/abstract/PR/v130/i1/p439_1.
- A Klein and B W Lee (1964). "http://prola.aps.org/abstract/PRL/v12/i10/p266_1|Does Spontaneous Breakdown of Symmetry Imply Zero-Mass Particles?". *Physical Review Letters* **12**: 266. doi: 10.1103/PhysRevLett.12.266 (<http://dx.doi.org/10.1103/PhysRevLett.12.266>). http://prola.aps.org/abstract/PRL/v12/i10/p266_1.
- W Gilbert (1964). "http://link.aps.org/abstract/PRL/v12/p713|Broken Symmetries and Massless Particles". *Physical Review Letters* **12**: 713. doi: 10.1103/PhysRevLett.12.713 (<http://dx.doi.org/10.1103/PhysRevLett.12.713>). <http://link.aps.org/abstract/PRL/v12/p713>.

External links

- At Fermilab, the Race Is on for the 'God Particle' (<http://www.nytimes.com/2007/07/24/science/24ferm.html>)
 - Physics World, Introducing the little Higgs (<http://physicsworld.com/cws/article/print/11353>)
 - A quasi-political Explanation of the Higgs Boson (<http://www.hep.ucl.ac.uk/~djm/higgsa.html>)
 - *The Atom Smashers*, a blog about the making of a documentary about the search for the Higgs boson (<http://www.theatomsmashers.blogspot.com/>)
 - In CERN Courier, Steven Weinberg reflects on spontaneous symmetry breaking (<http://cerncourier.com/cws/article/cern/32522>)
 - Steven Weinberg Praises Teams for Higgs Boson Theory (http://www.pas.rochester.edu/urpas/news/Hagen_030708)
 - Physical Review Letters - 50th Anniversary Milestone Papers (<http://prl.aps.org/50years/milestones#1964>)
 - Imperial College London on PRL 50th Anniversary Milestone Papers (http://www3.imperial.ac.uk/newsandeventspggrp/imperialcollege/newssummary/news_13-6-2008-12-42-20?newsid=38514)
 - *The God Particle*, from National Geographic Magazine (<http://ngm.nationalgeographic.com/2008/03/god-particle/achenbach-text>)
 - "Tevatron experiments double-team Higgs boson", sets lower bound at 170GeV (<http://www.physorg.com/news137076565.html>)
 - Englert-Brout-Higgs-Guralnik-Hagen-Kibble Mechanism on Scholarpedia (http://www.scholarpedia.org/article/Englert-Brout-Higgs-Guralnik-Hagen-Kibble_mechanism)
 - History of Englert-Brout-Higgs-Guralnik-Hagen-Kibble Mechanism on Scholarpedia ([http://www.scholarpedia.org/article/Englert-Brout-Higgs-Guralnik-Hagen-Kibble_mechanism_\(history\)](http://www.scholarpedia.org/article/Englert-Brout-Higgs-Guralnik-Hagen-Kibble_mechanism_(history)))
 - God Particle Overview (<http://www.godparticle.com/>)
 - Fermilab 'closing in' on the God particle (<http://www.newscientist.com/article/dn16618-fermilab-closing-in-on-the-god-particle.html>)
 - Provides a new and simple explanation of the mass and gravity enigma (<http://www.higgs-boson.org/>)
-

Quantum chemistry

Quantum chemistry is a branch of theoretical chemistry, which applies quantum mechanics and quantum field theory to address issues and problems in chemistry. The description of the electronic behavior of atoms and molecules as pertaining to their reactivity is one of the applications of quantum chemistry. Quantum chemistry lies on the border between chemistry and physics, and significant contributions have been made by scientists from both fields. It has a strong and active overlap with the field of atomic physics and molecular physics, as well as physical chemistry.

Quantum chemistry mathematically describes the fundamental behavior of matter at the molecular scale.^[1] It is, in principle, possible to describe all chemical systems using this theory. In practice, only the simplest chemical systems may realistically be investigated in purely quantum mechanical terms, and approximations must be made for most practical purposes (e.g., Hartree-Fock, post Hartree-Fock or Density functional theory, see computational chemistry for more details). Hence a detailed understanding of quantum mechanics is not necessary for most chemistry, as the important implications of the theory (principally the orbital approximation) can be understood and applied in simpler terms.

In quantum mechanics the Hamiltonian, or the physical state, of a particle can be expressed as the sum of two operators, one corresponding to kinetic energy and the other to potential energy. The Hamiltonian in the Schrödinger wave equation used in quantum chemistry does not contain terms for the spin of the electron.

Solutions of the Schrödinger equation for the hydrogen atom gives the form of the wave function for atomic orbitals, and the relative energy of the various orbitals. The orbital approximation can be used to understand the other atoms e.g. helium, lithium and carbon.

History

The **history of quantum chemistry** essentially began with the 1838 discovery of cathode rays by Michael Faraday, the 1859 statement of the black body radiation problem by Gustav Kirchhoff, the 1877 suggestion by Ludwig Boltzmann that the energy states of a physical system could be discrete, and the 1900 quantum hypothesis by Max Planck that any energy radiating atomic system can theoretically be divided into a number of discrete energy elements ϵ such that each of these energy elements is proportional to the frequency ν with which they each individually radiate energy, as defined by the following formula:

$$\epsilon = h\nu$$

where h is a numerical value called Planck's Constant. Then, in 1905, to explain the photoelectric effect (1839), i.e., that shining light on certain materials can function to eject electrons from the material, Albert Einstein postulated, based on Planck's quantum hypothesis, that light itself consists of individual quantum particles, which later came to be called photons (1926). In the years to follow, this theoretical basis slowly began to be applied to chemical structure, reactivity, and bonding.

Electronic structure

The first step in solving a quantum chemical problem is usually solving the Schrödinger equation (or Dirac equation in relativistic quantum chemistry) with the electronic molecular Hamiltonian. This is called determining the **electronic structure** of the molecule. It can be said that the electronic structure of a molecule or crystal implies essentially its chemical properties. An exact solution for the Schrödinger equation can only be obtained for the hydrogen atom. Since all other atomic, or molecular systems, involve the motions of three or more "particles", their Schrödinger equations cannot be solved exactly and so approximate solutions must be sought.

Wave model

The foundation of quantum mechanics and quantum chemistry is the **wave model**, in which the atom is a small, dense, positively charged nucleus surrounded by electrons. Unlike the earlier Bohr model of the atom, however, the wave model describes electrons as "clouds" moving in orbitals, and their positions are represented by probability distributions rather than discrete points. The strength of this model lies in its predictive power. Specifically, it predicts the pattern of chemically similar elements found in the periodic table. The wave model is so named because electrons exhibit properties (such as interference) traditionally associated with waves. See wave-particle duality.

Valence bond

Although the mathematical basis of quantum chemistry had been laid by Schrödinger in 1926, it is generally accepted that the first true calculation in quantum chemistry was that of the German physicists Walter Heitler and Fritz London on the hydrogen (H_2) molecule in 1927. Heitler and London's method was extended by the American theoretical physicist John C. Slater and the American theoretical chemist Linus Pauling to become the **Valence-Bond (VB)** [or **Heitler-London-Slater-Pauling (HLSP)**] method. In this method, attention is primarily devoted to the pairwise interactions between atoms, and this method therefore correlates closely with classical chemists' drawings of bonds.

Molecular orbital

An alternative approach was developed in 1929 by Friedrich Hund and Robert S. Mulliken, in which electrons are described by mathematical functions delocalized over an entire molecule. The **Hund-Mulliken** approach or **molecular orbital (MO) method** is less intuitive to chemists, but has turned out capable of predicting spectroscopic properties better than the VB method. This approach is the conceptional basis of the **Hartree-Fock method** and further post Hartree-Fock methods.

Density functional theory

The **Thomas-Fermi model** was developed independently by Thomas and Fermi in 1927. This was the first attempt to describe many-electron systems on the basis of electronic density instead of wave functions, although it was not very successful in the treatment of entire molecules. The method did provide the basis for what is now known as **density functional theory**. Though this method is less developed than post Hartree-Fock methods, its lower computational requirements allow it to tackle larger polyatomic molecules and even macromolecules, which has made it the most used method in computational chemistry

at present.

Chemical dynamics

A further step can consist of solving the Schrödinger equation with the total molecular Hamiltonian in order to study the motion of molecules. Direct solution of the Schrödinger equation is called *quantum molecular dynamics*, within the semiclassical approximation *semiclassical molecular dynamics*, and within the classical mechanics framework *molecular dynamics (MD)*. Statistical approaches, using for example Monte Carlo methods, are also possible.

Adiabatic chemical dynamics

Main article: Adiabatic formalism or Born-Oppenheimer approximation

In **adiabatic dynamics**, interatomic interactions are represented by single scalar potentials called potential energy surfaces. This is the Born-Oppenheimer approximation introduced by Born and Oppenheimer in 1927. Pioneering applications of this in chemistry were performed by Rice and Ramsperger in 1927 and Kassel in 1928, and generalized into the RRKM theory in 1952 by Marcus who took the transition state theory developed by Eyring in 1935 into account. These methods enable simple estimates of unimolecular reaction rates from a few characteristics of the potential surface.

Non-adiabatic chemical dynamics

Non-adiabatic dynamics consists of taking the interaction between several coupled potential energy surface (corresponding to different electronic quantum states of the molecule). The coupling terms are called **vibronic couplings**. The pioneering work in this field was done by Stueckelberg, Landau, and Zener in the 1930s, in their work on what is now known as the Landau-Zener transition. Their formula allows the transition probability between two diabatic potential curves in the neighborhood of an avoided crossing to be calculated.

Quantum chemistry and quantum field theory

The application of quantum field theory (QFT) to chemical systems and theories has become increasingly common in the modern physical sciences. One of the first and most fundamentally explicit appearances of this is seen in the theory of the photomagnetron. In this system, plasmas, which are ubiquitous in both physics and chemistry, are studied in order to determine the basic quantization of the underlying bosonic field. However, quantum field theory is of interest in many fields of chemistry, including: nuclear chemistry, astrochemistry, sonochemistry, and quantum hydrodynamics. Field theoretic methods have also been critical in developing the ab initio Effective Hamiltonian theory of semi-empirical pi-electron methods.

See also

- Atomic physics
- Computational chemistry
- Condensed matter physics
- International Academy of Quantum Molecular Science
- Physical chemistry
- Quantum chemistry computer programs
- Quantum electrochemistry
- QMC@Home
- Theoretical physics

Further reading

- Pauling, L. (1954). *General Chemistry*. Dover Publications. ISBN 0-486-65622-5.
- Pauling, L., and Wilson, E. B. *Introduction to Quantum Mechanics with Applications to Chemistry* (Dover Publications) ISBN 0-486-64871-0
- Atkins, P.W. *Physical Chemistry* (Oxford University Press) ISBN 0-19-879285-9
- McWeeny, R. *Coulson's Valence* (Oxford Science Publications) ISBN 0-19-855144-4
- Landau, L.D. and Lifshitz, E.M. *Quantum Mechanics:Non-relativistic Theory* (Course of Theoretical Physics vol.3) (Pergamon Press)
- Bernard Pullman and Alberte Pullman. 1963. *Quantum Biochemistry.*, New York and London: Academic Press.
- Eric R. Scerri, *The Periodic Table: Its Story and Its Significance*, Oxford University Press, 2006. Considers the extent to which chemistry and especially the periodic system has been reduced to quantum mechanics. ISBN 0-19-530573-6.
- Simon, Z. 1976. *Quantum Biochemistry and Specific Interactions.*, Taylor & Francis; ISBN-13: 978-0856260872 and ISBN 0-85-6260878 .

References

- [1] http://cmm.cit.nih.gov/modeling/guide_documents/quantum_mechanics_document.html|"Quantum Chemistry". *The NIH Guide to Molecular Modeling*. National Institutes of Health. http://cmm.cit.nih.gov/modeling/guide_documents/quantum_mechanics_document.html. Retrieved on 2007-09-08.

External links

- The Sherrill Group - Notes (<http://vergil.chemistry.gatech.edu/notes/index.html>)
 - ChemViz Curriculum Support Resources (<http://www.shodor.org/chemviz/>)
 - Early ideas in the history of quantum chemistry (<http://www.quantum-chemistry-history.com/>)
-

Nobel lectures by quantum chemists

- Walter Kohn's Nobel lecture (<http://nobelprize.org/chemistry/laureates/1998/kohn-lecture.html>)
 - Rudolph Marcus' Nobel lecture (<http://nobelprize.org/chemistry/laureates/1992/marcus-lecture.html>)
 - Robert Mulliken's Nobel lecture (<http://nobelprize.org/chemistry/laureates/1966/mulliken-lecture.html>)
 - Linus Pauling's Nobel lecture (<http://nobelprize.org/chemistry/laureates/1954/pauling-lecture.html>)
 - John Pople's Nobel lecture (<http://nobelprize.org/chemistry/laureates/1998/pople-lecture.html>)
-

Article Sources and Contributors

X-rays *Source:* <http://en.wikipedia.org/windex.php?oldid=175484653> *Contributors:* -

X-ray scattering techniques *Source:* <http://en.wikipedia.org/windex.php?oldid=295552122> *Contributors:* 168..., 2over0, Annabel, BevVincent, Bkraabel, Bullet2010, Coops1974, Crystal whacker, Darkstar78, Drbreznjev, EdJohnston, Gertlex, GregorB, Haimingli, Irene Ringworm, Jcwf, Jdrewitt, Jeff Dahl, Khb3rd, Kdliss, Kkmurray, La Pianista, Mikaey, Mspraveen, Nanotech18, Neparis, NerdyNSK, Nitrofev, Paul Henning, Pieter Kuiper, Rb82, RexNL, Rifleman 82, Romaioi, Selket, SellusGravius, Skier Dude, Slinky Puppet, Spellcast, Taras, Tpikonen, Uvainio, VTBushyTail, Webridge, Xstreamsys, 52 anonymous edits

Crystal *Source:* <http://en.wikipedia.org/windex.php?oldid=297401379> *Contributors:* 119, 13creek13, 2over0, 99of9, A Softer Answer, AGK, AHM, Aaronbrick, Abeg92, Acdx, Acroterion, Ael 2, Ahoerstemeier, Aitias, Ajaxkroon, Alansohn, Alexfusco5, Altenmann, Andrew Levine, Angusmclellan, Animum, Ann Stouter, Antandrus, Archer7, Arthena, Audioiv, Awickert, Az1568, B9 hummingbird hovering, Backslash Forwardslash, Badseed, Banano03, Bantman, Bauke, Bballerc28, Beaumont, Beland, Ben-Zin, Bencherlite, BlackHak, Bluezy, Bmg916, Bob f it, Bobo192, Boccobrock, Bomac, Bonez22, Bongwarrior, Bronzephoenix, Butane Goddess, Clreland, Call me Bubba, Caltas, Calvin 1998, CambridgeBayWeather, Can't sleep, clown will eat me, Capricorn42, CardinalDan, Carlosguitar, Cdcnc, Centrx, Cherryalexandra, Chowbok, Chris 73, Clicketyclack, Closedmouth, Cmichael, Cnguyen123, Cometstyles, Complexica, Conversion script, Crysandlg, Crystal whacker, Crystall94, Cutler, DJ Clayworth, DVD R W, Daarzniesk, Dancinstar, Daniel Case, Danski14, David.Monniaux, DeadEyeArrow, Debresser, Deglr6328, Dengero, DerHexer, Devshoppe, Dgrant, Digon3, Discospinster, Doctormatt, Doctorshim, Dolphinholmer, DrBob, Dreadstar, Drini, Ds13, Dschwen, Duckone, Dweller, Dylan Lake, Dysepision, Eclectology, El C, El aprendelenguas, ElusiveByte, Emerson7, Emote, Enviroboy, Eprh123, Espetkov, Everyking, Excirial, FaerieInGrey, Faradayplank, FastLizard4, Finavon, Flash176, FoRgEtFuLxLuV94, FooBar, Freestyle-69, GDonato, Galoubet, Gcm, Gentgeen, George The Dragon, Giftlite, Gilliam, Glen, Gogo Dodo, Govany, Gowtham99.9, GraYoshi2x, Gradbrad, GregorB, Gscshoyru, Gtstricky, Gurch, Gzkn, Hadal, Hagedis, Headbomb, Hellbus, Hempelmann, Hurricanehink, Husond, Hut 8.5, Huw Powell, Hydrogen Iodide, Icairns, Insanity Incarnate, Isnow, J.delanoy, J04n, Jamm.T, Janejellyroll, Jaxl, Jennavecia, Jiy, Jleela14, Jmath666, Jmundo, JoJan, John Stewart, John254, JohnCD, Jojhutton, Jose77, Jozal, Junglecat, Jurema Oliveira, KSmrq, Kaivosukeltaja, Kandar, Karol Langner, Kemiv, Kevin Murray, Kiia15, Kingykongy, KnowledgeOfSelf, Knuckles, Knulclunk, Kocoumlovesyou, Korg, Krawi, LAAFan, Latifshaikh20, Laurap414, Laurent1979, Lazyboi69, LeaveSleaves, LedgendGamer, Lemchesvej, Lights, Lisatwo, Logger9, Lowellian, MER-C, MPerel, Major:T, Majorly, Mani1, Matdrones, MaterialsScientist, Mav, Maxim, Mbz1, McSly, MeStevo, Meaningful Username, Mentifisto, Michael Hardy, Michaeldu, MickMacNee, Mike Rosoft, Mild Bill Hiccup, Minesweeper, Miquonranger03, Mirwin, Miscibleliquids, Mr. Lefty, Mr.pieface, Musashi miyamoto, N96, Namazu-tron, NawlinWiki, No Guru, Norm, Ochib, Oda Mari, Olivier, Olof, Omegatron, Ouishoebean, Outsider1994, Oxymoron83, PandaSaver, Pelo12354, Perdygal90210, Pharaoh of the Wizards, Philip Trueman, Physchim62, Piano non troppo, Plangent, Poeloc, Poluks, Pontifcake, PreRaphaelite, PrestonH, Puckly, PuppyGirl1508, PuzzletChung, Pyrospirit, Rachack, RainbowOfLight, Rapidfyre, RazorICE, Rdsmith4, Reciproco8, Recognizance, Recurring dreams, REIKEssentials, RememberMe?, Rettetast, Rhaneya, Rian-Koo, Rifleman 82, Riotrocket8676, Rocket000, Romanm, RoyBoy, Rror, RyGuy17, SEWilco, SMHC, Sahil shark, Samsara, Saperaud, Sarvil, Scasquatch, Savant13, Sceptre, Sean William, Secrets.of.the.skies, Selket, Sem-mem, Sergay, Shawnhac, Siim, Sir Arver, Sjakalle, Smack, Snowolf, Snowynight, Sonic3KMaster, SorryGuy, Soumyasch, Springnuts, Stephane29, Stephenb, Stevertigo, Strongbadmanofme, Suisui, Superdvd, Superm401, Swerdnaneb, T g7, TUF-KAT, Taemyr, Tagsantiago, Tantalate, TantalumTelluride, Tardigrade13, Tbone55, Techman224, Tekkenmasterbrendan, Tellyaddict, The undertow, TheCheeseManCan, Thehelpfulone, Tiddly Tom, Tinkerbellkait, Tinkerpersion, Tiptoety, Tom harrison, Tonmad, Tpb, Transisto, Ttony21, TutterMouse, UbUb, Ultatri, Until It Sleeps, Upholder, Vanzpunk0676, Vary, Ve4ernik, Veinor, Velela, Versus22, Vicki Rosenzweig, Voyagerfan5761, Vsmith, Vuong Ngan Ha, Wafflescakes, Walkerma, Wars, Weiguxp, Wenli, Willworkforicecream, Wisterlane, Wizard191, Wizardman, Wmahan, Wyatt915, Xanzzibar, YKWSG, Yamamoto Ichiro, Yidisheryid, Youandme, Z.E.R.O., ZX81, Zack, Zamphuor, Zsendukas, Zziuzz, Билецкий В.С., Куллер, 864 anonymous edits

Diffraction *Source:* <http://en.wikipedia.org/windex.php?oldid=296410849> *Contributors:* 2over0, A1call, Abiermans, Across.The.Synapse, Afrine, Ahmed1994, Alai, Alan Joe Skarda, Aleas, Ali, Amaltheus, Amosnomore, Andre Engels, AnnaFrance, Anoko moonlight, Anonymous Dissident, Army1987, Arnero, Atlant, Av99, Barney-12-3, Bazzargh, Bbatsell, Bcrowell, Beetstra, Birge, Bmicomp, Bryan Derksen, Buttsecks, Cambridgeincolour, Can't sleep, clown will eat me, Cdcnc, Charles Matthews, Charmed4ever, Complexica, Conversion script, Crowsnest, Cuardin, DMacks, Decibert, DerHexer, Dicklyon, Dino, DrBob, Egil, Ellywa, Enormousdude, Epzcaw, Erguvan7, Erudecorp, Eurion, Flowersofnight, Francs2000, Fredbauder, Fresheneesz, Garagebarrage27, Gfutia, Gholam, Giftlite, Gludwiczak, GregRM, Hadal, Headbomb, Hillbrand, Howabout1, Hunterd, Iecz, Igoldste, Instinct, Isnow, J.delanoy, JCraw, JForget, Jaganath, Jaxl, Jeff Dahl, Jermor, Jhbdel, Jjron, Jm smits, Karol Langner, Kdliss, KristianMolhave, Kurykh, LMB, La goutte de pluie, Laserheinz, Light current, Linus M., MER-C, Magnus Manske, Mani1, Mbz1, Mejor Los Indios, Michael Hardy, Moe Epsilon, Mufka, MuthuKutty, Narvalo, NawlinWiki, Neparis, Nghtwlkr, Nikai, Nk, Nuno Tavares, Odedee, OlavN, Omer88f, Orionus, OwenX, Oysteinp, P100011011, Pakaran, Pfaletra, Pflstad, Pflatau, Pps, ProhibitOnions, Pschemp, Quadell, RG2, Radiant chains, Ram-Man, Rbj, Reddi, RenamedUser2, Revilo314, Riceman3, Rnt20, Robert L, Ronbus, Rosuna, Rspanton, Rtcoles, RyanCross, Sakurambo, Sam Hocevar, Sango123, Saperaud, SebastianHelm, Sebrofb, Shadowjams, Shim'on, Shoessss, Siddhant, SimonP, Sinneed, Skarebo, Skoch3, Srleffler, Stirling Newberry, Stou, Strait, Sudiarta, Sverdrup, TakuyaMurata, The Anome, Thermochap, Tomruen, Trevorcox, Uncle Leo, V81, Wideofthemark, Wikiborg, Wikid77, Wingchi, Wolfkeeper, Xiahou, YxTay, Yyy, 百家姓之四, 237 anonymous edits

Uniform theory of diffraction *Source:* <http://en.wikipedia.org/windex.php?oldid=293154082> *Contributors:* CanadianCaesar, Difference engine, Edwin Carter, Jitse Niesen, Kalle, Mild Bill Hiccup, PEHowland, Paul D. Anderson, Pjvpjv, RHaworth, Ryachris, Thubing, Zscout370, 6 anonymous edits

Crystallography *Source:* <http://en.wikipedia.org/windex.php?oldid=294865893> *Contributors:* 168..., Addere, Ahoerstemeier, Alansohn, Alphachimp, Baldhur, Berland, BlindEagle42, Bluemask, C quest000, Cadmium, Cchoongcc, Cdcnc, Christopherlin, Ck lostsword, Commander Nemet, Constructive editor, Conversion script, Coolguy92591, Crystal whacker, Cstras, Cutler, Daarzniesk, Drue, Duncan.france, Gcm, Geologyguy, Giftlite, Gilliam, Glenn, Gombang, Gyrofrog, Headbomb, Heron, Hugh2414, Hugo-cs, Invitations, J.delanoy, Jimfbleak, Jitse Niesen, Jittat, JohnOwens, KSmrq, Kafuffle, Kalpanaitm, Karol Langner, Kcordina, Kdliss, Kokoriko, Krauss, Kurykh, Leonard G., Linas, Ling.Nut, Luna Santin, M stone, Mahlerite, Malcolm Farmer, Menchi, Mentifisto, Mhaitham.shammaa, Michael Hardy, MikeW25, Mikenorton, Mirokado, Mkosmul, Moonshiner, Mxpule, Olof, Oneforlogic, Oysteinp, Patrick, PhilKnight, Phys, Piano non troppo, Pion, Polyparadigm, Profjohn, PsiStar, Puchiko, Quantockgoblin, Quickbeam, Reciproco8, Rob Hooft, Robinh, Romaioi, SchiftyThree, Seanwall111111, Siim, Simesa, Substatique, Suisui, TantalumTelluride, TenOfAllTrades, Terrace4, Triops, Uber-Nerd, Van helsing, Vsmith, Walkerma, Walkiped, Wik, Zundark, Zzuuzz, 109 anonymous edits

Paracrystalline *Source:* <http://en.wikipedia.org/windex.php?oldid=291869326> *Contributors:* Bci2, CharlotteWebb, Furmanj, Giftlite, Sting au, Venny85, Warut, 1 anonymous edits

Synchrotron *Source:* <http://en.wikipedia.org/windex.php?oldid=291170914> *Contributors:* Alvinwc, Animum, Aottley, Benbest, Besselfunctions, Bevo, Bewebste, Boris Barowski, Brockert, BrokenSegue, BryanD, Cantus, Casey56, Choochus, Cirejcon, ConradPino, DV8 2XL, Dan100, Darkgecko, David.Monniaux, Dee Earley, Dlenmn, Drakmyth, E2m, EdwardEMeyer, Emerson7, Enquire, Estel, Eubulides, Excirial, Fantasi, Fredrik, Gbleem, Gene Nygaard, Gentoolligan, Gogo Dodo, Headbomb, JabberWok, Jaganath, Jeff G., Jjron, Jotel, Justpastalaska, Kdliss, Klaus, LSTech, Larkster, Laurascudder, Leonard G., Linas, Lokster, Macaddct1984, Mancune2001, MarkSweep, Mike Rosoft, Mjamja, Mjspe1, Mongerhedron, Mrpeauk, Mullet, Nahum Reduta, Nikai, Nunh-huh, Oleo007@gmail.com, P7lejo, PRehse, Palfrey, Pizza1512, Pj.debruin, Ptomato, RoyBoy, Rufua, RupertMillard, SDC4004, SSRF CHINA, SallyForth123, Smithbrenon, Stevenj, TPK, Teddybearspicnic, TheMaster42, Thinko, Timo Honkasalo, TimothyPilgrim, Tpikonen, Uvainio, WLU, Whitt35, Wolfkeeper, Xtreambar, Yk13, Zondor, Zowie, Zzedar, 朝彦, 141 anonymous edits

X-ray microscope *Source:* <http://en.wikipedia.org/windex.php?oldid=296734543> *Contributors:* AB, AndyBQ, Birge, Bouncingmolar, Can't sleep, clown will eat me, Chamal N, Deglr6328, Discospinster, Dratman, EbozMoore, Heron, Icairns, JTN, Marshman, NHSavage, Ptftft, RI, RoyBoy, Sommacal Alfonso, Stepp-Wulf, Stirling Newberry, The Anome, Топми Нёрд, 270 anonymous edits

Extended X-ray absorption fine structure *Source:* <http://en.wikipedia.org/windex.php?oldid=291227586> *Contributors:* Altenmann, Amhlope, Cadmium, Chaiken, D80s0q, Erguvan7, Jcwf, Kkmurray, Kommando, M A Mason, Pjvpjv, Rich Farmbrough, ShellyDKelly, Sketch-The-Fox, Skier Dude, Sumitash, Unimath, Vipuser, Xcomradex, 34 anonymous edits

Surface extended X-ray absorption fine structure *Source:* <http://en.wikipedia.org/windex.php?oldid=286284070> *Contributors:* LilHelpa, Peripitus, Skier Dude, Sumitash, THEN WHO WAS PHONE?, 5 anonymous edits

XANES *Source:* <http://en.wikipedia.org/windex.php?oldid=292783483> *Contributors:* Zover0, Agesworth, Agrestini, Azo bob, Bianconi, Cadmium, Chaiken, Coppertwig, Jcwf, Magioladitis, Pearle, Radagast83, Safalra, Skier Dude, Smolentsev, Wagggers, 66 anonymous edits

NEXAFS *Source:* <http://en.wikipedia.org/windex.php?oldid=193622849> *Contributors:* -

Small angle X-ray scattering *Source:* <http://en.wikipedia.org/windex.php?oldid=152888039> *Contributors:* -

Imaging *Source:* <http://en.wikipedia.org/windex.php?oldid=285115434> *Contributors:* Alai, Arcadian, Bact, Bme591wikiproject, Burt Harris, Carnildo, Chris the speller, David Shay, Dicklyon, Edcolins, Eleassar777, Kaeslin, Karol Langner, Kauczuk, Leonard G., Lights, Maikel, Nbarth, Oicumayberight, Patrick, Pde, Poweroid, Quantum2006, Quuxplusone, Qxz, Ringbang, Sander123, Seabhcan, Shawndkc, Srleffler, TBarregren, Tazmaniacs, Timitzeptel, Vladimir Drzik, Voicetalent, Wik, 18 anonymous edits

Compton scattering *Source:* <http://en.wikipedia.org/windex.php?oldid=297021831> *Contributors:* (jarbarf), Zover0, Alexbonaro, Allen McC., Alphachimp, Andrei Stroe, Anna512, AquaDTRS, Astrosona, AugPi, Batmanand, BenRG, Blainster, Borgx, Bryan Derksen, C.Bluck, CALR, Cburnett, Chapter11, Choihei, Chris Roy, Cortamears, Dchristle, Deltasct, Discospinster, Dungodung, El C, Eleassar777, Ellmist, Eman, Eteq, FentonGlass, Fordmadoxfraud, FourBlades, Freddie, Fresheneesz, Fuzzball!, Gene Nygaard, Gianluigi, Hairy Dude, Iwreckyou, JabberWok, Joke137, Junkinbomb, Keenan Pepper, Kiwi137, Kjolb, Kurykh, Kyng, Laurascudder, Linas, Looxix, Luis Sanchez, Lumidek, MakeRocketGoNow, Maliz, Mark Barnes, Mibchronicles, Mike Peel, Modest Genius, Mxn, NaNoMeTeR, Niven, Ojigiri, Omegatron, Owen214, Pentasyllabic, Peterlin, Pevernagie, Pfalstad, Pt, Pv42, RJHall, Reddi, Rogermong2, Sabbe, Sbyrnes321, SeanMon, Silenced, Stephen, Steve Wise, Stevertigo, StuTheSheep, The Smurfmeister, Tim314, Tpkonen, Uvainio, W.F.Galway, WMdeMuynck, Warlordwolf, Washburnmav, Wikiklrsc, Wikinu, Wikipedia brown, Youandme, Zereschk, 122 anonymous edits

Electron microscope *Source:* <http://en.wikipedia.org/windex.php?oldid=296877389> *Contributors:* 007 n1, 5Q5, A. Carty, ABF, Aaronsharpe, Acroterion, Adam Mihalyi, Adambiswanger1, Adjir, AdjustShift, Aillema, Aitias, Alan012, Alansohn, Albany NY, Alex Klotz, Amaltheus, Andre Engels, Andrei Stroe, Antonio Lopez, Apparition11, ArchonMagnus, Aurelius173, Average Earthman, Backslash Forwardslash, Banus, Bencherlite, Bender235, Bensaccount, Blechnic, Bobo192, Bongwarrior, Borgx, Brianga, C0nanPayne, Calabraxthis, Camembert, Can't sleep, clown will eat me, CanisRufus, Capricorn42, Captain-tucker, Chj77, Cetcher1159, Ceyockey, Cgarber, Chai, Chalm-awb, Chris G, Chrislk02, Chych, Closenplay, Conversion script, Corpx, Cstown, D, DVD R W, Daniel, DarkFalls, Darth Panda, Davewild, David R. Ingham, Davidbaca, Dcoetzee, Deglr6328, DeltaMicroscopyStudent, DerHexer, Dexarouskies, Dexter prog, Dgrant, Dicklyon, Dlohcierekim, Docu, DoubleBlue, Doyley, DrFO.Jr.Tn, DrMikeF, Dvratnam, Editor2020, El aprendelenguas, Elearning2000, Enchanter, Epr123, Ephram Shizgal, EricV89, Esem0, Evan1991, EyeSerene, Fabricationary, Ferengi, Fieldday-sunday, Fireice, Frank, Frank A, Frankatca, Frankenpuppy, Fueled, Funnybunny, Gaius Cornelius, Gary King, Gene Nygaard, George Burgess, Gh5046, Giflite, Gogo Dodo, Golfguy220-, GrahamColm, Grey Shadow, Ground, Hat'nCoat, Hedgemonkey, Heron, Horselover Frost, Hu, Hugo-cs, Hurricane Angel, Hydrogen Iodide, II MusLiM HyBRiD II, ILike2BeAnonymous, INKubusse, Ian Pitchford, IanOsgood, Imaninjapirate, Irfanhasmit, Isaac yagmoor, Itai, J.delanoy, JNighthawk, JRodeng, JTN, JaGa, Jaccardi, Jacopo Werther, Jeremiah, Jimp, Joelholdsworth, JohnOwens, JorgeGG, Joshua.morgan, Karnesky, Karol Langner, Keilana, Kesac, Kils, Kingpin13, Kissavos, KnowledgeOfSelf, Konsu, Kpjas, KristianMolhave, Kukini, Kuru, Kusunose, KyraVixen, Kzollman, LeilaniLad, Liferulez, Lindmere, Luna Santin, MER-C, Magnus Manske, MarcoTolo, Marek69, Mark.murphy, Maro91eg, Materialscientist, Mayapur, McSly, Mikaey, Mmxx, Monkeyknife, MooglegFan, Mschlindwein, Mwtoews, Myscrnm, Nate1481, Nath87, Ncemer, Netkinetic, Neurolysis, Nickfor1, Nihilitres, Nikai, Nmnogueira, Novalis, Oceano30, Oysteipn, Paulhaiti, Pengo, Perfecto, Pharaoh of the Wizards, Piano non troppo, Pip2andahalf, Plantsurfer, Plasticup, Pliable, PrestonH, Quadell, R.rommel, RainbowOfLight, Rajah, Richard Arthur Norton (1958-), Riflemann, Risk one, Rjwilmsi, RobHarding, Rror, Rurik3, Rustavo, S0uj1r0, STHayden, Sceptre, Scieurinae, Sean William, Selket, Shirulashem, Sikkema, Silsor, Simon Shek, Simonmn, Sludtke42, Snowmanradio, Snoyes, Sodium, Spbrandom, Spearhead, Speedyboy, Srdomingue, Srnc, Stahlkocher1, Steff, StephenBuxton, Steve Crossin, Stokerm, Sub-Angstrom, Svdmolen, Tacvek, Tahirlulislam, Tapir Terrific, Terrace4, The Anome, Thedjatclubrock, Thermochap, Thingg, Tijadr, Til.Bartel, TimVickers, Tjmayerinsf, Tmpokisn, Travelbird, Twisted86, Ulfbastel, Utcursch, Vossman, WahreJakob, Willking1979, Wtmitchell, Xy7, Zephyris, Zzuuzz, Кодекс, გოგა, 647 anonymous edits

Nanotechnology *Source:* <http://en.wikipedia.org/windex.php?oldid=297462263> *Contributors:* 04spicerc, 1234eatmoore, 2D, 450hondarider, 9.172, A Real Live One, A.Ou, Abune, Academic Challenger, AcademyAD, Actinman, AdamRetchless, AdamWeeden, Adashiel, Addshore, AdjustShift, Admiral Roo, AdnanSa, Aerothorn, Ahoerstemeier, Aim Here, AirBa, Ajdecon, AkSahota312, Akendall, Alansohn, AlexTheScot, Alexfusco5, Alexius08, Alexnye, Ali, AllanHainey, Almonit, Alsandro, Altenmann, Amaurea, Anaraug, Andonico, Andraeireinhardt, AndreiDukhin, Andrewpmk, Andrewrp, AngelOfSadness, Anirudh51, AnnaFrance, Anonymous editor, Anoxonian, Ant12344321, Ant123456789, Antandrus, Antonrojo, Antony-22, Antourourke, Apalaria, Apoorvbadami, Arabani, ArglebargleIV, Ariasne, Arifhussaintm, Arion 3x3, Arnoutf, Arpingstone, Art LaPella, Asbian513, Asmeurer, Aude, Average Earthman, Azlib77, B33R, Badgernet, Balsone1990, BananaFiend, Barbara Shack, Barticus88, Bathosrex, Bbatsell, Bedrokdamian, Beepu, Beetstra, Ben Tillman, Ben Wraith, Benstown, Bibliomaniac15, Big Bird, BlastOButter42, Blechnic, Blobblog, Blue520, Blueelectricstorm, Bmeguru, Bob, Bob rulz, Bobblewik, Bobo The Ninja, Bobo192, Bongwarrior, Bookandcoffee, Bornhj, Bornslippy, BradBeattie, Briaboru, Brianga, Bryan Derksen, Bschoott, Burgundavia, Butros, Bücherwürmlin, CNicol, CY3AHHA, Cacycle, Caddcreativity, Caiaffa, Cal 1234, Calair, Calvin 1998, Camw, Can't sleep, clown will eat me, CanadianLinuxUser, CandyPanda, Canthusus, Cantus, Capitalistroadster, Capricorn42, Captain-tucker, CardinalDan, Carlos-alberto-teixeira, Carlosguitar, CarolineFThornPhD, Catgut, Caulde, CecilPL, Cedars, Ceyockey, Chamal N, CharlesC, Charliebigpotatoes, CharlotteWebb, Chcknwnm, Cheaptubes, ChemGardener, Chicken Wing, Chill doubt, Chimpman, ChinoFireball, Chodges, Chooyimooyi, ChrassLovesEmma, Chris Roy, ChrisO, ChrisViper, Chrislk02, ChrisNHouston, Christopher Connor, Christopher Parham, Chubbychunk, Chun-hian, Chymicus, Clicketyclack, Closedmouth, Cole141299, Comestyles, Con0002, Conversion script, Corvidaeocorvus, CotyXD, Coumarin, Cp111, Cpichardo, Cpuwhiz11, CranfieldSAS, Cruittbuck, Cryonic07, Csjoier, Css, CtoheC, Cubic Hour, Cugerbrant, Cww, Cyberevil, Cyberman, DASonnenfeld, DLH, DV8 2XL, DVD R W, Da monster under your bed, Dado, Dag556, Damicatz, Dan100, Dancter, Daniel C, Daniel Shanefield, Dark Gaia, DarkFalls, Daveydweeb, David Levy, David.Monnaux, David44357, Davidfstr, Davidforrest, Dbfirs, Dbsherman, DeadEyeArrow, Deb, Deeb, Deligeyik, Dellidot, Dennis Valeev, DennisRobinson, Deor, DerHexer, Deselliers, Desiromeo107, Desplesda, Despotuli, Dethme0w, Dexterousg, Dhappe, Dhp1080, Dibbity Dan, Dicklyon, Dina, Discospinster, Djr32, Dkrogers, Dll99, Dmerrill, DouglasGreen, Dr SHOEB82, Dr-b-m, DrMikeF, Drat, Dreaded Walrus, Dskluz, Dynaflow, Dysepsion, E Wing, EBY3221, ERK, ESkog, EVGroup, Eclectology, Ecleveland, EdBever, Edcolins, Edison, Edkarpov, Eeon, Eequor, Efbfweborg, Ehn, Eivind, El C, Elamere, Electricitylikesme, Eliz81, Elwhy, Emiles93, Environ1561, Epastore, Epr123, Eric Holloway, Erpreeti, Escape Orbit, Esmash, Etxrge, Eve Hall, Everyking, Evlekis, Excirial, Exeunt, Fabrictramp, Fadierulez999, Falcorian, Fauncet, FayssalF, Femto, Feydey, Figarow, Filmz, Finlay McWalter, Firebladed, Fireplace, Flatline, Flewis, Floodamanny, FlyingTongger, Fock, Frank 76, Frankie1969, Frecklefoot, FreeKresge, FreplySpang, Fuhghettaboutit, FullMetal Falcon, Fvw, G.A.S, GChriss, GDonato, GJeffery, Gaff, Gail, Gakrivas, Garden, Garion96, Gatorguy13, Gchriss, Gcm, Gdo01, Geoffreyhunt, GermanX, Gheinen, Ghegwill, Giflite, Gilliam, Gioto, Gjd001, Gleeson 44, Glen, Glenn, Gllq, Globalhealth, Gogo Dodo, Granla, Greennature2, Gulhar, Gurch, Guyzero, Gwernol, H0D G, H0riz0n, HPSLPP, Hadal, HandyAndy, HappyCamper, Harry2big4u, Headbomb, Henry Flower, Hephaestos, Herbythyme, Heron, HexaChord, Hojmatt, Honeyzji, Howard547, Howcheng, Howdoesthiswo, Hreinn, Hu12, Hubert Wan, Hulagutten, Human.v2.0, Hupselpup, Husond, II MusLiM HyBRiD II, IRP, Iain99, Iam, Ian13, IanOsgood, Iandotcom, Icairns, Icarus, Ice Cold Beer, Icenie6, IddoGenuth, Illustria, Im a hustla, Imaninjapirate, ImperfectlyInformed, Imroy, InsertNameHere, Inwind, Ira Ko, Irishguy, Islander, IstvanWolf, Itschris, Itsmine, Iwilker, Ixf64, J.delanoy, JCOWens, JForget, JHMM13, Jaccardi, Jackol, Jaganath, Jamesmorrison, Jamesontai, Jamesooders, JanGlaenzer, Janastasopoulo, Jaxonowens, Jbw2, Jeffnichols, Jeffrey.Kleykamp, Jeffwarnika, Jenita JJ, Jfdwolff, JimVC3, Jj137, Jmanigold, Joachim Schrod, JoanneB, Joao.caprivi, Joeschmoe360, John.parkes007, Johnnyb82, Johnstex, Jon seah, Jose77, Joseph Solis in Australia, Jpeob, Jrockley, Jrsheehan, Jrugordon, Judicatus, Junglecat, KKul, Kaerondaes, Kami, Kamil101, Karenjc, Karnesky, Katula, Kbdank71, Kcordina, Keenan Pepper, Keith D, Kenneth M Burke, Kenyon, Khaydarian, Kilddevil, Kim Bruning, Kingpin13, Kiran b e, Kirsted, Kkmurray, Kku, Kmg90, Knotnic, KnowledgeOfSelf, Kosigrim, Koyo123, KrakatoaKatie, KramardanIkabu, Krawi, KristianMolhave, Ktsquare, Kubigula, Kukini, Kuru, Kuunavang, L Hamm, LC, Lady BlahDeBlah, Laogooli, Larry laptop, Latka, Laurascudder, Law, LeaveSleaves, Legeres, Les boys, Lfatehi, Lifeboatpres, Lights, Lightspeedchick, Ligulem, Likemike232, Lilgoni, Lizz379, Loupeter, Lowellian, Lstanley, Lucid, Luna Santin, Lunalona, Luvleme, M stone, MER-C, MITBeaverRocks, MMC, Mac, Mac Davis, MacGyverMagic, MacMed, Macewindu, Maha ts, Malerin, Malzees, Mandarax, Maniraptor, Manmantong2000, Manufacturing, Marshsie, MarsRover, Masschaos123, Master of Puppets, Matau, Materialscientist, Mateuszica, Math Champion, Mattcuk, Matticus78, Mattjharrison, Mauron, Mav, Maximus Rex, Mayoorezan, Mboverload, McGeddon, McVities, Mdebits, Meco, Meelosh, Melsaran, Memset, Menchi, Mentifisto, Metmathos, Mfskxseb, Michael Devore, Michael Hardy, Michael93555, Michaelas10, Michelle Roberts, Michellercrisp, Micke-sv, Mikastu, Mike Rosoft, Mike Treder, Mikeb87, Milesrulez, Mills89, Mimzy1990, Mindmatrix, Minipieper, Miranda, Mirondelta, Missing Ace, MisterSheik, Misza13, Mmm, Moink, MoonGod, Morgan-92,

Mormegil, Morven, Motor, Mr Bound, Mr strain, MrArt, Mrannanj, Mrmattyboy, Mschel, Mugless, Mwanner, Mww113, Mxb design, Mxn, Mysterymadman, NAHID, NHL09addict, NJGW, Nabeth, Naddy, Nakan, NanoIQP, NanoWorld, Nanobug, Nanodic, Nanojames, Nanoorg, Nanoshel, Nanotechthefuture, Naught101, Nauticashades, Naveenlingam, NawlinWiki, Ndenison, Neverquick, Newtownrocks, Nick Boulevard, Nickvalcke, Night Stalker, Nips, Nmnogueira, NoldeaNick, Noah Salzman, Noclevername, Noosphere, Notheruser, November05, Nuno Tavares, Nwerk, Obedium, Oda Mari, Ohnoitsjamie, Oldoneeye, Oleg Alexandrov, OllieFury, Omicronpersei8, Opelio, Optimale, OwenX, Oxymoron83, P4k, P99am, Palpatine, Paranoid, ParisianBlade, Passw0rd, Pat010, Patchimoo, Paul August, Paulk4, Pavan maddali, Pb30, Pechotat, Pedant17, Pedantic of Purley, Pegasus1138, Penubag, Peripitus, Perl, Persian Poet Gal, Peruvianllama, Petri Krohn, Pgan002, Philip Trueman, Phillipdison1891, Phound14, Physicist, Piano non troppo, Picaroon, Pip2andahalf, Piperh, Pizza1512, Plastic, Pmccray, Pmccray1, Porno, PranksterTurtle, Prettyperky, Primetime, Prolog, Prozhen, Quarl, Quintote, Qvqv, R'n'B, RDF, RG2, RHaworth, RMFan1, RadicalBender, Raeky, Rajamouli2000, Rama's Arrow, Raterman, Raul654, Raven4x4x, Rbarreira, Reaver789, Red Thunder, RedHillian, Reimarspohr, Remember, Remi0o, Rettetast, RexNL, ReyBrujo, Rholton, Rice888, Richard001, RichardF, Rifleman 82, Rknasc, Rlee1185, Rob-nick, Robert Merkel, RobertBradbury, Rocky rawstern, Rodolfou, Rogena, Rollerblade, RonUSMC, Ronaldo wanna b, Ronz, Rostislav Lapshin, Rothfuss, Roux-HG, RoyBoy, Royboycrashfan, Rrburke, Rxs, RyanCross, Ryanmcdaniel, Ryt, Ryulong, SFClancy, SFGatUMO, SJP, ST47, Sachinrocks, Saeed5252, Salsb, Sameerhansda, Sander123, Sandrider, Sarahmcd, Sarangdutt, Sarbruis, Saturday, Savidan, Scarian, Sceptre, SchubertCommunications, Scibaby, Scientific American, Scilit, Scorpionman, Scoutersig, Scullin, Sean122, Seddon, Seidenstud, Selket, Shadowjams, Shanes, SheffGruff, Shinseki, Shirulashem, Shmay, Shoeofdeath, Siliconov, Simon rjh, SiobhanHansa, Sionus, Sir Paul, Sir Vicious, Sirveaux, Sjö, SkerHawx, Skier Dude, Skysmith, Slaphappie, Smevy, Smilecolorsan, Smokefoot, Smokizzy, Snowolf, Snoyes, Solipsist, Sonett72, Soonerman1, Soxwon, Sp3ct3r, Speedoflightning, SpencerWilson, Spirallingspirit, SpuriousQ, Srividyakripakar, Srleffler, Stannered, Stardotboy, StephenBuxton, Stephenb, Stevage, SteveKSmith, StimsonGhetto1, SudhirP, Sumo42, Sumthin, Superstuntguy, SusanLesch, Sverdrup, Swaroopsr, Sweet2, Sweetpea2007, Sycthos, Syke22, T-borg, TNTfan101, Tabletop, Tamarkot, Tapir Terrific, Tarkovsky, TeamZissou, Tec2tec, Techguru, Tellyaddict, Template namespace initialisation script, Tempodivalse, Tennesboy, Texture, That Guy, From That Show!, The Evil Spartan, The Rambling Man, The Ungovernable Force, The wub, TheBilly, TheRanger, Thingg, Thunderstix, Thuresson, Tiddly Tom, Tide rolls, Tiggerjay, Tikar aum, Tilla2501, TimVickers, Timspencer1, Tirklf, Tisdalepardi, Tjmayerinsf, Tme42, Tohd8BohathuGh1, Tomshen, Tonym88, Torakuro, TotalSpaceshipGuy3, Tothebarricades.tk, Traal, TreasuryTag, Treisijs, Triwbe, Troels Arvin, Trounce, Tubedog, Tuffshagga, UberScienceNerd, Ukeexpat, Unconscious, Unixer, Uri, Useight, Utcursus, Uvi, Vary, Vegasciencetrust, Veinor, Vera Cruz, Vararapuajay, Vgy7ujm, Vinodm, Violentb0d, Vipuser, Viriditas, Viva dsK, VladimirKorablin, Vssun, Vuo, W bauman, WHSL, WLU, WadeSimMiser, Walker-IFR, Wangi, WarthogDemon, Wavelength, Waxigloo, Wazza28, WearyTraveller, WhatisFeelings?, Whitesaint, Whkoh, Wiki Raja, Wiki man55, WikiED, Wikiborg, Wikikrockiana, WillWare, Woohookitty, WpZurp, Waelgaest waeffe, Xcaliburn, Xen0phile, Yamamoto Ichiro, Ybbor, YellowMonkey, Yintan, Yngvarr, Ynhockey, Youandme, Youssefsan, Yst, Yupik, Zealotii, Zenith87, Zigger, Zundark, Zybez, Zygomorph, 2903 anonymous edits

DNA nanotechnology *Source:* <http://en.wikipedia.org/windex.php?oldid=294763628> *Contributors:* 0x38I9J*, Alnokta, Amaling, Anthonydelaware, Antony-22, Cyfal, Epb123, Giftlite, Gioto, Pwkr, ShawnDouglas, Thorwald, Tolosthemagician, ZayZayEM, 30 anonymous edits

DNA microarray *Source:* <http://en.wikipedia.org/windex.php?oldid=297570038> *Contributors:* 168..., 3 Löwi, Aciel, AdamRetchless, Adenosine, Afluegel, AlastairM3754, Albinpaulxavier, Amar kamath, Amarilla858, Amosfolarin, Andrew73, Andrewericolesman, Angr, Apers0n, Arcadian, Aremith, Artgen, Aurelduv, AxelBoldt, Bacterius88, Bender235, Bensaccout, Big Bird, Bioinformin, Blacksun, Brian Crawford, Broadbeer, Brooke618, Calmargulis, Carlsbad, Cathleenmrocco, Ceyockey, Chemist234, Ciar, Cmungall, Cobalt137cc, Crissmyass, DGG, Dacharle, Davidweiss, Denix13, Dicklyon, Discospinster, DoctorDNA, Dr. William Jacobs, Drdaveng, Duncharris, Environmatt, Fawcett5, Figma, GV wiki, GeeJo, Geno-Supremo, Giftlite, GiollaUidir, Glane23, Glashedy, GoldenTorc, Gurmukh.s, Gustavocarra, HankMansion, Hephaestos, Hgferman, Hraefen, Hu12, Hydkat, Iidnormal, Ilovemicroarrays, Ipodamos, Jack-A-Roe, Jackhynes, Jafield, Jahiegel, Jeff Marks, Jethero, Jfdwolff, Jgreene1305, Jgruszynski, JonHarder, Jonathan Hall, Jondel, JosephBarillari, Jotomicron, Jubal, Kantokano, Khalid hassani, KirbyRandolf, Klamber, Kurykh, La goutte de pluie, Lantonov, Larsson, Lassefolkersen, Lea Cleary, Lexor, Lfrench, Lightmouse, Lindsay658, Lisa230579, Lord.lucan, Luwo, Malljaja, MatthewBChambers, Mattpope, Michael Hardy, Miguel Andrade, Movado73, Mxn, Natarajanganesan, NicolasStransky, Nieselt, NoQuarter, Nrhoads, Nuptsey, Olympos, Paphrag, Parijata, Parkinson, Patrick Maitland, Peipei, PeterCanthropus, Pgan002, Pixelface, Postglock, Pvosta, Qinatan, Quartertone, Radagast83, RainbowOfLight, Raul654, Rebut, Rich Farmbrough, Rockner, Ruud no1, Sandrauesugi, Schutz, Scott.spillman, Sentausa, Shabd sound, Shamrocktuesday, Slustbader, Speedyboy, Spongebobsqpants, Squidonium, Srlasky, SteveChervitzTrutane, Tameeria, Terrace4, TestPilot, Thdog42, The Sunshine Man, TheiNhibition, Thingg, Thomas.Hentrich, Thrips, Thumperward, Toddmartinsky, Tombadog, Toniosky, Tstokes, Tstrobaugh, Tuskaloosa, Twisp, Typochimp, Tysi, Unint, Vegetarianrage, Venullian, Vladimir Pilný, Vrr, WAS 4.250, WMod-NS, Wavelength, Webridge, West Brom 4ever, Whosasking, Willia, Wk muriithi, Wleizero, Wli625, Woohookitty, WriterHound, Yaki-gaijin, Zven, 330 anonymous edits

DNA sequencing *Source:* <http://en.wikipedia.org/windex.php?oldid=294391714> *Contributors:* 25or6to4, 5piggies, Abanima, Abdullah mohammed, Abdull, Abizar, Agricola44, Akita86, Akjosh, Akriasas, AxelBoldt, BaChev, Bhar100101, Bjorn9800991, Brice one, Charles Gaudette, Cinnamon colbert, Clicketyclack, ConfuciusOrnis, Crana, Cremepuff222, Cspenser, CultureDrone, DWeißman, Dai mingjie, David Schacht, DerHexer, Discospinster, Dkropf, Dnacash, DoctorDNA, Dupz, DutchDevil, Dysmorodrepanis, ERcheck, ESanchez013, Eimeim, Ejwong, Eric-Wester, Eyu100, Fedra, Frankatca, Furbly100, Fuxx, George Church, God Emperor, Graminophile, Hoed4sho, Jacopo Werther, Johnuniq, Jvbishop, Keaka411, Ketil, Kku, Kymacpherson, Lantonov, Lenoxus, Lmsutton1, Loris, Lucas Blade, MBCF, Madeleine Price Ball, Magnus Manske, Malljaja, MarcoTolo, Mikael Häggström, Naturespace, Neffk, NewEnglandYankee, Nono64, Novangelis, Noveltyghost, Ohnoitsjamie, Omegatron, Oxymoron83, PDH, Peripitus, Pharos, Pixelface, Pvosta, RDBrown, RJaguar3, RRphys, Red89011, Rees11, Res2216firestar, Rjwilmsi, Robert K S, Robin klein, Robinatron, Rosyaraar, RoyBoy, SJP, Sandahl, Schnarr, Shtina, Seans Potato Business, Sentausa, Shrimp wong, Shymal, Sintaku, SomethingCatchy, Spellmaster, SteveChervitzTrutane, Su-no-G, Tammyz06, TestPilot, Trevyn, Tsmith423, Twas Now, Victor D, Vinylmeister, Xenon54, Yurivict, Zaimon, 189 anonymous edits

Neutron *Source:* <http://en.wikipedia.org/windex.php?oldid=296644176> *Contributors:* 2D, ABigGreenHippo, Aadal, Aarchiba, Abdullaais4u, Acalamari, AdjustShift, Aecarol, Ahoerstemeier, AlDragon, Alansohn, Alchie1, Andre Engels, Andres, Andrewa, Animum, AnonGuy, Antixt, Anyeverybody, Arjen Dijkstra, ArnoLagrange, Art Carlson, Aruton, Astavats, Asyndeton, Attilios, AxelBoldt, AySz88, Badseed, Bambaiah, Bender235, Bensaccount, Bobo192, Brainblaster52, Bsimmons666, Burntsauce, CDN99, Cabb99, Calypso, Can't sleep, clown will eat me, CanisRufus, Capricorn42, Cenarium, Cglassey, ChasingSol, Christofurio, Church of emacs, Citicat, Complexica, Conversion script, Cyp, DFriend, DV8 2XL, Danny, Dark Mage, Dbiel, Deansinclair, Demicx, Denni, DerHexer, Dev 176, DoctorPiouk, Donarreiskoffer, Doughboy, Doulos Christos, Dr.Science, Drilnoth, Drini, Dycedarg, Dlugosz, Ecko15, Eddideigel, Edgar181, El c, Ellywa, Enviroboy, Epb123, Everything, Femto, Forteblast, Frau Holle, Fredrik, FreeFull, Gaius Cornelius, Gentgeen, Geeking66, Giftlite, Gimmetrow, Glenn, Goods21, Goostyyy, Gopal81, Gordonrox24, Goudzovski, Hans Moravec, Hdehuer, Headbomb, Heavens is the world, HenryLi, Herbee, Icairns, Icek, Icewedge, Industrieman, Interiot, Ixf64, J.delanoy, JBukon, JWB, Jakew, Jaknouse, JarlaxleArtemis, Jeff G., JerrySteal, JetLover, Joelholdsworth, Jorge Stolfi, Joshmt, Jrockley, Ju7kik80l568r, Juancnuno, Karenjc, Karol Langner, Kbk, Kdliss, Keilana, Ketiltrout, King of Hearts, Kjkolb, Kjoonlee, Kkmurray, Knutux, KunalKathuria, Kuyabribri, KyleDantarin, LarryFrank, Lokal Profil, Looxix, Lord Shivan, M1ss1ontomars2k4, Martin451, Mav, Maximus Rex, Maxis ftw, Melchoir, Mennoblaauw, Merovingian, MetsFan76, Mike Rosoft, Mike Serfas, Mikez, Mkweise, Mocrine, Montazmeahii, Morgrimm, Mosaffa, Mother.earth, Mviduka4197, Nakon, Naturalnumber, Naturespace, Ncmvocalist, Neparis, Nergaal, Newone, Nick Y., NickMartin, Nicklcms, Nightscream, Nihiltres, Nikai, Nsaa, NuclearWinner, Obradovic Goran, Olivier, Oo64eva, Oxymoron83, Patrick, Patstuart, Paul Erik, Paula Pilcher, Pdbailey, Persian Poet Gal, Phylend, Pilotguy, Possum, Poupoune5, Prashanthns, RG2, RJHall, RadiantRay, Rajeevmass, Rangek, Raven1977, Reyk, Riana, Richard Arthur Norton (1958 -), Rmrfstar, Roadrunner, Romanm, Ronhones, Rursus, SDC, Safalra, Salsb, Satan's Kitchen, Sbarris, Sbowers3, Scarymaryfwfc, SchfiftyThree, Scottfisher, Seattle Skier, Sega381, Shoeofdeath, SkyLined, Slakr, Soarhead77, SouthernMan, Sparky2002b, SpeedyGonsales, Spencer, Spute, Srfleffer, Starkiller88, Stephenb, Strait, Subash.chandran007, Susvolans, TSO1D, TakuyaMurata, Tarosan, Tchaika, The Anome, TheEditrix2, Thedjatclubrock, Tide rolls, Tiptoety, Tobias Hoevekamp, Tohd8BohathuGh1, TomasBat, Trelvis, Triple333, Tsogo3, Until It Sleeps, Unyoyega, Valery Beaud, Vboo-belarus, Versus22, Voidxor, Vsmith, Vuo, W1k13rh3nry, Wafulz, WaveEtherSniffer, Whitepaw, Wigren, Wiki Tiki God, Wiki alf, WikiSlasher, Wknight94, XJamarastafire, Xerxes314, Yyy, Zfr, Велетень, 392 anonymous edits

Neutron scattering *Source:* <http://en.wikipedia.org/windex.php?oldid=297360408> *Contributors:* Andyfaff, Anonymous Dissident, Calltl, Cardamon, Chipmonker, EBlackburn, Grj23, Hellbus, J bellingham, Jdrewitt, Joachim Wuttke, Karol Langner, Kdliss, Kiyabg, Msiebuhr, NSR, Nitrous x, Paula Pilcher, PhilBentley, PranksterTurtle, Qwerty Binary, Sam8, Sanders muc, Soarhead77, 12 anonymous edits

Inelastic neutron scattering *Source:* <http://en.wikipedia.org/windex.php?oldid=297134738> *Contributors:* Chris the speller, D-rew, Jdrewitt, Joachim Wuttke, Kukini, Mkresch, Paradoxsociety, Paula Pilcher, 8 anonymous edits

ISIS *Source:* <http://en.wikipedia.org/windex.php?oldid=242282562> *Contributors:* -

ISIS neutron source *Source:* <http://en.wikipedia.org/windex.php?oldid=281693631> *Contributors:* 2over0, Andreww, Benjaminevans82, BigDukeSix, Bobblewik, CarolGray, Croquant, Florentino floró, Inglebat, Islander, J bellingham, Jll, Orlady, RLMCG, Stwalkerster, Superborsuk, Tikiwont, Tpikonen, Wurzelller, XR2TT, 15 anonymous edits

Sudbury Neutrino Observatory *Source:* <http://en.wikipedia.org/windex.php?oldid=296689818> *Contributors:* Bearcat, Blotto adrift, Boardhead, Bryan Derksen, CDN99, Ceyockey, Conversion script, Cstaffa, CyclePat, DMcanada, Duk, Euchiasmus, Falcorian, Fleurot, Flup, Flying fish, Gene Nygaard, Golfcam, HEL, Hadal, Hooperbloob, Hunor, Jag123, Jht4060, Jiminy pop, Joseph Dwayne, Judge Nutmge, Kelapstick, Kmccarty, Korandder, Linas, Looxix, M@sk, Maury Markowitz, Mindmatrix, Montrealais, Msh210, NeilFraser, Neparis, PeregrineAY, Quilche, Rich Farmbrough, Rnt20, Rotiro, RoySmith, Safalra, Sbharis, Scorbatt, ShakingSpirit, Shanes, Silsor, Stepa, Strait, Taxman, Tevatron, Tikiwont, Turtlejuice, Varnav, WISO, Wikibob, Wilmot1, 59 anonymous edits

ATLAS experiment *Source:* <http://en.wikipedia.org/windex.php?oldid=294908361> *Contributors:* 84user, AB, AcademyAD, Akamad, Amapelli, AndrewWatt, Andrius.v, Apis O-tang, Bcrowell, Bobblewik, Bovineone, Bridgeplayer, Bunchofgrapes, Charles Matthews, Ciphers, Col. Hauler, Cowman109, Curps, Cyberia23, Cynicism addict, Davdde, Djinn65, DragonflySixtyseven, Ehn, Erkan, Flying fish, Francs2000, Freakofnurture, Frencheigh, GangofOne, Gene Nygaard, Gregb, Gurch, Harp, Harryboyles, Jag123, Jmnbatista, Joopercoopers, Juhanson, Khukri, Kozuch, Kyurkewicz, Laurascudder, LeoNomis, Linas, Loodog, Lumidek, Lupin, MagdaGa, Mako098765, Mallorn, Mandavi, Manfalk, Martijn Hoekstra, Master z0b, Matt Crypto, Maxkramer, Mithridates, Mjaekel, Neparis, O. Harris, Orion11M87, Pediadeep, PeterMcCready, Plasticup, Rama, Rich Farmbrough, Rjwilmsi, Rob.derosa, SCZenz, SandyGeorgia, Sdedeo, Sfdan, Sheliak, SimonP, SinWin, Spellmaster, Splash, Ssayler, Suruena, Susvolans, The wub, Tony1, Tushar.bhatnagar, V9, Vald, WISO, Wayward, Wiki alf, Woodrowr, Z6, Zondor, 113 anonymous edits

Neutron spin echo *Source:* <http://en.wikipedia.org/windex.php?oldid=296628563> *Contributors:* Localoptimum, M.monkenbusch, Paula Pilcher, Satarsa, Shimgray, Tibor Horvath, Tpikonen, 9 anonymous edits

Muon *Source:* <http://en.wikipedia.org/windex.php?oldid=297037063> *Contributors:* 5Q5, Ahoerstemeier, Andrew Carlssin, Angela, Anonymous Dissident, Anthony Appleyard, Army1987, AxelBoldt, Bambaiah, Bennetto, Bkell, Bm gub, Bodhitha, Bryan Derksen, Bubba73, CYD, Can't sleep, clown will eat me, CapitalR, Ceyockey, Cjxc92, Conversion script, Coppertwig, Corpx, CrniBomber!!!, DannyWilde, Dauto, Deglr6328, Diberri, DnetSvg, Donarreiskoffer, DoubleBlue, Eb.hoop, EddEdmondson, Falcorian, Giftlite, Goudzovski, Graymornings, HEL, Headbomb, Herbee, JabberWok, Jarry1250, Kariteh, Keenan Pepper, Kjoonlee, LiDaobing, Looxix, Mani1, Mav, Melchoir, Merovingian, Mihaip, Mike Peel, Millosh, Misterigloo, Mother.earth, Ojigiri, Pjacobi, RDR, Ravedave, Rholton, Roadrunner, Rob Hooft, RobPlatt, Roscoe x, Rotiro, SCZenz, STGM, SalomonCeb, Salsb, Saritepe, Sbharis, Sbyrnes321, SchmittM, Scottfisher, Sheliak, Spencer, Srleffler, StewartMH, Stifle, Strait, Tarotcards, Tetracube, Thecinimod, Tigerhawkvok, Tim Starling, Vanderdecken, Xerxes314, Xinghuei, Yevgeny Kats, Youandme, Zundark, 119 anonymous edits

Ionization cooling *Source:* <http://en.wikipedia.org/windex.php?oldid=188728045> *Contributors:* Chrisrogers1234, Reyk

Deep inelastic scattering *Source:* <http://en.wikipedia.org/windex.php?oldid=292435681> *Contributors:* Alansohn, Anthony Appleyard, Batmanand, Charles Matthews, D.H, DerHexer, Dna-webmaster, E2m, Epbr123, Majorly, Nbach, Neparis, Peter Harriman, PeterReid, Phe, Quietly, SCZenz, Saga City, T@nn, Vb, 16 anonymous edits

Timeline of microphysics *Source:* <http://en.wikipedia.org/windex.php?oldid=295773233> *Contributors:* 0, 5.41, AjAldous, Aspects, Attilios, Bryan Derksen, Charles Matthews, Cutler, D6, DO'Neil, DannyWilde, Dave souza, DavidLevinson, Dirac66, Dstudent, EdH, Elektron, Elliskev, Fibonacci, Gareth Owen, Gregnguyen, Gretyl, HappyCamper, Harp, Headbomb, Hidaspal, Isomorphie, J.delanoy, JeffBobFrank, JeffW, Jheald, Kieran, Laurascudder, LeYaYa, Likebox, Looxix, Macumba, Michael Devore, Michael Zimmermann, MimirZero, Mr impossible, ObsidianOrder, Okedem, Onionmon, Paulleake, Physicistjedi, Piil, Pjacobi, Radagast83, RayTomes, Rmhermen, Ruud Koot, Safalra, Saga City, Selket, Smack, Stone, Tabletop, Tassedethe, Taxman, Timwi, Urhixidur, XJamRastafire, Yamara, 34 anonymous edits

Automatic calculation of particle interaction or decay *Source:* <http://en.wikipedia.org/windex.php?oldid=291744381> *Contributors:* Cricketgirl, EurekaMan, Freacafe, PigFlu Oink, Rhebus, SGGH, Victor Lopes, 7 anonymous edits

Neutrino *Source:* <http://en.wikipedia.org/windex.php?oldid=296914305> *Contributors:* A new name 2008, AWeishaupt, Abb3w, Abeneal, Ajgw56, Akriasas, Alansohn, Alastair301, Alfio, Alias Flood, Alton, Andre Engels, Andres, Angelastic, Anthony Appleyard, Anville, Apparentslug, Aqwis, Arbe, Astavats, Astralusetet, AxelBoldt, Baba476, Bambaiah, Bbx, Bcrowell, Benhocking, Blennow, Bobunf, BouhadeF, Bryan Derksen, Bunnyhop11, Cacycle, Calmargulis, Calton, Cenarium, Cgr1123, Charm, Chenyu, Christoph Scholz, ChristopherWillis, Cje, Cmprince, Conversion script, Cos111, CosineKitty, Curps, Cwitty, Cwolsheep, Cyde, Cydelin, DMcanada, DannyWilde, Dauto, Decowski, Deglr6328, Denis tarasov, Dirac66, DocWatson42, Donarreiskoffer, Doug Danner, DrWorm, Dratman, Dtgriscom, Duien, EddEdmondson, Eequor, Engwar, Ernsts, Esemono, Espetkov, Evercat, Fatal!ty, Fg2, Fibonacci, Findel, Fleurot, Flying fish, Foobaz, Fragman, Fredil Yupigo, Fxer, Gaius Cornelius, Galactor213, Gdarin, Gene Nygaard, Giftlite, Glenn, Gogo Dodo, GregorB, Gurch, HannesHultgren, Harp, Hdeasy, Headbomb, Heron, Hmmm, Hyperdeath, Ian Pitchford, Icairns, Icek, Intangir, Itinerant1, JWSchmidt, JabberWok, Jahilia, Jdlambert, Jht4060, Jimduck, Jjpcondor, Jmcc150, John fromer, John187, Joke137, Jonny-mt, Jorge Stolfi, Juliancolton, Jyfvalle, Kain Nihil, Ken Arromdee, Kharhaz, Kmarinas86, Kukini, La goutte de pluie, Laudaka, Lethe, LiDaobing, Libera, Ligulem, Looxix, LorenzoB, Lrenh, Lseixas, Lyuokdea, MER-C, Mac Davis, Mani1, Masoninman, Mattman723, Matty j, Mayrel, Mdob, Meekohi, Meelar, Melchoir, Mentifisto, Merovingian, Michael C Price, Mike Clough, Mike Peel, Mikez, MimirZero, Morangm, Morgan wascko, Mostargue, MrFizyx, Ms2ger, Mssgill, Nagytibi, Nakos2208, Nalumc, Nap, Naucer, Newone, Nickptar, Nikai, Ninja Wizard, Norbu19, Oblivious, Ohwilleke, Olaf Davis, Olsen-Fan, Otto ter Haar, PSimeon, Parande, Patrick, Pauli133, Phil John Hawkins, Philipump, Phr en, Pizza1512, Pjacobi, Plasticup, Pwjb, Quaoar, R.e.b., RC Master, RJFJR, RJHall, Ralfoide, Ravedave, Raymond Hill, RedBLAKandBURN, Reddi, Reedy, RexNL, Rhmtsang, Rhynchosaur, Ricima, Rjn, Rjwilmsi, Roadrunner, Rob Hooft, Rosenknospe, SCZenz, SDC, Sagredo, Salsb, Santaduck, Savant13, Sbharis, ScAvenger Iv, ScienceApologist, Scythe33, Sergio.ballestrero, Sheliak, Smithbrenon, Staecker, Strait, Sunborn, SuperLonghorn, Swamp Ig, Swamper777, SwordSmurf, Szdori, Tarquin, TenOfAllTrades, That Guy, From That Show!, The Original Wildbear, The assassin 47, TheMaster42, TheSeez, Thehotelambush, Thewayforward, Thuktun, Thunderbird2, Tom Loughheed, Tomaxer, TonyBermanseder, Trainbrain27, Vegaswikian, Vsmith, Vyznev Xnebara, WVhybrid, Wacko375, Warofdreams, Warut, Weasel5i2, Webmaster Pete, Wereon, Wikiborg, Witan, WolfmanSF, XJamRastafire, Xaonon, Xerxes314, Xihr, Xmantis, Yevgeny Kats, Yurigerhard, Zandperl, Zelab, Милан Леписавић, 387 anonymous edits

List of neutrino experiments *Source:* <http://en.wikipedia.org/windex.php?oldid=291370212> *Contributors:* DrCLN, Headbomb, Henbo, Hugo999, Neutrinoless, Pjacobi, Puttybrain, Vladis1av, 7 anonymous edits

List of materials analysis methods *Source:* <http://en.wikipedia.org/windex.php?oldid=296834157> *Contributors:* Amaltheus, Askewmind, Bvcrst, C.jeynes, Cardamon, CharlesC, Danski14, EdC2, Ein hesse, Excaliburhorn, Fredericks, Freecat, Garion96, Gimme danger, Gurch, HYPN2457, Hubble618, IanOsgood, IceKarma, JackSeoul, Jcwf, Kanzure, Karnesky, Karthikc123, Khatru2, Kkmurray, Korg, Materialsscientist, Michael Hardy, Mjmerriknight, Murray.booth, Neparis, Ohthelameness, Pegship, Pharmacomancer, Pythagoruz, Runningamok19, Twisp, XPh6, Yaotsan, 73 anonymous edits

Fourier transform spectroscopy *Source:* <http://en.wikipedia.org/windex.php?oldid=291868949> *Contributors:* Ajim, Asterion, Bci2, Berserkerus, BigFatBuddha, Bobby1011, Christopherlin, Damian Yerrick, Deglr6328, E104421, Epbr123, Graeme Bartlett, Guillom, Hankwang, Harold f, Haydarkustu, HelgeStenstrom, Jaraalbe, Jcwf, John.lindner, Jonathan F, Kcordina, Kingpin13, Kkmurray, Martyjmch, Michael Hardy, Nikai, Nitrogen15, Peter, Peterlewis, Rifleman 82, Rnt20, Ronningt, Roybb95, Seidenstud, Skier Dude, Slapidus, Smeyer1, Stannered, Sverdrup, Thepretenders22, Thinkinnng, Tim Starling, Veinor, Vectorsong, 69 anonymous edits

Chemical imaging *Source:* <http://en.wikipedia.org/windex.php?oldid=290927658> *Contributors:* Alansohn, Andyphil, AngelOfSadness, Annabel, Banus, Batykefer, Bci2, BierHerr, Chris the speller, Closedmouth, D6, Davewild, Editore99, GeeJo, HYPN2457, Iridescent, JIP, Jim.henderson, Kkmurray, Mdd, Mkansiz, Natalie Erin, Skysmith, Ultraexactzz, Wilson003, 38 anonymous edits

Atomic force microscope *Source:* <http://en.wikipedia.org/windex.php?oldid=297548215> *Contributors:* .:Ajvol.:, Admartch, Ahram, Ahram-kim, Alansohn, Allentchang, Alvestrand, Ambios, Ams627, Angela, Anthonydelaware, Antony-22, Arcfrk, Ase, Askewmind, Average Earthman, Bendzh, Bfollinprm, Bible, Biophys, Bobblewik, Bochica, Bryan Derksen, Canjth, CdnC, Chuckiesdad, Chych, Creepin475, Crm2kmsu, Crystallina, Cucumberslumber, Cyrus Grisham, Davidcastro, Dgrant, Doulos Christos, Edward, El C, Femto, Flipperinu, Fontissophy, Frosty0814snowman, Gaijinpl,

Gene Nygaard, Gene93k, Geodesic42, Graphene, Grmf, HYPN2457, Halibutt, Jatosado, Jaxl, Jcwf, Jni, Joechao, Joeyfox10, John, John Dalton, Kamukwam, Kariteh, Keenan Pepper, KristianMolhave, LMB, Lauranrg, Leifisme, Maximus Rex, Mormegil, NanoMamaForReal, Nmnogueira, Oreo Priest, Physicistjedi, Pieter Kuiper, Qef, Quadell, Qxz, Raymondwinn, Rhandley123, RoB, Rob Hooft, Ronz, Rostislav Lapshin, Ruder, SJP, Satish.murthy, Sbyrnes321, SecretDisc, Seraphchoir, Shniken1, Sisyphe happy man, Skier Dude, Switchsonic, Tai89ch, Think outside the box, Tim Starling, Uglygizmo, Vfranceschi, Wiki alf, Wikiborg, XarBiogeek, Yapete, Yurko, Yyy, Zeamays, Zureks, 176 anonymous edits

Nuclear magnetic resonance *Source:* <http://en.wikipedia.org/w/index.php?oldid=297583665> *Contributors:* 2lzSz, 63.192.137.xxx, Abecedare, Abrech, Agateller, Amitgujar, Amwestover, Arisa, Arthena, AutumnSnow, AxelBoldt, Baccyak4H, BailesB, Banano03, Bci2, Beetstra, BenFrantzDale, Bensaccount, Berland, Bigbadjoe, Biophysik, Bruker, Bssquirrel, CMuirPrice, Cacycle, Ceyockey, Charles Matthews, ChemistHans, Christopherlin, Conversion script, Crazy Demon, Cubbi, DJoe, DMacks, DV8 2XL, Daniel.Cardenas, Darrien, Davehi1, Deglr6328, DerHexer, Derlay, Dirac66, Djdaedalus, Dkentyko, Dreadstar, Dwmyers, Dynabee, DynamicDes, Dysprosia, ERcheck, Edgar181, Edupedro, Ejteye, Eraboin, Eras-mus, Fantumphool, Flogiston, Foobar, Franamax, G-W, G.hartig, Gehtnix, Gene Nygaard, Gentgeen, Ghiles, Giftlite, Glhann17, Gogo Dodo, GregorB, Greudin, Griffinofwales, Gurch, H Padleckas, Haham hanuka, Hankwang, Haydarkustu, Headbomb, Herbee, Hiberniantears, Hollgor, Iain99, Icairms, Ike9898, Ilws, IlyaV, Improv, Indiedan, Iorsh, Ixf64, Jayvyas, Jcepna, Jcm, Jcwf, Jens-Erik, Jketola, Jlin, Jmcc150, Jopires, Jpbowen, Jrizor8504, Jsmoreira, Jurgenfd, JustJuthan, Jxr, KasugaHuang, Katherine Folsom, Kaysette, Kc8ukw, Kevin Ryde, Khilari, King himself88, Kjaergaard, KrakatoaKatie, La goutte de pluie, Latch, Lee-Jon, Lexi Marie, Lfh, Linas, LinguisticDemographer, Linnhall, Little.pig.microphone, Loeffler, Loening, Lucamauri, M stone, Macholl, Markber, MartinSaunders, Marx Gomes, Mav, Michael Hardy, Mietchen, MikeW25, Mkeranat, Morten Cools, Mrmiller24, NamFohyr, Nergaal, Nick Mks, Nickptar, Nicolasbock, Nonoelmo, OMCV, Odie5533, Ole@look, Olivierlopez1, Orelena, Paintman, Paulyche, Pdbailey, Peregrine981, Peterlin, PhiRho, Potatoswatter, Pr3cursor, Pt, Quoeth, R'win, RSido, Ramamoor, Rednblu, Rich Farmbrough, Rijkbenik, Rintrah, Rjwilmsi, Rkising, Robert Hiller, Roy Hoffman, Rvlaw, SCZenz, Salsb, Shaddack, Sieg6529, Silverchemist, Skier Dude, SlipperyHippo, Snarfevs, Spincore, Spiralhighway, Spree4567, Stan Sykora, Stewartadcock, Tadin, TenOfAllTrades, Terhorstj, TheCoffee, Tim Starling, Timo Honkasalo, Timwi, TomyDuby, Tony Sidaway, Tony27587, VBrik, Van helsing, Varioustoxins, Voorlandt, Vuo, Wik, Wikiblaz, Wknight94, XRiffRaffx, Xiaopo, Yamamoto Ichiro, Zereshk, Zipz0p, 337 anonymous edits

2D-FT NMR and Spectroscopy *Source:* <http://en.wikipedia.org/w/index.php?oldid=297239250> *Contributors:* Bci2, Ched Davis, Drilnoth, H Padleckas, JaGa, Reedy, Rich Farmbrough, Rjwilmsi, Teeschmid, 2 anonymous edits

Infrared spectroscopy *Source:* <http://en.wikipedia.org/w/index.php?oldid=293726799> *Contributors:* 194.200.130.xxx, Aboalbiss, Ahoerstemeier, Annabel, Antandrus, Arcadian, Arnero, Ary29, Bensaccount, BigFatBuddha, Biophysik, Bobthebuilder37, Borgx, BountyTJ, Bubba hotep, CLW, Calaschym, Charles Matthews, Christopherlin, Chuck Sirloin, Cobi, Coffee, CommonsDelinker, Conversion script, Cwkmall, DMacks, DavidRKelly, Deglr6328, DerHexer, Dieter Baurecht, Dr.Soft, Drmies, El C, Eno-ja, Finalnight, Francs2000, Fresheneesz, Fuhghettaboutit, Fyver528, Gentgeen, GeorgHH, GermanX, Giftlite, Gilliam, Grimlock, Guillom, HYPN2457, Hankwang, HappyCamper, Haukurth, Heron, Hesacon, Hollgor, II MusLiM HyBRiD II, Ian Pitchford, J.delanoy, Jackol, Jaraalbe, Jcwf, Johnbrownsbody, Junglecatt, Kcordina, Kkmurray, Lifer21, Lightmouse, Littleghoti, Lorenzarius, LouisBB, LukeSurl, Martymjch, Materialschemist, Michael Hardy, Mjwlanics, Mythealias, Nakon, NewEnglandYankee, Nivix, Nmathew, Old Moonraker, Peterlewis, Pharmacomancer, Pit, Punctilius, Quadell, Rifleman 82, Rob Hooft, Sam Hocevar, SantoshS, Shalom Yechiel, Skier Dude, Someguy1221, Srnec, Stephenb, Stokerm, SuperTycoon, TechPurism, The wub, Tiago Becerra Paolini, Urbansky, VBrik, Vcelloho, Vector Potential, Vegaswikian, Veinor, Visor, Werson, Wmahan, Yashkochar, 218 anonymous edits

Near infrared spectroscopy *Source:* <http://en.wikipedia.org/w/index.php?oldid=295782647> *Contributors:* A2Kafir, Ameliorate!, Athene cunicularia, Bci2, Beetstra, BigSquareOne, Blimfark, Blueturtle01, Caltrop, CheekyMonkey, Dakeddie, Debrasser, Deglr6328, ElinorD, Gardenparty, Hankwang, Jaeger5432, Kjaergaard, Kkmurray, Kpmiyapuram, Martymjch, Njw, PaddyLeahy, Piano non troppo, Pinkadelica, RLDeran, Radagast83, RainbowOfLight, Rji, Silvonen, Srbauer, Tbonepsb, Tjr9898, Twas Now, Vegaswikian, Wayne Miller, 64 anonymous edits

Vibrational circular dichroism *Source:* <http://en.wikipedia.org/w/index.php?oldid=295070744> *Contributors:* Aktsu, Auntof6, Bci2, Buurma, Indurand, Slaweiks

Raman spectroscopy *Source:* <http://en.wikipedia.org/w/index.php?oldid=296991150> *Contributors:* Ajim, ARBradley4015, Afrine, Akv, Andrewavalon, Annabel, ArepoEn, Birdbrainscan, Brat32, Bullraker, Cdegallo, Charles Matthews, Christopherlin, Cyblor, D.Wardle, David Eppstein, Dazzaling69, Dfbaum, Editore99, Fang Aili, GT, Gabi bart, Gaius Cornelius, Galoubet, Gene Nygaard, Gene s, Gentgeen, Gerkleplex, GermanX, Giotto, Gunnar Larsson, Hankwang, Jaeger5432, Jaganath, Jameslh, Janke, Jll, Jmameren, Jofox, Jonnyapple, Judenicholson, Keramamide, Kkmurray, Kraftlu, Latch.r, LordDamarco, Loreshadow, LostLucidity, MARKELLOS, Magicalsauy, Manulinho72, MarcoTolo, Martin Hedegaard, Measly Swan, Meropie, Michbich, Mill haru, Mippi283, Mythealias, Nikai, Nmnogueira, Paul August, Paul venter, Pavlina2.0, Pcarbonn, Pericles899, Petergans, Piano non troppo, Pixeltoo, RTC, Ravi khanna, Redleaf, Rich Farmbrough, Rob Hooft, Rossheth, Rulie123, Shashang, Shreevatsa, Smalljim, Srosie68, TDogg310, Tantalate, Tha Stunna, The number c, The wub, Thue, Tillwe, Tmb4bd, Tomatoman, Tomgally, Uther Dhoul, Wilson003, Yasuakinaito, Zylorian, 138 anonymous edits

CARS *Source:* <http://en.wikipedia.org/w/index.php?oldid=271067073> *Contributors:* 2help, Ahunt, Ashtooamax, Bobo192, Bou, Can't sleep, clown will eat me, Ctjf83, Cureden, Danny1992, Delldot, Dreaded Walrus, Exor674, Ganeshk, Gerbrant, Glen 9x 2007, Gurchzilla, HQCentral, Hudicourt, Jcarle, Karlhahn, Kharker, Kukini, Metasquares, Neil Martin India, Ohnoitsjamie, Oldmanriver, Rich Farmbrough, Rrburke, Silver Edge, Skysmith, The wub, WestJet, 37 anonymous edits

Hyperspectral imaging *Source:* <http://en.wikipedia.org/w/index.php?oldid=291759304> *Contributors:* Adoniscik, Andrew c, Bci2, Cm the p, Dhaluza, Gcrisford, Geologicarka, Hankwang, Jprikkel, Lantonov, Moin95, Victorsong, 15 anonymous edits

Multispectral imaging *Source:* <http://en.wikipedia.org/w/index.php?oldid=243967330> *Contributors:* -

Confocal microscope *Source:* <http://en.wikipedia.org/w/index.php?oldid=47017285> *Contributors:* -

Fluorescence microscope *Source:* <http://en.wikipedia.org/w/index.php?oldid=283782950> *Contributors:* Andy Nestl, Bwbrian, Ch'marr, Chnickelfr, Coccxy Bloccxy, DO11.10, DerHexer, Ferh2os, Firehox, Gbleem, Graham87, Hetar, IlyaV, JSpung, Joechao, John, Kupirjo, Krynacpherson, Llbb, MarcoTolo, Mastermolch, Microscopist, Mysid, Nicolae Coman, Nmnogueira, OttoTheFish, Pjvpjv, Pvosta, Radagast83, Scrabbler, Stepa, SubwayEater, Utbg2008, Will-moore-dundee, Zeldaaot, 42 anonymous edits

Fluorescence correlation spectroscopy *Source:* <http://en.wikipedia.org/w/index.php?oldid=291763472> *Contributors:* Bci2, BenFrantzDale, Berkyl, Danrs, Ddkim, Gogowitsch, Hbayat, Jcwf, John, Karol Langner, Lightmouse, Maartend8, ST47, Skier Dude, Tizeff, Wisdom89, 32 anonymous edits

Fluorescence cross-correlation spectroscopy *Source:* <http://en.wikipedia.org/w/index.php?oldid=274364772> *Contributors:* Clicketyclack, Maartend8, 4 anonymous edits

Forster resonance energy transfer *Source:* <http://en.wikipedia.org/w/index.php?oldid=197657138> *Contributors:* -

Molecular graphics *Source:* <http://en.wikipedia.org/w/index.php?oldid=297452440> *Contributors:* ALoopingIcon, Agilemolecule, Altenmann, Arch dude, Chemistrannik, Chenmengen, CzarB, Dcrjsr, Dreftymac, Edguy99, Edward, EranHodis, Fvasconcellos, Harryboyles, Icep, JLSussman, Jweiss11, Karol Langner, Linforest, McVities, Mdd, Mobius, Mrug2, NapoliRoma, NicoV, Ohnoitsjamie, Outriggr, P99am, PBarak, Petermr, Provelt, Rjwilmsi, Rogerb67, SchuminWeb, Shura58, Sjoerd de Vries, SkyWalker, Thumperward, Timrollpickering, Vizbi, Vriend, Walkerma, WikiDan61, 16 anonymous edits

Molecular dynamics *Source:* <http://en.wikipedia.org/w/index.php?oldid=297629664> *Contributors:* Agilemolecule, Alex.g, Amire80, Ammatsun, Anthracene, Anxdo, ApJilly, Astavats, Ayucat, Bbullot, Bduke, BenFrantzDale, Bubba hotep, Chris the speller, Coastal593, Cortonin, Cwassman, DMacks, DRider, Dach, DeadEyeArrow, Demus Wiesbaden, Dicklyon, Dietmar.paschek, DragonflySixtyseven, Drswenson, Ebuchol, Ehdr, Gentgeen, Giftlite, Huckit, Itamblyn, Itub, JWSchmidt, Jerome Charles Potts, Jorgenumata, Jugander, Kaihsu, Karol Langner, Katherine Folsom, Kennylam, Kevyn, Kjaergaard, Knordlun, Laurent1979, Lexor, LiDaobing, Linas, Lomenoldur, Ludx, Maduixa, Marchuta, Marx Gomes, Mateusz Galuszka, Mattopia, Md Arshad Iqbal, Mihoopes, Mr Marie Weaver, Msuzen, Nicolasbock, Oiramrasac, Opabinia regalis, Ossi, P99am, Paul.raymond.brenner, Pedrito, Pelister, PhCOOH, Pksach, PrometheusX303, Raviwiki4, Rob Hooft, Roo1812, Sandycx, Shura58, Smoe, Smremde, Stewartadcock, Sudiarta, TStein, Themfromspace, Thorwald, Utcursch, Van helsing, Whanrott, Wikimcmd, Wittgenstein77, Wiz9999, Xavier andrade, Yrtgm, 200 anonymous edits

Quantum computer *Source:* <http://en.wikipedia.org/windex.php?oldid=294514216> *Contributors:* -Ozone-, 1mujin22, 4lex, AAAAA, AWeishaupt, Aarchiba, Abdullahazzam, Ajb, Albedo, Ale2006, Alex R S, Alksentrs, Alessandro, Amcfreely, Amwebb, AndrewStuckey, Andrewpmk, Andris, Antandrus, Antlegs, Anville, Anwar saadat, Arcfrk, Archelon, Arnero, ArnoldReinhold, Asmeurer, Asparagus, Atropos235, Auric, AxelBoldt, B9 hummingbird hovering, Bci2, Beagel, Beeban, Ben Standeven, Bencoder, Bevo, Bibliosapien, Bigmantonyd, Bihco, Bjohanson00, Bjweeks, Bletchley, Bobby D. Bryant, Bobo192, Bond4154, Booyabazooka, Brighterorange, Brilliant, Bryan Derksen, Bubba hotepe, BumbleFootClown, Burgaz, CBM, CSTAR, CYD, Captanpluto123, Card, Cenarium, Charles Matthews, CharlesGillingham, Chris 73, CloudNine, Cometstyles, Connelly, Couchpotato99, Count Caspian, Creidieki, Crunkcar, Cryptonaut, Cyan, Cyp, DV8 2XL, Dan Granahan, Danko Georgiev MD, Danny, Dar-Ape, DarkFalls, David Battle, David Gerard, David n m bond, DavidB, DavidLevinson, Davidgothberg, Davidmenz, Dead3y3, Dethme0w, Dgrant, DuckFeather, Durval, Dysprosia, Eaglizard, Edd Porter, Edonovan, Edward, Eigenlambda, El C, Elb2000, Eluchil, Epo, Eyu100, FKmailliW, Fattony77, Foxygirltamara, Frankenpuppy, Fullstop, Furrykef, Fyfer, G Colyer, GBL, GaaraMsg, GaeusOctavius, Gail, Gaius Cornelius, Galwhaa, Gary King, Gauge, Gentgeen, George100, Giftlite, Gioto, Glenn, Gnixon, Goldsmitharmy, Green caterpillar, GregorB, Gtg207u, HRV, Hadal, Hanjabba, Hannover.post, Hans Adler, Harold f, Harry Potter, Harryboyles, Hatethedj, Headbomb, Hfastedge, Hmrox, Hulagutten, HumphreyW, Husond, Hyandat, Hyperdivision, Iain David Stewart, Ihope127, Ik, Ilia Kr., Illspirit, Indosauros, Insurrectionist, Inwind, Isaacsurh, Iseeaboar, Isnow, Ispy1981, J.delanoy, JMK, JRGregory, Jao, JavOs, Jbw2, Jeargle, Jeff G., Jengod, Jitse Niesen, JJ137, Jksad, Jni, JohnCD, Jon513, JonHarder, Jorfer, Jotomicron, Jrockley, Justin Stafford, KD5TVI, Kannan karthik, Kate, Keegan, Keenan Pepper, Kevin Breitenstein, Kevyn, Kine, Kizeral, Ksn, Kuru, LC, Liftarn, Ligulem, Linas, Linus M., Looxix, Lostart, Lotu, LunatikOwl, Lunkwill, Lupin, MBisanz, MER-C, MagnaMopus, Manoliisfat, Marco de Mol, Marksuppes, Martaen, MartinSieg, Mat8989, Matt Crypto, Mattblack82, Matthewsism, Maurice Carbonaro, Mav, Maximus Rex, MementoVivere, Michael Hardy, MichaelMcGuffin, Michal Jurosz, Mike1024, Millerc, Mjager, Moment, Moonriddengirl, Mpassman, MrOllie, Mro, Muj0, MuncherOfSpleens, Nidckson, Nol888, Noldoaran, Norm mit, NotThatJamesBrown, Nurg, Nzv8fan, Octopus-Hands, Officialyover, Ojigiri, Oleg Alexandrov, Oliver Pereira, Onaillim, Oneyd, Pagrashtak, Pak21, Pakaran, Palfrey, PatrickHoo, PaulCook, Peter bertok, Peterdjones, Phil Boswell, Phoneused, Physis, Piano non troppo, Pietzsche, Poor Yorick, Populus, Powo, Pwjb, Pyrospirit, Quertyus, REQC, RG2, RHaworth, RJRocket53, RTC, Racklever, Ravedave, ReallyMale, Red Thunder, RedWolf, Remy B, Revived, Rich Farmbrough, Ripper234, Roadrunner, Robert Merkel, RobertG, RonanSandford, Ronz, RoyBoy, Ruud Koot, Rwww, Sajendra, Sam Hocevar, Sambarrows, Sanders muc, SandyGeorgia, Scott McNay, Scottcraig, Selain03, Seraph 31, Shoyer, Simetrical, SimonMayer, Skippydo, Sligocki, Smitte-Meister, Snakeyes, Snowolf, Spikeuk14, Spin-Half, Sploo22, Squiggle, Steamturn, Stevertigo, Tsang, Superm401, Susvolans, Symmetrysinger, TALlama, Taed, Taejo, Talon Artaime, Tarotcards, Thoosun, Techman224, Tellyaddict, That Guy, From That Show!, The Belgain, The Rogue Penguin, Tim Starling, Timwi, Tobyc75, Togo, Tom harrison, Tomstdenis, Tre1234, Tree Biting Conspiracy, Tricky Wiki44, Troelsj, Turdus, Turnstep, Ultra megatron, Uncle G, Undecided, Vaspian, Verbal, Vincenzo.romano, VodkaJazz, Wafulz, Weekwhom, Wereon, Whispering, Who, Wikiborg, Wikiklrc, Wikiscient, WilliamKF, Wim van Dam, WindOwl, Wish wellingtons, Wolfkeeper, Wrdavenport, Wtanaka, X1011, Xiong Chiamiov, Zlflood, 570 anonymous edits

Diffraction *Source:* <http://en.wikipedia.org/windex.php?oldid=296410849> *Contributors:* 2over0, A1call, Abiermans, Across.The.Synapse, Afrine, Ahmed1994, Alai, Alan Joe Skarda, Aleas, Ali, Amaltheus, Amosnomore, Andre Engels, AnnaFrance, Anoko moonlight, Anonymous Dissident, Army1987, Arnero, Atlant, Av99, Barney-12-3, Bazzargh, Bbatsell, Bcrowell, Beetstra, Birge, Bmicomp, Bryan Derksen, Buttseckks, Cambridgeincolour, Can't sleep, clown will eat me, Cdn, Charles Matthews, Charmed4ever, Complexica, Conversion script, Crowsnest, Cuardin, DMacks, Decibert, DerHexer, Dicklyon, Dino, DrBob, Egil, Ellyua, Enormousdude, Epzcaw, Erguvan7, Erudecorp, Eurion, Flowersofnight, Francs2000, Fredbauder, Fresheneesz, Garagebarrage27, Gftutia, Gholam, Giftlite, Gludwiczak, GregRM, Hadal, Headbomb, Hillbrand, Howabout1, Hunterd, Icez, Igoldste, Instinct, Isnow, J.delanoy, JCraw, JForget, Jaganath, Jaxl, Jeff Dahl, Jermor, Jhbdel, Jjron, Jm smits, Karol Langner, Kdliss, KristianMolhave, Kurykh, LMB, La goutte de pluie, Laserheinz, Light current, Linus M., MER-C, Magnus Manske, Mani1, Mbz1, Mejor Los Indios, Michael Hardy, Moe Epsilon, Mufka, MuthuKutty, Narvalo, NawlinWiki, Neparis, Ngthwlkr, Nikai, Nk, Nuno Tavares, Odedee, OlavN, Omer88f, Orionus, OwenX, Oysteinp, 1P00011011, Pakaran, Pfaletra, Pflstad, Pflatau, Pps, ProhibitOnions, Pschemp, Quadell, RG2, Radiant chains, Ram-Man, Rbj, Reddi, RenamedUser2, Revilo314, Riceman3, Rnt20, Robert L. Ronbus, Rosuna, Rspanton, Rtcoles, RyanCross, Sakurambo, Sam Hocevar, Sango123, Saperaud, SebastianHelm, Sebroff, Shadowjams, Shim'on, Shoessss, Siddhant, SimonP, Sinneed, Skarebo, Skoch3, Srleffler, Stirling Newberry, Stou, Strait, Sudiarta, Sverdrup, TakuyaMurata, The Anome, Thermochap, Tomruen, Trevorcox, Uncle Leo, V81, Wideofthemark, Wikiborg, Wikid77, Wingchi, Wolfkeeper, Xiahou, YxTay, Yyy, 百家姓之四, 237 anonymous edits

Quantum Mechanics *Source:* <http://en.wikipedia.org/windex.php?oldid=176798991> *Contributors:* -

S-matrix *Source:* <http://en.wikipedia.org/windex.php?oldid=289183367> *Contributors:* Abdull, Adjusting, Akriasas, AugPi, Berto, Bodera, BradBeattie, Businessman332211, Charles Matthews, Filemon, Giftlite, Hammer Raccoon, Headbomb, Hfastedge, Jeff3000, Likebox, Lumidek, MFH, Maliz, Matiasleoni, Michael Hardy, Ntस्प, Oleg Alexandrov, Pearle, Phys, PhysicsBob, Poli, QFT, RJFJR, Reuqr, Safalra, Secfan, SeventyThree, StephenWeber, StevenJohnston, Tbackstr, TimothyRias, Tothebarricades.tk, Tsiaojian lee, Tweet Tweet, 23 anonymous edits

Quantum logic *Source:* <http://en.wikipedia.org/windex.php?oldid=293018925> *Contributors:* Andris, Angela, Archelon, Aster Rainbow, Bci2, CSTAR, Charles Matthews, Cybercobra, DJIndica, David edwards, Dcoetsee, Dmr2, Dysprosia, Edward, Epsilon0, GTBacchus, Gaius Cornelius, Gene Ward Smith, Giftlite, GordonRoss, Hairy Dude, Headbomby, Icairns, Ilan770, Jengod, John Baez, Kimberlyg, KnightRider, Kuratowski's Ghost, Kzollman, Lethe, Linas, Lucidish, Mct mht, Mhss, Michael Hardy, Modify, Oerjan, Parkyere, Rsimmonds01, Sheliak, Shlomi Hillel, StevenJohnston, Stevertigo, T=0, Trovatore, V79, Zumbo, ىعىس, 36 anonymous edits

Spin *Source:* <http://en.wikipedia.org/windex.php?oldid=296006388> *Contributors:* 16@r, 1forhisnob, Alejo2083, Amtiss, Aquillion, Awesimo, AxelBoldt, BWDuncan, Barticus88, Bkberry, CBT, CYD, Cab88, Chairboy, Chenyu, Commander Keane, Conversion script, Craw-daddy, Cynicism addict, David R. Ingham, Dmmaus, Draeco, Emporole, Ewlyahoocom, Eyrian, Fabricationary, FlavrSavr, Fredrik, FreplySpang, Frznchckn, GRAHAMUK, HappyCamper, Hmwith, Howsaboutnow, Hraefen, Ihcoyc, Improv, IstvanWolf, JHunterJ, Jerzy, Jni, Josh Parris, Josiah Rowe, Jzylstra, Kaliber554, Kapahel, Karnesky, Kate, Kbk, Kostmo, Larry Sanger, LawrenceLo, MJD86, Mahdiislam, Mahjongg, Mangojuice, Mani1, MarSch, Marudubshinki, Mbadri, Mdale, MrRadioGuy, Mulad, Ohconfucius, P199, Patrick, Paul Erik, Ravn, Roadrunner, RobertG, Rodrigobelo, Scriberius, Serenity316, Skyman123, Slartibartfass, Spinningfounder, Stevertigo, Stux, Taestell, Ted87, Tedernst, Template namespace initialisation script, Thewayforward, Timo Laine, Tjfs, Wizard191, Zeramas, ^musaz, 40 anonymous edits

Fermion *Source:* <http://en.wikipedia.org/windex.php?oldid=295018942> *Contributors:* Abdullais4u, Alan Peakall, Andres, Anonymous Dissident, Antixt, Ashlux, BabuBhatt, Balaonair, Ben-Zin, Bevo, Bryan Derksen, CYD, Captaindan, Chenyu, Complexica, Conversion script, Dan Gluck, David Latapie, Dcljr, Dhatfield, Dominus, Donarreiskoffer, Drini, Drrngrvy, Enormousdude, Feebas factor, Flipperinu, Froppuff, Garry Denke, Giftlite, Glenn, HaeB, Haiviet, Happy-melon, Headbomb, Hidaspal, Icairns, JoJan, Jorisverbiest, Joshua Davis, Jrockley, Karol Langner, Kbdank71, Laurascudder, LearningKnight, Likebox, Lomn, Looxix, Lysdexia, MK8, Mav, Mbell, Meno25, Merovingian, Mixwell, Nikai, Nilradical, Olathe, Orionus, Oxymoron83, Paulfriedman7, Phys, Planlips, QFT, Rorro, Salsb, Seervoitek, Shalom Yechiel, Shlomi Hillel, SpuriousQ, Srleffler, Stormie, Strait, Syndicate, Tanhueiming, Tensegrity, The Anome, Tom Loughed, Tothebarricades.tk, TubularWorld, Vectorboson, Vivektewary, Vsmith, Wikeepedian, Wikiborg, Xerxes314, Zachorious, לוכי, 88 anonymous edits

Boson *Source:* <http://en.wikipedia.org/windex.php?oldid=295675183> *Contributors:* 217.126.156.xxx, Abdullais4u, Abtvctkt061, Aldie, Alexfusco5, Altenmann, Alxndr, Andres, Andrewa, Anonymous Dissident, Anthony Appleyard, Antixt, Beland, Ben-Zin, Bertrem, Bkalaf, Bradenripple, BriEnBest, Buckyboy314, Cakira, CYD, Candamir, Cenarium, Complexica, Conversion script, Cructacean, Dan Gluck, DanielCD, Danjel, Danthewhale, Dicklyon, Discospinster, Drxenocide, Enchanter, Enormousdude, Evil saltine, Froppuff, Frozenport, Giftlite, Gilliam, Glenn, Gravivitistically, GregorB, H2g2bob, Hadal, Hal peridol, Headbomb, Hidaspal, Hqb, Ianji, Icairns, Inertiatic076, Jensbn, Jeraaldo, Jlandahl, Jossi, Kaihsu, Kbdank71, Kbh3rd, Kingpin13, La goutte de pluie, Loeadec, Lisiate, Looxix, MK8, MagnaMopus, Master Justin, Mathninja, Mbell, Merovingian, Michael Hardy, MichaelMaggs, Mike2vzl, Minami Kana, Mormegil, Mpatel, Nakos2208, NawlinWiki, Nilradical, Noisy, Nsajiansajja, OlEnglish, Orionus, Ornil, Ouchitburns, Owhanow, Palica, Panoramix, Pharotic, Philvarner, Phys, Pkoppenn, Pyg, QFT, Roadrunner, Robinh, Rocastelo, Rorro, RuneSylvester, Salsb, Schneelocke, Senator Palpatine, Sreffer, Stebbins, Strait, Sunborn, T-dot, Tarotcards, The Anome, The Wild Falcon, The1physicist, TheEditrix2, Tim Starling, Ubrdude85, UltraHighVacuum, VashiDonsk, Voyajer, W.F.Galway, Ward3001, Welsh, WhiteHatLurker, Wikeepedian, Wikiborg, Zfr, Zzedar, 132 anonymous edits

Standard Model *Source:* <http://en.wikipedia.org/windex.php?oldid=297182670> *Contributors:* APH, Addshore, Agasicles, Agasides, AmarChandra, Andre Engels, Aosten, Arivero, AugPi, Awren, AxelBoldt, Axl, Bakken, Bambaiah, Bamkin, Barak Sh, Bassbonerocks, Benbest, Bender235, Bevo, Bodhiha, Bovineone, Brews ohare, Brim, Brockert, Bryan Derksen, Bubba73, C0nanPayne, CYD, Caco de vidro, CattleGirl, Chris the speller, ChristopherWillis, Complexica, Craig Bolon, Crazz bug 5, Crum375, D-Notice, DWHalliday, DannyWilde, Dauto, Dave1g, David Barnard, Dbenbenn, Deepmath, Derek Ross, Dextrose, Dfan, Dmmaus, Drhex, Drrngrvy, Dstudent, Dv82matt, Dysepsion, Eeekster, Egg, Ekjon Lok, El C, Elsweyn, Eprb123,

Ernsts, FT2, Faethon, Faethon34, Faethon36, Fences and windows, Fogger, FrankTobia, Gary King, Giftlite, Glenn, Gnixon, Goop Goop, Gparker, Gscshoyru, Guarracino, Guy Harris, H2g2bob, HEL, Hal peridol, Haotherb428, Harp, Harrigan, Headbomb, Herbee, Hexane2000, Hirak 99, HorsePunchKid, HungarianBarbarian, Icairns, Iomesus, Isis, Itinerant1, J Milburn, J.delanoy, JabberWok, Jagged 85, JarahE, JeffBobFrank, Jeodesic, Jgwacker, Jmnbatista, Joshmt, Julesd, Kacser, Kate, KathrynLybarger, Laurascudder, LeYaYa, Len Raymond, Leszek Jańczuk, Likebox, LilHelpa, Linas, Lomn, Looxix, Macumba, Mldmac, Melchoir, Metacommet, Michael C Price, Michael Hardy, Michaelbusch, Mindmatrix, Mjamja, Monedula, Moose-32, Mousaffa, MovGP0, Mpatel, Mxn, Nozzer42, Ohwilleke, Ordovico, Orion11M87, Orionus, Patrick, Pharotic, Phr, Phys, Physicist brazuca, Populus, QFT, Qwertyca, R.e.b., RG2, Ram-Man, Rama, Raven in Orbit, Rbj, Reddi, Rmrfstar, Roadrunner, Robdunst, Roscoe x, SCZenz, Schucker, SebastianHelm, Securiger, Setanta747 (locked), Setreset, SheepNotGoats, Sheliak, Silly rabbit, Sligocki, Soarhead77, Sonjaaa, Stannered, Stevertigo, Stillnotelf, Superm401, Swamy g, TPickup, Tarcieri, Tariqhada, Template namespace initialisation script, TenOfAllTrades, Tetracube, Texture, That Guy, From That Show!, The Anome, The Transliterator, Thunderboltz, Tom Loughheed, TriTertButoxy, Truthnlove, Twas Now, Van helsing, Verdy p, Vessels42, Voorlandt, VoxMoose, WJBScribe, Wagggers, Wwheaton, Xerxes314, YellowMonkey, Yevgeny Kats, Youandme, 238 anonymous edits

Quantum electrodynamics *Source:* <http://en.wikipedia.org/windex.php?oldid=296209448> *Contributors:* .:Ajvol.:, 130.64.83.xxx, 2over0, Achoo5000, Aeosynth, Ahoerstemeier, Alan Canon, Albertod4, Alexshag, Alro, AmarChandra, Ancheta Wis, Andrej.westermann, Aolanaonwaswronglyaccused, Aolanonawanabe, Bakken, Beland, Blaine Steinert, Bryan Derksen, Chipef, Complexica, Conversion script, DJIndica, DV8 2XL, DWeir, Daniel james, Daubigne, Dbachmann, DefLog, Diberri, Didymos, DnetSvg, Drini, EGGs, Enormousdude, Eyebum, F, Giftlite, Gravitophoton, HEL, Harley peters, Headbomb, Helix84, Iameukarya, Icairns, Ivanivanovich, JMK, JabberWok, JeffBobFrank, Joke137, Joshuaabowman, Jsldub, Keenan Pepper, Krapsin, Lambiam, Lethe, Light current, Linas, Looxix, Lucidish, Maliz, Mani1, Markus Kuhn, Mathieu Perrin, Matt McIrvin, Maurice Carbonaro, Max woolfson, Melchoir, Minestrone Soup, MobyDike, Mpatel, MuthuKutty, Neilrieck, ObsidianOrder, Omegaumber, Ortonmc, Ott2, Patrick Gill, PatrickOMoran, Peter484, Phys, Pjacobi, Plumpurple, QFT, RandomTool2, Rangek, Retune, Rex the first, Richwil, Rje, Rjtucke, Runningonbrains, SCZenz, Sadi Carnot, Salbers, Salix alba, Salsb, Sanders muc, Shyrnes321, Science5, Sctfn, Sheliak, Sj, Snafflekid, Speed8ump, Speedyboy, Spike Wilbury, Spsprez, Srleffler, Stannered, Stevertigo, Strait, Stripsi, Sukaël, Techibun, Tim Starling, Timb66, Tom Loughheed, Tooto, Tribaal, Triona, Truthnlove, UCSD3.14159, Ugha, Unyoyega, Urvabara, Van helsing, Viriditas, Voyajer, Waltpohl, Weihao.chiu, Wolfkeeper, Wooster, Yill577, Zarniwoot, 128 anonymous edits

Quantum field theory *Source:* <http://en.wikipedia.org/windex.php?oldid=296991585> *Contributors:* 130.64.83.xxx, 171.64.58.xxx, 9.86, APH, Ahoerstemeier, Albertod4, Alfred Centauri, Alison, AmarChandra, Amareto2, Amarvc, Ancheta Wis, Andrea Allais, Archelon, Arnero, AstroPig7, Bambaiah, Bananan, Banus, Bci2, BenRG, Bevo, Bkalafut, Bkennis2006, Bckavnger, Bob108, Brews ohare, Bt414, CALR, CYD, Caracolillo, Charles Matthews, Ciphers, Complexica, ConradPino, Conversion script, Custos0, Cyp, D6, DJIndica, Dan Gluck, Dauto, DefLog, Dj thegreat, Dmhowarth26, Docboat, Drschawrz, Egg, El C, Erik J, Etale, Four Dog Night, Gandalf61, Garion96, Gcbirzan, GeorgeLouis, Giftlite, Gjsreejith, Glenn, Graham87, GrahamHardy, HEL, Hairy Dude, Hanish.polavarapu, Headbomb, Helix84, Henry Delforn, HexaChord, HowardFrampton, Ht686rg90, IRP, IZAK, Igodard, Igorivanov, Iridescent, Itinerant1, J.delanoy, Jecht (Final Fantasy X), Jeepday, Jmnbatista, Joseph Solis in Australia, KarlHallowell, Karol Langner, Kasimann, Kenneth Dawson, Knowandgive, Kromatol, LLHolm, Leapold, Lerman, Lethe, Likebox, Looxix, Maliz, MarSch, Markisgreen, Marks, Martin Kostner, Masudr, Mav, Mbell, Mboverload, Mclid, Melchoir, Mendicus, Mentifisto, Mgiganteus1, Michael C Price, Michael Hardy, Moltrix, Mpatel, Msebast, MuDavid, N shaji, Neparis, Nikolas Karalis, Northgrove, Nvj, Oddmonster, Opie, PSimeon, Palpher, Paolo.dL, Pcarbonn, Phys, Physicistjedi, Pinkgoanna, Pjacobi, Pt, Puksik, QFT, R.ductor, R.e.b., RE, RG2, Raphtee, Rebooted, Roadrunner, Robert L, Rotem Dan, Rudminjd, RuudVisser, SCZenz, SebastianHelm, Semperf, Shanes, Sheliak, Shvav, Sietse Snel, SirFozzie, Skou, Spellage, Srleffler, Stephan Schneider, Stevertigo, StewartMH, Stupidmoran, Tamtamar, Template namespace initialisation script, The 80s chick, The Anome, The Wild West guy, Thialfi, Thingg, Threepounds, Tim Starling, TimNelson, Timwi, Tlabbshier, Tom Loughheed, Truthnlove, Tugjob, UkPaolo, Urvabara, Van helsing, Vanderdecken, Varuna, Victor Eremita, Wavelength, Wik, Witten Is God, Wwheaton, XJamRastafire, Yndurain, Zarniwoot, 211 anonymous edits

Quantum chromodynamics *Source:* <http://en.wikipedia.org/windex.php?oldid=296388344> *Contributors:* 130.199.3.xxx, AdamSolomon, Adoniscik, Ahoerstemeier, Alai, AndonicO, AnnaFrance, AxelBoldt, Azn king28, Bambaiah, Banus, Corvidae, Betsythedevine, BlackAndy, Brews ohare, CDN99, CYD, Capefeather, Chris the speller, Chrisfox8, Coemgenus, Complexica, Conversion script, Corvidaeacervus, DJIndica, DavidMcCabe, DKiernan, Ecucindler, Eep2, El C, Elroch, Emperorbma, Finell, Fredrik, Fwb22, GaeusOctavius, Garry Denke, Giftlite, Goplat, GrahamHardy, Guy Harris, HEL, Hairy Dude, Henriok, Hut 8.5, Icairns, JabberWok, Jaganath, JamesMLane, Jason Quinn, JeffBobFrank, Jitse Niesen, JonL, Kirill Lokshin, Kusma, Likebox, Lseixas, Lumidek, Maliz, Monedula, Moto Perpetuo, Mpatel, NNemec, Noclavername, Ojigiri, Petros000, Phys, Physicistjedi, Provelt, Pt, Ricky81682, Robomojo, Runningonbrains, Ryulong, Saibod, Salgueiro, Sam Hocevar, Sctfn, Seth Ilys, Shambolic Entity, Sheliak, Skullfunk, SkyLined, Skyring, Slakr, Slicky, Spike Wilbury, Stevertigo, Tamtamar, TenOfAllTrades, Thenewdeal87, Thiseye, TimBentley, Timmeken, TriTertButoxy, Truthnlove, Vald, VermillionBird, WDavis1911, WVhybrid, Whkoh, Xerxes314, Youandme, Zundark, Zzuuzz, 108 anonymous edits

Electron *Source:* <http://en.wikipedia.org/windex.php?oldid=296593681> *Contributors:* (aeropagitica), 16@r, A4, ABF, AVand, Aarchiba, Acalamari, Acelor, AcidHelmNun, Acrynim, Acroterion, Adam Rock, Ahoerstemeier, Aitias, Akamad, Al Wiseman, Ale jrb, AlexiusHoratius, AallyUnion, Almcraebotac, Anaraug, Andre Engels, Andres, Antonio Lopez, Ap, Ardonik, Army1987, Arpingstone, Artichoker, Asierra, AstroNomer, Atjesse, AtomicDragon, AxelBoldt, Bagel7, Bakanov, Bambaiah, Bart133, Bdesham, Beetle B., Ben Tillman, BenRG, Benjah-bmm27, Bennybp, Bessaccount, BernardH, Bert Hickman, BILIC, Blainstern, Bobo192, Bongwarrior, Booba5, Brews ohare, Brian0918, Bryan Derksen, Bvcrist, CYD, Calair, Camembert, CanadianLinuxUser, Cantras, CardinalDan, Ceranthor, Chamal N, Chekaz, ChemGardener, Chetvorno, Chill doubt, Chizkiyahavraham, Christopher Parham, ChristopherWillis, CircafuciX, Ckatz, Cometstyles, Complexica, Confusedmiked, Conversion script, Cool Blue, Correcting nonesense, Curps, D, DV8 2XL, Da monster under your bed, Daxude3320, Daniel.Cardenas, DannyWilde, Dar-Ape, DarthVader, Darthgriz98, Dauto, David Hochron, David edwards, DavidStern, Dawn Bard, Deh, Deryck Chan, Diberri, Dina, Dineshextreeme, Discospinster, Dispenser, Dissident, Dmn, Dmr2, DonJStevens, Donarreiskoffer, Droll, Drondent, E23, EJJ, Ealdgyth, Ed Poor, Edgar181, Edward Z. Yang, Egil, El C, Eleassar, Eleassar777, Elroch, Enviroboy, Eprb123, Equendil, Eric B, Eric-Wester, Evgeny, Fastfission, FeralDruid, Ferkelparade, FreplySpang, Fruge, Funnybunny, GDonato, Gaius Cornelius, Gary King, Gdo01, Gdr, Gef756, Gene Nygaard, Generalguy11, Gentgeen, GeometryGirl, Giftlite, Gil987, Gilgamesh, Glenn, Goplat, Graymornings, GreenSpigot, Greg L, Gtstricky, Gzuckier, H2g2bob, Hadal, HaeB, HappyVR, HcorEric X, Headbomb, Heavy bolter, Heimstern, Herbee, Heron, Hidaspal, Hongthay, Hqbb, Hurleymann1, Hveziris, IRP, Icairns, Ilikepie2221, Imaninjapirite, Inala, Iridescent, IrishChemistPride, IrishChemistPride2, Itub, Ixf64, J Di, J-stan, J.Sarfatti, J.delanoy, JLaTondre, JSpudeman, JabberWok, Jackal irl, Jaganath, James Trotter, Jamyricks, Jaques O. Carvalho, Jaxl, JayMars, Jebba, Jeff3000, JimQ, Jimp, JoanneB, John5955, JohnArmagh, JohnOwens, Joizashmo, Joncam, Jonnyapple, Jordi Burguet Castell, Joshmt, Jrockley, Jusjih, KPH2293, Kaiba, Kalivd, Kan8eDie, Karol Langner, Kingturtle, Kjoonlee, KnowledgeOfSelf, Knutux, KrakatoaKatie, Kriak, Krich, Kricotta, Kurtcobain321, Kurykh, Kurzon, Kwekubo, Lathrop, Latka, Light current, Lightmouse, Linas, Lkrujsw, Llort, LouisBB, Lucinos, Lunchscale, Lycaon, MEJG, Maliz, Malo, Mani1, Markhurd, Marlith, Martial75, Mattfont, Mav, Maximus Rex, Mbell, McVities, Megaboz, Melchoir, Melibarr05, Mermaid from the Baltic Sea, Merovingian, MetsFan76, Mgaarafan, Michael Devore, Michael H 34, Michael Hardy, Mike Peel, Mike Rosoft, Mindmatrix, Mindspillage, Miquonranger03, Mlouns, Monkey Bounce, Mote, Mr. Hallman, Mrhellcool, Ms2ger, Mxn, Mydickishuge24, Nabla, Naturalnumber, Neparis, Nergaal, Nergality, Neurolysis, Newone, Noel Streatfield, Nonagonal Spider, NovaDog, Nrccpm2026, NuclearWarfare, NuclearWinner, Numbo3, Obradovic Goran, Ocatecir, Omega21, Omegatron, Omnedon, Omnipedian, Opelio, Ori.livneh, Owlbuster, Ozielke, Palica, Pandion auk, Patrick, Patrick L. Goes, Pcarbonn, Pearle, Persian Poet Gal, Peter G Werner, Peter470, PeterisP, Peterlin, Peyna, Philip Trueman, PhilipO, Phillycheesesteaks, PhysSusie, Physchim62, Piano non troppo, PingPongBoy, Pingveno, Pnacutin, PoliticalJunkie, Ponyo, Potekhin, Prestonmag, Pt, RAlafritz, RG2, RJHall, RainbowOfLight, Rajeevmsa, RandomTREES, Ravedave, Rbdebole, RedRollerskate, Reddi, Rednblu, Redskunk, Redvers, Retired username, RetiredUser2, RexNL, Reywas92, Rgoodermote, Riana, Rich Farmbrough, RichBlinne, Ricky81682, RobertAustin, Rotational, RoyBoy, Royalguard11, Roybb95, Rurik3, Ruslik0, RyanOrdemann, Ryrivard, SCZenz, Sadi Carnot, Salsb, Sanders muc, SandyGeorgia, Shyrnes321, Scarian, Sean William, Secretlondon, Sergeanthuggy, Shadown, Sheliak, Shootbamboo, SimonP, Sjodenator, Skymt, Slartibartfast1992, Slowking Man, SmoothK, Spencer, Spike Wilbury, SpookyMulder, SpuriousQ, Srleffler, Ssd, Stepa, Stevertigo, Strait, StuTheSheep, Suisui, Susvolans, Swimallday, THEN WHO WAS PHONE?, Tcnvc, TechOutsider, Tellyaddict, Thadaddy3233, TheChrisD, Theonlyledge, Thereen, Thermocap, Thingg, Thisisborin9, Tim Starling, TimothyRias, Timwi, TomasBat, Tomdobb, Tonyfey, Tonyrex, Travelbird, TriTertButoxy, Trojancowboy, Tyco.skinner, UPS Truck Driver, Uncle G, Unclevortex, Uruk2008, V1adis1av, Ventolin, Versus22, Vespriстано, VictorP, Voorlandt, Voyajer, Vsmith, WFPm, WMSwiki, Wagggers, Wavelength, Wayward, Wereon, West Brom 4ever, Wigie, WikHead, Wikiborg, Wilt, WingkeeLEE, Wolfmankurd, Xl, Xantolus, Xerxes314, Xplat, Yamamoto Ichiro, Yath, Yoos, Zazou, Zeamays, ZeroOne, Zigger, ~K, 百家姓之四, 827 anonymous edits

Proton *Source:* <http://en.wikipedia.org/windex.php?oldid=296642458> *Contributors:* Aadal, Acalamari, Acroterion, Aeluwas, Ahoerstemeier, Aitias, Ale jrb, Alexalexalex123, Altenmann, Andre Engels, AndrewBuck, Antandrus, Anthony Appleyard, Anthony5429, Antixt, Anuran, Ap, Apoc2400, Arcturus87, ArglebargleIV, Army1987, Artaxiad, Astrangequark, Attilios, B41988, Bambaiah, Bayerischermann, Bebenko, Bensaccount, Bethling, Bjman, Blennow, Bobo192, Bongwarrior, Bryan Derksen, C.A.T.S. CEO, COMPFUNK2, Cacycle, can't sleep, clown will eat me, Carmelbuck, Cglassey, Cholerashot,

CiaPan, Ciju, Closedmouth, Complexica, Computerjoe, Conversion script, Crobzub, Cst17, Cureden, CyclePat, D-Day, Danny, David.Monniaux, DeadEyeArrow, Deathcakes, Deglr6328, Demmy100, Denny, Dhochron, Diagonalfish, DigitalSorceress, Dirac66, Discospinster, Donarreiskoffer, DragonflySixtyseven, Dvorak729, Dwmyers, Dwool99f, EarthPerson, Eddideigel, Edgar181, Egil, El C, El pobre Pedro, Elb2000, Elipongo, Ellissound, Ellmist, Epbr123, Eric-Wester, Excirial, Fang 23, Femto, F rien, Flauto Dolce, Fleminra, FooBar, Foobaz, Frank Lofaro Jr., Fresheneesz, GTubio, Geraki, Giftlite, GlassCobra, Glenn, GregorB, Grunt, Hadal, HairyDan, Headbomb, Heart of a Lion, Hellbus, Herbee, Heron, Herr apa, Homestarmy, Hveziris, Icairns, Injinera, Insanity Incarnate, Itsmine, Itub, J.delanoy, JaGa, Jacob.jose, Jaknouse, Jakohn, Jauerback, Jenlight, Jenswort, Jester2001, Jj137, Jordi Burguet Castell, Josh Cherry, Jpk, Jumbo Snails, Kaihsu, Kanxkawii, Kbdank71, Keilana, Kerotan, King of Hearts, Kjkolb, Kjoonlee, Knutux, Kusma, KyraVixen, Lo2u, Looxix, Lunchscale, Lupin, MER-C, MOble, Mani1, Manning Bartlett, Martin Ulfvik, Mattabat, Mattpickman, Maurice Carbonaro, Mav, Mayz, McVities, Melchoir, Merovingian, Mike Rosoft, Mikez, Mion, Mixwell, Mkweise, Mls1492, Mnemeson, Moe Epsilon, Moeron, Mozzura, Mr blabla, Munky2, Mxn, Myanw, Mygerardromance, Narayanese, Naturalnumber, Nekura, NeonMerlin, Newone, Nick Y., Nicklcms, Nivix, NuclearWarfare, NuclearWinner, Obradovic Goran, Oddworth, Odie5533, OllieFury, Omegatron, Omnipedian, Onevalefan, Oni Lukos, Orii, Oxymoron83, Patrick, Paul D. Anderson, Paul-L, Phroks13, Pdbailey, PeteShanosky, Petri Krohn, Phazvmk, Philip Trueman, Philippe, PhySusie, Pip2andahalf, PlatinumX, Plyn9, Poopmister91191, Pooryorick, Q43, RG2, RODERICKMOLASAR, Rain bowell, RainbowOfLight, Rajbboy69, Rajeevmass, RangeK, Rasheedy, Rdsmith4, Recurring dreams, Red Director, RedWolf, Regibox, Rettetast, RexNL, Rhethh, Richard Arthur Norton (1958-), Ronhjones, Rtcpenguin, Rueyfgugdij, S, Saga City, Salsa Shark, Salsb, Sbharis, Sbowers3, SchiftyThree, Shalom Yechiel, Silverxxx, Sir Vicious, SkyLined, Snurks, Sobekhotep, Soliloquial, Spacecadethailey, Spangineer, Specter01010, Squishywushy123, Srleffler, Stevertigo, Stewacide, Strait, Studnic12, Subash.chandran007, Swpb, Sycthos, TakuyaMurata, The Original Wildbear, The Rambling Man, The Real Marauder, Thehelpfulone, Thingg, Timwi, TomasBat, Tsogo3, Tuffcarrot, Umdunno, Until It Sleeps, Utcursch, Uucp, Vitalikk, Vortexrealm, Vsmith, WODUP, Waggars, Wandering Traveler, Weglarczyk, Weletahoozyzog, WickedwizarDOfoz, Wigie, WikHead, Wikiacc, Wikiwikiwiki3, Writtenright, XJamRastafire, Xe1881, Xerxes314, Xiahou, Yamamoto Ichiro, Yelyos, Zrules, Велетень, 560 anonymous edits

Hadrons *Source:* <http://en.wikipedia.org/windex.php?oldid=17027323> *Contributors:* -

Quarks *Source:* <http://en.wikipedia.org/windex.php?oldid=16090797> *Contributors:* -

Gluons *Source:* <http://en.wikipedia.org/windex.php?oldid=16236027> *Contributors:* -

Higgs boson *Source:* <http://en.wikipedia.org/windex.php?oldid=297612498> *Contributors:* -dennis-, A Man In Black, ABF, Abdullaish4u, Allstarecho, Altenmann, Alyjack, AnOddName, AndersFeder, Andrius.v, Anonymi, Antixt, Archelon, Artur80, Atomicthumbs, AxelBoldt, Baad, Bambaiah, Bcody80, Bcorr, BenRG, Benplowman, Betterusername, Bevo, BobertWABC, Bodhitha, Bookofjude, Boson15, Brian Fenton, Brians, Bryan Derksen, Bubba73, BullRangifer, C S, CYD, Cadmasteradam, Caknuck, CamB424, CamB4242, CesarB, Cgd8d, Cgwaldman, CharlesC, Chuckupd, Cinkcool, Closedmouth, Consumed Crustacean, CrazyInSane, Cructacean, D'Agosta, DBGustavson, DMurphy, Daniel C, DannyDaWriter, Dante Alighieri, Dauto, Dbachmann, DeadlyMETAL, Deceglie, Discospinster, Diza, Donarreiskoffer, DrGaellon, Dragon of the Pants, Dratman, Drmies, DÅugosz, EchetusXe, Ehn, Eikern, El C, ElfQrin, Eliga, Endersdouble, Epastore, Er ouz, Eritain, Ernsts, Excirial, Fatram, Fiziker, Fleisher, Fleminra, FooBar, Foobar, Frymaster, Gaurav, Giandrea, Giftlite, Gil987, Gobbledygeek, Goethean, Golbez, Goudzovski, GregorB, Gurch, Gwib, Hadal, Hairy Dude, Harold f, Harp, Headbomb, Herbee, Heron, Hippypink, Icairns, Iknowyourider, Impunv, Infestor, Itinerant, Itinerant1, Iwpg, J M Rice, J mcandrews, J.delanoy, JCSantos, JTiago, JabberWok, Jacques Antoine, JasonAQuest, Jc odcsmf, Jde123, Jehochman, Jfromcanada, Jgwacker, Jimtpat, Jkl, JohnArmagh, Jonathan D. Parshall, Jor63, Joriki, Josh Cherry, Jpod2, Jtuggle, Justinrossetti, Kaihsu, KapilTagore, Kbdank71, Kborland, Kencf0618, Kendrick7, Kenneth Dawson, Kgf0, Koavf, Konor org, Kooo, Kyng, La goutte de pluie, Lambiam, Laurascudder, Lee M, Lethe, LilHelpa, Linas, Loves martyr, M-Falcon, Mani1, Manning Bartlett, Marcel Kosko, Marcus Brute, Markdavid2000, Martaf, Martijn Hoekstra, Masterofpsi, Matan568, McVities, Mcorazao, Melchoir, Meldor, Merovingian, Mesons, Mgimpel, Michael C Price, Mike Peel, Mindmatrix, Moeron, Moose-32, Mukadderat, Mxn, N4tur4le, Nafhan, NawlinWiki, NeilN, Netrapt, Newzebras, Nightscream, Nihiltres, Nimur, Nondisclosure, Norm mit, Norvy, Novemberrain94, Now dance, fu.cker, dance!, Nsbinsnj, Nskillen, Nurg, Oddz, Ohnoitsjamie, Oreopriest, Orionus, Owain, Pagw, PeterTheWall, Peterbullockismynname, Phil Boswell, Photnh2o, Phys, PhysicsGrad2013, Pie4all88, Pip2andahalf, Pizza1512, Praveen pillay, ProjeX, Proofreader77, Pulickkal, Quadell, Qutezuze, R.e.b., Rangelov, Reinoutr, Resonance cascade, RetiredUser2, Reuben, RevendS, Rich Farmbrough, Rick7425, Rjwilmsi, Roadrunner, RobertG, Rotiro, Ruslik0, SCZenz, Salsb, Sasquatch, Shove, Sburke, ScAvenger, Selva, ShaneCavanaugh, Shawn@garbett.org, Shimgray, Sjdunn9, Slawojarek, Sligocki, Spemle, Splarka, SqueakBox, Srleffler, Strait, Superm401, Tburket, Tdent, TeunSpaans, Tevatron, The Original Wildbear, TheBendster, Thor Waldsen, Three887, Thruston, Ti-30X, Tigga en, Tom12519, TotoBaggins, TpbBradbury, TriTertButoxy, Tritium6, Twas Now, Universalsuffrage, Until It Sleeps, Usp, V1adis1av, Varlaam, WAS 4.250, WikiUserPedia, Wikiborg, Wmlschlotterer, Wnt, Xerxes314, Yevgeny Kats, Yoweigh, Zekemurdock, Zentropa, 346 anonymous edits

Quantum chemistry *Source:* <http://en.wikipedia.org/windex.php?oldid=296822991> *Contributors:* 144.189.40.xxx, 208.40.185.xxx, 4lex, Acroterion, Alansohn, Ayla, BTDenyer, Bci2, Bduke, Bob, BrianY, Bubbha, CDN99, Capecodeph, ChemGardener, CloudNine, Cmdrjameson, CommonsDelinker, Conversion script, Cool3, Cypa, EdJohnston, Edsanville, EmilyT, Euryalus, Gentgeen, Gershom, Giftlite, Glenn, GregorB, Haljolad, HappyCamper, Holdran, Hugo-cs, Ian Pitchford, Itub, James 007, Jantop, JerrySteal, Kaliumfredrik, Karol Langner, Keenan Pepper, Keilana, Koinut, Krash, La goutte de pluie, Lampuchi, Ligulem, Lijuni, Looxix, M stone, Martin Hedegaard, Meisfunny, Milo, Nickptar, Noisy, NzZl, Okedem, Perelaar, Ratol, Rifleman 82, SHL-at-Sv, SQL, Sadi Carnot, Salsb, Shalom Yechiel, Shanel, Sidhekin, Smoe, Sunev, Tasudrty, Terhorstj, Timwi, UninvitedCompany, Vb, Vgy7ujm, Vig vimarsh, Voigfda, Vsmith, W.F.Galway, Wiki alf, Xebvor, Yurik, Zarniwoot, Zeimusu, Александър, ملّاع بوبحم, 132 anonymous edits

Image Sources, Licenses and Contributors

Image:X-ray diffraction pattern 3clpro.jpg Source: http://en.wikipedia.org/windex.php?title=File:X-ray_diffraction_pattern_3clpro.jpg License: unknown Contributors: User:Jeff Dahl

Image:Unknown Quartz crystal 66.JPG Source: http://en.wikipedia.org/windex.php?title=File:Unknown_Quartz_crystal_66.JPG License: unknown Contributors: User:Digon3

Image:Insulincrystals.jpg Source: <http://en.wikipedia.org/windex.php?title=File:Insulincrystals.jpg> License: Public Domain Contributors: Chrumps, Jurema Oliveira, Photohound

Image:Halite(Salt)USGOV.jpg Source: [http://en.wikipedia.org/windex.php?title=File:Halite\(Salt\)USGOV.jpg](http://en.wikipedia.org/windex.php?title=File:Halite(Salt)USGOV.jpg) License: Public Domain Contributors: ARTE, Mschel, Quadro, Saperaud, Selphy, Str4nd, 6 anonymous edits

Image:Monocrystal dsc03676.jpg Source: http://en.wikipedia.org/windex.php?title=File:Monocrystal_dsc03676.jpg License: Creative Commons Attribution-Sharealike 2.0 Contributors: User:David.Monniaux

Image:Gallium1 640x480.jpg Source: http://en.wikipedia.org/windex.php?title=File:Gallium1_640x480.jpg License: GNU Free Documentation License Contributors: Dbc334, Frumpy, Greatpatton, Mattes, Saperaud, 1 anonymous edits

Image:Ice crystals.jpg Source: http://en.wikipedia.org/windex.php?title=File:Ice_crystals.jpg License: unknown Contributors: Mila Zinkova

Image:A fossil shell with calcite.jpg Source: http://en.wikipedia.org/windex.php?title=File:A_fossil_shell_with_calcite.jpg License: unknown Contributors: Mila

Image:Square diffraction.jpg Source: http://en.wikipedia.org/windex.php?title=File:Square_diffraction.jpg License: Public Domain Contributors: V81

Image:Diffraction pattern in spiderweb.JPG Source: http://en.wikipedia.org/windex.php?title=File:Diffraction_pattern_in_spiderweb.JPG License: unknown Contributors: Mila Zinkova

Image:Solar glory at the steam from hot spring.jpg Source: http://en.wikipedia.org/windex.php?title=File:Solar_glory_at_the_steam_from_hot_spring.jpg License: unknown Contributors: Mila Zinkova

Image:Young Diffraction.png Source: http://en.wikipedia.org/windex.php?title=File:Young_Diffraction.png License: Public Domain Contributors: DrKiernan, Glenn, Quatar

Image:Single-slit-diffraction-ripple-tank.jpg Source: <http://en.wikipedia.org/windex.php?title=File:Single-slit-diffraction-ripple-tank.jpg> License: unknown Contributors: User:Armedblowfish

Image:Wave Diffraction 4Lambda Slit.png Source: http://en.wikipedia.org/windex.php?title=File:Wave_Diffraction_4Lambda_Slit.png License: Public Domain Contributors: Original uploader was Dicklyon at en.wikipedia

Image:diffraction1.png Source: <http://en.wikipedia.org/windex.php?title=File:Diffraction1.png> License: unknown Contributors: Denniss, Rosarinagazo, Tony Wills, 2 anonymous edits

Image:Diffraction2vs5.jpg Source: <http://en.wikipedia.org/windex.php?title=File:Diffraction2vs5.jpg> License: GNU Free Documentation License Contributors: Original uploader was Bcrowell at en.wikipedia

Image:Diffraction 150 slits.jpg Source: http://en.wikipedia.org/windex.php?title=File:Diffraction_150_slits.jpg License: unknown Contributors: User:Shim'on

Image:Airy-pattern.svg Source: <http://en.wikipedia.org/windex.php?title=File:Airy-pattern.svg> License: Public Domain Contributors: User:Sakurambo

Image:Airy2.gif Source: <http://en.wikipedia.org/windex.php?title=File:Airy2.gif> License: unknown Contributors: MuthuKutty

Image:zboo lucky image 1pc.png Source: http://en.wikipedia.org/windex.php?title=File:Zboo_lucky_image_1pc.png License: Public Domain Contributors: Rnt20, Werckmeister

Image:Schéma de principe du synchrotron.jpg Source: http://en.wikipedia.org/windex.php?title=File:Schéma_de_principe_du_synchrotron.jpg License: Attribution Contributors: EPSIM 3D/JF Santarelli, Synchrotron Soleil

Image:Aust.-Synchrotron-Interior-Panorama,-14.06.2007.jpg Source: <http://en.wikipedia.org/windex.php?title=File:Aust.-Synchrotron-Interior-Panorama,-14.06.2007.jpg> License: unknown Contributors: User:Jiron

Image:SOLEIL le 01 juin 2005.jpg Source: http://en.wikipedia.org/windex.php?title=File:SOLEIL_le_01_juin_2005.jpg License: Attribution Contributors: David.Monniaux, Pieter Kuiper

Image:Hohlraum irradiation on NOVA laser.jpg Source: http://en.wikipedia.org/windex.php?title=File:Hohlraum_irradiation_on_NOVA_laser.jpg License: Public Domain Contributors: Deglr6328, DynV, Gumby600

Image:Be foil square.jpg Source: http://en.wikipedia.org/windex.php?title=File:Be_foil_square.jpg License: GNU Free Documentation License Contributors: Deglr6328

Image:Single multiple scattering.jpg Source: http://en.wikipedia.org/windex.php?title=File:Single_multiple_scattering.jpg License: Public Domain Contributors: Agrestini, Jarekt, Pieter Kuiper

Image:PuXANES.jpg Source: <http://en.wikipedia.org/windex.php?title=File:PuXANES.jpg> License: Public Domain Contributors: Bkell, Cadmium

Image:ComptonScattering-s.svg Source: <http://en.wikipedia.org/windex.php?title=File:ComptonScattering-s.svg> License: GNU Free Documentation License Contributors: Original uploader was JabberWok at en.wikipedia

Image:ComptonScattering-u.svg Source: <http://en.wikipedia.org/windex.php?title=File:ComptonScattering-u.svg> License: GNU Free Documentation License Contributors: Original uploader was JabberWok at en.wikipedia

Image:Compton-scattering.svg Source: <http://en.wikipedia.org/windex.php?title=File:Compton-scattering.svg> License: unknown Contributors: Original uploader was JabberWok at en.wikipedia

File:ComptonEnergy.jpg Source: <http://en.wikipedia.org/windex.php?title=File:ComptonEnergy.jpg> License: unknown Contributors: User:AllenMcC.

Image:Electron Microscope.png Source: http://en.wikipedia.org/windex.php?title=File:Electron_Microscope.png License: Public Domain Contributors: User:GrahamColm

Image:Ernst Ruska Electron Microscope - Deutsches Museum - Munich-edit.jpg Source: http://en.wikipedia.org/windex.php?title=File:Ernst_Ruska_Electron_Microscope_-_Deutsches_Museum_-_Munich-edit.jpg License: unknown Contributors: J Brew, uploaded on the English-speaking Wikipedia by .

Image:Ant SEM.jpg Source: http://en.wikipedia.org/windex.php?title=File:Ant_SEM.jpg License: unknown Contributors: Fanghong, Howcheng, Kersti Nebelsiek, Mattes, NEON ja, Neil916, Olei, Romary, Steff, 1 anonymous edits

Image:Golden insect 01 Pengo.jpg Source: http://en.wikipedia.org/windex.php?title=File:Golden_insect_01_Pengo.jpg License: unknown Contributors: Pengo

Image:Krillfilter2kils.jpg Source: <http://en.wikipedia.org/windex.php?title=File:Krillfilter2kils.jpg> License: GNU Free Documentation License Contributors: User:uwe kils

Image:C60a.png Source: <http://en.wikipedia.org/windex.php?title=File:C60a.png> License: GNU Free Documentation License Contributors: Original uploader was Mstroeck at en.wikipedia Later versions were uploaded by Bryn C at en.wikipedia.

Image:Rotaxane.jpg Source: <http://en.wikipedia.org/windex.php?title=File:Rotaxane.jpg> License: unknown Contributors: Keenan Pepper, M Stone

File:Sarfus.DNABiochip.jpg Source: <http://en.wikipedia.org/windex.php?title=File:Sarfus.DNABiochip.jpg> License: unknown Contributors: Nanolane

Image:Achermann7RED.jpg *Source:* <http://en.wikipedia.org/windex.php?title=File:Achermann7RED.jpg> *License:* Public Domain *Contributors:* Marc Achermann

Image:AFMsetup.jpg *Source:* <http://en.wikipedia.org/windex.php?title=File:AFMsetup.jpg> *License:* Creative Commons Attribution 2.5 *Contributors:* Inkwinia, Joey-das-WBF, KristianMolhave, Pieter Kuiper, 1 anonymous edits

Image:Holliday Junction.png *Source:* http://en.wikipedia.org/windex.php?title=File:Holliday_Junction.png *License:* Public Domain *Contributors:* Ahruman, Crux, Infrogmation, TimVickers, Wickey

Image:Holliday junction coloured.png *Source:* http://en.wikipedia.org/windex.php?title=File:Holliday_junction_coloured.png *License:* GNU Free Documentation License *Contributors:* Original uploader was Zephyris at en.wikipedia

Image:Mao-DX-schematic.jpg *Source:* <http://en.wikipedia.org/windex.php?title=File:Mao-DX-schematic.jpg> *License:* Creative Commons Attribution 2.5 *Contributors:* Antony-22

Image:Mao-DXarray-schematic.gif *Source:* <http://en.wikipedia.org/windex.php?title=File:Mao-DXarray-schematic.gif> *License:* Creative Commons Attribution 2.5 *Contributors:* Antony-22

Image:SierpinskiTriangle.svg *Source:* <http://en.wikipedia.org/windex.php?title=File:SierpinskiTriangle.svg> *License:* Public Domain *Contributors:* User:PiAndWhippedCream

Image:Rothemund-DNA-SierpinskiGasket.jpg *Source:* <http://en.wikipedia.org/windex.php?title=File:Rothemund-DNA-SierpinskiGasket.jpg> *License:* Creative Commons Attribution 2.5 *Contributors:* Antony-22

Image:Microarray2.gif *Source:* <http://en.wikipedia.org/windex.php?title=File:Microarray2.gif> *License:* Public Domain *Contributors:* Original uploader was Paphrag at en.wikipedia

Image:Affymetrix-microarray.jpg *Source:* <http://en.wikipedia.org/windex.php?title=File:Affymetrix-microarray.jpg> *License:* unknown *Contributors:* Schutz

Image:Microarray-schema.jpg *Source:* <http://en.wikipedia.org/windex.php?title=File:Microarray-schema.jpg> *License:* Public Domain *Contributors:* Larssono, Million Moments

Image:Heatmap.png *Source:* <http://en.wikipedia.org/windex.php?title=File:Heatmap.png> *License:* Public Domain *Contributors:* Original uploader was Miguel Andrade at en.wikipedia

Image:Mutation Surveyor Trace.jpg *Source:* http://en.wikipedia.org/windex.php?title=File:Mutation_Surveyor_Trace.jpg *License:* Public Domain *Contributors:* Tammyz06

Image:Sequencing.jpg *Source:* <http://en.wikipedia.org/windex.php?title=File:Sequencing.jpg> *License:* GNU Free Documentation License *Contributors:* John Schmidt

Image:DNA Sequencin 3 labeling methods.jpg *Source:* http://en.wikipedia.org/windex.php?title=File:DNA_Sequencin_3_labeling_methods.jpg *License:* Public Domain *Contributors:* Abizar

Image:Radioactive Fluorescent Seq.jpg *Source:* http://en.wikipedia.org/windex.php?title=File:Radioactive_Fluorescent_Seq.jpg *License:* unknown *Contributors:* Original uploader was Abizar at en.wikipedia

Image:CE Basic.jpg *Source:* http://en.wikipedia.org/windex.php?title=File:CE_Basic.jpg *License:* Public Domain *Contributors:* Abizar

Image:Sanger sequencing read display.gif *Source:* http://en.wikipedia.org/windex.php?title=File:Sanger_sequencing_read_display.gif *License:* Public Domain *Contributors:* Loris

Image:DNA Sequencing gDNA libraries.jpg *Source:* http://en.wikipedia.org/windex.php?title=File:DNA_Sequencing_gDNA_libraries.jpg *License:* Public Domain *Contributors:* Abizar

Image:Quark structure neutron.svg *Source:* http://en.wikipedia.org/windex.php?title=File:Quark_structure_neutron.svg *License:* unknown *Contributors:* User:Harp

Image:Beta Negative Decay.svg *Source:* http://en.wikipedia.org/windex.php?title=File:Beta_Negative_Decay.svg *License:* Public Domain *Contributors:* User:Joelholdsworth

Image:inelastic-neutron-scattering-basics.png *Source:* <http://en.wikipedia.org/windex.php?title=File:Inelastic-neutron-scattering-basics.png> *License:* Public Domain *Contributors:* Joachim Wuttke

Image:ISISLogo.png *Source:* <http://en.wikipedia.org/windex.php?title=File:ISISLogo.png> *License:* unknown *Contributors:* Islander

Image:ISIS_exptal_hall.jpg *Source:* http://en.wikipedia.org/windex.php?title=File:ISIS_exptal_hall.jpg *License:* unknown *Contributors:* wurzeller

Image:ISIS_neutron_hall.jpg *Source:* http://en.wikipedia.org/windex.php?title=File:ISIS_neutron_hall.jpg *License:* unknown *Contributors:* User:Sandig

Image:Sudbury Neutrino Observatory.artist concept of detector.jpg *Source:* http://en.wikipedia.org/windex.php?title=File:Sudbury_Neutrino_Observatory.artist_concept_of_detector.jpg *License:* unknown *Contributors:* Bearcat, Duk, Joseph Dwayne, 1 anonymous edits

File:Sudbury sno.jpg *Source:* http://en.wikipedia.org/windex.php?title=File:Sudbury_sno.jpg *License:* Public Domain *Contributors:* Original uploader was Srbauser at de.wikipedia

Image:LHC.svg *Source:* <http://en.wikipedia.org/windex.php?title=File:LHC.svg> *License:* unknown *Contributors:* User:Harp

Image:ATLAS-logo.jpg *Source:* <http://en.wikipedia.org/windex.php?title=File:ATLAS-logo.jpg> *License:* logo *Contributors:* Andrius.v

Image:CERN Atlas Caverne.jpg *Source:* http://en.wikipedia.org/windex.php?title=File:CERN_Atlas_Caverne.jpg *License:* GNU Free Documentation License *Contributors:* Nikolai Schwerg

Image:gg to ttH.jpg *Source:* http://en.wikipedia.org/windex.php?title=File:Gg_to_ttH.jpg *License:* Public Domain *Contributors:* Harp, Helix84, Joelholdsworth, Pieter Kuiper

Image:ATLAS TRT.jpg *Source:* http://en.wikipedia.org/windex.php?title=File:ATLAS_TRT.jpg *License:* GNU Free Documentation License *Contributors:* Gorgo, Harp

Image:ATLAS HCal.jpg *Source:* http://en.wikipedia.org/windex.php?title=File:ATLAS_HCal.jpg *License:* GNU Free Documentation License *Contributors:* Mdd, Skaller, 1 anonymous edits

Image:CERN-Rama-33.jpg *Source:* <http://en.wikipedia.org/windex.php?title=File:CERN-Rama-33.jpg> *License:* Creative Commons Attribution-Sharealike 2.0 *Contributors:* User:Rama

Image:ATLAS Above.jpg *Source:* http://en.wikipedia.org/windex.php?title=File:ATLAS_Above.jpg *License:* GNU Free Documentation License *Contributors:* Gorgo, Harp

Image:Atlas detector CERN feb2007.jpg *Source:* http://en.wikipedia.org/windex.php?title=File:Atlas_detector_CERN_feb2007.jpg *License:* Public Domain *Contributors:* Sindre Skrede

Image:Moons shodow in muons.gif *Source:* http://en.wikipedia.org/windex.php?title=File:Moons_shodow_in_muons.gif *License:* unknown *Contributors:* Deglr6328, Headbomb, Stifle, Vanderdecken, 1 anonymous edits

Image:Muon Decay.png *Source:* http://en.wikipedia.org/windex.php?title=File:Muon_Decay.png *License:* Public Domain *Contributors:* User:Thymo

Image:DIS.svg *Source:* <http://en.wikipedia.org/windex.php?title=File:DIS.svg> *License:* Public Domain *Contributors:* Belfer00, E2m

Image:First neutrino observation.jpg *Source:* http://en.wikipedia.org/windex.php?title=File:First_neutrino_observation.jpg *License:* Public Domain *Contributors:* Harp, Pieter Kuiper, Svdmlen, 1 anonymous edits

Image:Proton proton cycle.png *Source:* http://en.wikipedia.org/windex.php?title=File:Proton_proton_cycle.png *License:* unknown *Contributors:* Bryan Derksen, Harp

Image:Supernova-1987a.jpg *Source:* <http://en.wikipedia.org/windex.php?title=File:Supernova-1987a.jpg> *License:* unknown *Contributors:* First image: Dr. Christopher Burrows, w:European Space AgencyESA/w:Space Telescope Science InstituteSTScI and w:NASANASA; Second image: w:Hubble Heritage ProjectHubble Heritage team.

Image:Interferometer.svg Source: <http://en.wikipedia.org/windex.php?title=File:Interferometer.svg> License: unknown Contributors: User:Stannered

Image:FIRST measurement of SF6 and NH3.jpg Source: http://en.wikipedia.org/windex.php?title=File:FIRST_measurement_of_SF6_and_NH3.jpg License: Creative Commons Attribution-Sharealike 3.0 Contributors: Andre Villemaire

Image:AFMimageRoughGlass20x20.png Source: <http://en.wikipedia.org/windex.php?title=File:AFMimageRoughGlass20x20.png> License: Public Domain Contributors: Chych

Image:Atomic force microscope by Zureks.jpg Source: http://en.wikipedia.org/windex.php?title=File:Atomic_force_microscope_by_Zureks.jpg License: unknown Contributors: User:Zureks

Image:Atomic force microscope block diagram.svg Source: http://en.wikipedia.org/windex.php?title=File:Atomic_force_microscope_block_diagram.svg License: Public Domain Contributors: Twisp

Image:AFM (used) cantilever in Scanning Electron Microscope, magnification 1000x.GIF Source: [http://en.wikipedia.org/windex.php?title=File:AFM_\(used\)_cantilever_in_Scanning_Electron_Microscope,_magnification_1000x.GIF](http://en.wikipedia.org/windex.php?title=File:AFM_(used)_cantilever_in_Scanning_Electron_Microscope,_magnification_1000x.GIF) License: unknown Contributors: User:SecretDisc

Image:AFM (used) cantilever in Scanning Electron Microscope, magnification 3000x.GIF Source: [http://en.wikipedia.org/windex.php?title=File:AFM_\(used\)_cantilever_in_Scanning_Electron_Microscope,_magnification_3000x.GIF](http://en.wikipedia.org/windex.php?title=File:AFM_(used)_cantilever_in_Scanning_Electron_Microscope,_magnification_3000x.GIF) License: unknown Contributors: User:SecretDisc

Image:Single-Molecule-Under-Water-AFM-Tapping-Mode.jpg Source: <http://en.wikipedia.org/windex.php?title=File:Single-Molecule-Under-Water-AFM-Tapping-Mode.jpg> License: unknown Contributors: User:Yurko

Image:AFM noncontactmode.jpg Source: http://en.wikipedia.org/windex.php?title=File:AFM_noncontactmode.jpg License: unknown Contributors: User:Creepin475

Image:AFM beamdetection.jpg Source: http://en.wikipedia.org/windex.php?title=File:AFM_beamdetection.jpg License: unknown Contributors: User:Creepin475

Image:AFM view of sodium chloride.gif Source: http://en.wikipedia.org/windex.php?title=File:AFM_view_of_sodium_chloride.gif License: Public Domain Contributors: Courtesy of prof. Ernst Meyer, university of Basel

Image:Atomic Force Microscope Science Museum London.jpg Source: http://en.wikipedia.org/windex.php?title=File:Atomic_Force_Microscope_Science_Museum_London.jpg License: GNU Free Documentation License Contributors: John Dalton

Image:Piezoscanner.JPG Source: <http://en.wikipedia.org/windex.php?title=File:Piezoscanner.JPG> License: unknown Contributors: User:Creepin475

Image:Bruker Avance1000.jpg Source: http://en.wikipedia.org/windex.php?title=File:Bruker_Avance1000.jpg License: unknown Contributors: Haydarkustu

Image:Nuclear Magnetic Resonance Spectrometer.jpg Source: http://en.wikipedia.org/windex.php?title=File:Nuclear_Magnetic_Resonance_Spectrometer.jpg License: Public Domain Contributors: EMSL at Pacific Northwest National Laboratory

Image:EPR splitting.jpg Source: http://en.wikipedia.org/windex.php?title=File:EPR_splitting.jpg License: Public Domain Contributors: Original uploader was Astrochemist at en.wikipedia

Image:HWB-NMRv900.jpg Source: <http://en.wikipedia.org/windex.php?title=File:HWB-NMRv900.jpg> License: Public Domain Contributors: MartinSaunders

Image:Modern 3T MRI.JPG Source: http://en.wikipedia.org/windex.php?title=File:Modern_3T_MRI.JPG License: unknown Contributors: User:KasugaHuang

Image:Symmetrical stretching.gif Source: http://en.wikipedia.org/windex.php?title=File:Symmetrical_stretching.gif License: Public Domain Contributors: Tiago Becerra Paolini, 1 anonymous edits

Image:Asymmetrical stretching.gif Source: http://en.wikipedia.org/windex.php?title=File:Asymmetrical_stretching.gif License: Public Domain Contributors: Tiago Becerra Paolini

Image:Scissoring.gif Source: <http://en.wikipedia.org/windex.php?title=File:Scissoring.gif> License: Public Domain Contributors: Tiago Becerra Paolini

Image:Modo rotacao.gif Source: http://en.wikipedia.org/windex.php?title=File:Modo_rotacao.gif License: Public Domain Contributors: Original uploader was Tiago Becerra Paolini at pt.wikipedia

Image:Wagging.gif Source: <http://en.wikipedia.org/windex.php?title=File:Wagging.gif> License: Public Domain Contributors: Tiago Becerra Paolini

Image:Twisting.gif Source: <http://en.wikipedia.org/windex.php?title=File:Twisting.gif> License: Public Domain Contributors: Tiago Becerra Paolini

Image:IR spectroscopy apparatus.jpg Source: http://en.wikipedia.org/windex.php?title=File:IR_spectroscopy_apparatus.jpg License: GNU Free Documentation License Contributors: Ewen

Image:IR summary version 2.gif Source: http://en.wikipedia.org/windex.php?title=File:IR_summary_version_2.gif License: unknown Contributors: DavidRKelly, Devon Fyson

Image:2dir_pulse_sequence_newversion.png Source: http://en.wikipedia.org/windex.php?title=File:2dir_pulse_sequence_newversion.png License: Creative Commons Attribution-Sharealike 3.0 Contributors: Pharmacomancer (talk) Original uploader was Pharmacomancer at en.wikipedia

Image:Dichloromethane near IR spectrum.png Source: http://en.wikipedia.org/windex.php?title=File:Dichloromethane_near_IR_spectrum.png License: GNU Free Documentation License Contributors: Original uploader was Deglr6328 at en.wikipedia

Image:Ethanol near IR spectrum.png Source: http://en.wikipedia.org/windex.php?title=File:Ethanol_near_IR_spectrum.png License: unknown Contributors: Original uploader was Deglr6328 at en.wikipedia

File:Symmetrical stretching.gif Source: http://en.wikipedia.org/windex.php?title=File:Symmetrical_stretching.gif License: Public Domain Contributors: Tiago Becerra Paolini, 1 anonymous edits

File:Asymmetrical stretching.gif Source: http://en.wikipedia.org/windex.php?title=File:Asymmetrical_stretching.gif License: Public Domain Contributors: Tiago Becerra Paolini

File:Scissoring.gif Source: <http://en.wikipedia.org/windex.php?title=File:Scissoring.gif> License: Public Domain Contributors: Tiago Becerra Paolini

File:Twisting.gif Source: <http://en.wikipedia.org/windex.php?title=File:Twisting.gif> License: Public Domain Contributors: Tiago Becerra Paolini

File:Wagging.gif Source: <http://en.wikipedia.org/windex.php?title=File:Wagging.gif> License: Public Domain Contributors: Tiago Becerra Paolini

File:Agitation moléculaire en milieu aqueux.PNG Source: http://en.wikipedia.org/windex.php?title=File:Agitation_moléculaire_en_milieu_aqueux.PNG License: unknown Contributors: User:H'arnet

File:Amino-CORN.png Source: <http://en.wikipedia.org/windex.php?title=File:Amino-CORN.png> License: unknown Contributors: Original uploader was Password at en.wikipedia

File:GeneticCode21.svg Source: <http://en.wikipedia.org/windex.php?title=File:GeneticCode21.svg> License: unknown Contributors: Original uploader was Kosigrim at en.wikipedia

File:Monosodium-glutamate.png Source: <http://en.wikipedia.org/windex.php?title=File:Monosodium-glutamate.png> License: GNU Free Documentation License Contributors: Cacycle, Rob Hooft, Samulili

File:H-Gly-Ala-OH.jpg Source: <http://en.wikipedia.org/windex.php?title=File:H-Gly-Ala-OH.jpg> License: unknown Contributors: Csatazs

File:Zuiterionball.svg Source: <http://en.wikipedia.org/windex.php?title=File:Zuiterionball.svg> License: Public Domain Contributors: user:YassineMrabet

File:Peptidformationball.svg Source: <http://en.wikipedia.org/windex.php?title=File:Peptidformationball.svg> License: Public Domain Contributors: user:YassineMrabet

File:Aa structure function.svg Source: http://en.wikipedia.org/windex.php?title=File:Aa_structure_function.svg License: Public Domain Contributors: Jonathan

File:Protein Dynamics Cytochrome C 2NEW smaller.gif *Source:*

http://en.wikipedia.org/windex.php?title=File:Protein_Dynamics_Cytochrome_C_2NEW_smaller.gif *License:* GNU Free Documentation License
Contributors: Original uploader was Zephyris at en.wikipedia

File:Protein-primary-structure.png *Source:* <http://en.wikipedia.org/windex.php?title=File:Protein-primary-structure.png> *License:* Public Domain
Contributors: National Human Genome Research Institute (NHGRI)

File:Lysozyme crystal1.JPG *Source:* http://en.wikipedia.org/windex.php?title=File:Lysozyme_crystal1.JPG *License:* unknown *Contributors:* Chrumps, Lode

File:1ezg Tenebrio molitor.png *Source:* http://en.wikipedia.org/windex.php?title=File:1ezg_Tenebrio_molitor.png *License:* GNU Free Documentation License
Contributors: Original uploader was WillowW at en.wikipedia

File:Concanavalin A.png *Source:* http://en.wikipedia.org/windex.php?title=File:Concanavalin_A.png *License:* Public Domain *Contributors:* User:Lijealso

File:Porin.qutemol.ao.png *Source:* <http://en.wikipedia.org/windex.php?title=File:Porin.qutemol.ao.png> *License:* unknown *Contributors:* ALoopingIcon

File:Sucrose porin 1a0s.png *Source:* http://en.wikipedia.org/windex.php?title=File:Sucrose_porin_1a0s.png *License:* unknown *Contributors:* Opabinia regalis

File:Sucrose specific porin 1A0S.png *Source:* http://en.wikipedia.org/windex.php?title=File:Sucrose_specific_porin_1A0S.png *License:* GNU Free Documentation License *Contributors:* Snow64

File:StrictosidineSynthase.png *Source:* <http://en.wikipedia.org/windex.php?title=File:StrictosidineSynthase.png> *License:* unknown *Contributors:* User:Hannes Röst

File:Calmodulin 1CLL.png *Source:* http://en.wikipedia.org/windex.php?title=File:Calmodulin_1CLL.png *License:* Public Domain *Contributors:* Joolz, Lateiner, LeaMaimone, Lode, 1 anonymous edits

File:Haemoglobin-3D-ribbons.png *Source:* <http://en.wikipedia.org/windex.php?title=File:Haemoglobin-3D-ribbons.png> *License:* Public Domain
Contributors: Benjah-bmm27

File:Hemoglobin t-r state ani.gif *Source:* http://en.wikipedia.org/windex.php?title=File:Hemoglobin_t-r_state_ani.gif *License:* GNU Free Documentation License
Contributors: Conscious, Dbenbenn, Editor at Large, Habj, Lennert B, Noca2plus, Tomia, 2 anonymous edits

File:Clostridium perfringens Alpha Toxin Rotate.rsh.gif *Source:*

http://en.wikipedia.org/windex.php?title=File:Clostridium_perfringens_Alpha_Toxin_Rotate.rsh.gif *License:* Public Domain *Contributors:* Ramin Herati

File:Bcl-2 Family.jpg *Source:* http://en.wikipedia.org/windex.php?title=File:Bcl-2_Family.jpg *License:* unknown *Contributors:* Hoffmeier

File:Bcl-2 3D.jpg *Source:* http://en.wikipedia.org/windex.php?title=File:Bcl-2_3D.jpg *License:* GNU Free Documentation License *Contributors:* CN3D

File:PBB Protein THPO image.jpg *Source:* http://en.wikipedia.org/windex.php?title=File:PBB_Protein_THPO_image.jpg *License:* unknown
Contributors:

File:Bence Jones Protein MLE1.jpg *Source:* http://en.wikipedia.org/windex.php?title=File:Bence_Jones_Protein_MLE1.jpg *License:* Public Domain
Contributors: Alex McPherson, University of California, Irvine

File:Duck Delta 1 Crystallin.jpg *Source:* http://en.wikipedia.org/windex.php?title=File:Duck_Delta_1_Crystallin.jpg *License:* Public Domain
Contributors: Ragesoss

File:Michelson-morley.png *Source:* <http://en.wikipedia.org/windex.php?title=File:Michelson-morley.png> *License:* GNU Free Documentation License
Contributors: user:bighead

File:Interferometer.JPG *Source:* <http://en.wikipedia.org/windex.php?title=File:Interferometer.JPG> *License:* unknown *Contributors:* User:Brews ohare

File:Michelson interferometer schematic.png *Source:* http://en.wikipedia.org/windex.php?title=File:Michelson_interferometer_schematic.png *License:* GNU Free Documentation License *Contributors:* Teebeutel

File:IR spectroscopy apparatus.jpg *Source:* http://en.wikipedia.org/windex.php?title=File:IR_spectroscopy_apparatus.jpg *License:* GNU Free Documentation License *Contributors:* Ewen

File:IR spectrometer.jpg *Source:* http://en.wikipedia.org/windex.php?title=File:IR_spectrometer.jpg *License:* Public Domain *Contributors:* S.Levchenkov

File:Michelson Interferometer.jpg *Source:* http://en.wikipedia.org/windex.php?title=File:Michelson_Interferometer.jpg *License:* unknown
Contributors: Falcorian, Juiced lemon, Teebeutel

File:Ir hcl rot-vib mrtz.svg *Source:* http://en.wikipedia.org/windex.php?title=File:Ir_hcl_rot-vib_mrtz.svg *License:* unknown *Contributors:* mrtz

File:BandeIR.png *Source:* <http://en.wikipedia.org/windex.php?title=File:BandeIR.png> *License:* GNU Free Documentation License *Contributors:* User:Grimlock

File:Michelsoninterferometer.jpg *Source:* <http://en.wikipedia.org/windex.php?title=File:Michelsoninterferometer.jpg> *License:* Copyrighted free use
Contributors: Juiced lemon, Skygazer, Tano4595, Teebeutel, Umherirrender, Xorx

File:Michelson couleur.jpg *Source:* http://en.wikipedia.org/windex.php?title=File:Michelson_couleur.jpg *License:* unknown *Contributors:* NicoB, Teebeutel

File:Bismuthine-2D-IR-MMW-dimensions.png *Source:* <http://en.wikipedia.org/windex.php?title=File:Bismuthine-2D-IR-MMW-dimensions.png> *License:* Public Domain *Contributors:* Ben Mills

File:Infrared spectrometer.jpg *Source:* http://en.wikipedia.org/windex.php?title=File:Infrared_spectrometer.jpg *License:* unknown *Contributors:* ishikawa

Image:Raman energy levels.jpg *Source:* http://en.wikipedia.org/windex.php?title=File:Raman_energy_levels.jpg *License:* Creative Commons Attribution-Sharealike 2.5 *Contributors:* w:User:Pavlina2.0

Image:HyperspectralCube.jpg *Source:* <http://en.wikipedia.org/windex.php?title=File:HyperspectralCube.jpg> *License:* Public Domain *Contributors:* Dr. Nicholas M. Short, Sr.

Image:MultispectralComparedToHyperspectral.jpg *Source:*

<http://en.wikipedia.org/windex.php?title=File:MultispectralComparedToHyperspectral.jpg> *License:* Public Domain *Contributors:* Dr. Nicholas M. Short, Sr.

Image:Fluorescence microscop.jpg *Source:* http://en.wikipedia.org/windex.php?title=File:Fluorescence_microscop.jpg *License:* unknown
Contributors: Masur

Image:Inverted microscope.jpg *Source:* http://en.wikipedia.org/windex.php?title=File:Inverted_microscope.jpg *License:* unknown *Contributors:* Nuno Nogueira (Nmnogueira) Original uploader was Nmnogueira at en.wikipedia

Image:FluorescenceFilters 2008-09-28.svg *Source:* http://en.wikipedia.org/windex.php?title=File:FluorescenceFilters_2008-09-28.svg *License:* unknown *Contributors:* User:Mastermolch

Image:Dividing Cell Fluorescence.jpg *Source:* http://en.wikipedia.org/windex.php?title=File:Dividing_Cell_Fluorescence.jpg *License:* unknown
Contributors: Will-moore-dundee

Image:FluorescentCells.jpg *Source:* <http://en.wikipedia.org/windex.php?title=File:FluorescentCells.jpg> *License:* Public Domain *Contributors:* DO11.10, Emijrp, NEON ja, Origamiemensch, Splette, Tolanor, 5 anonymous edits

Image:FISH 13 21.jpg *Source:* http://en.wikipedia.org/windex.php?title=File:FISH_13_21.jpg *License:* Public Domain *Contributors:* Gregor1976

Image:Yeast membrane proteins.jpg *Source:* http://en.wikipedia.org/windex.php?title=File:Yeast_membrane_proteins.jpg *License:* unknown
Contributors: User:Masur

Image:jmol1.png *Source:* <http://en.wikipedia.org/windex.php?title=File:jmol1.png> *License:* unknown *Contributors:* Peter Murray-Rust

Image:Hemagglutinin_molecule.png Source: http://en.wikipedia.org/windex.php?title=File:Hemagglutinin_molecule.png License: GNU Free Documentation License Contributors: U.S. National Institutes of Health.

Image:FormicAcid.pdb.png Source: <http://en.wikipedia.org/windex.php?title=File:FormicAcid.pdb.png> License: Public Domain Contributors: Csörföly D, Cwbm (commons)

Image:Isosurface on molecule.jpg Source: http://en.wikipedia.org/windex.php?title=File:Isosurface_on_molecule.jpg License: unknown Contributors: StoatBringer

Image:porin.qutemol.dl.png Source: <http://en.wikipedia.org/windex.php?title=File:Porin.qutemol.dl.png> License: unknown Contributors: ALoopingIcon

Image:porin.qutemol.ao.png Source: <http://en.wikipedia.org/windex.php?title=File:Porin.qutemol.ao.png> License: unknown Contributors: ALoopingIcon

Image:JmolStick.PNG Source: <http://en.wikipedia.org/windex.php?title=File:JmolStick.PNG> License: unknown Contributors: Peter Murray-Rust

Image:Mdalgorith.PNG Source: <http://en.wikipedia.org/windex.php?title=File:Mdalgorith.PNG> License: Public Domain Contributors: User:Knordlun

Image:Bloch sphere.svg Source: http://en.wikipedia.org/windex.php?title=File:Bloch_sphere.svg License: unknown Contributors: User:Smite-Meister

Image:Quantum computer.jpg Source: http://en.wikipedia.org/windex.php?title=File:Quantum_computer.jpg License: unknown Contributors: Original uploader was Jbw2 at en.wikipedia

Image:BQP complexity class diagram.svg Source: http://en.wikipedia.org/windex.php?title=File:BQP_complexity_class_diagram.svg License: Public Domain Contributors: User:Mike1024

Image:Standard Model of Elementary Particles.svg Source: http://en.wikipedia.org/windex.php?title=File:Standard_Model_of_Elementary_Particles.svg License: unknown Contributors: User:MissMJ

Image:Elementary particle interactions.svg Source: http://en.wikipedia.org/windex.php?title=File:Elementary_particle_interactions.svg License: unknown Contributors: User:Stannered

Image:Particle chart Log.svg Source: http://en.wikipedia.org/windex.php?title=File:Particle_chart_Log.svg License: Public Domain Contributors: Arivero, 1 anonymous edits

Image:Question mark2.svg Source: http://en.wikipedia.org/windex.php?title=File:Question_mark2.svg License: Public Domain Contributors: Original uploader was Acdx at en.wikipedia

Image:vacuum polarization.svg Source: http://en.wikipedia.org/windex.php?title=File:Vacuum_polarization.svg License: Public Domain Contributors: User:Stannered

Image:electron self energy.svg Source: http://en.wikipedia.org/windex.php?title=File:Electron_self_energy.svg License: Public Domain Contributors: User:DnetSvg, User:Phys

Image:vertex correction.svg Source: http://en.wikipedia.org/windex.php?title=File:Vertex_correction.svg License: Public Domain Contributors: User:Harmaa

Image:Schattenkreuzröhre-in use-lateral view-standing cross.jpg Source: http://en.wikipedia.org/windex.php?title=File:Schattenkreuzröhre-in_use-lateral_view-standing_cross.jpg License: unknown Contributors: User:D-Kuru

File:Cyclotron motion wider view.jpg Source: http://en.wikipedia.org/windex.php?title=File:Cyclotron_motion_wider_view.jpg License: unknown Contributors: User:Sfu

Image:Bohr atom model English.svg Source: http://en.wikipedia.org/windex.php?title=File:Bohr_atom_model_English.svg License: unknown Contributors: User:Brighterorange

Image:Orbital s1.png Source: http://en.wikipedia.org/windex.php?title=File:Orbital_s1.png License: unknown Contributors: User:RJHall

Image:Asymmetricwave2.png Source: <http://en.wikipedia.org/windex.php?title=File:Asymmetricwave2.png> License: unknown Contributors: User:TimothyRias

Image:Virtual pairs near electron.png Source: http://en.wikipedia.org/windex.php?title=File:Virtual_pairs_near_electron.png License: unknown Contributors: User:RJHall

Image:Lorentz force.svg Source: http://en.wikipedia.org/windex.php?title=File:Lorentz_force.svg License: GNU Free Documentation License Contributors: User:Jaro.p

Image:Bremstrahlung.svg Source: <http://en.wikipedia.org/windex.php?title=File:Bremstrahlung.svg> License: Public Domain Contributors: Journey234, Pieter Kuiper, RJHall

Image:Hydrogen Density Plots.png Source: http://en.wikipedia.org/windex.php?title=File:Hydrogen_Density_Plots.png License: Public Domain Contributors: User:PoorLeno

Image:Lightning over Oradea Romania cropped.jpg Source: http://en.wikipedia.org/windex.php?title=File:Lightning_over_Oradea_Romania_cropped.jpg License: Public Domain Contributors: User:Lucas

Image:Lorentz factor.svg Source: http://en.wikipedia.org/windex.php?title=File:Lorentz_factor.svg License: Public Domain Contributors: User:egg

Image:Pairproduction.png Source: <http://en.wikipedia.org/windex.php?title=File:Pairproduction.png> License: GNU Free Documentation License Contributors: Davidhorman, Falcorian, RJHall

Image:AirShower.svg Source: <http://en.wikipedia.org/windex.php?title=File:AirShower.svg> License: GNU Free Documentation License Contributors: User:Mpfiz

Image:Polarlicht 2.jpg Source: http://en.wikipedia.org/windex.php?title=File:Polarlicht_2.jpg License: Public Domain Contributors: United States Air Force photo by Senior Airman Joshua Strang

Image:GPN-2000-003012.png Source: <http://en.wikipedia.org/windex.php?title=File:GPN-2000-003012.png> License: Public Domain Contributors: NASA

Image:Quark structure proton.svg Source: http://en.wikipedia.org/windex.php?title=File:Quark_structure_proton.svg License: unknown Contributors: User:Harp

Image:One-loop-diagram.svg Source: <http://en.wikipedia.org/windex.php?title=File:One-loop-diagram.svg> License: GNU Free Documentation License Contributors: JabberWok

Image:Gluon-top-higgs.svg Source: <http://en.wikipedia.org/windex.php?title=File:Gluon-top-higgs.svg> License: GNU Free Documentation License Contributors: JabberWok

License

GNU Free Documentation License
<http://www.gnu.org/copyleft/fdl.html>
